

Late-Stage Functionalization of 1,2-Dihydro-1,2-Azaborines

Author: Alec Nathaniel Brown

Persistent link: <http://hdl.handle.net/2345/bc-ir:104564>

This work is posted on [eScholarship@BC](#),
Boston College University Libraries.

Boston College Electronic Thesis or Dissertation, 2015

Copyright is held by the author. This work is licensed under a Creative Commons Attribution-NonCommercial 4.0 International License (<http://creativecommons.org/licenses/by-nc/4.0>).

Boston College

The Graduate School of Arts and Sciences

Department of Chemistry

LATE-STAGE FUNCTIONALIZATION OF 1,2-DIHYDRO-1,2-AZABORINES

a dissertation

by

ALEC NATHANIEL BROWN

submitted in partial fulfillment of the requirements

for the degree of

Doctor of Philosophy

August 2015

© copyright by ALEC NATHANIEL BROWN

2015

LATE-STAGE FUNCTIONALIZATION OF 1,2-DIHYDRO-1,2-AZABORINES

by

ALEC NATHANIEL BROWN

Dissertation Advisor:

Professor Shih-Yuan Liu

ABSTRACT: Described herein are two distinct research projects focused on the development of metal-catalyzed late-stage functionalization strategies for 1,2-dihydro-1,2-azaborines separated into three chapters. The first chapter discusses the development, synthesis, and recent contributions to the field of azaborine chemistry. The second chapter details the development of rhodium catalyzed *B*-H bond activation for the synthesis of a new class of BN-stilbenes as well as the discovery of a novel *B*-H to *B*-Cl transformation that is successful both with *B*-H azaborines as well as other *B*-H containing compounds. The third chapter pertains to the development of a *B*-H and *B*-Cl tolerant C(3) functionalization strategy through the use of Negishi cross-coupling. Using this methodology, previously unreported isomers of BN-naphthalene and BN-indenyl have been synthesized and characterized.

Dedicated to:

Mom, Dad, Keith, and the crazy extended family we have who have all handled the lack
of vacations and distances in their own way

ACKNOWLEDGMENTS

I would first like to acknowledge Professor Liu for providing a mentally stimulating and satisfying research program to be a part of, with plenty of opportunities to broaden my chemical experience. I would also like to thank Professor Morken and Professor Byers for acting as readers of my thesis and members of my committee, despite my relatively short time here at Boston College. I would like to thank the members of the Liu lab, the present and the past, the East and the West for providing thoughtful discussion and ways to keep the work fresh and exciting. I am indebted to Professor Branchaud for sharing his outlook on effective teaching, science, and life philosophy and his message of continuous improvement, especially when it comes to providing students with the best experience tailored to their own needs that you can give.

Thanks to Jacob Ishibashi for reading sometimes illegible drafts and providing feedback.

To the members of the “weekend group” who were always willing to have a bit of fun and get together to tell stories together despite grad school, thank you for the long nights, we can all strive to be more like Monty.

The best part about graduate school was the conflux of intellectual discussion and talking about chemistry. I would like to thank everyone I have had the pleasure of bouncing ideas off of and discussing science, those times are what makes everything worth it.

List of Abbreviations

Å: angstrom	DMA: dimethyl acetamide
Φ: quantum yield of fluorescence	DMF: dimethylformamide
9-BBN: 9-Borabicyclo[3.3.1]nonane	DMSO: dimethylsulfoxide
Ac: acetate	dppb: 1,2-Bis(diphenylphosphino)butane
API: active pharmaceutical ingredient	dppe: 1,2-Bis(diphenylphosphino)ethane
B ₂ Pin ₂ : bispinacalatodiboron	dppf: 1,1'-Bis(diphenylphosphino) ferrocene
BDE: bond disassociation energy	dtbpy: 4,4'-Di- <i>tert</i> -butyl-2,2'-dipyridyl
BINAP: 2,2'-bis(diphenylphosphino)- 1,1'-binaphthyl	EbDH: ethylbenzene dehydrogenase
bn: benzyl	<i>ee.</i> : enantiomeric excess
Bu: n-butyl	Eq.: equation
cod: cyclooctadiene	equiv: equivalent
cot: cyclooctatetraene	ESI: electrospray ionization
Cp: cyclopentadienyl	eV: electron volts
Cp*: pentamethylcyclopentadienyl	GC/FID: gas chromatography/ flame ionization detector
CPME: cyclopropyl methyl ether	HBcat: catecholborane
cy: cyclohexyl	HBpin: 4,4,5,5-Tetramethyl-1,3,2- dioxaborolane
D: dalton	HOMO: highest occupied molecular orbital
DAIB: (Diacetoxyiodo)benzene	HPLC: high performance liquid chromatography
dan: 1,8-diaminonaphthalene	HRMS: high resolution mass spectrometry
DART: direct analysis in real time	
dba: dibenzylacetone	
DDQ: 2,3-Dichloro-5,6-dicyano-1,4- benzoquinone	

IR: infrared

KHMDS: potassium bis(trimethylsilyl)amide

LAH: lithium aluminum hydride

LDA: Lithium diisopropylamide

LUMO: lowest unoccupied molecular orbital

M: molar

mes: mesityl, 2,4,6-trimethylphenyl

mes-H: 1,3,5-trimethylbenzene

MTBE: methyl tertbutyl ether

nbd: norbornadiene

NCS: *N*-chloro succinamide

nm: nanometer

NMI: *N*-methylimidazole

NMR: nuclear magnetic resonance

NR: no reaction

OFET: organic field effect transistor

OLED: organic light-emitting diode

ORTEP: Oak Ridge Thermal Ellipsoid Plot

Pd/C: palladium on carbon

Pd G2: Chloro [2-(2'-amino-1,1'-biphenyl)]palladium(II)

Ph: phenyl

PHOLED: Phosphorescent organic light-emitting diode

PPh₃: triphenylphosphine

RCM: ring-closing metathesis

rt: room temperature

T0: initial time

TBAF: tetrabutylammonium fluoride

TBS: tert-butyl dimethyl silyl

TD-DFT: time dependent density functional theory

TEA: triethylamine

Tf: triflate

THF: tetrahydrofuran

TMEDA; tetramethylethylenediamine

TMP: tetramethyl piperadine

TMS: trimethylsilyl

TMS-Cl: chlorotrimethylsilane

Trp: tris(pyrazolyl)borate

UV: ultraviolet

V: volt

Xphos: 2-dicyclohexylphosphino-2',4',6'-triisopropyl-1,1'-biphenyl

xs: excess

Table of Contents

Chapter 1	1
Introduction to the Chemistry of 1,2-Azaborines	1
1.1 BN/CC-Isosterism	1
1.2 The development of 1,2-azaborine chemistry	3
1.3 Modern synthesis of monocyclic 1,2-azaborines	7
1.4 Recent developments in azaborine chemistry	13
1.4.1 Warren Piers, University of Calgary, Canada	13
1.4.2 Holger Bettinger, University of Tübingen, Germany	14
1.4.3 Suning Wang, Queen's University, Canada	17
1.4.4 Paul Pringle, University of Bristol, United Kingdom	18
1.4.5 Qichun Zhang, Nanyang Technological University, Singapore	19
1.4.6 Masaharu Nakamura, Kyoto University, Japan	21
1.4.7 Jian Pei, Peking University, China	22
1.4.8 Shih-Yuan Liu, Boston College, United States	25
1.5 The Future of BN-Arenes	29
Chapter 2	30
Metal-Catalyzed <i>B</i> -H Activation of 1,2-Azaborines: Dehydrogenative Borylation to Generate BN-Isosteres of Stilbene and a Unique Metal-Catalyzed <i>B</i> -H to <i>B</i> -Cl Conversion Using an Alkyl Chloride as the Chloride Source	30
2.1 Introduction	30
2.2 Background	32
2.2.1 The development of metal-catalyzed hydroboration and the discovery of metal-catalyzed dehydrogenative borylation	32
2.2.2 The development and scope of metal-catalyzed dehydrogenative borylation of alkenes and alkynes	41
2.2.3 Metal-catalyzed dehydrogenative borylation of alkynes	52
2.2.4 Known <i>B</i> -H to <i>B</i> -Cl transformations	53
2.2.4.1 Electrophilic chlorination of carborane anions	54
2.2.4.2 <i>B</i> -H to <i>B</i> -Cl using HCl	55

2.2.4.3	<i>B</i> -H to <i>B</i> -Cl through conproportionation	55
2.2.4.4	<i>B</i> -H to <i>B</i> -Cl in borate metal complexes	56
2.3	Development of the Dehydrogenative Borylation of 1,2-Azaborines With Styrenes: Synthesis and Characterization of BN-Stilbenes	57
2.4	Development of a novel catalytic <i>B</i> -H to <i>B</i> -Cl with an alkyl chloride as the chloride source	70
2.4	Summary and Conclusions.....	77
2.5	Experimental Section	79
2.5.1	General Information.....	79
2.5.2	Procedure for the preparation of 4-dimethylamino styrene [2039-80-7]....	80
2.5.3	Catalyst Survey (Table 2.1)	81
2.5.4	Preparation of compounds 2.95-2.111 (Scheme 2.32).....	83
2.5.5	Oxygen and water stability study of compound 2.111	89
2.5.6	Synthesis of carbonaceous 2.112-2.114	90
2.5.7	Photophysical data and measurement	92
2.5.8	Crystallographic Data for Compound 2.95 :.....	93
2.5.9	Computational Approach and Results (with Professor David Dixon).....	106
2.5.10	Optimization of <i>B</i> -H to <i>B</i> -Cl Reaction.....	209
2.5.11	Gram-Scale <i>B</i> -H to <i>B</i> -Cl	211
2.5.12	<i>B</i> -H to <i>B</i> -Cl with 9-BBN and HBpin	212
2.5.11	NMR Spectral Library	212
Chapter 3	250
	Development of the Negishi Cross-Coupling of 1,2-Azaborines Containing <i>B</i> -H and <i>B</i> -Cl Bonds and Its Application to the Synthesis of New Extended BN-Arenes.....	250
3.1	Introduction	250
3.2	Background	251
3.2.1	BN-Naphthalenes	251
3.2.1.1	Synthesis of 2,1-Borazaronaphthalenes.....	252
3.2.1.2	Synthesis of 10,9-Borazaronaphthalenes.....	255
3.2.1.3	Synthesis of 1,2-Borazaronaphthalenes.....	256

3.2.2	BN-Indene.....	257
3.2.3	Halogenation Reactions of BN-Heterocycles	259
3.2.4	The Application of Cross-Coupling Reactions for the Modification of BN-Heterocycles.....	261
3.2.5	Boron-Zinc Exchange	265
3.2.6	Known Reactivity Between Boron and Zinc Reagents: Boron-Tolerant Negishi Coupling	268
3.3	Development of Functional Group Tolerant Negishi Cross-Coupling	271
3.3.1	Synthesis of C(3) Brominated <i>B</i> -H and <i>B</i> -Cl Azaborines.....	271
3.3.2	Stability of BN-Arenes to Zinc Reagents	273
3.3.3	Optimization and Substrate Scope of <i>B</i> -H Tolerant Negishi Coupling ..	274
3.3.4	Optimization and Substrate Scope of <i>B</i> -Cl Tolerant Negishi Coupling .	283
3.3.5	Synthesis of and Characterization of New Extended BN-Arenes	287
3.4	Summary and Conclusions.....	293
3.5	Experimental Section	293
3.5.0	General Information.....	293
3.5.1	Experimental Procedures	295
3.5.1.1	Qualitative <i>B</i> -Cl Bond Reactivity with Alkyl Zinc Tests (scheme 2)	295
3.5.1.2	Screening of phosphine ligands for <i>B</i> -H tolerant cross-coupling (Table 3.1).....	297
3.5.1.3	Optimization of PdCl ₂ (P ^o tol ₃) ₂ catalyst system (Table 3.2)	299
3.5.1.4	Preparation of C3 substituted <i>B</i> -H azaborines (schemes 3.21-3.22) 303 Procedures for coupling of R ₂ Zn and RZnX reagents:	303
3.5.1.5	Crystallographic data for compound 3.83	317
3.5.1.6	Survey of catalysts and solvents for the Negishi cross-coupling reaction of 1,2-azaborine 3.71 (Table 3.3).....	326
3.5.1.7	NMR yields of <i>B</i> -Cl azaborines 3.90-3.95 (Scheme 3.23).....	329
3.5.1.8	Preparation of <i>B</i> -Me azaborines 3.96-3.101 (Scheme 3.23).....	336
3.5.1.9	Large-scale preparation of 3.92 (Scheme 3.25).....	343
3.5.1.10	Synthesis of BN-indenyl 3.106 from 3.92 (Scheme 3.26).....	344

3.5.1.11	X-ray crystal data for 3.106	347
3.5.1.12	Synthesis of 9,1-borazaronaphthalene 3.2 from 3.92 (Scheme 3.27).....	361
3.5.1.13	Procedure for the determination of the quantum yield of 3.2	364
3.5.1.13	Crystallographic information for 3.2	366
3.6	NMR Spectral Library	370
Appendix 1: Standard Operating Procedures for the Synthesis of Azaborines Used Throughout This Work		463
A.1	Synthesis of Triallylborane	463
A.1.1	Introductory Scale Procedure for Triallylborane	465
A.1.2	Large-scale Synthesis of Triallylborane	468
A.2	Synthesis of 1,2-Azaborines.....	471
A.2.1	Synthesis of ring-closing precursor A1	471
A.2.2	Synthesis of ring-closed A2	475
A.2.3	Synthesis of N-TBS B-Cl A3	478
A.2.4	Synthesis of C(3) brominated B-Cl azaborine A4	481
A.2.4	Synthesis of C(3) brominated B-H azaborine A5	486

Chapter 1

Introduction to the Chemistry of 1,2-Azaborines

1.1 BN/CC-Isosterism¹

A boron-nitrogen single bond has the same number of valence electrons as a carbon-carbon double bond (C=C bond), while the hybridization and steric environment of the boron and nitrogen system closely mimics that of the C=C bond (Figure 1.1). The replacement of a C=C bond with a B–N bond results in a new BN/CC isostere.² When considered in the context of an extended conjugated system, the effects of BN/CC isosterism are of particular interest for potential biomedical³ and materials science applications.

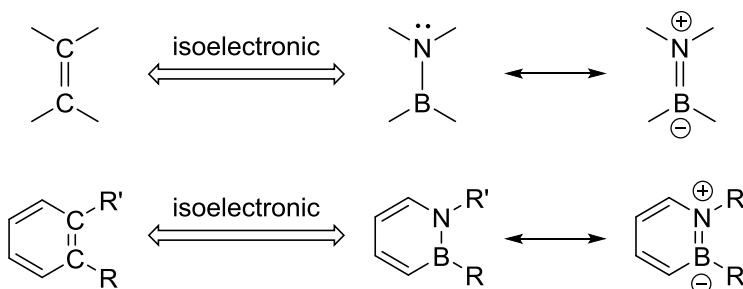


Figure 1.1: Isoelectronic nature of the C=C bond and B–N bond.

¹ The chemistry of BN/CC isosterism has been previously reviewed: (a) Bosdet, M. J. .; Piers, W. E. *Can. J. Chem.* **2009**, *87*, 8-29. (b) Campbell, P. G.; Marwitz, A. J. V.; Liu, S.-Y. *Angew. Chem. Int. Ed.* **2012**, *51*, 6074-6092.

² Langmuir, I. *J. Am. Chem. Soc.* **1919**, *41*, 1543-1559.

³ (a) Liu, L.; Marwitz, A. J. V.; Matthews, B. W.; Liu, S.-Y. *Angew. Chem. Int. Ed.* **2009**, *48*, 6817-6819. (b) Abbey, E. R.; Zakharov, L. N.; Liu, S.-Y. *J. Am. Chem. Soc.* **2010**, *132*, 16340-16342. (c) Abbey, E. R.; Zakharov, L. N.; Liu, S.-Y. *J. Am. Chem. Soc.* **2011**, *133*, 11508-11511. (d) Knack, D. H.; Marshall, J. L.; Harlow, G. P.; Dudzik, A.; Szaleniec, M.; Liu, S.-Y.; Heider, J. *Angew. Chem. Int. Ed.* **2013**, *52*, 2599-2601. (e) Abbey, E. R.; Liu, S.-Y. *Org. Biomol. Chem.* **2013**, *11*, 2060-2069.

In fact, the replacement of any two carbons with boron and nitrogen in a six-membered aromatic structure has the potential to produce three different isomeric BN-isosteres of benzene: 1,2-azaborine (**1.A**), 1,4-azaborine (**1.B**), or 1,3-azaborine (**1.C**) (Figure 1.2). **1.A** is the thermodynamically most stable and most studied isomer, yet displays the lowest aromaticity.⁴ **1.B** is known as part of polycyclic⁵ structures as well as very limited monocyclic⁶ structures, however knowledge of the overall effects of the 1,4-azaborine structure are still limited.

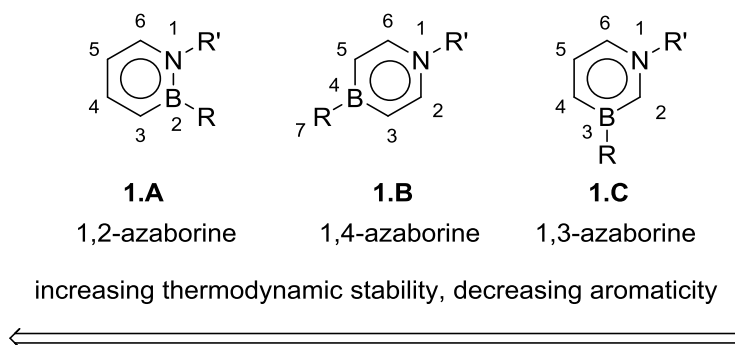


Figure 1.2: The three isomeric BN-arene structures

⁴ For calculated estimates please see: Ghosh, D.; Periyasamy, G.; Pati, S. K. *Phys. Chem. Chem. Phys.* **2011**, *13*, 20627-20636. (b) Baranac-Stojanović, M. *Chem. Eur. J.* **2014**, *20*, 16558-16565. For an experimental measurement of the resonance stabilization energy of a 1,2-azaborine please see: Campbell, P. G.; Abbey, E. R.; Neiner, D.; Grant, D. J.; Dixon, D. A.; Liu, S.-Y. *J. Am. Chem. Soc.* **2010**, *132*, 18048-18050. For a solid-state discussion of the aromaticity of 1,2-azaborines please see: Abbey, E. R.; Zakharov, L. N.; Liu, S.-Y. *J. Am. Chem. Soc.* **2008**, *130*, 7250-7252.

⁵ Maitlis, P. M. *J. Chem. Soc.* **1961**, No. 0, 425-429. (b) Kranz, M.; Hampel, F.; Clark, T. *J. Chem. Soc., Chem. Commun.* **1992**, No. 17, 1247-1248. (c) Agou, T.; Sekine, M.; Kobayashi, J.; Kawashima, T. *Chem. Commun.* **2009**, No. 14, 1894-1896. (d) Agou, T.; Sekine, M.; Kobayashi, J.; Kawashima, T. *Chem. Eur. J.* **2009**, *15*, 5056-5062. (e) Agou, T.; Arai, H.; Kawashima, T. *Chem. Lett.* **2010**, *39*, 612-613. (f) Dimitrijević, E.; Taylor, M. S. *Chem. Sci.* **2013**, *4*, 3298-3303. (g) Dimitrijević, E.; Cusimano, M.; Taylor, M. S. *Org. Biomol. Chem.* **2014**, *12*, 1391-1394. (g) Xu, S.; Haeffner, F.; Li, B.; Zakharov, L. N.; Liu, S.-Y. *Angew. Chem. Int. Ed.* **2014**, *53*, 6795-6799. (h) Chinnapattu, M.; Sathiyarayanan, K. I.; Iyer, P. S. *RSC Adv.* **2015**, *5*, 37716-37720.

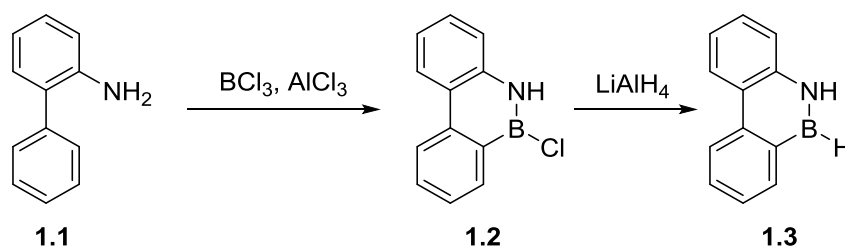
⁶ (a) Braunschweig, H.; Damme, A.; Jimenez-Halla, J. O. C.; Pfaffinger, B.; Radacki, K.; Wolf, J. *Angew. Chem. Int. Ed.* **2012**, *51*, 10034-10037. (b) Holzmeier, F.; Lang, M.; Hemberger, P.; Bodi, A.; Schäfer, M.; Dewhurst, R. D.; Braunschweig, H.; Fischer, I. *Chem. Eur. J.* **2014**, *20*, 9683-9692.

1.C is similarly understudied,⁷ likely due to its difficult synthesis and lower calculated stability. This body of work will focus on the synthesis and functionalization of compounds containing an adjacent BN-unit, the 1,2-azaborine structure.

1.2 The development of 1,2-azaborine chemistry

In 1958, Dewar⁸ reported the synthesis of 9-aza-10-boraphenanthrene (**1.3**), the first reported example of a 1,2-azaborine and the first incorporation of the 1,2-azaborine moiety into an extended arene. N-directed electrophilic aromatic substitution of 2-phenyl aniline (**1.1**) with boron trichloride in the presence of aluminum trichloride generated B–Cl intermediate (**1.2**). Treatment of **1.2** with lithium aluminum hydride produced N–H and B–H containing **1.3** after acidic workup (Scheme 1.1). Dewar demonstrated the reactivity of **1.3** and its derivatives in nucleophilic⁹ and electrophilic¹⁰ aromatic substitution reactions as well as deprotonation studies of the nitrogen atom.¹¹

Scheme 1.1: Dewar’s synthesis of 9-aza-10-boraphenanthrene 1.3, the first 1,2-azaborine



⁷ (a) Xu, S.; Zakharov, L. N.; Liu, S.-Y. *J. Am. Chem. Soc.* **2011**, *133*, 20152-20155. (b) Xu, S.; Mikulas, T. C.; Zakharov, L. N.; Dixon, D. A.; Liu, S.-Y. *Angew. Chem. Int. Ed.* **2013**, *52*, 7527-7531.

⁸ Dewar, M. J. S.; Kubba, V. P.; Pettit, R. *J. Chem. Soc.* **1958**, No. 0, 3073-3076.

⁹ Dewar, M. J. S.; Maitlis, P. M. *J. Am. Chem. Soc.* **1961**, *83*, 187-193.

¹⁰ (a) Dewar, M. J. S.; Kubba, V. P. *Tetrahedron* **1959**, *7*, 213-222. (b) Dewar, M. J. S.; Kubba, V. P. *J. Org. Chem.* **1960**, *25*, 1722-1724. (c) Dewar, M. J. S.; Kubba, V. P. *J. Am. Chem. Soc.* **1961**, *83*, 1757-1760.

¹¹ Dewar, M. J. S.; Maitlis, P. M. *Tetrahedron* **1961**, *15*, 35-45.

Dewar's groundbreaking study of 1,2-azaborine systems led to the discovery of other polycyclic 1,2-azaborines including, for example, 2,1-borazaronaphthalene (**1.4**)¹² and 10,9-borazaronaphthalene (**1.5**) as shown in Figure 1.3.^{13,14}

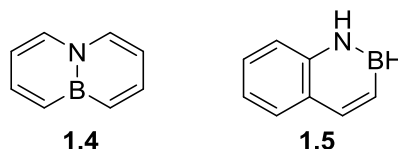
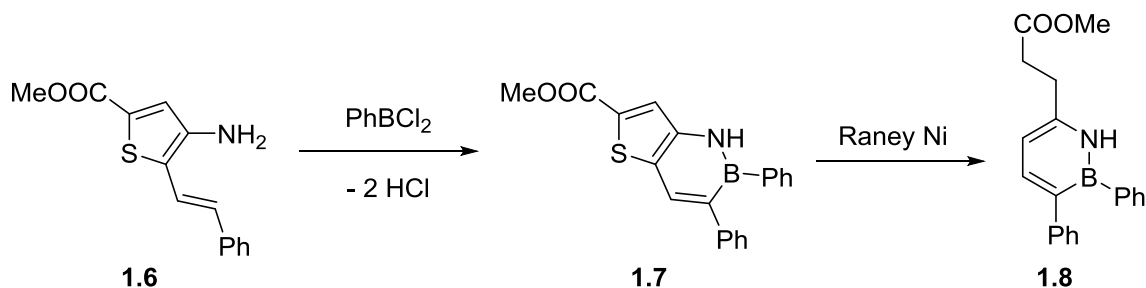


Figure 1.3: Additional ring-fused BN-naphthalenes synthesized by Dewar

Dewar also synthesized the first example of a monocyclic, unfused 1,2-azaborine in 1962 through a reductive desulfurization route.¹⁵ Compound **1.6** underwent electrophilic borylation to generate compound **1.7**. Desulfurization with Raney nickel led to the production of the first highly substituted monocyclic azaborine **1.8** (Scheme 1.2).

Scheme 1.2: The first synthesis of a monocyclic azaborine, 1.8



¹² Dewar, M. J. S.; Dietz, R. *J. Chem. Soc.* **1959**, No. 0, 2728-2730.

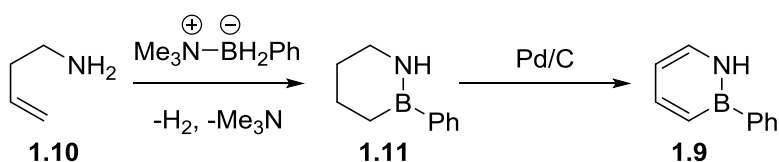
¹³ Dewar, M. J. S.; Gleicher, G. J.; Robinson, B. P. *J. Am. Chem. Soc.* **1964**, *86*, 5698-5699.

¹⁴ For a more detailed description of the chemistry of BN-naphthalenes, please see chapter 3.

¹⁵ Dewar, M. J. S.; Marr, P. A. *J. Am. Chem. Soc.* **1962**, *84*, 3782.

White¹⁶ soon reported the synthesis of a monosubstituted monocyclic *B*-Ph azaborine (**1.9**) through an intramolecular hydroboration followed by palladium-catalyzed oxidation. Treatment of homoallylamine with trimethylaminephenylborane under dilute conditions at 120 °C generated BN cyclohexene **1.11**. Oxidation of neat **1.11** over palladium on carbon at high temperature (>200 °C) under a stream of nitrogen gas produced monocyclic biphenyl isostere **1.9**.

Scheme 1.3: Whites synthesis of *B*-Ph 1.9



From 1970-2000, the field of azaborine chemistry remained rather dormant (13 publications vs. 41 from 1958-1970¹⁷). At the dawn of the new millennium, Ashe and Fang¹⁸ demonstrated a new, mild approach to the synthesis of 6-membered 1,2-azaborine **1.16** (Scheme 1.4, Eq. 1) and 5-membered azaborolide **1.19** (Scheme 1.4, Eq. 2) through a ring-closing metathesis route.

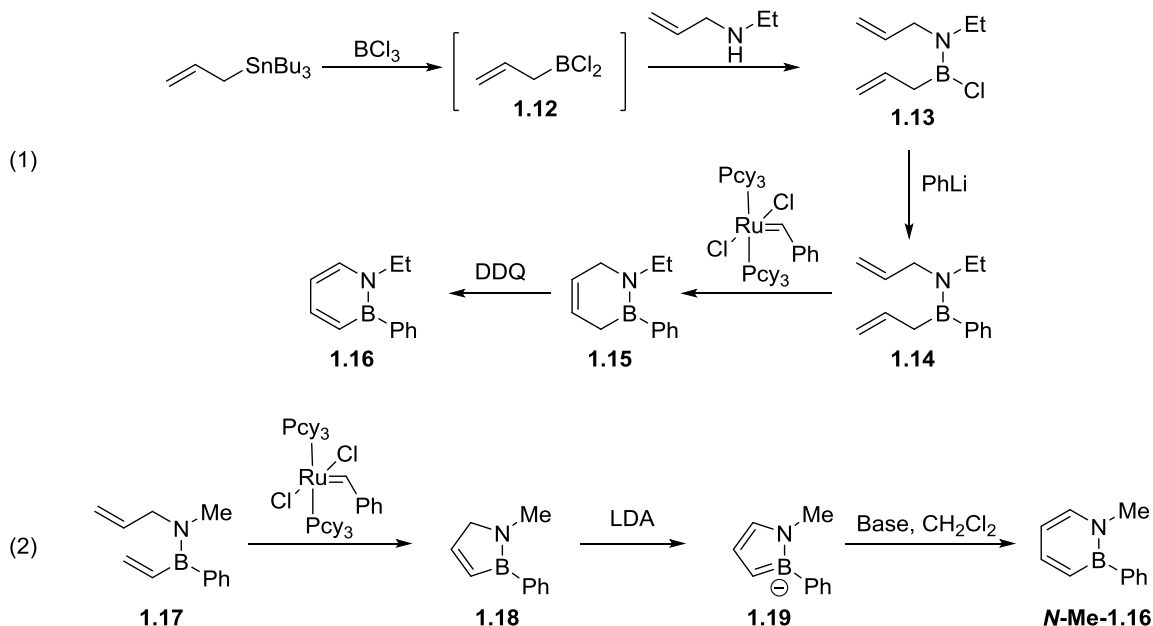
Allylborondichloride **1.12** was generated via transmetalation of allyltributylstannane and boron trichloride. Addition of *N*-ethylallylamine and elimination of HCl provided *B*-N containing **1.13**. Substitution of the *B*-Cl bond with phenyllithium generated diene **1.14**.

¹⁶ White, D. G. *J. Am. Chem. Soc.* **1963**, *85*, 3634-3636.

¹⁷ Data obtained from a scifinder scholar search performed 5/22/2015 for articles containing the concept "azaborine"

¹⁸ Ashe, A. J.; Fang. *Org. Lett.* **2000**, *2*, 2089-2091.

Scheme 1.4: Ashe and Fang's ring-closing metathesis route to 1,2-azaborines



Ring-closing metathesis with Grubb's first generation catalyst produced compound **1.15**. Oxidation using DDQ produced aromatized **1.16**. *B*-vinyl **1.17** was also amenable to ring-closing metathesis generating the 5-membered-ring-containing **1.18**. Deprotonation with LDA furnished azaborolide **1.19** which the authors later¹⁹ demonstrated could be converted to the 6-membered *N*-Me-**1.16** through a carbene-mediated ring expansion.

The Ashe group studied the chemistry of boron-substituted azaborines in metal complexes²⁰ as well as novel syntheses of other ring-fused BN-arenes.²¹ The work of the

¹⁹ Ashe, A. J.; Fang, X.; Fang, X.; Kampf, J. W. *Organometallics* **2001**, *20*, 5413-5418.

²⁰ (a) Ashe, A. J.; Fang, X.; Fang, X.; Kampf, J. W. *Organometallics* **2001**, *20*, 5413-5418. (b) Pan, J.; Kampf, J. W.; Ashe, A. J. *Organometallics* **2004**, *23*, 5626-5629. (c) Pan, J.; Kampf, J. W.; Ashe III, A. J. *Organometallics* **2008**, *27*, 1345-1347. (d) Pan, J.; Kampf, J. W.; Ashe, A. J. *Organometallics* **2009**, *28*, 506-511. (e) Ashe, A. J. *Organometallics* **2009**, *28*, 4236-4248.

²¹ (a) Fang, X.; Yang, H.; Kampf, J. W.; Banaszak Holl, M. M.; Ashe, A. J. *Organometallics* **2006**, *25*, 513-518. (b) Rohr, A. D.; Kampf, J. W.; Ashe, A. J. *Organometallics* **2014**, *33*, 1318-1321.

Ashe group generated a renewed interest in monocyclic azaborines by providing a simple synthetic route to substituted azaborines and demonstrating the potential for modern methodology to be applied to systems containing a B–N bond. The pioneering work of Dewar, White, and Ashe was instrumental in the Liu group’s development and continued interest in a research program focusing on the design, synthesis, and application of BN-arenes.

1.3 Modern synthesis of monocyclic 1,2-azaborines

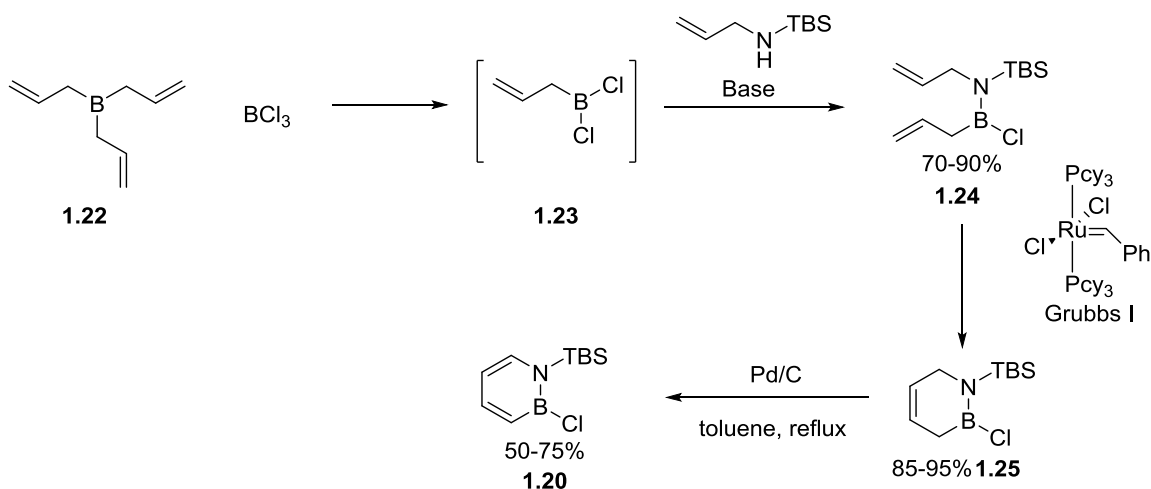
Ashe’s contributions led to a renaissance in the field of BN-arenes. Our group has refined and expanded upon their improved synthesis of monocyclic azaborines. We have developed two complementary azaborine synthons: *N*-TBS *B*-Cl azaborine **1.20**²² as well as *N*-H *B*-OBu azaborine **1.21**.²³ In the Ashe inspired synthesis of **1.20**, the generation of allylboron dichloride **1.23** with triallylborane and boron trichloride circumvents the use of toxic tin and generally gives higher yields²⁴ after condensation with *N*-TBS allylamine to generate diene **1.24**. The *B*-Cl bond is maintained during ring-closing metathesis using Grubbs’ first generation catalyst to give **1.25**. Oxidation of **1.25** over palladium on carbon generates synthon **1.20** which features the removable *N*-TBS group and the functionalizable *B*-Cl bond (Scheme 1.5).

²² Marwitz, A. J. V.; Abbey, E. R.; Jenkins, J. T.; Zakharov, L. N.; Liu, S.-Y. *Org. Lett.* **2007**, *9*, 4905-4908.

²³ Abbey, E. R.; Lamm, A. N.; Baggett, A. W.; Zakharov, L. N.; Liu, S.-Y. *J. Am. Chem. Soc.* **2013**, *135*, 12908-12913.

²⁴ Unpublished results, details in appendix 1.

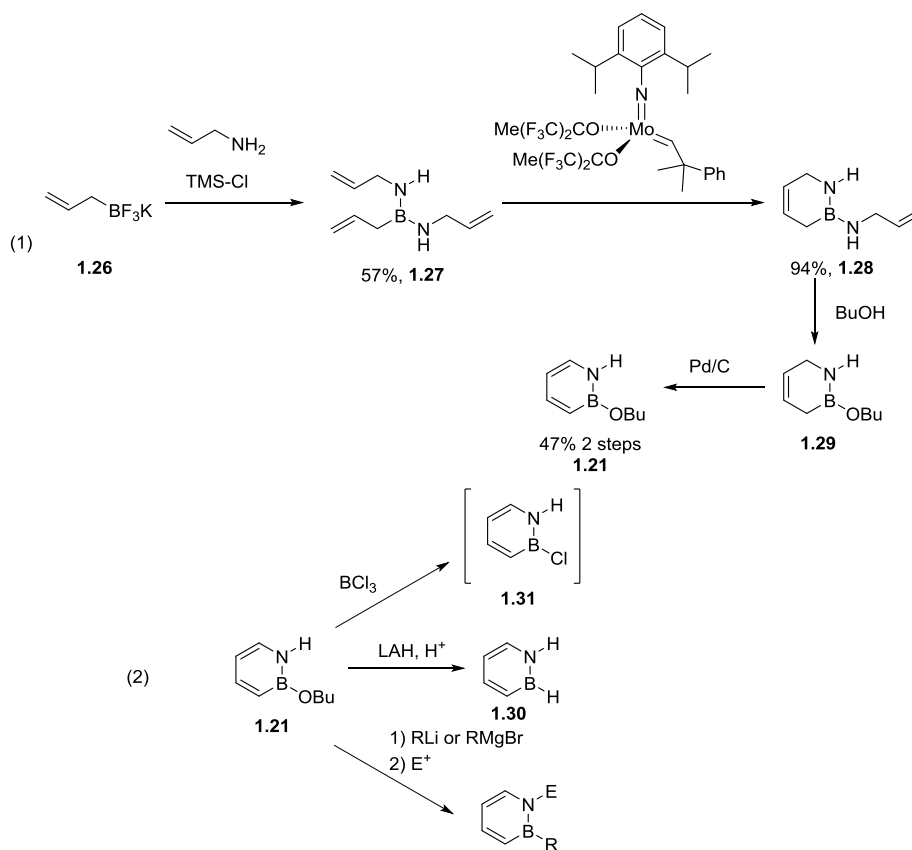
Scheme 1.5: Modern synthesis of B–Cl synthon 1.20



The synthesis of **1.21** begins with the double substitution of allyl potassium trifluoroborate **1.26** by allylamine under action of chlorotrimethylsilane to generate **1.27**. Ring-closing metathesis using a Schrock-type molybdenum catalyst preferentially generates the six-membered ring in **1.28**. Substitution of the exocyclic allylamine with butanol generated **1.29** which is oxidized over palladium on carbon to generate synthon **1.21** (Scheme 1.6, Eq. 1). Protecting-group free **1.21** is amenable to many functional group transformations and can be used to synthesize the parental 1,2-dihydro-1,2-azaborine **1.30** on gram scale (**1.30** is only obtainable from **1.20** on relatively small scale²⁵) as well as to introduce a variety of other substitutions at boron and nitrogen (Scheme 1.6, Eq. 2).

²⁵ Marwitz, A. J. V.; Matus, M. H.; Zakharov, L. N.; Dixon, D. A.; Liu, S.-Y. *Angew. Chem. Int. Ed.* **2009**, *48*, 973-977.

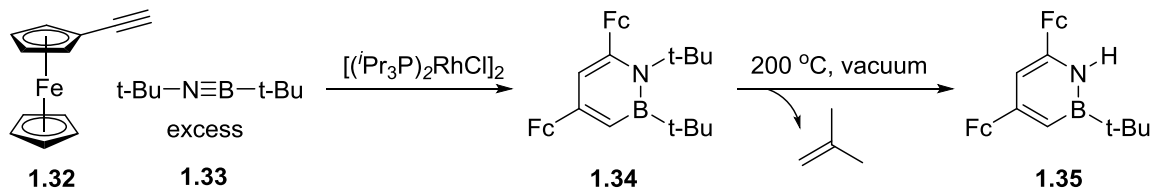
Scheme 1.6: Modern synthesis and reactivity of *N*-H *B*-OBu synthon 1.21



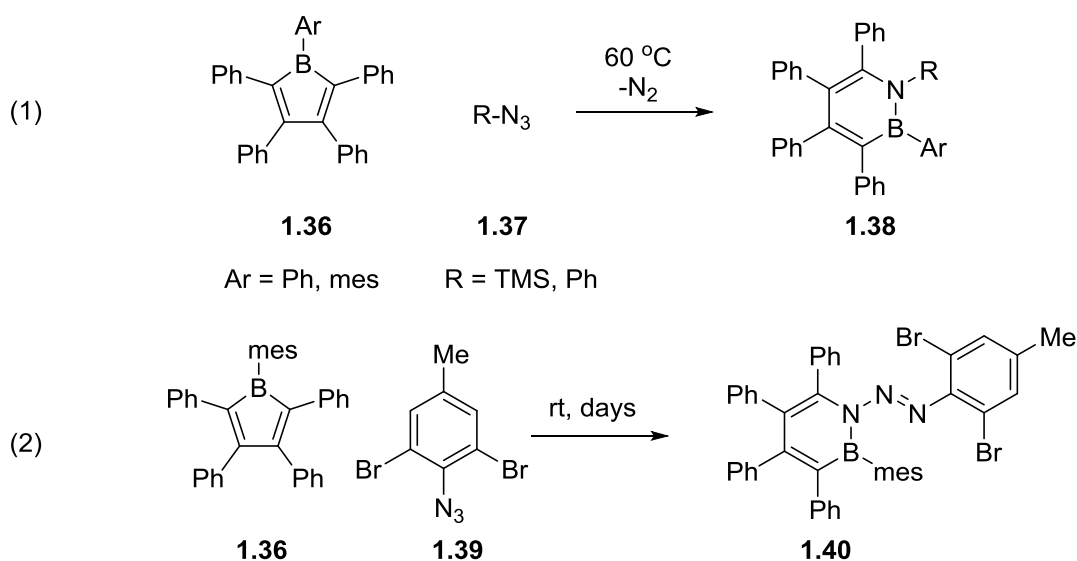
Braunschweig²⁶ has recently developed a novel “cyclotrimerization” route to substituted azaborines from ferrocenyl alkynes **1.32** and iminoborane **1.33** to generate azaborine **1.34** (Scheme 1.7). Upon heating to 200 °C under reduced pressure compound **1.34** eliminates an equivalent of isobutylene to generate **1.35**.

²⁶ Braunschweig, H.; Geetharani, K.; Jimenez-Halla, J. O. C.; Schäfer, M. *Angew. Chem. Int. Ed.* **2014**, *53*, 3500-3504.

Scheme 1.7: Rhodium-catalyzed “cyclotrimerization” route to 1.35



Scheme 1.8: Ring-expansion of boroles with azides to generate azaborines



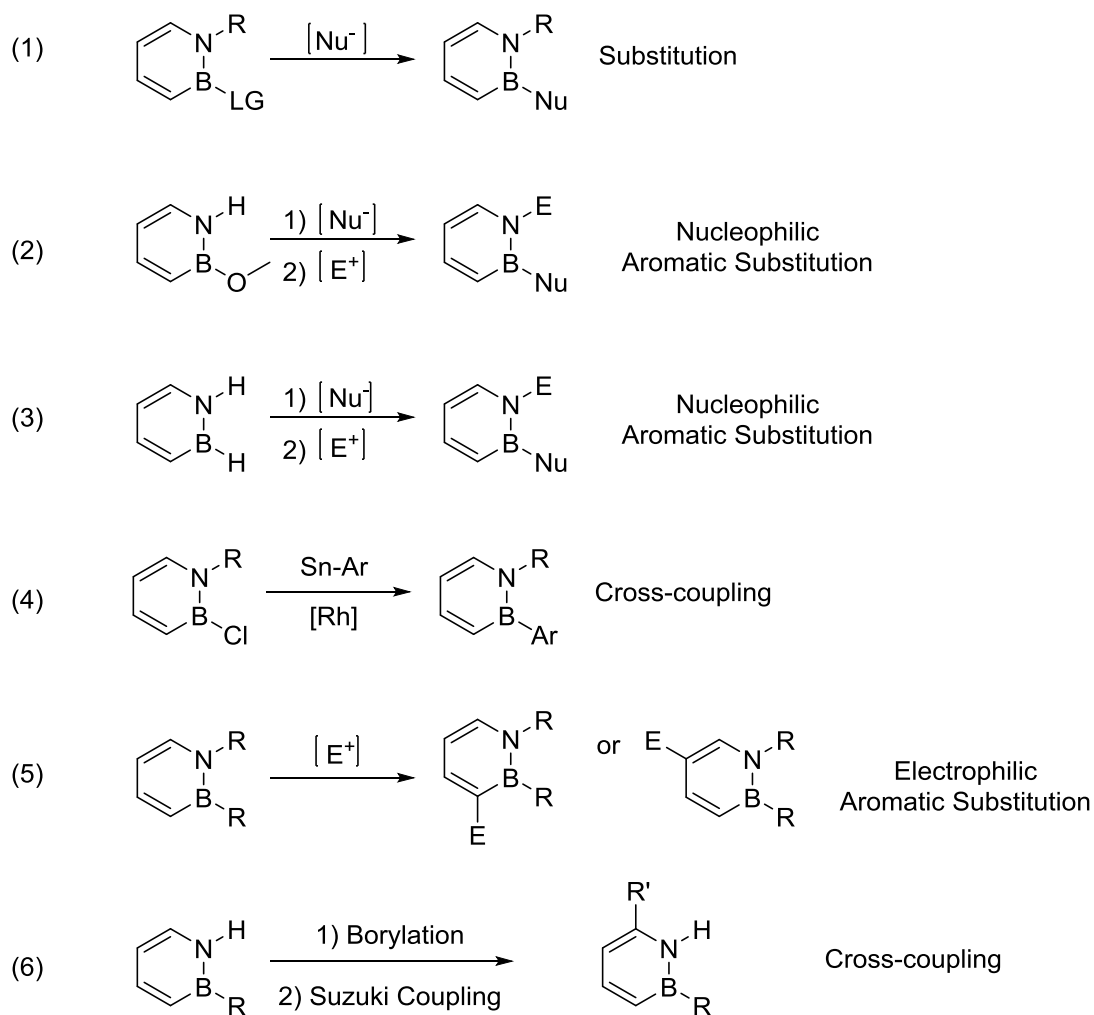
Braunschweig²⁷ and Martin²⁸ have also separately demonstrated a limited ring-expansion of highly substituted boroles (**1.36**) with azides (**1.37**) in order to generate highly substituted monocyclic azaborines **1.38** with concomitant extrusion of nitrogen

²⁷ Braunschweig, H.; Hörl, C.; Mailänder, L.; Radacki, K.; Wahler, J. *Chem. Eur. J.* **2014**, *20*, 9858-9861.

²⁸ Couchman, S. A.; Thompson, T. K.; Wilson, D. J. D.; Dutton, J. L.; Martin, C. D. *Chem. Commun.* **2014**, *50*, 11724-11726.

gas (Scheme 1.8 Eq. 1). When suitably substituted azides are used (**1.39**),²⁹ a unique *N*-azo substituted azaborine structure is obtained (**1.40**, Scheme 1.8, Eq. 2).

Scheme 1.9: Late-stage functionalization strategies for monocyclic azaborines



²⁹ Braunschweig, H.; Celik, M. A.; Hupp, F.; Krummenacher, I.; Mailänder, L. *Angew. Chem. Int. Ed.* **2015**, *54*, 6347-6351.

The simplest method³⁰ for the late-stage functionalization of azaborines is the nucleophilic substitution at boron (LG = either –Cl, –OTf, or OR; Scheme 1.9, Eq. 1). Concurrent boron and nitrogen substitution can be achieved through nucleophilic aromatic substitution,³¹ however the range of electrophiles is limited (Scheme 1.9, Eq. 2-3). Boron substitution through a rhodium-catalyzed Stille-inspired B–Cl cross-coupling³² is another viable method for substitution at boron with a higher functional group tolerance than the nucleophilic methods (Scheme 1.9, Eq. 6). Ashe³³ first demonstrated the electrophilic aromatic substitution reaction of monocyclic 1,2-azaborines which displayed a regioselectivity based upon the nature of the electrophile. Our group³⁴ later expanded this methodology to include B–Cl containing azaborines (Scheme 1.9, Eq. 5).³⁵ Most recently, our group³⁶ demonstrated a regioselective borylation/Suzuki cross-coupling sequence as a method for the synthesis of diverse C(6) aryl-substituted azaborines (Scheme 1.9, Eq. 6). The reviews³⁷ by Piers and our group have discussed the development of the chemistry of BN-systems through 2012, thus the remaining discussion of 1,2-azaborine chemistry will cover more recent developments in the field.

³⁰ (a) Marwitz, A. J. V.; Abbey, E. R.; Jenkins, J. T.; Zakharov, L. N.; Liu, S.-Y. *Org. Lett.* **2007**, *9*, 4905-4908. (b) Marwitz, A. J. V.; McClintock, S. P.; Zakharov, L. N.; Liu, S.-Y. *Chem. Commun.* **2010**, *46*, 779-781. (c) Marwitz, A. J. V.; Jenkins, J. T.; Zakharov, L. N.; Liu, S.-Y. *Angew. Chem. Int. Ed.* **2010**, *49*, 7444-7447 (d) Marwitz, A. J. V.; Jenkins, J. T.; Zakharov, L. N.; Liu, S.-Y. *Organometallics* **2011**, *30*, 52-54. (e) Marwitz, A. J. V.; Lamm, A. N.; Zakharov, L. N.; Vasiliu, M.; Dixon, D. A.; Liu, S.-Y. *Chem. Sci.* **2012**, *3*, 825-829.

³¹ (a) Lamm, A. N.; Garner, E. B.; Dixon, D. A.; Liu, S.-Y. *Angew. Chem. Int. Ed.* **2011**, *50*, 8157-8160. (b) Abbey, E. R.; Lamm, A. N.; Baggett, A. W.; Zakharov, L. N.; Liu, S.-Y. *J. Am. Chem. Soc.* **2013**, *135*, 12908-12913.

³² Rudebusch, G. E.; Zakharov, L. N.; Liu, S.-Y. *Angew. Chem. Int. Ed.* **2013**, *52*, 9316-9319.

³³ Pan, J.; Kampf, J. W.; Ashe, A. J. *Org. Lett.* **2007**, *9*, 679-681.

³⁴ Lamm, A. N.; Liu, S.-Y. *Mol. BioSyst.* **2009**, *5*, 1303-1305.

³⁵ For further discussion of electrophilic aromatic substitution reactions of BN-arenes please see chapter 3

³⁶ Baggett, A. W.; Vasiliu, M.; Li, B.; Dixon, D. A.; Liu, S.-Y. *J. Am. Chem. Soc.* **2015**, *137*, 5536-5541.

³⁷ (a) Bosdet, M. J. ; Piers, W. E. *Can. J. Chem.* **2009**, *87*, 8-29. (b) Campbell, P. G.; Marwitz, A. J. V.; Liu, S.-Y. *Angew. Chem. Int. Ed.* **2012**, *51*, 6074-6092.

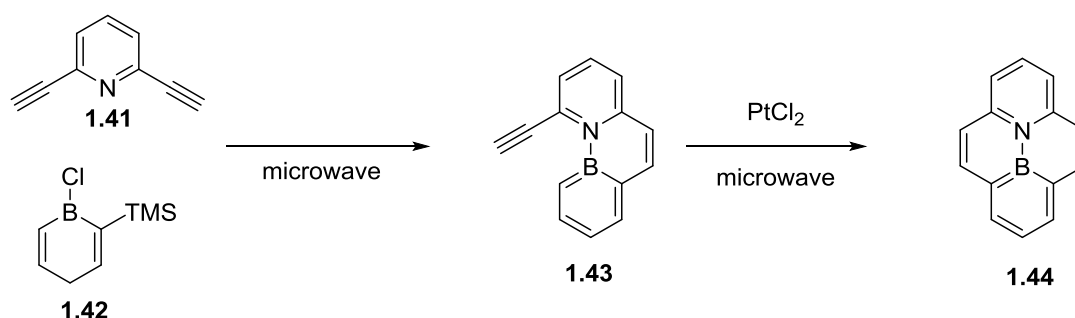
1.4 Recent developments in azaborine chemistry

In recent years, the incorporation of a BN unit into extended arenes in order to fine tune the electronic properties and probe the applications of BN/CC isosterism in materials science has received a great deal of attention. Labs from all over the world including the Piers, Pei, Nakamura, Zhang, Wang, Feng, and our lab have recently contributed to the study of extended arene systems containing a well-defined BN-unit.

1.4.1 Warren Piers, University of Calgary, Canada

The Piers lab³⁸ has developed a cyclization route (which was later improved by the Fort lab³⁹ through the use of microwave irradiation) to BN-arenes containing an internal B–N bond using 2-alkynyl pyridines such as **1.41** and Fu's⁴⁰ borabenzene precursor **1.42**. The original application of this methodology allowed the preparation of BN-pyrene **1.44** (Scheme 1.10).

Scheme 1.10: Synthesis of BN-pyrene **1.44**.



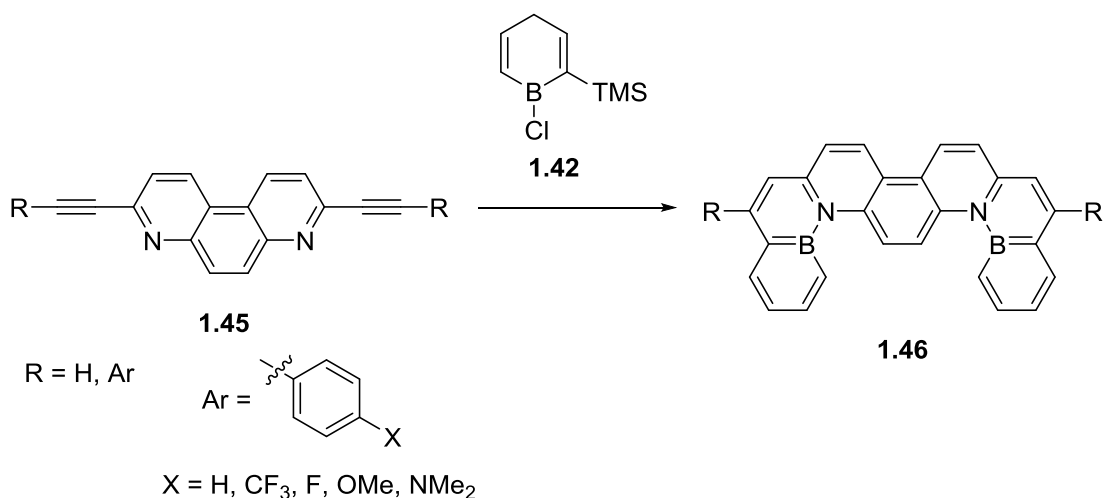
³⁸ Bosdet, M. J. D.; Piers, W. E.; Sorensen, T. S.; Parvez, M. *Angew. Chem. Int. Ed.* **2007**, *46*, 4940-4943.

³⁹ Wadle, J. J.; McDermott, L. B.; Fort, E. H. *Tetrahedron Lett.* **2014**, *55*, 445-447.

⁴⁰ Hoic, D. A.; Wolf, J. R.; Davis, W. M.; Fu, G. C. *Organometallics* **1996**, *15*, 1315-1318.

More recently, Piers⁴¹ has applied a similar synthetic approach to the synthesis of a bis-BN analogue of an isomer of heptacene **1.46** from the double ring-closing of symmetric **1.45** with **1.42** (Scheme 1.11). The carbonaceous isomer of **1.46** has yet to be synthesized; in some cases the selective synthesis of a BN-containing polyarene may be easier than the all-carbon counterpart due to the different methodologies available for the synthesis of BN-systems.

Scheme 1.11: Synthesis of bis-BN-heptacene isomer 1.46



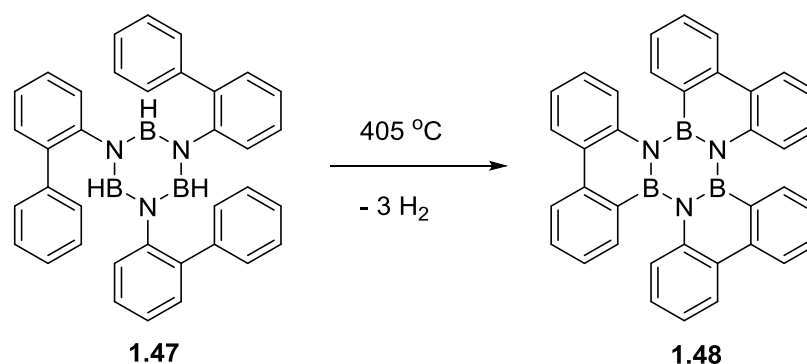
1.4.2 Holger Bettinger, University of Tübingen, Germany

The Bettinger lab⁴² has demonstrated the synthesis of a borazine trimer of Dewar's BN-phenanthrene. When *N*-orthobiphenyl borazine **1.47** was heated above 400 °C, three equivalents of hydrogen were lost to generate the BN-phenanthrene trimer **1.48** (Scheme 1.12).

⁴¹ Neue, B.; Araneda, J. F.; Piers, W. E.; Parvez, M. *Angew. Chem. Int. Ed.* **2013**, *52*, 9966-9969.

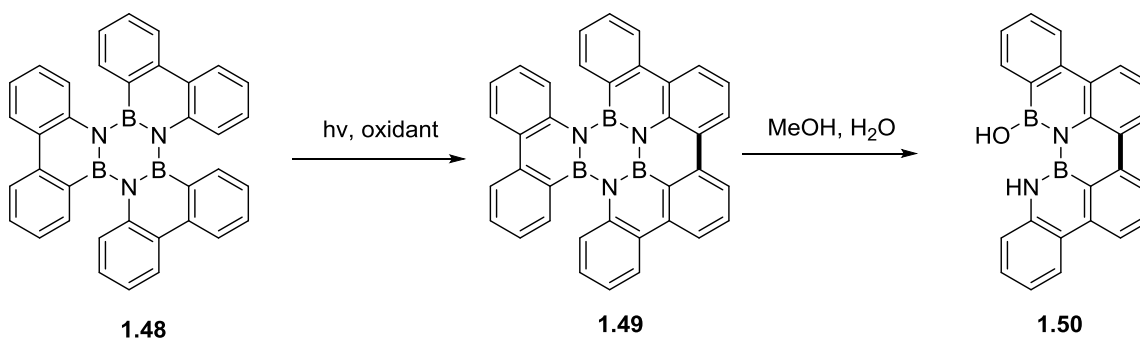
⁴² Müller, M.; Behnle, S.; Maichle-Mössmer, C.; Bettinger, H. F. *Chem. Commun.* **2014**, *50*, 7821-7823.

Scheme 1.12: Synthesis of trimeric BN-phenanthrene 1.48



When irradiated in the presence of an oxidant, **1.48** generated **1.49** which contains a new carbon-carbon bond (attempts at obtaining more than a single C–C bond formation were unsuccessful). Interestingly, the borazine core of **1.49** could be digested with water and methanol to generate compound **1.50** without breaking the newly-tethered B–N bond (Scheme 1.13).

Scheme 1.13: Synthesis of compound 1.50

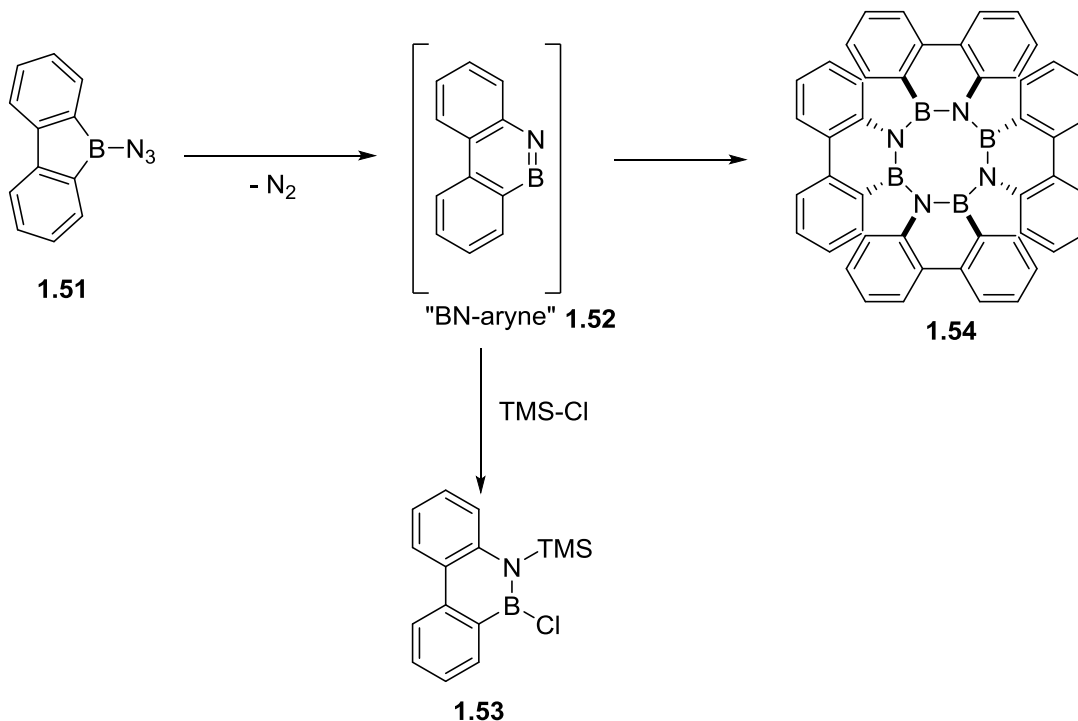


The Bettinger group⁴³ is also able to access BN-tetramer **1.54** through the transient BN-phenanthryne intermediate **1.52** (Scheme 1.14). The authors have supported

⁴³ Müller, M.; Maichle-Mössmer, C.; Bettinger, H. F. *Angew. Chem. Int. Ed.* **2014**, *53*, 9380-9383.

the existence of intermediate **1.52** both experimentally by trapping **1.52** with TMS-Cl to generate compound **1.53** as well as computationally.⁴⁴ Previously synthesized *B*-azide borole **1.51**⁴⁵ is thermally unstable in refluxing heptane, decomposing to a mixture of products from which the BN-tetramer **1.54** can be isolated in low yield. In the solid state, tetramer **1.54** adopts a nonplanar conformation similar to that observed with nonaromatic cyclooctatetraene⁴⁶ to minimize steric interactions as well as avoid the antiaromatic nature of the 8 π electron system.

Scheme 1.14: Synthesis of tetramer 1.54 from BN-aryne 1.52



⁴⁴ Bettinger, H. F.; Müller, M. *J. Phys. Org. Chem.* **2015**, *28*, 97-103.

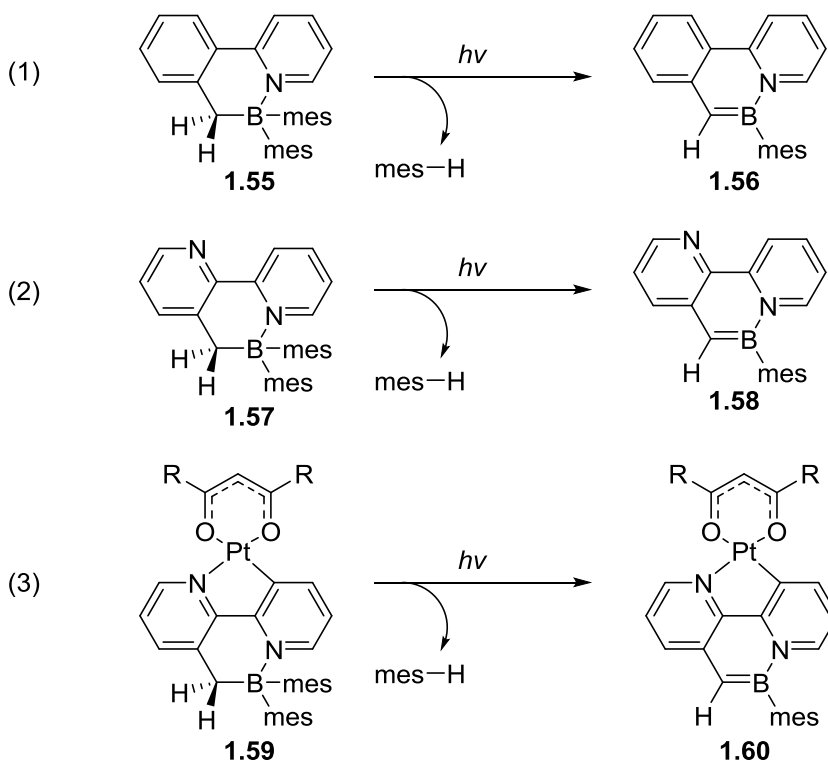
⁴⁵ Biswas, S.; Oppel, I. M.; Bettinger, H. F. *Inorg. Chem.* **2010**, *49*, 4499-4506.

⁴⁶ (a) Kaufman, H. S.; Fankuchen, I.; Mark, H. *Nature* **1948**, *161*, 165.

1.4.3 Suning Wang, Queen's University, Canada

The Wang lab⁴⁷ has observed a photoelimination of mesitylene in substituted phenylpyridine **1.55** to generate aromatized **1.56** (Scheme 1.15, Eq. 1). In a subsequent study,⁴⁸ the authors discovered that similarly substituted bipyridine **1.57** also undergoes this aromatization to yield compound **1.58** (Scheme 1.15, Eq. 2)

Scheme 1.15: Photoelimination aromatization generating azaborines



Cyclometallation of compound **1.57** with platinum gives complex **1.59** (Scheme 1.15, Eq. 3) which undergoes a more facile photoelimination at a higher wavelength

⁴⁷ Lu, J.-S.; Ko, S.-B.; Walters, N. R.; Kang, Y.; Sauriol, F.; Wang, S. *Angew. Chem. Int. Ed.* **2013**, *52*, 4544-4548.

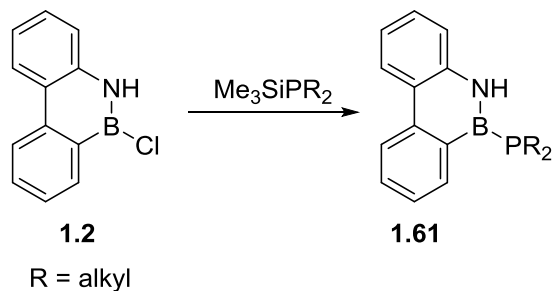
⁴⁸ Ko, S.-B.; Lu, J.-S.; Wang, S. *Org. Lett.* **2014**, *16*, 616-619.

(lower energy) to generate aromatized **1.60** due to a lower activation barrier to achieve the necessary transition state for photoelimination to take place.

1.4.4 Paul Pringle, University of Bristol, United Kingdom

Pringle et al.⁴⁹ have developed a method for the synthesis of BN-phosphine ligands which contain a *P*-B bond. Starting with Dewar's *B*-Cl BN-phenanthrene **1.2**, the authors performed a metathesis reaction with Me_3SiPR_2 ($\text{R}=\text{alkyl}$) reagents to generate the *P*-B bond in **1.61**. **1.61** is a competent ligand for rhodium and is more active in hydrogenation reactions than its carbonaceous isostere.

Scheme 1.16: Synthesis of BN-phosphines



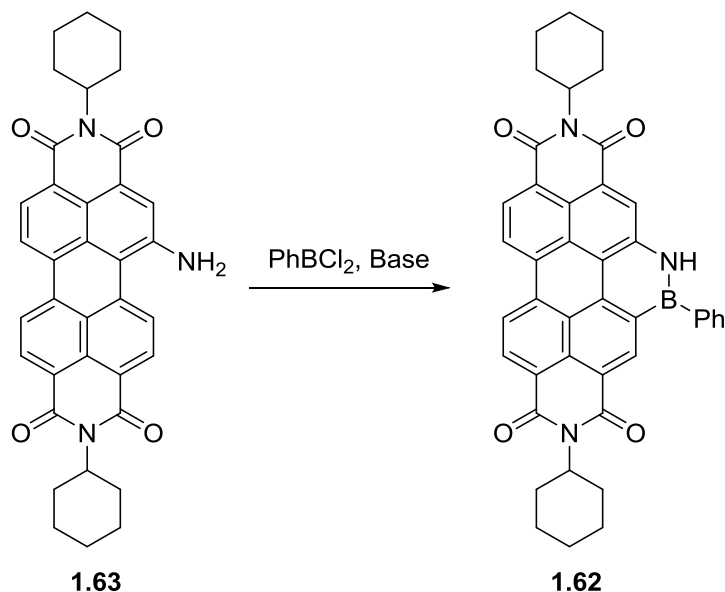
Unfortunately, the *P*-B bond in these systems is quite labile, liberating R_2PH and *B*-OH within 5 minutes upon treatment with water. Complexation to rhodium alleviated this problem somewhat; however the full possibility of BN-phosphines has not yet been systematically probed.

⁴⁹ Bailey, J. A.; Haddow, M. F.; Pringle, P. G. *Chem. Commun.* **2014**, 50, 1432-1434.

1.4.5 Qichun Zhang, Nanyang Technological University, Singapore

The Zhang lab⁵⁰ has recently demonstrated the synthesis of a BN-fused perylene (1.62) diimide which can be synthesized from monoaminated 1.63 and phenylboron dichloride (Scheme 1.17). The compound exhibits selective binding of fluoride over other anions (Cl^- , Br^- , I^- , SO_4^- , NO_3^- , CH_3COO^- , H_2PO_4^- , CN^- , BF_4^- , ClO_4^- , and PF_6^-) displaying a colorimetric (red-green) response with an on-off fluorescence response in chloroform.

Scheme 1.17: Synthesis of BN-fused perylene



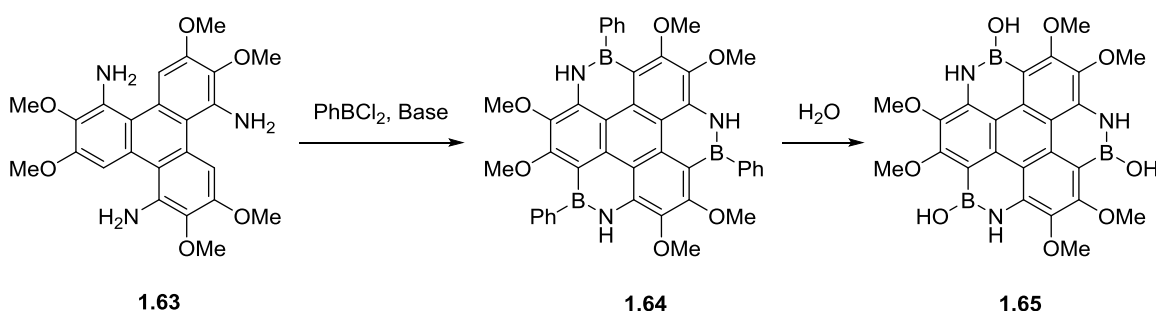
The authors also fabricated an OLED (organic light-emitting diode) device using 1.62 as the active element with an external quantum efficiency of up to 1.57%.

⁵⁰ Li, G.; Zhao, Y.; Li, J.; Cao, J.; Zhu, J.; Sun, X. W.; Zhang, Q. *J. Org. Chem.* **2015**, *80*, 196-203.

Compound **1.62** displays a high thermal stability, with 5% weight loss decomposition (thermogravimetric analysis, TGA) at 402 °C.

Early this year, both the Zhang lab⁵¹ and the Pei lab⁵² simultaneously released a near-identical synthesis of a tris-BN-coronene (**1.64**) from triamine **1.63** (Scheme 1.18). Compound **1.64** undergoes a protodeborylation with the loss of phenyl to produce **1.65** in water. **1.65** represents another example of a BN-substituted arene where the all-carbon isostere is still unknown.

Scheme 1.18: Synthesis of tris-BN-coronene 1.64



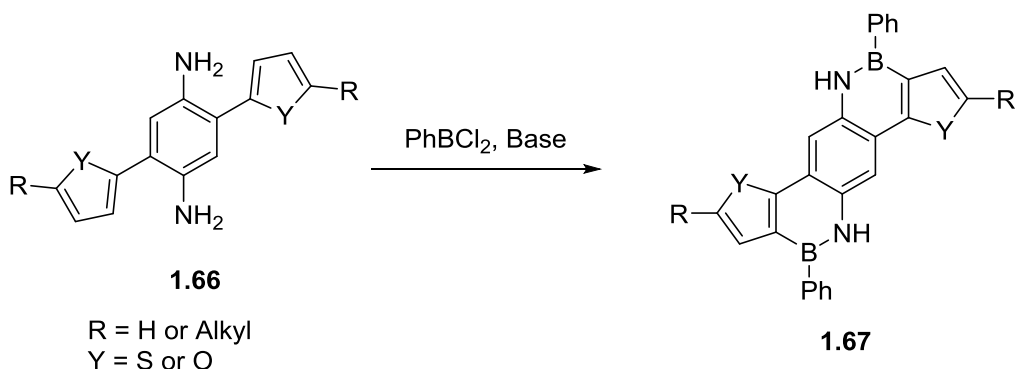
The Feng group⁵³ has utilized an amine directed electrophilic borylation of tetrasubstituted bis-aniline **1.66** to generate ladder-type acenes **1.67** (Scheme 1.19). The authors prepared a blue-OLED device with **1.67** as the active element with an external quantum efficiency of up to 1.4% (where $\text{Y}=\text{S}$ and $\text{R}=\text{Bu}$).

⁵¹ Li, G.; Xiong, W.-W.; Gu, P.-Y.; Cao, J.; Zhu, J.; Ganguly, R.; Li, Y.; Grimsdale, A. C.; Zhang, Q. *Org. Lett.* **2015**, *17*, 560-563.

⁵² Wang, X.-Y.; Zhuang, F.-D.; Wang, X.-C.; Cao, X.-Y.; Wang, J.-Y.; Pei, J. *Chem. Commun.* **2015**, *51*, 4368-4371.

⁵³ Wang, X.; Zhang, F.; Liu, J.; Tang, R.; Fu, Y.; Wu, D.; Xu, Q.; Zhuang, X.; He, G.; Feng, X. *Org. Lett.* **2013**, *15*, 5714-5717.

Scheme 1.19: Synthesis of ladder-type BN-acenes **1.67**



1.4.6 Masaharu Nakamura, Kyoto University, Japan

Nakamura et al.⁵⁴ have synthesized BN-helicene **1.69** as a racemic mixture from the amine-directed electrophilic borylation of **1.68** (Scheme 1.20, Eq. 1). The authors observed a dramatic change in the semiconductor properties between thin-films of racemic **1.69** and enantiomerically pure **1.69-(P)**. The racemic mixture was a p-type semiconductor (large hole mobility), while the enantiomerically pure compound displayed properties of an n-type semiconductor (large electron mobility).

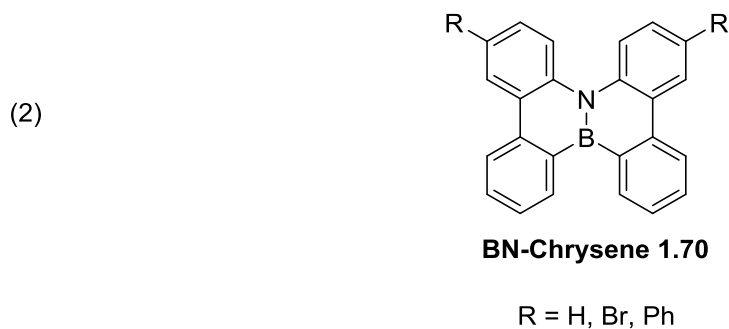
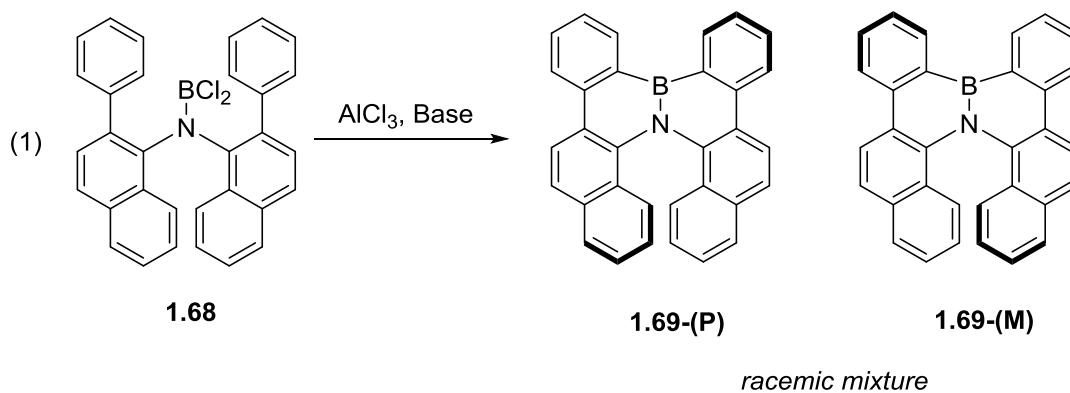
More recently, Nakamura et al.⁵⁵ have synthesized a series of substituted BN-chrysenes (**1.70**) in a similar fashion to the synthesis of **1.69** (Scheme 1.20, Eq. 2). The authors hypothesized and verified that the inclusion of the BN moiety would sufficiently increase the singlet–triplet excitation energy of the chrysene system to stabilize a device. PHOLED (phosphorescent organic light-emitting diode) devices fabricated with the BN-

⁵⁴ Hatakeyama, T.; Hashimoto, S.; Oba, T.; Nakamura, M. *J. Am. Chem. Soc.* **2012**, *134*, 19600-19603.

⁵⁵ Hashimoto, S.; Ikuta, T.; Shiren, K.; Nakatsuka, S.; Ni, J.; Nakamura, M.; Hatakeyama, T. *Chem. Mater.* **2014**, *26*, 6265-6271.

chrysenes also showed vastly improved efficiencies (external quantum efficiency of up to 19.5%) and lifetime₈₀ values (up to 226 hours) over the all-carbon chrysene.

Scheme 1.20: Synthesis of ladder-type BN-acenes 1.69



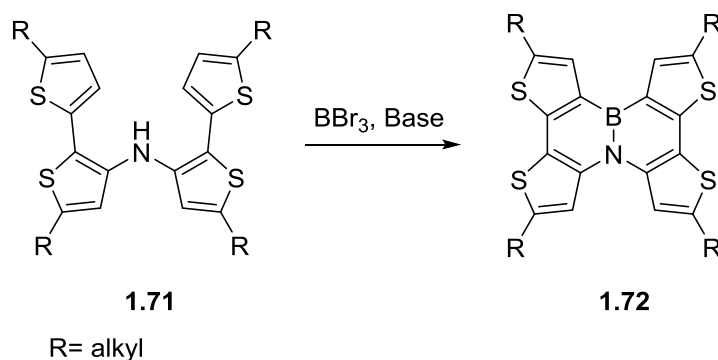
1.4.7 Jian Pei, Peking University, China

Pei et al.⁵⁶ have been at the forefront of the study and innovation of BN-fused polycyclic aromatic compounds for use in materials science. They have also developed a number of BN-arene based devices. The first BN-based electronic device

⁵⁶ Wang, X.-Y.; Wang, J.-Y.; Pei, J. *Chem. Eur. J.* **2015**, *21*, 3528-3539.

was fabricated in their laboratory⁵⁷ and is based upon BN-fused tetrathiophene **1.72** which can be synthesized by the twofold electrophilic borylation of amine **1.71** (Scheme 1.21). The skeleton of **1.72** displayed a high thermal stability (as high as 400 °C for 5% weight loss by thermogravimetric analysis, R=hexyl). Surprisingly, there was no indication of an interaction with F⁻, which has been observed with other thiophene-fused azaborines.⁵⁸

Scheme 1.21: Pei's tetrathiophene-fused compound 1.72



Organic field effect transistor (OFET) devices were prepared with **1.72** acting as a hole transporter with a maximum hole mobility of 0.15 cm²/V·s. In a subsequent study⁵⁹ the authors were able to fine tune the solid-state electronic properties of **1.72** by systematically varying the length of the alkyl chain. Through their alkyl-chain engineering, the authors were able to demonstrate a previously unobserved pronounced effect of chain-length on the properties of their OFET devices, namely that odd-

⁵⁷ Wang, X.-Y.; Lin, H.-R.; Lei, T.; Yang, D.-C.; Zhuang, F.-D.; Wang, J.-Y.; Yuan, S.-C.; Pei, J. *Angew. Chem. Int. Ed.* **2013**, *52*, 3117-3120.

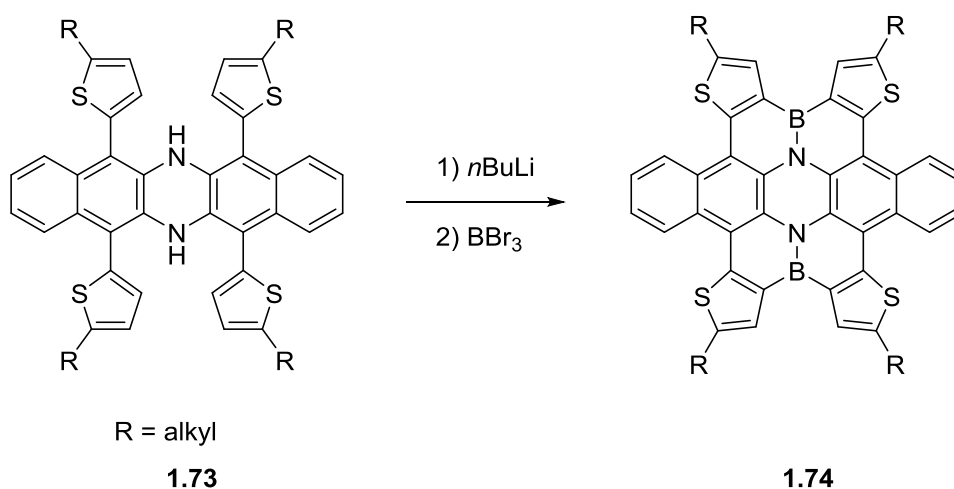
⁵⁸ Lepeltier, M.; Lukoyanova, O.; Jacobson, A.; Jeeva, S.; Perepichka, D. F. *Chem. Commun.* **2010**, *46*, 7007-7009.

⁵⁹ Wang, X.-Y.; Zhuang, F.-D.; Zhou, X.; Yang, D.-C.; Wang, J.-Y.; Pei, J. *J. Mater. Chem. C* **2014**, *2*, 8152-8161.

numbered chain lengths gave a higher hole mobility and a more crystalline thin-film leading to overall better devices.

In a continued effort to expand the understanding and efficiency of BN-containing devices, the Pei group⁶⁰ synthesized azacene-based **1.74** from tetrathiophene **1.73** (Scheme 1.22). In the solid state, compound **1.74** adopts a nonplanar saddle-type structure which self-assembles to generate a 1-dimensional microribbon. The authors were able to fabricate a field-effect transistor using microribbons of **1.74** which demonstrated an increased conductivity upon irradiation and a maximum hole mobility of 0.23 cm²/V·s.

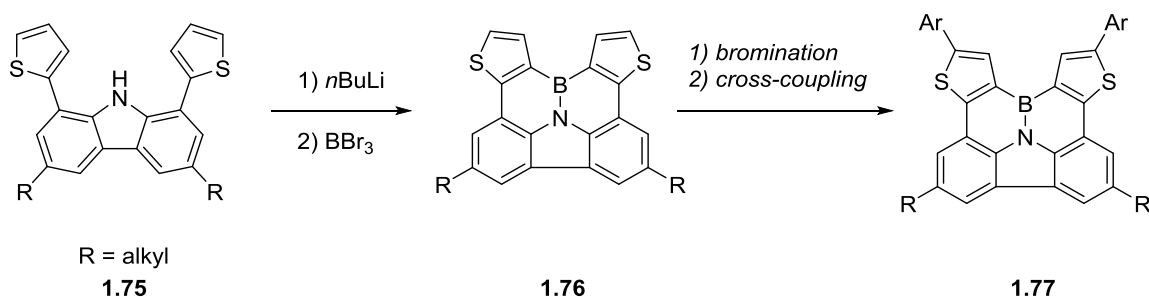
Scheme 1.22: Pei's synthesis of azacene-based 1.74



⁶⁰ Wang, X.-Y.; Zhuang, F.-D.; Wang, R.-B.; Wang, X.-C.; Cao, X.-Y.; Wang, J.-Y.; Pei, J. *J. Am. Chem. Soc.* **2014**, *136*, 3764-3767.

Very recently, Pei et al.⁶¹ have reported a late-stage functionalization strategy for the synthesis of carbazole-centered BN-fused **1.77** (Scheme 1.23). Electrophilic borylation of carbazole **1.75** generated BN-fused **1.76**. Selective bromination at the two most accessible positions followed by cross-coupling allows for the facile modular synthesis of a variety of new systems with tunable optoelectronic properties from a single common intermediate.

Scheme 1.23: Pei's modular synthesis of carbazole-based 1.77



1.4.8 Shih-Yuan Liu, Boston College, United States

In recent years, the Liu lab has continued to study the basic science and applications of monocyclic and extended BN-arenes. In a continued effort to understand the electronic structures of BN-arenes, our group has collaborated with the Chrostowska group in order to perform UV-photoelectron spectroscopy studies of 1,2- and 1,3-azaborines (**1.78-1.80**),⁶² BN-anthracenes (**1.83** and **1.84**),⁶³ as well as BN-isosteres of

⁶¹ Wang, X.-Y.; Yang, D.-C.; Zhuang, F.-D.; Liu, J.-J.; Wang, J.-Y.; Pei, J. *Chem. Eur. J.* **2015**, *21*, 8867-8873.

⁶² Chrostowska, A.; Xu, S.; Lamm, A. N.; Mazière, A.; Weber, C. D.; Dargelos, A.; Baylère, P.; Graciaa, A.; Liu, S.-Y. *J. Am. Chem. Soc.* **2012**, *134*, 10279-10285.

indole (**1.86** and **1.87**)⁶⁴ to experimentally measure the electronic structure of these compounds.

The experimentally measured HOMO energies of **1.78** (−8.0 eV), **1.79** (−8.45 eV), and **1.80** (−8.6 eV) were found to be higher in energy than toluene (**1.81**, −8.83 eV) or benzene (**1.82**, −9.25 eV) suggesting a destabilizing effect on the HOMO for BN-heterocycles likely due to desymmetrization from the inclusion of the BN-unit (Figure 1.4). In the case of BN-anthracenes **1.83** (−8.0 eV) and **1.84** (−7.7 eV), the inclusion of BN units had a stabilizing effect on the HOMO when compared to anthracene **1.85** (−7.4 eV).

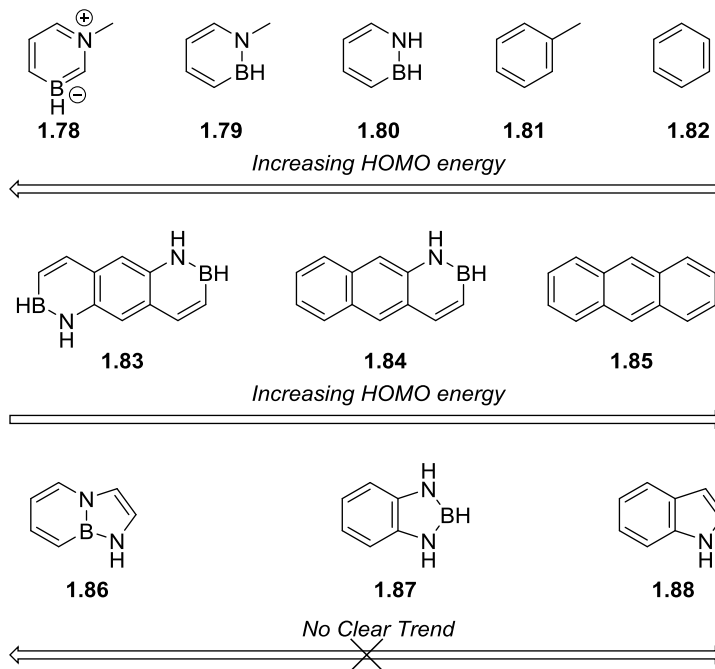


Figure 1.4: HOMO trends of a few series of BN-arenes

⁶³ Ishibashi, J. S. A.; Marshall, J. L.; Mazière, A.; Lovinger, G. J.; Li, B.; Zakharov, L. N.; Dargelos, A.; Graciaa, A.; Chrostowska, A.; Liu, S.-Y. *J. Am. Chem. Soc.* **2014**, *136*, 15414-15421.

⁶⁴ Chrostowska, A.; Xu, S.; Mazière, A.; Boknevitz, K.; Li, B.; Abbey, E. R.; Dargelos, A.; Graciaa, A.; Liu, S.-Y. *J. Am. Chem. Soc.* **2014**, *136*, 11813-11820.

The effect of BN-substitution was less pronounced in BN-indoles⁶⁵ **1.86** (−8.05 eV) and **1.87** (−7.9 eV) when compared to parental indole **1.88** (−7.9 eV). The results of these studies have not displayed a clear HOMO energy trend based upon different BN-substitution patterns, and suggest that the electronic structure consequences of BN/CC isosterism need to be studied individually and cannot yet be generally predicted.

Compounds **1.83** and **1.84** exhibit very similar absorption and emission profiles when compared to parental anthracene. In contrast to this observation, monocyclic azaborines generally exhibit a bathochromic shift in both absorption and emission.⁶⁶ In addition to exploring the electronic properties of BN-anthracenes **1.83** and **1.84**, the reactivity of B–Me derivatives was investigated and was found to be generally unreactive under Diels-Alder or Friedel-Crafts conditions (anthracene readily undergoes both Diels-Alder and Friedel-Crafts reactions). We are still unable to predict the reactivity of BN-isosteres of extended π -systems because there are not enough examples to generate an effective model. As our understanding of the basic science and reactivity of BN-isosteres grows through synthesis and characterization, so too will our ability to predict target molecules with desirable properties.

Our group provided the difficult to synthesize parental 1,2-dihydro-1,2-azaborine **1.80** to the Bettinger group,⁶⁷ who performed a matrix isolation study on the

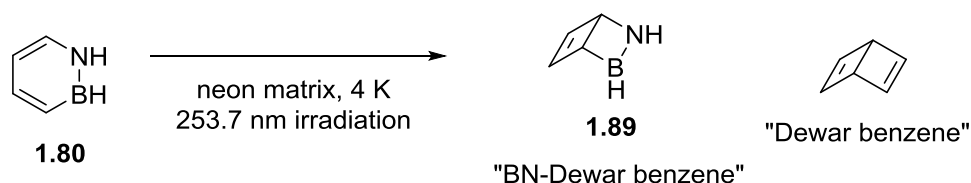
⁶⁵ For a review of BN isosteres of indole please see: Abbey, E. R.; Liu, S.-Y. *Org. Biomol. Chem.* **2013**, *11*, 2060-2069.

⁶⁶ (a) Marwitz, A. J. V.; Matus, M. H.; Zakharov, L. N.; Dixon, D. A.; Liu, S.-Y. *Angew. Chem., Int. Ed.* **2009**, *48*, 973–977. (b) Marwitz, A. J. V.; Lamm, A. N.; Zakharov, L. N.; Vasiliu, M.; Dixon, D. A.; Liu, S.-Y. *Chem. Sci.* **2012**, *3*, 825–829. (c) Taniguchi, T.; Yamaguchi, S. *Organometallics* **2010**, *29*, 5732–5735.

⁶⁷ Brough, S. A.; Lamm, A. N.; Liu, S.-Y.; Bettinger, H. F. *Angew. Chem. Int. Ed.* **2012**, *51*, 10880-10883.

photoisomerization of parental azaborine **1.80** to generate the BN-Dewar benzene structure **1.89** (Scheme 1.24).

Scheme 1.24: Matrix isolation formation of BN-Dewar benzene 1.89.

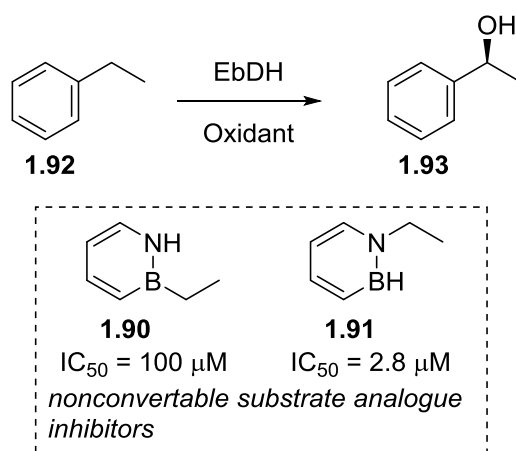


When sublimed into a solid neon matrix and irradiated with 253.7 nm light, BN-Dewar benzene **1.89** can be detected by IR-spectroscopy (versus computationally predicted spectra) as the only photoisomerization product after 22 hours of irradiation.

In an effort to probe the effect of BN-substitution on biological activity, our group prepared BN-isosteres of ethylbenzene **1.90** and **1.91** for collaboration with the Heider group.⁶⁸ Ethylbenzene dehydrogenase (EbdH) is known to oxidize ethylbenzene (**1.92**) to (S)-1-phenylethanol (**1.93**). When incubated with low concentrations of **1.90** or **1.91** the activity of the enzyme is lowered. This result verified that BN-arenes are capable of having vastly different biological properties to their carbonaceous isosteres. The effect of BN/CC isosterism on biological activity is still in its infancy; continued study could allow for the development of BN-containing APIs (active pharmaceutical ingredients).

⁶⁸ Knack, D. H.; Marshall, J. L.; Harlow, G. P.; Dudzik, A.; Szaleniec, M.; Liu, S.-Y.; Heider, J. *Angew. Chem. Int. Ed.* **2013**, *52*, 2599-2601.

Scheme 1.25: BN-ethylbenzenes 1.90 and 1.91 inhibit EbdH



1.5 The Future of BN-Arenes

While the understanding and application of extended BN-arenes has increased dramatically in the last 5 years, the synthesis and functionalization of unfused monocyclic azaborines has been much less explored. It is important to develop varied and complementary strategies for the substitution of 1,2-azaborines. Regioselective and functional-group tolerant methodologies to enable selective late-stage functionalization of 1,2-azaborines at any position will allow for the rational design of complicated systems containing monocyclic BN-arenes. When the problem of 1,2-azaborine chemistry evolves from “*will this reaction work*” to “*what target should we make*,” the fundamental properties that have been observed with BN-arenes will be incorporated and harnessed in the development of new compounds for use in biomedical and materials science.

Chapter 2

Metal-Catalyzed *B*-H Activation of 1,2-Azaborines: Dehydrogenative Borylation to Generate BN-Isosteres of Stilbene and a Unique Metal-Catalyzed *B*-H to *B*-Cl Conversion Using an Alkyl Chloride as the Chloride Source

2.1 Introduction

The chemistry of the *B*-H bond has enabled powerful synthetic techniques. *B*-H bonds in 3-coordinate boron species are traditionally Lewis-acidic at boron and hydridic at hydrogen. In the aromatic parental 1,2-dihydro-1,2-azaborine **2.1**, some hydridic character would be expected due to the resonance forms and nature of the *B*-N bond. However, this *B*-H unit does not display the same level of reactivity towards aldehydes (Scheme 2.1, Eq. 1)⁶⁹ as either the less aromatic borazine **2.2** (Scheme 2.1, Eq. 2) or 1-*H*-boratabenzene **2.3** (Scheme 2.1, Eq. 3).⁷⁰

Azaborine **2.1** is reactive to nucleophiles, reacting with two equivalents of *n*BuLi to generate *N*-Li **2.4** and one equivalent of LiH (Scheme 2.1, Eq. 4).⁷¹ This reactivity with nucleophiles is similar to that observed with borazine which has been shown to react with organolithium and organomagnesium reagents to generate *B*-substitution from *B*-H and *B*-R substituted borazines.⁷²

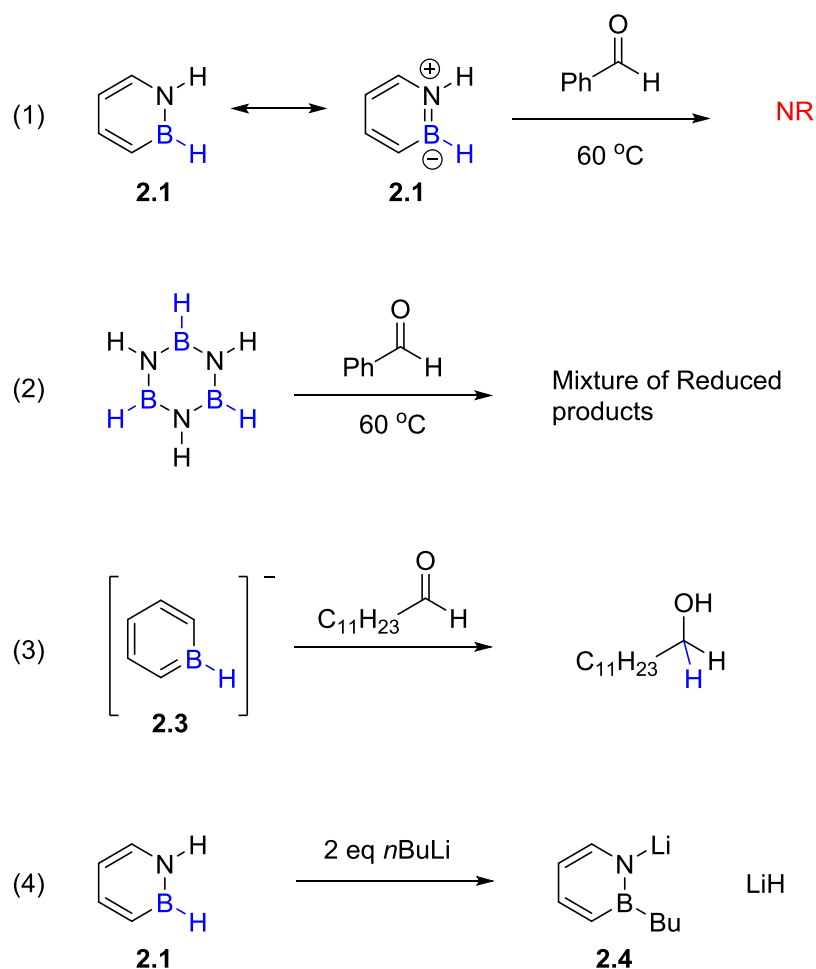
⁶⁹ Marwitz, A. J. V.; Matus, M. H.; Zakharov, L. N.; Dixon, D. A.; Liu, S.-Y. *Angew. Chem. Int. Ed.* **2009**, *48*, 973-977.

⁷⁰ Hoic, D. A.; Davis, W. M.; Fu, G. C. *J. Am. Chem. Soc.* **1995**, *117*, 8480-8481.

⁷¹ Lamm, A. N.; Garner, E. B.; Dixon, D. A.; Liu, S.-Y. *Angew. Chem. Int. Ed.* **2011**, *50*, 8157-8160.

⁷² (a) Smalley, J. H.; Stafiej, S. F. *J. Am. Chem. Soc.* **1959**, *81*, 582-586. (b) Moews, P. C.; Laubengayer, A. W. *Inorg. Chem.* **1963**, *2*, 1072-1073. (c) Powell, P.; Semlyen, J. A.; Blofeld, R. E.; Phillips, C. S. G. *J. Chem. Soc.* **1964**, No. 0, 280-283. (d) Nöth, H.; Rojas-Lima, S.; Troll, A. *Eur. J. Inorg. Chem.* **2005**, 1895-1906. (e) Nöth, H.; Troll, A. *Eur. J. Inorg. Chem.* **2005**, 3524-3535.

Scheme 2.1: Hydridic reactivity of *B*-H species with aldehydes and electrophilic reactivity of 2.1



We were interested in exploring the reactivity of the azaborine *B*-H bond in metal-mediated reactions in order to better understand the nature of the *B*-H bond in BN-arenes. This chapter will discuss: 1) the development of metal-catalyzed *B*-H activation strategies in 1,2-azaborines for the synthesis of a new class of BN-stilbene compounds, 2) the study of the effect of electron-rich and electron-poor substituents on the optical properties of these BN-stilbenes, and 3) the discovery and optimization of a novel, metal-catalyzed *B*-H to *B*-Cl transformation using alkyl chlorides as the chloride source.

2.2 Background

2.2.1 The development of metal-catalyzed hydroboration and the discovery of metal-catalyzed dehydrogenative borylation

With the development of oxygen-stabilized and less reactive hydroboration reagents such as 9-BBN (**2.5**),⁷³ catecholborane (**2.6**),⁷⁴ and 4,4,6-trimethyl-1,3,2-dioxaborinane (**2.7**)⁷⁵ (Figure 2.1), interest in performing metal-catalyzed hydroborations became more attractive due to the benefits of using the more stable, yet less reactive alkoxyboranes.

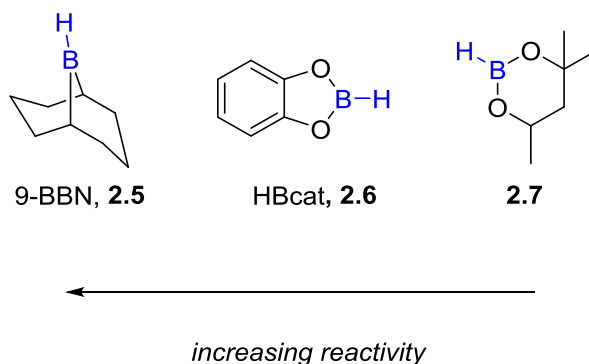


Figure 2.1: Selected hydroboration reagents in order of reactivity

The first metal-catalyzed hydroboration reaction was demonstrated by Sneddon et al.,⁷⁶ who were able to perform a hydroboration using pentaborane **2.8** to generate the

⁷³ (a) Brown, H. C. "Organic Syntheses via Boranes" John Wiley & Sons, Inc. New York: 1975. (b) Soderquist, J. A.; Brown, H. C. *J. Org. Chem.* **1981**, *46*, 4599-4600.

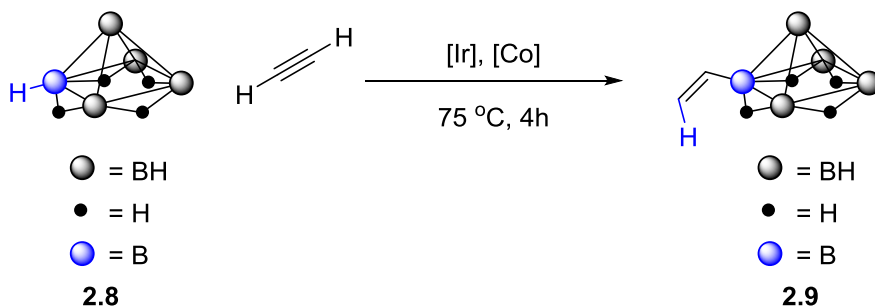
⁷⁴ Brown, H. C.; Gupta, S. K. *J. Am. Chem. Soc.* **1971**, *93*, 1816-1818.

⁷⁵ (a) Woods, W. G.; Strong, P. L. *J. Am. Chem. Soc.* **1966**, *88*, 4667-4671. (b) Fish, R. H. *J. Am. Chem. Soc.* **1968**, *90*, 4435-4439. (c) Fish, R. H. *J. Org. Chem.* **1973**, *38*, 158.

⁷⁶ (a) Wilczynski, R.; Sneddon, L. G. *J. Am. Chem. Soc.* **1980**, *102*, 2857-2858. (b) Wilczynski, R.; Sneddon, L. G. *Inorg. Chem.* **1981**, *20*, 3955-3962.

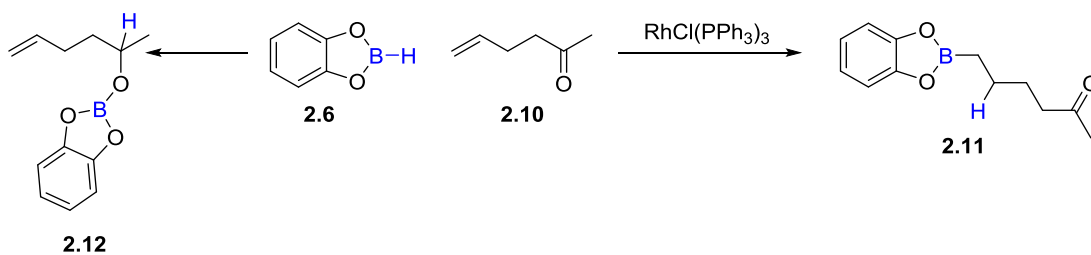
B-vinyl product **2.9** in the presence of $\text{Ir}(\text{CO})\text{Cl}(\text{PPh}_3)_2$ or $(\text{R}\equiv\text{R}')\text{Co}_2(\text{CO})_6$ catalysts at 70°C (Scheme 2.2).

Scheme 2.2: First reported metal-catalyzed hydroboration with pentaborane 2.8



Expanded interest in metal-catalyzed hydroboration reactions was kindled by the seminal report by Männig and Nöth.⁷⁷ The authors demonstrated a complete reversal in selectivity for the hydroboration of 5-hexen-2-one (**2.10**) with **2.6** when performed in the presence of Wilkinson's catalyst ($\text{RhCl}(\text{PPh}_3)_3$) (Scheme 2.3). The uncatalyzed reaction was selective for the reduction of the carbonyl to generate species **2.12** while the catalyzed reaction was selective for the formation of terminal alkylboronic ester **2.11**. The authors noted that dialkylboranes did not display the same level of selectivity towards alkenes under their catalytic conditions.

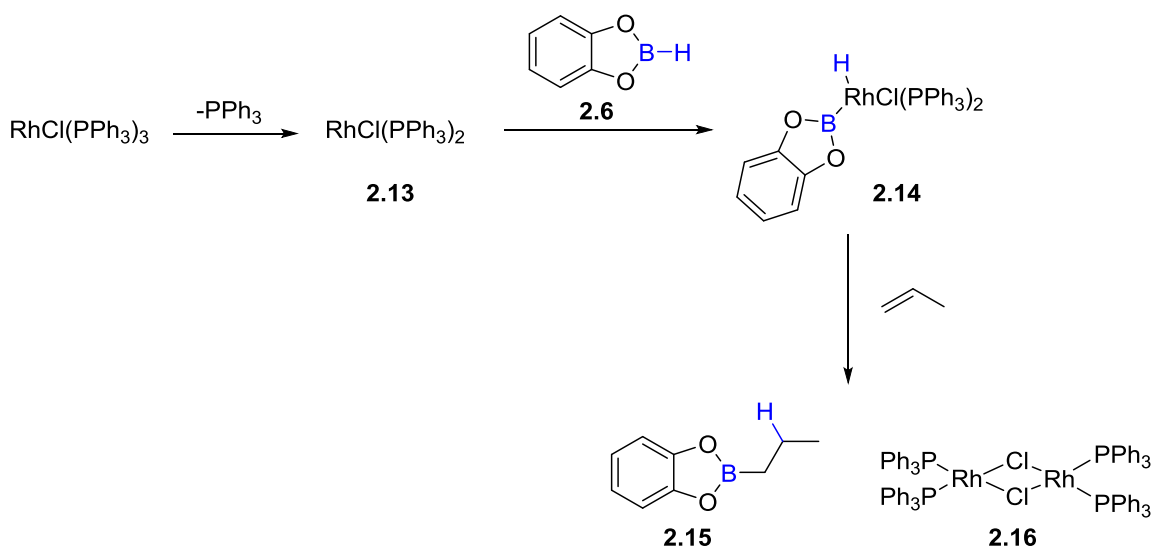
Scheme 2.3: Selectivity of metal-catalyzed hydroboration



⁷⁷ Männig, D.; Nöth, H. *Angew. Chem. Int. Ed. Engl.* **1985**, *24*, 878-879.

The authors were also able to characterize the product of the oxidative addition to the B–H bond (complex **2.14**) from the stoichiometric reaction of **2.6** and Wilkinson’s catalyst.⁷⁸ When treated with 1-propene, **2.14** generated compound **2.15** and rhodium dimer **2.16** (Scheme 2.4).

Scheme 2.4: Stoichiometric reactions of Wilkinson’s catalyst with 2.6

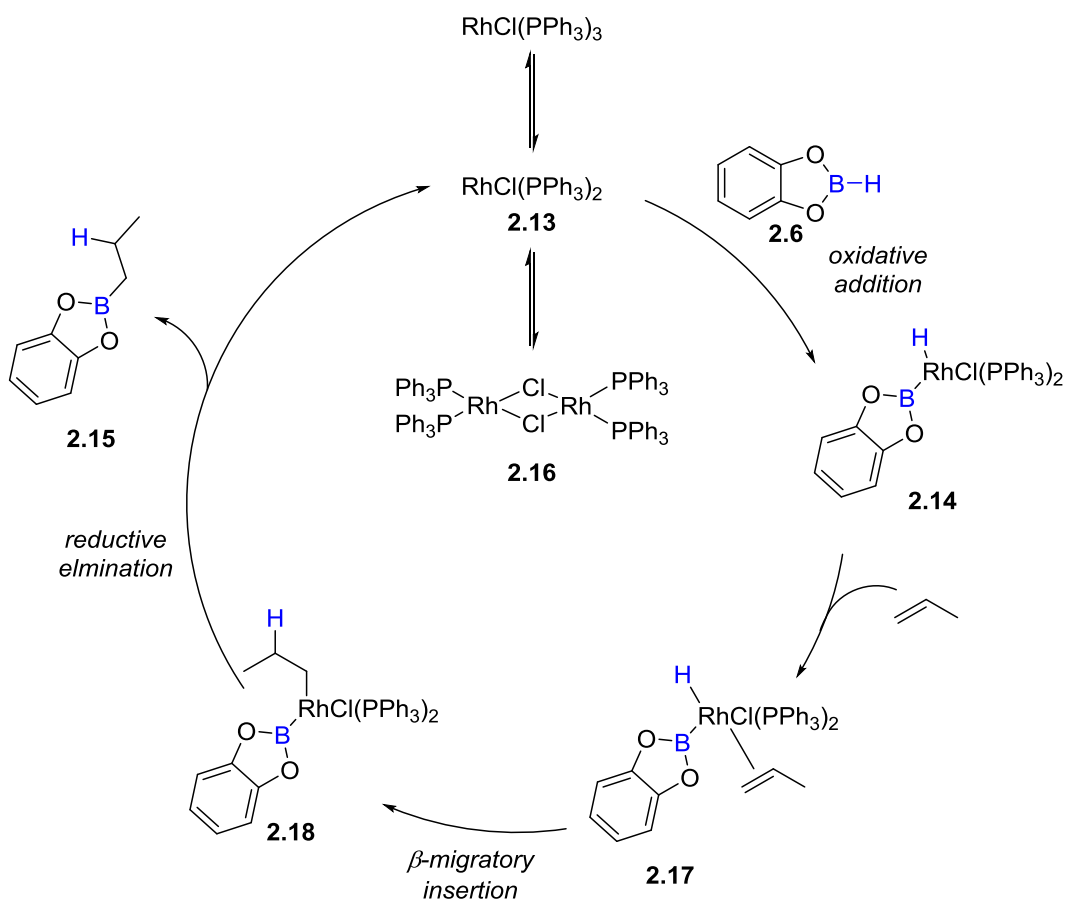


The authors proposed a catalytic cycle involving the oxidative addition of **2.6** to in-situ formed **2.13** to generate **2.14**. Ligand association of the alkene generates **2.17** followed by β -migratory insertion into the Rh-H bond to generate intermediate **2.18**. Reductive elimination provides **2.15** and complex **2.13** (which dimerizes to **2.16**) as shown in Scheme 2.5. A more detailed analysis of this mechanism was undertaken by

⁷⁸ Kono and Ito first discovered this rapid oxidative addition in 1975: Kono, H.; Ito, K. *Chem. Lett.* **1975**, 4, 1095-1096.

Evans et al.⁷⁹ and later Burgess et al.⁸⁰ through extensive labeling and product distribution studies.

Scheme 2.5: Initially proposed catalytic cycle for rhodium (I) catalyzed hydroboration of alkenes



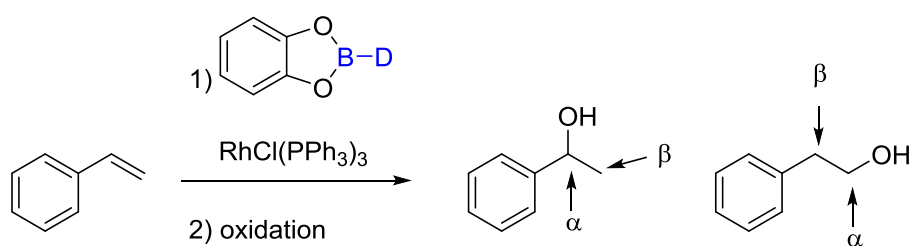
Initially, the two groups disagreed on the distribution of deuterium atoms in the rhodium-catalyzed hydroboration using deuterio-2.6, especially in the case of the hydroboration of styrene. This incongruity was later established to be due to oxidation of

⁷⁹ (a) Evans, D. A.; Fu, G. C. *J. Org. Chem.* **1990**, *55*, 2280-2282. (b) Evans, D. A.; Fu, G. C.; Anderson, B. A. *J. Am. Chem. Soc.* **1992**, *114*, 6679-6685.

⁸⁰ (a) Burgess, K.; Van der Donk, W. A.; Kook, A. M. *J. Org. Chem.* **1991**, *56*, 2949-2951. (b) Burgess, K.; Ohlmeyer, M. J. *Chem. Rev.* **1991**, *91*, 1179-1191. (c) Burgess, K.; Van der Donk, W. A.; Westcott, S. A.; Marder, T. B.; Baker, R. T.; Calabrese, J. C. *J. Am. Chem. Soc.* **1992**, *114*, 9350-9359.

“aged” Wilkinson’s catalyst (which Burgess et al. used) versus the use of freshly prepared, vigorously air free catalyst (which Evans et al. used). The “aged” catalyst showed a degraded selectivity, and a higher propensity to undergo deleterious side-reactions than its pure counterpart. The addition of PPh₃ to the aged catalyst restored its selectivity (Scheme 2.6). Another factor which degraded the selectivity of the catalyzed hydroboration was the use of impure alkenes which often contain trace oxidative impurities which also contributed to a lowered selectivity. The authors often observed vinyl boronic esters as minor side products stemming from dehydrogenative borylation.

Scheme 2.6: Selectivity of deuterium incorporation during catalyzed hydroboration of styrene



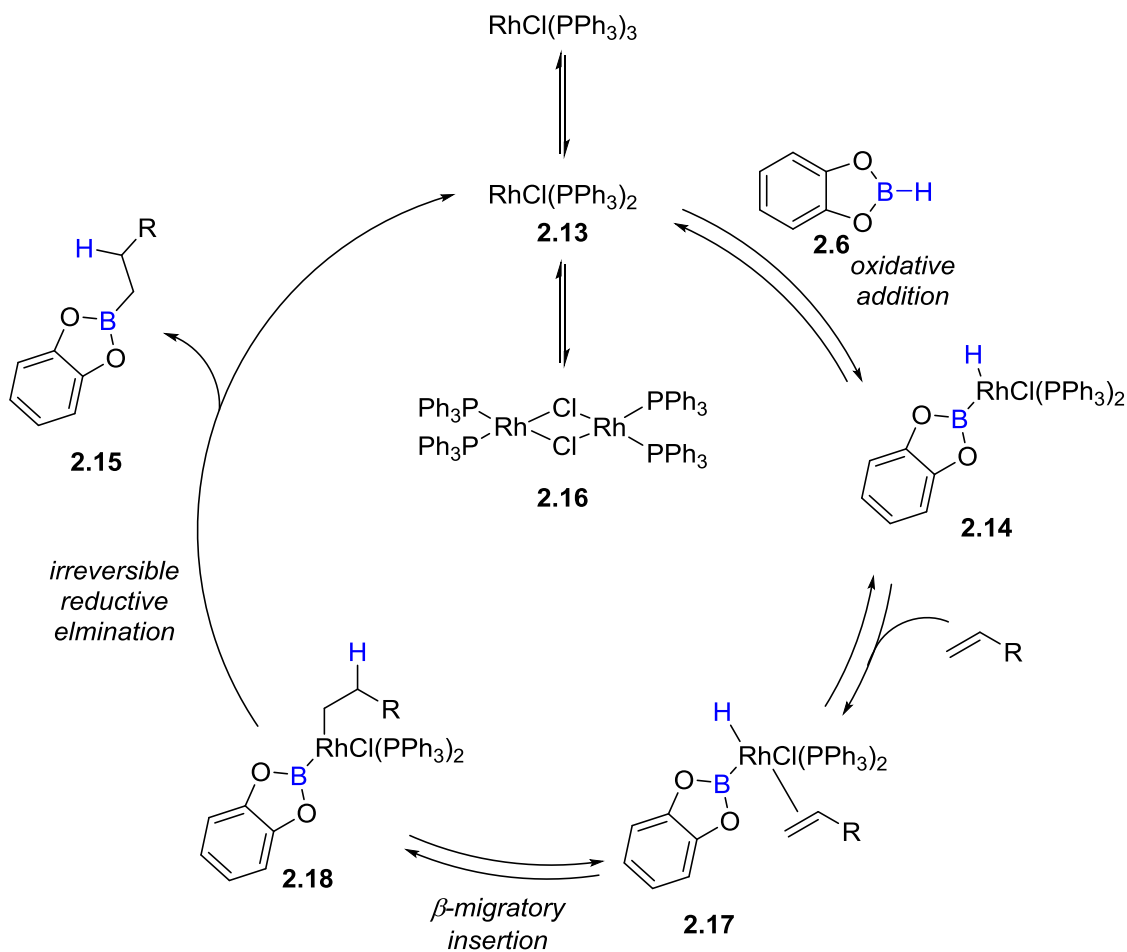
pure [Rh]	98 % α : β D 0:100	2 % α : β D 0:100
aged [Rh]	14 % α : β D 0:100	46 % α : β D 40:60
aged [Rh]+PPh ₃	96 % α : β D 0:100	4 % α : β D 0:100

missing % corresponds to recovered starting material

The most consistent mechanism for this rhodium catalyzed hydroboration consists of reversible steps preceding the final B–C bond-forming reductive elimination and has

been corroborated by DFT calculations.⁸¹ The original hypothesis by Männig and Nöth stood up to more robust scrutiny (Scheme 2.7).

Scheme 2.7: Most consistent catalytic cycle for rhodium (I) catalyzed hydroboration of alkenes



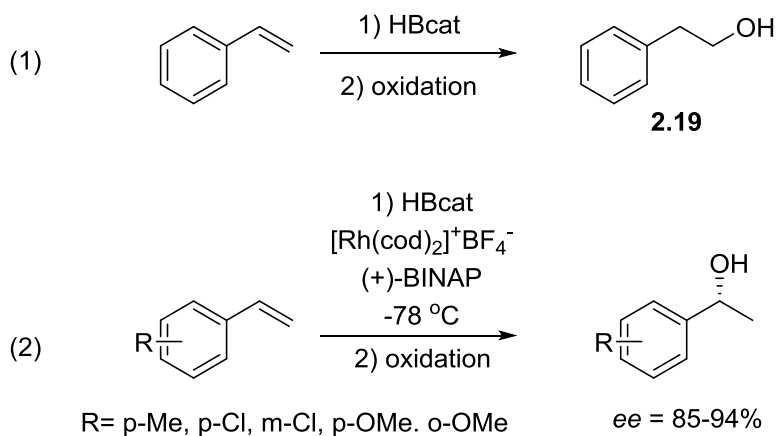
The selectivity for catalyzed hydroboration of styrenes is important to note. As demonstrated by Brown et al.,⁸² the traditional selectivity for uncatalyzed hydroboration of styrene gives a preference for the formation of **2.19** (Scheme 2.8, Eq. 1). Hayashi et

⁸¹ (a) Musaev, D. G.; Mebel, A. M.; Morokuma, K. *J. Am. Chem. Soc.* **1994**, *116*, 10693-10702. (b) Dorigo, A. E.; von Ragué Schleyer, P. *Angew. Chem. Int. Ed. Engl.* **1995**, *34*, 115-118. (c) Widauer, C.; Grützmacher, H.; Ziegler, T. *Organometallics* **2000**, *19*, 2097-2107.

⁸² Brown, H. C.; Gupta, S. K. *J. Am. Chem. Soc.* **1975**, *97*, 5249-5255.

al.⁸³ later demonstrated that the hydroboration of styrene with **2.6** with screened rhodium species $[\text{RhCl}(\text{cod})]_2$, $[\text{Rh}(\text{cod})_2]^+\text{BF}_4^-$, $[\text{Rh}(\text{cod})_2]^+\text{BF}_4^- + 2\text{PPh}_3$, $[\text{RhCl}(\text{cod})_2]^+\text{BF}_4^- + \text{dppe}$, $[\text{RhCl}(\text{cod})]_2 + \text{dppb}$, $[\text{Rh}(\text{cod})_2]^+\text{BF}_4^- + \text{dppb}$, and $[\text{Rh}(\text{cod})(\text{dppb})]^+\text{BF}_4^-$ could generate the benzylic hydroboration product selectively. The authors initially used “aged” Wilkinson’s catalyst, and observed almost no selectivity for the desired internal product, consistent with the observations of Burgess et al. The authors found that the $[\text{Rh}(\text{cod})_2]^+\text{BF}_4^- + \text{dppb}$ system was most selective, and were able to demonstrate the enantioselective synthesis of benzylic alcohols using $[\text{RhCl}(\text{cod})_2]^+\text{BF}_4^- + \text{Noyori's (+)-BINAP}$ at $-78\text{ }^\circ\text{C}$ under catalyst control (Scheme 2.8 Eq. 2).

Scheme 2.8: Catalyzed and uncatalyzed hydroboration of styrenes



Around the same time, the field of asymmetric metal-catalyzed hydroborations was beginning to be studied by many groups. The first asymmetric metal-catalyzed hydroboration was reported by Burgess et al. in 1988,⁸⁴ and was also promoted by a

⁸³ (a) Hayashi, T.; Matsumoto, Y.; Ito, Y. *J. Am. Chem. Soc.* **1989**, *111*, 3426-3428. (b) Hayashi, T.; Matsumoto, Y.; Ito, Y. *Tetrahedron: Asymmetry* **1991**, *2*, 601-612.

⁸⁴ Burgess, K.; Ohlmeyer, M. J. *J. Org. Chem.* **1988**, *53*, 5178-5179.

BINAP-based catalyst. This was followed quickly by Evans et al.,⁸⁵ who showed a complimentary and better regio- and diastereoselectivity for the catalyzed substrate-directed hydroboration of protected and unprotected allylic alcohols. Suzuki et al.⁸⁶ were working concurrently with Hayashi and coworkers to develop similar enantioselective catalyzed hydroboration of a larger yet still limited range of alkenes and chiral phosphines, however the reactions did not have as high of enantioselectivities as those demonstrated with styrenes and cationic rhodium complexes. Burgess and Ohlmeyer⁸⁷ developed a substrate-directed metal-catalyzed hydroboration of protected allylic amines, which gave complimentary selectivity to the uncatalyzed reaction. Evans and Fu⁸⁸ then developed an intramolecular amide-directed rhodium-catalyzed hydroboration of cyclic alkenes with high diastereoselectivity (up to 95:5).

Since both catalyst control and substrate control had been demonstrated using exclusively catecholborane, Brown and Lloyd-Jones⁸⁹ studied borane controlled metal-catalyzed hydroboration using ephedrine (**2.20**) and pseudoephedrine (**2.21**) derived oxazaborolidines. In this initial study, they observed multiple products from the reaction with 4-methoxystyrene, and, unfortunately only the reaction with **2.21** and [Rh(nbd)(dppf)]SO₃CF₃ as the catalyst gave high yield of **2.22** with moderate *ee*. **2.20** exists as a dimer in solution which inhibited catalysis. In all cases, some amount of hydrogenated styrene **2.23** was observed (Scheme 2.9).

⁸⁵ Evans, D. A.; Fu, G. C.; Hoveyda, A. H. *J. Am. Chem. Soc.* **1988**, *110*, 6917-6918.

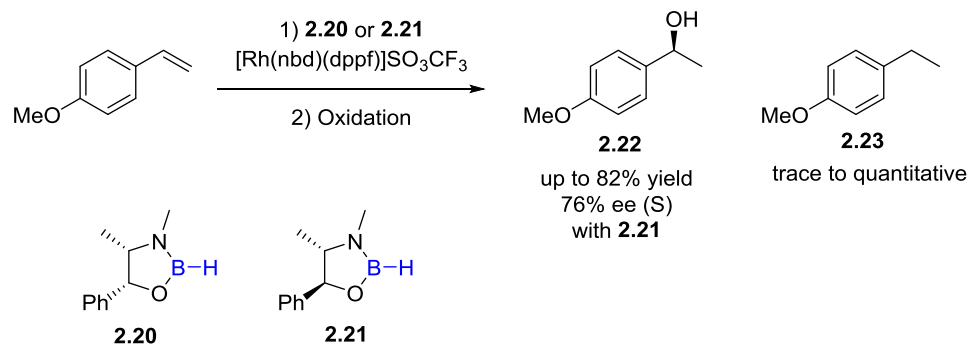
⁸⁶ Sato, M.; Miyaura, N.; Suzuki, A. *Tetrahedron Lett.* **1990**, *31*, 231-234.

⁸⁷ Burgess, K.; Ohlmeyer, M. J. *Tetrahedron Lett.* **1989**, *30*, 5857-5860.

⁸⁸ Evans, D. A.; Fu, G. C. *J. Am. Chem. Soc.* **1991**, *113*, 4042-4043.

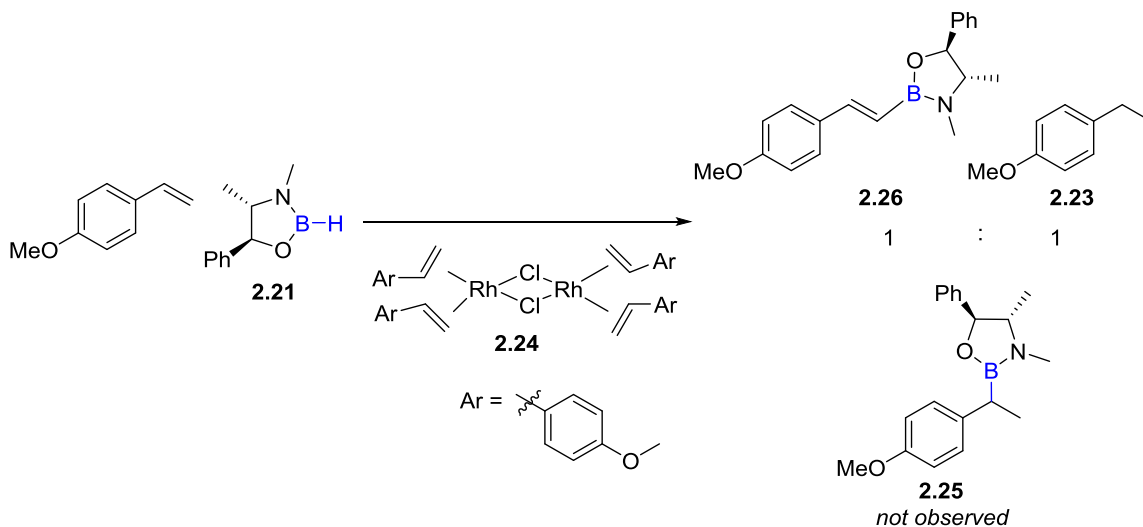
⁸⁹ Brown, J. M.; Lloyd-Jones, G. C. *Tetrahedron: Asymmetry* **1990**, *1*, 869-872.

Scheme 2.9: Borane controlled enantioselective metal-catalyzed hydroboration



While searching for an improvement to the oxazaborolidine hydroboration chemistry, Brown and Lloyd-Jones⁹⁰ developed a novel dehydrogenative borylation. During their continued reaction screening, they saw a unique reactivity mode when they treated **2.21** with tetrastirenyl rhodium dimer **2.24**. Instead of the hydroboration product **2.25**, a 1:1 formation of 4-methoxy ethylbenzene **2.23** and the E-vinylboronate **2.26** was observed (Scheme 2.10).

Scheme 2.10: Dehydrogenative borylation of 4-methoxystyrene

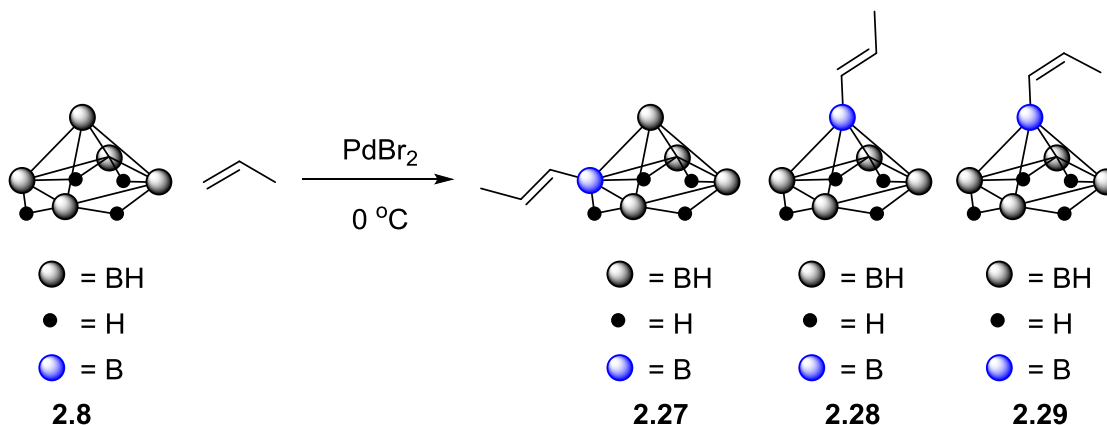


⁹⁰ Brown, J. M.; Lloyd-Jones, G. C. *J. Chem. Soc., Chem. Commun.* **1992**, 9, 710-712.

2.2.2 The development and scope of metal-catalyzed dehydrogenative borylation of alkenes and alkynes⁹¹

The aforementioned report by Brown and Lloyd-Jones was the first selective homogeneous dehydrogenative borylation. The first reported dehydrogenative borylation was reported earlier by Sneddon et al. in 1983.⁹² Upon action of propene and PdBr₂, pentaborane **2.8** undergoes dehydrogenative borylation to generate a mixture of products **2.27-2.29** in good yield at 0 °C (87% combined yield, Scheme 2.11).

Scheme 2.11: Dehydrogenative borylation of pentaborane



Brown and Lloyd-Jones⁹³ continued their investigation into the dehydrogenative borylation of aryl alkenes and were able to expand the scope to include 4-vinylchlorobenzene and vinylferrocene with N-isopropyl **2.21** and catalyst **2.24**. Upon

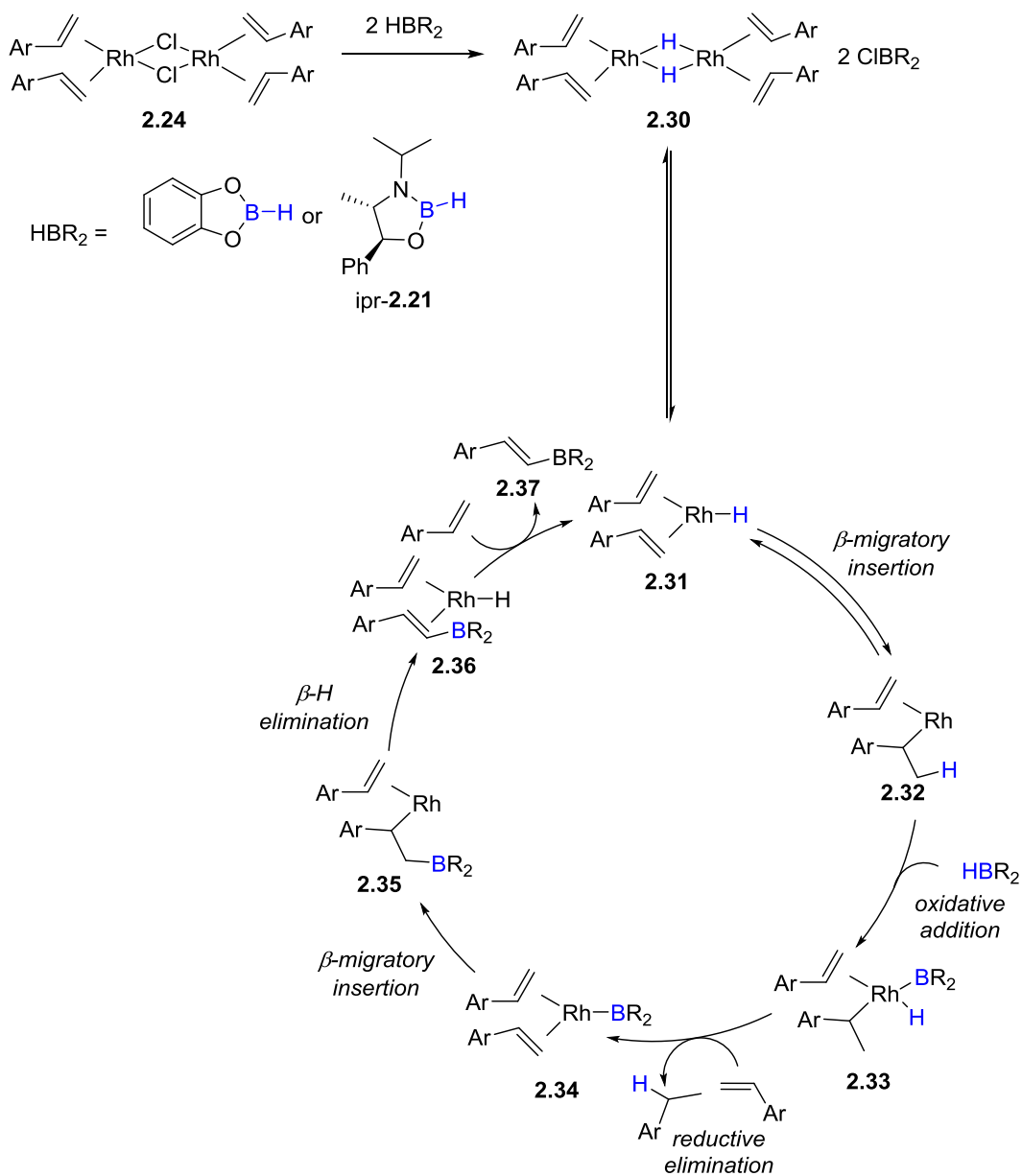
⁹¹ For an in-depth review of C–H activation towards the formation of C–B bonds please see: Mkhaliid, I. A. I.; Barnard, J. H.; Marder, T. B.; Murphy, J. M.; Hartwig, J. F. *Chem. Rev.* **2010**, *110*, 890-931.

⁹² Davan, T.; Corcoran, E. W.; Sneddon, L. G. *Organometallics* **1983**, *2*, 1693-1694.

⁹³ Brown, J. M.; Lloyd-Jones, G. C. *J. Am. Chem. Soc.* **1994**, *116*, 866-878.

studying the mechanism through deuterium labeling and kinetic measurements, they proposed a mechanism for dehydrogenative borylation using catalyst **2.24** as shown in Scheme 2.12.

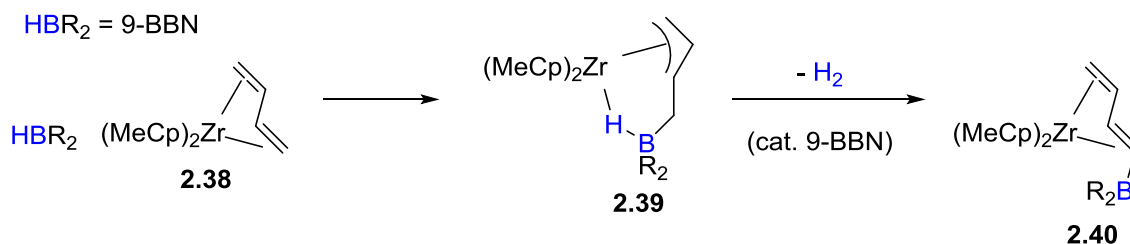
Scheme 2.12: Mechanism of dehydrogenative borylation



Rhodium dimer **2.24** is first reduced by two equivalents of the borane to generate dimeric species **2.30** and two equivalents of the respective chloroborane. Monomer **2.31** is hypothesized to be the active catalytic species, which undergoes reversible migratory insertion to generate **2.32**. Oxidative addition of HBR_2 generates proposed 4-coordinate **2.33**, which can undergo reductive elimination to give one equivalent of the hydrogenated styrene and complex **2.34**. β -Migratory insertion to the preferred benzylic-rhodium species **2.35** prepares the system for β -hydride elimination to generate complex **2.36** which undergoes a ligand exchange to generate the vinylboronicester **2.37**, regenerating active species **2.31**. In 1993, Marder et al.⁹⁴ showed that a vinylarene could insert directly into a Rh-B bond *if there was no hydride on the metal*, lending support to the Rh-B migratory insertion step to generate the terminal borane.

In 1993, Erker et al.⁹⁵ showed that (butadiene)zirconocene **2.38** reacts with 9-BBN in order to generate compound **2.39**. Vinylborane **2.40** is formed upon 9-BBN-catalyzed loss of H_2 (Scheme 2.13).

Scheme 2.13: Dehydrogenative borylation of $(\text{MeCp})_2\text{Zr}$ with 9-BBN

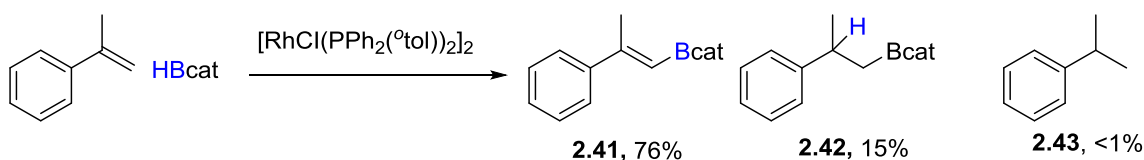


⁹⁴ Baker, R. T.; Calabrese, J. C.; Westcott, S. A.; Nguyen, P.; Marder, T. B. *J. Am. Chem. Soc.* **1993**, *115*, 4367-4368.

⁹⁵ Erker, G.; Noe, R.; Wingbermühle, D.; Petersen, J. L. *Angew. Chem. Int. Ed. Engl.* **1993**, *32*, 1213-1215.

Also in 1993, Marder et al.⁹⁶ demonstrated the first selective dehydrogenative borylation without the observation of a significant amount of hydrogenated alkene substrate. The use of hindered styrene compounds allowed for dehydrogenative borylation with minimal hydrogenation of the styrene with loss of H₂. [RhCl(PPh₂(^otol))₂]₂ gave the highest selectivity for the dehydrogenative borylation product **2.41**, however >10% of the hydroboration product **2.42** was always present. Under the optimized conditions, <1% of hydrogenated alkene **2.43** was observed (Scheme 2.14).

Scheme 2.14: Dehydrogenative borylation of α -Me styrene



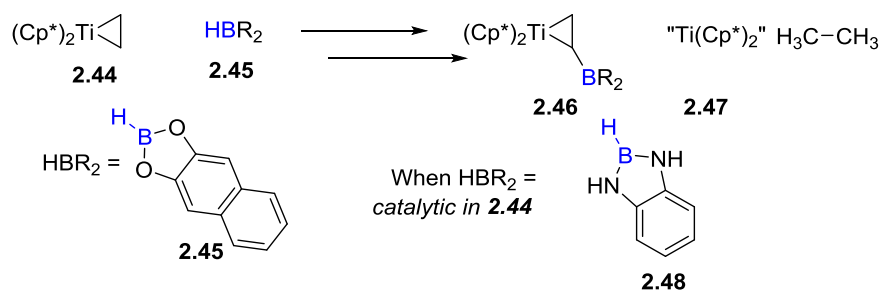
In 1995, Smith and Motry⁹⁷ demonstrated the stoichiometric dehydrogenative borylation of $(\eta^5\text{-Cp}^*)_2\text{Ti}(\eta^2\text{CH}_2\text{CH}_2)$ **2.44** with borane **2.45** (Scheme 2.15) to generate complex **2.46**. This reaction proceeded with the sacrificial hydrogenation of one equivalent of $(\eta^5\text{-Cp}^*)_2\text{Ti}(\eta^2\text{CH}_2\text{CH}_2)$ to generate $(\eta^5\text{-Cp}^*)_2\text{Ti}$ **2.47** and ethane in addition to **2.46**. The same group⁹⁸ later expanded the methodology to be catalytic in **2.44**, achieving turnover by substituting borane **2.45** with **2.48**. This substitution allowed for the reformation of **2.44** from **2.46** upon treatment with ethylene.

⁹⁶ Westcott, S. A.; Marder, T. B.; Baker, R. T. *Organometallics* **1993**, *12*, 975-979.

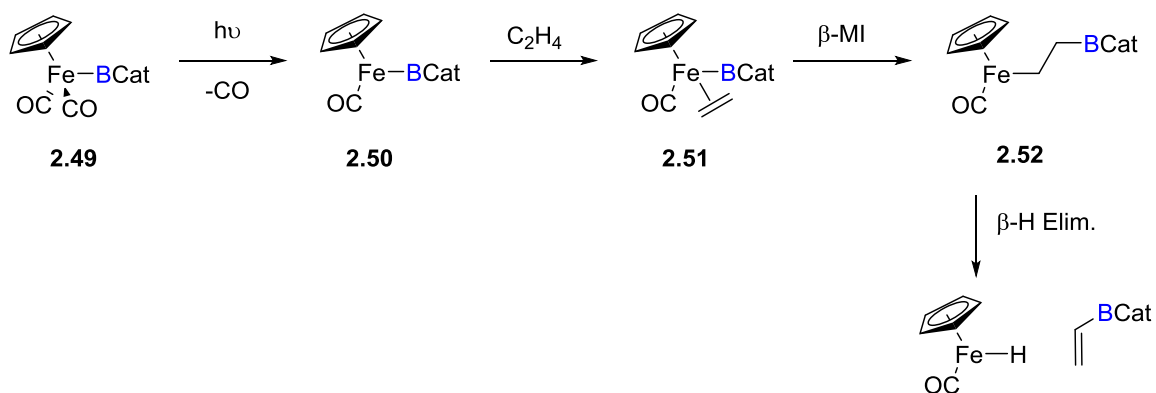
⁹⁷ Motry, D. H.; Smith, M. R. *J. Am. Chem. Soc.* **1995**, *117*, 6615-6616.

⁹⁸ Motry, D. H.; Brazil, A. G.; Smith, M. R. *J. Am. Chem. Soc.* **1997**, *119*, 2743-2744.

Scheme 2.15: Stoichiometric titanocene dehydrogenative borylation



Scheme 2.16: Stoichiometric iron-boryl dehydrogenative borylation



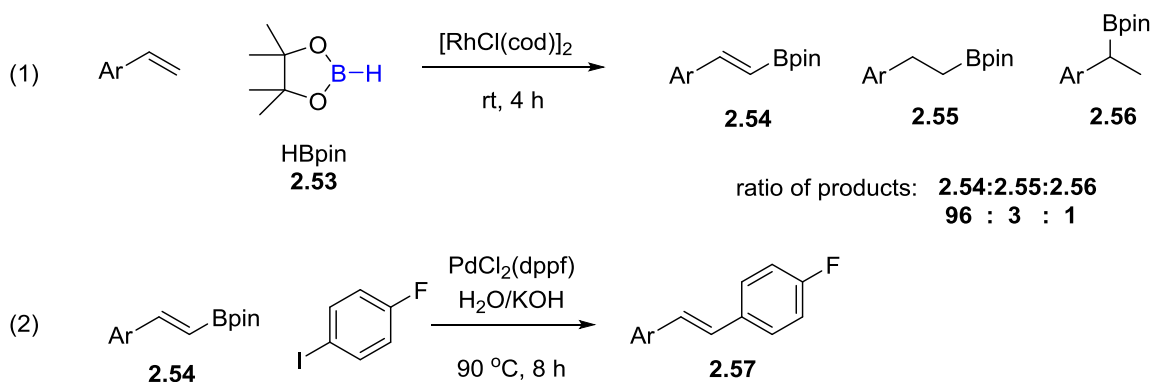
The Hartwig group⁹⁹ developed metal-boryl (M=Re, Mn, Fe) complexes which, under UV irradiation, were able to perform C–H activation of alkyl, aryl, and alkenyl C–H bonds to generate C–B bonds (Scheme 2.16). Pianostool boryl complex **2.49** ejects carbon monoxide under UV irradiation to generate reactive complex **2.50**. This complex then reacts with ethylene to generate complex **2.51**. Insertion of ethylene into the Fe–B bond of **2.51** generates intermediate **2.52**. β -Hydride elimination then produces vinyl boronic acid catechol ester. Later mechanistic study was inconclusive on the mechanism

⁹⁹ Waltz, K. M.; He, X.; Muhoro, C.; Hartwig, J. F. *J. Am. Chem. Soc.* **1995**, *117*, 11357-11358.

of dehydrogenative borylation of ethylene due to no discernable intra- or intermolecular isotope effect from deuterium labeling studies.¹⁰⁰

In 1999, Masuda et al.¹⁰¹ reported a synthesis of vinyl boronic esters using $[\text{RhCl}(\text{cod})]_2$ as the precatalyst with HBpin **2.53** (Scheme 2.17, Eq. 1). They observed selective formation of vinylboronic ester **2.54** over hydroboration products **2.55** and **2.56**. The authors were able to synthesize unsymmetrical stilbene **2.57** by using this methodology combined with Suzuki cross-coupling (Scheme 2.17, Eq. 2).

Scheme 2.17: Dehydrogenative borylation of styrenes with HBpin and subsequent Suzuki cross-coupling



Masuda and coworkers¹⁰² later expanded their dehydrogenative borylation reaction to include $\text{Ru}(\text{cod})(\text{cot})/4\text{PR}_3$ as the precatalyst, however they were unable to generate favorable selectivity for dehydrogenative borylation over side reactivities. Sabo-Etienne and Caballero¹⁰³ also demonstrated that $\text{Ru}(\text{H})_2(\text{H}_2)_2(\text{Pcy}_3)_2$ could serve as

¹⁰⁰ Waltz, K. M.; Muhoro, C. N.; Hartwig, J. F. *Organometallics* **1999**, *18*, 3383-3393.

¹⁰¹ Murata, M.; Watanabe, S.; Masuda, Y. *Tetrahedron Letters* **1999**, *40*, 2585-2588.

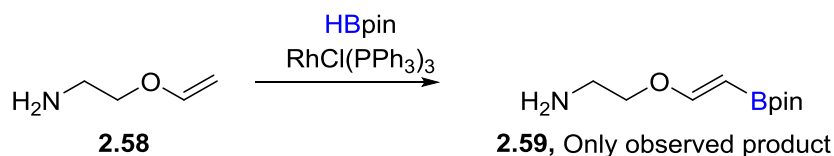
¹⁰² Murata, M.; Kawakita, K.; Asana, T.; Watanabe, S.; Masuda, Y. *Bull. Chem. Soc. of Jpn.* **2002**, *75*, 825-829.

¹⁰³ Caballero, A.; Sabo-Etienne, S. *Organometallics* **2007**, *26*, 1191-1195.

catalyst for both hydroboration and dehydrogenative borylation reactions, although the selectivity was similarly low to that observed by Masuda.

At the turn of the century, Westcott et al.¹⁰⁴ demonstrated a highly selective dehydrogenative borylation of aminopropyl vinyl ethers **2.58** with pinacolborane and Wilkinson's catalyst. No boron-containing products other than the vinyl boronic ester **2.59** were observed (Scheme 2.18).

Scheme 2.18: Selective dehydrogenative borylation of aminopropyl vinyl ethers



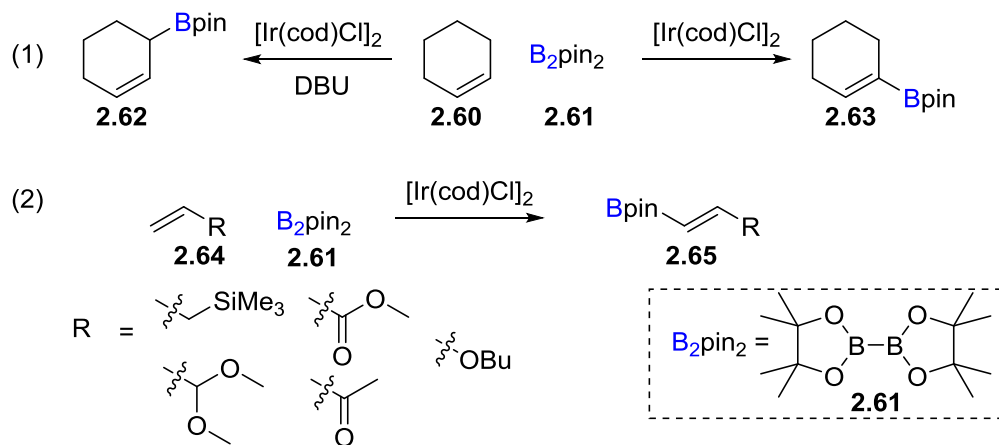
Marder et al.¹⁰⁵ were interested in the continued development of dehydrogenative borylation strategies that did not sacrifice a significant amount of alkene to hydrogenation. They discovered that *trans*-[RhCl(CO)(PPh₃)₂] was a suitable precatalyst for generating vinyl boronic esters from bis-boronate reagents such as B₂pin₂ without significant hydrogenation of the alkene or vinyl boronic ester using either conventional or microwave heating. The reaction times and conversions however, were beyond the realm of practicality in synthesis (conventional heated reactions were on the order of 5 days while the conversions were inconsistent and substrate dependent).

¹⁰⁴ Vogels, C. M.; Hayes, P. G.; Shaver, M. P.; Westcott, S. A. *Chem. Commun.* **2000**, 1, 51-52.

¹⁰⁵ (a) Coapes, R. B.; Souza, F. E. S.; Thomas, R. L.; Hall, J. J.; Marder, T. B. *Chem. Commun.* **2003**, No. 5, 614-615. (b) Mkhaliid, I. A. I.; Coapes, R. B.; Edes, S. N.; Coventry, D. N.; Souza, F. E. S.; Thomas, R. L.; Hall, J. J.; Bi, S.-W.; Lin, Z.; Marder, T. B. *Dalton Trans.* **2008**, No. 8, 1055-1064.

In 2007, Szabó and Olsson¹⁰⁶ demonstrated a conditions-dependent borylation of cyclic alkenes **2.60** with B₂pin₂ **2.61** and [Ir(cod)Cl]₂ (Scheme 2.19, Eq. 1). The use of diboron reagents avoided side reactivity associated with the B–H bond such as unwanted hydroboration. When treated with DBU the conditions generated allylic boronic esters **2.62**, and with no base present the conditions generated the vinyl boronic ester **2.63**. The group later expanded the reaction conditions to include acyclic primary alkenes **2.64** (Scheme 2.19, Eq. 2).¹⁰⁷ They were able to demonstrate Suzuki cross-coupling with the generated vinyl boronic esters **2.65**, as well as allylboron addition to aldehydes with the allylic boronic esters. A mechanistic study in their 2009 paper suggested that their system likely undergoes a dehydrogenative borylation mechanism with a rate-limiting alkene insertion to the Ir–B bond due to a lack of a k_H/k_D kinetic isotope effect.

Scheme 2.19: Iridium-catalyzed dehydrogenative borylation of alkenes

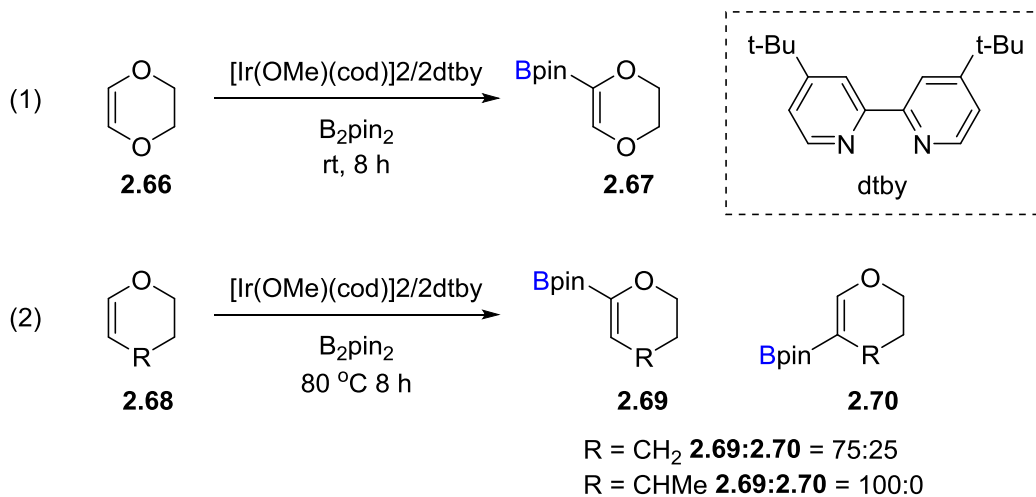


¹⁰⁶ Olsson, V. J.; Szabó, K. J. *Angew. Chemie Int. Ed.* **2007**, *46*, 6891-6893.

¹⁰⁷ (a) Olsson, V. J.; Szabó, K. J. *Org. Lett.* **2008**, *10*, 3129-3131. (b) Olsson, V. J.; Szabó, K. J. *J. Org. Chem.* **2009**, *74*, 7715-7723.

In 2008 Miyaura et al.¹⁰⁸ demonstrated an iridium-catalyzed dehydrogenative borylation of cyclic vinylic ethers using the [Ir(OMe)(cod)]₂/2dtby catalyst system they had developed in collaboration with Hartwig¹⁰⁹ for the stoichiometric, ambient temperature, direct C–H borylation of arenes. Miyaura et al. found that the C–H borylation reaction of 1,4-dioxene **2.66** proceeded at room temperature to generate the vinyl boronic ester **2.67** (Scheme 2.20, Eq. 1). Cyclic vinylic monoethers **2.68** required elevated temperature to react, and selectivity for the generation of α -borylated **2.69** over β -borylated **2.70** was only achieved with γ -substitution (Scheme 2.20, Eq. 2).

Scheme 2.20: Iridium-catalyzed dehydrogenative borylation of cyclic vinyl ethers



Unlike Szabó's iridium-catalyzed dehydrogenative borylation, a measurable kinetic isotope effect $k_{\text{H/D}} = 3.2$ was observed. This suggests a mechanism involving

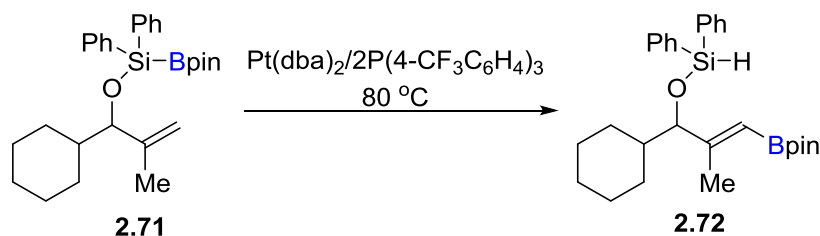
¹⁰⁸ (a) Kikuchi, T.; Takagi, J.; Ishiyama, T.; Miyaura, N. *Chemistry Letters* **2008**, 37, 664-665. (b) Kikuchi, T.; Takagi, J.; Isou, H.; Ishiyama, T.; Miyaura, N. *Chem. Asian J.* **2008**, 3, 2082-2090.

¹⁰⁹ (a) Ishiyama, T.; Takagi, J.; Ishida, K.; Miyaura, N.; Anastasi, N. R.; Hartwig, J. F. *J. Am. Chem. Soc.* **2002**, 124, 390-391. (b) Ishiyama, T.; Takagi, J.; Hartwig, J. F.; Miyaura, N. *Angew. Chem. Int. Ed.* **2002**, 41, 3056-3058.

direct C–H activation, more similar to the mechanism postulated by Hartwig and coworkers in the C–H borylation of arenes.¹¹⁰ As is often the case the mechanism of the reaction is dependent upon the nature of the catalyst and the substrate.

In 2009, the Suginome lab¹¹¹ demonstrated an intramolecular platinum catalyzed dehydrogenative borylation using methallyl silylboronic esters **2.71**¹¹² to selectively generate vinylboronic esters with the boron cis- to the methyl group **2.72** (Scheme 2.21).

Scheme 2.21: Platinum catalyzed intramolecular vinyl boronic ester formation



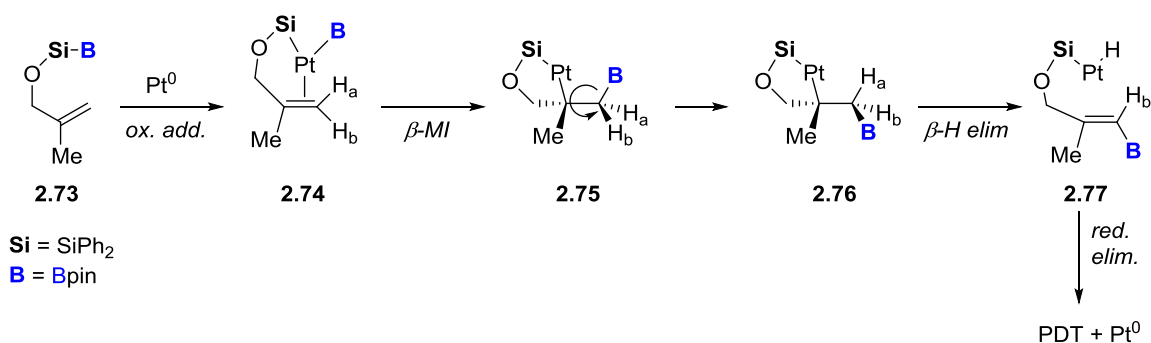
The authors propose the following mechanism to account for the high selectivity for the *syn* arrangement of the Bpin and Me substituents. Silaborane **2.73** oxidatively adds to the platinum (0) center to generate **2.74**. β -Migratory insertion of the alkene into the Pt–B bond generates intermediate **2.75**. After bond rotation to generate the more stable eclipsed conformer **2.76**, a β -hydride elimination occurs to generate vinyl boronic ester **2.77** which upon reductive elimination to form the Si–H bond gives product while regenerating the platinum (0) species.

¹¹⁰ Boller, T. M.; Murphy, J. M.; Hapke, M.; Ishiyama, T.; Miyaura, N.; Hartwig, J. F. *J. Am. Chem. Soc.* **2005**, *127*, 14263-14278.

¹¹¹ Ohmura, T.; Takasaki, Y.; Furukawa, H.; Suginome, M. *Angew. Chem. Int. Ed.* **2009**, *48*, 2372-2375.

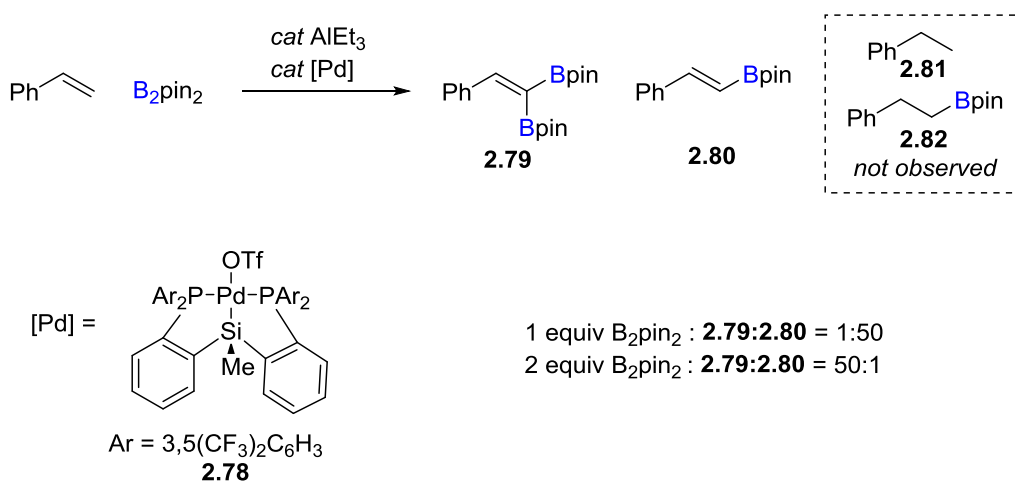
¹¹² For preparation of silylboronic esters please see: Ohmura, T.; Masuda, K.; Furukawa, H.; Suginome, M. *Organometallics* **2007**, *26*, 1291-1294.

Scheme 2.22: Proposed mechanism for platinum catalyzed intramolecular vinyl boronic ester formation from methallyl silyboronic esters



More recently Iwasawa et al.¹¹³ demonstrated a selective double dehydrogenative borylation of styrene using triethylaluminum activated PSiP-pincer palladium catalyst **2.78** (Scheme 2.23). The reaction showed the selective formation of double dehydrogenative borylation product **2.79** when 2 equivalents of B_2pin_2 were used, and a high selectivity for dehydrogenative borylation product **2.80** with one equivalent of B_2pin_2 .

Scheme 2.23: Selective double dehydrogenative borylation with PSiP-Pd 2.78



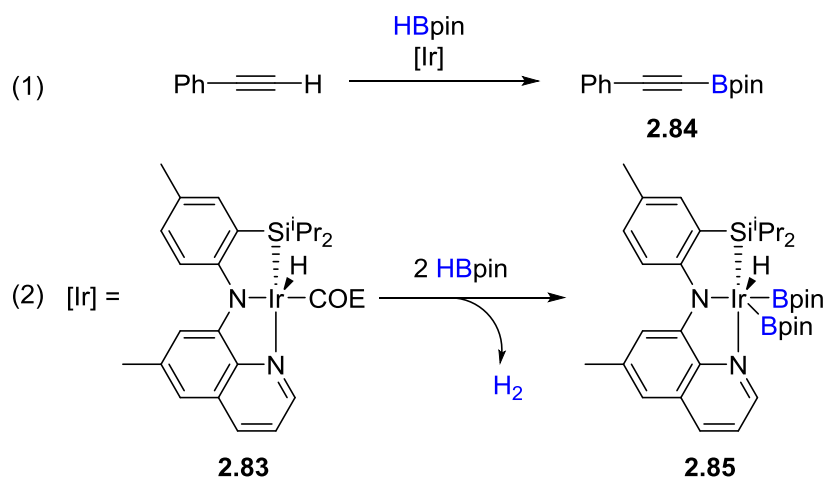
¹¹³ Takaya, J.; Kirai, N.; Iwasawa, N. *J. Am. Chem. Soc.* **2011**, *133*, 12980-12983.

The reaction took place without the formation of hydrogenation (**2.81**) or hydroboration (**2.82**) products. The reaction generates one or two equivalents of HBpin, which are not activated under the reaction conditions. A continued study¹¹⁴ expanded the scope of the reaction to include selective single- and double- dehydrogenative borylation reactions of unactivated alkenes.

2.2.3 Metal-catalyzed dehydrogenative borylation of alkynes

In 2013, Ozerov et al.¹¹⁵ demonstrated the first dehydrogenative borylation of a terminal alkyne using HBpin and a SiNN pincer iridium catalyst **2.83** at room temperature in 10 minutes to generate alkynyl Bpin **2.84** (Scheme 2.24, Eq. 1). Interestingly, this catalyst rapidly releases hydrogen gas from HBpin to generate the active species **2.85** (Scheme 2.24, Eq. 2).

Scheme 2.24: Selective dehydrogenative borylation of primary alkynes with SiNN-Ir

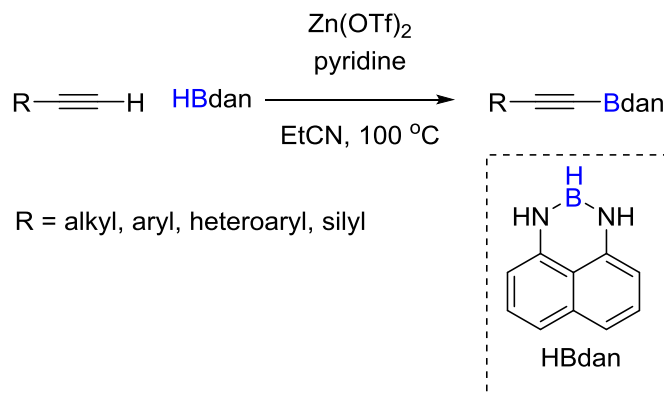


¹¹⁴ Kirai, N.; Iguchi, S.; Ito, T.; Takaya, J.; Iwasawa, N. *Bull. Chem. Soc. Jpn.* **2013**, *86*, 784-799.

¹¹⁵ Lee, C.-I.; Zhou, J.; Ozerov, O. V. *J. Am. Chem. Soc.* **2013**, *135*, 3560-3566.

Tsuchimoto and coworkers¹¹⁶ were more recently able to demonstrate the dehydrogenative borylation of a large range of terminal alkynes with HBdan and a Zn/pyridine Lewis acid catalyst system in refluxing propionitrile (Scheme 2.25).

Scheme 2.25: Selective dehydrogenative borylation of primary alkynes with SiNN-Ir



Catalytic transformations of *B*-H bonds have generated many ways to access new organoborane species. The development of hydroboration, dehydrogenative borylation, and aryl *C*-H borylation (which has dramatically increased the synthetic toolbox for the synthesis of functionalized arenes) has been driven by the success and scope of the Nobel prize winning Suzuki cross-coupling.

2.2.4 Known *B*-H to *B*-Cl transformations

The replacement of a *B*-H bond (BDE of *B*-H in $\text{BH}_3=105.2 \text{ kcal/mol}$ ¹¹⁷) with a *B*-Cl (BDE of *B*-Cl in $\text{BCl}_3=102.1 \text{ kcal/mol}$ ¹¹⁸) bond is nearly thermoneutral. However, the high electrophilicity of the polarized *B*-Cl generally makes it susceptible to

¹¹⁶ Tsuchimoto, T.; Utsugi, H.; Sugiura, T.; Horio, S. *Adv. Synth. Catal.* **2015**, *357*, 77-82.

¹¹⁷ Rablen, P. R.; Hartwig, J. F. *J. Am. Chem. Soc.* **1996**, *118*, 4648-4653.

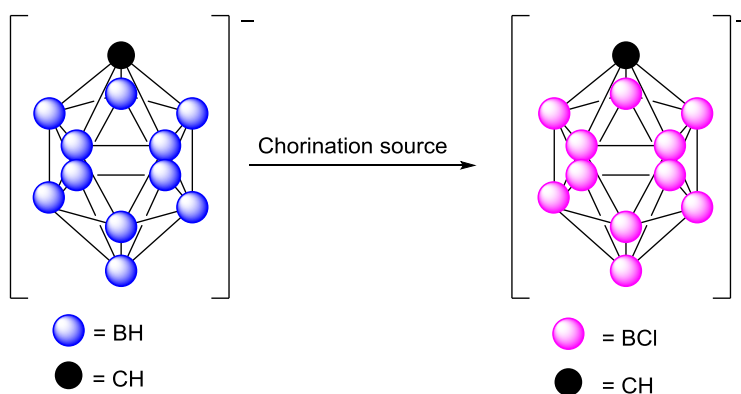
¹¹⁸ Luo, Y. R., *Comprehensive Handbook of Chemical Bond Energies*, CRC Press, Boca Raton, FL, 2007.

substitution reactions with nucleophiles in three-coordinate boron. Although postulated by Brown and Lloyd-Jones as the initial step in generating active catalytic species in dehydrogenative borylation, the chemistry of selectively transforming $B-H$ bonds to $B-Cl$ bonds is underexplored.

2.2.4.1 Electrophilic chlorination of carborane anions

The icosahedral carba-*closo*-dodecaborate (carborane) anion $[CHB_{11}H_{11}]^-$ undergoes $B-H$ displacement reactions when treated with Cl_2 , NCS, or ICl to generate $B-Cl$ containing carboranes with 1-11 Cl units depending on the specific conditions used (Scheme 2.26).¹¹⁹ Although this represents the most studied $B-H$ to $B-Cl$ transformation, the extreme stability and unique reactivity of the carborane anion does not allow for many parallels to be made with other systems.

Scheme 2.25: Electrophilic chlorination of carborane anions



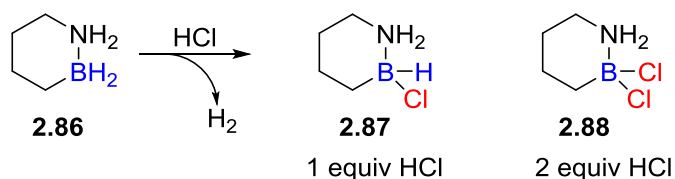
¹¹⁹ (a) Jelínek, T.; Plešek, J.; Heřmánek, S.; Štíbr, B. *Coll. of Czech. Chem. Comm.* **1986**, *51*, 819-829. (b) Xie, Z.; Tsang, C.-W.; Xue, F.; Mak, T. C. W. *Inorg. Chem.* **1997**, *36*, 2246-2247. (c) Xie, Z.; Tsang, C.-W.; Xue, F.; Mak, T. C. W. *Journal of Organometallic Chemistry* **1999**, *577*, 197-204. (d) Vyakaranam, K.; Körbe, S.; Divišová, H.; Michl, J. *J. Am. Chem. Soc.* **2004**, *126* (48), 15795-15801. (e) Körbe, S.; Schreiber, P. J.; Michl, J. *Chem. Rev.* **2006**, *106*, 5208-5249.

2.2.4.2 *B–H* to *B–Cl* using HCl

When $\text{BH}_3 \cdot \text{THF}$ is treated with HCl, $\text{BHCl}_2 \cdot \text{THF}$ or $\text{BH}_2\text{Cl} \cdot \text{THF}$ is produced through concomitant release of hydrogen gas (from the combination of the protic HCl and hydridic *B–H*) depending on the stoichiometry.¹²⁰

In a similar fashion, 1,2-BN cyclohexane¹²¹ **2.86** undergoes either mono- or bis-chlorination by release of hydrogen gas to generate **2.87** or **2.88** when treated with one or two equivalents of HCl respectively (Scheme 2.26).

Scheme 2.26: Hydrogen release in 1,2-BN cyclohexane



2.2.4.3 *B–H* to *B–Cl* through comproportionation

In order to synthesize the hydroborating agents BHCl_2 and BH_2Cl , H. C. Brown demonstrated a comproportionation methodology (Scheme 2.27). When diborane was mixed with $\text{BCl}_3 \cdot \text{OEt}_2$ in appropriate stoichiometry the $\text{BHCl}_2 \cdot \text{OEt}_2$ and $\text{BH}_2\text{Cl} \cdot \text{OEt}_2$ species were generated.¹²² This methodology works for the solid weighable

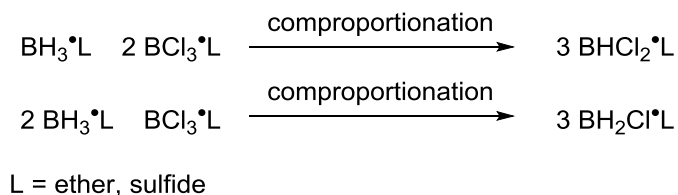
¹²⁰ G. Zweifel, *J. Organomet. Chem.* **1967**, *9*, 215-221.

¹²¹ Luo, W.; Zakharov, L. N.; Liu, S.-Y. *J. Am. Chem. Soc.* **2011**, *133*, 13006-13009.

¹²² Brown, H. C.; Tierney, P. A. *J. Inorg. Nucl. Chem.* **1959**, *9*, 51-55.

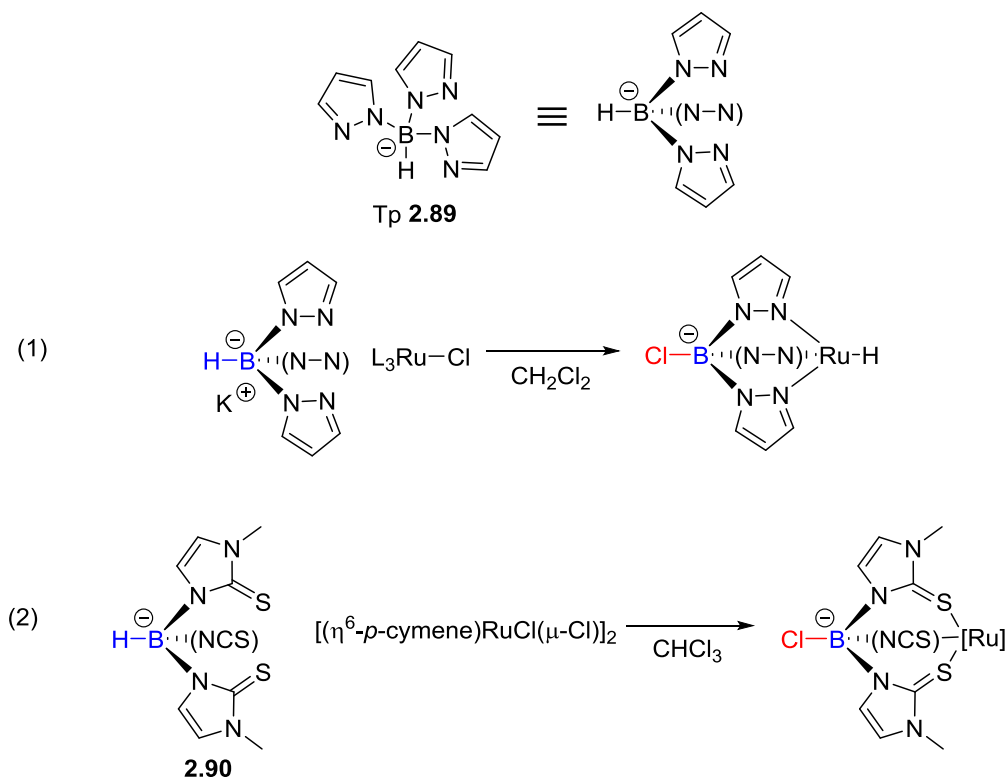
dimethylsulfide complexes as well as other stabilizing ligands.¹²³ The extent of reaction and selectivity are dependent on the nature of the stabilizing ligand, L.

Scheme 2.27: Comproportionation of B–H and B–Cl bonds



2.2.4.4 B–H to B–Cl in borate metal complexes

Scheme 2.28: B–H to B–Cl in the presence of metal centers



¹²³ (a) Brown, H. C. "Organic Syntheses via Boranes" John Wiley & Sons, Inc. New York: 1975 pp. 45-47.
 (b) Kanth, J. V. B.; Brown, H. C. *J. Org. Chem.* **2001**, *66*, 5359-5365.

The tris(pyrazolyl)borate (Tp, **2.89**) ligands are anionic chelating ligands containing a *B*–H bond commonly used in coordination chemistry.¹²⁴ In some rare cases,¹²⁵ complexation of Tp to a metal containing a *Ru*–Cl bond instigates a *B*–H to *B*–Cl exchange to generate a *Ru*–H bond (Scheme 2.28, Eq. 1). There is also a single example of structurally related tris(mercaptomethimazolyl)borate ligands (**2.90**) undergoing a similar transformation upon complexation to a ruthenium center (Scheme 2.28, Eq. 2).¹²⁶ The mechanism for these reactions is unknown and unstudied.

2.3 Development of the Dehydrogenative Borylation of 1,2-Azaborines With Styrenes: Synthesis and Characterization of BN-Stilbenes

We were interested in studying the basic science of catalysis at the boron center in 1,2-azaborines. There have been two reported catalytic activations of a *B*–X bond (X=Cl or X=Ar) in 1,2-azaborines: the rhodium-catalyzed *B*–Cl activation with aryl stannanes to generate *B*–Ar species;¹²⁷ and the palladium-catalyzed self-arylation¹²⁸ of C(3)-Br, *B*–Ar 2,1-borazaranaphthalenes under Suzuki cross-coupling conditions to generate *B*–OH bonds. Before this work, the catalytic activation of an azaborine *B*–H bond had not been demonstrated.

In order to probe the inherent reactivity of the *B*–H bond in 1,2-azaborines, we decided to use *N*–Bn *B*–H azaborine **2.91** as a model *B*–H system for our studies. 4-

¹²⁴ For a review covering coordination complexes of the so-called “scorpionate” ligands please see: Trofimenko, S. *Chem. Rev.* **1993**, 93 (3), 943.

¹²⁵ (a) Burtscher, D.; Perner, B.; Mereiter, K.; Slugovc, C. *J. Organomet. Chem.* **2006**, 691, 5423-5430. (b) Foley, N. A.; Abernethy, R. J.; Gunnoe, T. B.; Hill, A. F.; Boyle, P. D.; Sabat, M. *Organometallics* **2009**, 28, 374-377. (c) Page, M. J.; Messerle, B. A.; Wagler, J. *Organometallics* **2009**, 28, 6145-6151.

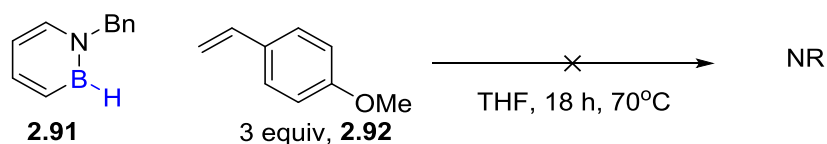
¹²⁶ Wang, X.-Y.; Shi, H.-T.; Wu, F.-H.; Zhang, Q.-F. *J. Mol. Struct.* **2010**, 982, 66-72.

¹²⁷ Rudebusch, G. E.; Zakharov, L. N.; Liu, S. -Y. *Angew. Chem. Int. Ed. Engl.* **2013**, 52, 9316-9319.

¹²⁸ Molander, G. A.; Wisniewski, S. R. *J. Org. Chem.* **2014**, 79, 8339-8347.

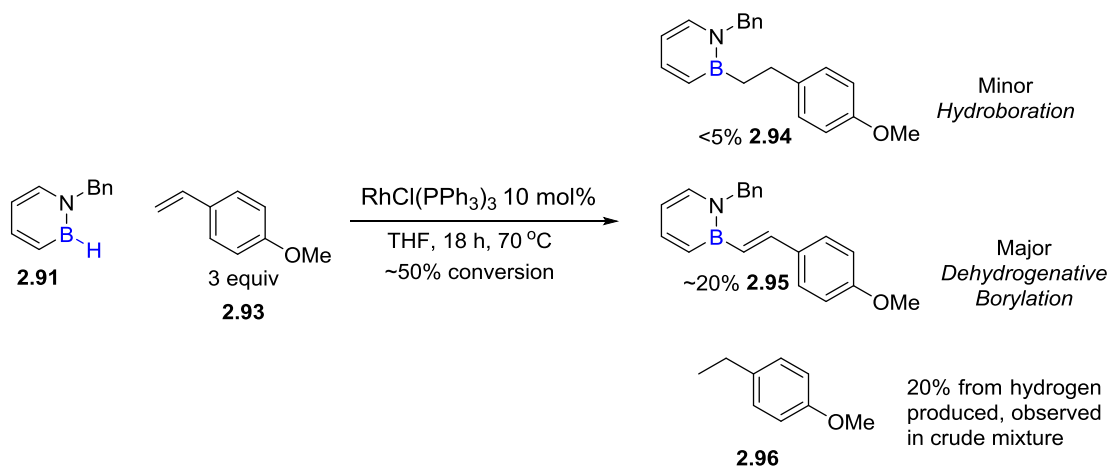
methoxy styrene **2.92** was chosen as a model alkene because the additional polarity of the methoxy unit would allow for facile separation by column chromatography and styrenes often exhibit interesting selectivities in borylation chemistry. Reaction of **2.91** with 1 equivalent of **2.92** in THF for 18 hours at 70 °C in an unregulated pressure vessel resulted in no reaction and recovery of the starting materials (Scheme 2.29).¹²⁹

Scheme 2.29: Uncatalyzed reaction of 2.91 and 2.92



When Wilkinson's catalyst was introduced to this reaction under identical conditions, we were able to isolate the hydroboration product **2.94** as a minor product (<5% isolated yield).

Scheme 2.30: B-H activation of 2.91 using Wilkinson's catalyst



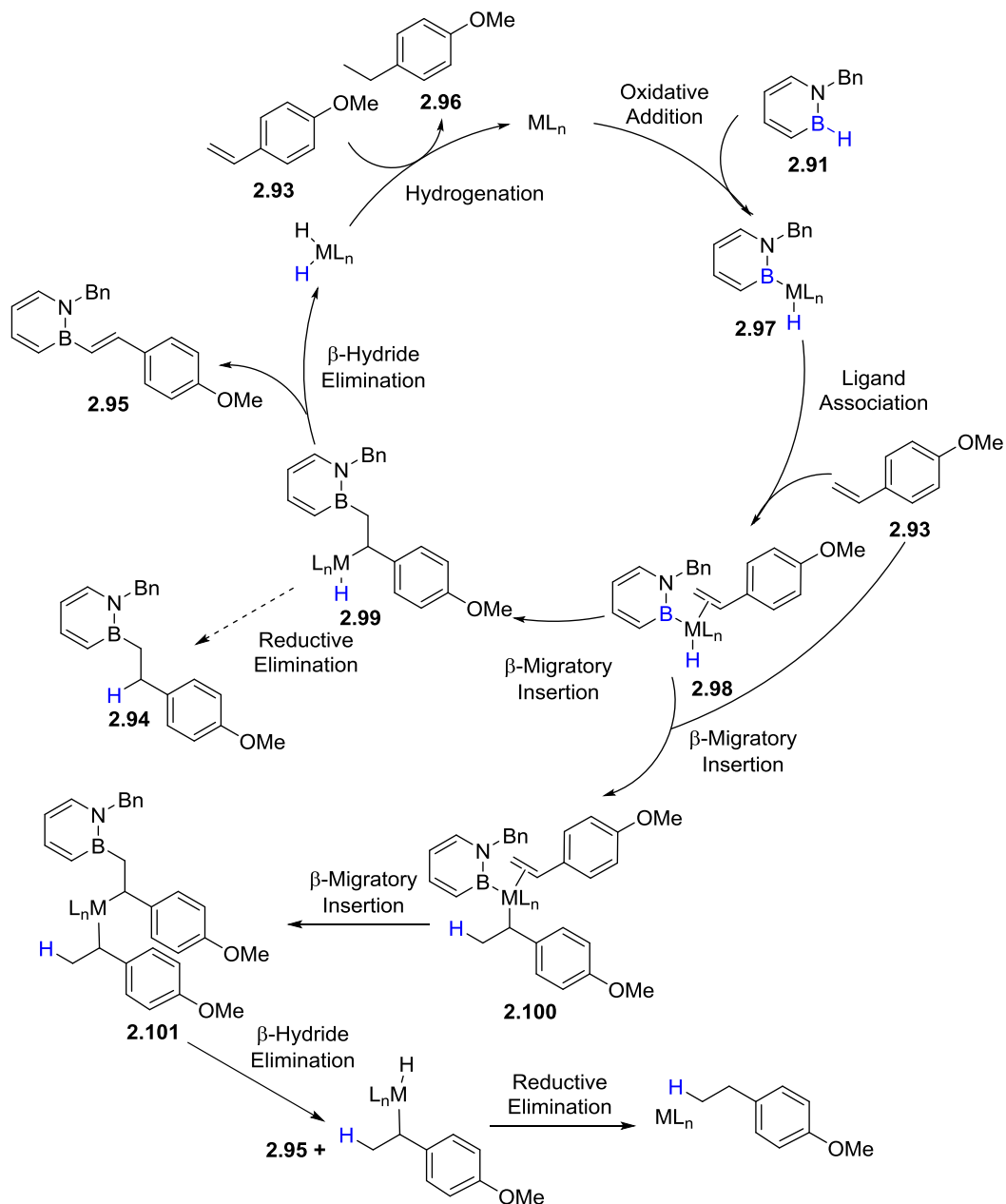
¹²⁹ 1-hexene was also unreactive under these reaction conditions

We did not expect the major product to be BN-stilbene **2.95** from dehydrogenative borylation (Wilkinson's catalyst generally gives major hydroboration and minor dehydrogenative borylation products, Scheme 2.30). We also observed a 1:1 mixture of **2.95** to 4-methoxy ethylbenzene **2.96** which would be expected from a traditional dehydrogenative borylation reaction.

We hypothesize that the mechanism for the selective formation of **2.95** follows a similar mechanism to that proposed by Brown and Lloyd-Jones in their initial report and mechanistic study of dehydrogenative borylation discussed above. Our hypothetical mechanism is as follows.

Oxidative addition of the metal to the *B*-H bond generates metal hydride **2.97**. Ligand association with **2.93** proffers intermediate **2.98**. Since the only observed products are the terminal boranes **2.94** and **2.95** a preferential β -migratory insertion of the alkene into the *B*-M bond over the *M*-H bond is possible to generate **2.99**, followed by a β -hydride elimination to generate the conjugated BN-stilbene **2.95**. Hydrogenation of another unit of **2.93** regenerates the catalyst and restarts the cycle. An alternative pathway could involve two styrene units undergoing β -migratory insertion from intermediate **2.98**, first into the *M*-H bond to generate *B*-M-alkyl species **2.100**, then a second into the *B*-M bond to generate the alkyl-M-alkyl species **2.101** (Scheme 2.31). β -Hydride elimination to generate the BN-stilbene followed by reductive elimination of the H-M-alkyl species regenerates the catalyst and restarts the cycle. The selectivity for dehydrogenative borylation could arise from the increased relative stability of the *B*-vinyl bond due to its conjugation into the aromatic backbone of the 1,2-azaborine.

Scheme 2.31: Possible mechanism for dehydrogenative borylation of 2.91



We were interested in targeting the initially unexpected BN-stilbene structure because carbonaceous stilbene compounds are common in biologically active¹³⁰ and

¹³⁰ Roupe, K. A.; Remsberg, C. M.; Yáñez, J. A.; Davies, N. M. *Curr. Clin. Pharmacol.* **2006**, *1*, 81-101.

natural products such as resveratrol and other stilbenoids.¹³¹ In addition, stilbenes are often used in materials science applications as model systems due to their properties upon interaction with light.¹³² Stilbenes are widely studied for applications in scintillators,¹³³ photoresists,¹³⁴ light emitting diodes,¹³⁵ optical brighteners,¹³⁶ and non-linear optics.¹³⁷

The incorporation of BN and other heteroarene units into conjugated systems for materials science applications is an emerging field.¹³⁸ The integration of monocyclic 1,2-azaborines into extended π -systems is even more limited;¹³⁹ the ability to study a larger

¹³¹ For recent reviews on resveratrol see: (a) Baur, J. A.; Sinclair, D. A. *Nat Rev Drug Discov* **2006**, *5*, 493. (b) Cottart, C.-H.; Nivet-Antoine, V.; Beaudeau, J.-L. *Mol. Nutr. Food Res.* **2014**, *58*, 7-21.

¹³² For pioneering mechanistic work on the photoisomerization of stilbenes:, see (a) Saltiel, J. *J. Am. Chem. Soc.* **1967**, *89*, 1036-1037. (b) Saltiel, J. *J. Am. Chem. Soc.* **1968**, *90*, 6394-6400. (c) Saltiel, J.; Waller, A. S.; Sears Jr, D. F.; Garrett, C. Z. *J. Phys. Chem.* **1993**, *97*, 2516-2522. For an overview, see: (d) Meier, H. *Angew. Chem. Int. Ed. Engl.* **1992**, *31*, 1399-1420..

¹³³ Zaitseva, N. P.; Newby, J.; Hamel, S.; Carman, L.; Faust, M.; Lordi, V.; Cherepy, N. J.; Stoeffl, W.; Payne, S. A. *Proc. SPIE.* **2009**, *7449*, 744911.

¹³⁴ For a leading reference, see: (a) Stuber, F. A.; Ulrich, H.; Rao, D. V.; Sayigh, A. A. R. *J. Appl. Polym. Sci.* **1969**, *13*, 2247-2255. (b) Soomro, S. A.; Benmouna, R.; Berger, R.; Meier, H. *Eur. J. Org. Chem.* **2005**, *2005*, 3586-3593.

¹³⁵ (a) Lo, S.-C.; Burn, P. L. *Chem. Rev.* **2007**, *107*, 1097-1116. (b) Likhtenshtein, G. *Stilbenes: Applications in Chemistry, Life Sciences, and Materials science*; Wiley: New York, 2010.

¹³⁶ Dorlars, A.; Schellhammer, C. -W.; Schroeder, J. *Angew. Chem. Int. Ed. Engl.* **1975**, *14*, 665-679.

¹³⁷ Cheng, L. T.; Tam, W.; Stevenson, S. H.; Meredith, G. R.; Rikken, G.; Marder, S. R. *J. Phys. Chem.* **1991**, *95*, 10631-10643.

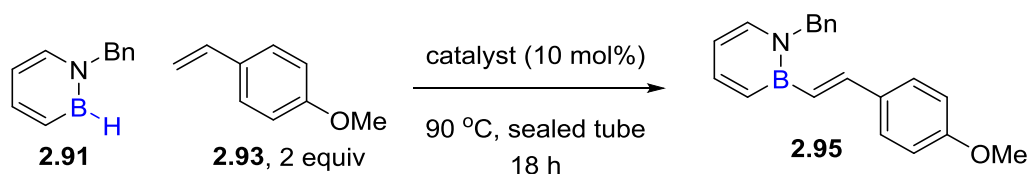
¹³⁸ (a) Jäkle, F. *Chem. Rev.* **2010**, *110*, 3985-4022. (b) Campbell, P. G.; Marwitz, A. J.; Liu, S. Y. *Angew. Chem., Int. Ed.* **2012**, *51*, 6074-6092. (c) Jiang, W.; Li, Y.; Wang, Z. *Chem. Soc. Rev.* **2013**, *42*, 6113-6127. For more recent examples please see the following as leading references: (d) Wang, X.; Zhang, F.; Liu, J.; Tang, R.; Fu, Y.; Wu, D.; Xu, Q.; Zhuang, X.; He, G.; Feng, X. *Org. Lett.* **2013**, *15*, 5714-5717. (e) Müller, M.; Behnle, S.; Maichle-Mössmer, C.; Bettinger, H. F. *Chem. Commun.* **2014**, *50*, 7821-7823. (f) Wang, X.-Y.; Zhuang, F.-D.; Wang, R.-B.; Wang, X.-C.; Cao, X.-Y.; Wang, J.-Y.; Pei, J. *J. Am. Chem. Soc.* **2014**, *136*, 3764-3767. (g) Ishibashi, J. S. A.; Marshall, J. L.; Maziere, A.; Lovinger, G. J.; Li, B.; Zakharov, L. N.; Dargelos, A.; Graciaa, A.; Chrostowska, A.; Liu, S.-Y. *J. Am. Chem. Soc.* **2014**, *136*, 15414-15421. (h) Li, G.; Xiong, W.-W.; Gu, P.-Y.; Cao, J.; Zhu, J.; Ganguly, R.; Li, Y.; Grimsdale, A. C.; Zhang, Q. *Org. Lett.* **2015**, *17*, 560-563. (i) Wang, X.-Y.; Yang, D.-C.; Zhuang, F.-D.; Liu, J.-J.; Wang, J.-Y.; Pei, J. *Chem. Eur. J.* **2015**, ASAP: 10.1002/chem.201501161

¹³⁹ (a) Marwitz, A. J. V.; Jenkins, J. T.; Zakharov, L. N.; Liu, S.-Y. *Angew. Chem. Int. Ed.* **2010**, *49*, 7444-7447. (b) Taniguchi, T.; Yamaguchi, S. *Organometallics* **2010**, *29*, 5732-5735. (c) Marwitz, A. J. V.; Lamm, A. N.; Zakharov, L. N.; Vasiliu, M.; Dixon, D. A.; Liu, S.-Y. *Chem. Sci.* **2012**, *3*, 825-829. (d) Neue, B.; Fröhlich, R.; Wibbeling, B.; Fukazawa, A.; Wakamiya, A.; Yamaguchi, S.; Würthwein, E.-U. *J. Org. Chem.* **2012**, *77* (5), 2176-2184.

range of π -conjugated BN-arenes would allow for the development and fine-tuning of favorable optical and materials properties.

In order to pursue the formation of BN-stilbenes, we surveyed a number of commercially available catalysts known to promote *B*-H activation and dehydrogenative borylation to optimize the formation of BN stilbene **2.95**.

Table 2.1. Survey of catalysts and solvents for the dehydrogenative borylation reaction between 1,2-azaborine **2.91 and styrene **2.93**.**



entry	catalyst	solvent	yield (%) ^a
1	RhCl(PPh ₃) ₃	THF	15
2	RhH(CO)(PPh ₃) ₃	THF	0
3	[Rh(dppb)(cod)] ⁺ BF ₄ ⁻	THF	0
4	[Ir(cod)(py)(Pcy ₃)] ⁺ PF ₆ ⁻	THF	51
5	[Rh(cod) ₂] ⁺ BF ₄ ⁻	THF	64
6	[Rh(nbd)Cl] ₂	THF	80
7	[Rh(cod) ₂] ⁺ BF ₄ ⁻	toluene	60
8	[Rh(cod) ₂] ⁺ BF ₄ ⁻	acetonitrile	23
9	[Rh(cod) ₂] ⁺ BF ₄ ⁻	CH ₂ Cl ₂	75
10	[Rh(nbd)Cl] ₂	toluene	94
11	[Rh(nbd)Cl] ₂	acetonitrile	52
12	[Rh(nbd)Cl] ₂	CH ₂ Cl ₂	98 (83) ^b
13	[Rh(nbd)Cl] ₂ (2.5 mol %)	CH ₂ Cl ₂	(86) ^{b,c}

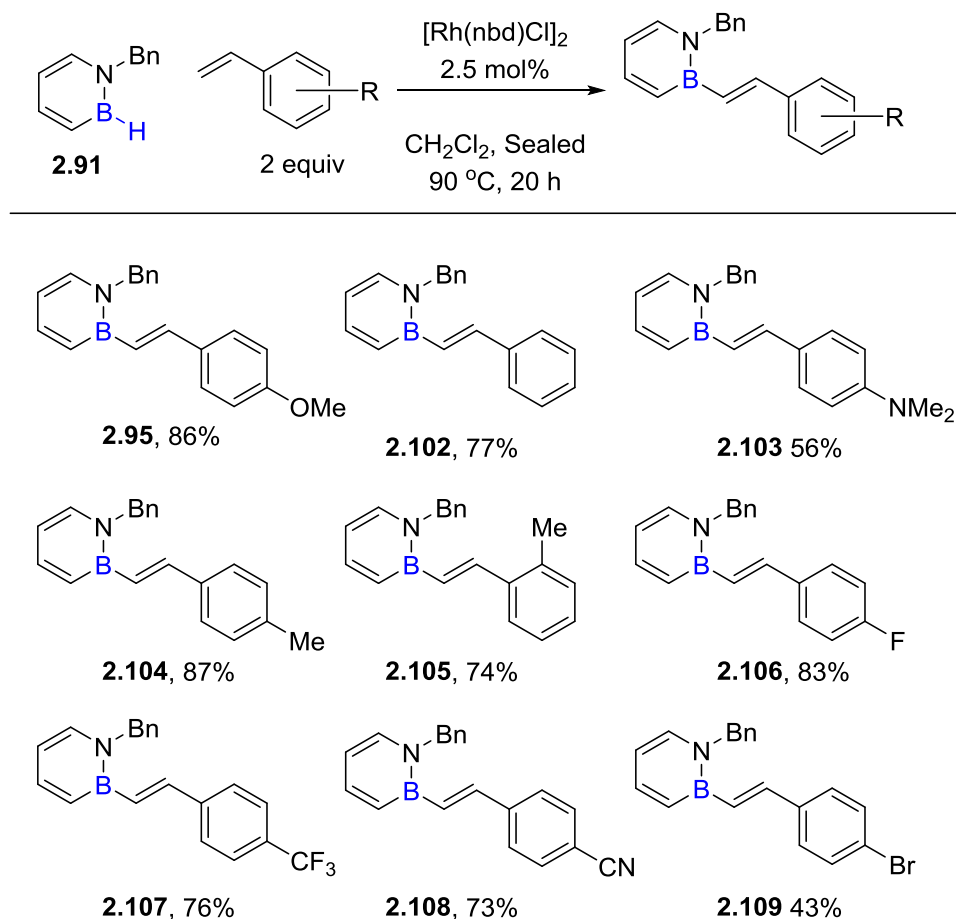
^a Yield determined by HPLC versus a calibrated internal standard, average of two runs. ^b Isolated yields in parentheses, average of two runs. ^c 20 h reaction time.

Wilkinson's catalyst gave the desired stilbene as the major product in just 15% yield (Table 2.1, entry 1). Other phosphine-ligated rhodium complexes successfully used in *B*-H activation reactions were ineffective for this reaction (Table 2.1, entries 2 and 3). On the other hand, Crabtree's complex furnished the product in 51% yield (Table 2.1, entry 4). Gratifyingly, we found that phosphine-free rhodium alkene complexes similar to those used in Brown and Lloyd-Jones' original report such as $[\text{Rh}(\text{cod})_2]^+\text{BF}_4^-$ or $[\text{Rh}(\text{nbd})(\text{Cl})]_2$ were suitable catalysts for our model dehydrogenative borylation reaction (Table 2.1, entries 5 and 6). We thus chose those two complexes for further solvent optimization studies. We determined that methylene chloride was the best performing solvent for both rhodium complexes (Table 2.1, entries 7-12) providing the desired product in up to 98% HPLC yield (83% isolated yield) in the case of $[\text{Rh}(\text{nbd})(\text{Cl})]_2$ (Table 2.1, entry 12). A reduction of the catalyst loading to 2.5 mol% $[\text{Rh}(\text{nbd})(\text{Cl})]_2$ was not detrimental with respect to the isolated yield of **2.95** (Table 2.1, entry 13). Two equivalents of the styrene **2.93** were necessary to achieve full conversion to the BN-stilbene because one equivalent of styrene was hydrogenated during the catalytic cycle under all effective conditions. Neither 1-hexene nor phenylacetylene were active under these conditions.

With the optimized conditions determined, we next turned our attention to the scope of the dehydrogenative borylation reaction (Scheme 2.32). The reaction with the parent styrene furnished **2.102** in 77% yield. While the electron rich 4-methoxystyrene was a suitable substrate for the reaction in good yield (**2.95**, 86% yield), 4-dimethylaminostyrene produced the corresponding BN stilbene **2.103** in moderate 56% yield. Steric influences on styrene do not appear to affect the yield of BN stilbene

products as both 4- and 2-tolylstyrene are suitable substrates (**2.104**, 87% yield and **2.105**, 74% yield). Electron-withdrawing substituents are tolerated in good yield (**2.106**, 83% yield; **2.107**, 76% yield; and **2.108**, 73% yield). Finally, 4-bromostyrene couples with **2.91** in low yield to generate a BN stilbene that can be potentially further functionalized through cross-coupling (**2.109**, 43% yield). The low yield of **2.109** can be attributed to side reactions stemming from C–Br activation.

Scheme 2.32 Synthesis of BN stilbenes through Rh-catalyzed dehydrogenative borylation.

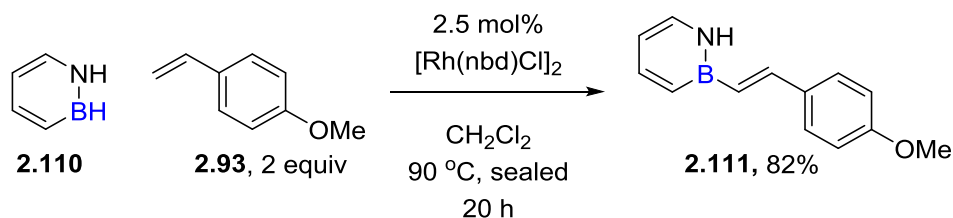


Percent yields are isolated and the average of two runs.

We sought to demonstrate the utility of this dehydrogenative coupling in the synthesis of a BN isostere of a biologically active molecule. We identified 4-methoxy-*trans*-stilbene as a suitable biologically active structure¹⁴⁰ to incorporate the azaborine motif in order to demonstrate BN/CC isosterism because it was found to be active in two separate screenings by two separate groups for two separate biological assays. Treatment of the parent 1,2-azaborine **2.110** with *para*-methoxystyrene under the optimized conditions results in the formation of the BN stilbene **2.111** in 82% isolated yield as a crystalline solid (Scheme 2.33). Thus, the reaction conditions are compatible with the protic N–H functional group in **2.110**.

In order to probe the viability of this compound for biological studies, we performed oxygen and water stability studies as we have previously established.¹⁴¹ BN stilbene **2.111** showed <5% decomposition under an oxygen atmosphere in C₆D₆ at 50 °C for 4 hours or at room temperature under ambient atmosphere for 16 hours. The compound was also stable with <5% decomposition to 8.5 equivalents of water in DMSO-d₆ at room temperature for 2 hours; then 50 °C for 2 hours.

Scheme 2.33 Synthesis of *N*–H BN-stilbene **2.111** from **2.110**



¹⁴⁰ (a) Roman, B. I.; De Coen, L. M.; Thérèse F C Mortier, S.; De Ryck, T.; Vanhoecke, B. W.; Katritzky, A. R.; Bracke, M. E.; Stevens, C. V. *Bioorg. Med. Chem.* **2013**, *21*, 5054-5063. (b) Martí-Centelles, R.; Cejudo-Marín, R.; Falomir, E.; Murga, J.; Carda, M.; Marco, J. A. *Bioorg. Med. Chem.* **2013**, *21*, 3010-3015.

¹⁴¹ As monitored against hexamethylbenzene as an internal NMR standard: Lamm, A. N.; Liu, S.-Y. *Mol. Biosyst.* **2009**, *5*, 1303-1305.

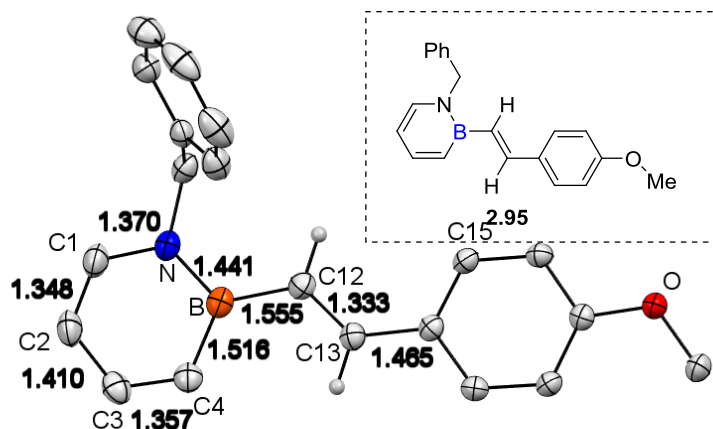


Figure 2.2: ORTEP illustration, with thermal ellipsoids drawn at the 35% probability level, of BN-stilbene **2.95** and selected bond distances. All hydrogens except for the alkenyl hydrogens attached to C12 and C13 have been omitted for clarity.

We were able to isolate only the *trans*- BN stilbene isomers among possible reaction products under our optimized conditions (e.g., *B*-alkyl species and *cis*- BN stilbene isomers). Single crystal X-ray diffraction analysis unambiguously confirms our structural assignment for **2.95** as the *trans*-isomer (Figure 2.2). The molecule adopts a relatively planar structure in the solid state. The \angle N-B-C12-C13 and \angle C12-C13-C14-C15 dihedral angles are $170.4(1)^\circ$ and $2.3(2)^\circ$, respectively. The heterocyclic intra-ring distances are similar to a typical 1,2-azaborine motif.¹⁴² The C12–C13 distance of $1.333(2)$ Å is also consistent with distances normally observed in stilbenes.¹⁴³ On the

¹⁴² For a structural study of 1,2-azaborines, see: Abbey, E. R.; Zakharov, L. N.; Liu, S. -Y. *J. Am. Chem. Soc.* **2008**, *130*, 7250-7252.

¹⁴³ Bis(*p*-methoxy)-*trans*-stilbene has a CC–double bond length of 1.32 Å: Theocharis, C. R.; Jones, W.; Rao, C. N. R. *J. Chem. Soc., Chem. Commun.* **1984**, 1291-1293.

other hand, the B–C12 distance of 1.555(2) Å is significantly longer than a typical arene C(sp²)–alkene C(sp²) single bond distance of ~1.47 Å.¹⁴⁴

We then investigated the impact of BN/CC isosterism on the photophysical properties of stilbene derivatives. We chose a representative set of BN stilbenes containing an electron-withdrawing (**2.107**, (–CF₃) black in Figure 2.3), electron-neutral (**2.102**, (–H) green in Figure 2), and electron-rich (**2.95**, (–OMe) blue in Figure 2.3) arene for direct comparison with the corresponding carbonaceous stilbene analogues (**2.112** (–CF₃, pink), **2.113** (–H, orange), **2.114** (–OMe, red)).

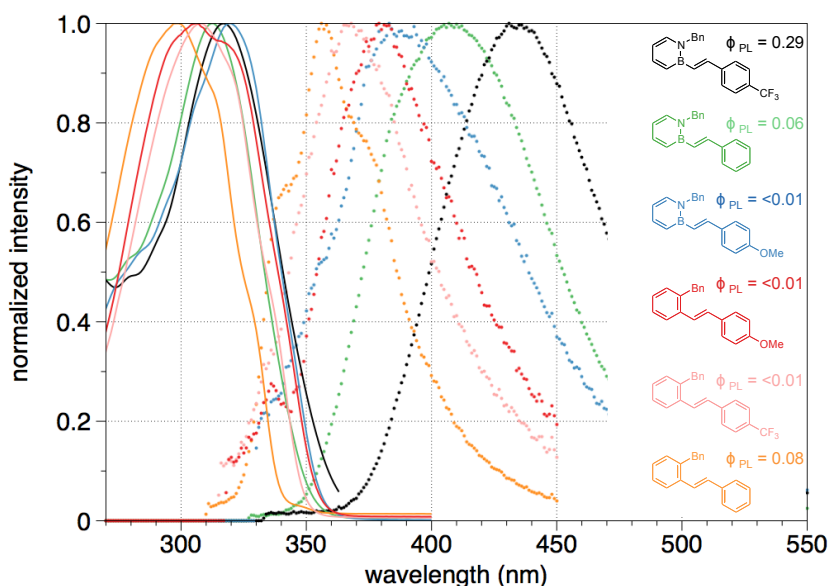


Figure 2.3: Normalized absorption and emission spectra (in MeCN) of select BN stilbenes in direct comparison with their corresponding carbonaceous counterparts. Quantum yields were determined in EtOH at room temperature in comparison to diphenylanthracene and anthracene as standards.

As can be seen from Figure 2.3, BN-stilbenes exhibit a bathochromic shift in both the absorption and emission spectra. The substituent effect is more pronounced in the emission relative to the absorption. In particular, the effect of the substituents on the

¹⁴⁴ This observation is consistent with the larger covalent radius of boron (0.85 Å) vs. carbon (0.75 Å), see: Pyykkö, P.; Atsumi, M. *Chem. Eur. J.* **2009**, *15*, 12770-12779.

emission peak is significantly stronger in BN stilbenes (**2.95**(λ_{em}): 390 nm; **2.107**(λ_{em}): 431 nm; Δ : 2439 cm^{-1}) than in all-carbon series **2.113**(λ_{em}): 357 nm; **2.114**(λ_{em}): 380 nm; Δ : 1695 cm^{-1}). The photophysical properties of BN stilbene **2.107** ($-\text{CF}_3$, black trace) is particularly intriguing. Compound **2.107** exhibits a large Stokes shift (8340 cm^{-1}) and the highest quantum yield (Φ_{PL} : 0.29) among the stilbene compounds that we have investigated.

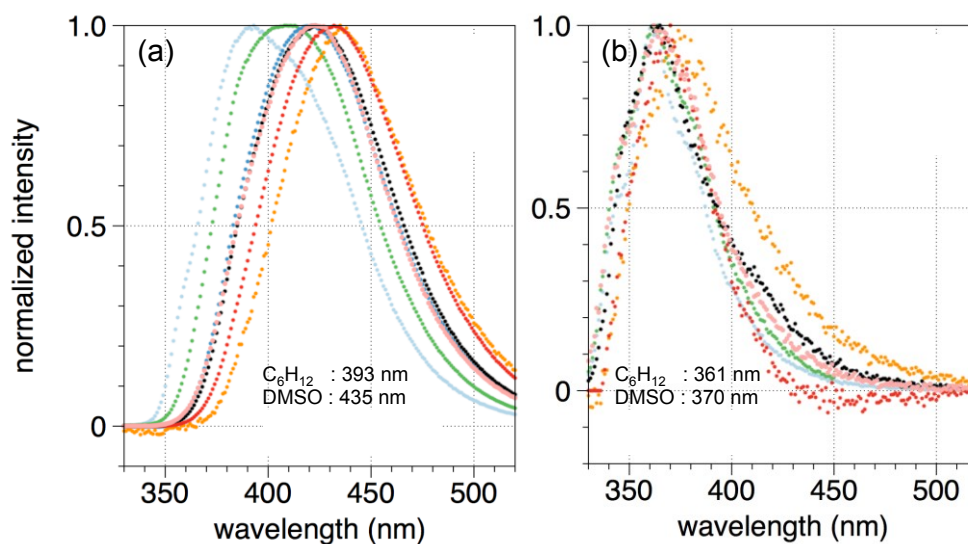


Figure 2.4: Normalized emission spectra of (a) BN stilbene **2.107** and (b) carbonaceous analogue **2.112** in various solvents (orange:DMSO, red:MeCN, black: CH_2Cl_2 , pink: EtOH, blue: THF, green: Et_2O , pale blue: cyclohexane). All measurements were taken at $1 \times 10^{-5}\text{M}$.

We performed emission solvatochromism studies on BN stilbene **2.107** and its carbonaceous analogue **2.112** to elucidate the nature of the excited state. Figure 2.4 illustrates a significant positive solvatochromism on the emission maxima of BN stilbene **2.107** (a red shift of 2457 cm^{-1} going from cyclohexane (λ_{em} : 393 nm) to DMSO (λ_{em} : 435 nm)) as compared to the carbonaceous stilbene **2.112** (a red shift of 674 cm^{-1} from

cyclohexane to DMSO).²⁹ The results of the solvatochromic study are consistent with a stronger charge transfer character of the excited state for **2.107** than for **2.112**, which also presumably involves a larger structural reorganization from ground state leading to the large observed Stokes shift for **2.107**. We observed little perturbation of the absorbance λ_{\max} in relation to solvent polarity. The relatively high photoluminescence quantum yield for BN-stilbene **2.107** may be due to destabilization of biradical states relative to the charge-transfer state.¹⁴⁵ The charge-transfer state is still active towards radiative decay while the biradical states are associated with nonradiative decay pathways. If the biradical states are higher in energy, the relative increased population of the charge-transfer state will result in a higher quantum yield. TD-DFT calculations performed in collaboration with Professor David Dixon at The University of Alabama for compound **2.107** reveal that the HOMO-LUMO transition is the predominant one with an oscillator strength of 0.57.¹⁴⁶

Figure 2.5 shows that the *N*-benzyl group does not significantly interact with either the HOMO or LUMO. The HOMO-LUMO diagrams are also consistent with **2.107** exhibiting a stronger charge transfer character than the carbonaceous **2.112** through a larger electron shift from the azaborine ring to the $-\text{CF}_3$ aryl than the phenyl in **2.112**. Thus, our studies suggest that BN/CC isosterism in the context of stilbenes can promote charge transfer transitions in which the 1,2-azaborine heterocycle can be considered a better electron donor than the corresponding phenyl ring.

¹⁴⁵ Biradical states include singlet phantom state, triplet excited state, and triplet phantom state. Lewis, F. D.; Weigel, W. *J. Phys. Chem. A*. **2000**, *104*, 8146-8153.

¹⁴⁶ Hilborn, R. C. *Am. J. Phys.* **1982**, *50*, 982-986.

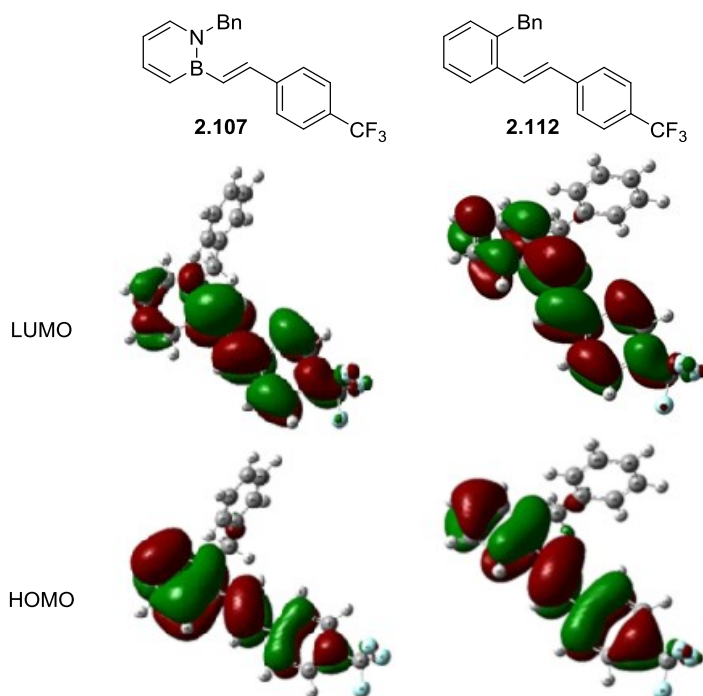


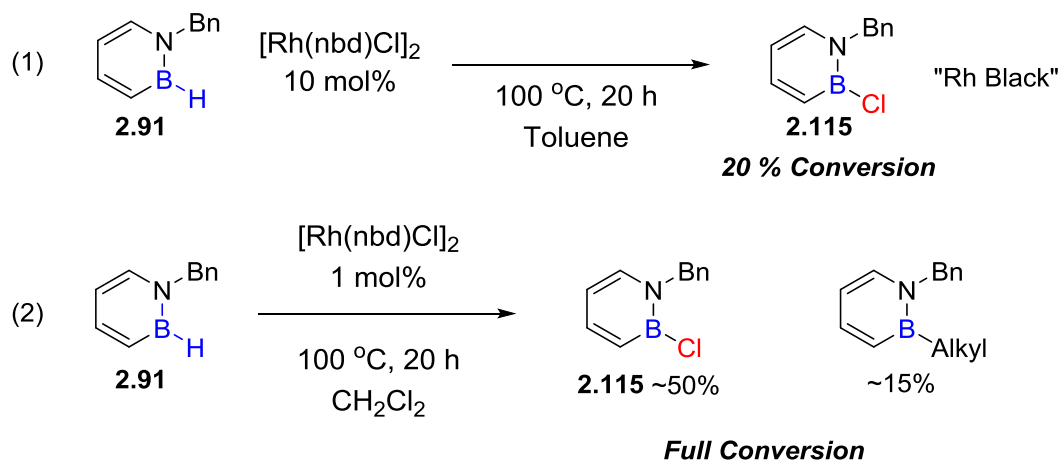
Figure 2.5. HOMO and LUMO (B3LYP Kohn-Sham orbitals) of **2.107** and **2.112**.

2.4 Development of a novel catalytic *B*-H to *B*-Cl with an alkyl chloride as the chloride source.

During the course of our studies of the dehydrogenative borylation of 1,2-azaborines, we were able to observe a stoichiometric reaction between the $[\text{Rh}(\text{nbd})\text{Cl}]_2$ catalyst and *B*-H azaborine **2.91** to generate *B*-Cl **2.115** (Scheme 2.34, Eq. 1). More interestingly, we were also able to observe *catalytic* formation of **2.115** when the reaction was performed in methylene chloride (Scheme 2.34, Eq. 2). We also observed the production of a new *B*-alkyl product which did not contain any signals consistent with incorporation of a norbornane fragment, likely resulting from the *C*-Cl activation of

methylene chloride. Rhodium-catalyzed methylene chloride or chloroform activation is not uncommon, but generally requires an electron-rich ligand system.¹⁴⁷

Scheme 2.34 Initial observations regarding the B–H to B–Cl conversion

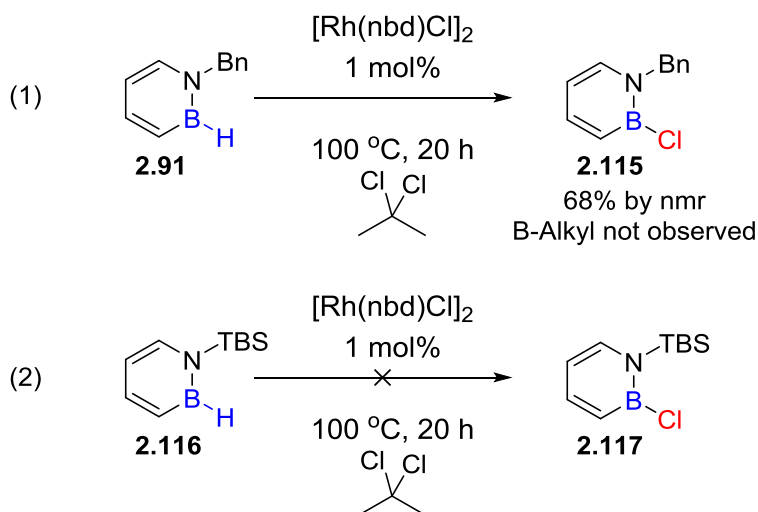


In an attempt to improve this reaction, we initially screened different chloride sources as additives. Unfortunately, the yield of **2.115** was not affected in an appreciable amount in relation to the additive-free reaction with ammonium chloride, sodium chloride, calcium chloride, lithium chloride or hydrochloric acid. Other additives such as cadmium chloride, zinc chloride, trimethylamine, N-chlorosuccinimide, or phenylacetylene gave intractable mixtures of products.

¹⁴⁷ (a) Burns, E. G.; Chu, S. S. C.; De Meester, P.; Lattman, M. *Organometallics* **1986**, *5*, 2383-2384. (b) Nishiyama, H.; Horihata, M.; Hirai, T.; Wakamatsu, S.; Itoh, K. *Organometallics* **1991**, *10*, 2706-2708. (c) Ball, G. E.; Cullen, W. R.; Fryzuk, M. D.; James, B. R.; Rettig, S. J. *Organometallics* **1991**, *10*, 3767-3769. (d) Haarman, H. F.; Ernsting, J. M.; Kranenburg, M.; Kooijman, H.; Veldman, N.; Spek, A. L.; van Leeuwen, P. W. N. M.; Vrieze, K. *Organometallics* **1997**, *16*, 887-900. (e) Bradd, K. J.; Heaton, B. T.; Jacob, C.; Sampanthar, J. T.; Steiner, A. *J. Chem. Soc., Dalton Trans.* **1999**, No. 7, 1109-1112. (f) Tejel, C.; Ciriano, M. A.; Oro, L. A.; Tiripicchio, A.; Ugozzoli, F. *Organometallics* **2001**, *20*, 1676-1682. (g) Dorta, R.; Shimon, L. J. W.; Rozenberg, H.; Milstein, D. *Eur. J. Inorg. Chem.* **2002**, *2002*, 1827-1834. (h) Chan, K. T. K.; Spencer, L. P.; Masuda, J. D.; McCahill, J. S. J.; Wei, P.; Stephan, D. W. *Organometallics* **2004**, *23*, 381-390. (i) Zeng, J. Y.; Hsieh, M.-H.; Lee, H. M. *J. Organomet. Chem.* **2005**, *690*, 5662-5671. (j) Tejel, C.; Ciriano, M. A.; López, J. A.; Jiménez, S.; Bordonaba, M.; Oro, L. A. *Chem. Eur. J.* **2007**, *13*, 2044-2053. (k) Blank, B.; Glatz, G.; Kempe, R. *Chem. Asian J.* **2009**, *4*, 321-327. (l) Vetter, A. J.; Rieth, R. D.; Brennessel, W. W.; Jones, W. D. *J. Am. Chem. Soc.* **2009**, *131*, 10742-10752. (m) Ho, H.-A.; Dunne, J. F.; Ellern, A.; Sadow, A. D. *Organometallics* **2010**, *29*, 4105-4114.

The initial results of adding Cl⁻ sources were not particularly positive and were still accompanied by the formation of unidentified *B*-alkyl species, so we looked at 2,2-dichloropropane as an alternative solvent to methylene chloride for the synthesis of **2.115**. 2,2-dichloropropane was a successful chloride source, generating **2.115** in 69% ¹H NMR yield, and avoided the formation of *B*-alkyl species (Scheme 2.35 Eq. 1). Unfortunately, this reaction was prone to the formation of heterogeneous metal species and, under identical conditions, was not suitable for the transformation of *N*-TBS *B*-H azaborine **2.116** to the *B*-Cl containing **2.117** (Scheme 2.35 Eq. 2).

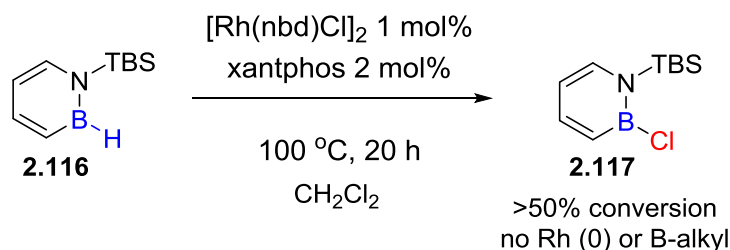
Scheme 2.35: Identical conditions did not generate 2.117 from 2.116



We sought to develop a system which would: 1) convert **2.116** to **2.117**, 2) avoid the production of Rh(0) species, and 3) be amenable to the use of stoichiometric chloride source rather than a large excess. In order to probe the feasibility of this reaction with compound **2.116**, we screened a small number of stabilizing phosphines for the reaction

in CH₂Cl₂.¹⁴⁸ Fortuitously xantphos generated the desired product with >50% conversion and no sign of Rh(0) byproducts (Scheme 2.36, all other phosphines screened were inactive under the reaction conditions).

Scheme 2.36: Initial hit for the generation of 2.117



We determined that the reaction took place with 1.1 equiv. of methylene chloride in deuterated benzene sealed at 110 °C in 19% yield (Table 2.2, entry 1). We then systematically studied the effect of inclusion of additional alkyl, aryl, -H, and -Cl groups to the -CCl₂- fragment. The replacement of a C-H bond with a C-Cl bond in chloroform gave a similarly low yield of 11% (Table 2.2, entry 2). Carbon tetrachloride, however, showed a significant increase in yield to 33% compared to methylene chloride (Table 2.2, entry 3). An increase in the steric bulk in 2,2-dichloropropane and 2,2-dichlorobutane gave moderate yields of 63% and 59% respectively (Table 2.2, entries 4 and 5). Primary-chloride containing 1,2-dichloroethane gave a low 24% yield (Table 2.2, entry 7). Both 1-chloropentane and α -chlorotoluene gave <10% yields, and were accompanied by insoluble side products (Table 2.4, entries 6 and 8). Benzal chloride gave a 41% yield (Table 2.2, entry 9) while benzotrichloride gave a higher yield of 53% (Table 2.2, entry

¹⁴⁸ Phosphines screened include: biphep, xantphos, PCy₃, and P^tBu₃.

10). Benzhydryl chloride generated **2.117** in 64% yield (Table 2.2, entry 11), while α -chloroparaxylene did not show an improvement over α -chlorotoluene (Table 2.2, entry 12). (1-Chloroethyl)Benzene was highly successful, giving a 92% yield after 20 hours, or a 96% yield after 1 hour (Table 2.2, entry 13). 1 equivalent of ethylbenzene was also cleanly produced during this reaction from the reduction of the C–Cl bond.

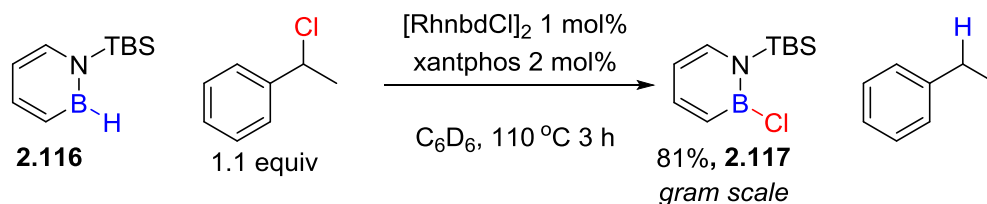
Table 2.2: Optimization of B–H to B–Cl reaction

Entry	Chloride Source	% Yield ^a	Entry	Chloride Source	% Yield ^a
1		19	8		9
2		11	9		41
3		33	10		53
4		63	11		64
5		59	12		10
6		24	13		92, 96 ^b
7		6			

^a ¹H NMR yield determined versus hexamethylbenzene as internal standard, average of two runs. ^b Yield at 1 hour.

With optimized conditions in hand, we demonstrated that this reaction can be carried out on gram scale with an 81% yield after distillation (Scheme 2.37).

Scheme 2.35: Gram-scale synthesis of 2.117



We were interested in expanding this optimized reaction to include C(3) substitution, however all attempts at performing the B-H to B-Cl with a C(3) substituted azaborine returned starting material. We were also curious if this methodology could be applied to other, nonaromatic boranes such as 9-BBN or pinacolborane. In order to probe this possibility, we submitted both 9-BBN (Figure 2.6) and pinacolborane (Figure 2.7) to our reaction conditions at a reduced temperature of 50 °C. Gratifyingly, ^{11}B NMR analysis of both reaction mixtures was consistent with a complete B-H to B-Cl conversion. 9-BBN dimer ($\delta_{11\text{B}}=27.8$) was converted to a new species consistent with 9-BBN-Cl ($\delta_{11\text{B}}=80.6^{149}$) over the course of 5 hours. There was also a small indication of the minor formation of an unknown BR_3 ($\delta_{11\text{B}}=88.2$) species. When pinacolborane ($\delta_{11\text{B}}=28.1$ (d, $J_{\text{BH}}=175.2$)) was subjected to our reaction conditions a fast conversion to a single species consistent with ClBpin ($\delta_{11\text{B}}=27.8^{150}$) was observed. In order to rule out a possible B_2pin_2 side product, we spiked the mixture with a known sample of B_2pin_2 , and

¹⁴⁹ Brown, H. C.; Soderquist, J. A. *J. Org. Chem.* **1980**, *45*, 846-849.

¹⁵⁰ Bettinger, H. F.; Filthaus, M.; Bornemann, H.; Oppel, I. M. *Angew. Chem. Int. Ed.* **2008**, *47*, 4744-4747.

were able to observe the expected ^{11}B resonance ($\delta_{11\text{B}}=30.9$). Upon treatment with excess water at room temperature the ClBpin converted entirely to a $\text{B}(\text{OR})_3$ species ($\delta_{11\text{B}}=19.4$). ^1H NMR was consistent with a single ClBpin species as well. Despite numerous attempts we were unable to obtain a mass spectrum of the ClBpin, observing only the $\text{B}(\text{OR})_3$ species. It is likely that derivitization of the $\text{B}-\text{Cl}$ will be necessary in order to demonstrate the applicability of this reaction.

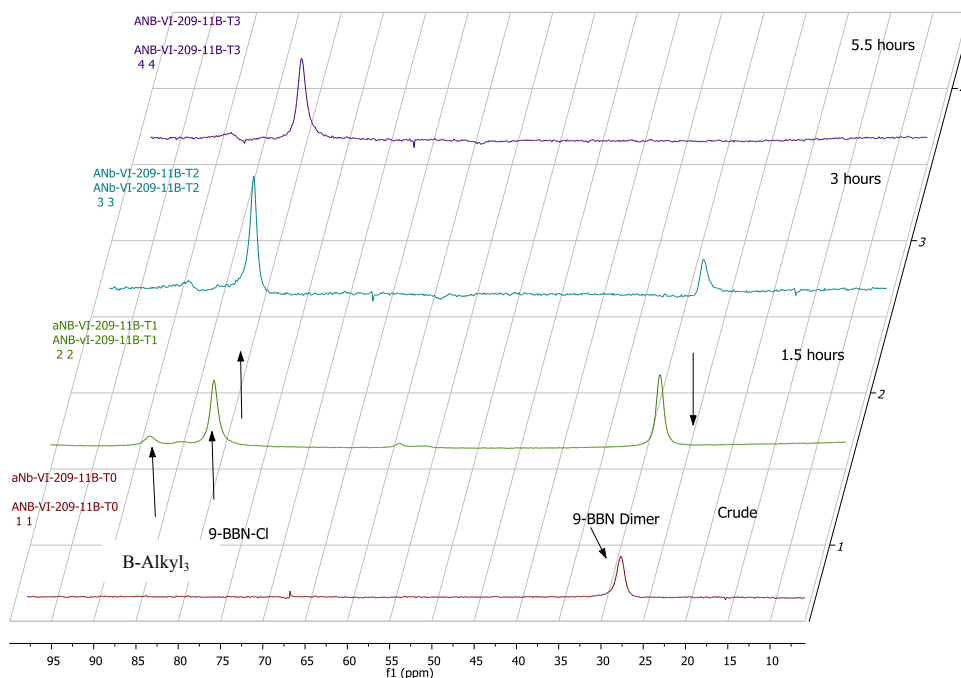
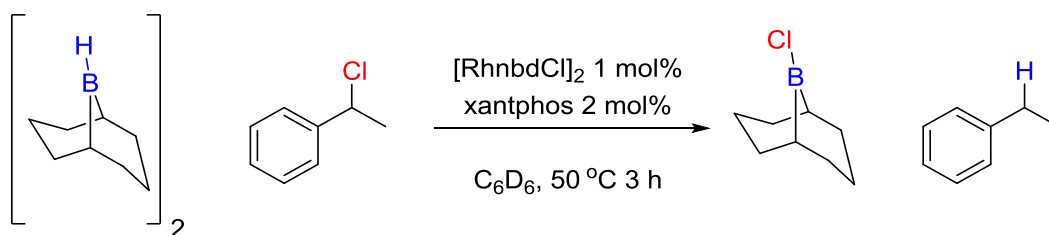


Figure 2.6: ^{11}B NMR indication of 9-BBN-Cl formation

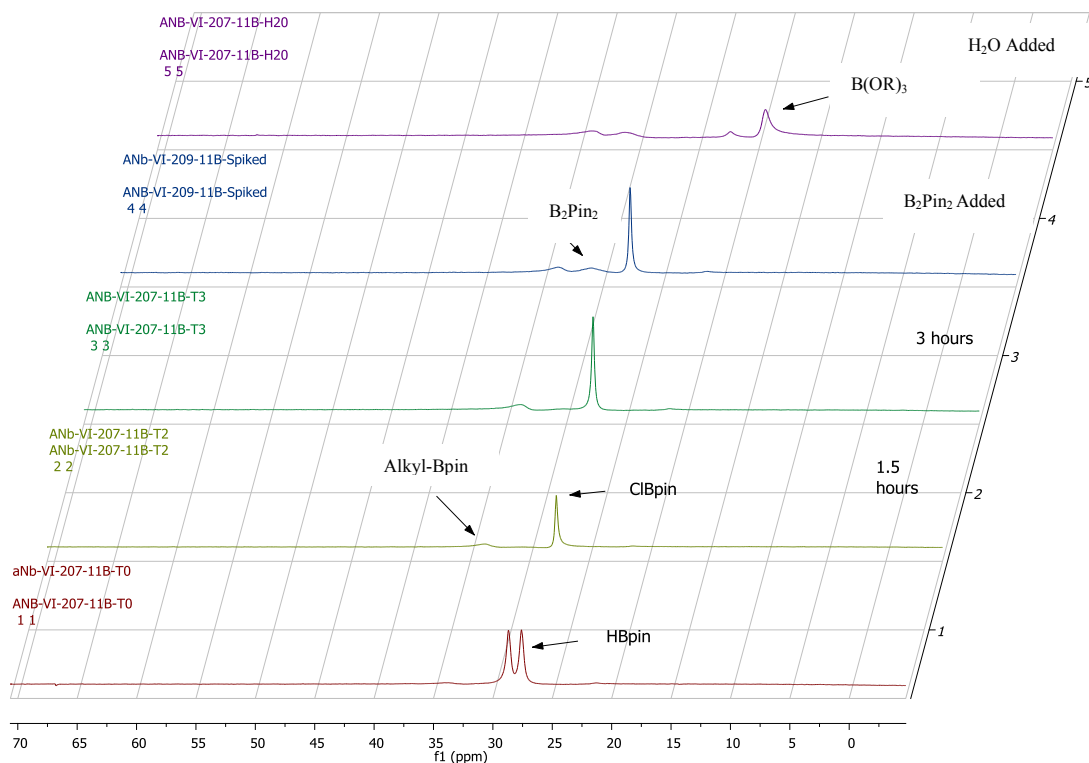
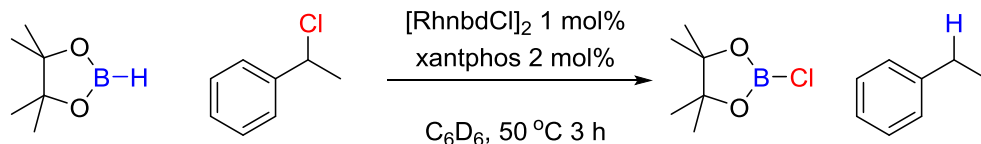


Figure 2.7: ¹¹B NMR indication of ClBpin formation

2.4 Summary and Conclusions

We have demonstrated two methods for the metal-catalyzed *B*-H activation of 1,2-azaborines including a dehydrogenative borylation of styrenes to selectively generate new BN-stilbenes and a novel *B*-H to *B*-Cl transformation. We have investigated the optical properties of select BN-stilbenes and compared them to their carbonaceous counterparts. In the case of the BN-stilbenes, the azaborine ring is acting as a stronger electron donor than phenyl, leading to an increased charge-transfer character of the

excitation of BN-stilbenes compared their carbon isosteres, resulting in a larger Stoke's shift and solvatachromic effects for electron withdrawing substituents than electron donating substituents.

We have observed a novel rhodium/xantphos catalyzed $B-H$ to $B-Cl$ conversion using an alkyl chloride as the chloride source and found that (1-chloroethyl)benzene is the optimal chloride source. We have demonstrated the use of this methodology on gram scale as well as preliminarily observed the $B-H$ to $B-Cl$ with other dialkyl and dialkoxy $B-H$ systems.

The $B-H$ bond of 1,2-azaborines can undergo traditional $B-H$ activation as well as act as a model $B-H$ for discovery of new transformations. In this sense, the stability and nonreactivity of the 1,2-azaborine to traditional uncatalyzed $B-H$ reactions can allow for the development and design of new catalytic reactions and functional group transformations beyond the narrow scope of 1,2-azaborine chemistry.

While the mechanism for the $B-H$ to $B-Cl$ transformation is unknown, we hypothesize that a transmetallation from the $Rh-Cl$ starting material to generate an equivalent of the $B-Cl$ product is taking place following the dehydrogenative borylation mechanism proposed by Brown and Lloyd-Jones. The resulting $Rh-H$ could reduce the alkyl chloride by 1) oxidative addition/reductive elimination pathway to regenerate the $Rh-Cl$, or alternatively 2) the $R-Cl$ bond could homolytically cleave, generating an $R\cdot$ which could abstract a $H\cdot$ from the $Rh-H$ species generating a $Rh\cdot$ which could combine with the $Cl\cdot$ to regenerate the active $Rh-Cl$ species. Further mechanistic study is required to elucidate the most likely scenario.

2.5 Experimental Section

2.5.1 General Information

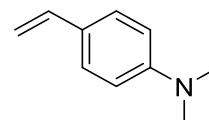
All oxygen- and moisture-sensitive manipulations were carried out under an inert atmosphere (N_2) using either standard Schlenk techniques or a glove box. THF, Et_2O , CH_2Cl_2 , toluene, and pentane were purified by passing through a neutral alumina column under argon. C_6D_6 was dried and distilled over sodium/benzophenone, 4-dimethylamino styrene was prepared via a Wittig olefination of 4-dimethylamino benzaldehyde and distilled before use,¹⁵¹ alkyl chlorides were distilled and were passed through a dry neutral alumina column immediately before use. All other chemicals were purchased (Aldrich or TCI) and used as received. All styrenes were run through a dry neutral alumina column immediately before use. Silica and alumina were dried overnight at 120 °C under high vacuum. ^{11}B NMR spectra were recorded on a Varian Unity/Inova 300 spectrometer at ambient temperature. 1H NMR spectra were recorded on a Varian Unity/Inova 300 or Varian Unity/Inova 600 spectrometer. ^{13}C NMR spectra were recorded on a Varian Unity/Inova 500 spectrometer or Varian Unity/Inova 600 spectrometer. NMR spectra for compound **2.111** were collected on either a Varian Inova 500 or a Varian INOVA 500 spectrometer. ^{11}B NMR spectra were externally referenced to $BF_3 \cdot Et_2O$ (δ 0). Fluorescence emission spectra were collected on a Jobin Yvon Horiba Fluoromax 4 spectrometer in dry degassed acetonitrile or ethanol. Photoluminescence quantum yields were calculated using anthracene and 9,10-diphenylanthracene standards

¹⁵¹ Frstrup, P.; Le Quement, S.; Tanner, D.; Norrby, P.-O. *Organometallics* **2004**, *23*, 6160- 6165.

by standard procedures.¹⁵² UV-Vis spectra were collected on an Agilent 8453 spectrophotometer with ChemStation software. Extinction coefficients were calculated by finding the slope of the absorbance plot at different known concentrations using the Beer-Lambert Law. HPLC measurements were taken using an Agilent 1100 system equipped with a G1315B DAD detector at 254 nm with reference wavelength at 420 nm, an inline G1379A degasser, and an Econosil semi-prep 250 by 10 mm silica normal-phase column (catalog 6233) at 3 mL/min with 99:1 hexanes:THF as eluent. High-resolution mass spectroscopy data were obtained at the Mass Spectroscopy Facilities and Services Core of the Environmental Health Sciences Center at Oregon State University. High resolution mass spectroscopy for compound **2.111** was carried out on a JEOL AccuTOF instrument (JEOL USA, Peabody, MA), equipped with a DART ion source (IonSense, Inc., Danvers, MA) in positive ion mode.

2.5.2 Procedure for the preparation of 4-dimethylamino styrene [2039-80-7]:¹⁵³

n-butyl lithium (12.8 mL, 32.0 mmol, 2.5 M in THF) was added dropwise to a solution of methyltriphenylphosphonium bromide (9.5 g, 27 mmol) in THF (65 mL). The red solution was allowed to stir until fully dissolved before addition of the aldehyde (4.0 g, 27 mmol in 24 mL THF), upon which, the mixture turned white or pale yellow. After 4 h stirring at room temperature, the THF was removed under reduced pressure, replaced with ether and the solution was passed through a short silica gel plug (the material is not very stable on



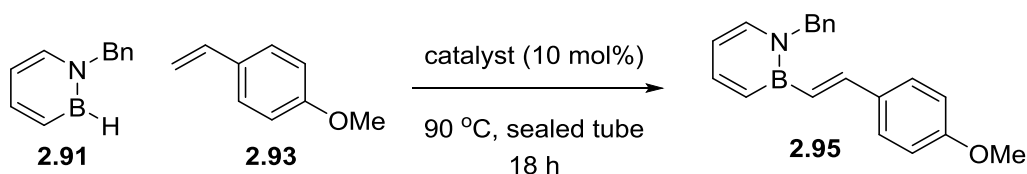
¹⁵² Jobin Yvon Ltd. *A Guide to Recording Fluorescence Quantum Yields* (accessed March 2014). <http://www.horiba.com/fileadmin/uploads/Scientific/Documents/Fluorescence/quantumyieldstrad.pdf>

¹⁵³ Fristrup, P.; Le Quement, S.; Tanner, D.; Norrby, P.-O. *Organometallics* **2004**, *23*, 6160- 6165.

silica gel). The solvent was removed and the mixture was distilled in a short-path distillation apparatus under reduced pressure over CaH₂ (bp: 62-65 °C at 300 mTorr) yielding a clear colorless oil (3.0 g, 76% yield). This material was passed through a plug of dry neutral alumina immediately before use (leaving a yellow impurity at the baseline). Spectra matched those previously reported after distillation.

¹H NMR (300 MHz, CDCl₃): 7.36 (d, ³J_{HH} = 7 Hz, 2H) 6.6-6.71 (m, 3H), 5.60 (d, ³J_{HH} = 17.6 Hz, 1H), 5.08 (d, ³J_{HH} = 10.9 Hz, 1H), 2.99 (s, 6H).

2.5.3 Catalyst Survey (Table 2.1)



General Procedure: In a glove box under a nitrogen atmosphere, *N*-Bn-*BH*-azaborine **2.91** (25 mg, 0.15 mmol) was added to an 8 mL pressure tube containing 0.1 equivalent (0.015 mmol) of appropriate catalyst. To this mixture was added 2.1 equiv. (43 mg, 0.31 mmol) of *p*-methoxy styrene **2.93**, and the system was charged with 2.0 mL of appropriate solvent. The reaction tube was sealed and allowed to react for 18 hours at 90 °C. Upon completion, a known amount of hexaethylbenzene was added as an internal standard to the reaction mixture and mixed thoroughly. An aliquot from this mixture was prepared for HPLC analysis, and yields were calculated based upon response curves from known concentrations of product versus internal standard.

Entry 1: The general procedure was followed, using Wilkinson's catalyst, $\text{RhCl}(\text{PPh}_3)_3$ (14 mg, 0.015 mmol) with 2.0 mL of THF as solvent. HPLC analysis indicated 15% product formation (average of two runs, 1st run: 14%, 2nd run: 15%).

Entry 2: The general procedure was followed, using $\text{RhH}(\text{CO})(\text{PPh}_3)_3$ (14 mg, 0.015 mmol) with 2.0 mL of THF as solvent. HPLC analysis indicated no product formation (average of two runs).

Entry 3: The general procedure was followed, using $[\text{Rh}(\text{dppb})(\text{cod})]^+\text{BF}_4^-$ (11 mg, 0.015 mmol) with 2.0 mL of THF as solvent. HPLC analysis indicated no product formation (average of two runs).

Entry 4: The general procedure was followed, using Crabtree's catalyst, $[\text{Ir}(\text{cod})(\text{Py})(\text{PCy}_3)]\text{PF}_6$ (11 mg, 0.015 mmol) with 2.0 mL of THF as solvent. HPLC analysis indicated 51% product formation (average of two runs, 1st run: 52%, 2nd run: 51%).

Entry 5: The general procedure was followed, using $[\text{Rh}(\text{cod})_2]^+\text{BF}_4^-$ (3.0 mg, 0.015 mmol) with 2.0 mL of THF as solvent. HPLC analysis indicated 64% product formation (average of two runs, 1st run: 66%, 2nd run: 62%).

Entry 6: The general procedure was followed, using $[\text{Rh}(\text{nbd})\text{Cl}]_2$ (3.4 mg, 0.015 mmol) with 2.0 mL of THF as solvent. HPLC analysis indicated 80% product formation (average of two runs, 1st run: 85%, 2nd run: 75%).

Entry 7: The general procedure was followed, using $[\text{Rh}(\text{cod})_2]^+\text{BF}_4^-$ (3.0 mg, 0.015 mmol) with 2.0 mL of toluene as solvent. HPLC analysis indicated 60% product formation (average of two runs, 1st run: 64%, 2nd run: 56%).

Entry 8: The general procedure was followed, using $[\text{Rh}(\text{cod})_2]^+\text{BF}_4^-$ (3.0 mg, 0.015 mmol) with 2.0 mL of acetonitrile as solvent. HPLC analysis indicated 23% product formation (average of two runs, 1st run: 24%, 2nd run: 22%).

Entry 9: The general procedure was followed, using $[\text{Rh}(\text{cod})_2]^+\text{BF}_4^-$ (3.0 mg, 0.015 mmol) with 2.0 mL of methylene chloride as solvent. HPLC analysis indicated 75% product formation (average of two runs, 1st run: 79%, 2nd run: 71%).

Entry 10: The general procedure was followed, using $[\text{Rh}(\text{nbd})\text{Cl}]_2$ (3.4 mg, 0.015 mmol) with 2.0 mL of toluene as solvent. HPLC analysis indicated 94% product formation (average of two runs, 1st run: 94%, 2nd run: 94%).

Entry 11: The general procedure was followed, using $[\text{Rh}(\text{nbd})\text{Cl}]_2$ (3.4 mg, 0.015 mmol) with 2.0 mL of acetonitrile as solvent. HPLC analysis indicated 52% product formation (average of two runs, 1st run: 48%, 2nd run: 56%).

Entry 12: The general procedure was followed, using $[\text{Rh}(\text{nbd})\text{Cl}]_2$ (3.4 mg, 0.015 mmol) with 2.0 mL of methylene chloride as solvent. HPLC analysis indicated 98% product formation (average of two runs, 1st run: 96%, 2nd run: 99%).

Entry 13: See Synthesis of compound **2.95**.

2.5.4 Preparation of compounds 2.95-2.111 (Scheme 2.32)

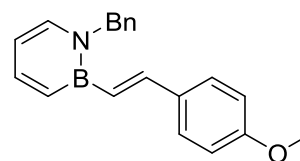


General procedure: In a glove box under a nitrogen atmosphere a pressure tube was charged with **2.91** (50.0 mg, 0.296 mmol), $[\text{Rh}(\text{nbd})\text{Cl}]_2$ (1.7 mg, 0.0074 mmol), 2.1

equiv. of appropriate styrene, and 2.5 mL of methylene chloride. The sealed reaction vessel was then placed in a 90 °C oil bath for 20 hours. At the conclusion of the reaction, the solvent was removed under reduced pressure, and the desired BN stilbene product was isolated by column chromatography under inert atmosphere as a white crystalline solid (eluent: Et₂O/pentane).

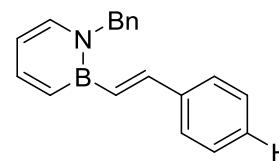
Compound 2.95, *p*-OMe:

The general procedure was followed using 4-vinylanisole (90.0 mg, 0.620 mmol), column eluent 10:90 Et₂O:pentane (86% average yield of two runs (76.4 mg, 86% and 75.5 mg 85%)). ¹H NMR (600 MHz, CD₂Cl₂): δ 7.60-7.62 (m, 1H), 7.39 (d, ³J_{HH} = 18 Hz, 1H), 7.32 (app t, ³J_{HH} = 7.8 Hz, 2H), 7.25 (t, ³J_{HH} = 7.2 Hz, 1H), 7.18-7.20 (m, 5H), 7.11 (d, ³J_{HH} = 10.8 Hz, 1H), 6.87 (d, ³J_{HH} = 9 Hz, 2H), 6.76 (d, ³J_{HH} = 18 Hz, 1H), 6.25 (td, ³J_{HH} = 7.8 Hz, 1.2 Hz, 1H), 5.13 (s, 2H), 3.80 (s, 3H). ¹¹B NMR (96 MHz, CD₂Cl₂) δ 33.8 (s). ¹³C NMR (150 MHz, CD₂Cl₂): δ 160.3, 144.8, 142.9, 140.3, 139.8, 132.2, 129.2 (2C), 128.5, 127.8, 127.4, 125.2 (br), 114.5, 111.5, 57.4, 55.8. UV/Vis: (Acetonitrile) λ_{max} = 320 nm, ε = 27040 M⁻¹ cm⁻¹. HRMS (EI) calcd for C₂₀H₂₀BNO (M⁺): 301.16380; found: 301.16476.



Compound 2.102, *p*-H:

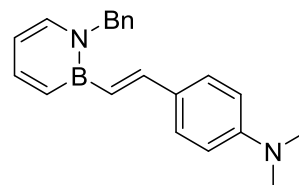
The general procedure was followed using styrene (65.0 mg, 0.620 mmol), column eluent 3:97 Et₂O:pentane (77% average yield of two runs (58.5 mg, 73% and 65.0 mg 81%)). ¹H NMR (300 MHz, CD₂Cl₂): δ 7.66-7.72 (m, 1H), 7.19-7.40 (m, 13H), 6.99 (d, 18.1 Hz, 1H), 6.36 (td, ³J_{HH} = 6.7 Hz, 1.5 Hz, 1H), 5.18 (s, 2H). ¹¹B NMR (96 MHz, CD₂Cl₂): δ



33.4 (s). ^{13}C NMR (150 MHz, CD_2Cl_2): δ 57.5, 111.8, 127.2, 127.4, 127.9, 128.5, 129.1, 127.3, 139.4, 139.8, 140.3, 143.2, 145.1. 2 Carbons next to boron were not observed. UV/Vis: (Acetonitrile) $\lambda_{\text{max}} = 313 \text{ nm}$, $\epsilon = 24627 \text{ M}^{-1} \text{ cm}^{-1}$. HRMS (EI+) calcd for $\text{C}_{19}\text{H}_{18}\text{BN}$ (M+): 271.15323; found: 271.15354.

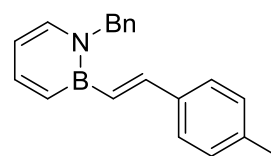
Compound 2.103, *p*-NMe₂:

The general procedure was followed using 4-*N,N*-dimethylamino styrene (93.0 mg, 0.621 mmol), column eluent 10:90–30:70 Et₂O:pentane (56% average yield of two runs (53 mg, 57% and 50 mg, 54%)). ^1H NMR (300 MHz, CD_2Cl_2): δ 7.62-7.64 (m, 1H), 7.11-7.49 (m, 9H), 6.71-6.79 (m, 4H), 6.34 (t, $^3J_{\text{HH}} = 6.6 \text{ Hz}$, 1H), 5.18 (s, 2H), 3.02 (s, 6H). ^{11}B NMR (96 MHz, CD_2Cl_2): δ 33.8 (s). ^{13}C NMR (125 MHz, CD_2Cl_2): δ 151.2, 145.7, 142.6, 140.5, 139.7, 129.2 (2C), 128.4, 127.7, 127.7, 127.4, 122.2 (br), 112.6, 111.1, 57.3, 40.7. UV/Vis: (Acetonitrile) $\lambda_{\text{max}} = 350 \text{ nm}$, $\epsilon = 42776 \text{ M}^{-1} \text{ cm}^{-1}$. HRMS (EI+) calcd for $\text{C}_{21}\text{H}_{24}\text{BN}_2$ (M+): 315.2033; found: 315.2027.



Compound 2.104, *p*-Me:

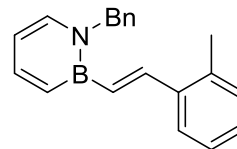
The general procedure was followed using 4-methyl styrene (74.0 mg, 0.619 mmol), column eluent 3:97 Et₂O:pentane (87% average yield of two runs, (71.1 mg, 85% and 73.9 mg, 88%)). ^1H NMR (300 MHz, CD_2Cl_2): δ 7.604-7.663 (m, 1H), 7.01-7.34 (m, 12H), 6.76 (d, $^3J_{\text{HH}} = 17.8 \text{ Hz}$, 1H), 6.20 (td, $^3J_{\text{HH}} = 6.8 \text{ Hz}$, 1.5 Hz, 1H), 5.02 (s, 2H), 2.23 (s, 3H). ^{11}B NMR (96 MHz, CD_2Cl_2): δ 33.9 (s). ^{13}C NMR (150 MHz, CD_2Cl_2): δ 144.2, 142.0, 139.3, 138.8, 137.6, 135.7, 128.8, 128.2 (2C), 126.9, 126.4, 126.2, 125 (br), 110.6, 56.5,



20.6. UV/Vis: (Acetonitrile) $\lambda_{\text{max}} = 315 \text{ nm}$, $\epsilon = 24659 \text{ M}^{-1} \text{ cm}^{-1}$. HRMS (EI+) calcd for $\text{C}_{20}\text{H}_{20}\text{BN}$ (M+): 285.16888; found: 285.16952.

Compound 2.105, *o*-Me:

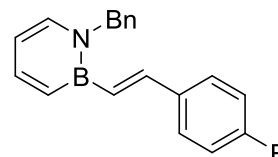
The general procedure was followed using 2-methyl styrene (74.0 mg, 0.619 mmol), column eluent 3:97 Et₂O:pentane (74% average yield of two runs, (60 mg, 71% and 65 mg 77%)). ¹H NMR



(300 MHz, CD₂Cl₂): δ 7.41-7.62 (m, 4H), 7.04-7.30 (m, 9H), 6.74 (d, ³J_{HH} = 18 Hz, 1H), 6.21 (td, ³J_{HH} = 7.2 Hz, 1.5 Hz, 1H) 5.02 (s, 2H), 2.34 (s, 3H). ¹¹B NMR (96 MHz, CD₂Cl₂): δ 33.9 (s). ¹³C NMR (150 MHz, CD₂Cl₂): δ 143.1, 142.8, 140.3, 139.8, 138.6, 136.4, 130.9, 129.2 (2C), 128.3, 127.9, 127.4, 126.6, 125.9, 111.7, 57.5, 20.1. (One C-B not directly visible) UV/Vis: (Acetonitrile) $\lambda_{\text{max}} = 313 \text{ nm}$, $\epsilon = 19625 \text{ M}^{-1} \text{ cm}^{-1}$. HRMS (EI+) calcd for $\text{C}_{20}\text{H}_{20}\text{BN}$ (M+): 285.16888; found: 285.17011.

Compound 2.106, *p*-F:

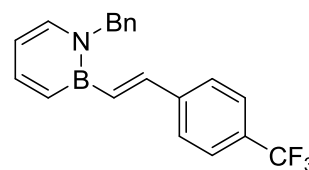
The general procedure was followed using 4-fluoro styrene (76.0 mg, 0.619 mmol), column eluent 3:97 Et₂O:pentane (83% average yield of two runs, (77 mg, 90% and 64 mg, 75%)).



¹H NMR (300 MHz, CD₂Cl₂): δ 7.49-7.55 (m, 4H), 6.88-7.40 (m, 9H), 6.72 (d, ³J_{HH} = 17.8 Hz, 1H), 6.20 (td, ³J_{HH} = 6.4 Hz, 1.8 Hz, 1H), 5.01 (s, 2H). ¹¹B NMR (96 MHz, CD₂Cl₂): δ 33.9 (s). ¹³C NMR (150 MHz, CD₂Cl₂): δ 164.0, 162.3, 143.8, 143.2, 140.2, 139.8, 135.7, 129.2, 128.8, 127.9, 127.3, 116.0, 115.8, 111.8, 57.5, UV/Vis: (Acetonitrile) $\lambda_{\text{max}} = 312 \text{ nm}$, $\epsilon = 88842 \text{ M}^{-1} \text{ cm}^{-1}$. HRMS (EI+) calcd for $\text{C}_{19}\text{H}_{17}\text{BNF}$ (M+): 289.14381; found: 289.14473.

Compound 2.107, *p*-CF₃:

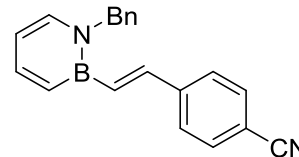
The general procedure was followed using 4-(trifluoromethyl) styrene (107 mg, 0.619 mmol), column eluent 3:97 Et₂O:pentane (76% average yield of two runs, (79.7 mg,



80% and 72.6 mg 73%). ¹H NMR (300 MHz, CD₂Cl₂): δ 7.63-7.76 (m, 5H), 7.50 (d, ³J_{HH} = 18 Hz, 1H), 7.19-7.42 (m, 7H), 7.11 (d, ³J_{HH} = 18.3 Hz, 1H), 6.42 (td, ³J_{HH} = 6.9 Hz, 1.8 Hz, 1H), 5.21 (s, 2H). ¹¹B NMR (96 MHz, CD₂Cl₂): δ 33.6 (s). ¹³C NMR (150 MHz, CD₂Cl₂): δ 142.5, 142.3, 141.9, 139.1, 138.9, 130.0 (br), 128.8 (q, CF₃), 128.3, 127.0, 126.4 (2C) 125.1, 125.0, 124.9, 111.2, 56.6. UV/Vis: (Acetonitrile) λ_{max} = 317 nm, ε = 21291 M⁻¹ cm⁻¹. HRMS (EI+) calcd for C₂₀H₁₇BNF₃ (M⁺): 339.14062; found: 339.14031.

Compound 2.108, *p*-CN:

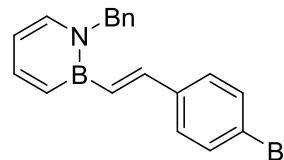
The general procedure was followed using 4-cyano styrene (80.0 mg, 0.619 mmol), column eluent 10:90 Et₂O:pentane (73% average yield of two runs, (69.4 mg, 79%



and 58.7 mg 67%). ¹H NMR (300 MHz, CD₂Cl₂): δ 7.07-7.74 (m, 14H), 6.41 (t, ³J_{HH} = 6.3 Hz, 1H), 5.18 (s, 2H). ¹¹B NMR (96 MHz, CD₂Cl₂): δ 32.2(s). ¹³C NMR (125 MHz, CD₂Cl₂): 143.6, 143.5, 142.9, 140.0, 139.9, 132.9, 130 (br), 129.3 (2C), 128.0, 127.6, 127.3, 119.6, 112.3, 111.5, 57.7. UV/Vis: (Acetonitrile) λ_{max} = 326 nm, ε = 23757 M⁻¹ cm⁻¹. HRMS (EI+) calcd for C₂₀H₁₈BN₂ (M⁺): 297.1536; found: 297.1574.

Compound 2.109, *p*-Br:

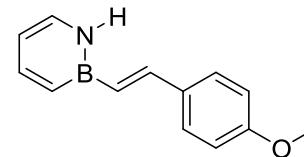
The general procedure was followed using 4-bromo styrene (110 mg, .619 mmol), column eluent 3:97 Et₂O:pentane (43% average yield of two runs, (43 mg, 43% and 44 mg



43%). ¹H NMR (600 MHz, CD₂Cl₂): δ 7.62-7.65 (m, 1H), 7.09-7.41 (d, ³J_{HH} = 7.8 Hz, 2H), 7.31-7.39 (m, 5H) 7.22-7.27 (m, 2H), 7.16-7.18 (m, 2H), 7.10-7.12 (d, ³J_{HH} = 11.4 Hz, 1H), 6.90-6.93 (d, ³J_{HH} = 18 Hz, 1H), 6.331 (t, ³J_{HH} = 6.6 Hz, 1H), 5.14 (s, 2H). ¹¹B NMR (96 MHz, CD₂Cl₂): δ 33.8 (s). ¹³C NMR (150 MHz, CD₂Cl₂): δ 143.6, 143.3, 140.2, 139.8, 138.4, 132.2, 129.3 (2C), 128.8 (2C), 127.9, 127.3, 122.1, 111.9, 57.5. UV/Vis: (Acetonitrile) λ_{max} = 317 nm, ε = 24502 M⁻¹ cm⁻¹. HRMS (EI+) calcd for C₁₉H₁₇BNBr (M⁺): 349.06374; found: 349.06540.

Compound 2.111, N-H *p*-OMe:

In a glove box under a nitrogen atmosphere a pressure tube was charged with 1,2-dihydro-1,2-azaborine **2.110** (102 mg, 1.36 mmol), 0.025 equiv. of [Rh(nbd)Cl]₂ (16 mg, 0.034



mmol), 2.1 equiv. of 4-vinylanisole (383 mg, 2.86 mmol), and 3.0 mL of methylene chloride. This was placed at 90 °C in an oil bath for 20 hours. Upon cooling the product crystallizes from solution. Methylene chloride was added to the solution in order to dissolve the precipitate and the mixture was passed through a silica gel plug and recrystallized from methylene chloride/pentane mixture in a -30 °C freezer. The product was collected and a second recrystallization of the concentrated mother liquor was combined with the first batch to give the total mass of compound **5** (237 mg, 82% yield).

^1H NMR (500 MHz, CD_2Cl_2): δ 8.07 (br s, 1H), 7.71 (dd, $^3J_{\text{HH}} = 6.4, 11.2$ Hz, 1H), 7.54 (d, $^3J_{\text{HH}} = 9$ Hz, 2H), 7.33-7.38 (m, 2H), 7.08 (d, $^3J_{\text{HH}} = 11$ Hz, 1H), 6.94 (d, $^3J_{\text{HH}} = 9$ Hz, 2H), 6.63 (d, $^3J_{\text{HH}} = 19$ Hz, 1H), 6.33 (t, $^3J_{\text{HH}} = 5.4$ Hz, 1H), 3.82 (s, 3H). ^{11}B NMR (160 MHz, CD_2Cl_2): δ 33.8 (s). ^{13}C NMR (125 MHz, CD_2Cl_2): δ 160.3, 144.3, 143.2, 134.5, 132.0, 128.5 (br), 128.4, 125.5 (br), 114.5, 110.0, 55.8. HRMS (EI+) calcd for $\text{C}_{19}\text{H}_{17}\text{BNBr}$ (M+1): 212.12467; found: 212.12438.

2.5.5 Oxygen and water stability study of compound **2.111**¹⁵⁴

In a glovebox an NMR tube equipped with a J-Young valve was charged with compound **2.111** (11 mg, 0.052 mmole, 1 equiv), internal standard hexamethylbenzene (0.8 mg, 0.1 equiv, 0.005 mmole), and 0.5 mL of dried and degassed C_6D_6 . This was degassed via freeze-pump-thaw cycles until no gas evolution was apparent. The NMR tube was maintained under static vacuum and the atmosphere was replaced with oxygen. An NMR spectra was taken immediately following introduction of O_2 but before vigorous shaking to establish a time_0 . When this was measured the sample was vigorously shaken and heated to 50 °C in an oil bath for 1 hour. Nmr analysis indicated no decomposition. The NMR tube was again flushed with an excess of oxygen via balloon to ensure complete saturation, sealed, and heated to 50 °C for another hour--NMR analysis showed no decomposition. The tube was shaken vigorously and heated for another 2 hours at 50 °C—NMR analysis showed no decomposition. Visually the only change was a slight brownish color appearing, but any decomposition products were indistinguishable by NMR and integration versus the internal standard showed a

¹⁵⁴ Lamm, A. N.; Liu, S.-Y. *Mol. Biosyst.* **2009**, *5*, 1303-1305.

consistent ratio. We then poured the NMR tube into a scintillation vial and allowed it to sit for 16 hours at room temperature under ambient atmosphere to see if the material was stable for longer periods of time at increasing concentration. Nmr analysis of the crystalline residue showed no decomposition.

In a glovebox, an NMR tube equipped with a J-Young valve was charged with compound **5** (11 mg, 0.052 mmole, 1 equiv), internal standard hexamethylbenzene (0.8 mg, 0.1 equiv, 0.005 mmole), and 0.5 mL of DMSO- d_6 . A t_{me_0} NMR was taken to establish integral values and the spectrum of the compound in DMSO- d_6 . Water was added to this solution via microsyringe (8 μ L, 8.5 equiv). We observed no change either visually or by NMR analysis at room temperature for 2 hours. The mixture was then heated to 50 °C for 2 hours. Nmr analysis indicated no decomposition products.

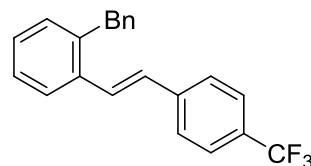
2.5.6 Synthesis of carbonaceous 2.112-2.114

Procedure for Suzuki-Miyaura coupling:

Under nitrogen, a 25 mL round bottom flask equipped with a reflux condenser and a stir bar was charged with 1.1 equiv. (1.1 mmol, 272 mg) of 2-benzylbromobenzene, 1 equiv. (1 mmol) of appropriate styrylboronic acid, 0.02 equiv. (0.02 mmol, 15 mg) of $PdCl_2(PPh_3)_2$, and 1.5 mL of toluene. To this was added 2.67 equiv. of KOH (5.0 M in H_2O). This mixture was heated to 70 °C overnight (18 hours) with stirring. Upon completion, hexanes was added, and the layers were partitioned. The organic layer was washed 3x with water and then 3x with brine and dried over sodium sulfate. The products were isolated via column chromatography (Et_2O and hexanes as eluent).

Compound 2.112, *p*-CF₃:

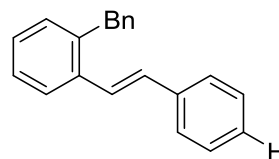
The general procedure was followed using (E)-4-(trifluoromethyl)styrylboronic acid (216 mg, 1.0 mmol), column eluent pentane (90.2 mg, 27%). ¹H NMR (300 MHz,



CDCl₃): δ 4.21(s, 2H), 7.02 (d, ³J_{HH} = 16.1 Hz, 1H), 7.20-7.69 (m, 12H), 4.35 (s, 2H). ¹³C NMR (600 MHz, CDCl₃): δ 141.2, 140.7, 138.8, 136.1, 131.1, 129.3, 129.2, 128.99, 128.9, 128.8, 128.6, 127.2, 126.8, 126.4, 126.3, 125.8, 125.8, 39.7. CF₃ group is overlapping with the aromatic region. UV/Vis: (Acetonitrile) λ_{max} = 303 nm, ε = 24018 M⁻¹ cm⁻¹. HRMS (EI+) calcd for C₂₂H₁₇F₃ (M⁺): 339.1361; found: 339.1345.

Compound 2.113, *p*-H:

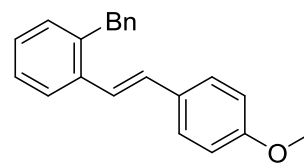
The general procedure was followed using (E)-styrylboronic acid (148 mg, 1.0 mmol), column eluent pentane (70.4 mg, 26%). ¹H



NMR (300 MHz, CDCl₃): δ 7.76 (d, ³J_{HH} = 8 Hz, 1H), 7.28-7.54 (m, 14H), 7.05 (d, ³J_{HH} = 16 Hz, 1H), 4.26 (s, 2H). ¹³C NMR (600 MHz, CDCl₃): δ 138.7, 136.95, 130.99, 130.8, 129.0, 128.9, 128.1, 127.9, 127.2, 127.1, 126.9, 126.8, 126.4, 126.3, 126.2, 126.1, 39.7. UV/Vis: (Acetonitrile) λ_{max} = 299 nm, ε = 21199 M⁻¹ cm⁻¹. HRMS (EI+) calcd for C₂₁H₁₉ (M⁺): 271.1487; found: 271.1475.

Compound 2.114, *p*-OMe:

The general procedure was followed using *p*-methoxy (E)-styrylboronic acid (196 mg, 1.0 mmol), column eluent 5:95 Et₂O:pentane (32 mg, 10%). ¹H NMR (300 MHz, CDCl₃): δ



7.55(d, ³J_{HH} = 8 Hz, 1H), 7.25 (d, ³J_{HH} = 9 Hz, 2H), 7.09-7.23 (m, 8H), 6.79-7.07 (m,

3H), 4.06 (s, 3H), 3.74 (s, 3H). ¹³C NMR (600 MHz, CDCl₃): δ 159.5, 140.9, 138.2, 137.0, 130.8, 130.6, 130.4, 129.1, 128.7, 127.9, 127.5, 126.8, 126.9, 125.9, 124.5, 114.3, 55.5, 39.5. UV/Vis: (Acetonitrile) λ_{max} = 306 nm, ε = 28422 M⁻¹ cm⁻¹. HRMS (EI+) calcd for C₂₂H₂₁O (M⁺): 301.1592; found: 301.1587.

2.5.7 Photophysical data and measurement

Photophysical data for compounds **2.95**, **2.102**, **2.107**, **2.112**, **2.113**, and **2.114**.

Compound	Absorption		Emission λ _{max} (nm)	Stokes Shift (cm ⁻¹)	Quantum Yield Φ
	λ _{max} (nm)	ε (LM ⁻¹ cm ⁻¹)			
2.95	320	28422	390	5610	>.01
2.102	313	24953	407	7380	.06
2.107	317	22253	431	8340	.29
2.114	303	24018	368	5830	.01
2.113	299	21199	357	5430	.08
2.112	306	28422	380	6360	.01

Procedure for measuring quantum yields:¹⁵⁵

Flourescence quantum yield, Φ, was measured according to the principles outlined in “*A Guide to Recording Fluorescence Quantum Yields*” from Horiba Inc. Measurements were taken in degassed ethanol with constant slit widths. Two compounds of known quantum yield in ethanol (anthracene (Φ= 0.27) and 9-10-diphenyl anthracene (Φ=0.95)) were used to calibrate the measurement following the outlined procedure below.

¹⁵⁵ Jobin Yvon Ltd. *A Guide to Recording Fluorescence Quantum Yields* (accessed March 2014).

Empirical formula	C ₂₀ H ₂₀ B N O	
Formula weight	301.18	
Temperature	173(2) K	
Wavelength	0.71073 Å	
Crystal system	Monoclinic	
Space group	P2(1)/c	
Unit cell dimensions	a = 23.009(4) Å	α = 90°.
	b = 5.4564(10) Å	β = 103.943(3)°.
	c = 13.699(3) Å	γ = 90°.
Volume	1669.2(5) Å ³	
Z	4	
Density (calculated)	1.198 Mg/m ³	
Absorption coefficient	0.072 mm ⁻¹	
F(000)	640	
Crystal size	0.23 x 0.17 x 0.13 mm ³	
Theta range for data collection	0.91 to 25.00°.	
Index ranges	-27 ≤ h ≤ 27, -6 ≤ k ≤ 6, -16 ≤ l ≤ 16	
Reflections collected	15265	
Independent reflections	2959 [R(int) = 0.0200]	
Completeness to theta = 25.00°	100.0 %	
Absorption correction	Semi-empirical from equivalents	
Max. and min. transmission	0.9907 and 0.9836	
Refinement method	Full-matrix least-squares on F ²	

Data / restraints / parameters	2959 / 0 / 288
Goodness-of-fit on F^2	1.026
Final R indices [$I > 2\sigma(I)$]	R1 = 0.0345, wR2 = 0.0994
R indices (all data)	R1 = 0.0418, wR2 = 0.1152
Largest diff. peak and hole	0.154 and -0.150 e.Å ⁻³

Table 2. Atomic coordinates ($\times 10^4$) and equivalent isotropic displacement parameters ($\text{Å}^2 \times 10^3$)

for liu79a. $U(\text{eq})$ is defined as one third of the trace of the orthogonalized U^{ij} tensor.

	x	y	z	$U(\text{eq})$
O(1)	4490(1)	4401(2)	13688(1)	39(1)
N(1)	2003(1)	7028(2)	7515(1)	41(1)
B(1)	2517(1)	5563(3)	7974(1)	38(1)
C(1)	1674(1)	6554(3)	6559(1)	52(1)
C(2)	1814(1)	4744(3)	5986(1)	55(1)
C(3)	2322(1)	3262(3)	6351(1)	49(1)
C(4)	2669(1)	3598(3)	7293(1)	44(1)
C(5)	1782(1)	9100(3)	8013(1)	43(1)
C(6)	1220(1)	8543(2)	8350(1)	38(1)
C(7)	750(1)	10185(3)	8148(1)	47(1)
C(8)	243(1)	9803(4)	8498(1)	63(1)

C(9)	204(1)	7748(4)	9056(1)	70(1)
C(10)	668(1)	6065(4)	9253(1)	65(1)
C(11)	1173(1)	6447(3)	8899(1)	51(1)
C(12)	2858(1)	5941(3)	9090(1)	41(1)
C(13)	3281(1)	4422(3)	9585(1)	37(1)
C(14)	3606(1)	4480(2)	10646(1)	34(1)
C(15)	3524(1)	6310(2)	11320(1)	36(1)
C(16)	3825(1)	6236(2)	12318(1)	35(1)
C(17)	4220(1)	4323(2)	12682(1)	32(1)
C(18)	4313(1)	2506(2)	12032(1)	34(1)
C(19)	4006(1)	2607(2)	11029(1)	35(1)
C(20)	4871(1)	2386(3)	14087(1)	42(1)

__Table 3. Bond lengths [Å] and angles [°] for **2.95**.

O(1)-C(17)	1.3694(15)
O(1)-C(20)	1.4292(16)
N(1)-C(1)	1.3703(18)
N(1)-B(1)	1.4405(19)
N(1)-C(5)	1.4735(19)
B(1)-C(4)	1.516(2)
B(1)-C(12)	1.555(2)
C(1)-C(2)	1.348(2)

C(1)-H(1)	1.005(17)
C(2)-C(3)	1.410(2)
C(2)-H(2)	0.983(18)
C(3)-C(4)	1.357(2)
C(3)-H(3)	0.975(18)
C(4)-H(4)	0.957(16)
C(5)-C(6)	1.505(2)
C(5)-H(5A)	0.991(15)
C(5)-H(5B)	0.980(16)
C(6)-C(7)	1.380(2)
C(6)-C(11)	1.388(2)
C(7)-C(8)	1.381(2)
C(7)-H(7)	0.976(17)
C(8)-C(9)	1.372(3)
C(8)-H(8)	0.99(2)
C(9)-C(10)	1.385(3)
C(9)-H(9)	0.93(2)
C(10)-C(11)	1.376(2)
C(10)-H(10)	0.95(2)
C(11)-H(11)	0.996(18)
C(12)-C(13)	1.333(2)
C(12)-H(12)	1.004(18)
C(13)-C(14)	1.4655(18)

C(13)-H(13)	0.981(16)
C(14)-C(19)	1.3907(18)
C(14)-C(15)	1.4028(18)
C(15)-C(16)	1.3766(19)
C(15)-H(15)	0.976(15)
C(16)-C(17)	1.3944(18)
C(16)-H(16)	0.975(15)
C(17)-C(18)	1.3833(18)
C(18)-C(19)	1.3866(18)
C(18)-H(18)	0.956(14)
C(19)-H(19)	0.953(15)
C(20)-H(20A)	0.990(16)
C(20)-H(20B)	1.006(16)
C(20)-H(20C)	0.976(17)
C(17)-O(1)-C(20)	116.66(10)
C(1)-N(1)-B(1)	121.31(13)
C(1)-N(1)-C(5)	114.47(12)
B(1)-N(1)-C(5)	124.22(12)
N(1)-B(1)-C(4)	114.22(13)
N(1)-B(1)-C(12)	121.46(13)
C(4)-B(1)-C(12)	124.26(13)
C(2)-C(1)-N(1)	122.70(14)

C(2)-C(1)-H(1)	122.2(10)
N(1)-C(1)-H(1)	115.1(10)
C(1)-C(2)-C(3)	120.46(14)
C(1)-C(2)-H(2)	118.3(10)
C(3)-C(2)-H(2)	121.3(10)
C(4)-C(3)-C(2)	120.53(15)
C(4)-C(3)-H(3)	120.6(10)
C(2)-C(3)-H(3)	118.9(10)
C(3)-C(4)-B(1)	120.71(14)
C(3)-C(4)-H(4)	116.8(10)
B(1)-C(4)-H(4)	122.4(10)
N(1)-C(5)-C(6)	113.90(12)
N(1)-C(5)-H(5A)	107.9(8)
C(6)-C(5)-H(5A)	108.8(8)
N(1)-C(5)-H(5B)	108.9(9)
C(6)-C(5)-H(5B)	108.6(9)
H(5A)-C(5)-H(5B)	108.6(12)
C(7)-C(6)-C(11)	118.89(14)
C(7)-C(6)-C(5)	119.79(13)
C(11)-C(6)-C(5)	121.27(13)
C(6)-C(7)-C(8)	121.32(16)
C(6)-C(7)-H(7)	118.0(10)
C(8)-C(7)-H(7)	120.7(10)

C(9)-C(8)-C(7)	119.37(18)
C(9)-C(8)-H(8)	119.1(12)
C(7)-C(8)-H(8)	121.5(12)
C(8)-C(9)-C(10)	119.99(17)
C(8)-C(9)-H(9)	119.9(13)
C(10)-C(9)-H(9)	120.1(13)
C(11)-C(10)-C(9)	120.49(18)
C(11)-C(10)-H(10)	117.1(11)
C(9)-C(10)-H(10)	122.4(11)
C(10)-C(11)-C(6)	119.91(17)
C(10)-C(11)-H(11)	119.2(10)
C(6)-C(11)-H(11)	120.9(10)
C(13)-C(12)-B(1)	123.43(14)
C(13)-C(12)-H(12)	116.9(10)
B(1)-C(12)-H(12)	119.6(10)
C(12)-C(13)-C(14)	128.80(13)
C(12)-C(13)-H(13)	117.4(9)
C(14)-C(13)-H(13)	113.8(9)
C(19)-C(14)-C(15)	117.14(12)
C(19)-C(14)-C(13)	119.42(12)
C(15)-C(14)-C(13)	123.42(12)
C(16)-C(15)-C(14)	121.19(12)
C(16)-C(15)-H(15)	118.3(8)

C(14)-C(15)-H(15)	120.5(8)
C(15)-C(16)-C(17)	120.36(12)
C(15)-C(16)-H(16)	120.8(8)
C(17)-C(16)-H(16)	118.8(8)
O(1)-C(17)-C(18)	124.53(11)
O(1)-C(17)-C(16)	115.81(11)
C(18)-C(17)-C(16)	119.66(12)
C(17)-C(18)-C(19)	119.25(12)
C(17)-C(18)-H(18)	120.5(8)
C(19)-C(18)-H(18)	120.3(8)
C(18)-C(19)-C(14)	122.40(12)
C(18)-C(19)-H(19)	118.9(8)
C(14)-C(19)-H(19)	118.7(9)
O(1)-C(20)-H(20A)	109.0(9)
O(1)-C(20)-H(20B)	110.6(9)
H(20A)-C(20)-H(20B)	110.7(13)
O(1)-C(20)-H(20C)	106.4(10)
H(20A)-C(20)-H(20C)	113.2(13)
H(20B)-C(20)-H(20C)	107.0(13)

Symmetry transformations used to generate equivalent atoms:

Table 4. Anisotropic displacement parameters ($\text{\AA}^2 \times 10^3$) for **2.95**. The anisotropic displacement factor exponent takes the form: $-2 \sum h^2 a^{*2} U^{11} + \dots + 2 h k a^* b^* U^{12}$]

	U11	U22	U33	U23	U13	U12
O(1)	43(1)	38(1)	33(1)	0(1)	5(1)	6(1)
N(1)	39(1)	46(1)	36(1)	6(1)	5(1)	1(1)
B(1)	33(1)	44(1)	39(1)	7(1)	9(1)	-4(1)
C(1)	49(1)	64(1)	38(1)	8(1)	1(1)	7(1)
C(2)	56(1)	74(1)	31(1)	2(1)	4(1)	-1(1)
C(3)	49(1)	61(1)	40(1)	-4(1)	18(1)	-6(1)
C(4)	37(1)	54(1)	42(1)	1(1)	12(1)	0(1)
C(5)	40(1)	38(1)	46(1)	7(1)	4(1)	2(1)
C(6)	43(1)	38(1)	30(1)	-2(1)	3(1)	-4(1)
C(7)	47(1)	46(1)	45(1)	-4(1)	7(1)	0(1)
C(8)	52(1)	70(1)	70(1)	-18(1)	22(1)	-5(1)
C(9)	73(1)	85(1)	64(1)	-29(1)	39(1)	-32(1)
C(10)	94(1)	58(1)	50(1)	-5(1)	30(1)	-27(1)
C(11)	66(1)	44(1)	43(1)	3(1)	11(1)	-8(1)
C(12)	37(1)	45(1)	40(1)	0(1)	7(1)	2(1)
C(13)	35(1)	39(1)	36(1)	0(1)	8(1)	-2(1)
C(14)	30(1)	34(1)	37(1)	2(1)	7(1)	-1(1)
C(15)	33(1)	31(1)	42(1)	3(1)	6(1)	3(1)
C(16)	37(1)	30(1)	39(1)	-2(1)	10(1)	1(1)
C(17)	30(1)	33(1)	34(1)	1(1)	7(1)	-3(1)

C(18)	33(1)	31(1)	38(1)	3(1)	7(1)	4(1)
C(19)	37(1)	33(1)	37(1)	-2(1)	11(1)	2(1)
C(20)	47(1)	41(1)	36(1)	5(1)	4(1)	6(1)

Table 5. Hydrogen coordinates ($\times 10^4$) and isotropic displacement parameters ($\text{\AA}^2 \times 10^3$) for **2.95**.

	x	y	z	U(eq)
H(1)	1329(7)	7700(30)	6304(13)	62(5)
H(2)	1553(7)	4490(30)	5310(14)	63(5)
H(3)	2410(7)	1950(30)	5925(13)	60(5)
H(4)	3003(7)	2510(30)	7506(12)	53(4)
H(5A)	2102(6)	9570(30)	8608(11)	43(4)
H(5B)	1704(6)	10490(30)	7548(11)	47(4)
H(7)	789(7)	11650(30)	7758(12)	56(5)
H(8)	-93(9)	10980(40)	8360(15)	79(6)
H(9)	-135(9)	7490(40)	9301(15)	82(6)
H(10)	659(8)	4620(40)	9639(14)	69(5)
H(11)	1498(7)	5200(40)	9039(12)	63(5)

H(12)	2742(7)	7330(30)	9485(13)	61(5)
H(13)	3388(7)	3030(30)	9211(12)	51(4)
H(15)	3245(6)	7660(30)	11093(11)	40(4)
H(16)	3763(6)	7500(30)	12785(10)	43(4)
H(18)	4581(6)	1180(30)	12273(10)	39(4)
H(19)	4066(6)	1330(30)	10587(11)	40(4)
H(20A)	4632(7)	860(30)	13982(12)	49(4)
H(20B)	5216(7)	2270(30)	13756(12)	51(4)
H(20C)	5040(7)	2760(30)	14796(13)	54(4)

Table 6. Torsion angles [°] for **2.95**.

C(1)-N(1)-B(1)-C(4)	2.89(19)
C(5)-N(1)-B(1)-C(4)	-177.76(12)
C(1)-N(1)-B(1)-C(12)	-174.40(13)
C(5)-N(1)-B(1)-C(12)	5.0(2)
B(1)-N(1)-C(1)-C(2)	-1.3(2)
C(5)-N(1)-C(1)-C(2)	179.33(15)
N(1)-C(1)-C(2)-C(3)	-1.1(3)
C(1)-C(2)-C(3)-C(4)	1.6(2)
C(2)-C(3)-C(4)-B(1)	0.2(2)
N(1)-B(1)-C(4)-C(3)	-2.4(2)

C(12)-B(1)-C(4)-C(3)	174.81(13)
C(1)-N(1)-C(5)-C(6)	73.91(16)
B(1)-N(1)-C(5)-C(6)	-105.47(15)
N(1)-C(5)-C(6)-C(7)	-133.41(13)
N(1)-C(5)-C(6)-C(11)	49.23(18)
C(11)-C(6)-C(7)-C(8)	1.3(2)
C(5)-C(6)-C(7)-C(8)	-176.09(14)
C(6)-C(7)-C(8)-C(9)	-0.2(2)
C(7)-C(8)-C(9)-C(10)	-0.8(3)
C(8)-C(9)-C(10)-C(11)	0.6(3)
C(9)-C(10)-C(11)-C(6)	0.6(2)
C(7)-C(6)-C(11)-C(10)	-1.6(2)
C(5)-C(6)-C(11)-C(10)	175.82(14)
N(1)-B(1)-C(12)-C(13)	170.39(13)
C(4)-B(1)-C(12)-C(13)	-6.6(2)
B(1)-C(12)-C(13)-C(14)	-175.74(12)
C(12)-C(13)-C(14)-C(19)	175.79(14)
C(12)-C(13)-C(14)-C(15)	-2.3(2)
C(19)-C(14)-C(15)-C(16)	-0.49(19)
C(13)-C(14)-C(15)-C(16)	177.65(12)
C(14)-C(15)-C(16)-C(17)	0.0(2)
C(20)-O(1)-C(17)-C(18)	-3.10(17)
C(20)-O(1)-C(17)-C(16)	176.58(11)

C(15)-C(16)-C(17)-O(1)	-179.14(11)
C(15)-C(16)-C(17)-C(18)	0.56(19)
O(1)-C(17)-C(18)-C(19)	179.09(11)
C(16)-C(17)-C(18)-C(19)	-0.58(18)
C(17)-C(18)-C(19)-C(14)	0.06(19)
C(15)-C(14)-C(19)-C(18)	0.47(19)
C(13)-C(14)-C(19)-C(18)	-177.75(11)

Symmetry transformations used to generate equivalent atoms:

2.5.9 Computational Approach and Results (with Professor David Dixon)

The calculations were done at the density functional theory (DFT) level on substituted stilbenes with a benzyl group on the *ortho* carbon for the stilbene (type **6**) and on the BN isoster stilbene (type **3**) with a benzyl group on the N. The substituents are Br, CF₃, CH₃, CN, F, NMe₂, and OCH₃. The geometries were optimized at the DFT B3LYP/DZVP2 level.¹⁵⁶ Vibrational frequencies were calculated to show that the optimized structures were minima on the potential energy surface. The UV-visible spectra were calculated using time dependent DFT (TD-DFT).¹⁵⁷ In the first step, TD-DFT provides vertical excitation energies, the energy from the ground state to the excited

¹⁵⁶ (a) Becke, A. D. *J. Chem. Phys.* **1993**, *98*, 5648-5652. (b) C. Lee, W. Yang, R. G. Parr, *Phys. Rev. B* **1988**, *37*, 785-789. (c) N. Godbout, D. R. Salahub, J. Andzelm, E. Wimmer, *Can. J. Chem.* **1992**, *70*, 560-571.

¹⁵⁷(a) R. Bauernschmitt, R. Ahlrichs, *Chem. Phys. Lett.*, 1996, **256**, 454. (b) M. E. Casida, C. Jamorski, K. C. Casida, and D. R. Salahub, *J. Chem. Phys.*, 1998, **108**, 4439-4449.

state at the ground state geometry. The first excited state was then optimized to provide adiabatic excitation energies (ground state to optimized excited state) and fluorescence (emission) energies (transition from the optimized excited state to the ground state at the excited state geometry). In order to model the effect of solvent, the TD-DFT calculations were also performed using the self-consistent reaction field approach¹⁵⁸ implemented in Gaussian09¹⁵⁹ at the CPCM level with the Klamt radii¹⁶⁰ for R = H and CF₃. The solvents were acetonitrile cyclohexane, CH₂Cl₂, diethyl ether, DMSO, and EtOH. The ground state and first excited singlet state were also optimized in the different solvents. All calculations were done with Gaussian09.

We focus on the compounds with substituents R = H, CF₃, and OCH₃ (Table S1 and Figure S1) The data for the remaining compounds is also given (Figure S1). The calculated first singlet excitations are dominated by the HOMO-LUMO (the HOMO and LUMO are the B3LYP Kohn-Sham orbitals) transition and are predicted to be intense (Table S4). We predict vertical absorptions in reasonable agreement with the experimental data between 329 and 347 nm in the gas phase for the different substituents. In acetonitrile, for R = H and CF₃, the range is 330 to 370 nm.

¹⁵⁸ Tomasi, J.; Mennucci, B.; Cammi, R. *Chem. Rev.* **2005**, *105*, 2999-3093; G. Scalmani, M. J. Frisch, B. Mennucci, J. Tomasi, R. Cammi, and V. Barone, *J. Chem. Phys.*, **2006**, *124*, 094107: 1-15.

¹⁵⁹ Gaussian 09, Revision B.1, Frisch, M. J.; Trucks, G. W.; Schlegel, H. B.; Scuseria, G. E.; Robb, M. A.; Cheeseman, J. R.; Scalmani, G.; Barone, V.; Mennucci, B.; Petersson, G. A.; Nakatsuji, H.; Caricato, M.; Li, X.; Hratchian, H. P.; Izmaylov, A. F.; Bloino, J.; Zheng, G.; Sonnenberg, J. L.; Hada, M.; Ehara, M.; Toyota, K.; Fukuda, R.; Hasegawa, J.; Ishida, M.; Nakajima, T.; Honda, Y.; Kitao, O.; Nakai, H.; Vreven, T.; Montgomery, Jr., J. A.; Peralta, J. E.; Ogliaro, F.; Bearpark, M.; Heyd, J. J.; Brothers, E.; Kudin, K. N.; Staroverov, V. N.; Kobayashi, R.; Normand, J.; Raghavachari, K.; Rendell, A.; Burant, J. C.; Iyengar, S. S.; Tomasi, J.; Cossi, M.; Rega, N.; Millam, N. J.; Klene, M.; Knox, J. E.; Cross, J. B.; Bakken, V.; Adamo, C.; Jaramillo, J.; Gomperts, R.; Stratmann, R. E.; Yazyev, O.; Austin, A. J.; Cammi, R.; Pomelli, C.; Ochterski, J. W.; Martin, R. L.; Morokuma, K.; Zakrzewski, V. G.; Voth, G. A.; Salvador, P.; Dannenberg, J. J.; Dapprich, S.; Daniels, A. D.; Farkas, Ö.; Foresman, J. B.; Ortiz, J. V.; Cioslowski, J.; Fox, D. J. Gaussian, Inc., Wallingford CT, 2009.

¹⁶⁰ (a) Klamt, A.; Schürmann, G. *J. Chem. Soc. Perkin Trans. 2*, **1993**, 799-805; (b) Klamt, A. *COSMO-RS From Quantum Chemistry to Fluid Phase Thermodynamics and Drug Design* Elsevier: Amsterdam, **2005**

The HOMO for **2.102**, **2.113**, **2.107**, and **2.112** can be described as being delocalized over the two benzene rings (BN-ring) bonded to the C=C and including the C=C carbons. The LUMO is delocalized over the same atoms. For R = H, there is little difference between the gas phase and acetonitrile for the stilbene or the BN isostere. For R= CF₃, the effect of acetonitrile solvent is minimal for **6g**. However for **3g**, the HOMO has a larger component on the ring containing the BN group than does the ring with the CF₃ substituent. The effect of the solvent acetonitrile is noticeable as it localizes the HOMO more onto the ring containing the BN moiety. In contrast the LUMO is more localized on the ring with the CF₃ group.

The difference in the emission spectra for **2.107** and **2.95** is 0.18 eV as compared to the experimental value of 0.30 eV and the difference in the emission spectra between **2.114** and **2.113** is predicted to be 0.24 eV as compared to the experimental value of 0.21 eV. The gas phase Stokes shifts range from 0.47 to 0.62 eV and do not show as large a shift as experimentally observed in solution as the emission peaks are predicted to have too small a red shift. The calculated Stokes shifts in acetonitrile are larger but we do not see a significant difference between the stilbene and the BN isoster (Table S2). In addition, the peaks in acetonitrile are red-shifted as compared to experiment. For R= H, the peak absorption is red-shifted by 0.12 eV to 330 nm in acetonitrile as compared to the gas phase for **3b** and for **6b**, the red-shift is 0.10 eV to 338 nm. The red-shift of the first excitation peak is approximately constant for the different solvents. The Stokes shifts do correlate with the size of the dielectric constant with the largest Stokes shifts found for the solvents with the highest dielectric constants. We predict that the emission spectra do shift in the solvents for both **2.107** and **2.112**. The effect of solvent is not surprising as the

molecular dipole moments (Table S3) are large (>4 D) for **2.112** and **2.113** due to the CF₃ group.

Table S1. Calculated 1st singlet excitation energies for vertical absorption and emission in the gas phase.

Molecule	R	Vertical Absorption (eV)	Vertical Absorption (nm)	Oscillator strength	Vertical Emission (eV)	Vertical Emission (nm)	Stokes shift (eV)
BN isoster	H	3.76	329	0.63	3.16	393	0.60
BN isoster	CF ₃	3.58	347	0.57	2.96	419	0.62
BN isoster	OCH ₃	3.73	332	0.85	3.14	395	0.59
stilbene	H	3.84	323	0.77	3.37	367	0.47
stilbene	CF ₃	3.75	330	0.83	3.16	392	0.59
stilbene	OCH ₃	3.69	336	0.87	3.13	396	0.56

Table S2. Calculated 1st singlet excitation energies for vertical absorption and emission in solvents for R= CF₃ for the stilbene and the BN isoster.

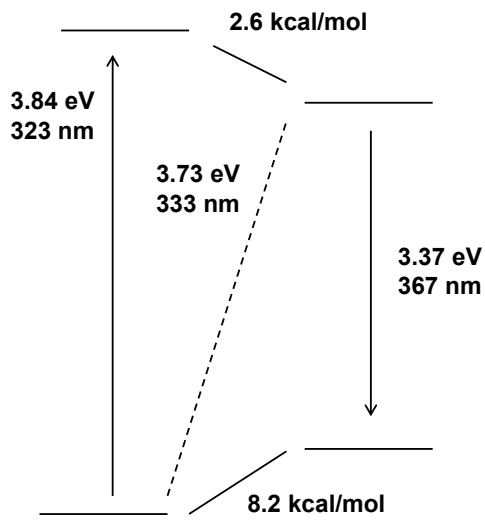
Molecule	solvent	ϵ	Vertical Absorption (eV)	Vertical Absorption (nm)	Oscillator strength	Vertical Emission (eV)	Vertical Emission (nm)	Stokes shift (eV)
BN isoster	gas		3.76	329	0.63	3.16	393	0.60

BN isoster	cyclohexane	2.0165	3.45	360	0.71	2.80	443	0.65
BN isoster	diethyl ether	4.24	3.44	361	0.68	2.73	453	0.71
BN isoster	CH ₂ Cl ₂	8.93	3.42	363	0.70	2.68	463	0.74
BN isoster	EtOH	24.852	3.41	364	0.67	2.64	469	0.77
BN isoster	acetonitrile.	35.688	3.48	356	0.69	2.64	470	0.84
BN isoster	DMSO	46.826	3.40	365	0.69	2.63	470	0.77
stilbene	gas		3.75	330	0.83	3.16	392	0.59
stilbene	cyclohexane	2.0165	3.55	350	1.00	2.95	420	0.60
stilbene	diethyl ether	4.24	3.55	349	1.00	2.82	440	0.73
stilbene	CH ₂ Cl ₂	8.93	3.53	352	1.00	2.74	452	0.79
stilbene	EtOH	24.852	3.54	350	1.00	2.70	460	0.84
stilbene	acetonitrile.	35.688	3.63	342	0.98	2.69	461	0.94
stilbene	DMSO	46.826	3.53	352	1.00	2.68	462	0.85

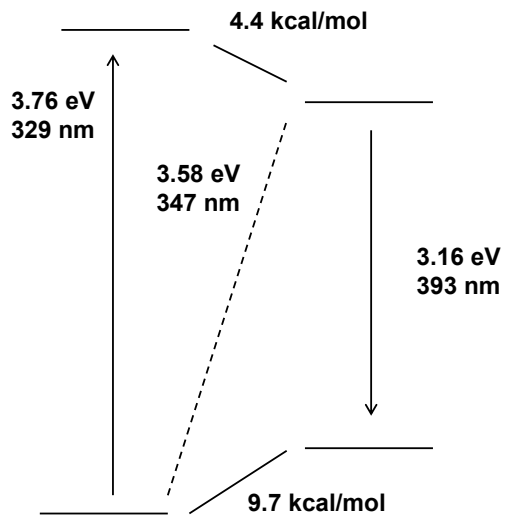
Table S3. Dipole moments (D) for the ground state for R = H, CF₃, and OCH₃.

Molecule	R	μ (D)
----------	---	-----------

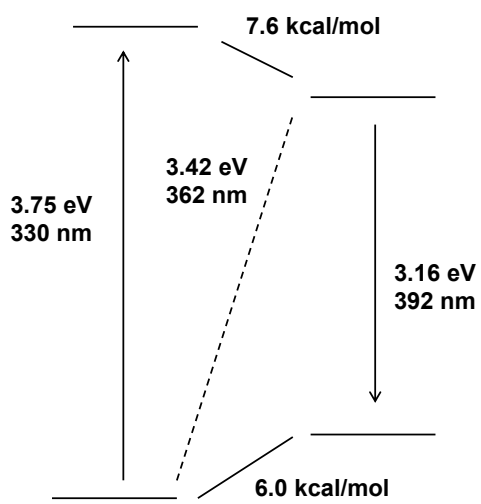
BN isoster	H	1.86
BN isoster	CF ₃	4.91
BN isoster	OCH ₃	0.82
stilbene	H	0.23
stilbene	CF ₃	4.17
stilbene	OCH ₃	1.77



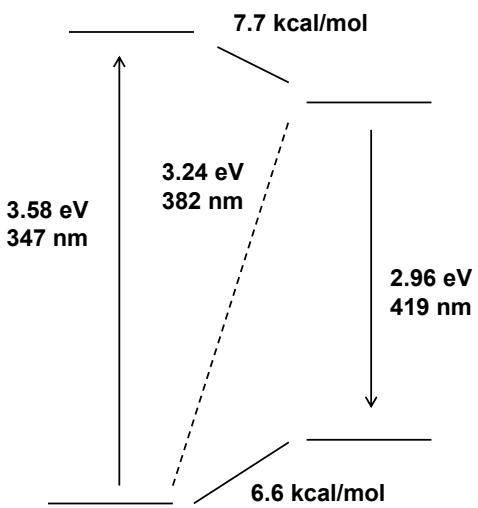
$C_{21}H_{18}$



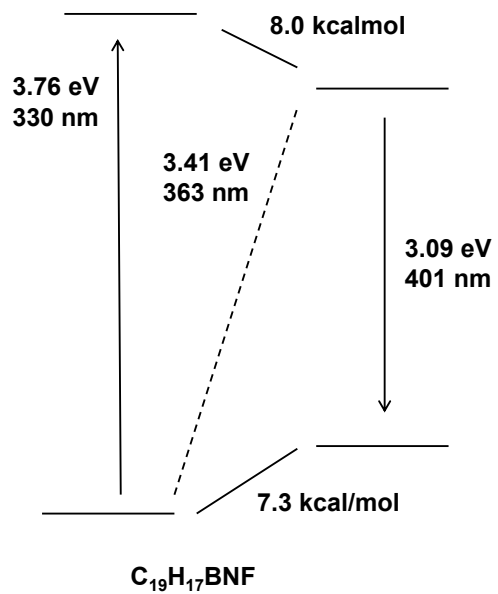
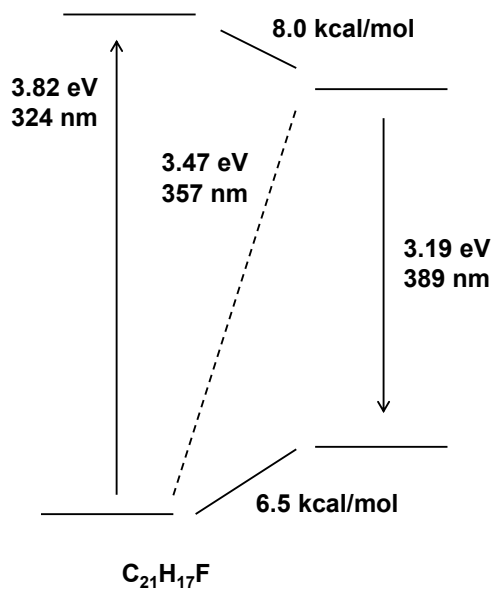
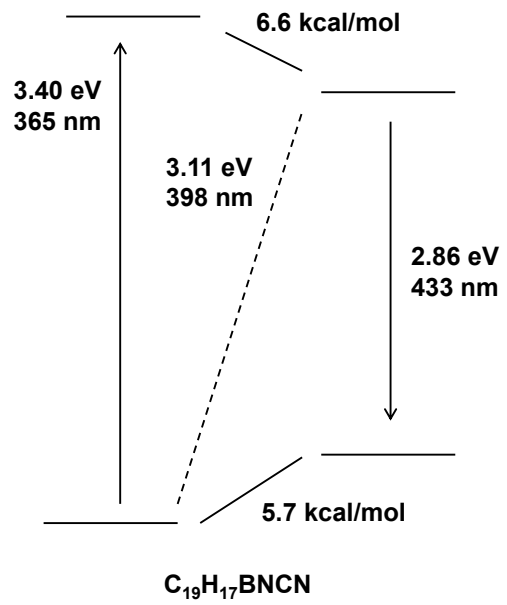
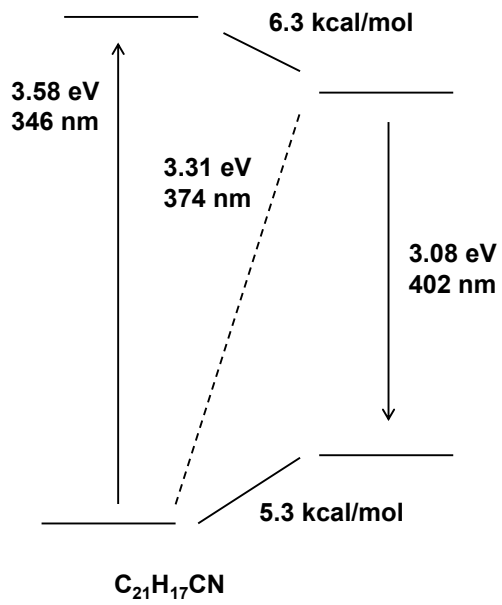
$C_{19}H_{18}BN$

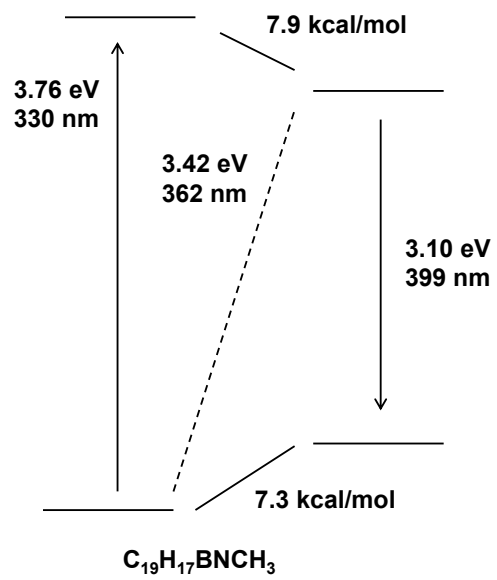
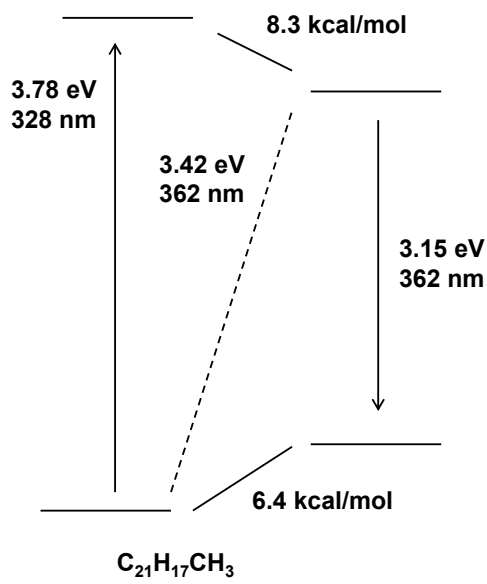
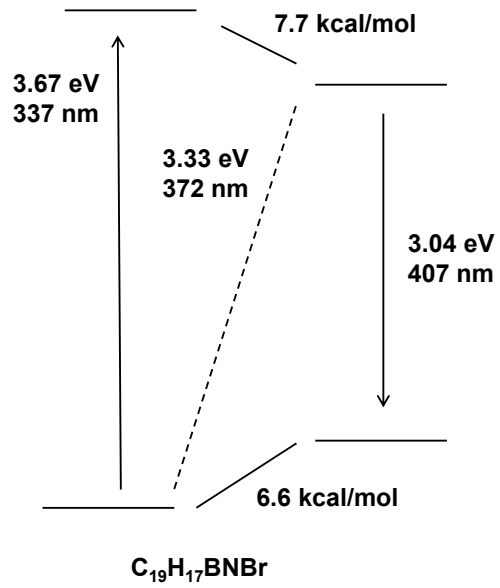
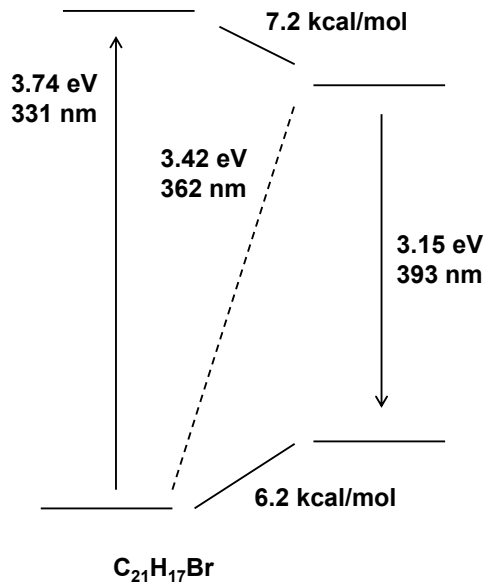


$C_{21}H_{17}CF_3$



$C_{19}H_{17}BNCF_3$





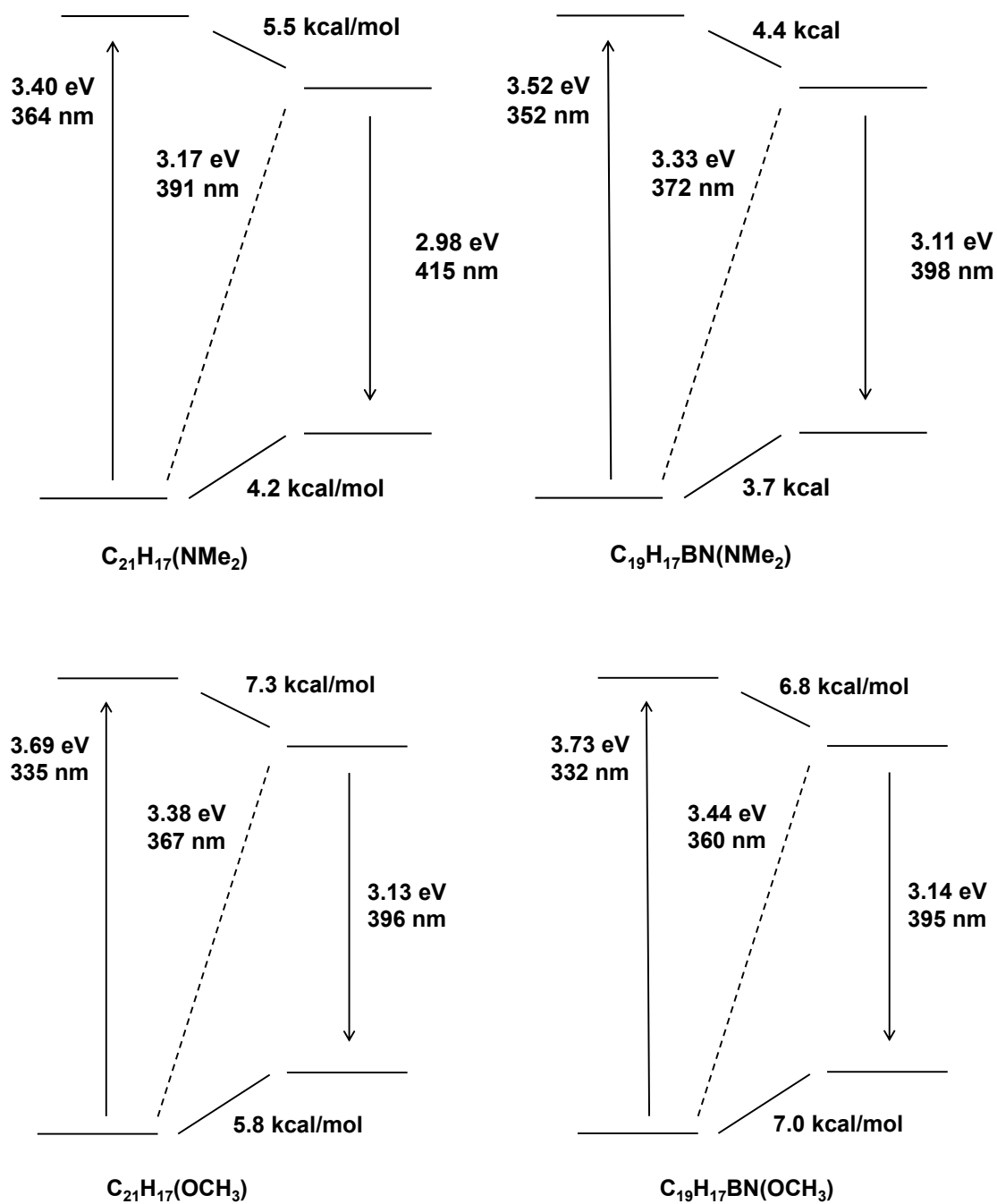


Figure S1. TD-DFT gas phase excitation energies to the 1st excited state.

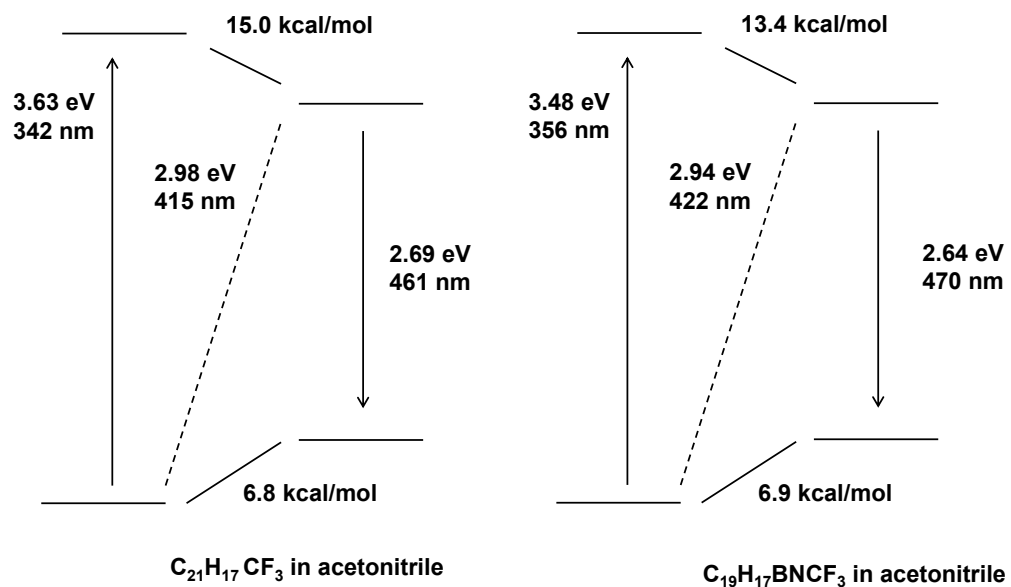


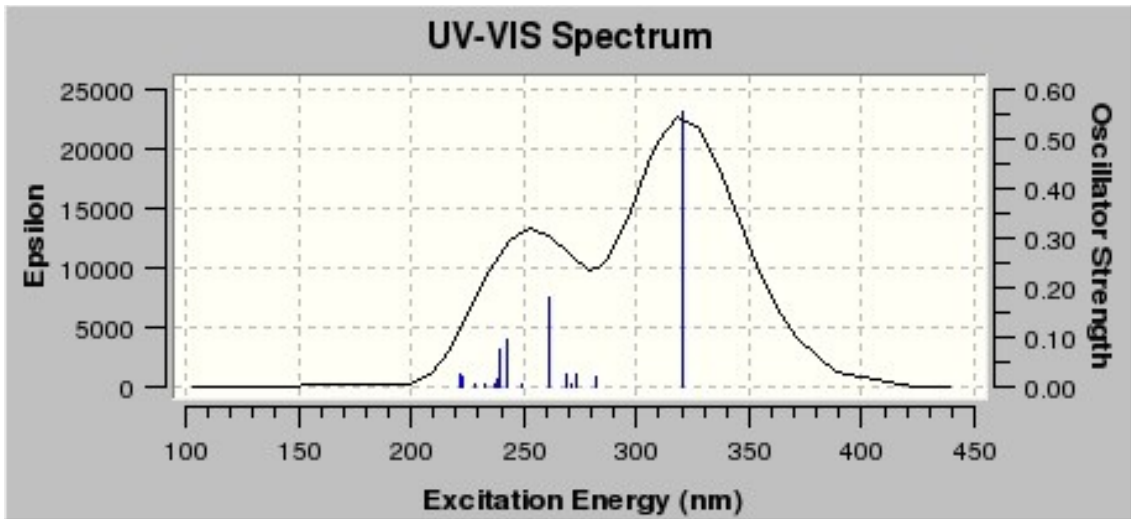
Figure S2. TD-DFT excitation energies for the 1st excited state in acetonitrile.

Table S4: Individual molecule excitation energies**C₁₉H₁₈BN (R = H)**

Excited	State 1	3.76 eV	329.4 nm	f=0.6321
72 →73	0.69844	HOMO→LUMO		
Excited	State 2	4.30 eV	288.0nm	f=0.0473
72 →74	0.68501			
Excited	State 3	4.51 eV	275.1 nm	f=0.0007
69 →73	0.39991			
70 →73	-0.18867			
71 →77	-0.14932			
72 →75	0.20829			
72 →76	-0.10765			
72 →77	0.45893			
Excited	State 4	4.56 eV	271.9 nm	f=0.0674
71 →73	0.45607			
72 →75	0.50763			
72 →77	-0.12208			
Excited	State 5	4.62 eV	268.4 nm	f=0.0011

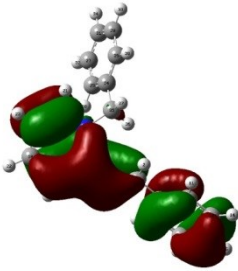
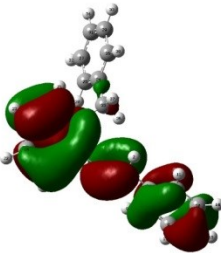
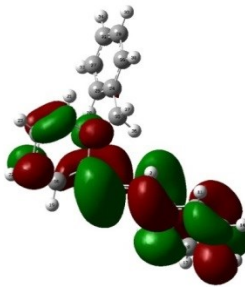
72 → 75 0.14766

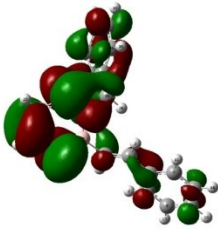
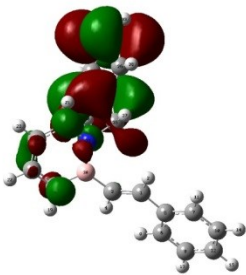
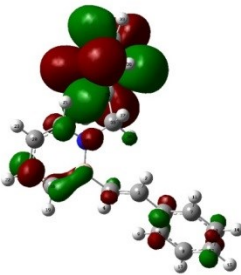
72 → 76 0.68394



orbitals

HOMO -4 (no 68) – 7.15 eV	HOMO -3 (no 69) – 6.98 eV	HOMO -2 (no 70) -6.95 eV

HOMO -1 (no 71) -6.50 eV	HOMO (no 72) -5.74 eV	LUMO (no 73) -1.47 eV
		

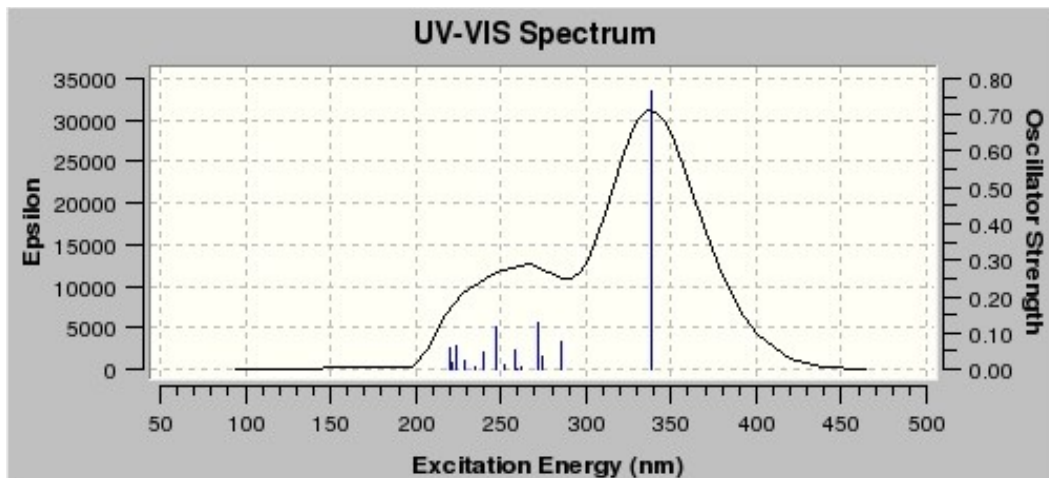
LUMO +1 (no 74) -0.84 eV	LUMO +2 (no 75) -0.66 eV	LUMO +3 (no 76) -0.57 eV
		

C₁₉H₁₈BN (R = H) in acetonitrile

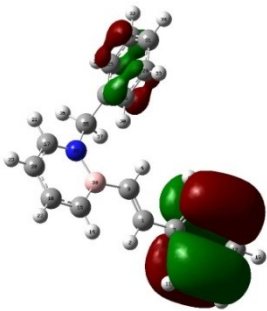
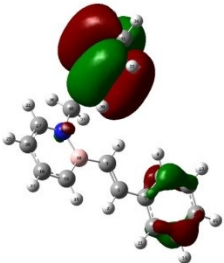
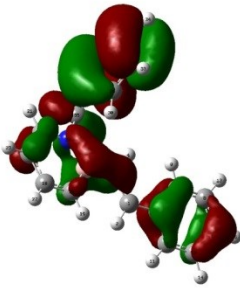
Excited	State 1	3.66 eV	338.5 nm	f=0.7657
72 →73	0.70286	HOMO→LUMO		
Excited	State 2	4.34 eV	285.9 nm	f=0.0752
72 →74	0.68399			
Excited	State 3	4.51 eV	274.8 nm	f=0.0356
68 →73	0.36164			
71 →73	0.37643			
71 →76	0.10504			
72 →75	0.25488			
72 →76	0.33436			
72 →77	0.10243			
Excited	State 4	4.55 eV	272.5 nm	f=0.1248
68 →73	-0.25875			
71 →73	0.56470			
72 →75	-0.24965			
72 →76	-0.12931			
Excited	State 5	4.73 eV	262.2 nm	f=0.0031
70 →73	-0.40383			

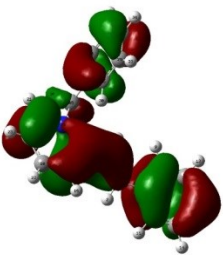
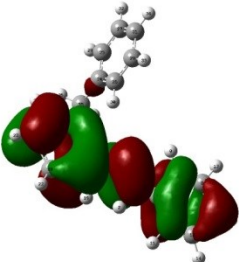
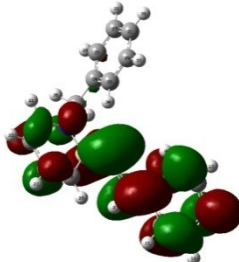
72 → 75 0.45388

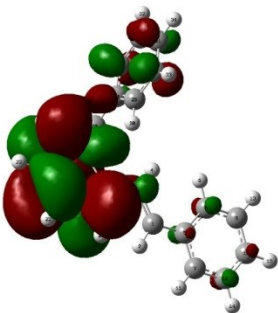
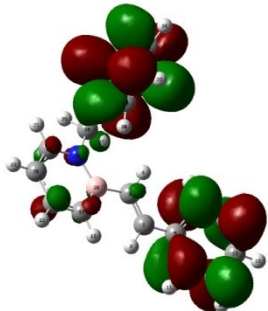
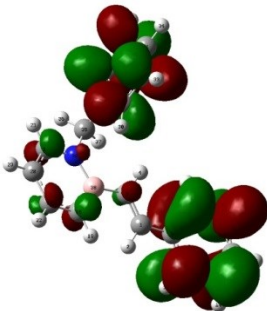
72 → 76 -0.33284



orbitals

HOMO -4 (no 68) -7.12 eV	HOMO -3 (no 69) -7.10 eV	HOMO -2 (no 70) -6.94 eV
		

HOMO -1 (no 71) - 6.71 eV	HOMO (no 72) -5.79 eV	LUMO (no 73) -1.68 eV
		

LUMO +1 (no 74) -0.94 eV	LUMO +2 (no 75) - 0.53 eV	LUMO +3 (no 76) - 0.49 eV
		

C₁₉H₁₇BNCF₃ (R = CF₃)

Excited	State 1	3.58 eV	346.6 nm	f=0.5725
88 → 89	0.70010	HOMO→LUMO		
Excited	State 2	4.40 eV	281.5 nm	f=0.0282
84 → 89	0.21421			
87 → 89	-0.10302			
88 → 90	0.55348	HOMO→LUMO+1		
88 → 91	0.31651			
Excited	State 3	4.45 eV	278.7 nm	f=0.1684
84 → 89	-0.15157			
87 → 89	0.50216	HOMO-1→LUMO		
88 → 90	0.32873			
88 → 91	-0.29800			
Excited	State 4	4.48 eV	276.8 nm	f=0.0504
84 → 89	0.24688			
86 → 89	0.22862			
87 → 89	0.41331	HOMO-1→LUMO		
88 → 90	-0.1994			
88 → 91	0.38124	HOMO→LUMO+2		

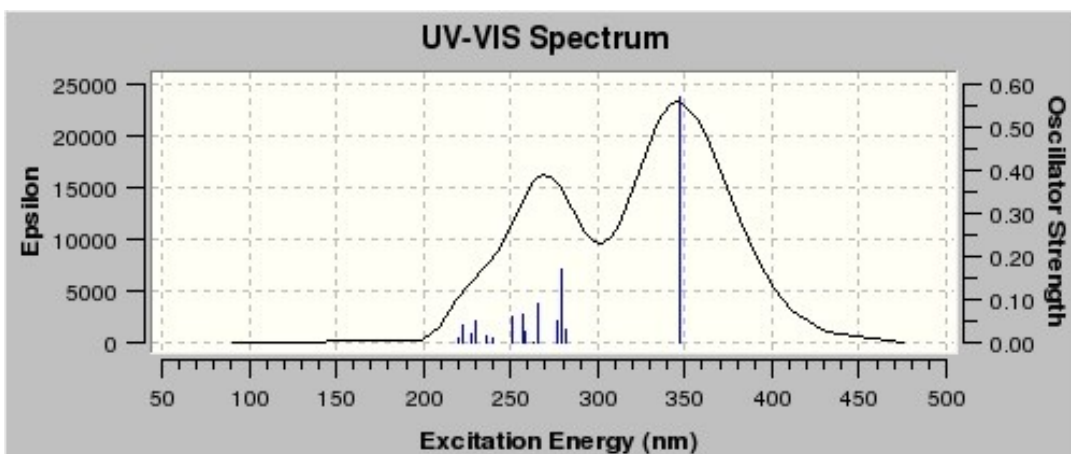
Excited State 5 4.66 eV 266.0 nm f=0.0877

85 → 89 -0.10997

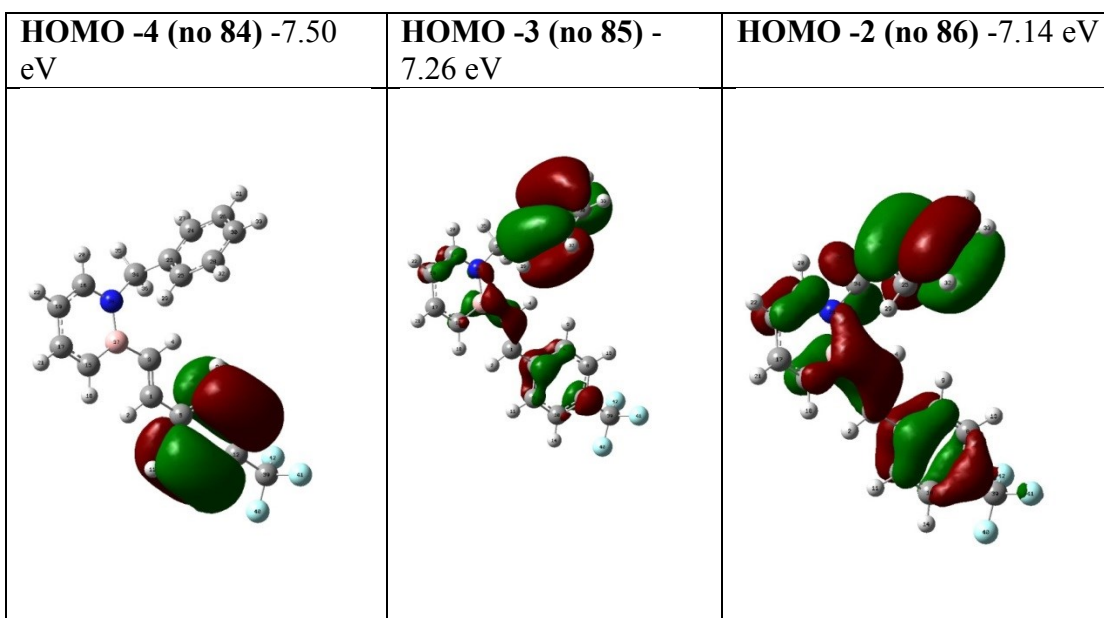
86 → 89 0.56023 HOMO-2→LUMO

87 → 89 -0.12798

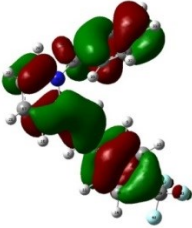
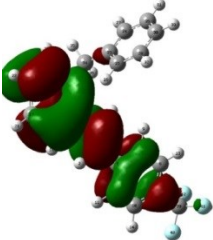
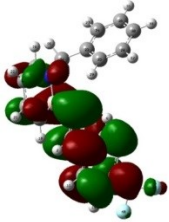
88 → 92 0.37789

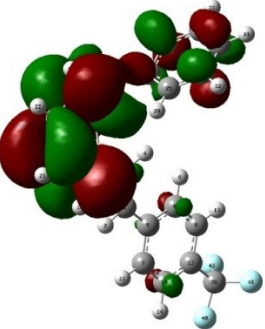
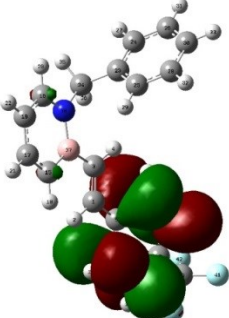
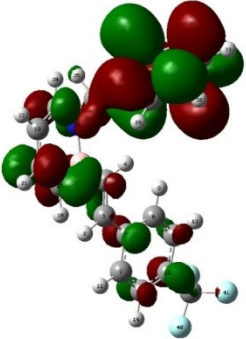


orbitals



--	--	--

HOMO -1 (no 87) -6.93 eV	HOMO (no 88) -5.97 eV	LUMO (no 89) -2.04 eV
		

LUMO +1 (no 90) -1.08 eV	LUMO +2 (no 91) -0.86 eV	LUMO +3 (no 92) -0.72 eV
		

C₁₉H₁₇BNCF₃ in acetonitrile

Excited State 1 3.48 eV 356.3 nm f=0.6944

88 → 89 0.7037 HOMO→LUMO

Excited State 2 4.35 eV 285.0 nm f=0.1039

87 → 89 0.68316 HOMO-1→LUMO

Excited State 3 4.40 eV 281.6 nm f=0.1191

83 → 89 0.1106

84 → 89 0.17462

87 → 89 0.12903

88 → 90 0.61148 HOMO→LUMO+1

88 → 91 0.22268

Excited State 4 4.46 eV 277.8 nm f=0.0288

84 → 89 0.31303

86 → 89 0.14972

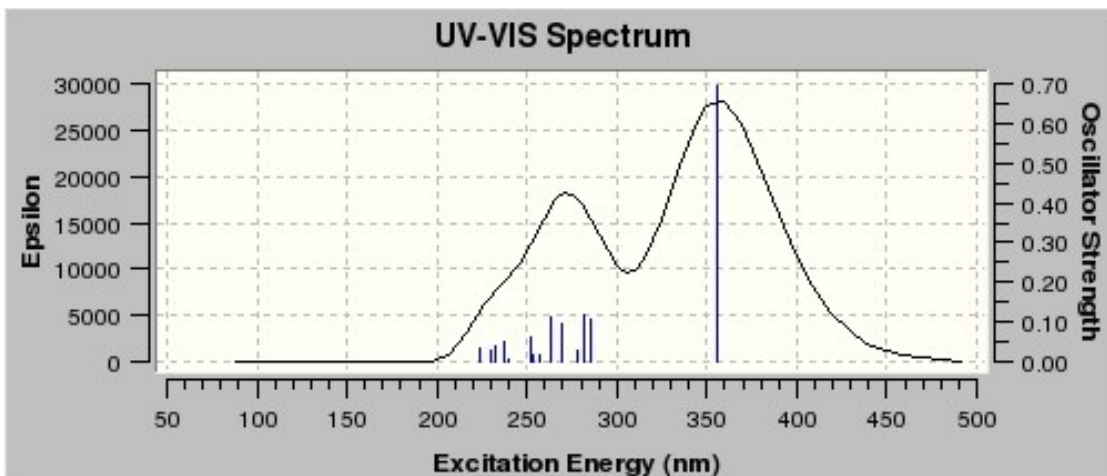
88 → 90 -0.27001

88 → 91 0.52061 HOMO→LUMO+2

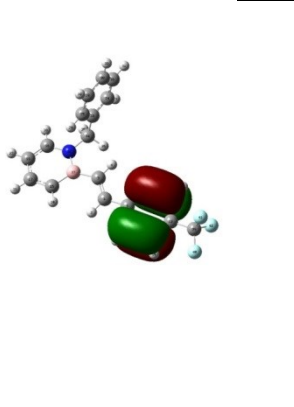
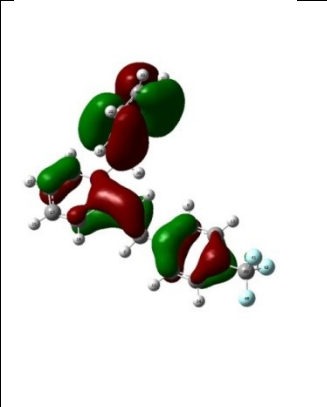
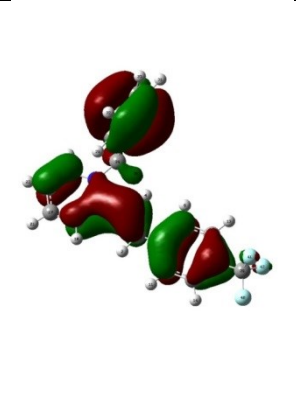
Excited State 5 4.59 eV 269.9 nm f=0.0956

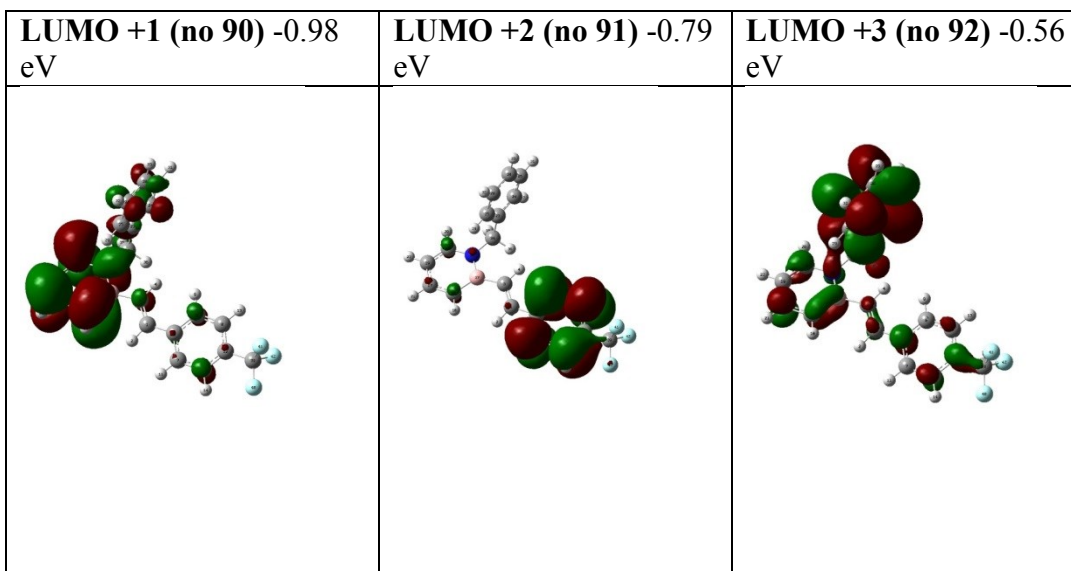
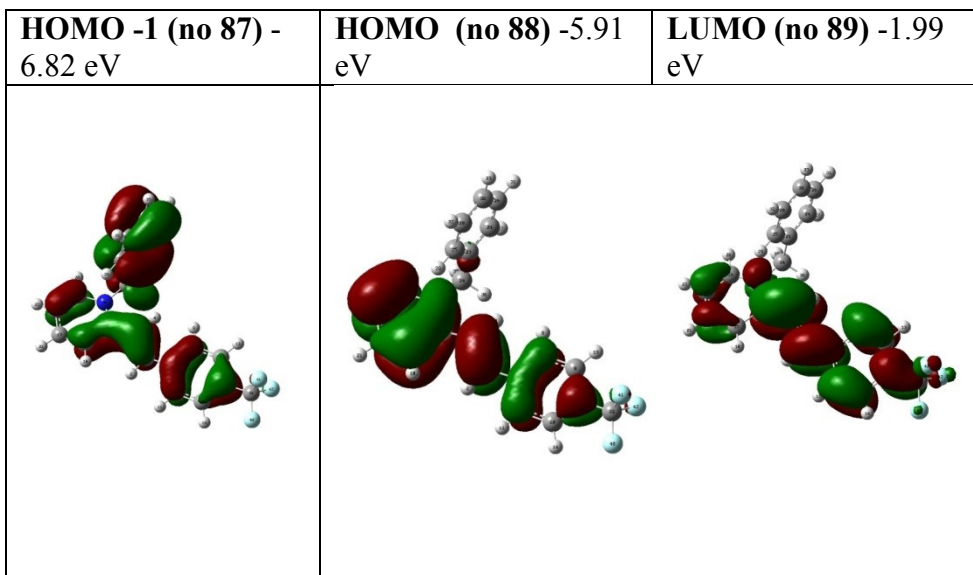
85 → 89 -0.21175

86 → 89 0.65139 HOMO-2→LUMO



Orbitals

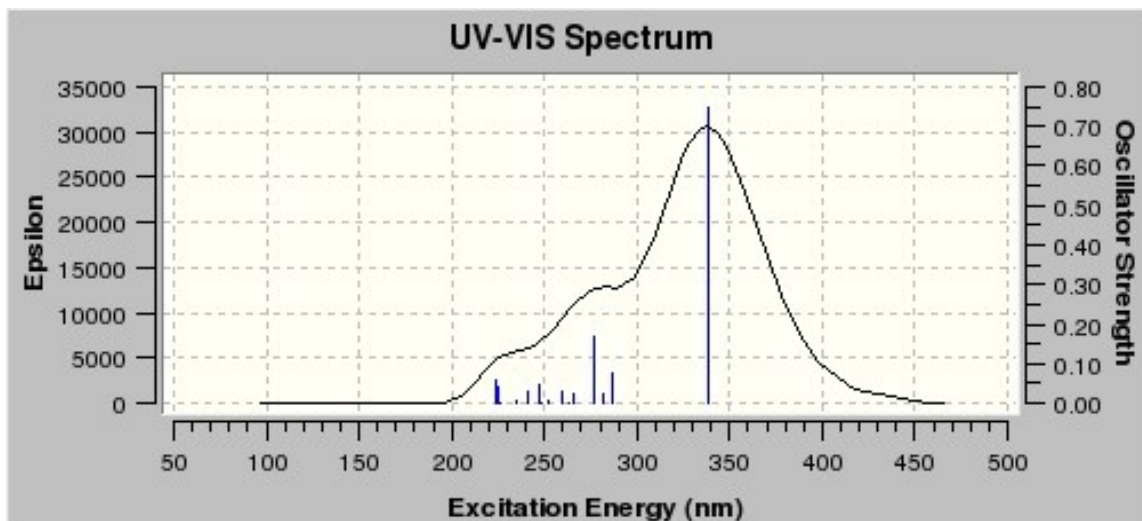
HOMO -4 (no 84) - 7.44 eV	HOMO -3 (no 85) - 7.14 eV	HOMO -2 (no 86) - 7.02 eV
		



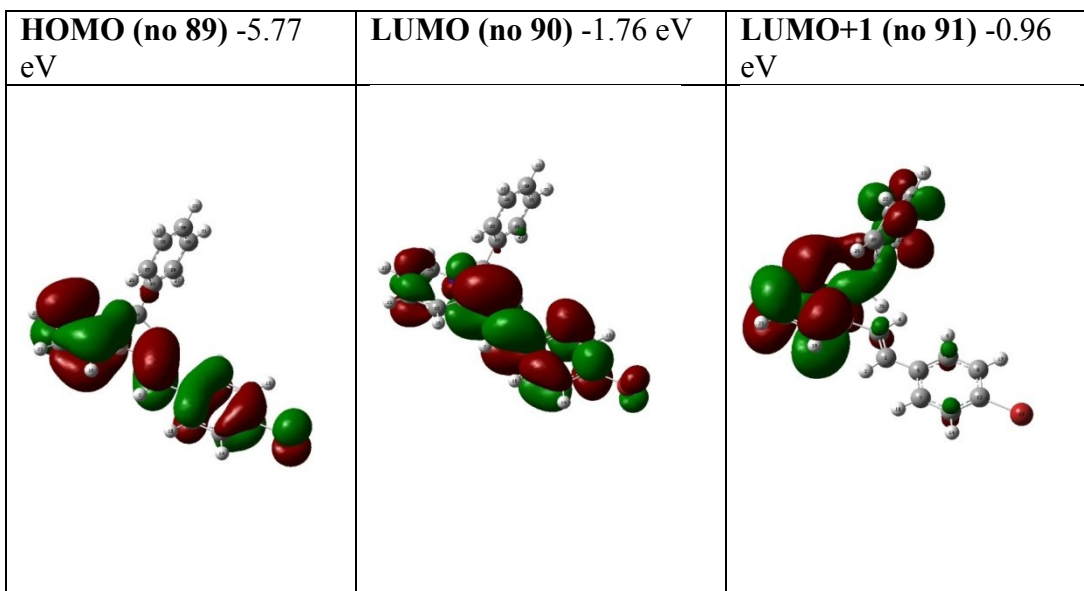
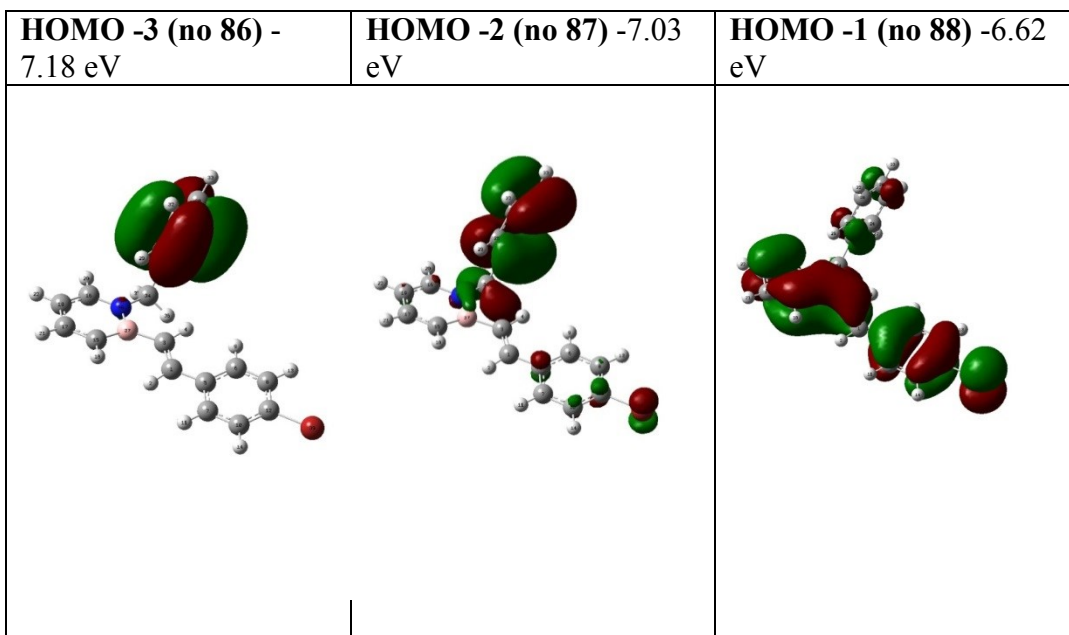
C₁₉H₁₇BNBr (R = Br)

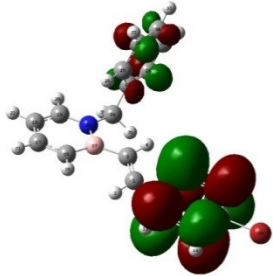
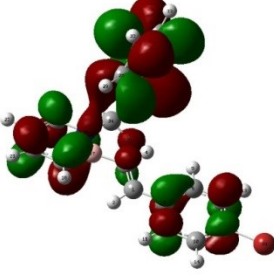
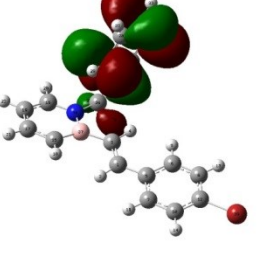
Excited	State 1	3.66 eV	338.3 nm	f=0.7466
89 →90	0.69897	HOMO→LUMO		
Excited	State 2	4.33 eV	286.3 nm	f=0.0750
88 →90	0.13574			
89 →91	0.65938			
89 →92	0.12170			
Excited	State 3	4.40 eV	281.9 nm	f=0.0259
85 →90	-0.25640			
88 →90	-0.38777			
88 →92	0.11510			
89 →92	0.48437			
89 →93	0.13937			
Excited	State 4	4.47 eV	277.1 nm	f=0.1660
85 →90	-0.16370			
88 →90	0.51541			
89 →91	-0.17937			
89 →92	0.35158			
89 →93	-0.15969			

Excited State 5 4.67 eV 265.4 nm f=0.0248
87 → 90 0.23559
88 → 90 0.15397
89 → 93 0.61370



Orbitals



LUMO +2 (no 92) -0.69 eV	LUMO +3 (no 93) -0.59 eV	LUMO +4 (no 94) -0.52 eV
		

C₁₉H₁₇BNCH₃ (R = CH₃)

Excited	State 1	3.76 eV	329.8 nm	f=0.7381
76 → 77	0.69866	HOMO → LUMO		
Excited	State 2	4.22 eV	293.7 nm	f=0.0391
76 → 78	0.69047	HOMO → LUMO+1		
Excited	State 3	4.45 eV	278.5 nm	f=0.0004
74 → 77	0.38524			
75 → 77	-0.1128			
75 → 81	-0.13482			
76 → 79	0.19470			

76 →81 0.50947 HOMO→LUMO+4

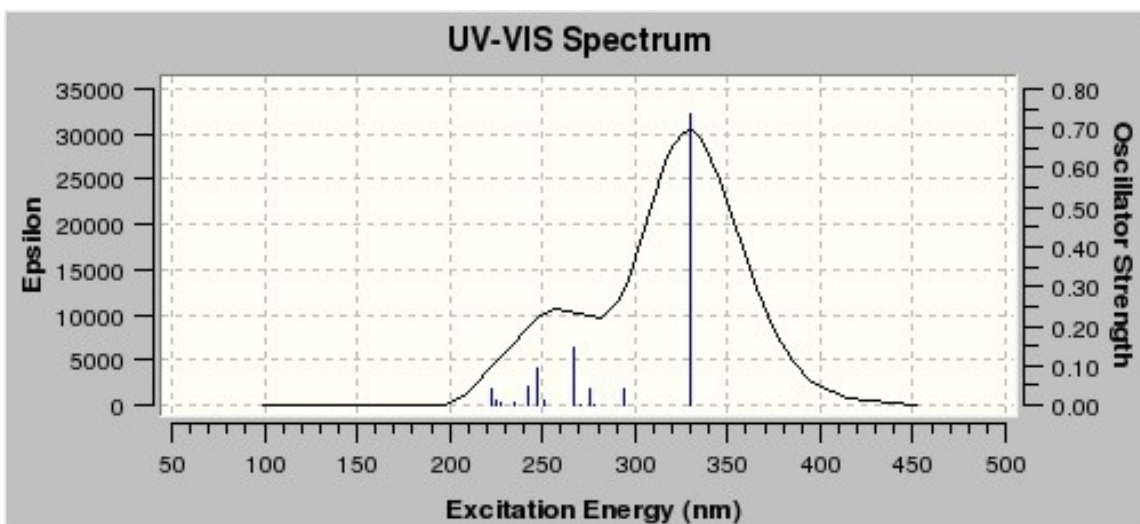
Excited State 4 4.50 eV 275.5 nm f=0.0400

75 →77 0.43525

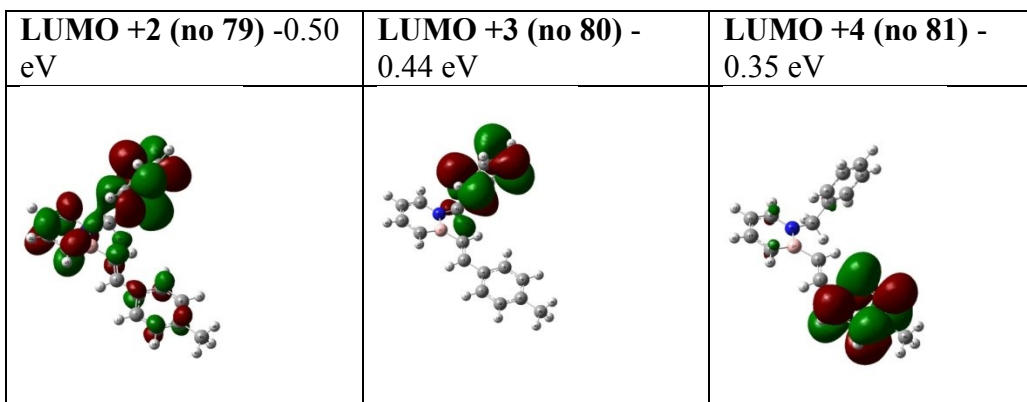
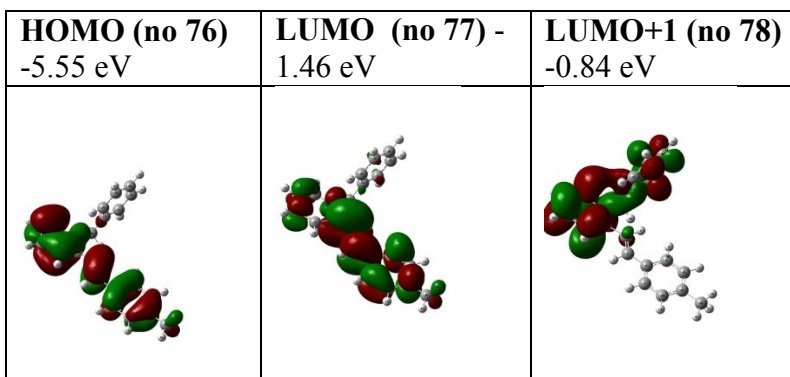
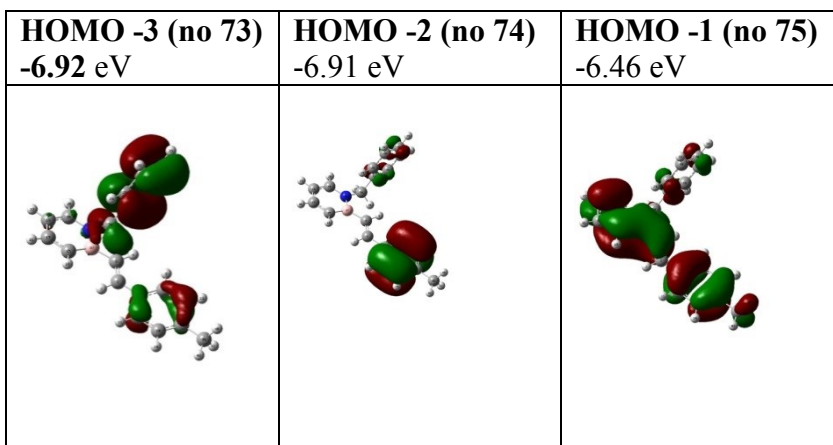
76 →79 0.53622 HOMO→LUMO+2

Excited State 5 4.58 eV 270.8 nm f=0.0003

76 →80 0.69857 HOMO→LUMO+3



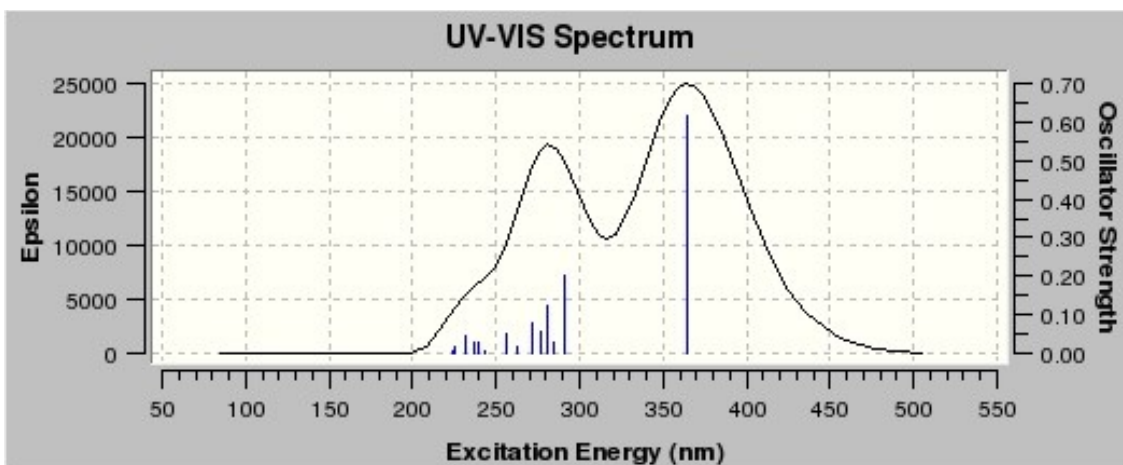
Orbitals



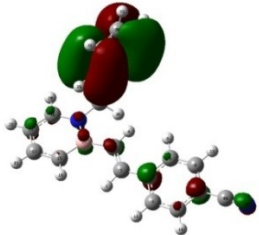
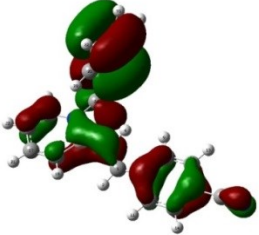
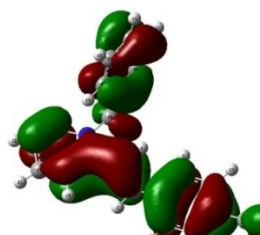
C₁₉H₁₇BNCN (R = CN)

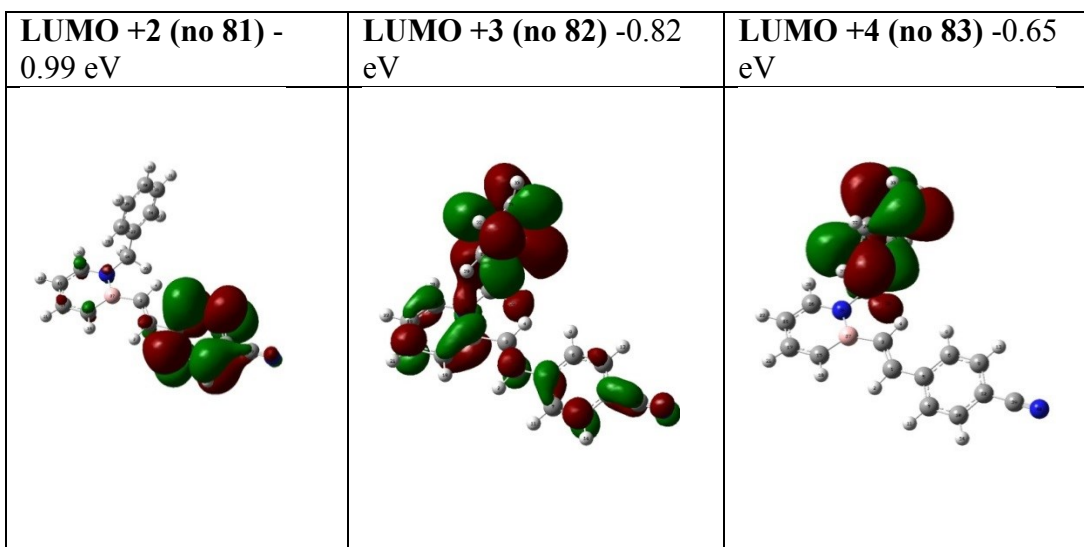
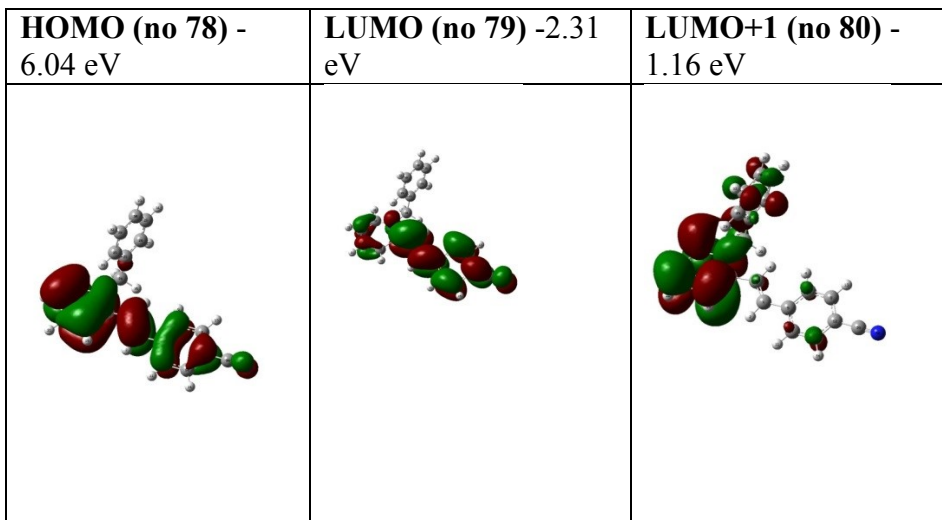
Excited	State 1	3.40 eV	365.0 nm	f=0.6135
78 →79	0.69986	HOMO→LUMO		
Excited	State 2	4.26 eV	291.1 nm	f=0.2021
76 →79	0.25085			
77 →79	0.63597			
78 →81	0.10580			
Excited	State 3	4.35 eV	284.8 nm	f=0.0282
74 →79	0.35432			
77 →81	0.12776			
78 →80	0.30666			
78 →81	0.48905			
Excited	State 4	4.41 eV	281.2 nm	f=0.1253
73 →79	0.10850			
76 →79	0.39862			
77 →79	-0.10719			
78 →80	0.49963			
78 →81	-0.20696			
Excited	State 5	4.48 eV	276.6 nm	f=0.0567

74 → 79 0.11094
 75 → 79 0.34583
 76 → 79 0.46387
 77 → 79 -0.15577
 78 → 80 -0.28122
 78 → 81 0.13452
 78 → 82 -0.12564



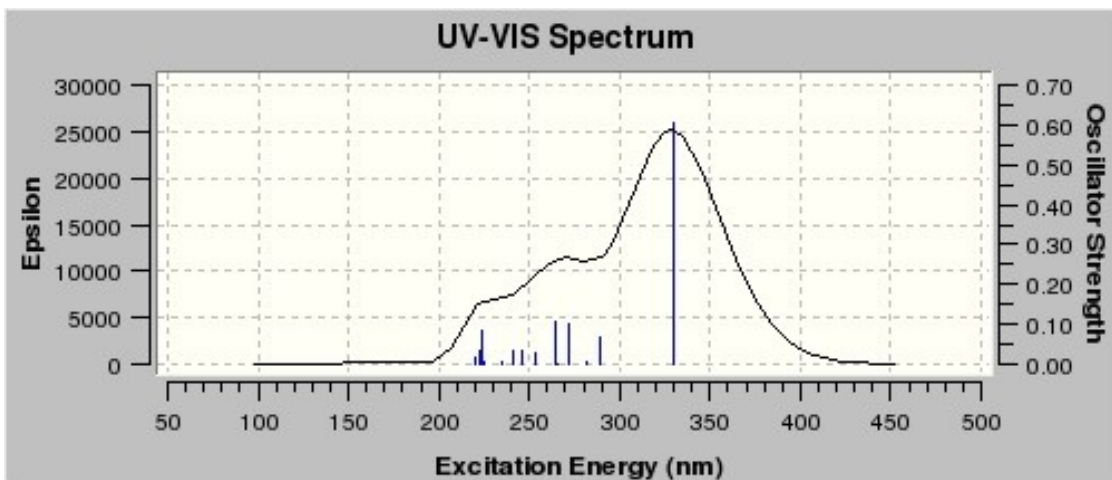
itals

HOMO -3 (no 75) - 7.30eV	HOMO -2 (no 76) - 7.17 eV	HOMO -1 (no 77) - 6.95 eV
		

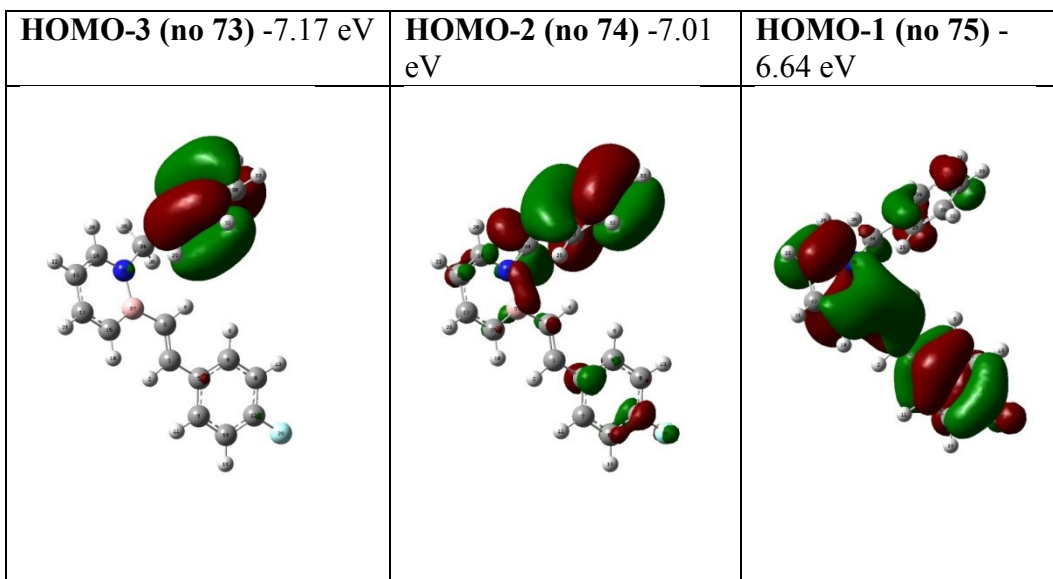


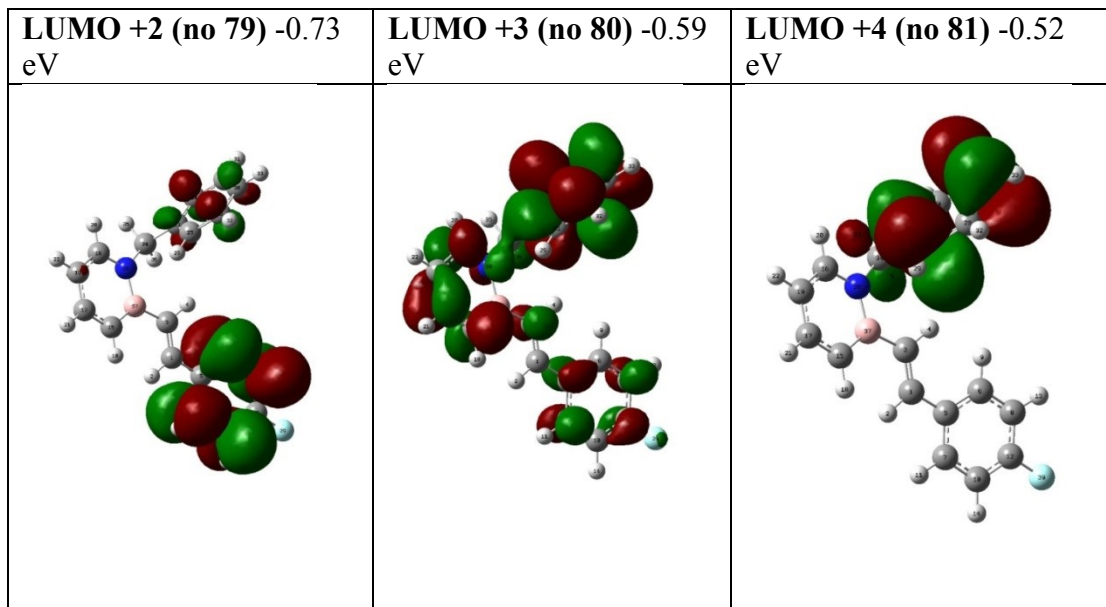
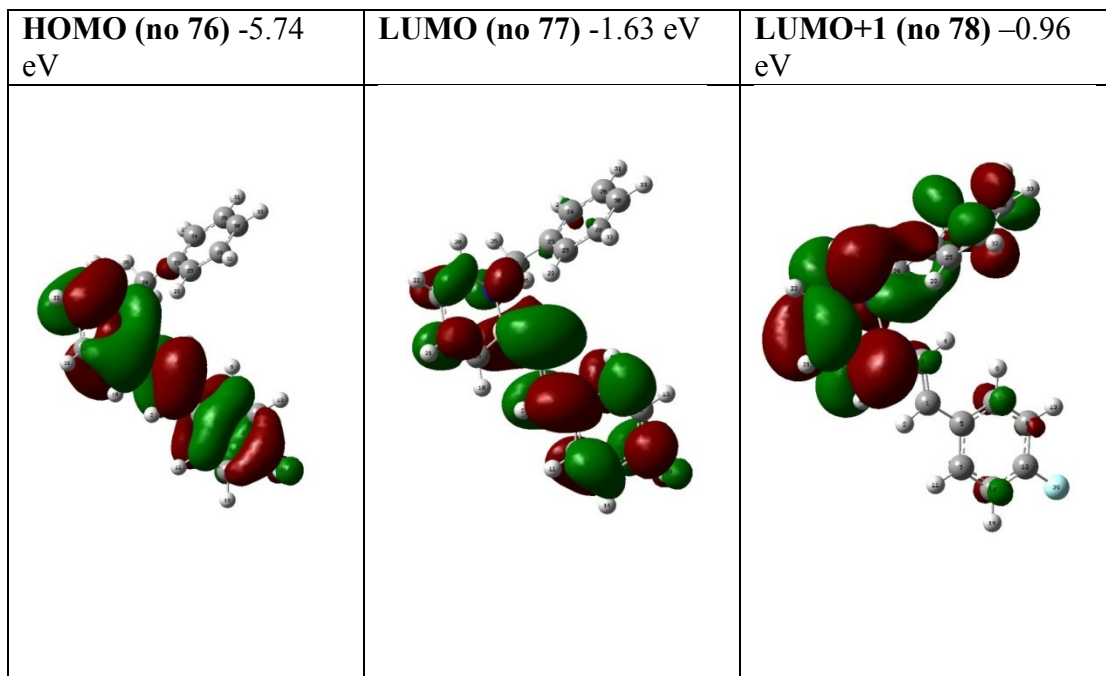
C₁₉H₁₇BNF (R = F)

Excited	State 1	3.76 eV	330.0 nm	f=0.6071
76 →77	0.69729	HOMO→LUMO		
Excited	State 2	4.29 eV	288.7 nm	f=0.0663
76 →78	0.67483	HOMO→LUMO+1		
76 →79	0.11332			
Excited	State 3	4.40 eV	281.7 nm	f=0.0040
72 →77	0.23520			
75 →77	-0.15578			
76 →78	-0.12734			
76 →79	0.61916	HOMO→LUMO+2		
Excited	State 4	4.56 eV	272.1 nm	f=0.0983
75 →77	0.51461	HOMO-1→LUMO		
76 →79	0.15423			
76 →80	0.43830			
Excited	State 5	4.67 eV	265.4 nm	f=0.0005
76 →81	0.69818	HOMO→LUMO+4		



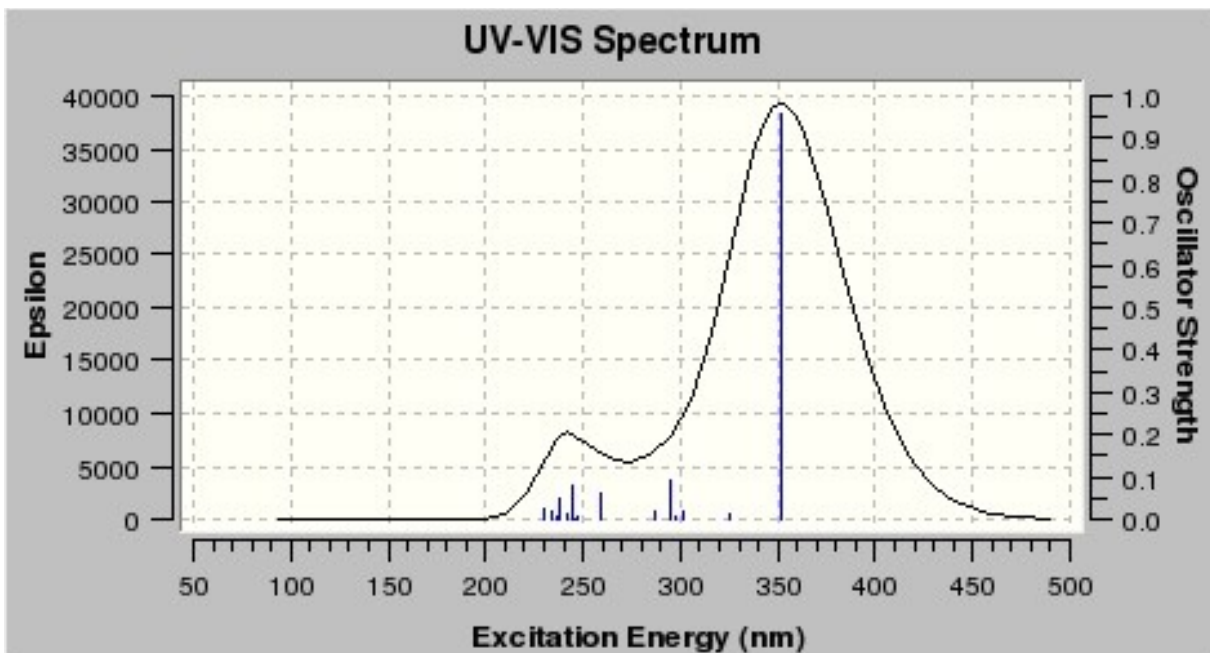
orbitals



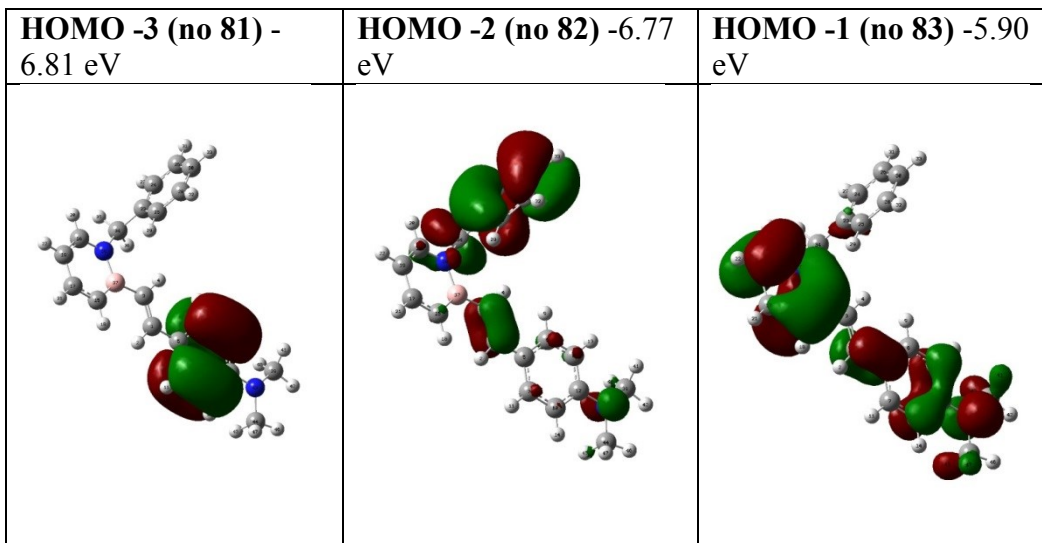


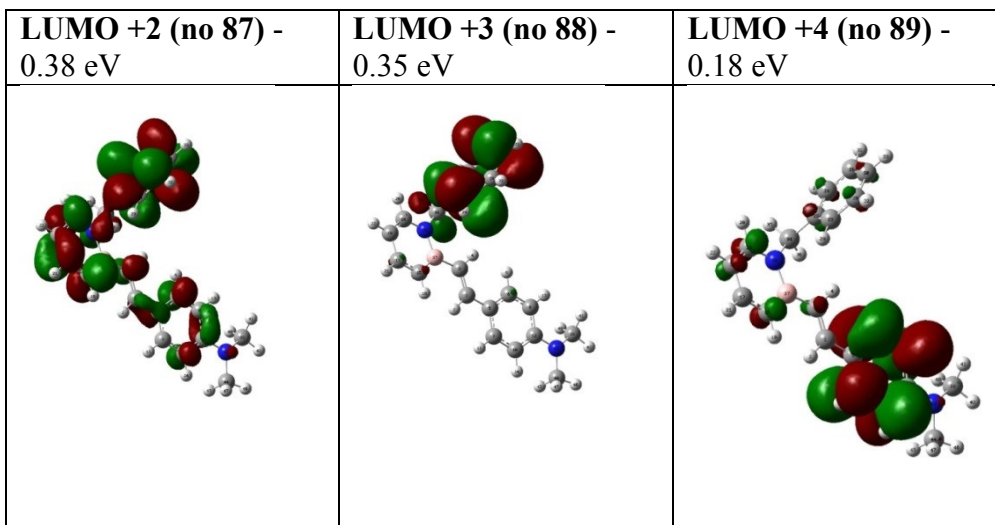
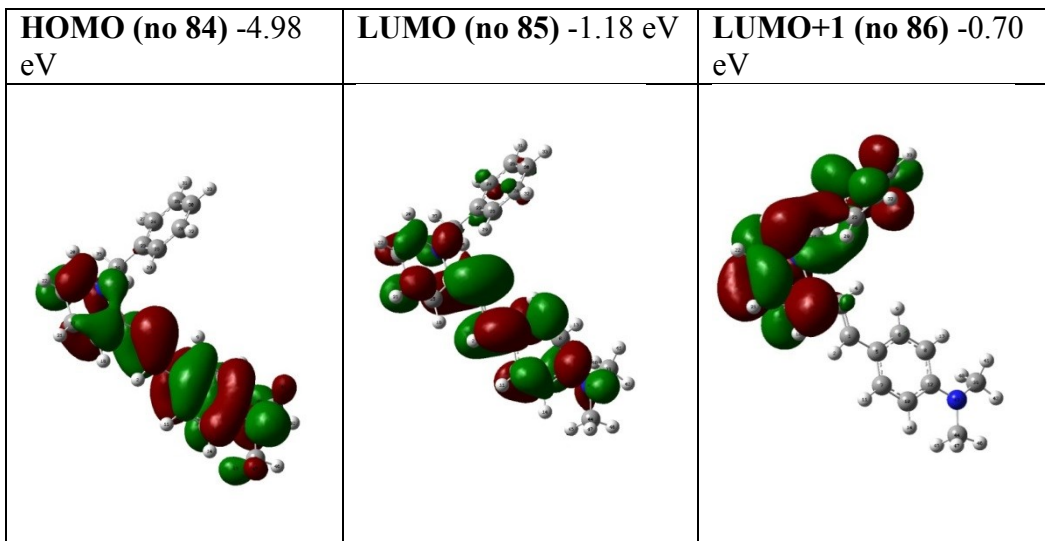
C₁₉H₁₇BNNMe₂ (R = NMe₂)

Excited	State 1	3.52 eV	352.4 nm	f=0.9587
84 →85	0.6996	HOMO→LUMO		
Excited	State 2	3.82 eV	324.9 nm	f=0.0104
84 →86	0.70009	HOMO→LUMO+1		
Excited	State 3	4.11 eV	301.8 nm	f=0.0176
81 →85	-0.14873			
84 →87	0.55088	HOMO→LUMO+2		
84 →88	-0.15245			
84 →89	-0.36588			
Excited	State 4	4.17 eV	297.1 nm	f=0.0059
84 →87	0.24426			
84 →88	0.64729	HOMO→LUMO+3		
Excited	State 5	4.20 eV	295.1 nm	f=0.0902
81 →85	0.1429			
83 →85	-0.3108			
84 →87	0.27532			
84 →88	-0.21903			
84 →89	0.49563	HOMO→LUMO+4		



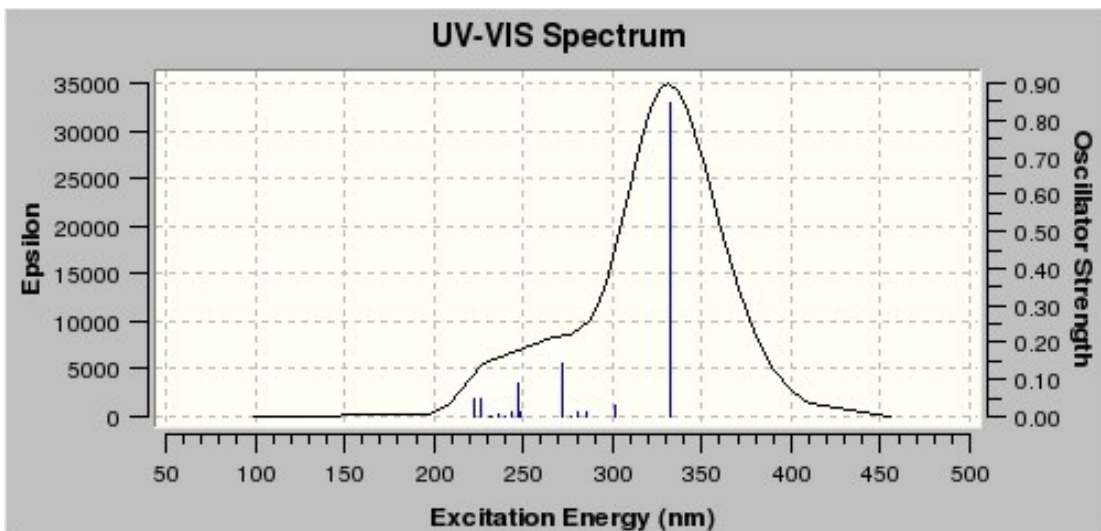
Orbitals



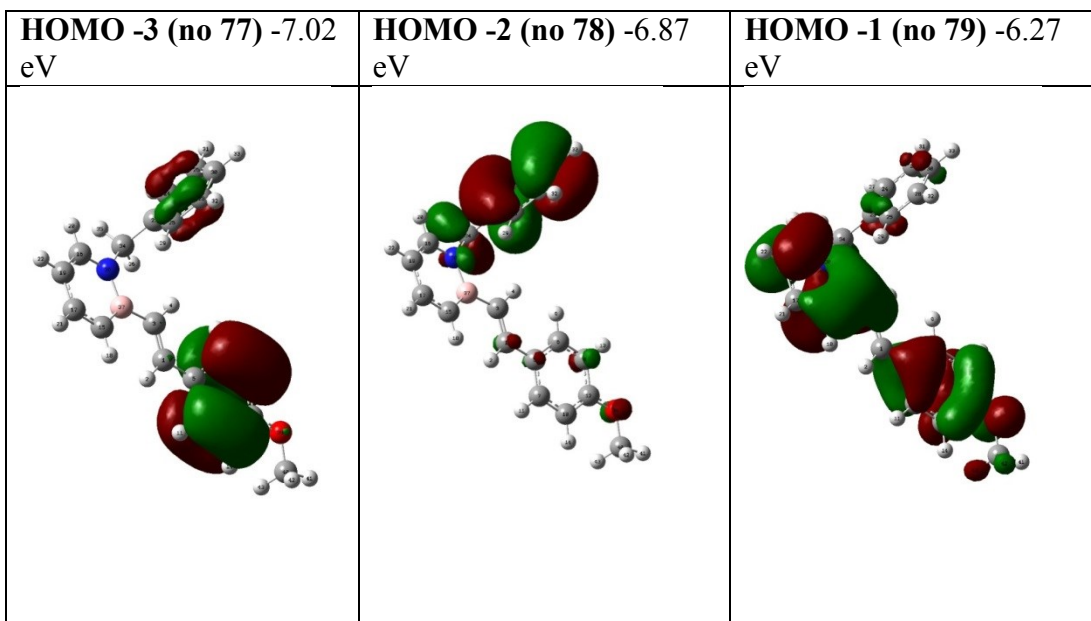


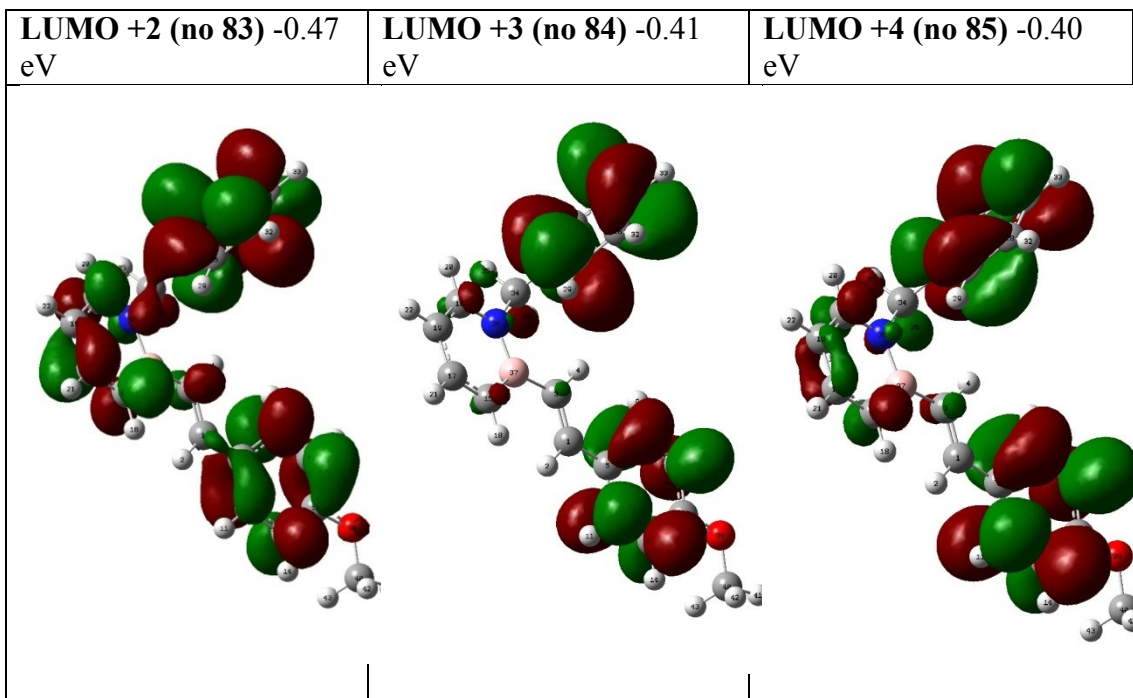
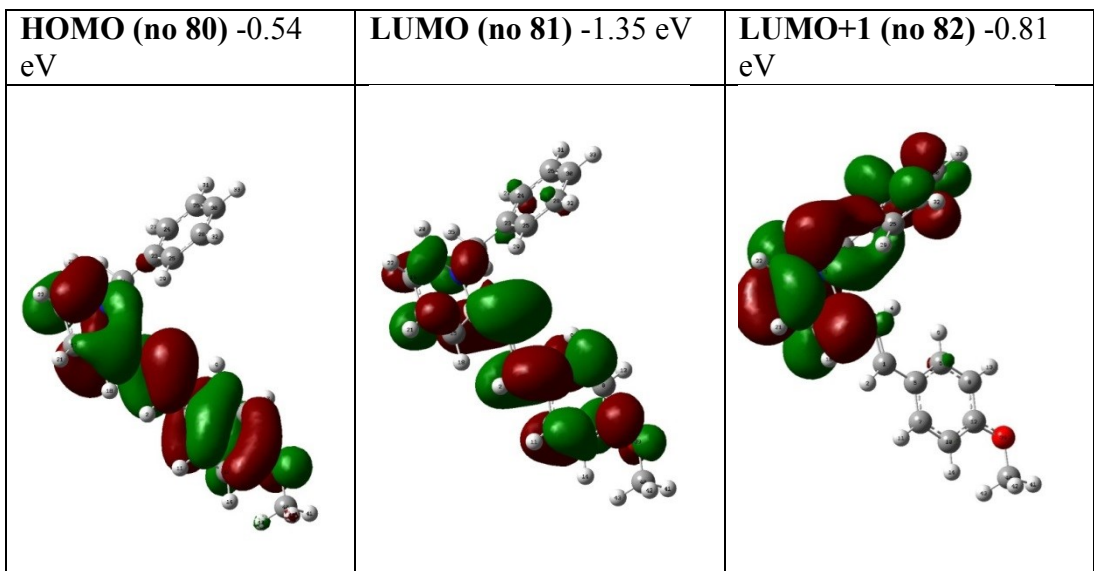
C₁₉H₁₈BNOCH₃ (R = OCH₃)

Excited	State 1	3.73 eV	332.0 nm	f=0.8456
80 →81	0.69799	HOMO→LUMO		
Excited	State 2	4.11 eV	301.8 nm	f=0.0280
80 →82	0.69466	HOMO→LUMO+1		
Excited	State 3	4.34 eV	285.7 nm	f=0.0148
77 →81	-0.24061			
79 →81	0.16000			
80 →83	0.40004	HOMO→LUMO+2		
80 →84	0.31879	HOMO→LUMO+3		
80 →85	0.36240	HOMO→LUMO+4		
Excited	State 4	4.41 eV	281.1 nm	f=0.0102
80 →81	-0.44746			
80 →83	0.47700			
80 →84	-0.12886			
80 →85	-0.20914			
Excited	State 5	4.48 eV	276.5 nm	f=0.0001
80 →84	0.56157			
80 →85	-0.41997			



Orbitals



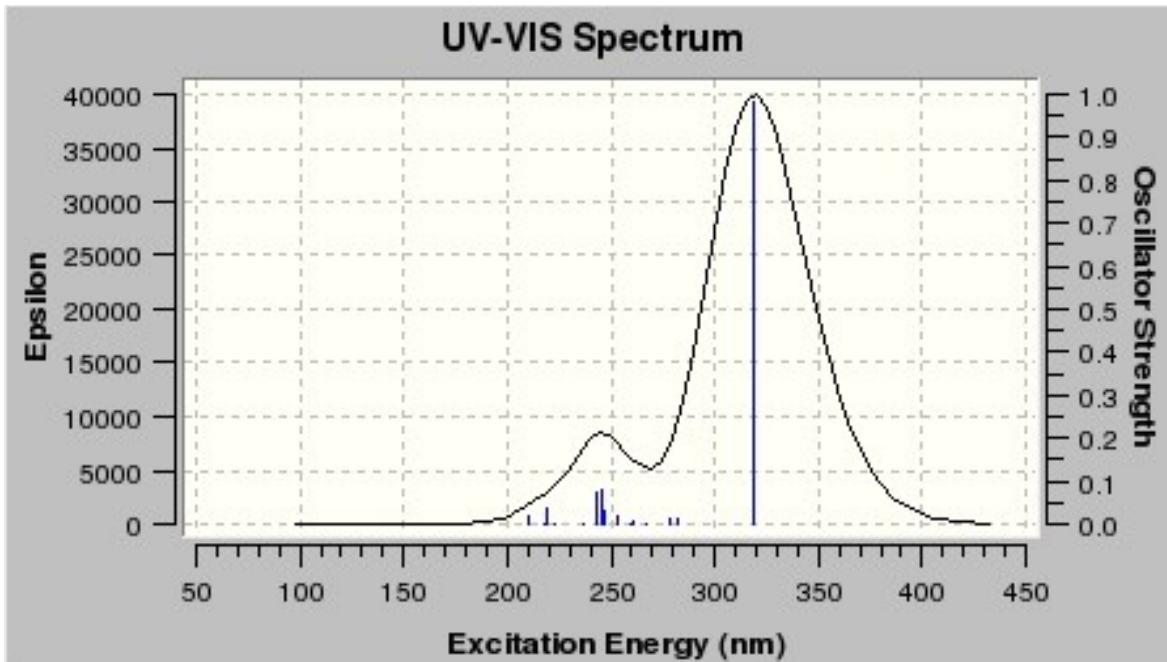


Hydrocarbon C₂₁H₁₈ (R = H)

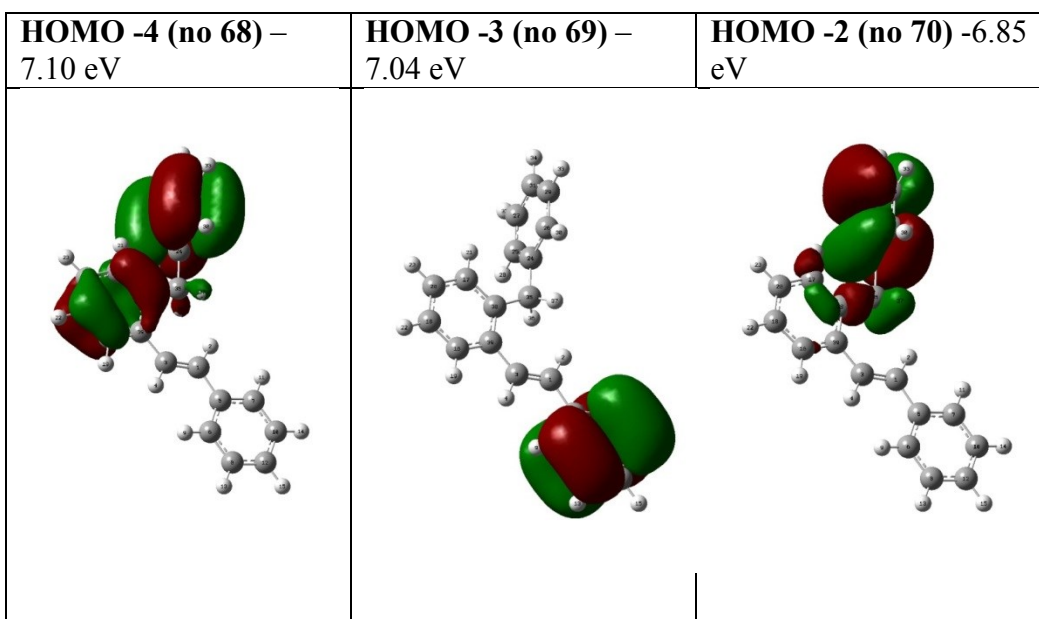
Excited	State 1	3.84 eV	323.2 nm	f=0.7749
72 →73	0.70203	HOMO→LUMO		
Excited	State 2	4.39 eV	282.7 nm	f=0.0165
70 →73	-0.34212			
71 →73	0.44438	HOMO -1→LUMO		
72 →74	0.34431			
72 →77	0.19074			
Excited	State 3	4.47 eV	277.2 nm	f=0.0078
68 →73	0.48448	HOMO -4→LUMO +1		
72 →75	0.47054	HOMO→LUMO +3		
Excited	State 4	4.51 eV	275.1 nm	f=0.0000
70 →73	0.36247			
71 →73	0.53334	HOMO -1→LUMO		
72 →74	-0.23816			
Excited	State 5	4.73 eV	262.2 nm	f=0.0188
69 →73	-0.28448			
70 →73	0.37869			
72 →74	0.45901	HOMO→LUMO +1		

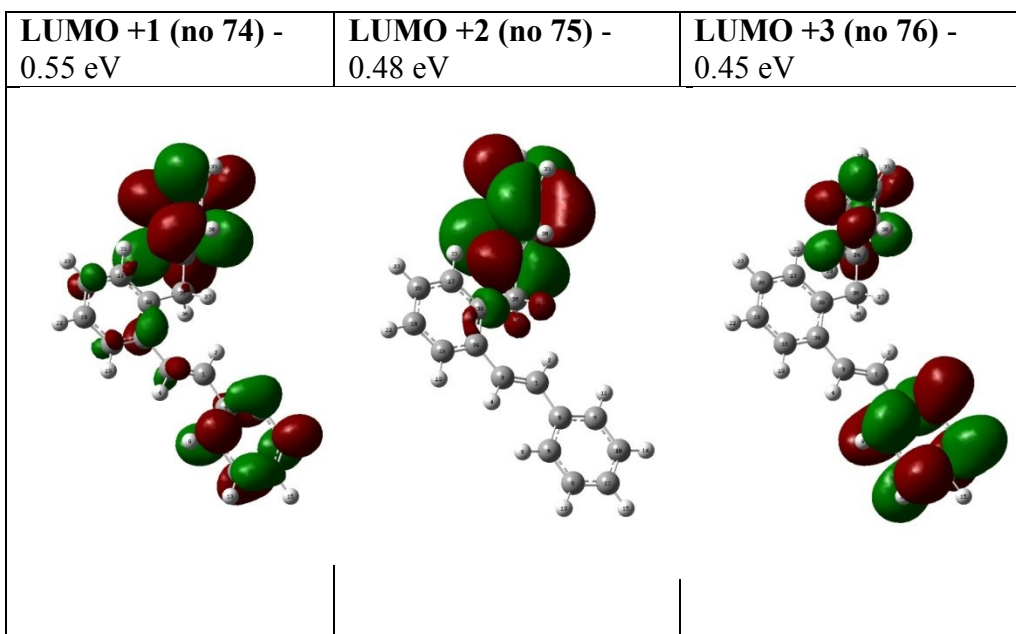
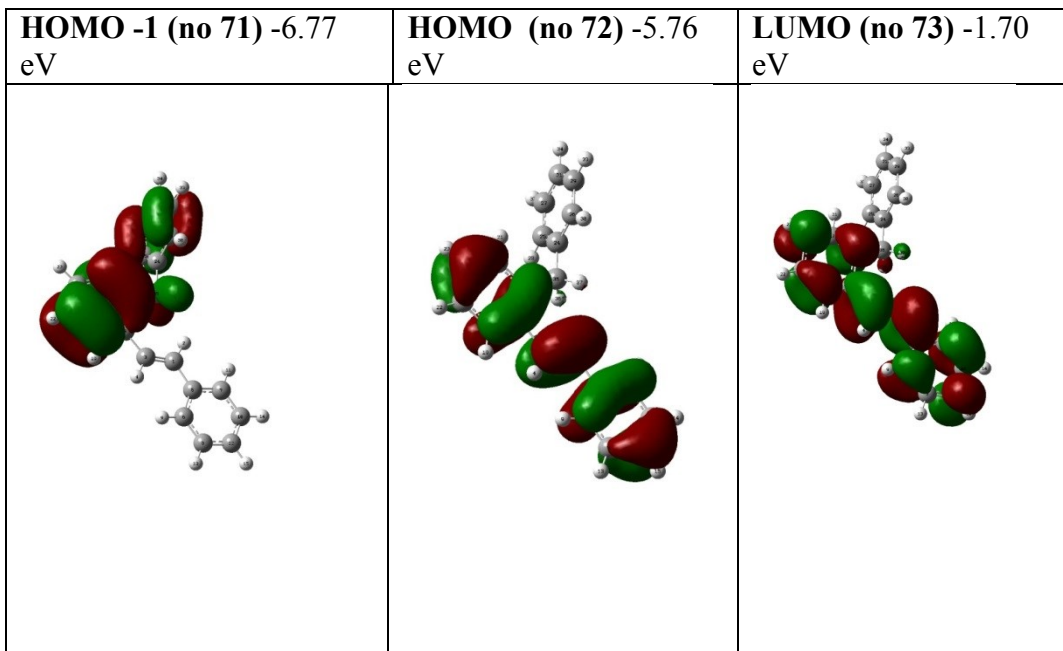
72 → 76 -0.10722

72 → 77 -0.18635



Orbitals





Hydrocarbon C₂₁H₁₈ (R = H) in Acetonitrile

Excited	State 1	3.72 eV	333.1 nm	f=0.9340
72 →73	0.70441	HOMO→LUMO		
Excited	State 2	4.37 eV	283.8 nm	f=0.0123
70 →73	-0.30698			
71 →73	0.54457	HOMO -1→LUMO		
72 →74	0.25263			
72 →77	0.15273			
Excited	State 3	4.47 eV	277.1 nm	f=0.0029
68 →73	-0.12952			
69 →73	0.10636			
70 →73	0.43648	HOMO -2→LUMO		
71 →73	0.42079	HOMO -1→LUMO		
72 →74	-0.26576			
72 →75	-0.10314			
72 →77	-0.11258			
Excited	State 4	4.49 eV	276.3 nm	f=0.0068
68 →73	0.46291	HOMO -4→LUMO		
70 →73	0.14058			
71 →73	0.12384			

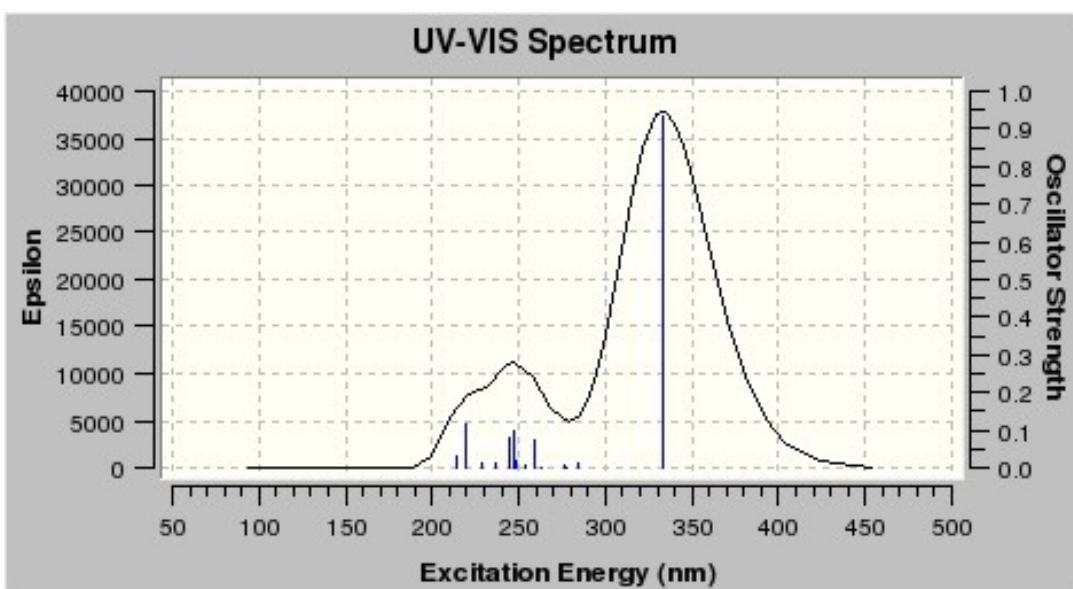
72 →75 0.48222 HOMO→LUMO +2

Excited State 5 4.72 eV 262.5 nm f=0.0013


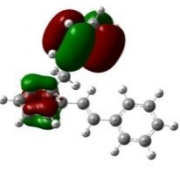
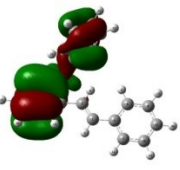
69 →73 0.61755 HOMO -3→LUMO

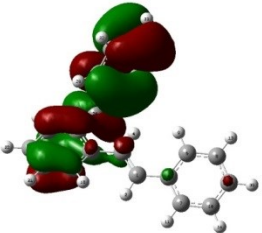
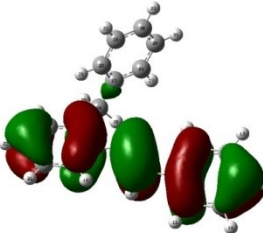
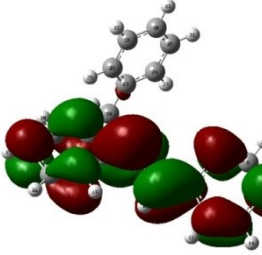
70 →73 -0.26481

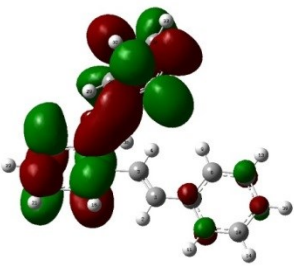
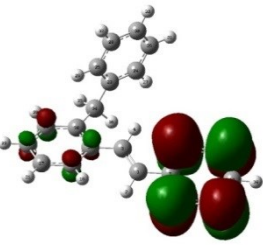
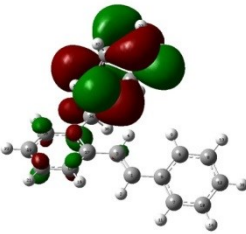
72 →74 -0.19674



Orbitals

HOMO -4 (no 68) -7.13 eV	HOMO -3 (no 69) -7.04 eV	HOMO -2 (no 70) -6.95 eV
		

HOMO -1 (no 71) -6.77 eV	HOMO (no 72) -5.87 eV	LUMO (no 73) -1.77 eV
		

LUMO +1 (no 74) -0.61 eV	LUMO +2 (no 75) -0.52 eV	LUMO +3 (no 76) -0.45 eV
		

Hydrocarbon C₂₁H₁₇CF₃ (R = CF₃)

Excited State 1 3.75 eV 330.4 nm f=0.8264

88 → 89 0.70118 HOMO→LUMO

Excited State 2 4.19 eV 296.1 nm f=0.0224

87 → 89 0.68794 HOMO-1→LUMO

Excited State 3 4.33 eV 286.25 nm f=0.0076

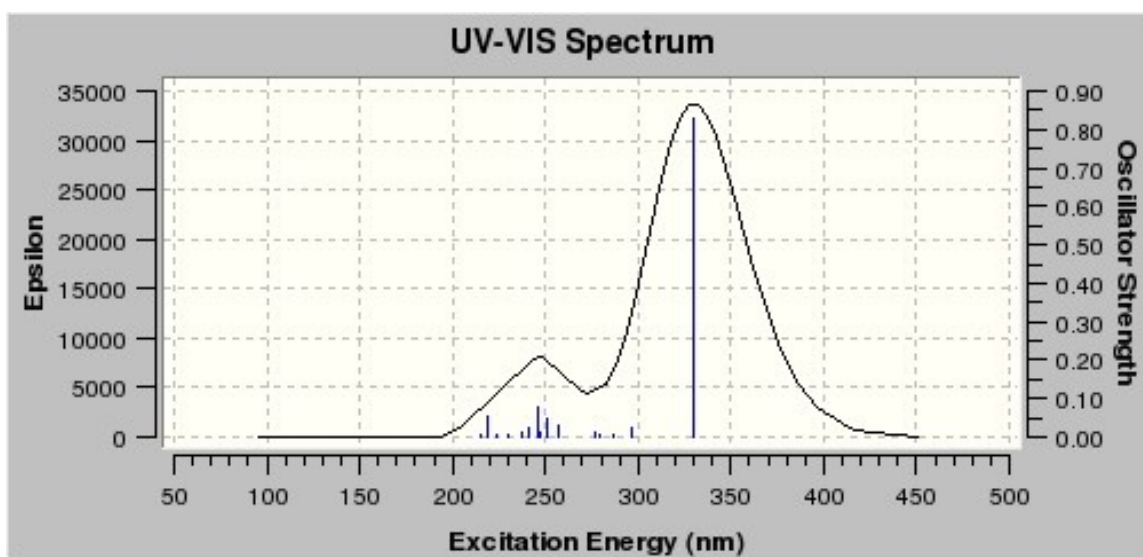
85 → 89 -0.35873

86 → 89 0.51997 HOMO-2→LUMO

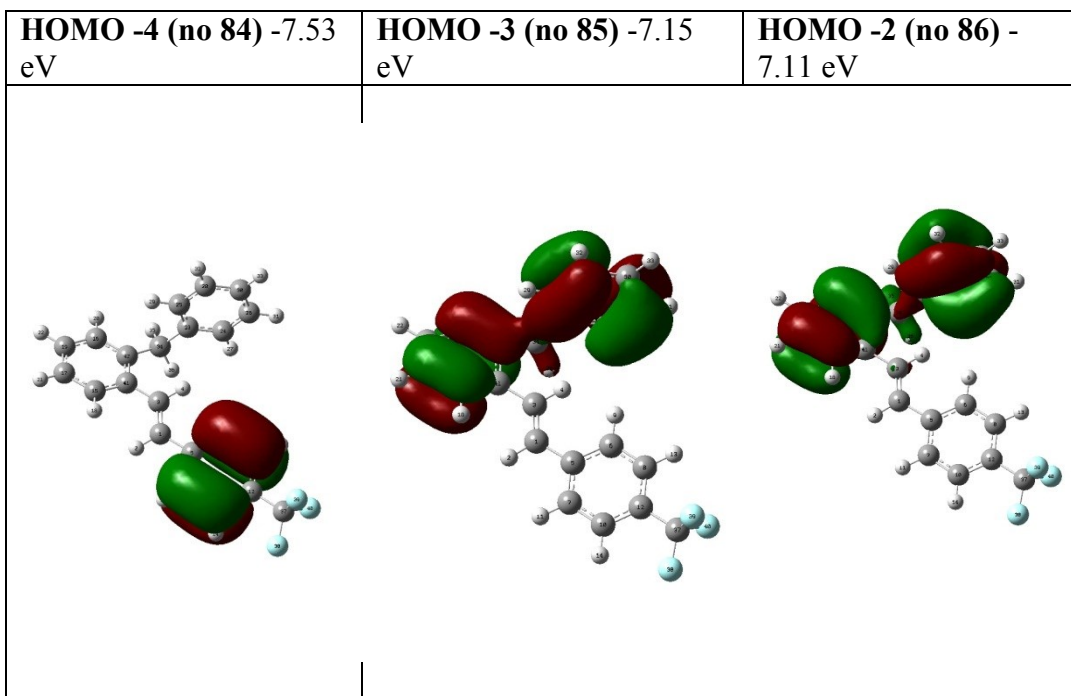
87 → 89 0.13116

88 → 91 -0.2135

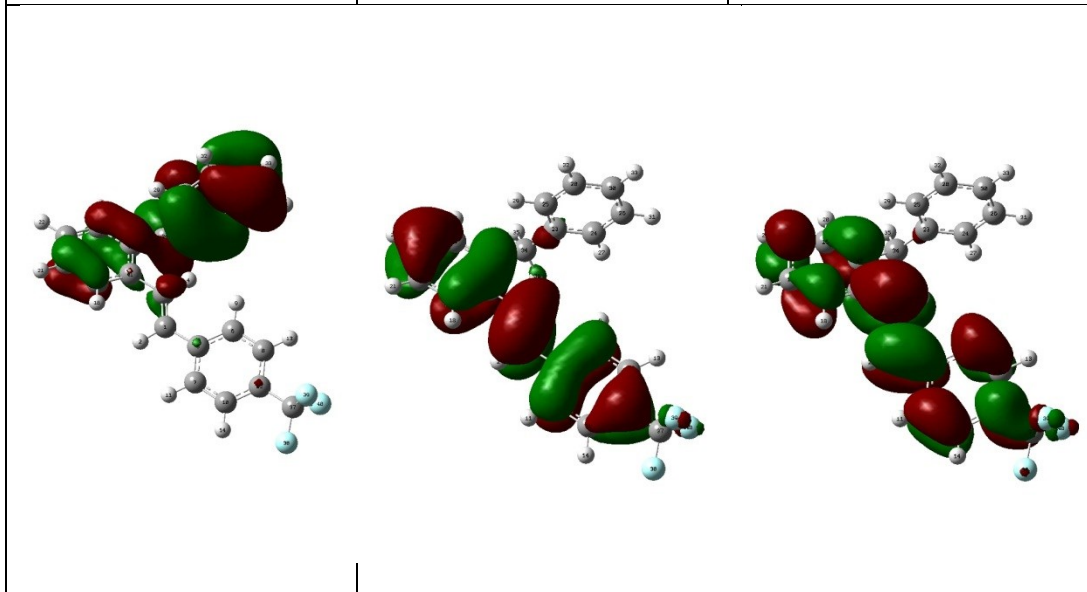
88 → 94 -0.12905



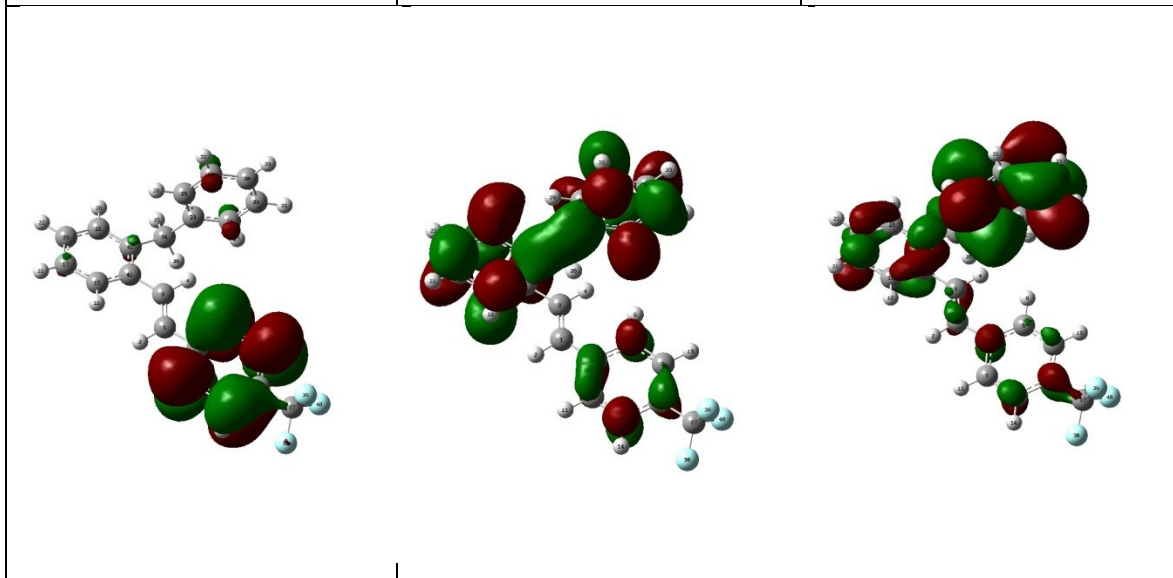
Orbitals



HOMO -1 (no 87) -6.90 eV	HOMO (no 88) -6.15 eV	LUMO (no 89) -2.14 eV
---------------------------------	------------------------------	------------------------------



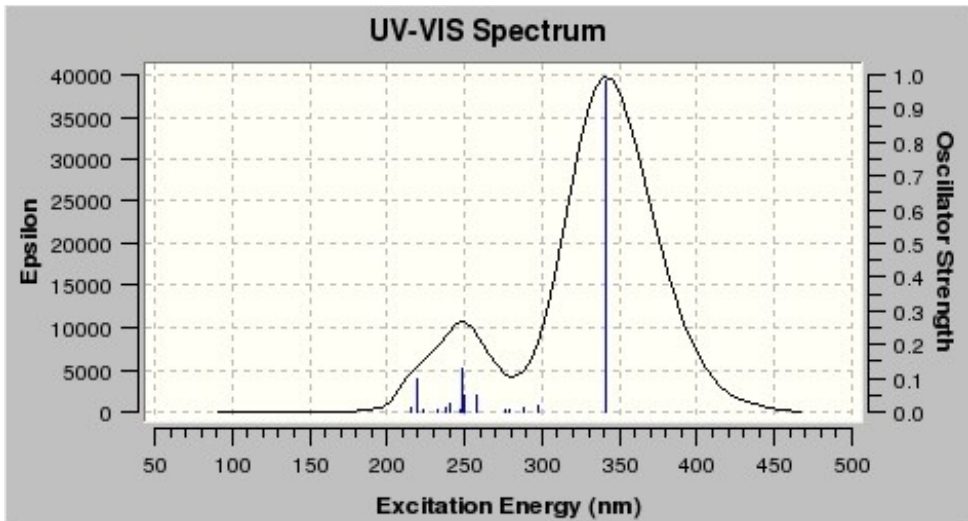
LUMO +1 (no 90) -0.90 eV	LUMO +2 (no 91) -0.77 eV	LUMO +3 (no 92) -0.59 eV
---------------------------------	---------------------------------	---------------------------------



C₂₁H₁₇CF₃ in acetonitrile

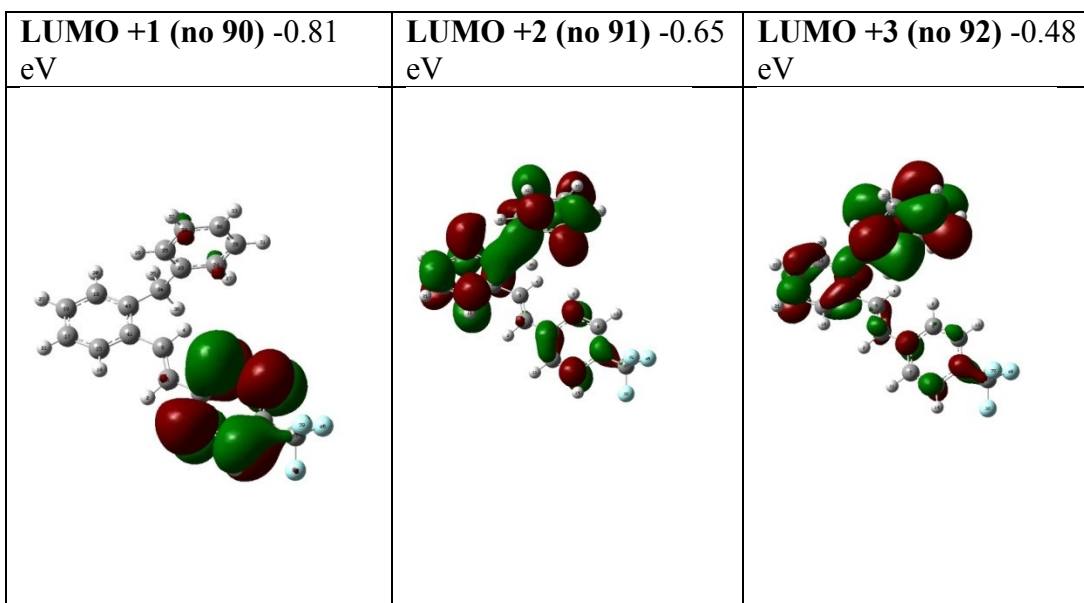
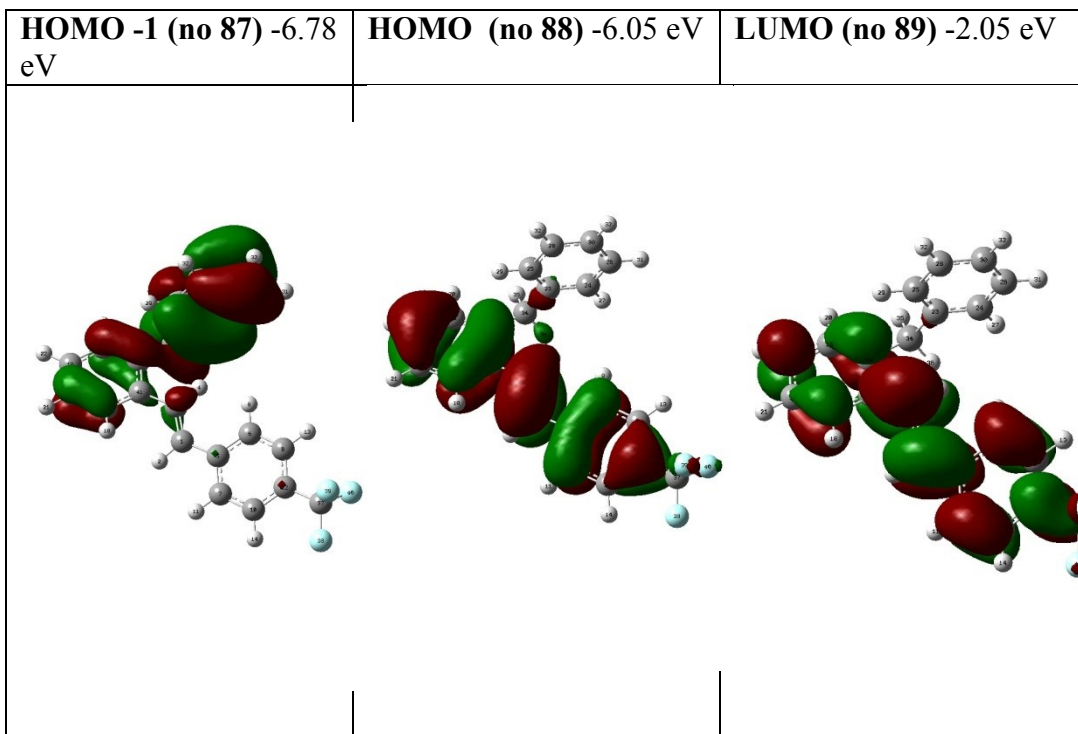
Excited	State 1	3.63 eV	341.7 nm	f=0.9788
88 → 89	0.70423	HOMO→LUMO		
Excited	State 2	4.16 eV	297.7 nm	f=0.0183
86 → 89	0.10245			
87 → 89	0.68758	HOMO-1→LUMO		
Excited	State 3	4.31 eV	287.7 nm	f=0.0114
85 → 89	0.17169			
86 → 89	0.62239	HOMO-2→LUMO		
87 → 90	-0.14015			
88 → 91	-0.17632			
88 → 94	0.12301			
Excited	State 4	4.45 eV	278.8 nm	f=0.0064
84 → 89	-0.40517			
85 → 89	0.13536			
88 → 90	0.54128	HOMO→LUMO+1		
Excited	State 5	4.48 eV	276.9 nm	f=0.0091
85 → 89	0.65945	HOMO-3→LUMO		
86 → 89	-0.19767			

88 → 90 -0.10595



acn.C₂₁H₁₈.CF₃

HOMO -4 (no 84) - 7.44 eV	HOMO -3 (no 85) - 7.06 eV	HOMO -2 (no 86) -6.99 eV



Hydrocarbon C₂₁H₁₇Br (R = Br)

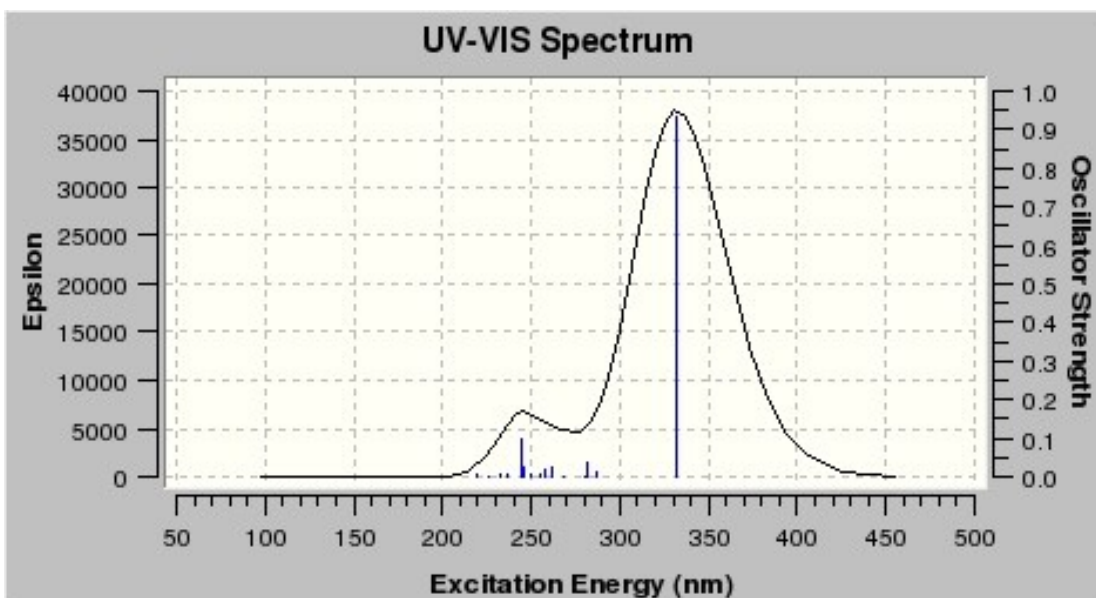
Excited	State 1	3.73 eV	332.4 nm	f=0.9351
89 →90	0.0.70259	HOMO→LUMO		

Excited	State 2	4.32 eV	287.1 nm	f=0.0112
86 →90	0.11333			
87 →90	0.19131			
88 →90	0.61473			
89 →92	0.19701			
89 →94	-0.13013			

Excited	State 3	4.40 eV	282.1 nm	f=0.0343
84 →90	-0.34856			
89 →91	0.59444			

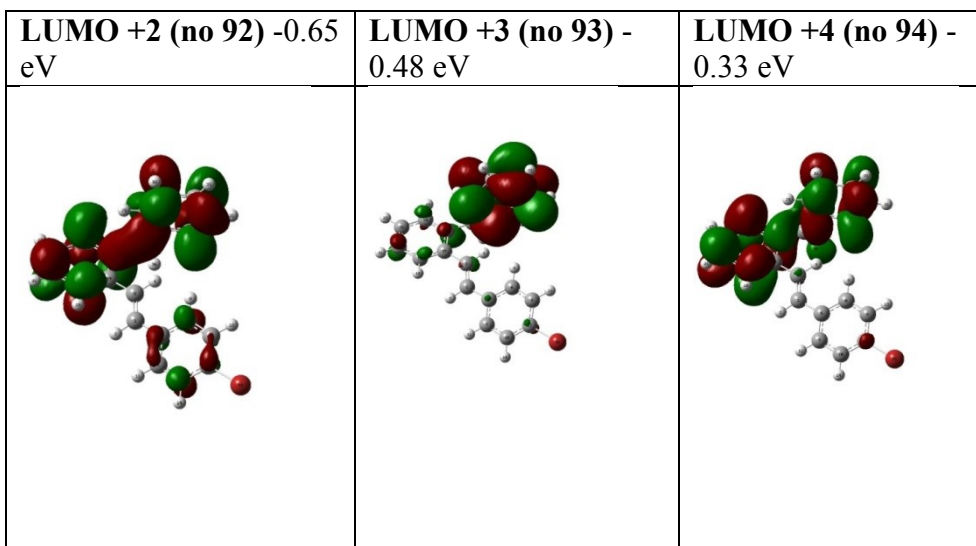
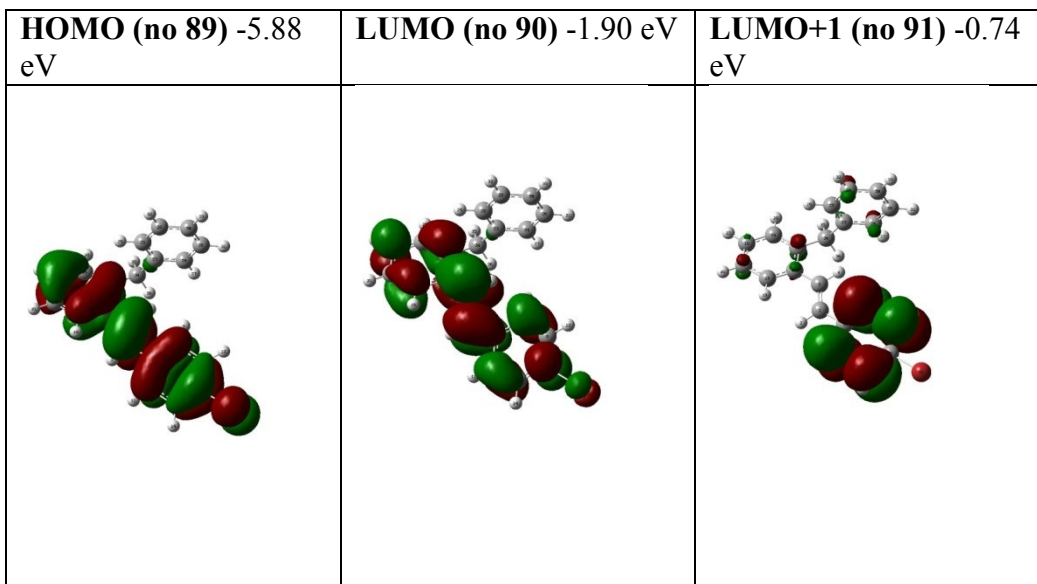
Excited	State 4	4.43 eV	279.7 nm	f=0.0015
86 →90	0.21713			
87 →90	0.47691			
88 →90	-0.32617			
89 →92	0.29209			
89 →94	-0.13407			

Excited State 5 4.63 eV 267.9 nm f=0.0011
 86 → 90 0.59332
 87 → 90 -0.36579
 89 → 92 0.13044



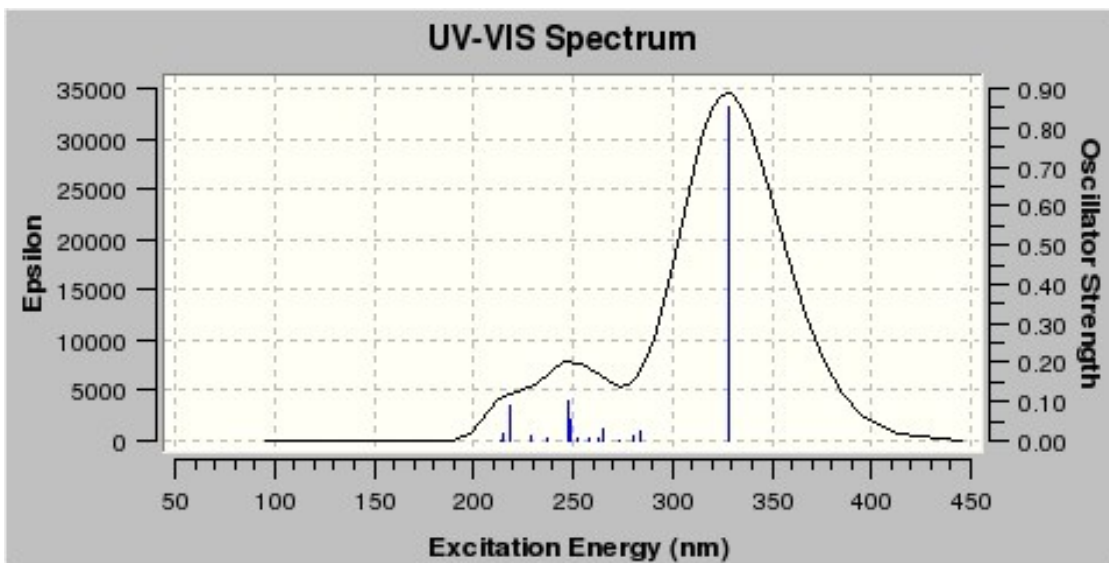
Orbitals

HOMO -3 (no 86) - 7.07 eV	HOMO -2 (no 87) - 7.02 eV	HOMO -1 (no 88) -6.82 eV

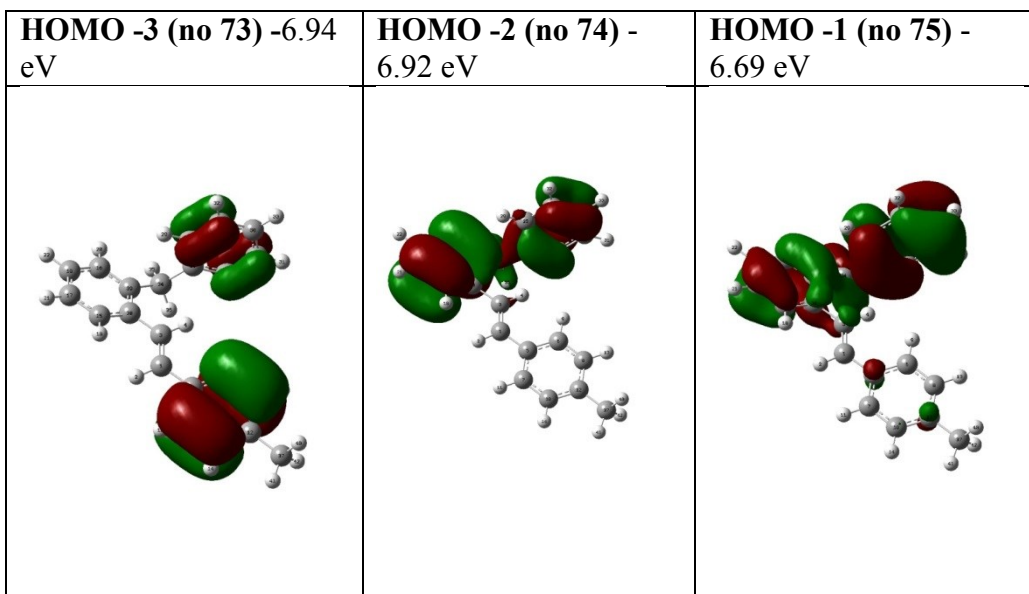


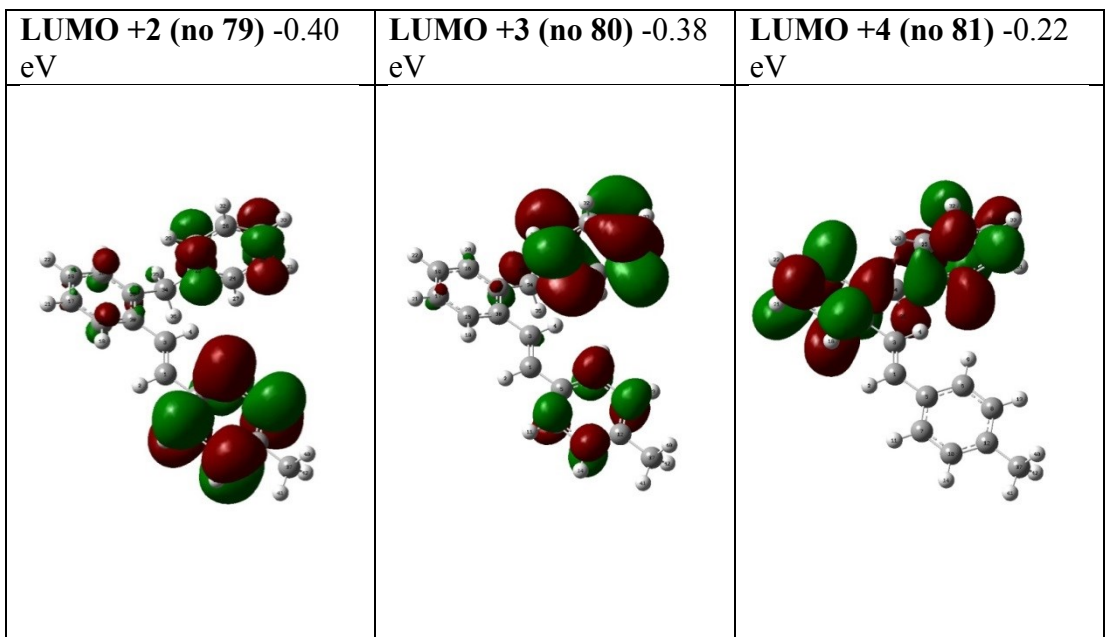
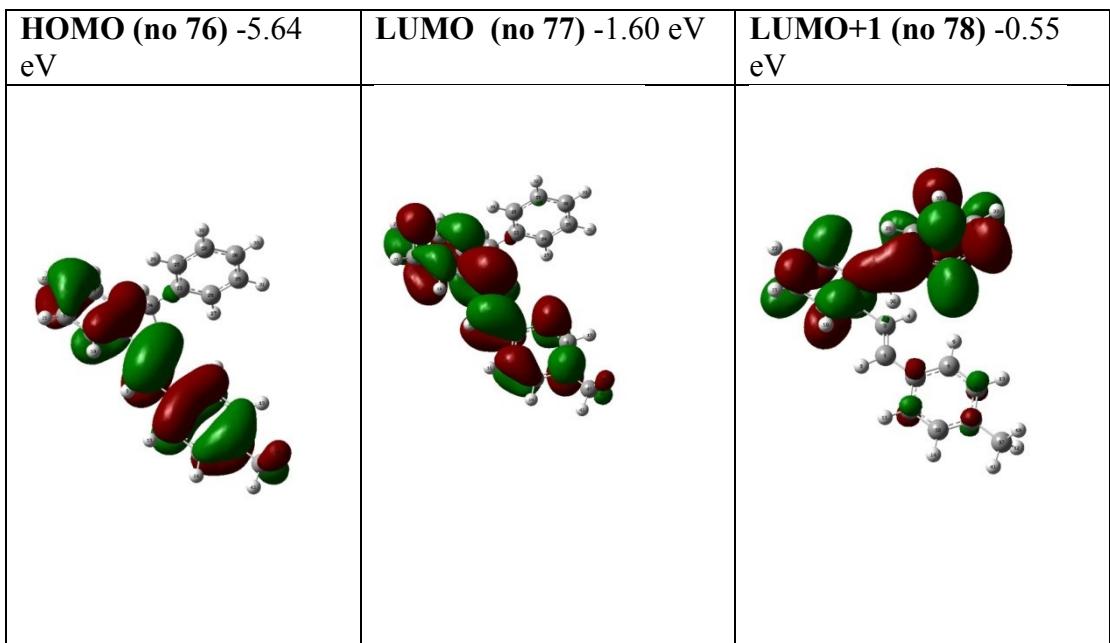
Hydrocarbon C₂₁H₁₇CH₃ (R = CH₃)

Excited	State 1	3.76 eV	329.8 nm	f=0.7381
76 →77	0.69866	HOMO→LUMO		
Excited	State 2	4.22 eV	293.7 nm	f=0.0391
76 →78	0.69047	HOMO→LUMO+1		
Excited	State 3	4.45 eV	278.5 nm	f=0.0004
74 →77	0.38524			
75 →77	-0.1128			
75 →81	-0.13482			
76 →79	0.1947			
76 →81	0.50947	HOMO→LUMO+4		
Excited	State 4	4.50 eV	275.5 nm	f=0.0400
75 →77	0.43525			
76 →79	0.53622	HOMO→LUMO+2		
Excited	State 5	4.58 eV	270.8 nm	f=0.0003
76 →80	0.69857	HOMO→LUMO+3		



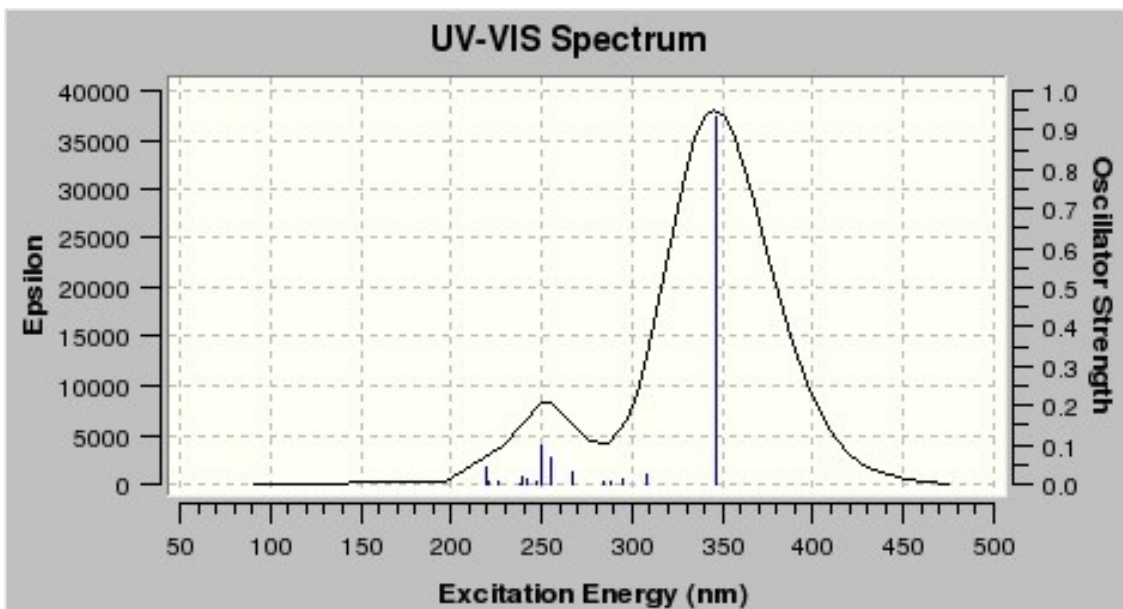
orbitals



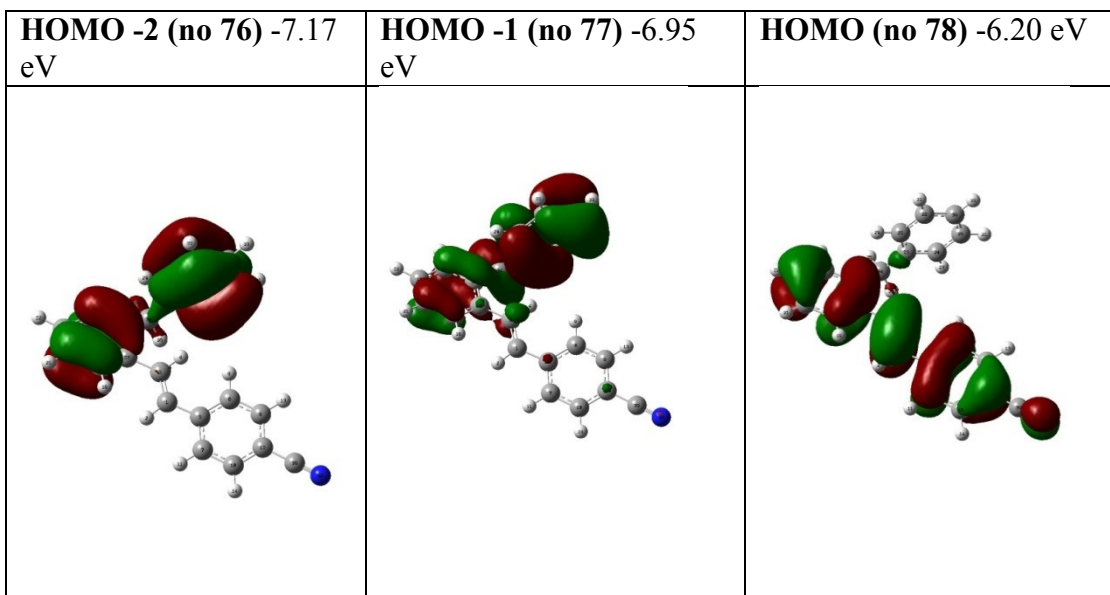
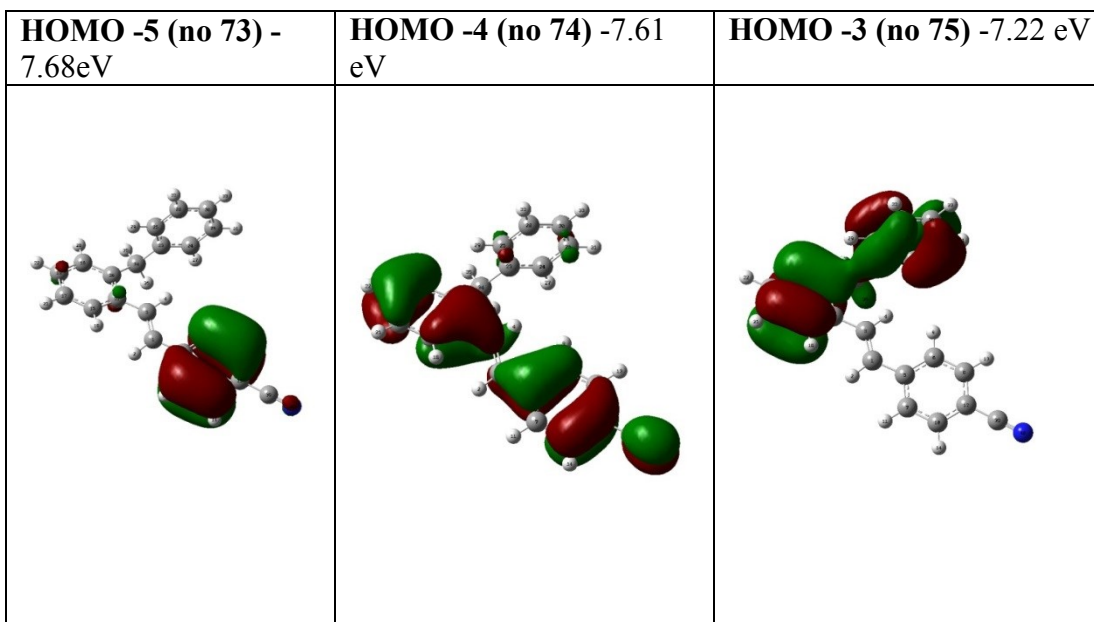


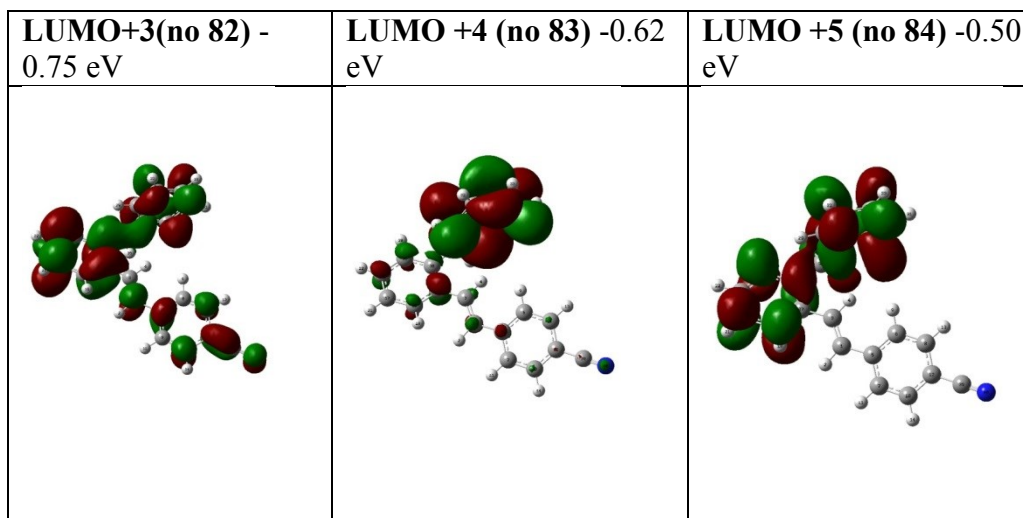
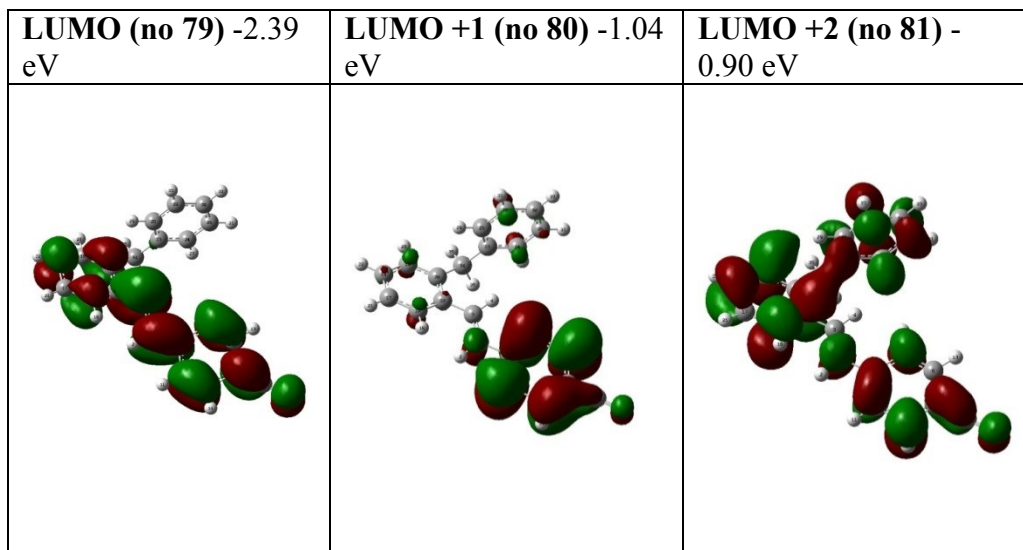
Hydrocarbon C₂₁H₁₇CN (R = CN)

Excited	State 1	3.58 eV	346.0 nm	f=0.9324
78 →79	0.70184	HOMO→LUMO		
Excited	State 2	4.02 eV	308.1 nm	f=0.0238
77 →79	0.69805			
Excited	State 3	4.21 eV	294.4 nm	f=0.0097
75 →79	-0.43675			
76 →79	0.49745			
78 →81	-0.11277			
78 →82	0.1424			
78 →84	-0.10948			
Excited	State 4	4.30 eV	288.6 nm	f=0.0059
75 →79	0.507			
76 →79	0.48014			
Excited	State 5	4.36 eV	284.5 nm	f=0.0080
73 →79	-0.42698			
78 →80	0.5264			
78 →81	-0.13537			



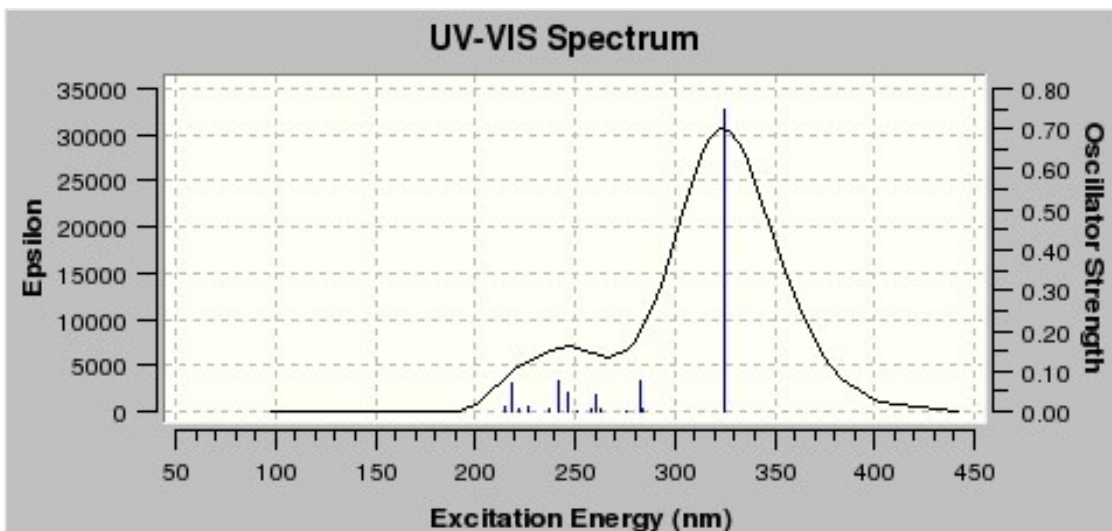
Orbitals





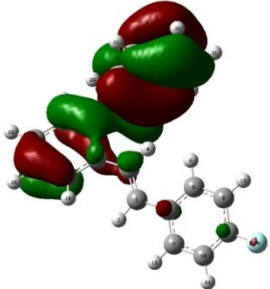
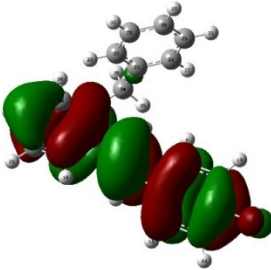
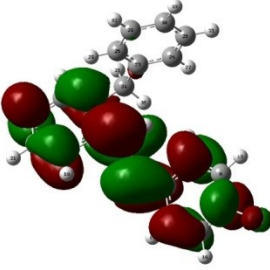
Hydrocarbon C₂₁H₁₇F (R = F)

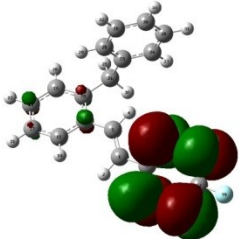
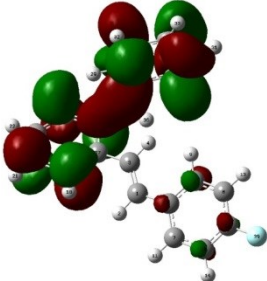
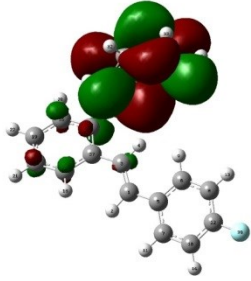
Excited	State 1	3.76 eV	330.0 nm	f=0.6071
76 →77	0.69729	HOMO→LUMO		
Excited	State 2	4.29 eV	288.7 nm	f=0.0663
76 →78	0.67483	HOMO→LUMO+1		
76 →79	0.11332			
Excited	State 3	4.40 eV	281.7 nm	f=0.0040
72 →77	0.2352			
75 →77	-0.15578			
76 →78	-0.12734			
76 →79	0.61916	HOMO→LUMO+2		
Excited	State 4	4.56 eV	272.1 nm	f=0.0983
75 →77	.051461	HOMO-1→LUMO		
76 →79	0.15423			
76 →80	0.4383			
Excited	State 5	4.67 eV	265.4 nm	f=0.0005
76 →81	0.69818	HOMO→LUMO+4		



orbitals

HOMO -4 (no 72) -7.32 eV	HOMO -3 (no 73) -7.05 eV	HOMO -2 (no 74) -6.98 eV

HOMO -1 (no 75) -6.79 eV	HOMO (no 76) -5.84 eV	LUMO (no 77) -1.77 eV
		

LUMO +1 (no 78) -0.78 eV	LUMO +2 (no 79) -0.64 eV	LUMO +3 (no 80) -0.48 eV
		

Hydrocarbon C₂₁H₁₇NMe₂ (R = NMe₂)

Excited State 1 3.52 eV 352.4 nm f=0.9587

84 →85 0.6996 HOMO→LUMO

Excited State 2 3.82 eV 324.9 nm f=0.0104

84 →86 0.70009

Excited State 3 4.11 eV 301.8 nm f=0.0176

81 →85 -0.17873

84 →87 0.55088

84 →88 -0.15245

84 →89 -0.36588

Excited State 4 4.17 eV 297.1 nm f=0.0059

84 →87 0.24426

84 →88 0.64729

Excited State 5 4.20 eV 295.1 nm f=0.0902

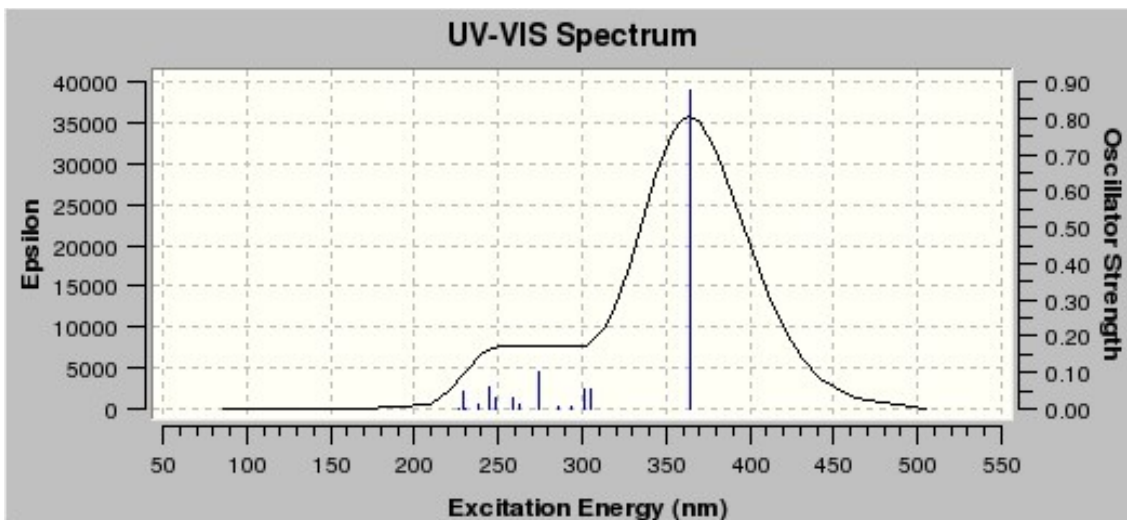
81 →85 0.14290

83 →85 -0.31080

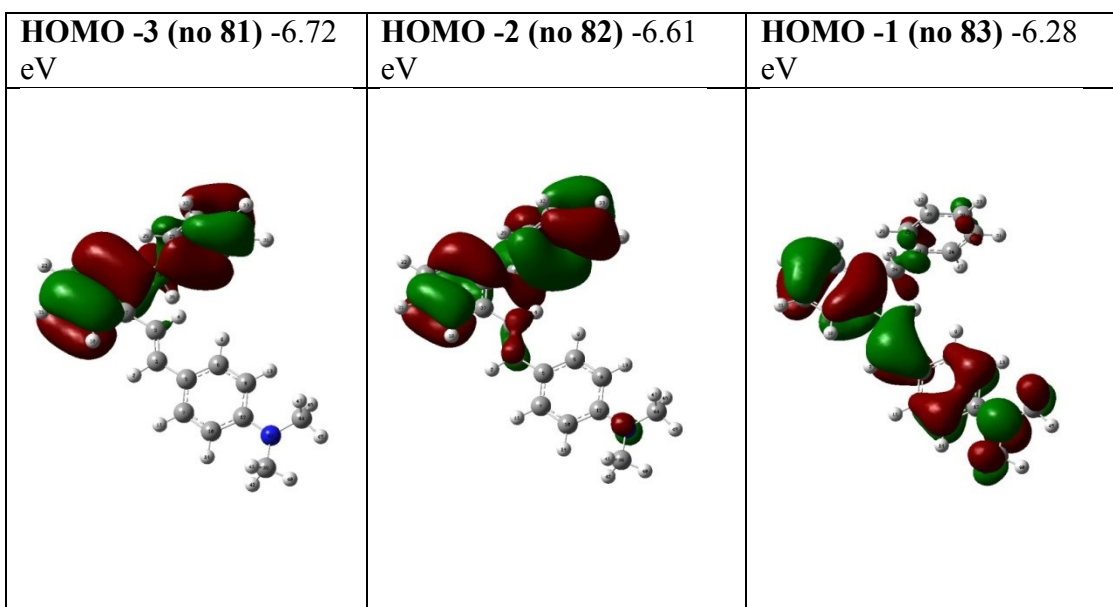
84 →87 0.27532

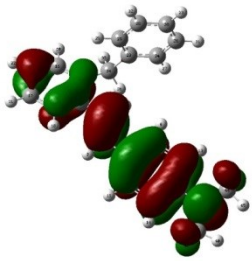
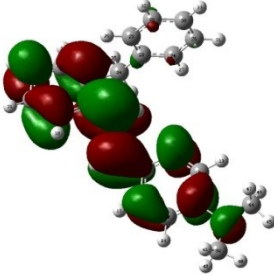
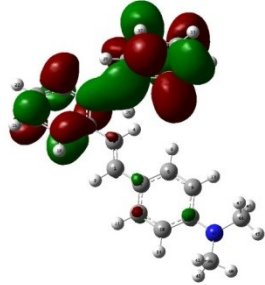
84 →88 -0.21903

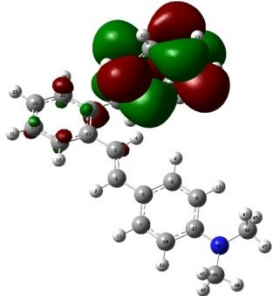
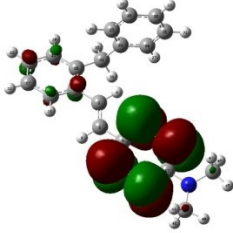
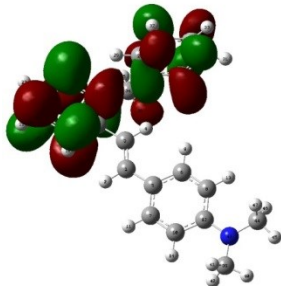
84 →89 0.49563



${}_{21}\text{H}_{18}\cdot\text{NMe}_2$



HOMO (no 84) -4.99 eV	LUMO (no 85) -1.34 eV	LUMO +1 (no 86) -0.42 eV
		

LUMO +2 (no 87) -0.29 eV	LUMO +3 (no 88) -0.25 eV	LUMO +4 (no 89) -0.09 eV
		

Hydrocarbon C₂₁H₁₇OCH₃ (R = OCH₃)

Excited State 1 3.69 eV 335.6 nm f=0.8697

80 →81 0.70044 HOMO→LUMO

Excited State 2 4.32 eV 287.1 nm f=0.0892

75 →81 -0.22351

77 →81 -0.15384

80 →82 0.48230

80 →83 0.38475

Excited State 3 4.33 eV 286.4 nm f=0.0006

75 →81 -0.15586

77 →81 0.15498

78 →81 0.17131

79 →81 0.19962

80 →82 -0.31243

80 →83 0.49075

80 →85 -0.16292

Excited State 4 4.54 eV 272.9 nm f=0.0132

79 →81 0.49784

80 →82 0.32311

80 →83 -0.14269

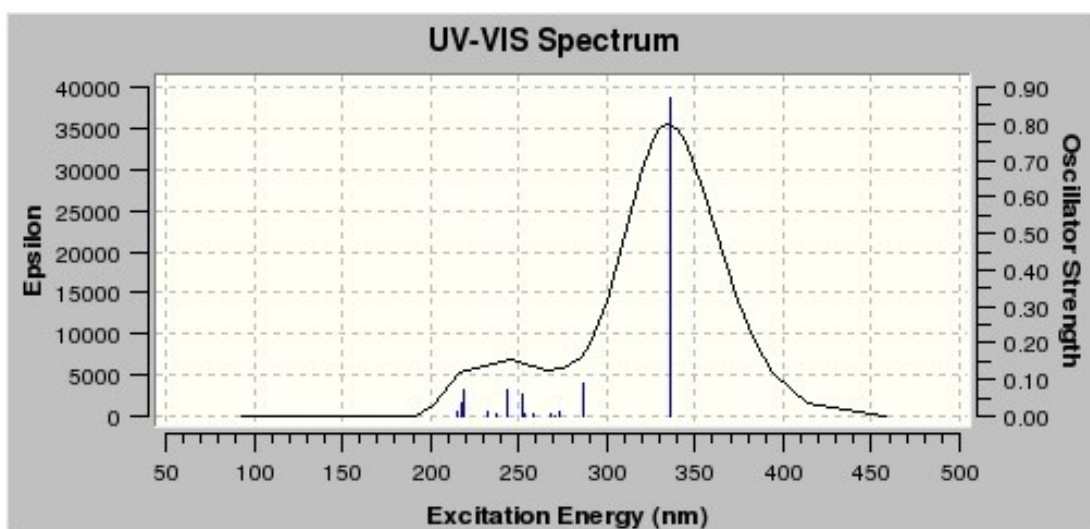
80 → 84 -0.21699

80 → 85 -0.2526

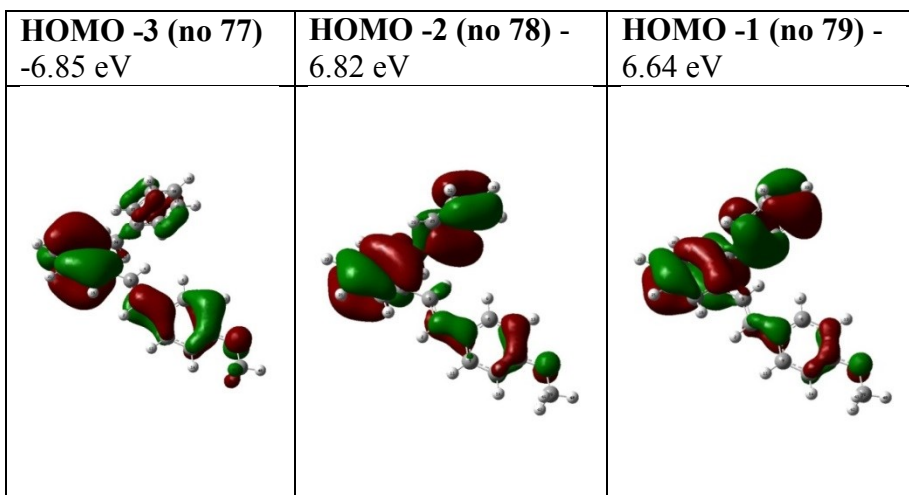
Excited State 5 4.58 eV 270.8 nm f=0.0022

79 → 81 0.25217

80 → 84 0.64854



Orbitals



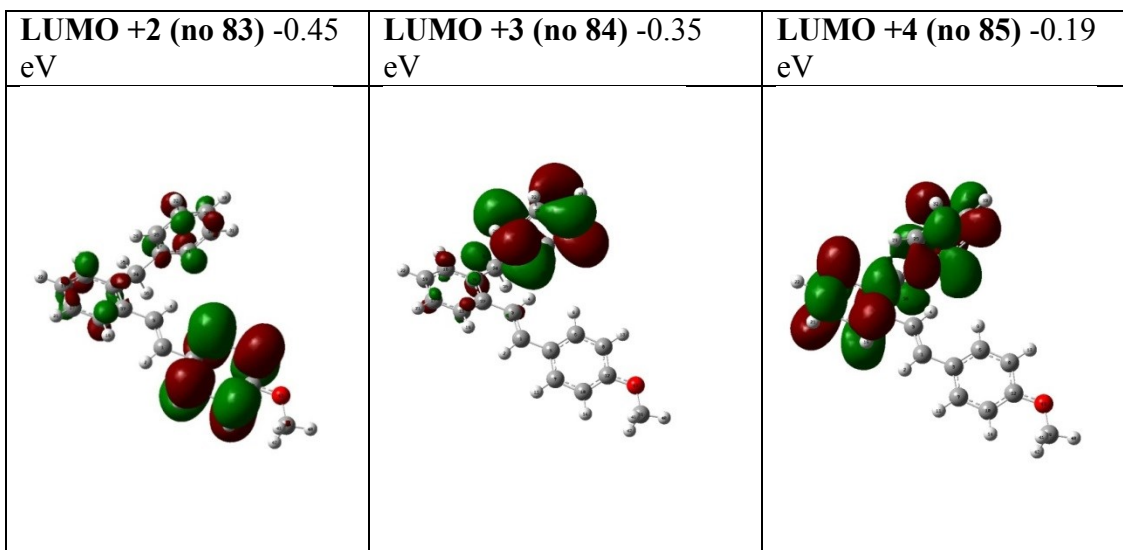
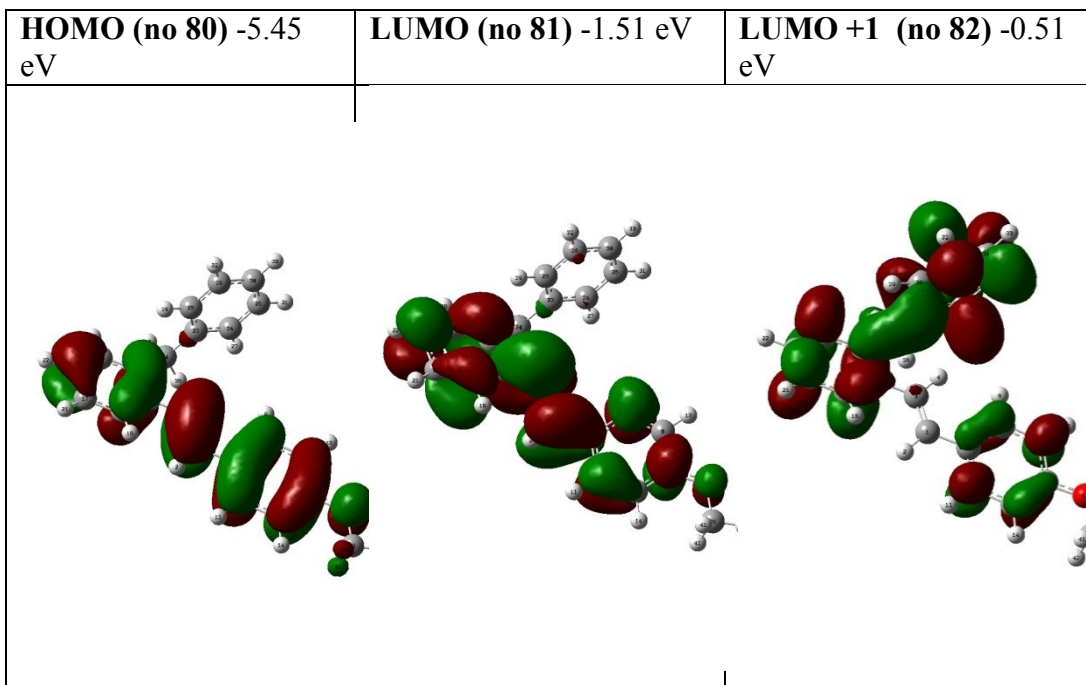


Table S5. Optimized Cartesian x, y, z Coordinates in Å.

C₂₁H₁₇CF₃

E = -1148.3779206 Hartrees

C	0.013833	1.728456	-0.048948
H	-0.053954	2.808226	-0.163648
C	-1.123673	1.011736	0.088862
H	-1.046356	-0.057108	0.260605
C	1.382641	1.197603	-0.029984
C	1.682016	-0.184345	-0.000153
C	2.462158	2.103237	-0.048038
C	2.999481	-0.630989	0.020221
H	0.881072	-0.915999	-0.005705
C	3.787463	1.662622	-0.027422
H	2.257694	3.170065	-0.073252
C	4.058562	0.291875	0.009726
H	3.210769	-1.695378	0.043330
H	4.602178	2.377928	-0.036708
C	-2.764716	2.765085	-0.633672
C	-4.859288	1.391567	0.565335
C	-4.056317	3.289051	-0.697401
H	-1.956966	3.289685	-1.133994
C	-5.114337	2.599648	-0.092862
H	-5.680751	0.858728	1.037386

H	-4.238463	4.220813	-1.224682
H	-6.125245	2.993786	-0.137924
C	-3.038716	-1.678490	0.549385
C	-2.256022	-2.713514	1.088625
C	-3.544874	-1.829741	-0.751437
C	-1.989704	-3.874299	0.352094
H	-1.853260	-2.613257	2.093752
C	-3.281199	-2.989274	-1.491003
H	-4.141209	-1.035969	-1.190693
C	-2.503031	-4.016864	-0.943562
H	-1.382676	-4.663616	0.786702
H	-3.680005	-3.088861	-2.496598
H	-2.296850	-4.914282	-1.519250
C	-3.357522	-0.449359	1.397123
H	-4.267604	-0.656433	1.972095
H	-2.561067	-0.321256	2.138143
C	5.476417	-0.219567	0.000050
F	6.388050	0.761922	0.224752
F	5.804246	-0.793413	-1.196423
F	5.679729	-1.179438	0.947185
C	-2.491022	1.552336	0.033598
C	-3.568074	0.850108	0.637932

C₂₁H₁₈

E = -811.2184631 Hartrees

C	1.638559	-1.355412	0.051196
H	1.769986	-2.431819	0.146529
C	0.386203	-0.862886	-0.073002
H	0.258744	0.204160	-0.225878
C	2.889510	-0.584079	0.039975
C	2.931153	0.828235	0.031401
C	4.116378	-1.279932	0.043030
C	4.149962	1.507507	0.015107
H	2.008625	1.399585	0.050053
C	5.338549	-0.599847	0.026678
H	4.107797	-2.366901	0.054107
C	5.361831	0.799456	0.010959
H	4.159538	2.593802	0.011940
H	6.269586	-1.159635	0.027031
C	-0.897205	-2.896229	0.643511
C	-3.203716	-1.956231	-0.584089
C	-2.065248	-3.658200	0.697800
H	-0.008876	-3.253280	1.154780
C	-3.230044	-3.187851	0.079498
H	-4.106577	-1.592421	-1.068187
H	-2.070635	-4.605437	1.229219
H	-4.146959	-3.768578	0.117440
C	-2.054708	1.404089	-0.556941
C	-1.503428	2.587233	-1.077711

C	-2.621057	1.438884	0.727169
C	-1.523744	3.777470	-0.340361
H	-1.055496	2.578715	-2.068612
C	-2.643827	2.627316	1.467675
H	-3.040041	0.532330	1.152606
C	-2.096355	3.802333	0.938058
H	-1.091934	4.681619	-0.760622
H	-3.085311	2.634748	2.460300
H	-2.111590	4.722759	1.514256
C	-2.071943	0.136576	-1.408445
H	-2.980118	0.150498	-2.022603
H	-1.234866	0.178998	-2.113291
C	-0.853303	-1.655934	-0.027874
C	-2.039124	-1.177865	-0.646896
H	6.307473	1.333051	0.000503

$C_{19}H_{18}BN$

$E = -814.6547494$ Hartrees

C	2.129703	0.961822	-0.032637
H	2.371780	2.009067	-0.213239

C	0.829960	0.628550	0.150321
H	0.616894	-0.425383	0.336024
C	3.302576	0.071563	-0.006795
C	3.210922	-1.325605	0.177802
C	4.585898	0.630973	-0.176410
C	4.355834	-2.123170	0.192225
H	2.239604	-1.792422	0.305425
C	5.735203	-0.166535	-0.160826
H	4.679054	1.704374	-0.320646
C	5.625743	-1.549477	0.024010
H	4.262939	-3.196382	0.333105
H	6.712535	0.288990	-0.293157
H	6.514291	-2.173600	0.035884
C	-0.252881	3.034400	-0.574880
C	-2.703608	2.209848	0.555960
C	-1.359765	3.853476	-0.619007
H	0.660977	3.395903	-1.043095
C	-2.601697	3.436905	-0.048270
H	-3.641424	1.880025	0.993469
H	-1.317168	4.832707	-1.093972
H	-3.474811	4.079096	-0.084755
C	-2.547324	-1.017534	0.478785
C	-3.169026	-2.107285	1.112146
C	-2.496842	-0.987748	-0.921452

C	-3.720230	-3.151717	0.362483
H	-3.223410	-2.140309	2.198004
C	-3.050723	-2.031818	-1.674225
H	-2.029361	-0.149253	-1.427158
C	-3.662369	-3.117382	-1.037613
H	-4.197978	-3.986738	0.867045
H	-3.004717	-1.994585	-2.758776
H	-4.092587	-3.924627	-1.622868
C	-1.923364	0.072903	1.342721
H	-2.585158	0.274699	2.191432
H	-0.985039	-0.291283	1.767178
B	-0.340978	1.661320	0.084909
N	-1.647087	1.338587	0.648505

$C_{19}H_{17}BNCF_3$

E = -1151.8142196 Hartrees

C	0.417085	1.617052	-0.058802
H	0.402667	2.682923	-0.283030
C	-0.761331	0.991378	0.168843
H	-0.715780	-0.075525	0.391367

C	1.765195	1.026753	-0.031944
C	2.008315	-0.340236	0.233154
C	2.876726	1.855450	-0.280175
C	3.303196	-0.848096	0.249416
H	1.178488	-1.011751	0.425000
C	4.181189	1.354187	-0.265946
H	2.714072	2.909776	-0.486547
C	4.395863	-0.000456	0.000870
H	3.472634	-1.900404	0.455080
H	5.022274	2.010380	-0.459083
C	-2.394486	3.063962	-0.556030
C	-4.567294	1.676838	0.592863
C	-3.666444	3.594026	-0.590550
H	-1.598023	3.635082	-1.029674
C	-4.766729	2.892969	-0.010371
H	-5.395361	1.133324	1.038178
H	-3.863121	4.554989	-1.063682
H	-5.768291	3.307727	-0.037808
C	-3.558141	-1.426944	0.474690
C	-3.730902	-2.680232	1.087728
C	-3.620854	-1.342687	-0.922159
C	-3.954117	-3.827345	0.319911
H	-3.691154	-2.760627	2.171810
C	-3.846253	-2.491513	-1.693340

H	-3.495548	-0.383427	-1.413149
C	-4.012441	-3.736487	-1.078072
H	-4.085585	-4.788508	0.808625
H	-3.891414	-2.410606	-2.775502
H	-4.187313	-4.625123	-1.677112
C	-3.291665	-0.215051	1.361743
H	-4.024537	-0.202506	2.175228
H	-2.313028	-0.320055	1.835840
B	-2.148133	1.712541	0.104052
N	-3.332742	1.084137	0.675925
C	5.786491	-0.582422	0.015367
F	6.750338	0.357464	-0.160339
F	5.959062	-1.515218	-0.967527
F	6.060427	-1.219379	1.191150

C₁₉H₁₇BNBr

E = -3387.64959860 Hartree

C	0.341373	-1.624216	0.058867
H	0.321038	-2.689991	0.283095
C	-0.833551	-0.992010	-0.168778
H	-0.782078	0.074624	-0.391302
C	1.692739	-1.041410	0.032009
C	1.943445	0.324208	-0.233089
C	2.799653	-1.876266	0.280240

C	3.241125	0.824871	-0.249351
H	1.117359	1.000319	-0.424935
C	4.106878	-1.382252	0.266011
H	2.631148	-2.929672	0.486612
C	4.329070	-0.028822	-0.000805
H	3.416403	1.876222	-0.455015
H	4.944308	-2.043104	0.459148
C	-2.478187	-3.055495	0.556095
C	-4.643261	-1.656330	-0.592798
C	-3.753068	-3.578489	0.590615
H	-1.684907	-3.631028	1.029739
C	-4.849444	-2.871335	0.010436
H	-5.468298	-1.108227	-1.038113
H	-3.955077	-4.538346	1.063747
H	-5.853294	-3.280526	0.037873
C	-3.616892	1.441802	-0.474625
C	-3.782693	2.696030	-1.087663
C	-3.680072	1.357894	0.922224
C	-3.999536	3.844364	-0.319846
H	-3.742499	2.776203	-2.171745
C	-3.899090	2.507954	1.693405
H	-3.560094	0.397954	1.413214
C	-4.058364	3.753832	1.078137
H	-4.125666	4.806242	-0.808560

H	-3.944699	2.427299	2.775567
H	-4.228300	4.643425	1.677177
C	-3.357149	0.228448	-1.361678
H	-4.090079	0.219972	-2.175163
H	-2.377944	0.328018	-1.835775
B	-2.224335	-1.705462	-0.103987
N	-3.405438	-1.070492	-0.675860
BR	6.094988	0.698706	-0.019172

C₁₉H₁₇BNCH₃

E = -853.982592809 Hartree

C	-1.558966	1.315355	0.039996
H	-1.662922	2.374891	0.273303
C	-0.315162	0.831354	-0.191969
H	-0.239605	-0.231818	-0.424875
C	-2.834123	0.582596	0.012438
C	-2.933385	-0.801433	-0.252495
C	-4.031084	1.279302	0.264549
C	-4.169203	-1.443887	-0.261262
H	-2.036645	-1.380797	-0.448275
C	-5.271103	0.630925	0.254137
H	-3.988060	2.345758	0.471893
C	-5.364880	-0.742624	-0.008123
H	-4.213009	-2.511053	-0.466639

H	-6.174856	1.201213	0.453149
C	1.060359	3.080156	0.546551
C	3.394022	1.948598	-0.565995
C	2.262491	3.750393	0.600401
H	0.196703	3.557991	1.005708
C	3.445617	3.178472	0.038645
H	4.285040	1.502665	-0.998384
H	2.341608	4.727566	1.074972
H	4.393203	3.704117	0.081154
C	2.738833	-1.252251	-0.474134
C	3.041379	-2.479297	-1.089812
C	2.792065	-1.165324	0.922882
C	3.383281	-3.598788	-0.324868
H	3.009216	-2.560516	-2.174115
C	3.135972	-2.286172	1.691366
H	2.565558	-0.225505	1.415047
C	3.431867	-3.505584	1.073405
H	3.614211	-4.539926	-0.815823
H	3.171567	-2.203673	2.773819
H	3.698578	-4.372501	1.670556
C	2.349857	-0.071555	-1.358147
H	3.087046	0.026870	-2.162149
H	1.394459	-0.282911	-1.844055
B	0.975712	1.706126	-0.113327

N	2.235548	1.219260	-0.667264
C	-6.697468	-1.458349	-0.016280
H	-6.736027	-2.229844	0.761197
H	-6.873640	-1.956517	-0.976099
H	-7.522032	-0.762783	0.159378

C₁₉H₁₇BNCN

E = -906.912478876 Hartree

C	1.265720	-1.453596	0.048032
H	1.315488	-2.518331	0.272219
C	0.051059	-0.900053	-0.178555
H	0.031208	0.167069	-0.403698
C	2.573804	-0.782047	0.021275
C	2.730409	0.600587	-0.226019
C	3.737158	-1.545973	0.255128
C	3.988922	1.191152	-0.239889
H	1.858981	1.221472	-0.403698
C	5.005086	-0.967330	0.243401
H	3.639982	-2.610763	0.448255
C	5.140379	0.410502	-0.005486
H	4.095740	2.254246	-0.428737
H	5.889222	-1.569425	0.424909
C	-1.452445	-3.063923	0.558924
C	-3.709120	-1.809571	-0.581102

C	-2.691537	-3.666729	0.603599
H	-0.621239	-3.586062	1.029350
C	-3.833865	-3.032881	0.028179
H	-4.569886	-1.317691	-1.024386
H	-2.829096	-4.635754	1.081058
H	-4.809399	-3.505096	0.062937
C	-2.842667	1.354016	-0.478006
C	-3.024543	2.606498	-1.090237
C	-2.929288	1.263696	0.917038
C	-3.281356	3.746842	-0.323083
H	-2.965460	2.691506	-2.173106
C	-3.188032	2.406052	1.687633
H	-2.795867	0.305328	1.407533
C	-3.364042	3.650052	1.073390
H	-3.419242	4.707492	-0.810992
H	-3.251168	2.320689	2.768542
H	-3.564443	4.533602	1.671929
C	-2.547415	0.149395	-1.365928
H	-3.301436	0.098587	-2.158314
H	-1.588030	0.295132	-1.868043
B	-1.290082	-1.702886	-0.106247
N	-2.511905	-1.146326	-0.673440
C	6.442214	1.020440	-0.019681
N	7.499391	1.517707	-0.031732

C₁₉H₁₇BNF

E = -913.927381680 Hartree

C	-1.580929	1.296274	0.030896
H	-1.699025	2.360856	0.231161
C	-0.330397	0.819213	-0.172441
H	-0.238161	-0.248644	-0.376451
C	-2.848532	0.548042	0.009159
C	-2.922394	-0.847154	-0.198569
C	-4.056554	1.246966	0.209929
C	-4.146922	-1.515299	-0.206552
H	-2.014756	-1.421865	-0.349284
C	-5.294520	0.596087	0.204362
H	-4.026269	2.320849	0.373059
C	-5.315113	-0.779109	-0.004989
H	-4.209763	-2.586986	-0.362361
H	-6.224217	1.133187	0.358519
C	1.025218	3.080605	0.564070
C	3.364067	1.974888	-0.564450
C	2.221656	3.762237	0.613683
H	0.159614	3.547682	1.030621
C	3.406755	3.203438	0.044262
H	4.256828	1.539309	-1.003621
H	2.294017	4.738351	1.091346

H	4.349460	3.737953	0.083787
C	2.715959	-1.237800	-0.480545
C	2.994420	-2.468045	-1.101336
C	2.790001	-1.152501	0.915561
C	3.333474	-3.592090	-0.341992
H	2.945824	-2.548176	-2.185106
C	3.131087	-2.278178	1.678446
H	2.582054	-0.210539	1.411837
C	3.403121	-3.500538	1.055557
H	3.545580	-4.535645	-0.836722
H	3.183195	-2.197005	2.760309
H	3.667494	-4.371177	1.648258
C	2.331908	-0.051769	-1.359507
H	3.073867	0.052706	-2.158240
H	1.379707	-0.260624	-1.852966
B	0.952217	1.708874	-0.099266
N	2.212225	1.235068	-0.661569
F	-6.511770	-1.430188	-0.012234

C₁₉H₁₇BNNMe₂

E = -948.656875355 Hartree

C	0.749926	-1.536874	0.058498
H	0.758219	-2.598482	0.306309
C	-0.447321	-0.954024	-0.202623

H	-0.427641	0.109484	-0.446189
C	2.079382	-0.919918	0.047437
C	2.312756	0.441251	-0.244422
C	3.215012	-1.702817	0.334612
C	3.591845	0.985717	-0.242021
H	1.477542	1.093003	-0.481439
C	4.504739	-1.174843	0.340381
H	3.083576	-2.759649	0.555056
C	4.730514	0.195635	0.066574
H	3.706199	2.036042	-0.480462
H	5.334978	-1.834024	0.562103
C	-2.011418	-3.094076	0.481533
C	-4.236430	-1.744112	-0.609258
C	-3.265047	-3.661940	0.515734
H	-1.193143	-3.655156	0.929650
C	-4.394440	-2.978930	-0.035134
H	-5.085094	-1.213941	-1.031894
H	-3.428127	-4.640561	0.965535
H	-5.383123	-3.423723	-0.007480
C	-3.349399	1.384015	-0.450351
C	-3.617107	2.629017	-1.045541
C	-3.369267	1.284675	0.946924
C	-3.890951	3.753907	-0.260916
H	-3.611605	2.720078	-2.129531

C	-3.645220	2.410407	1.735025
H	-3.169893	0.330406	1.422835
C	-3.905834	3.647963	1.137039
H	-4.096167	4.708864	-0.736487
H	-3.655888	2.317793	2.817227
H	-4.120344	4.518675	1.749575
C	-3.026221	0.197855	-1.353284
H	-3.750000	0.172098	-2.174995
H	-2.047199	0.350408	-1.813394
B	-1.805463	-1.715045	-0.145385
N	-3.020151	-1.112403	-0.691136
C	6.221239	2.084994	-0.424281
H	5.996905	2.153588	-1.500523
H	5.605490	2.821870	0.101168
H	7.265095	2.365372	-0.273330
N	6.007063	0.749589	0.116136
C	7.158857	-0.139714	0.174103
H	7.234202	-0.800468	-0.703993
H	8.068499	0.460533	0.230928
H	7.122757	-0.766417	1.071078

$C_{19}H_{17}BNOCH_3$

E = -929.211654903 Hartree

C	1.147437	-1.360714	0.035200
---	----------	-----------	----------

H	1.227509	-2.416045	0.295431
C	-0.086058	-0.857269	-0.213689
H	-0.138520	0.201211	-0.472763
C	2.436811	-0.658315	-0.006177
C	2.568155	0.719581	-0.303138
C	3.618245	-1.371328	0.261901
C	3.810596	1.338630	-0.328921
H	1.685257	1.315106	-0.511817
C	4.880189	-0.763896	0.239442
H	3.553071	-2.431288	0.494678
C	4.980957	0.601637	-0.058412
H	3.906825	2.395731	-0.555188
H	5.761074	-1.357679	0.452852
C	-1.500772	-3.076262	0.540669
C	-3.820269	-1.900080	-0.554285
C	-2.715027	-3.722792	0.604512
H	-0.643213	-3.571645	0.992720
C	-3.891409	-3.128266	0.051388
H	-4.705879	-1.436894	-0.979643
H	-2.809429	-4.698094	1.080219
H	-4.848720	-3.635294	0.101511
C	-3.101663	1.287144	-0.465715
C	-3.381904	2.521726	-1.076872
C	-3.147395	1.198494	0.931451

C	-3.694619	3.646679	-0.307431
H	-3.355113	2.604630	-2.161203
C	-3.462076	2.324799	1.704448
H	-2.937387	0.253042	1.420087
C	-3.735886	3.551596	1.090938
H	-3.908278	4.593666	-0.794957
H	-3.491952	2.240825	2.786969
H	-3.979652	4.422841	1.691591
C	-2.744811	0.099761	-1.354429
H	-3.492318	0.016326	-2.150633
H	-1.790831	0.293212	-1.850428
B	-1.393301	-1.704040	-0.121406
N	-2.648613	-1.193350	-0.665559
O	6.155439	1.306685	-0.111018
C	7.366715	0.601164	0.152892
H	8.167063	1.336488	0.056604
H	7.375076	0.186287	1.168588
H	7.525398	-0.205987	-0.573172

C₂₁H₁₇Br

E = -3384.21428948 Hartree

C	0.056374	-1.729650	-0.049683
H	0.128640	-2.809131	-0.164373
C	1.190882	-1.008248	0.088413

H	1.109118	0.060267	0.260143
C	-1.314615	-1.204444	-0.031056
C	-1.619691	0.176258	-0.001292
C	-2.390385	-2.114520	-0.049384
C	-2.938991	0.617468	0.018757
H	-0.821768	0.911207	-0.006641
C	-3.717500	-1.679371	-0.029094
H	-2.181519	-3.180496	-0.074553
C	-3.994256	-0.309754	0.007994
H	-3.154670	1.680977	0.041820
H	-4.529257	-2.398029	-0.038587
C	2.839318	-2.754814	-0.633723
C	4.927913	-1.372682	0.565812
C	4.133083	-3.273451	-0.697134
H	2.033861	-3.282735	-1.134249
C	5.188103	-2.579697	-0.092329
H	5.747055	-0.836464	1.038070
H	4.319199	-4.204451	-1.224375
H	6.200638	-2.969664	-0.137142
C	3.094706	1.689845	0.549427
C	2.307618	2.721631	1.088478
C	3.600559	1.843190	-0.751268
C	2.036701	3.881313	0.351888
H	1.905023	2.619708	2.093505

C	3.332291	3.001631	-1.490893
H	4.200270	1.051886	-1.190381
C	2.549758	4.026001	-0.943640
H	1.426317	4.668118	0.786350
H	3.730932	3.102868	-2.496389
H	2.340022	4.922566	-1.519374
C	3.418365	0.462033	1.397237
H	4.327443	0.672853	1.972436
H	2.622261	0.330643	2.138059
C	2.560462	-1.543207	0.033486
C	3.634460	-0.836550	0.638091
BR	-5.793557	0.330914	-0.004710

$C_{21}H_{17}CH_3$

E = -850.546287494 Hartree

C	-1.101154	-1.573921	-0.050768
H	-1.118428	-2.656088	-0.167049
C	0.091955	-0.954031	0.089547
H	0.103838	0.117471	0.261002
C	-2.425415	-0.939758	-0.035374
C	-2.621883	0.459125	0.006121
C	-3.574656	-1.752368	-0.069093
C	-3.904118	1.002989	0.022678
H	-1.767309	1.128443	0.012905

C	-4.860898	-1.201477	-0.051970
H	-3.458030	-2.832826	-0.104847
C	-5.051749	0.186087	-0.004779
H	-4.021912	2.083764	0.050951
H	-5.724966	-1.860596	-0.076788
C	1.585519	-2.839798	-0.628862
C	3.783406	-1.646340	0.576355
C	2.829296	-3.469964	-0.687730
H	0.738400	-3.295146	-1.131843
C	3.940120	-2.871896	-0.080334
H	4.644542	-1.182557	1.050985
H	2.934159	-4.414154	-1.214275
H	4.914714	-3.349197	-0.121729
C	2.253391	1.567824	0.546529
C	1.598715	2.687747	1.087180
C	2.761154	1.655800	-0.759281
C	1.460313	3.868487	0.347744
H	1.194003	2.636618	2.095267
C	2.624685	2.835013	-1.502377
H	3.257840	0.796756	-1.199384
C	1.974798	3.947099	-0.953138
H	0.950345	4.723259	0.783488
H	3.022254	2.883862	-2.512254
H	1.866955	4.860098	-1.531268

C	2.436550	0.314544	1.399622
H	3.349335	0.437423	1.994474
H	1.614848	0.263852	2.121989
C	-6.435947	0.796120	0.008381
C	1.409596	-1.608201	0.037349
C	2.541078	-0.999849	0.644521
H	-6.595490	1.433489	-0.868722
H	-7.209525	0.023944	0.007878
H	-6.584096	1.422200	0.895301

C₂₁H₁₇CN

E = -903.476212288 Hartree

C	-0.794191	-1.665000	-0.060945
H	-0.758858	-2.744302	-0.191991
C	0.363717	-0.984162	0.095221
H	0.315866	0.083411	0.283662
C	-2.143874	-1.091359	-0.041948
C	-2.397455	0.299365	0.000488
C	-3.253956	-1.963136	-0.075324
C	-3.697166	0.792337	0.020526
H	-1.572181	1.003452	0.003191
C	-4.561205	-1.481401	-0.055270
H	-3.083571	-3.035570	-0.112927
C	-4.793736	-0.094737	-0.005309

H	-3.877499	1.861822	0.049129
H	-5.402489	-2.166159	-0.078684
C	1.957965	-2.782104	-0.622812
C	4.087421	-1.456915	0.569718
C	3.235869	-3.338176	-0.686037
H	1.137096	-3.288771	-1.120160
C	4.311267	-2.673190	-0.084642
H	4.922585	-0.943292	1.038916
H	3.394289	-4.276088	-1.209985
H	5.311921	-3.092708	-0.129093
C	2.332807	1.656306	0.546873
C	1.569868	2.705965	1.086152
C	2.836048	1.794942	-0.756498
C	1.319857	3.868696	0.346902
H	1.170344	2.616044	2.093558
C	2.588441	2.956246	-1.498800
H	3.417435	0.990060	-1.195605
C	1.829777	3.998387	-0.951437
H	0.728500	4.669750	0.781624
H	2.984729	3.046054	-2.506294
H	1.636272	4.897324	-1.529125
C	2.634132	0.424333	1.396815
H	3.553967	0.614390	1.961940
H	1.842821	0.316187	2.146517

C	1.715500	-1.560326	0.040379
C	2.810412	-0.882873	0.641654
C	-6.137485	0.415342	0.013084
N	-7.229329	0.831023	0.028940

C₂₁H₁₇F

E = -910.490957685 Hartree

C	-1.113288	-1.565484	-0.051597
H	-1.135649	-2.647319	-0.167388
C	0.081310	-0.949601	0.089279
H	0.096647	0.121499	0.263004
C	-2.434642	-0.923115	-0.036826
C	-2.616729	0.478112	-0.018452
C	-3.587875	-1.734849	-0.048522
C	-3.892300	1.042622	-0.000233
H	-1.757115	1.139913	-0.032372
C	-4.874849	-1.187423	-0.030146
H	-3.475798	-2.815539	-0.067432
C	-5.002530	0.197588	-0.004225
H	-4.037188	2.117561	0.009271
H	-5.761665	-1.812062	-0.036641
C	1.570539	-2.836395	-0.633084
C	3.771668	-1.646313	0.570150
C	2.813452	-3.467978	-0.694501

H	0.722227	-3.290126	-1.135579
C	3.925489	-2.871428	-0.088058
H	4.634269	-1.184290	1.043669
H	2.916689	-4.411658	-1.222147
H	4.899486	-3.349722	-0.131503
C	2.223297	1.567598	0.550008
C	1.546504	2.673429	1.092279
C	2.731947	1.668321	-0.754661
C	1.386750	3.853146	0.355231
H	1.142116	2.612725	2.099957
C	2.574156	2.846404	-1.495193
H	3.246188	0.820176	-1.195890
C	1.901744	3.944439	-0.944532
H	0.860524	4.697294	0.792295
H	2.972952	2.905627	-2.504008
H	1.777689	4.856591	-1.520691
C	2.428384	0.315093	1.398966
H	3.349143	0.443194	1.980108
H	1.618346	0.257712	2.133994
C	1.397898	-1.605499	0.034786
C	2.530372	-0.998233	0.641037
F	-6.248516	0.748425	0.011235

C₂₁H₁₇NMe₂

E = -945.220421074 Hartree

C	0.347875	-1.686097	0.028076
H	0.303515	-2.767514	0.147540
C	-0.813085	-1.003036	-0.105195
H	-0.768321	0.066669	-0.282857
C	1.703067	-1.133725	0.001293
C	1.991519	0.248000	-0.039410
C	2.810221	-2.004620	0.029665
C	3.296942	0.725304	-0.067800
H	1.181477	0.970964	-0.030488
C	4.124978	-1.543104	0.001064
H	2.636598	-3.077190	0.076561
C	4.408468	-0.157804	-0.066391
H	3.452730	1.796902	-0.084771
H	4.929615	-2.267375	0.031219
C	-2.396499	-2.807853	0.631702
C	-4.542619	-1.500768	-0.547043
C	-3.670597	-3.372555	0.703789
H	-1.569259	-3.307770	1.125458
C	-4.756612	-2.717329	0.110265
H	-5.383396	-0.991568	-1.011815
H	-3.817969	-4.310799	1.231042
H	-5.754258	-3.143108	0.162891
C	-2.861473	1.631871	-0.539651

C	-2.173505	2.725668	-1.092537
C	-3.345317	1.741191	0.773523
C	-1.979849	3.901863	-0.358453
H	-1.786050	2.657197	-2.106373
C	-3.153815	2.916084	1.511444
H	-3.866372	0.901697	1.222979
C	-2.471531	4.002249	0.949808
H	-1.445008	4.736173	-0.804060
H	-3.533690	2.981572	2.527219
H	-2.321252	4.911800	1.523979
C	-3.105049	0.385576	-1.387824
H	-4.012668	0.550384	-1.980667
H	-2.288265	0.294359	-2.111899
C	-2.161888	-1.586165	-0.036323
C	-3.268848	-0.920628	-0.629891
C	6.813969	-0.596769	0.133473
H	7.759052	-0.066936	0.002858
H	6.784784	-1.006195	1.155736
H	6.808282	-1.434954	-0.570656
N	5.715364	0.318701	-0.142077
C	5.963411	1.738565	0.068215
H	7.029928	1.934531	-0.055327
H	5.431995	2.341406	-0.674991
H	5.662405	2.083348	1.070173

C₂₁H₁₇OCH₃

E = -925.775187301 Hartree

C	0.749749	-1.553991	0.047911
H	0.776105	-2.635713	0.167181
C	-0.449922	-0.946115	-0.093179
H	-0.473147	0.124931	-0.266062
C	2.067595	-0.910572	0.031014
C	2.254563	0.492017	-0.027431
C	3.223339	-1.709475	0.079639
C	3.525210	1.051300	-0.045657
H	1.395527	1.155032	-0.047099
C	4.512604	-1.161777	0.061758
H	3.116830	-2.790343	0.128616
C	4.668838	0.229028	-0.003234
H	3.663169	2.126973	-0.086077
H	5.371518	-1.821279	0.099444
C	-1.924312	-2.847372	0.625976
C	-4.135192	-1.674615	-0.575207
C	-3.161701	-3.489951	0.685403
H	-1.072461	-3.295030	1.127930
C	-4.279351	-2.902455	0.080133
H	-5.001353	-1.218556	-1.048249
H	-3.256522	-4.435695	1.211152

H	-5.249141	-3.389371	0.122218
C	-2.637206	1.554278	-0.543479
C	-1.993973	2.681388	-1.082930
C	-3.144830	1.635436	0.762824
C	-1.866506	3.862350	-0.341825
H	-1.589417	2.635686	-2.091354
C	-3.019416	2.814841	1.507542
H	-3.632483	0.770770	1.202007
C	-2.380810	3.934053	0.959525
H	-1.364868	4.722566	-0.776522
H	-3.416567	2.858256	2.517844
H	-2.281143	4.847120	1.539014
C	-2.808654	0.300267	-1.397949
H	-3.723162	0.414851	-1.991857
H	-1.986979	0.258699	-2.120971
C	-1.760672	-1.613331	-0.039182
C	-2.899300	-1.015995	-0.644327
C	7.059684	0.088807	0.022070
H	7.891496	0.794405	-0.004742
H	7.111071	-0.498470	0.947448
H	7.125908	-0.584018	-0.842137
O	5.874650	0.881311	-0.025520

2.5.10 Optimization of B–H to B–Cl Reaction

Initial observations were qualitative in nature. Reactions were run on 25 mg scale in unregulated pressure vessels

General Procedure: In a nitrogen glovebox, an NMR tube fitted with a J-Young valve was charged with 100 μL of a stock solutions in C_6D_6 of the following: an internal standard of hexamethylbenzene (253.8 mg : 10 mL, 2.53 mg, .0154 mmol : 100 μL), N–TBS–B–H–azaborine (2.496 g : 10mL, 24.9 mg, .129 mmol : 100 μL), $[\text{Rh}(\text{nbd})\text{Cl}]_2$ (57.5 mg :10 mL, .575 mg, .00125 mmol), and xantphos (155.3 mg : 10mL, 1.51 mg, .00261 mmole) and an appropriate amount of chloride source (1.1 equiv to azaborine) was added via microsyringe. A time zero ^1H NMR was taken and the integrations of the starting material to internal standard were compared with integrations of the starting material, product, and internal standard after 24 hours in an oil bath at 110 $^\circ\text{C}$. No reaction was observable at room temperature. Because the yields reported in table 2.4 are the average of two runs, the yields that are reported below for a specific experiment may differ from the values presented in the paper.

Entry 1: Methylene chloride: The general procedure was followed with the addition of 9 μL of methylene chloride (12 mg, 0.141 mmole). Nmr analysis after 24 hours indicated an 18% yield. A duplicate run gave 19% yield.

Entry 2: Chloroform: The general procedure was followed with the addition of 12 μL of chloroform (17.8 mg, 0.149 mmole). Nmr analysis after 24 hours indicated a 13% yield. A duplicate run gave 10% yield.

Entry 3: Carbon tetrachloride: The general procedure was followed with the addition of 14 μL of carbon tetrachloride (22.2 mg, 0.144 mmole). Nmr analysis after 24 hours indicated a 32% yield. A duplicate run gave 33% yield.

Entry 4: 2,2-Dichloropropane: The general procedure was followed with the addition of 15 μL of 2,2-dichloropropane (16.2 mg, 0.144 mmole). Nmr analysis after 24 hours indicated a 64% yield. A duplicate run gave 62% yield.

Entry 5: 2,2-Dichlorobutane: The general procedure was followed with the addition of 17 μL of 2,2-dichlorobutane (18.5 mg, 0.146 mmole). Nmr analysis after 24 hours indicated a 60% yield. A duplicate run gave 58% yield.

Entry 6: 1-Chloropentane: The general procedure was followed with the addition of 15 μL of 1-chloropentane (13.2 mg, .124 mmole). Nmr analysis after 24 hours indicated an 5% yield. A duplicate run gave 6% yield.

Entry 7: 1,2-Dichloroethane: The general procedure was followed with the addition of 12 μL of 1,2-dichloroethane (15.0 mg, 0.152 mmole). Nmr analysis after 24 hours indicated a 25% yield. A duplicate run gave 23% yield.

Entry 8: α -Chlorotoluene: The general procedure was followed with the addition of 17 μL of α -chlorotoluene (18.7 mg, 0.148 mmole). Nmr analysis after 24 hours indicated an 8% yield. A duplicate run gave 10% yield.

Entry 9: Benzal Chloride: The general procedure was followed with the addition of 18 μL of benzal chloride (22.6 mg, 0.140 mmole) Nmr analysis after 24 hours indicated a 46% yield. A duplicate run gave 36% yield.

Entry 10: Benzotrichloride: The general procedure was followed with the addition of 20 μL of benzotrichloride (27.5 mg, 0.141 mmole). Nmr analysis after 24 hours indicated a 58% yield. A second run gave 48% yield.

Entry 11: Benzhydryl Chloride: The general procedure was followed with the addition of 25 μL of benzhydryl chloride (28.5 mg, .0141 mmole). Nmr analysis after 24 hours indicated a 63% yield. A duplicate run gave 64% yield.

Entry 12: α -Chloro-*p*-Xylene: The general procedure was followed with the addition of 19 μL of α -chloro-*p*-xylene (20.1 mg, 0.143 mmole). Nmr analysis after 24 hours indicated a 10% yield. A duplicate run gave 10% yield.

Entry 13: (1-Chloroethyl)Benzene: The general procedure was followed with the following modification: The reaction was run for 1 hour after addition of 20 μL of 1-Chloroethyl)benzene (21.2 mg, .151 mmole). Nmr analysis after 1 hour indicated a 96% yield. Two additional runs with 24 hour reaction time gave gave 90% yield and 94% yield.

2.5.11 Gram-Scale *B-H* to *B-Cl*

An unregulated pressure vessel was charged with 1.0 equiv of **2.116** (1g, 5.18 mmole), 0.01 equiv $[\text{Rh}(\text{nbd})\text{Cl}]_2$ (24 mg, .0518 mmole), 0.02 equiv xantphos (60 mg,

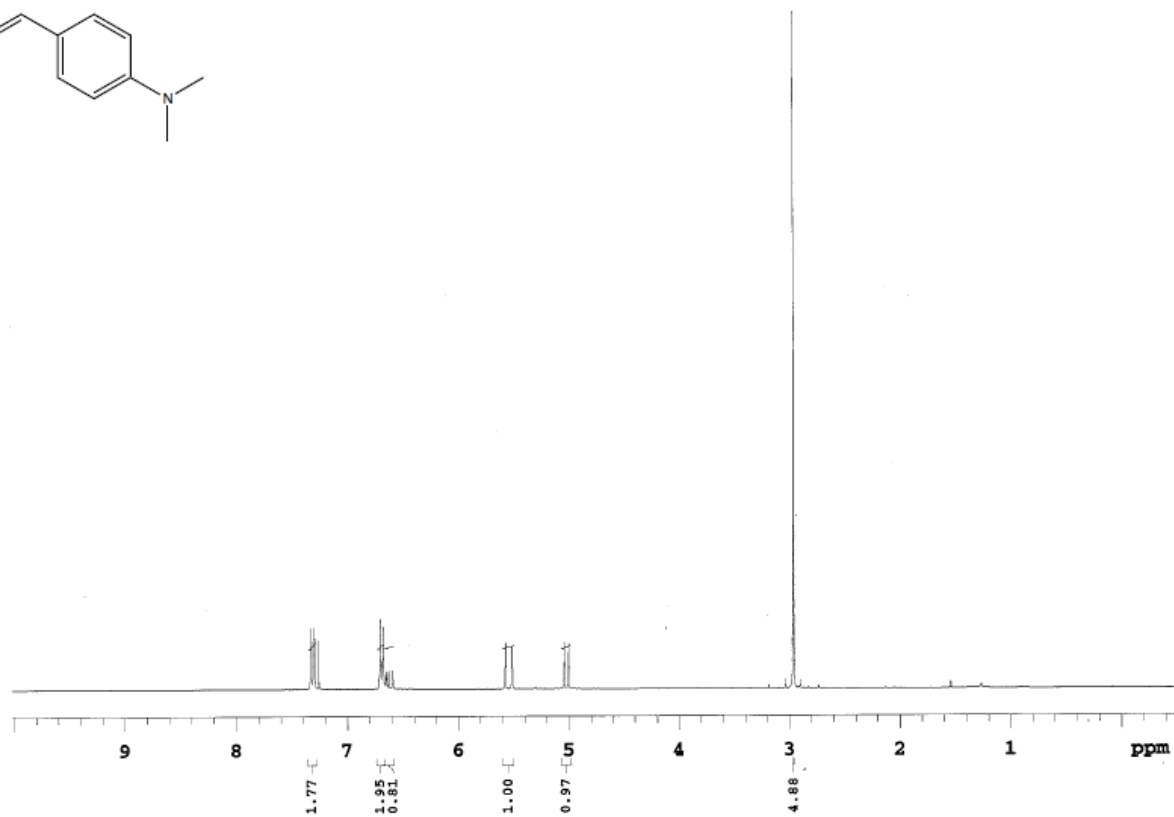
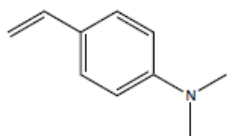
0.104 mmole), 1.1 equiv (1-chloroethyl)benzene (801 mg, 5.69 mmole) and 5 mL of C₆D₆. The system was sealed and heated to 110 °C until completion (~3 h). Upon completion the volatiles were removed and **2.117** was isolated by vacuum distillation. (955 mg, 81% yield.) The NMR spectra were identical to those previously reported.

2.5.12 *B–H* to *B–Cl* with 9-BBN and HBpin

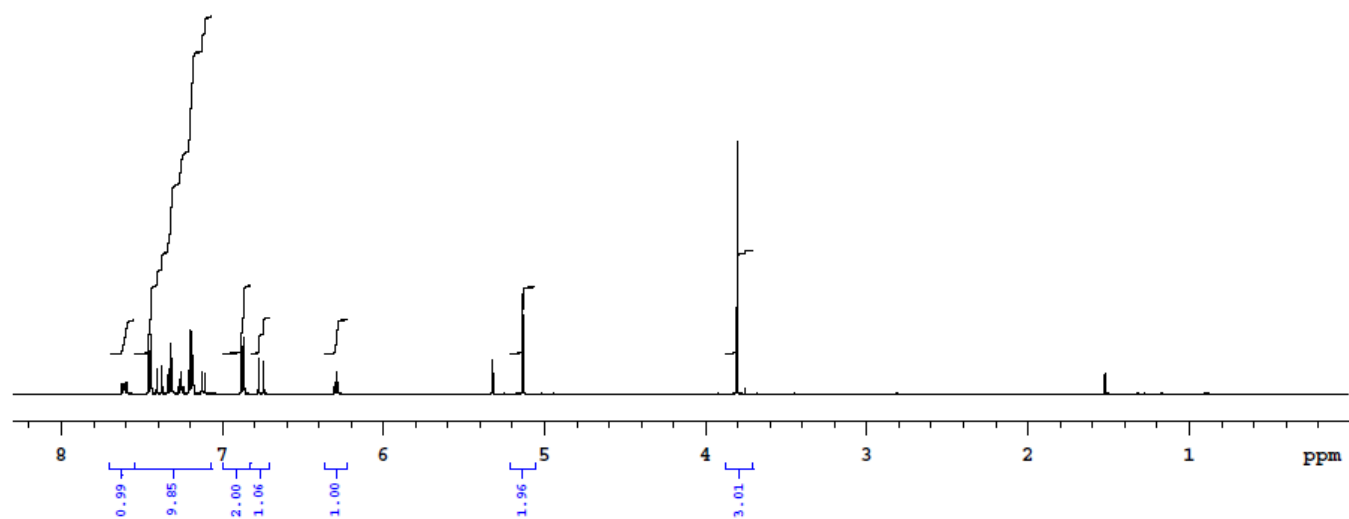
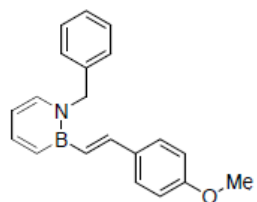
9-BBN: In a nitrogen glovebox, an NMR tube fitted with a J-Young valve was charged with 1 equiv of 9-BBN in hexanes (0.4M, 188 μL, 0.075 mmole), 0.05 equiv [Rh(nbd)Cl]₂ (1.7 mg, .0038 mmole), 0.1 equiv xantphos (4.3 mg, 0.0075 mmole), and 1.1 equiv of (1-chloroethyl)benzene (11.6 mg, 0.0824 mmole) and 0.6 mL of C₆D₆. An initial T0 ¹¹B NMR was taken, followed by heating to 50 °C with timepoint analysis indicated in Figure 2.6. Full conversion to the desired 9-BBN-Cl was observed in 5 hours of reaction time.

HBpin: In a nitrogen glovebox, an NMR tube fitted with a J-Young valve was charged with 1 equiv of HBpin (20 mg, 0.156 mmole), 0.05 equiv [Rh(nbd)Cl]₂ (3.6 mg, .0078 mmole), 0.1 equiv xantphos (9.1 mg, 0.016 mmole), and 1.1 equiv of (1-chloroethyl)benzene (24.1 mg, 0.172 mmole) and 0.7 mL of C₆D₆. An initial ¹¹B NMR was taken, followed by heating to 50 °C with timepoint analysis indicated in Figure 2.7. Full conversion to the desired ClBpin was observed in 1.5 hours of reaction time.

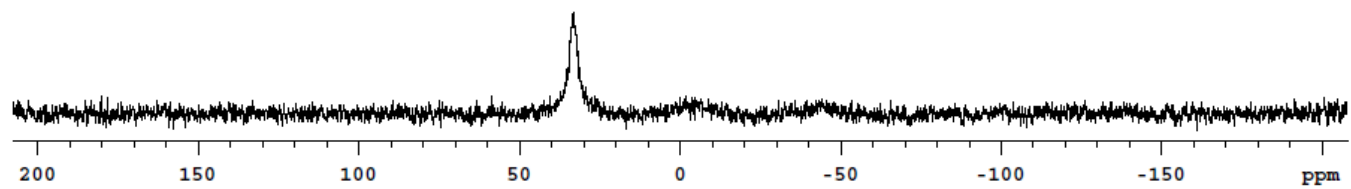
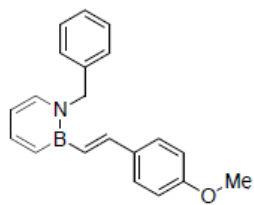
2.5.11 NMR Spectral Library



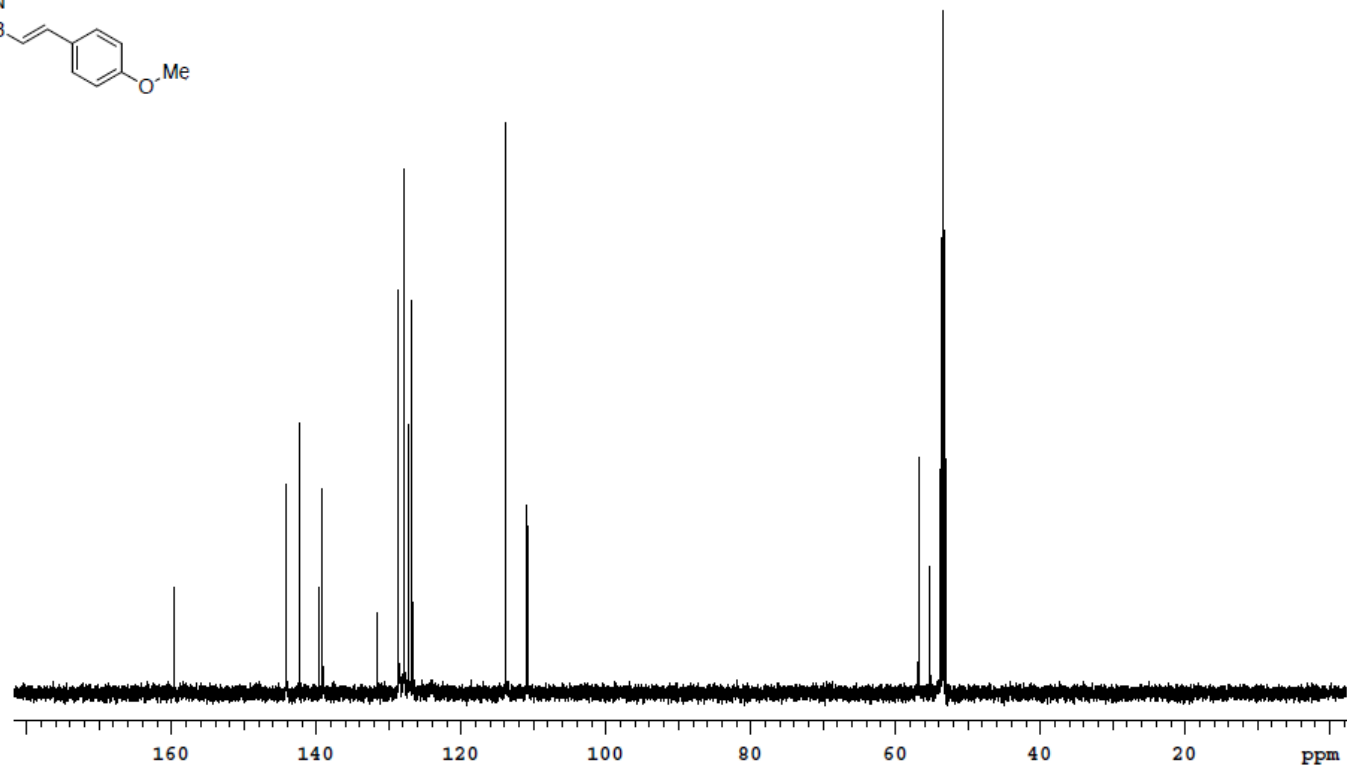
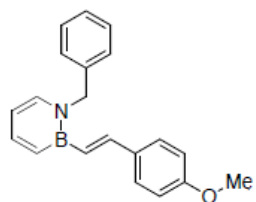
PULSE SEQUENCE Relax. delay 1.000 sec Pulse 45.0 degrees Acq. time 3.000 sec Width 4799.0 Hz 8 repetitions	OBSERVE H1, 299.9325271	DATA PROCESSING Line broadening 0.2 Hz FT size 32768 Total time 1 minute	UO Inova-300 Standard-1H Solvent: cdcl3 Temp. 25.0 C / 298.1 K Operator: abrown INOVA-300 "carbon.uoregon.edu"
--	--------------------------------	--	---



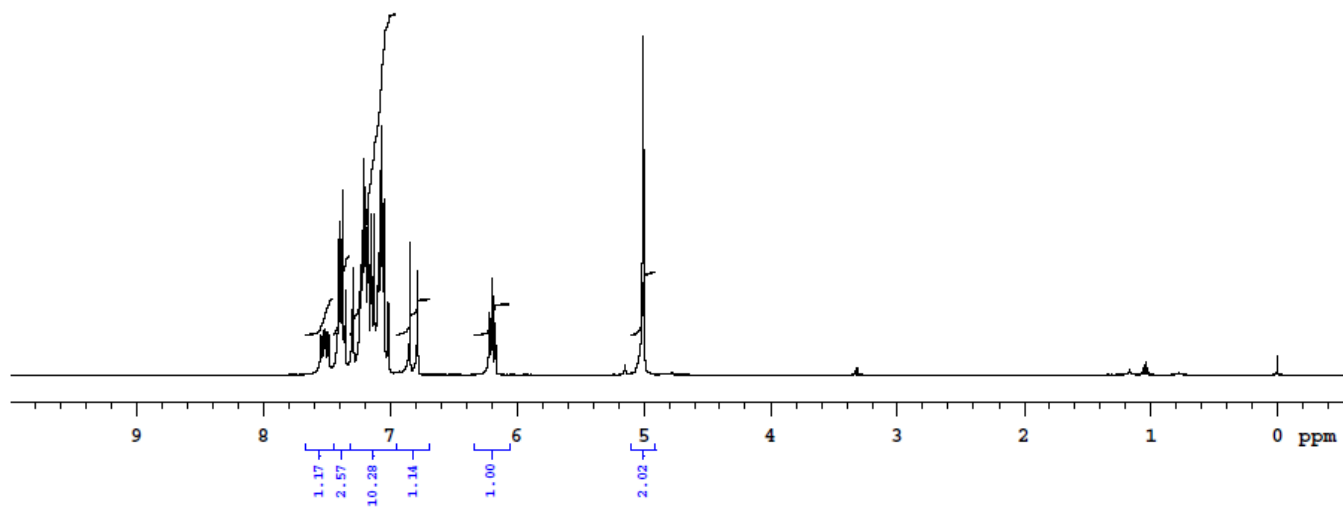
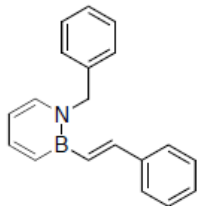
PULSE SEQUENCE Relax. delay 10.000 sec Pulse 45.0 degrees Acq. time 5.190 sec Width 6313.1 Hz 8 repetitions	OBSERVE H1, 599.9795419	DATA PROCESSING FT size 65536 Total time 2 minutes	UO VNMRS-600 standard 1H P-MeO for publication <hr/> Solvent: cd2cl2 Temp. 25.0 C / 298.1 K Operator: abrown File: ANB-PMeO-H1-Publication VNMRS-500 "hotwax.uoregon.edu"
---	--------------------------------	---	---



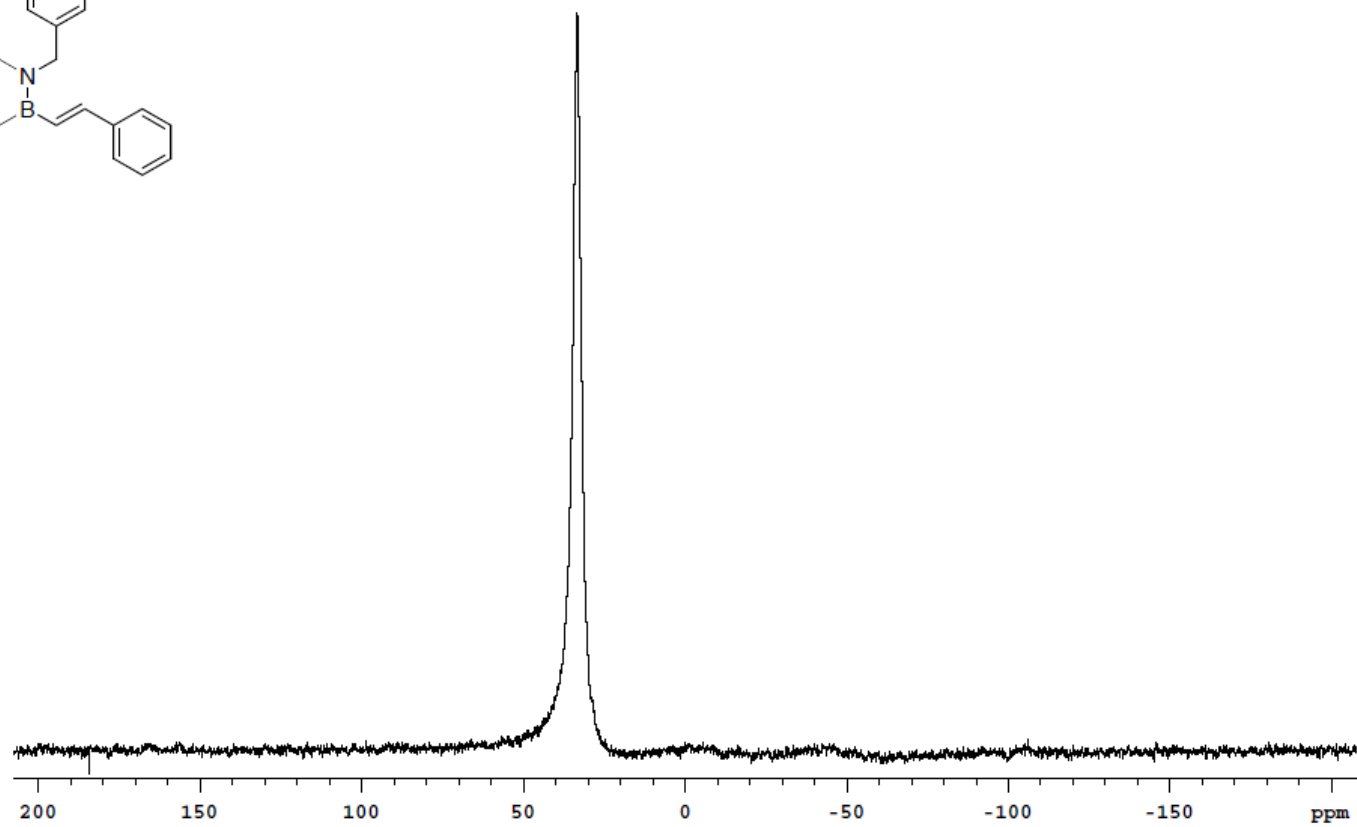
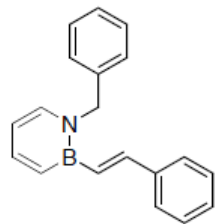
PULSE SEQUENCE Relax. delay 0.200 sec Pulse 60.0 degrees Acq. time 0.200 sec Width 40000.0 Hz 360 repetitions	OBSERVE E11, 96.2692069	DATA PROCESSING Line broadening 10.0 Hz FT size 16384 Total time 2 minutes	UO Inova-300-N Boron-11 Solvent: cd2cl2 Temp. 25.0 C / 298.1 K Operator: abrown File: ANB-PMeO-E11-Publication INOVA-500 "hotwax.uoregon.edu"
---	--------------------------------	--	---



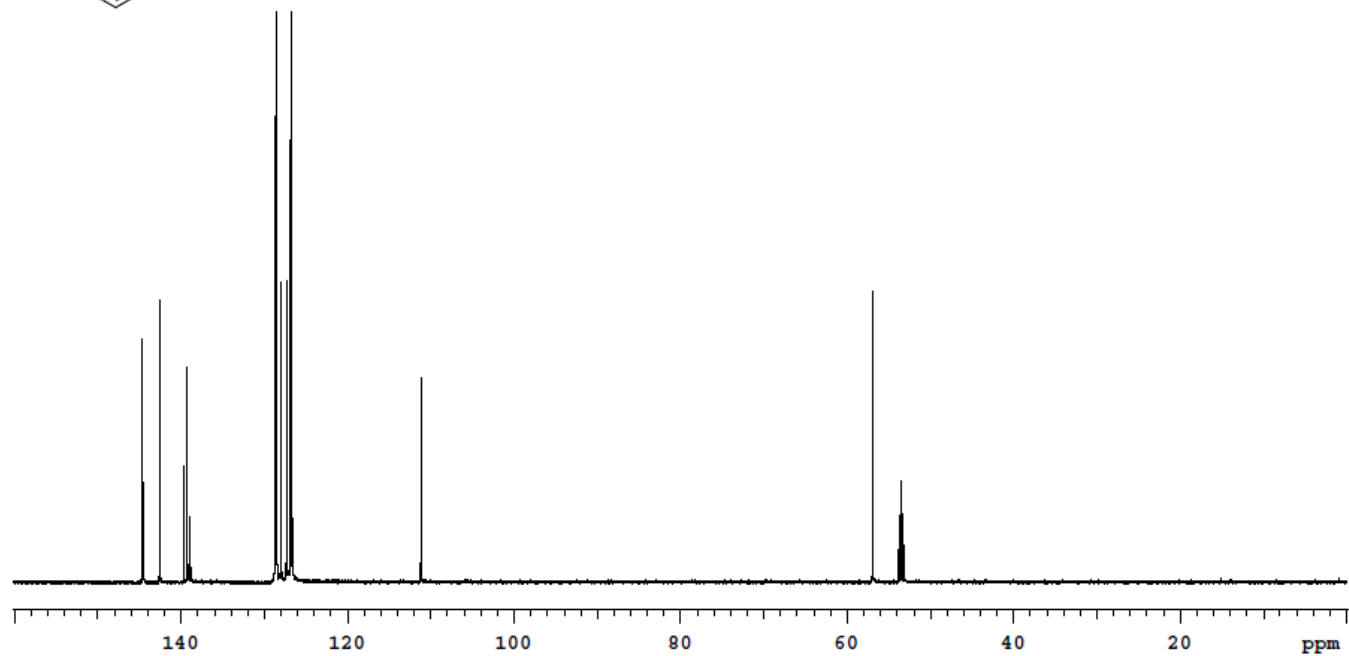
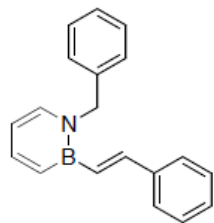
PULSE SEQUENCE Relax. delay 1.000 sec Pulse 45.0 degrees Acq. time 0.865 sec Width 27777.8 Hz 316 repetitions	OBSERVE C13, 150.8649758 DECOUPLE H1, 599.9825418 Power 43 dB continuously on WALTZ-16 modulated	DATA PROCESSING Line broadening 1.0 Hz FT size 131072 Total time 9 minutes	UO VNMR5-600 standard 13C P-MeO for Publication <hr/> Solvent: cd2cl2 Temp. 25.0 C / 298.1 K Operator: abrown File: ANB-PMeO-Cl3-Publication VNMR5-500 *hotwax.uoregon.edu*
---	---	--	---



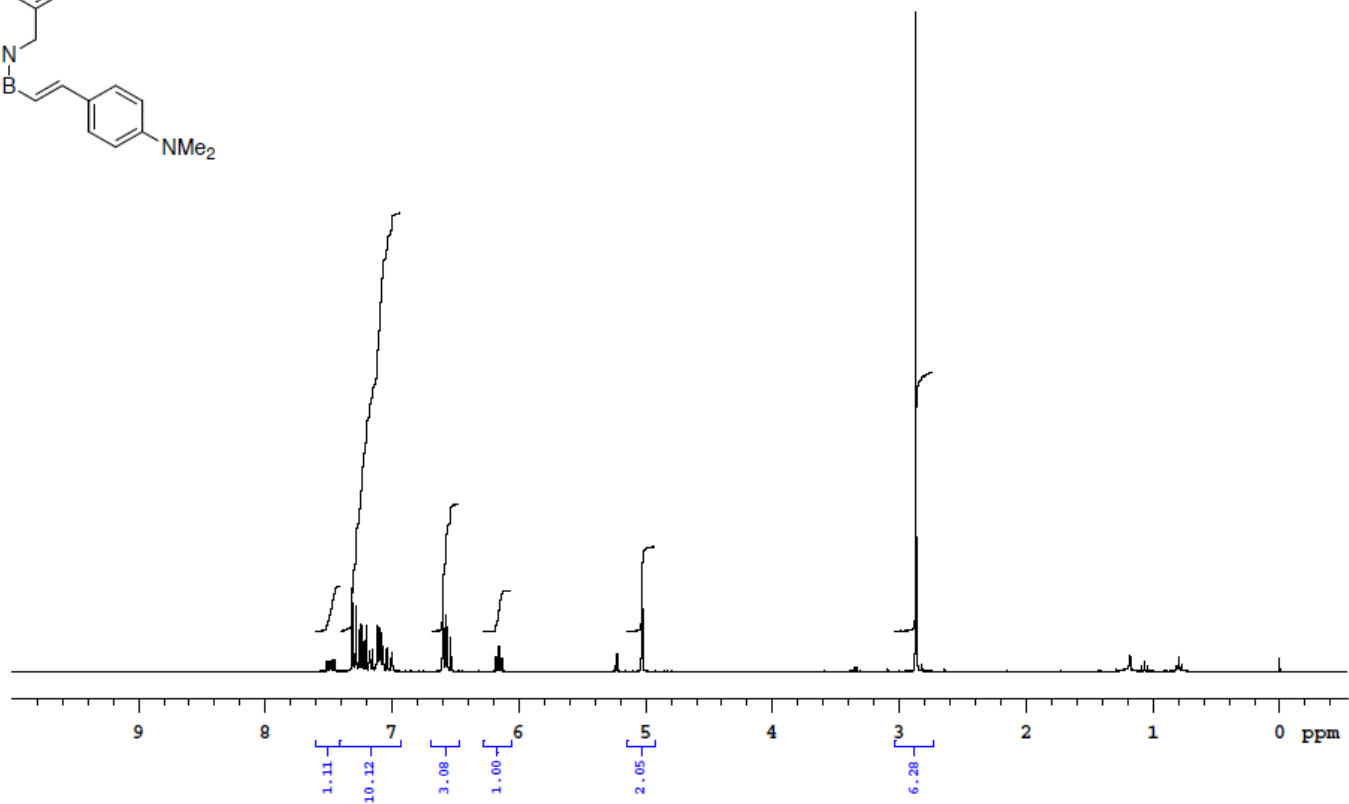
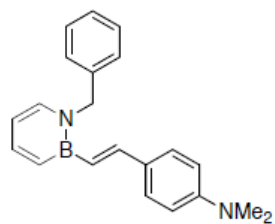
PULSE SEQUENCE Relax. delay 10.000 sec Pulse 45.0 degrees Acq. time 3.000 sec Width 4799.0 Hz 8 repetitions	OBSERVE H1, 299.9331583	DATA PROCESSING Line broadening 0.2 Hz FT size 32768 Total time 1 minutes	UO Inova-300 Standard-1H ANB-II-145- For Publication <hr/> Solvent: cd2cl2 Temp. 25.0 C / 298.1 K Operator: abrown File: ANB-II-145-H1-Publication
---	--------------------------------	---	--



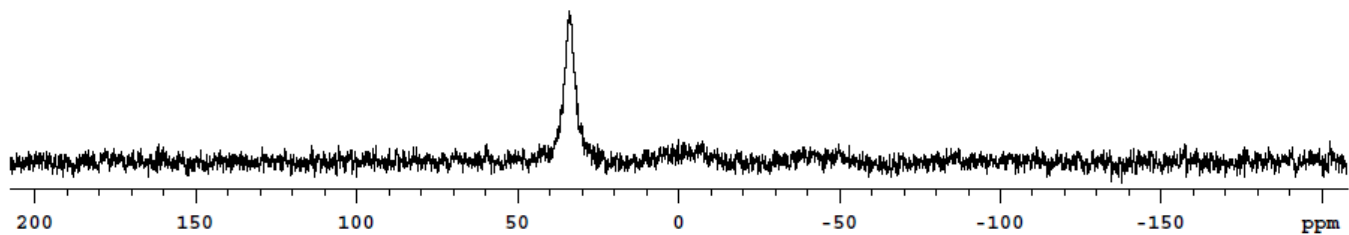
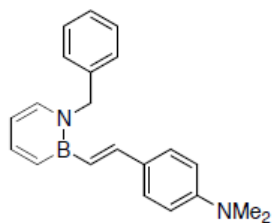
PULSE SEQUENCE Relax. delay 0.200 sec Pulse 60.0 degrees Acq. time 0.200 sec Width 40000.0 Hz 80 repetitions	OBSERVE B11, 96.2683493	DATA PROCESSING Line broadening 10.0 Hz FT size 16384 Total time 1 minute	UO Inova-300-N Boron-11 Solvent: D2O Temp. 25.0 C / 298.1 K Operator: abrown File: ANB-II-145-B11-Publication INOVA-500 "hotwax.uoregon.edu"
--	--------------------------------	---	--



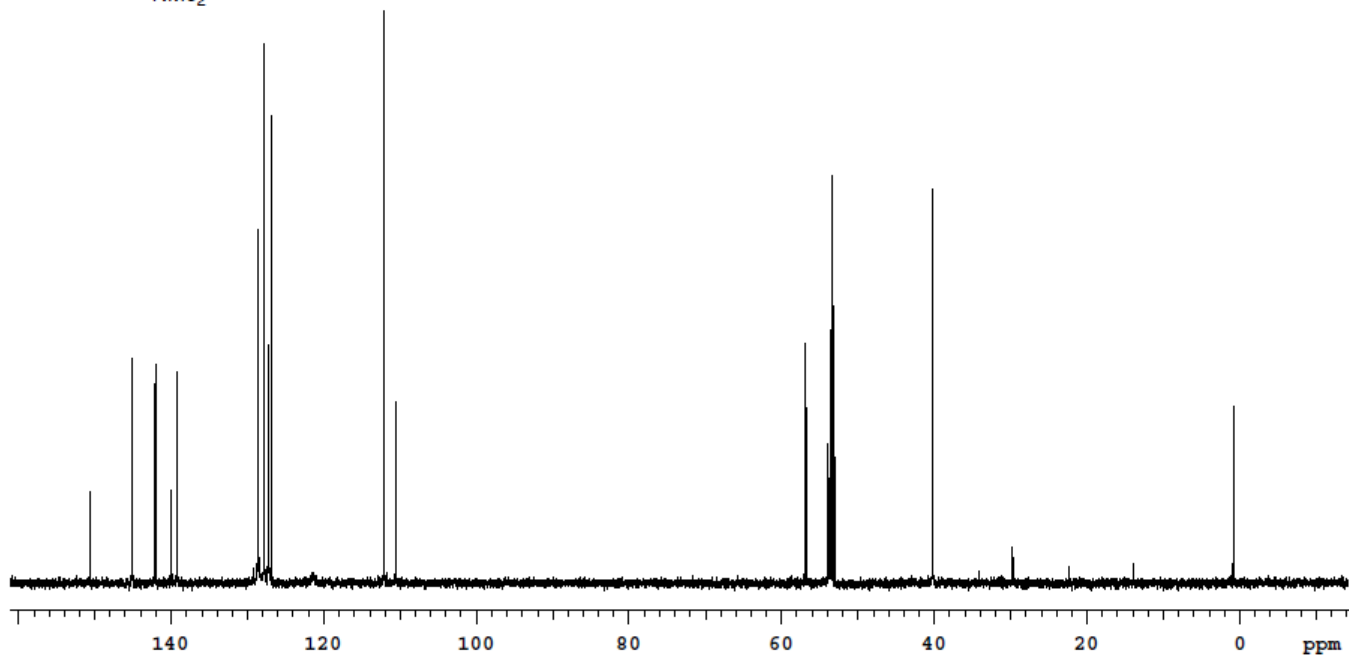
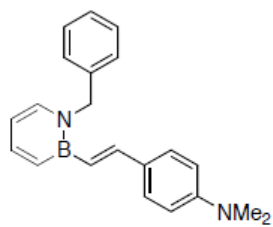
PULSE SEQUENCE Relax. delay 1.000 sec Pulse 45.0 degrees Acq. time 0.865 sec Width 37878.8 Hz 224 repetitions	OBSERVE C13, 150.8649570 DECOUPLE H1, 599.9824669 Power 44 dB continuously on WALTZ-16 modulated	DATA PROCESSING Line broadening 1.0 Hz FT size 131072 Total time 6 minutes	UO VNMR5-600 standard 13C ANB-II-145-For Publication Solvent: cd2cl2 Temp. 25.0 C / 298.1 K Operator: abrown File: ANB-II-145-C13-Publication VNMR5-500 "hotwax.uoregon.edu"
---	---	--	--



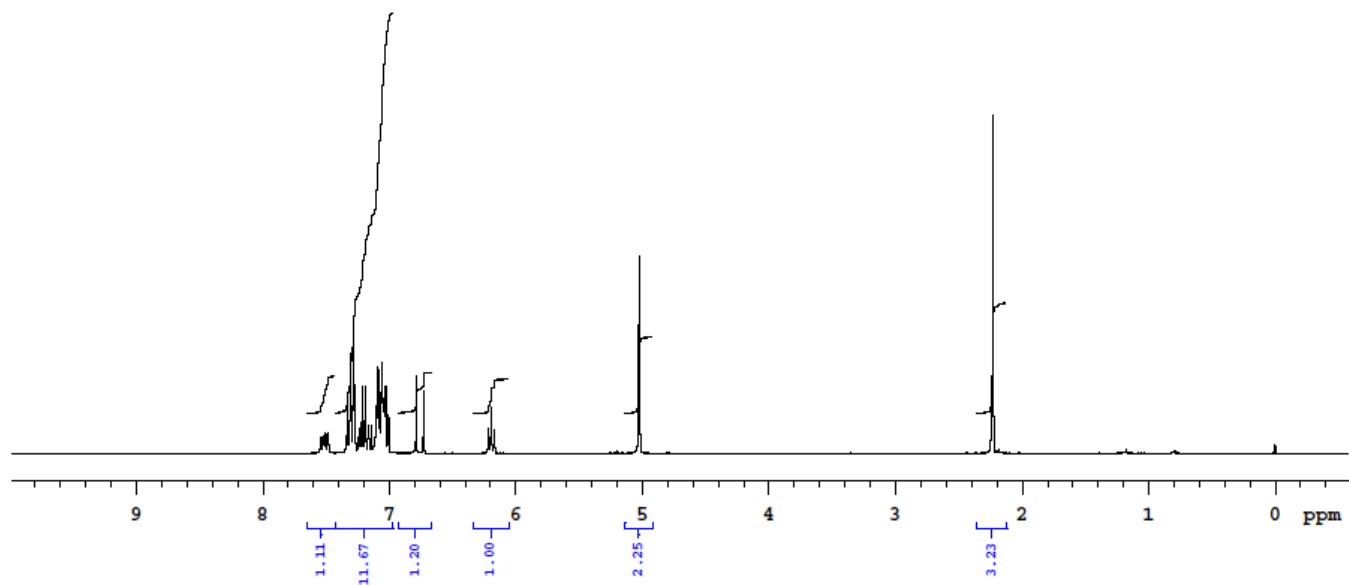
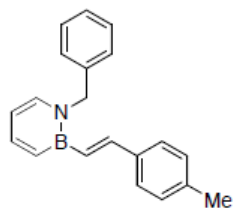
PULSE SEQUENCE Relax. delay 10.000 sec Pulse 45.0 degrees Acq. time 3.000 sec Width 4799.0 Hz 8 repetitions	OBSERVE H1, 299.9331355	DATA PROCESSING Line broadening 0.2 Hz FT size 32768 Total time 1 minutes	UO Inova-300 Standard-1H Solvent: cd2cl2 Temp. 25.0 C / 298.1 K Operator: abrown File: ANB-II-177-H1-PUBLICATION INOVA-500 "hotwax.uoregon.edu"
---	--------------------------------	---	---



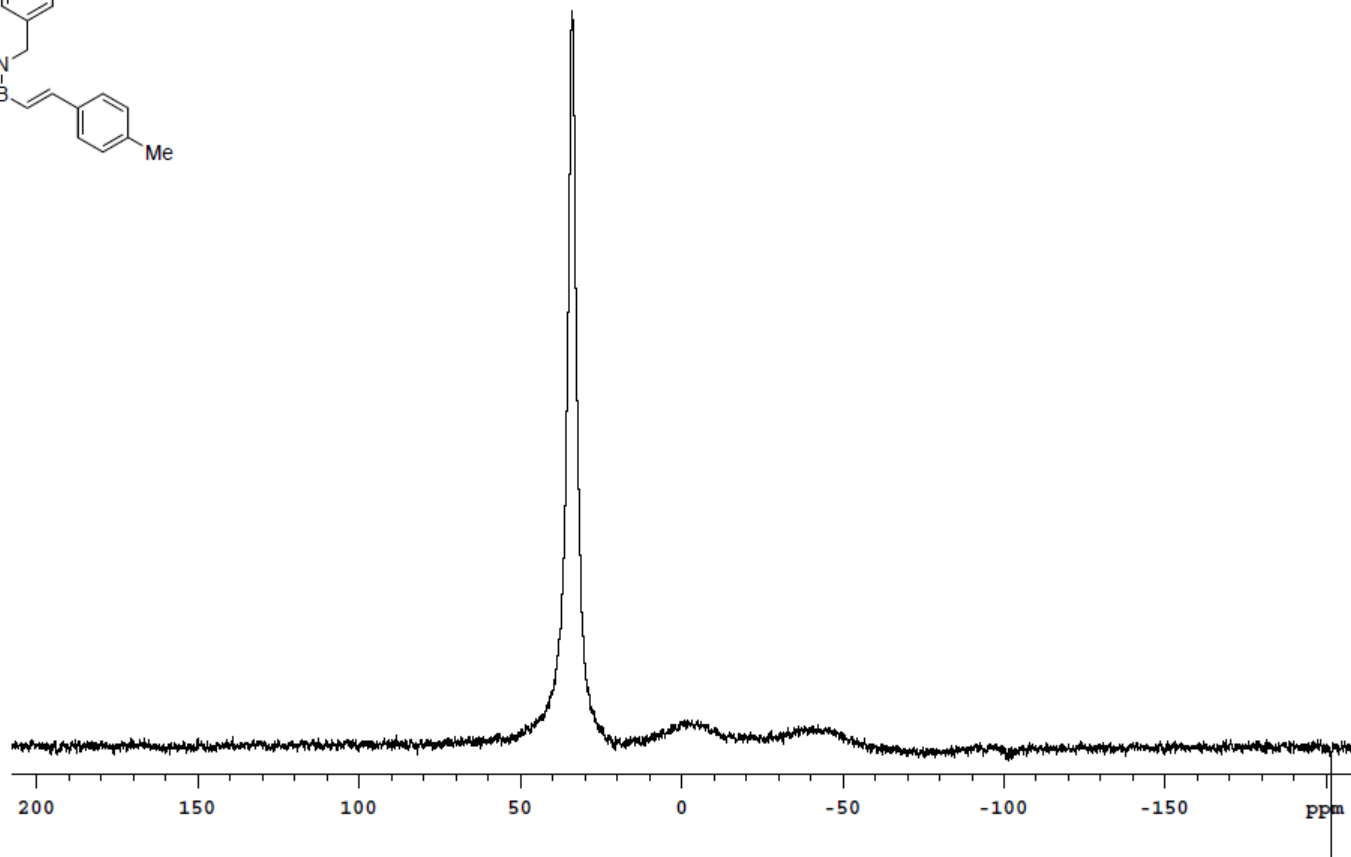
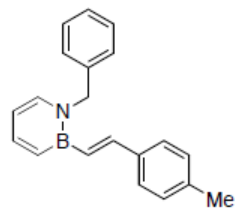
PULSE SEQUENCE Relax. delay 0.200 sec Pulse 60.0 degrees Acq. time 0.200 sec Width 40000.0 Hz 536 repetitions	OBSERVE B11, 96.2692868	DATA PROCESSING Line broadening 10.0 Hz FT size 16384 Total time 3 minutes	UO Inova-300-N Boron-11 ANB-II-177-PUBLICATION Solvent: CD2Cl2 Temp. 25.0 C / 298.1 K Operator: abrown File: ANB-II-177-B11-PUBLICATION INNOVA-500 "hotwax.uoregon.edu"
---	--------------------------------	--	---



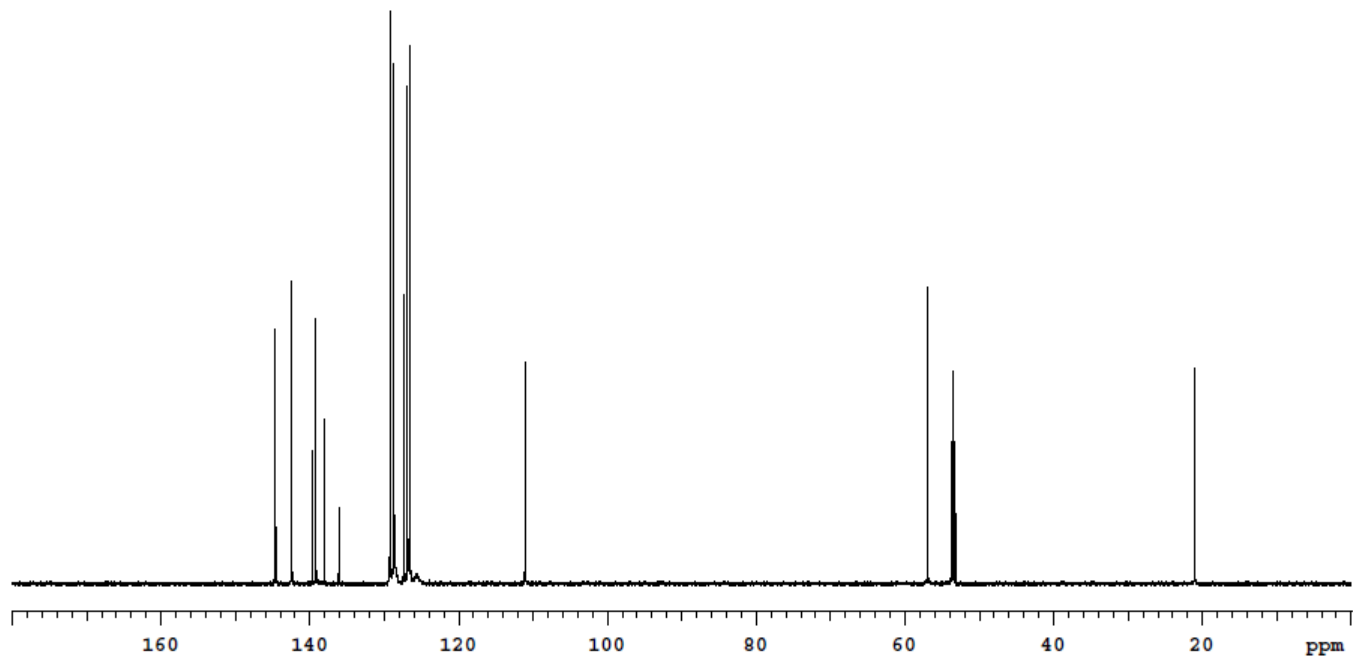
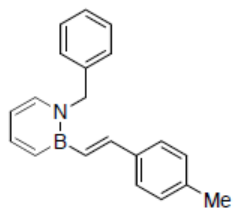
PULSE SEQUENCE Relax. delay 2.000 sec Pulse 45.0 degrees Acq. time 1.000 sec Width 31434.2 Hz 156 repetitions	OBSERVE C13, 125.7515537 DECOUPLE H1, 500.1077051 Power 39 dB continuously on WALTZ-16 modulated	DATA PROCESSING Line broadening 1.0 Hz FT size 65536 Total time 7 minutes	UO Inova-500 Carbon-13 ANB-II-301 P NMe2 Solvent: cd2cl2 Temp. 25.0 C / 298.1 K Operator: abrown File: ANB-PNMe2Stilbene-C13-Publication INOVA-500 "hotwax.uoregon.edu"
---	--	---	---



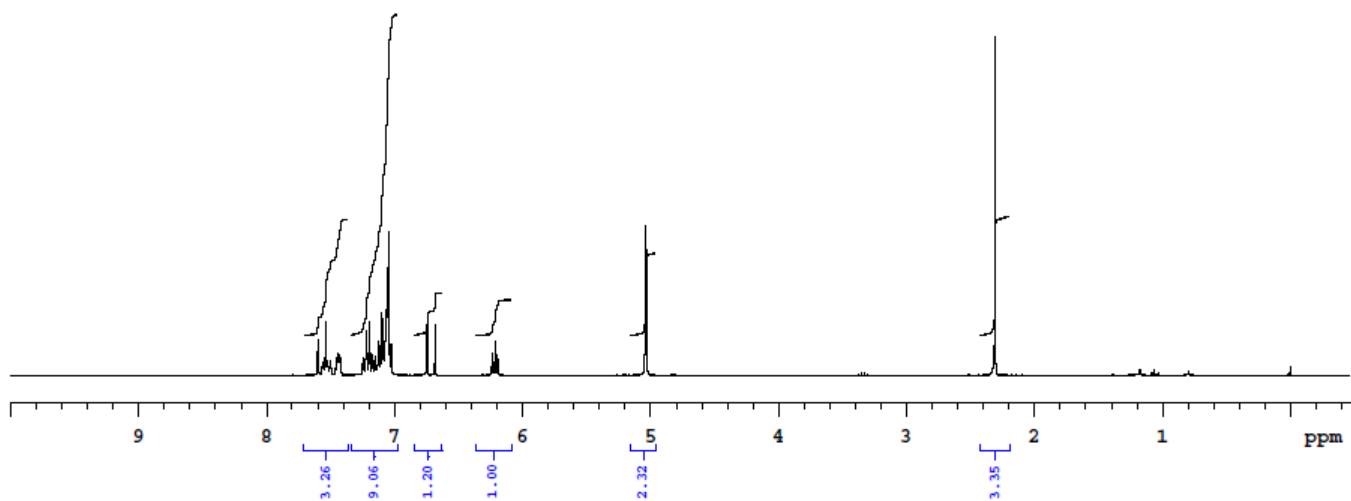
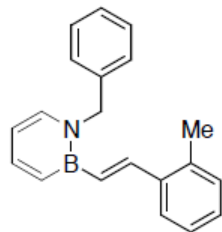
<p>PULSE SEQUENCE Relax. delay 10.000 sec Pulse 45.0 degrees Acq. time 3.000 sec Width 4800.8 Hz 8 repetitions</p>	<p>OBSERVE H1, 300.0510588</p>	<p>DATA PROCESSING Line broadening 0.2 Hz FT size 32768 Total time 1 minutes</p>	<p>UO Inova-300-N standard 1H ANB-II-129-FOR PUBLICATION Solvent: cd2cl2 Temp. 25.0 C / 298.1 K Operator: abrown File: ANB-II-129-H1-Publication</p>
--	--------------------------------	--	--



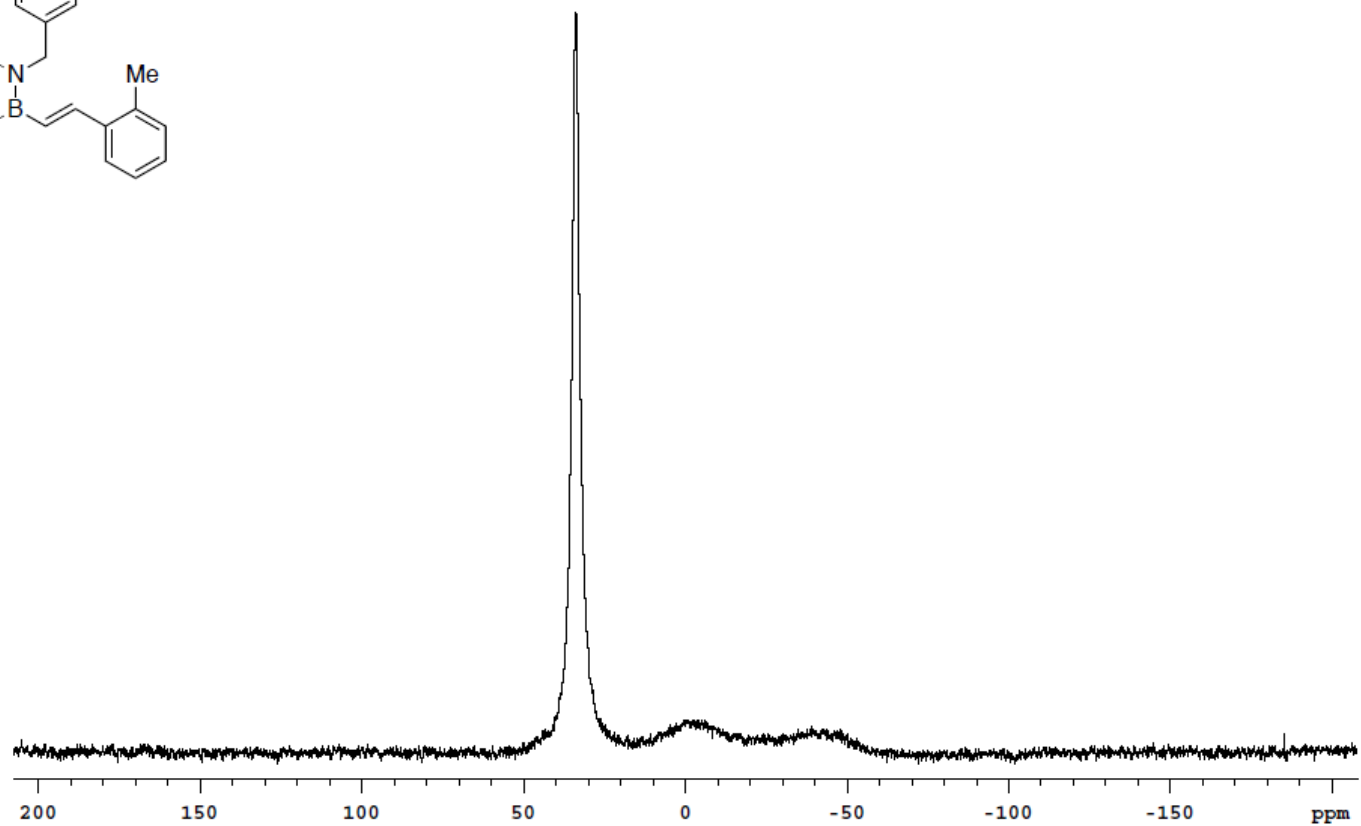
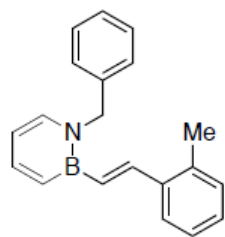
PULSE SEQUENCE Relax. delay 0.200 sec Pulse 60.0 degrees Acq. time 0.200 sec Width 40000.0 Hz 400 repetitions	OBSERVE B11, 96.2692968	DATA PROCESSING Line broadening 10.0 Hz FT size 16384 Total time 2 minutes	UO Inova-300-N Boron-11 ANB-II-129-FOR Publication Solvent: cd2c12 Temp. 25.0 C / 298.1 K Operator: abrown File: ANB-II-129-B11-Publication INOVA-500 "hotwax.uoregon.edu"
---	--------------------------------	--	--



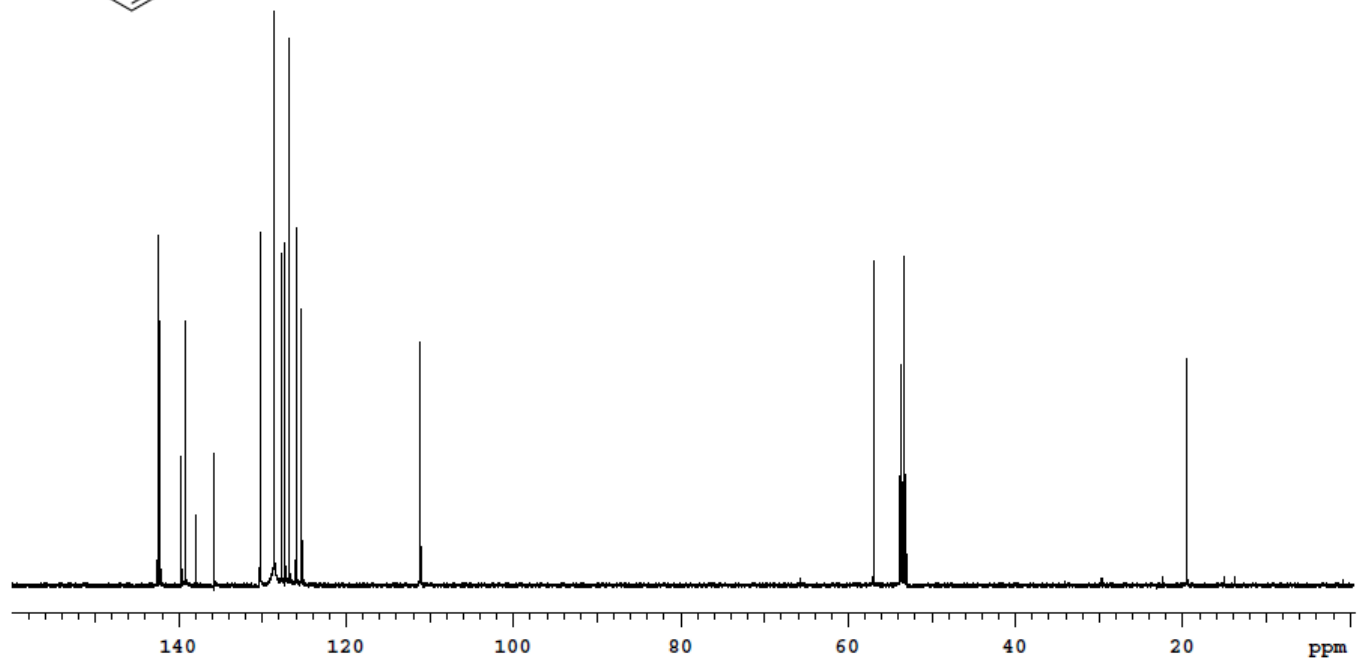
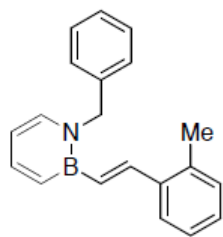
PULSE SEQUENCE Relax. delay 2.000 sec Pulse 45.0 degrees Acq. time 0.865 sec Width 37878.8 Hz 236 repetitions	OBSERVE C13, 150.8649570 DECOUPLE H1, 599.9824669 Power 44 dB continuously on WALTZ-16 modulated	DATA PROCESSING Line broadening 1.0 Hz FT size 131072 Total time 11 minutes	UO VNMR5-600 standard 13C ANB-II-141-For Publication Solvent: cd2c12 Temp. 25.0 C / 298.1 K Operator: abrown File: ANB-II-129-C13-Publication VNMR5-500 "hotwax.uoregon.edu"
---	---	---	--



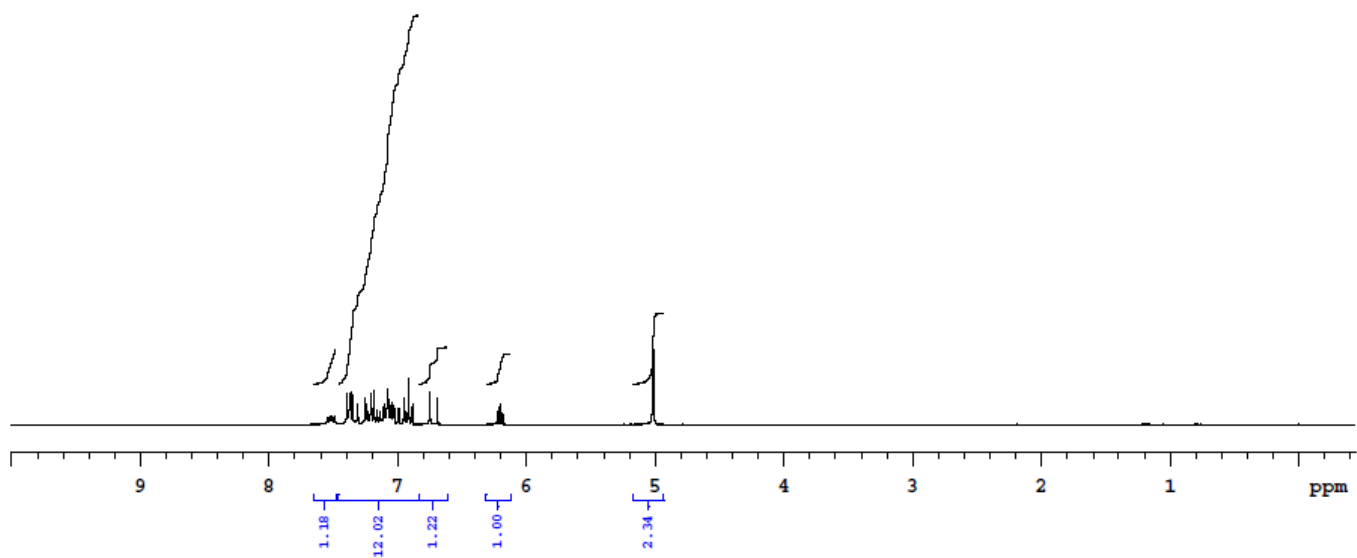
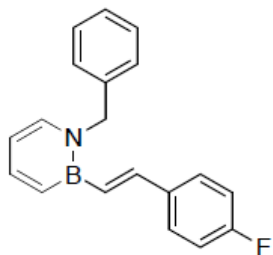
PULSE SEQUENCE Relax. delay 10.000 sec Pulse 45.0 degrees Acq. time 3.000 sec Width 4800.8 Hz 8 repetitions	OBSERVE H1, 300.0510586	DATA PROCESSING Line broadening 0.2 Hz FT size 32768 Total time 1 minutes	UO Inova-300-N standard 1H ANB-II-131-For Publication <hr/> Solvent: D2O Temp. 25.0 C / 298.1 K Operator: abrown File: ANB-II-131-H1-Publication
---	--------------------------------	---	--



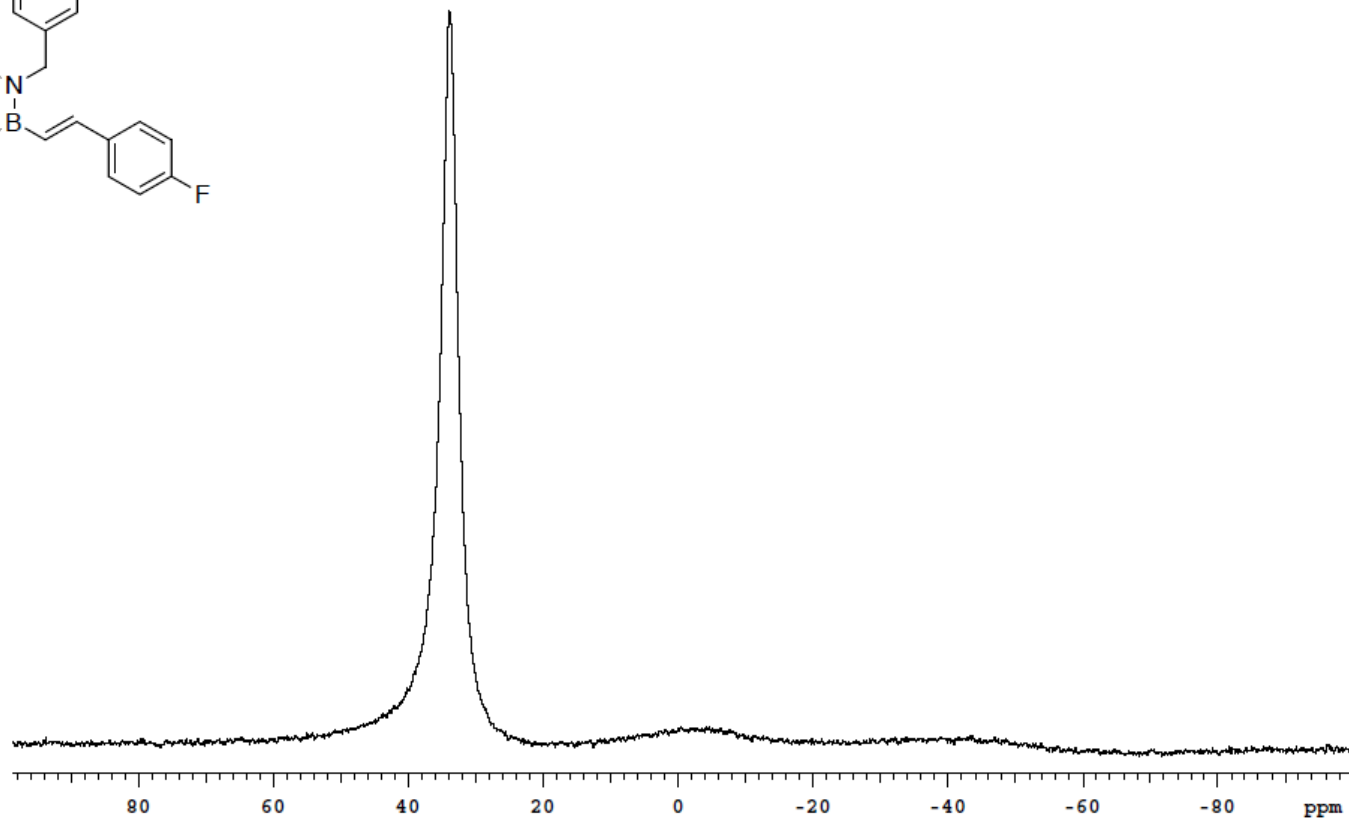
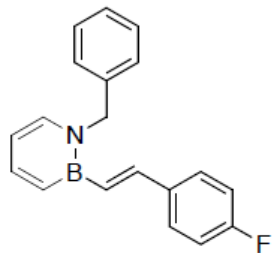
PULSE SEQUENCE Relax. delay 0.200 sec Pulse 60.0 degrees Acq. time 0.200 sec Width 40000.0 Hz 272 repetitions	OBSERVE B11, 96.2692868	DATA PROCESSING Line broadening 10.0 Hz FT size 16384 Total time 1 minutes	Solvent: cd2cl2 Temp. 25.0 C / 298.1 K Operator: abrown File: ANB-II-131-B11-Publication INOVA-500 "hotwax.uoregon.edu"
---	--------------------------------	--	--



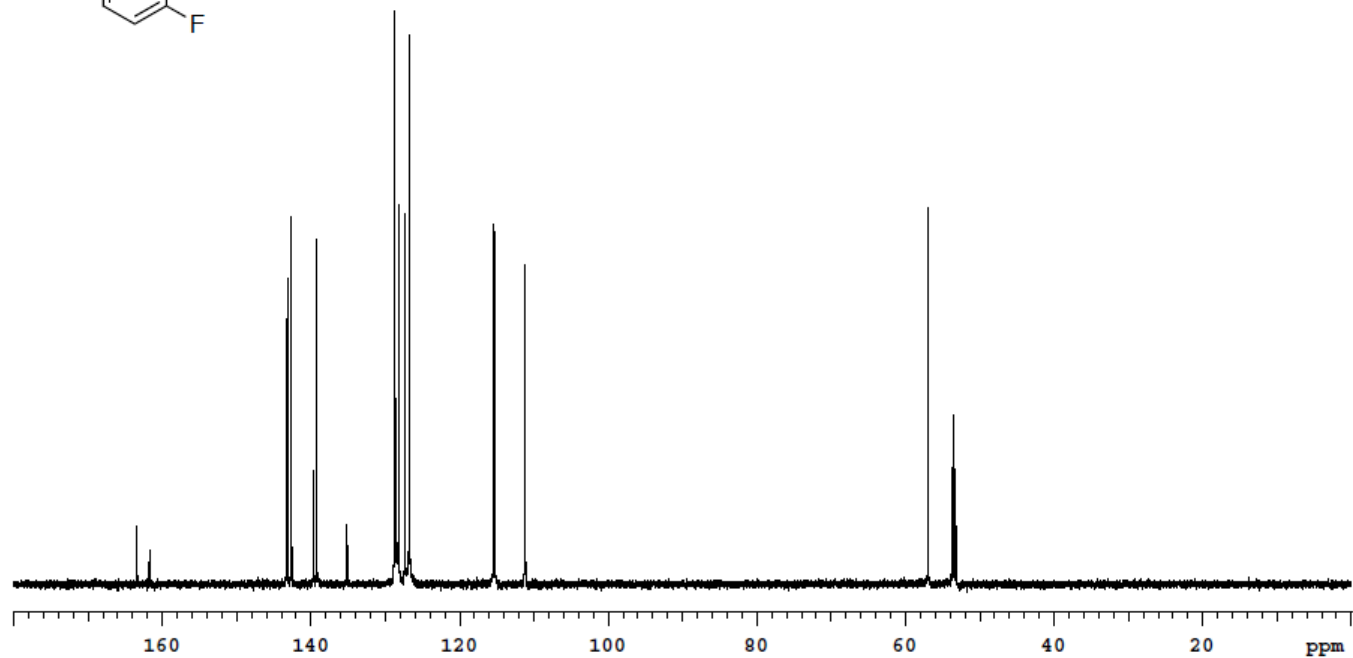
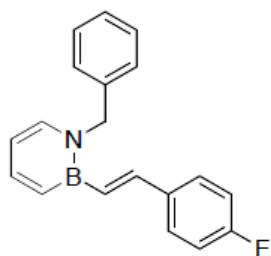
PULSE SEQUENCE Relax. delay 1.000 sec Pulse 45.0 degrees Acq. time 0.865 sec Width 37878.8 Hz 836 repetitions	OBSERVE C13, 150.8649570 DECOUPLE H1, 599.9824669 Power 44 dB continuously on WALTZ-16 modulated	DATA PROCESSING Line broadening 1.0 Hz FT size 131072 Total time 25 minutes	UO VNMR5-600 standard 13C ANB-II-131-For Publication Solvent: cd2c12 Temp. 25.0 C / 298.1 K Operator: abrown File: ANB-II-131-C13-Publication VNMR5-500 "hotwax.uoregon.edu"
---	---	---	--



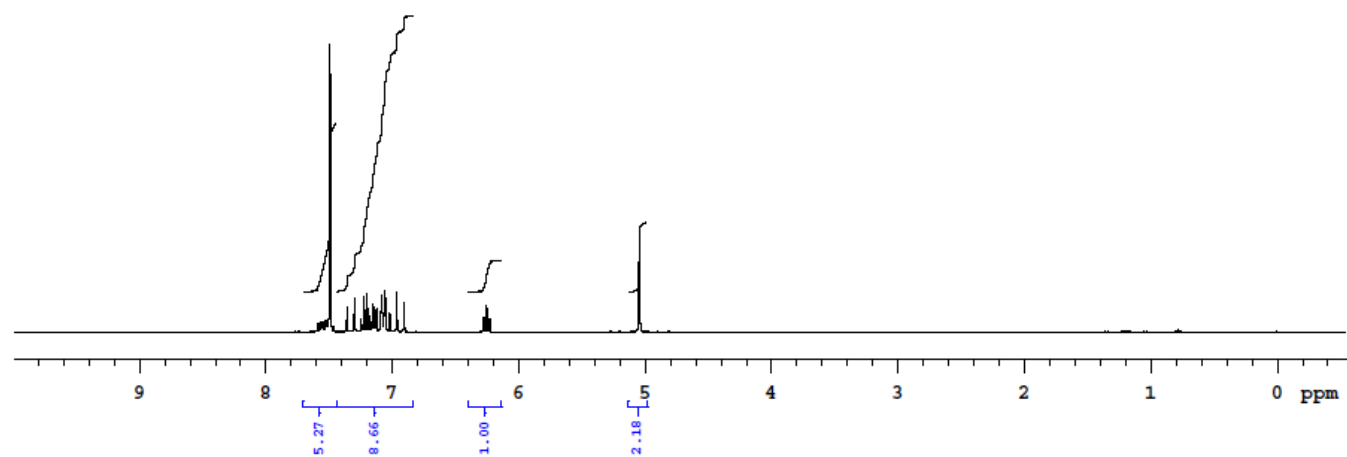
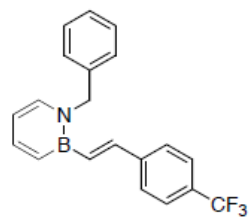
PULSE SEQUENCE Relax. delay 10.000 sec Pulse 45.0 degrees Acq. time 3.000 sec Width 4900.8 Hz 8 repetitions	OBSERVE H1, 300.0510632	DATA PROCESSING Line broadening 0.2 Hz FT size 32768 Total time 1 minutes	UO Inova-300-N standard 1H ANB-II-141-FOR PUBLICATION <hr/> Solvent: cd2cl2 Temp. 25.0 C / 298.1 K Operator: abrown File: ANB-II-141-H1-Publication
---	--------------------------------	---	---



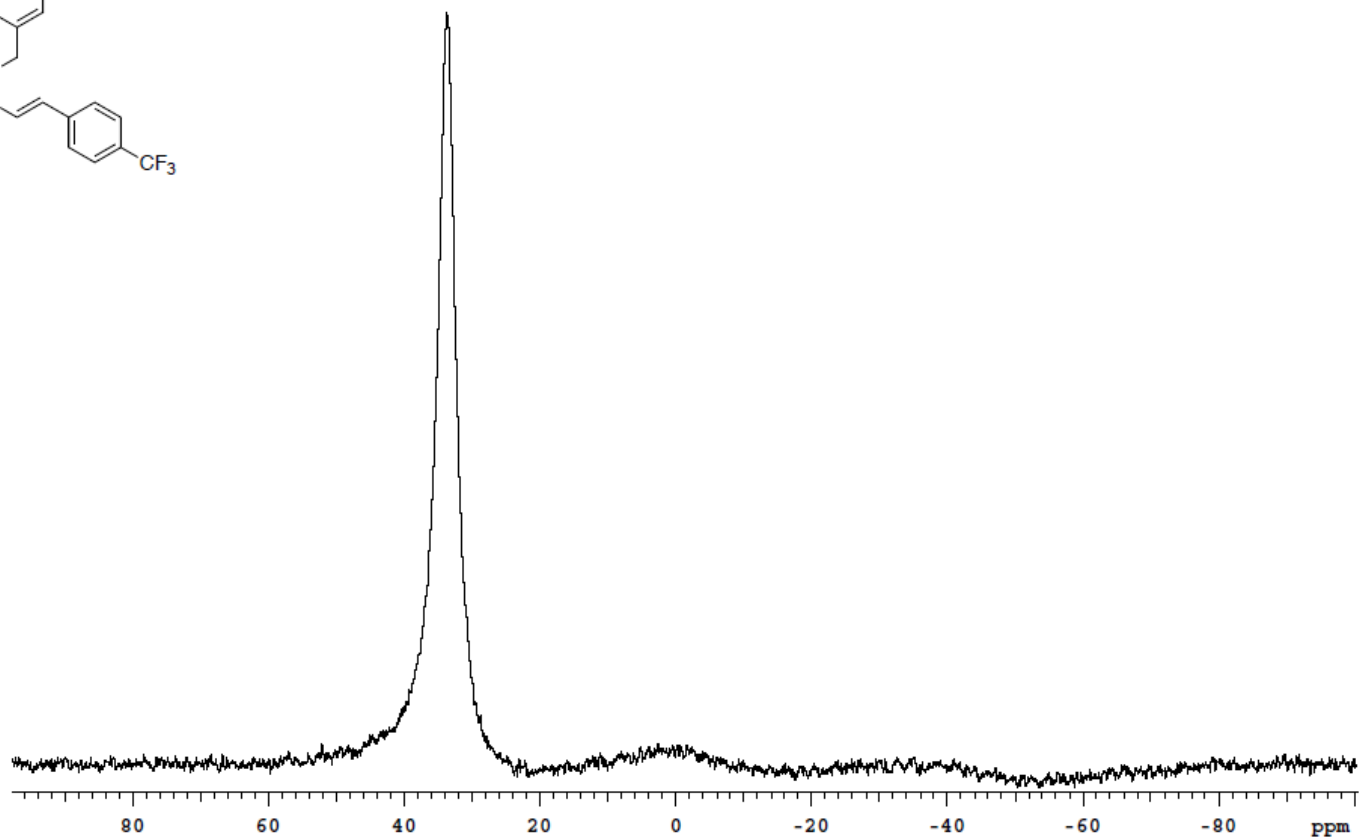
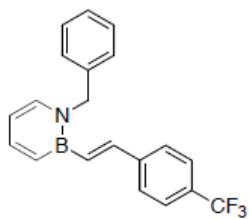
PULSE SEQUENCE Relax. delay 0.200 sec Pulse 60.0 degrees Acq. time 0.200 sec Width 40000.0 Hz 400 repetitions	OBSERVE B11, 96.2692868	DATA PROCESSING Line broadening 10.0 Hz FT size 16384 Total time 2 minutes	UO Inova-300-N Boron-11 ANB-II-141-FOR Publication Solvent: cd2cl2 Temp. 25.0 C / 298.1 K Operator: abrown File: ANB-II-141-B11-Publication INOVA-500 *hotwax.uoregon.edu*
---	--------------------------------	--	--



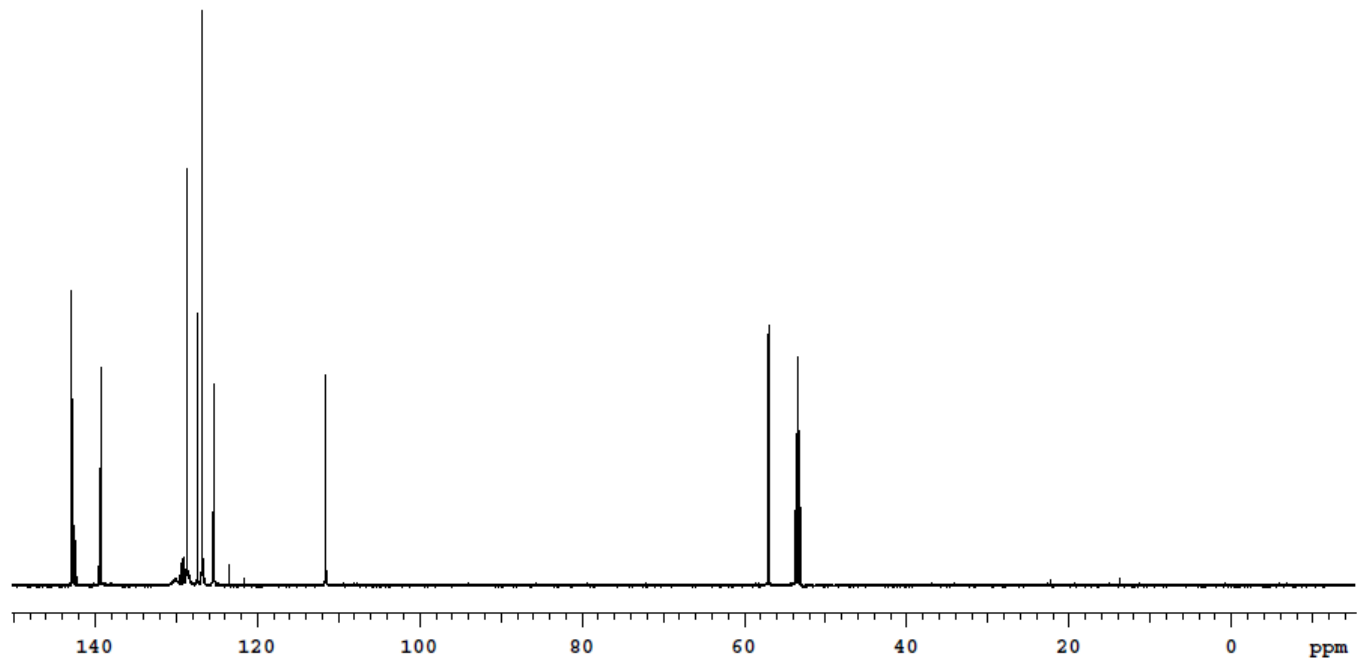
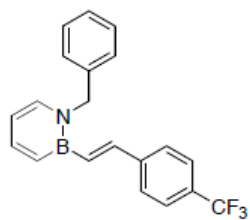
PULSE SEQUENCE Relax. delay 1.000 sec Pulse 45.0 degrees Acq. time 0.965 sec Width 37878.8 Hz 236 repetitions	OBSERVE C13, 150.9649570 DECOUPLE H1, 599.9824669 Power 44 dB continuously on WALTZ-16 modulated	DATA PROCESSING Line broadening 1.0 Hz FT size 131072 Total time 7 minutes	UO VNMR5-600 standard 13C ANB-II-141-For Publication Solvent: cd2c12 Temp. 25.0 C / 298.1 K Operator: abrown File: ANB-II-141-C13-Publication VNMR5-500 "hotwax.uoregon.edu"
---	--	--	--



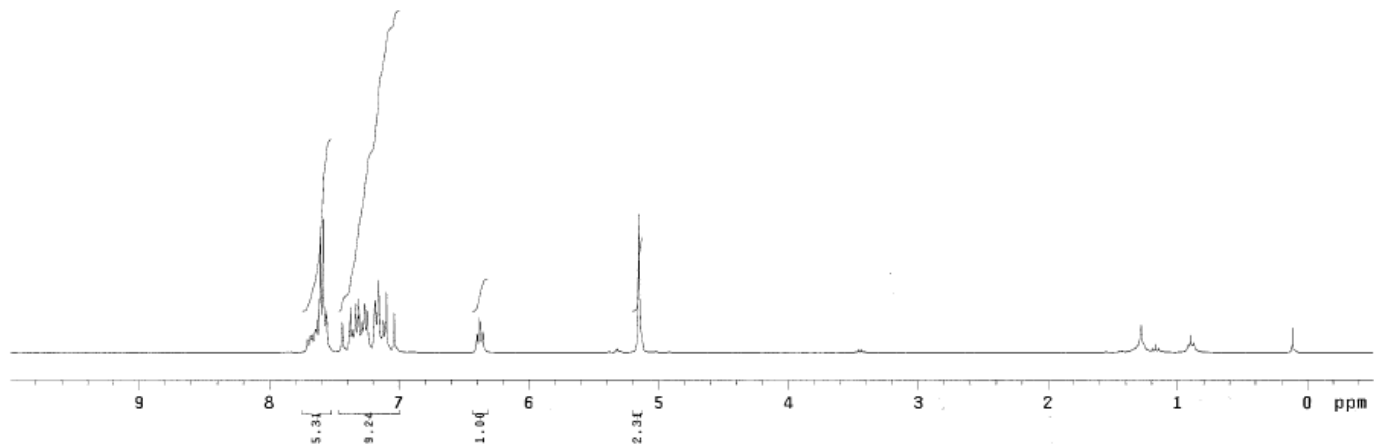
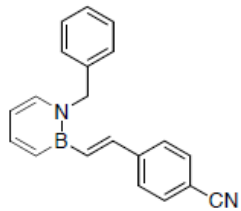
PULSE SEQUENCE Relax. delay 10.000 sec Pulse 45.0 degrees Acq. time 3.000 sec Width 4900.9 Hz 8 repetitions	OBSERVE H1, 300.0510573	DATA PROCESSING Line broadening 0.2 Hz FT size 32768 Total time 1 minutes	UO Inova-300-N standard 1H Solvent: cd2cl2 Temp. 25.0 C / 298.1 K Operator: abrown File: ANB-II-133-H1-Publication INOVA-500 "hotwax.uoregon.edu"
---	--------------------------------	---	---



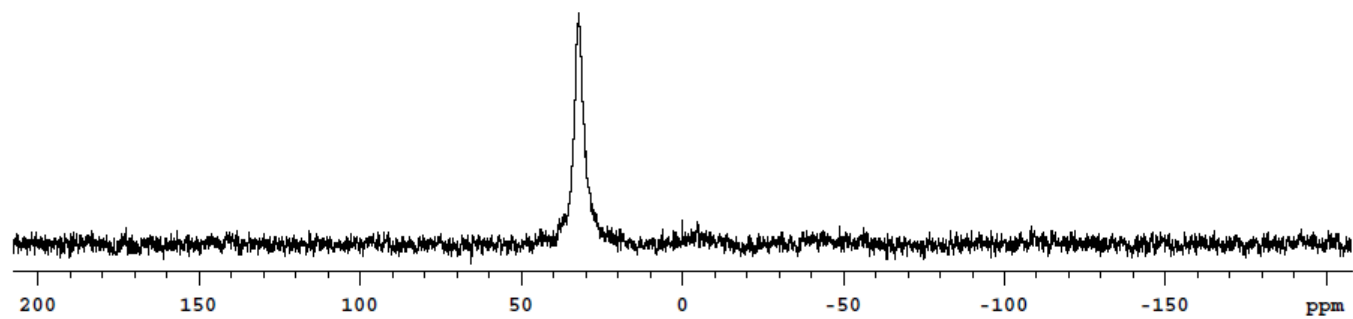
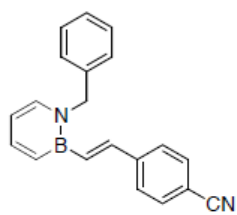
<p>PULSE SEQUENCE Relax. delay 0.200 sec Pulse 60.0 degrees Acq. time 0.200 sec Width 40000.0 Hz 176 repetitions</p>	<p>OBSERVE B11, 96.2682868</p>	<p>DATA PROCESSING Line broadening 10.0 Hz FT size 16384 Total time 1 minute</p>	<p>UO Inova-300-N Boron-11 ANB-I-133 for Publication</p> <hr/> <p>Solvent: cd2cl2 Temp. 25.0 C / 298.1 K Operator: abrown File: ANB-II-133-B11-Publication INOVA-500 *hotwax.uoregon.edu*</p>
--	--------------------------------	--	---



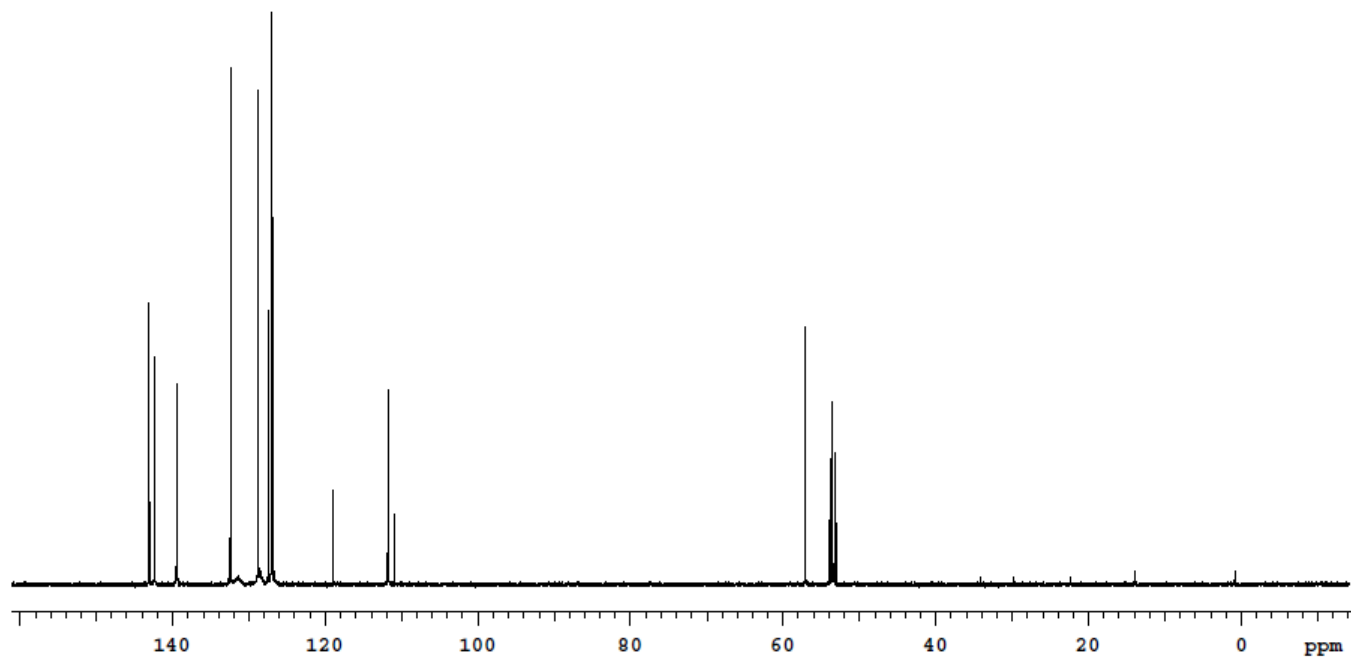
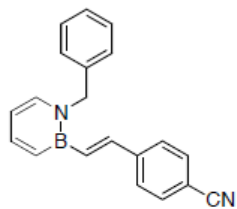
PULSE SEQUENCE Relax. delay 1.000 sec Pulse 45.0 degrees Acq. time 0.865 sec Width 37878.8 Hz 1056 repetitions	OBSERVE C13, 150.9649570 DECOUPLE H1, 599.9824669 Power 44 dB continuously on WALTZ-16 modulated	DATA PROCESSING Line broadening 1.0 Hz FT size 131072 Total time 32 minutes	UO VNMR5-600 standard 13C ANB-II-133-For Publication Solvent: cd2cl2 Temp. 25.0 C / 298.1 K Operator: abrown File: ANB-II-133-C13-Publication VNMR5-500 "hotwax.uoregon.edu"
--	---	---	--



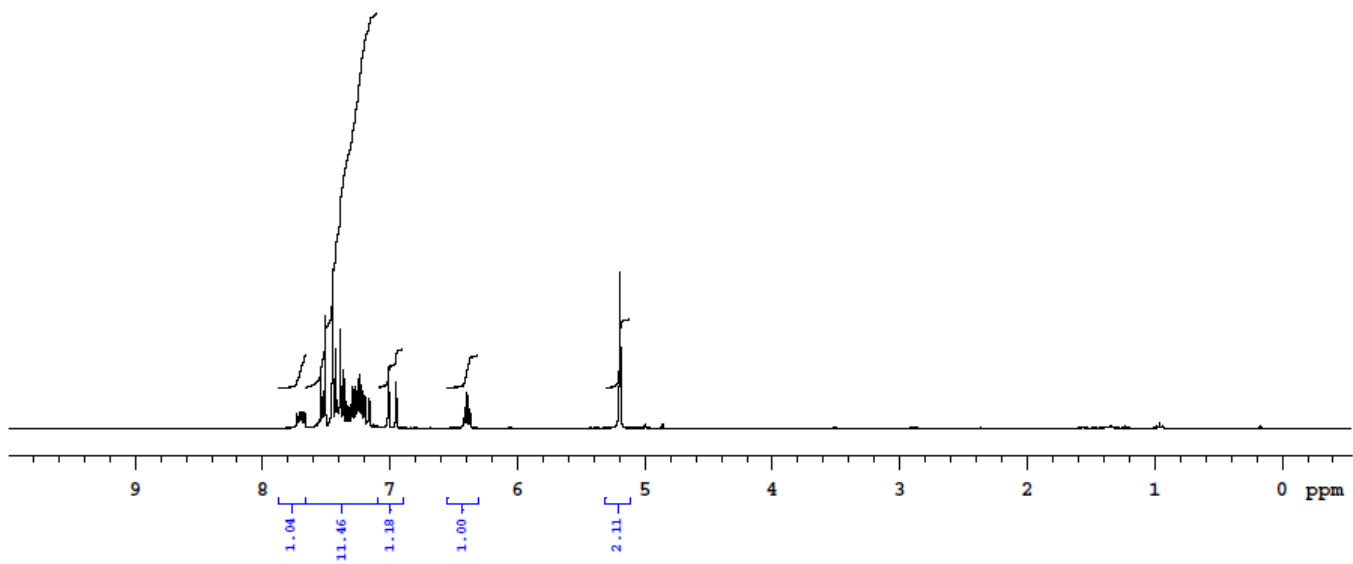
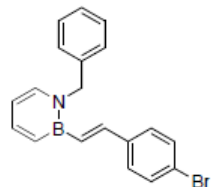
PULSE SEQUENCE Relax. delay 1.000 sec Pulse 45.0 degrees Acq. time 3.000 sec Width 4798.0 Hz 8 repetitions	OBSERVE H1, 299.9331082	DATA PROCESSING Line broadening 0.2 Hz FT size 32768 Total time 1 minute	UO Inova-300 Standard-1H Solvent: cdcl3 Temp. 25.0 C / 298.1 K Operator: abrown File: P-CN62yield INOVA-500 "nmr16"
---	-------------------------	---	--



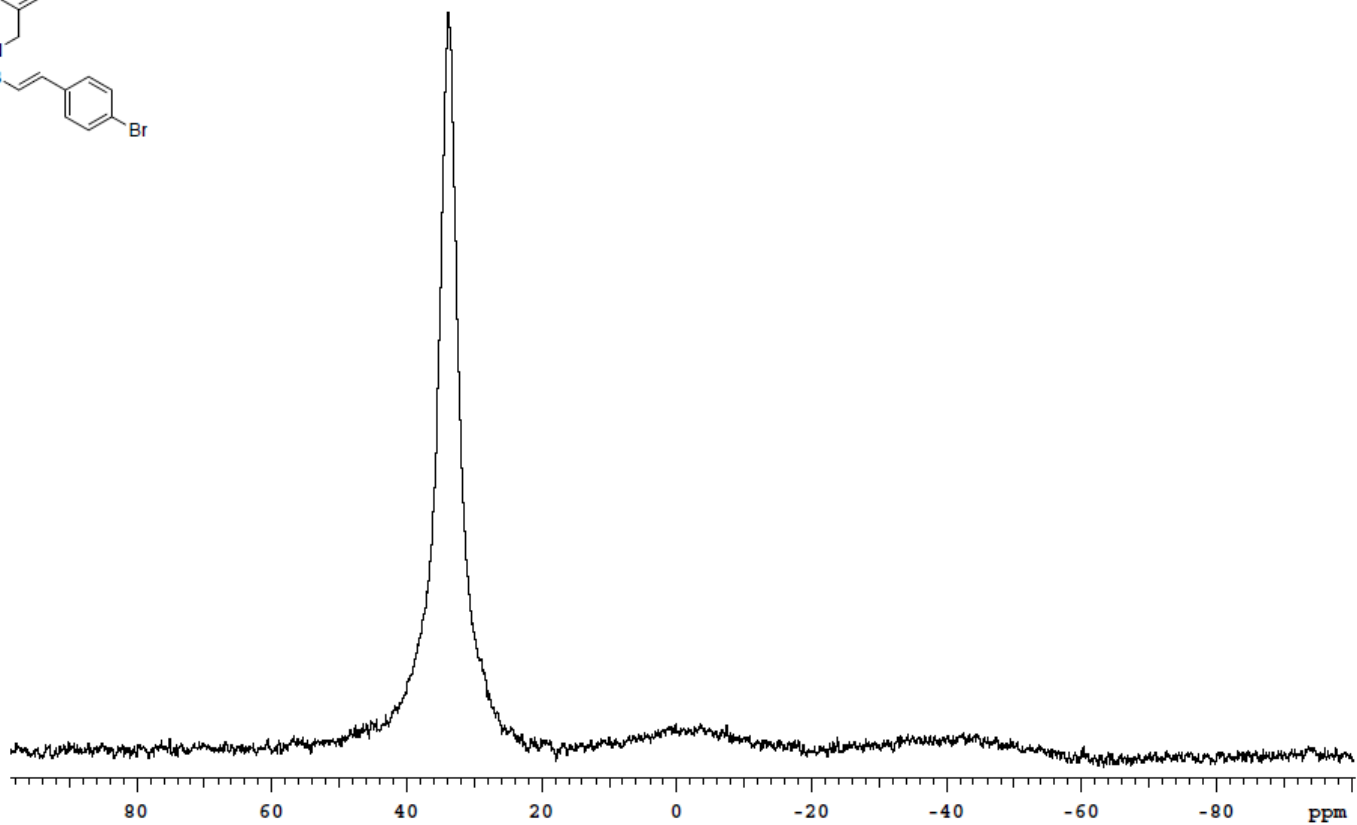
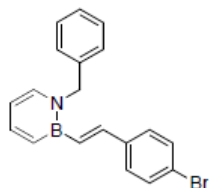
PULSE SEQUENCE Relax. delay 0.200 sec Pulse 60.0 degrees Acq. time 0.200 sec Width 40000.0 Hz 288 repetitions	OBSERVE B11, 96.2692869	DATA PROCESSING Line broadening 10.0 Hz FT size 16384 Total time 1 minutes	UO Inova-300-N Boron-11 Solvent: CD2Cl2 Temp. 25.0 C / 298.1 K Operator: abrown File: ANB-II-187-B11-PUBLICATION INOVA-500 *hotwax.uoregon.edu*
---	--------------------------------	--	---



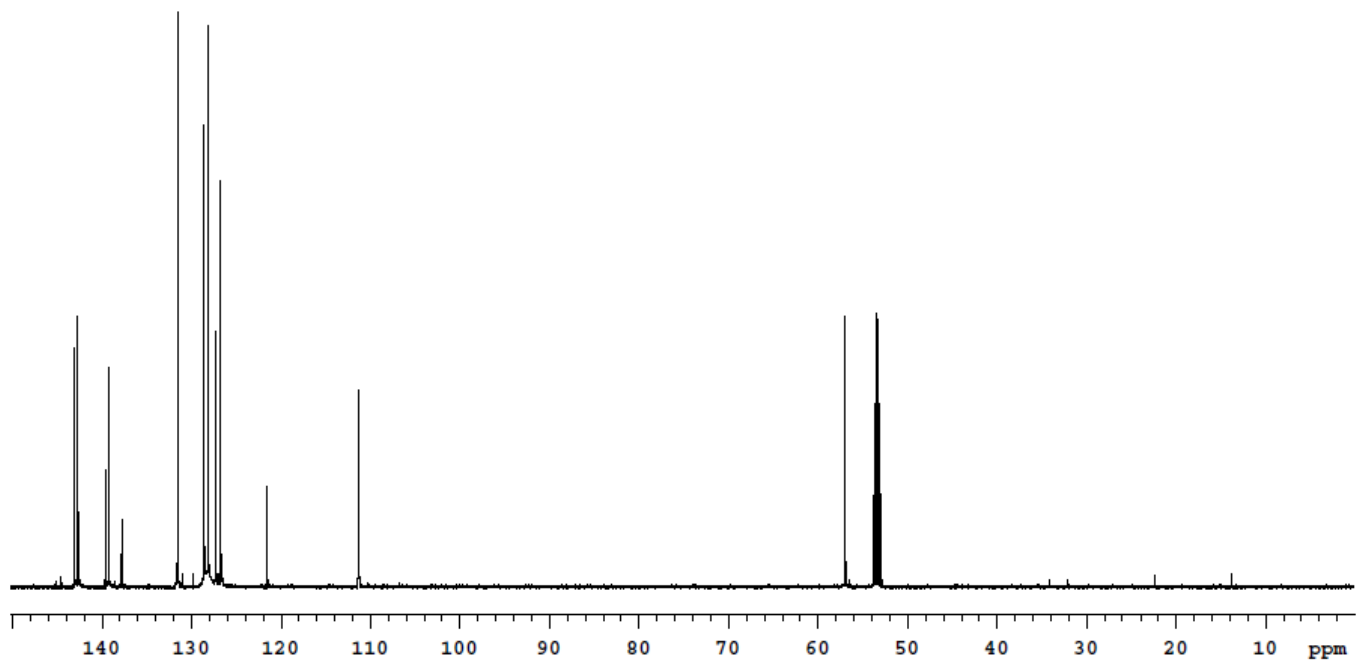
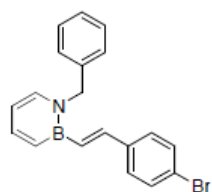
PULSE SEQUENCE Relax. delay 2.000 sec Pulse 45.0 degrees Acq. time 1.000 sec Width 31434.2 Hz 304 repetitions	OBSERVE C13, 125.7515537 DECOUPLE H1, 500.1077051 Power 39 dB continuously on WALTZ-16 modulated	DATA PROCESSING Line broadening 1.0 Hz FT size 65536 Total time 15 minutes	UO Inova-500 Carbon-13 ANB-II--PCN-Pub Solvent: cd2cl2 Temp. 25.0 C / 298.1 K Operator: abrown File: ANB-PCNStilbene-C13-Publication INOVA-500 "hotwax.uoregon.edu"
---	---	--	---



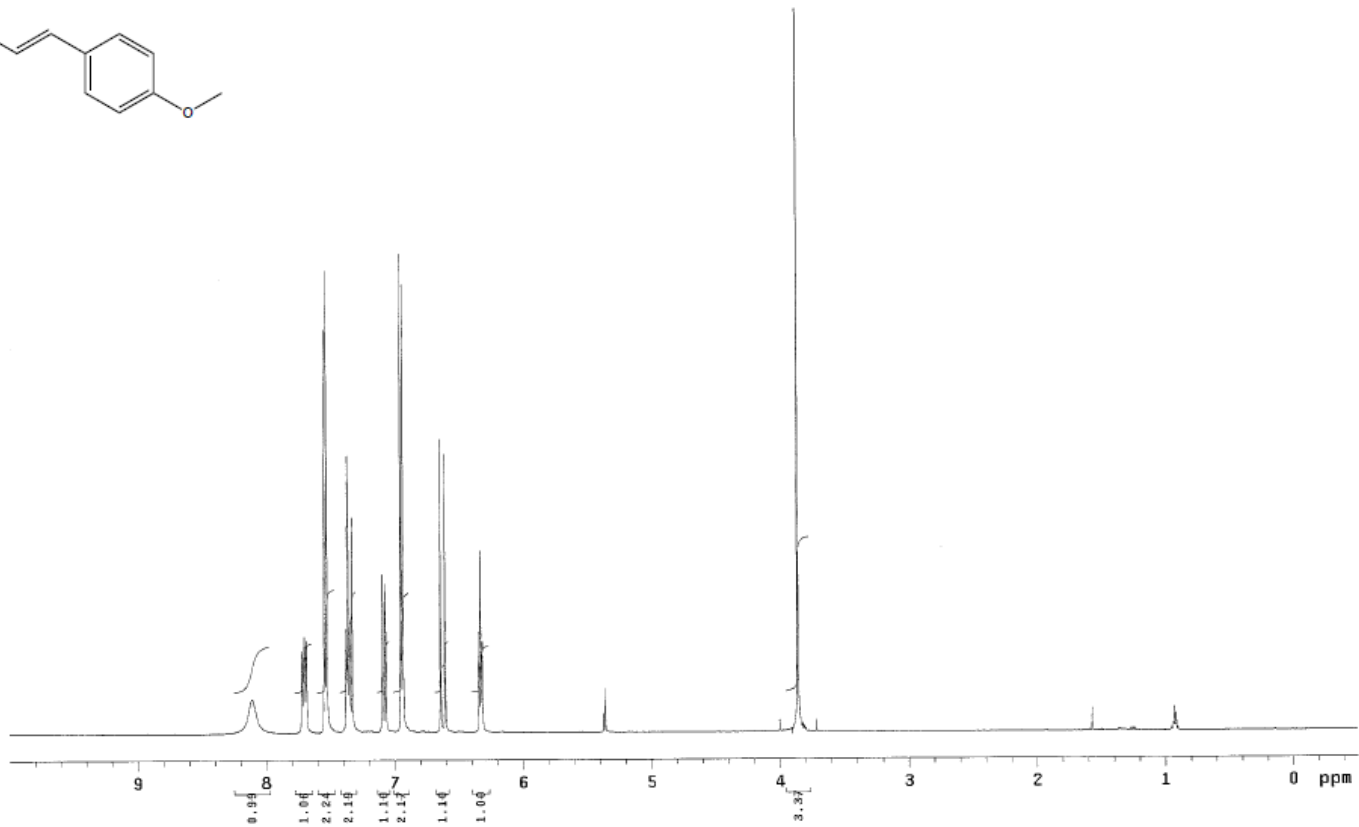
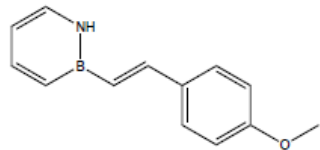
PULSE SEQUENCE Relax. delay 10.000 sec Pulse 45.0 degrees Acq. time 3.000 sec Width 4800.8 Hz 9 repetitions	OBSERVE H1, 300.0510060	DATA PROCESSING Line broadening 0.2 Hz FT size 32768 Total time 1 minutes	UO Inova-300-N standard 1H Solvent: cd2cl2 Temp. 25.0 C / 298.1 K Operator: abrown File: ANB-II-137-H1-bestssofar INOVA-500 *hotwax.uoregon.edu
--	-------------------------	--	---



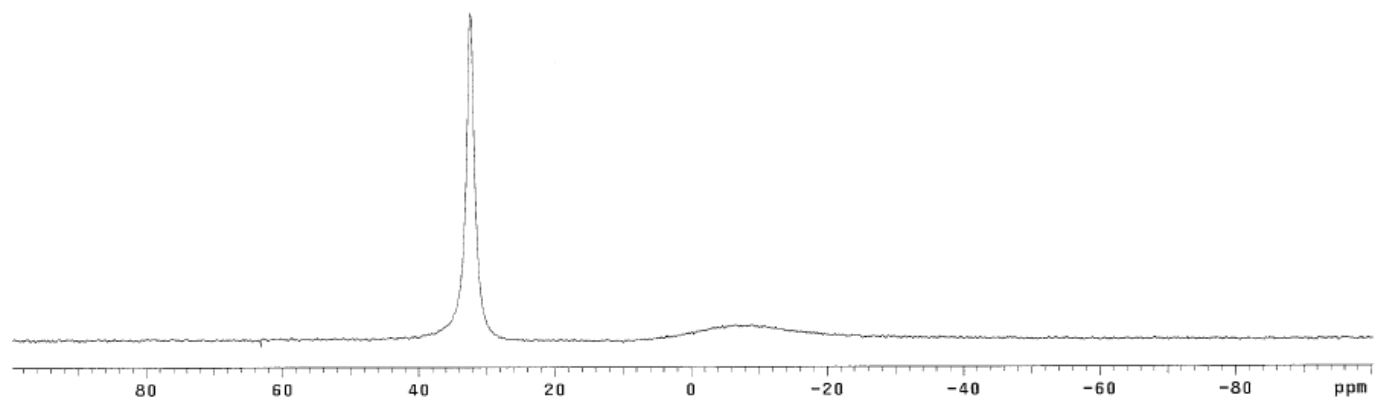
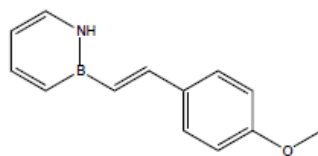
PULSE SEQUENCE Relax. delay 0.200 sec Pulse 60.0 degrees Acq. time 0.200 sec Width 40000.0 Hz 328 repetitions	OBSERVE B11, 96.2682868	DATA PROCESSING Line broadening 10.0 Hz FT size 16384 Total time 2 minutes	UO Inova-300-N Boron-11 ANB-I-137 for Publication Solvent: cd2c12 Temp. 25.0 C / 298.1 K Operator: abrown File: ANB-II-137-B11-Publication INOVA-500 "hotwax.uoregon.edu"
--	-------------------------	---	---



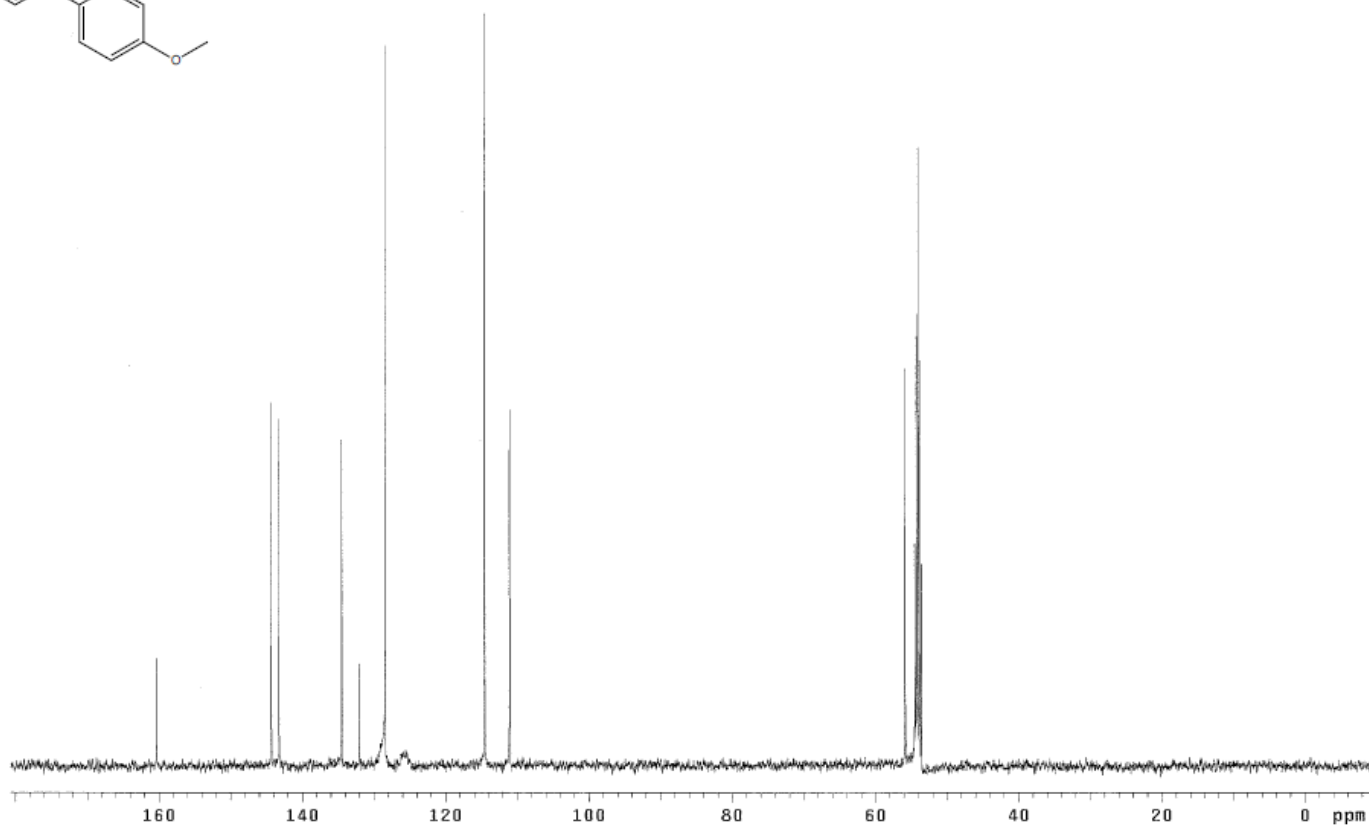
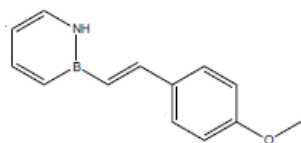
PULSE SEQUENCE Relax. delay 1.000 sec Pulse 45.0 degrees Acq. time 0.865 sec Width 37878.8 Hz 1140 repetitions	OBSERVE C13, 150.8649570 DECOUPLE H1, 599.9824669 Power 44 dB continuously on WALTZ-16 modulated	DATA PROCESSING Line broadening 1.0 Hz FT size 131072 Total time 35 minutes	UO VNMR5-600 standard 13C ANB-II-137-bestsofar Solvent: cd2c12 Temp. 25.0 C / 298.1 K Operator: abrown File: ANB-II-137-C13-bestsofar VNMR5-500 "hotwax.uoregon.edu"
--	---	---	--



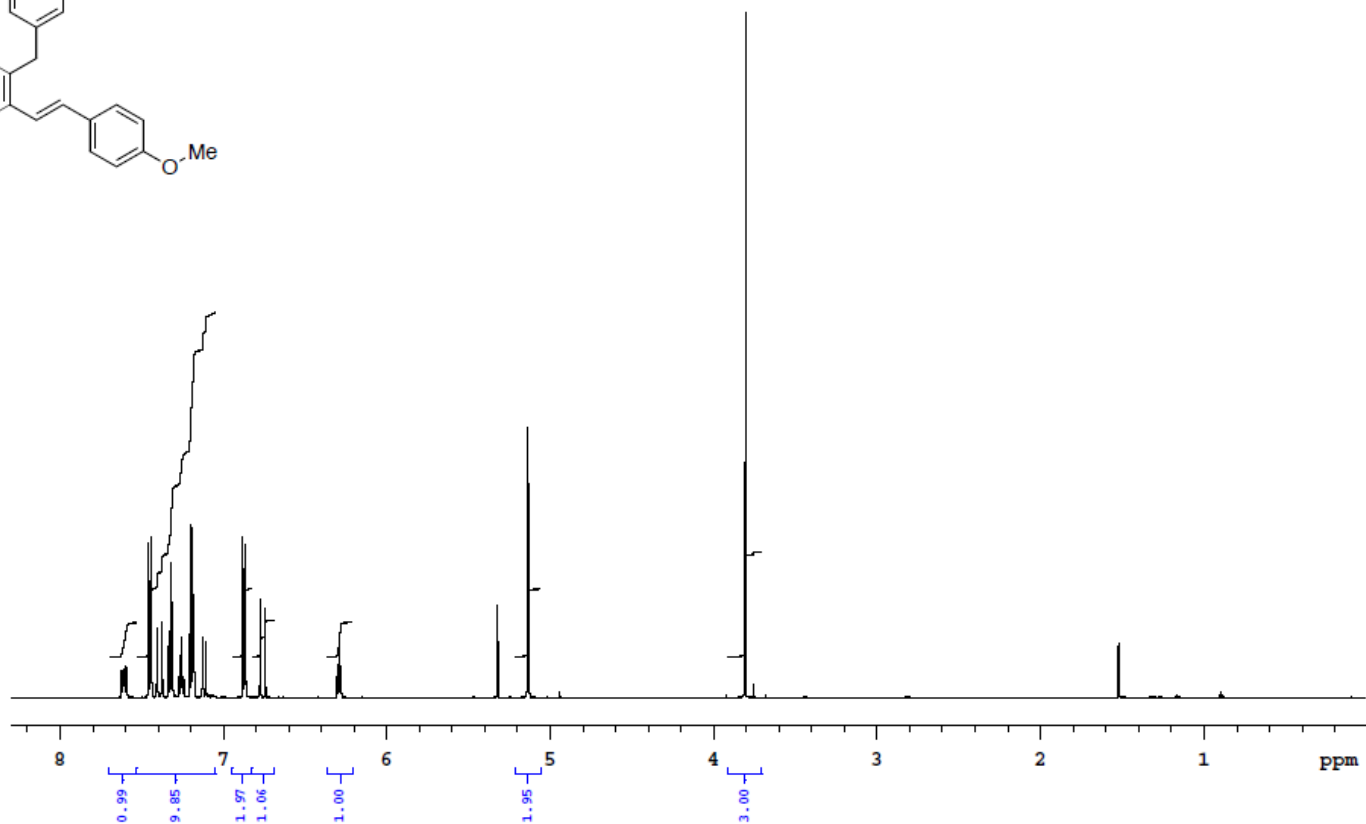
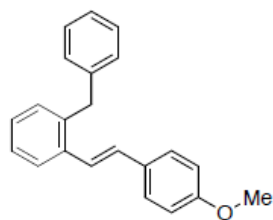
PULSE SEQUENCE Relax. delay 10.000 sec Pulse 45.0 degrees Acq. time 2.049 sec Width 7996.0 Hz 8 repetitions	OBSERVE H1, 499.7729719	DATA PROCESSING FT size 32768 Total time 1 minutes	ANb-V-297-1H-Pub Solvent: cd2c12 Temp. 25.0 C / 298.1 K Operator: Liu INOVA-500 "mer11"
---	--------------------------------	---	--



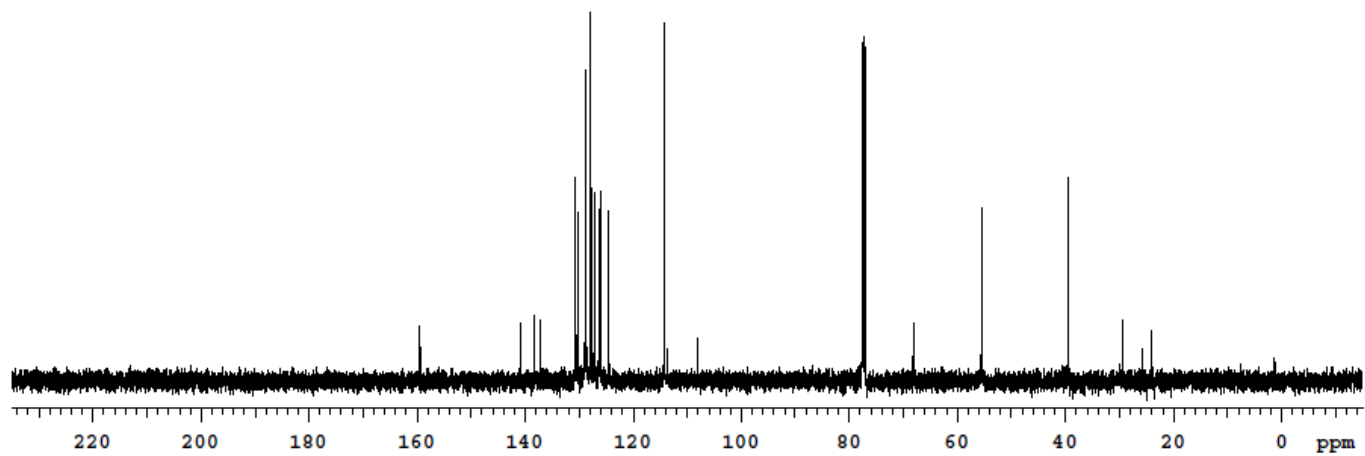
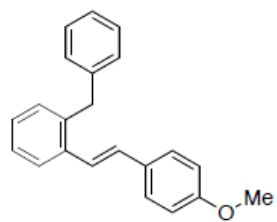
PULSE SEQUENCE Relax. delay 0.100 sec Pulse 00.6 degrees Acq. time 0.100 sec Width 32051.3 Hz 56 repetitions	OBSERVE B11, 160.3470852	DATA PROCESSING Line broadening 15.0 Hz FT size 6132 Total time 1 minute		ANb-V-297-118-1 Solvent: cd2cl2 Temp. 25.0 C / 298.1 K Operator: Liu INOVA-500 "nrr11"
--	---------------------------------	--	--	--



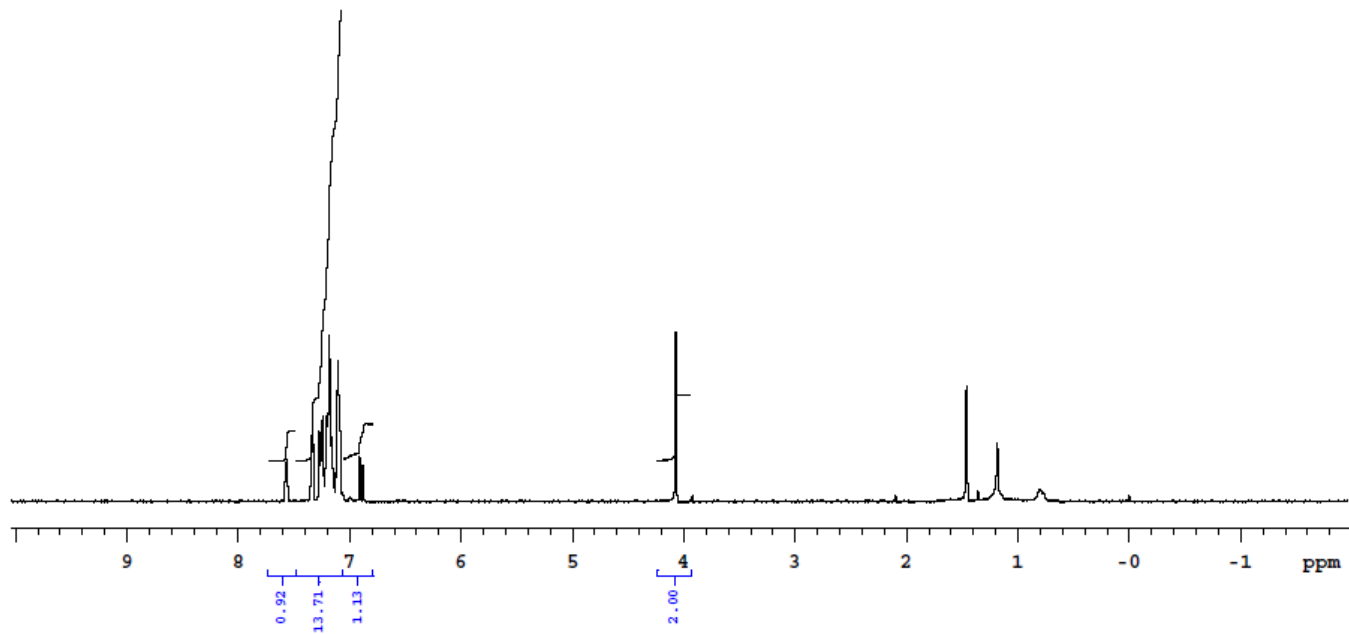
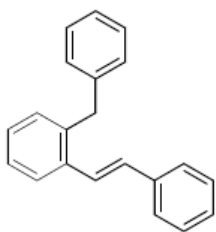
PULSE SEQUENCE Relax. delay 1.000 sec Pulse 45.0 degrees Acq. time 1.049 sec Width 31250.0 Hz 512 repetitions	OBSERVE C13, 125.6952926 DECOUPLE H1, 499.8842612 Power 40 dB continuously on WALTZ-16 modulated	DATA PROCESSING Line broadening 4.0 Hz FT size 65536 Total time 17 minutes	ANB-V-297-13C-Pub Solvent: cd2cl2 Temp. 25.0 C / 298.1 K Operator: Liu VNMR5-500 "nmr18"
---	--	--	---



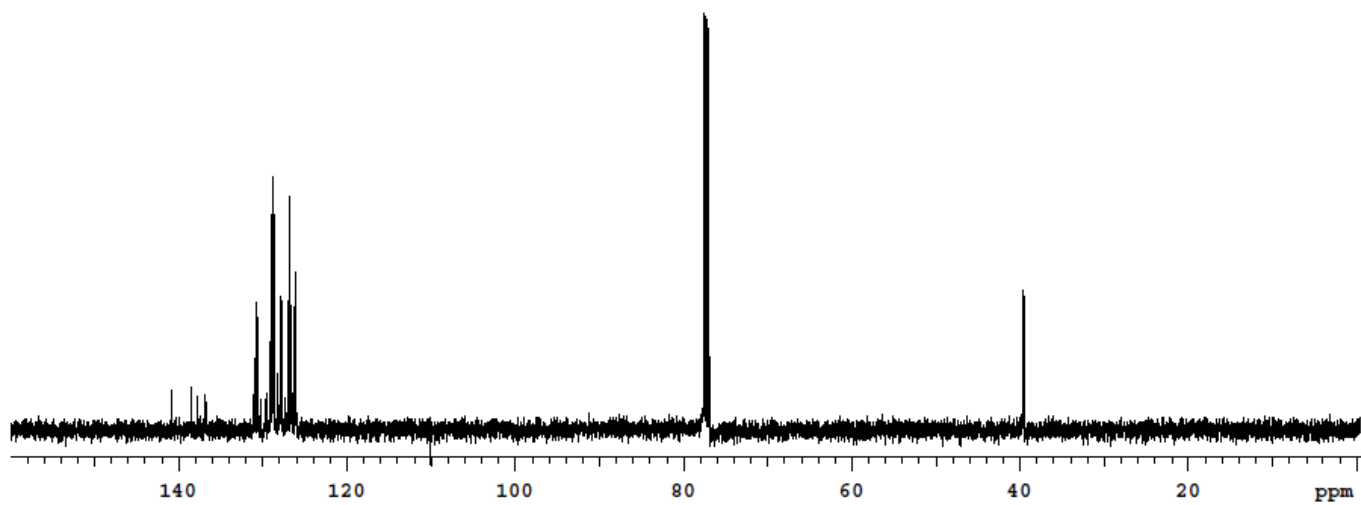
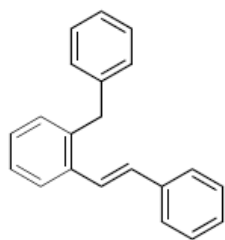
PULSE SEQUENCE Relax. delay 10.000 sec Pulse 45.0 degrees Acq. time 5.190 sec Width 6313.1 Hz 8 repetitions	OBSERVE H1, 599.9795419	DATA PROCESSING FT size 65536 Total time 2 minutes	UO VNMR5-600 standard 1H P-MeO for publication <hr/> Solvent: cd2cl2 Temp. 25.0 C / 298.1 K Operator: abrown File: ANB-PMeO-H1-Publication VNMR5-500 "hotwax.uoregon.edu"
---	--------------------------------	---	---



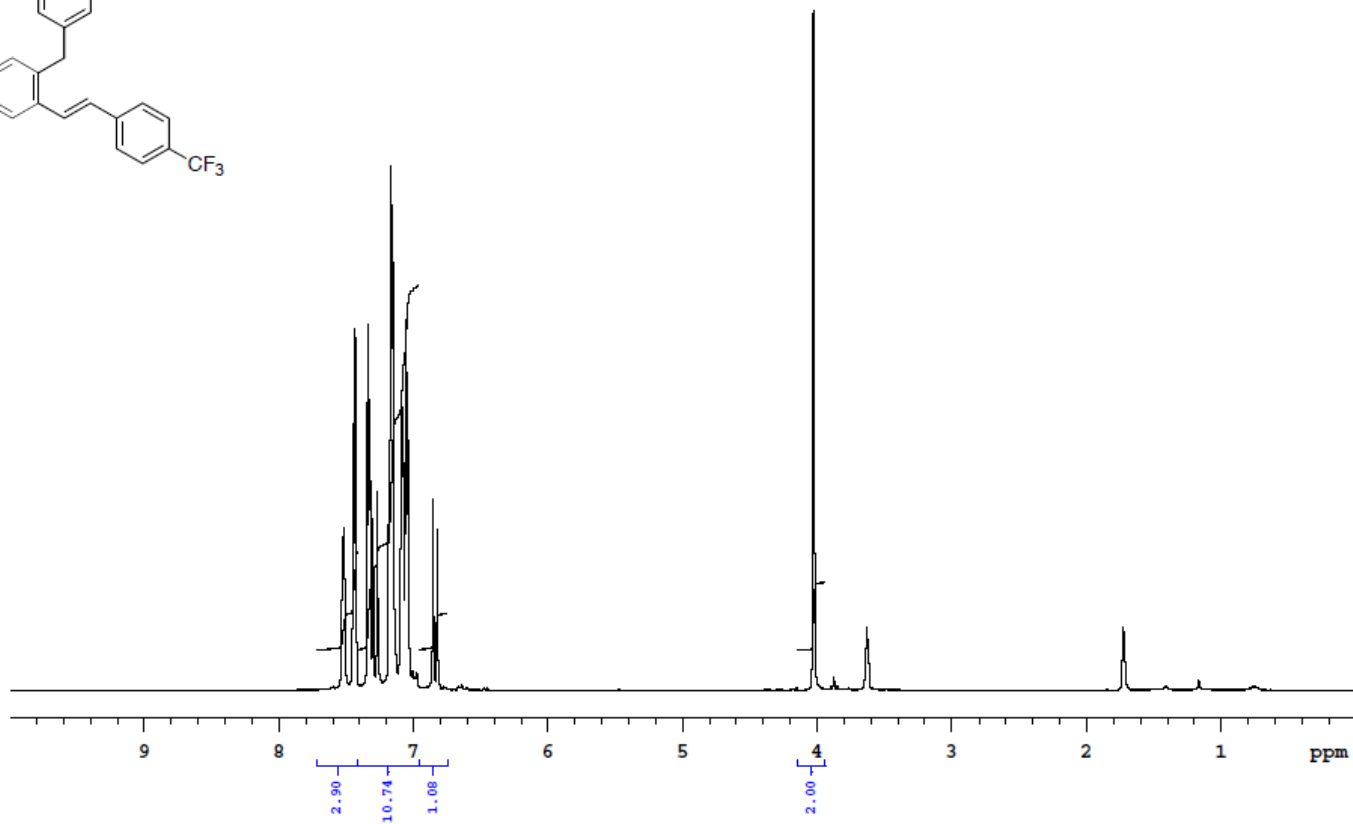
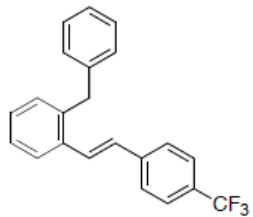
PULSE SEQUENCE Relax. delay 1.000 sec Pulse 45.0 degrees Acq. time 1.000 sec Width 31434.2 Hz 156 repetitions	OBSERVE C13, 125.7513123 DECOUPLE H1, 500.1067449 Power 39 dB continuously on WALTZ-16 modulated	DATA PROCESSING Line broadening 1.0 Hz FT size 65536 Total time 5 minutes	UO Inova-500 Carbon-13 Solvent: cdcl3 Temp. 25.0 C / 298.1 K Operator: abrown File: ANB-II-253-13c-Publication INOVA-500 *hotwax.uoregon.edu*
---	--	---	---



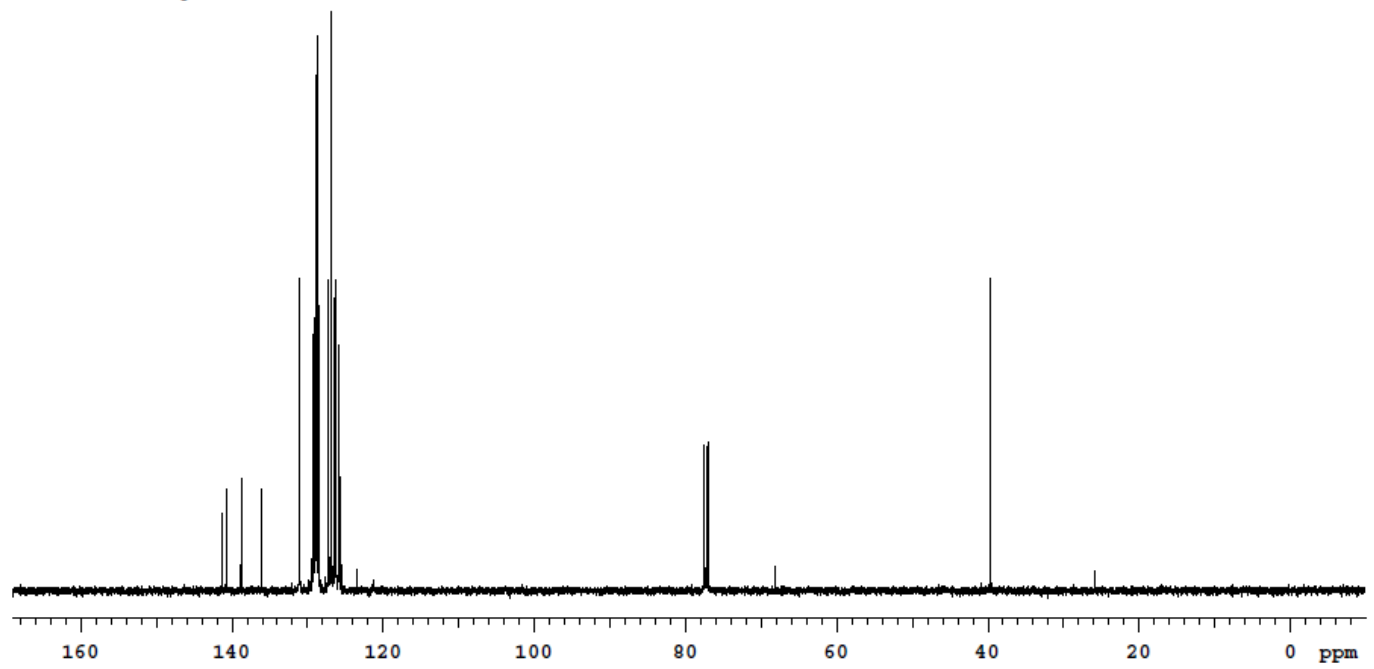
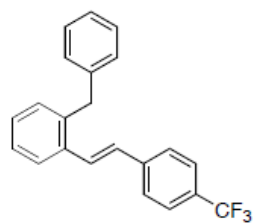
PULSE SEQUENCE Relax. delay 1.000 sec Pulse 45.0 degrees Acq. time 2.048 sec Width 8001.6 Hz 8 repetitions	OBSERVE H1, 500.1043401	DATA PROCESSING FT size 32768 Total time 1 minute	UO Inova-500 standard 1H AllCarbonParaH Solvent: cdcl3 Temp. 25.0 C / 298.1 K Operator: abrown File: ANB-allCarbonParaH-PUBLICATIONREA INOVA-500 "hotwax.uoregon.edu"
--	--------------------------------	--	---



PULSE SEQUENCE Relax. delay 1.000 sec Pulse 45.0 degrees Acq. time 1.000 sec Width 31434.2 Hz 184 repetitions	OBSERVE C13, 125.7513123 DECOUPLE H1, 500.1067449 Power 39 dB continuously on WALTZ-16 modulated	DATA PROCESSING Line broadening 1.0 Hz FT size 65536 Total time 6 minutes	UO Inova-500 Carbon-13 Solvent: cdc13 Temp. 25.0 C / 298.1 K Operator: abrown File: ANB-ALLCARBONPARAH-C13Publication INOVA-500 *hotwax.uoregon.edu*
---	--	---	--



PULSE SEQUENCE Relax. delay 1.000 sec Pulse 45.0 degrees Acq. time 2.048 sec Width 8001.6 Hz 8 repetitions	OBSERVE H1, 500.1044075	DATA PROCESSING FT size 32768 Total time 1 minute	UO Inova-500 standard 1H Solvent: cdcl3 Temp. 25.0 C / 298.1 K Operator: abrown File: ANB-II-AllcarbonPCF3H1-Pub INOVA-500 "hotwax.uoregon.edu"
--	--------------------------------	--	---



PULSE SEQUENCE Relax. delay 1.000 sec Pulse 45.0 degrees Acq. time 1.000 sec Width 31434.2 Hz 108 repetitions	OBSERVE C13, 125.7513123 DECOUPLE H1, 500.1067449 Power 39 dB continuously on WALTZ-16 modulated	DATA PROCESSING Line broadening 1.0 Hz FT size 65536 Total time 3 minutes	UO Inova-500 Carbon-13 Solvent: cdcl3 Temp. 25.0 C / 298.1 K Operator: abrown File: ANB-II-AllcarbonPCF3-C13-Pub INOVA-500 *hotwax.uoregon.edu
---	--	---	--

Chapter 3

Development of the Negishi Cross-Coupling of 1,2-Azaborines Containing *B*-H and *B*-Cl Bonds and Its Application to the Synthesis of New Extended BN-Arenes

3.1 Introduction

In order to study and be able to predict the effects of BN/CC isosterism,¹⁶¹ it is necessary to develop methodology which allows for total control over the location of the BN unit in extended and monocyclic arenes. To this end, the Liu¹⁶² group has extensively studied late-stage functionalization strategies of monocyclic 1,2-azaborines at the boron and nitrogen centers. In order to develop the synthetic toolbox necessary to synthesize specific compounds of interest in any of their isomeric forms, it is necessary to expand the synthetic methodology to include selective functionalization at any of the ring positions.

This chapter will discuss the optimization of Negishi cross-coupling at the C(3) position of brominated azaborines in the presence of reactive *B*-H and *B*-Cl bonds and its application in the synthesis of new extended BN-arenes including parental 9,1-borazaronaphthalene and a new BN-indenyl.

¹⁶¹ For an overview of BN/CC isosterism please see the following reviews: (a) Liu, Z.; Marder, T. B. *Angew. Chem. Int. Ed. Engl.* **2008**, *47*, 242-244. (b) Bosdet, M. J. D.; Piers, W. E. *Can. J. Chem.* **2009**, *87*, 8-29. (c) Campbell, P. G.; Marwitz, A. J.; Liu, S.-Y. *Angew. Chem. Int. Ed. Engl.* **2012**, *51*, 6074-6092.

¹⁶² Late-stage functionalization strategies for monocyclic 1,2-azaborines include: **Nucleophilic Substitution of B-Cl**: (a) Marwitz, A. J. V.; Abbey, E. R.; Jenkins, J. T.; Zakharov, L. N.; Liu, S.-Y. *Org. Lett.* **2007**, *9*, 4905-4908. (b) Marwitz, A. J. V.; McClintock, S. P.; Zakharov, L. N.; Liu, S.-Y. *Chem. Commun.* **2010**, *46*, 779-781. **Nucleophilic Aromatic Substitution**: (c) Lamm, A. N.; Garner, E. B.; Dixon, D. A.; Liu, S.-Y. *Angew. Chem. Int. Ed.* **2011**, *50*, 8157-8160. (d) Abbey, E. R.; Lamm, A. N.; Baggett, A. W.; Zakharov, L. N.; Liu, S.-Y. *J. Am. Chem. Soc.* **2013**, *135*, 12908-12913. **Catalyzed B-Cl Activation**: (e) Rudebusch, G. E.; Zakharov, L. N.; Liu, S.-Y. *Angew. Chem. Int. Ed.* **2013**, *52*, 9316-9319. **Catalyzed B-H Activation**: (f) Brown, A. N.; Zakharov, L. N.; Mikulas, T.; Dixon, D. A.; Liu, S.-Y. *Org. Lett.* **2014**, *16*, 3340-3343.

3.2 Background

3.2.1 BN-Naphthalenes

By replacing a single carbon-carbon double bond in the backbone of naphthalene it should be possible to obtain six possible isomers of BN-naphthalenes. Scheiner calculated the relative thermodynamic stabilities of five of the six isomers of BN-naphthalene (**3.1-3.5**) as shown in Figure 3.1.¹⁶³ 1,9-borazaronaphthalene **3.5** is predicted to be the least stable of the isomers while 1,2-borazaronaphthalene **3.1** is predicted to be the most stable. Experimental verification of this is difficult because the selective synthesis of BN-naphthalenes is still an unsolved problem.

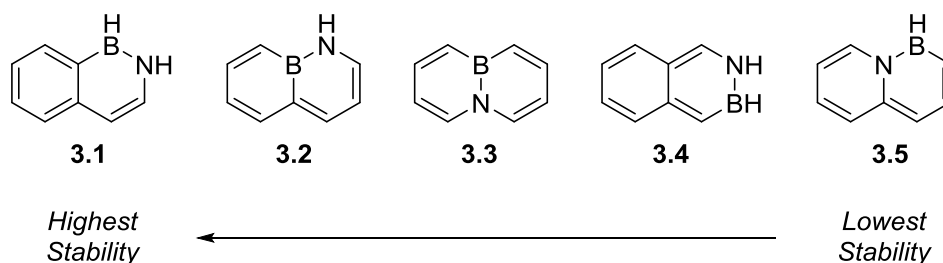


Figure 3.1: Scheiner's Calculated Relative Stabilities of BN-Naphthalenes

Of the six possible isomers, only two unsubstituted BN-naphthalenes have been synthesized: 2,1-borazaronaphthalene **3.6** and 10,9-borazaronaphthalene **3.3** (Figure 3.2). Substituted compounds with the 1,2-borazaronaphthalene core (**3.1x**) have recently been

¹⁶³ Kar, T.; Elmore, D. E.; Scheiner, S. *Journal of Molecular Structure: THEOCHEM* **1997**, 392, 65-74.

reported by Cui,¹⁶⁴ however the parental structure is not known, and Cui's synthesis may not be amenable to the synthesis of the parental structure **3.1**.

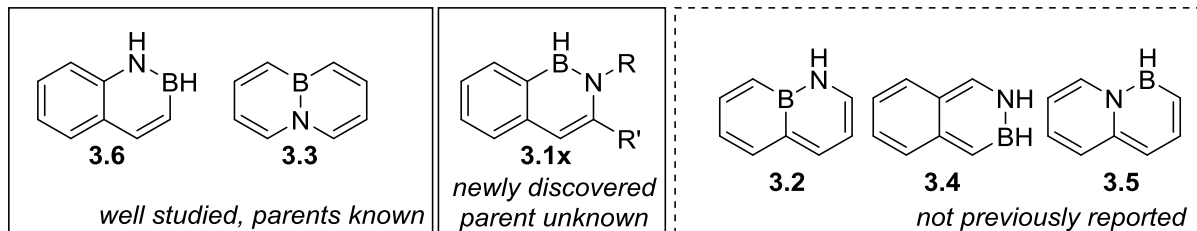


Figure 3.2: Known and unknown BN-naphthalenes

Prior to the work disclosed herein, there were no examples of compounds containing structures **3.2-3.5**.

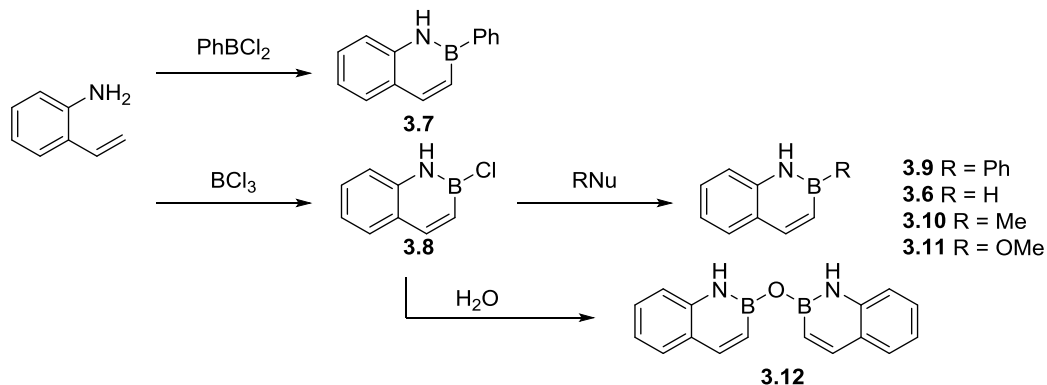
3.2.1.1 Synthesis of 2,1-Borazaronaphthalenes

Dewar reported the first BN-naphthalene, a derivative of 2,1-borazaronaphthalene in 1959.¹⁶⁵ Treatment of 2-aminostyrene with phenyl boron dichloride or boron trichloride led to the generation of **3.7** or **3.8** respectively (Scheme 3.1). **3.8** could be substituted by alkyl, alkoxide, or hydride nucleophiles in order to generate *B*-Ph **3.9**, *B*-H **3.6**, *B*-Me **3.10**, and *B*-OMe **3.11**. When exposed to water **3.8** generates the *B*-O-*B* dimeric structure **3.12** which was stable to further hydrolysis.

¹⁶⁴ Liu, X.; Wu, P.; Li, J.; Cui, C. *J. Org. Chem.* **2015**, *80* (8), 3737-3744.

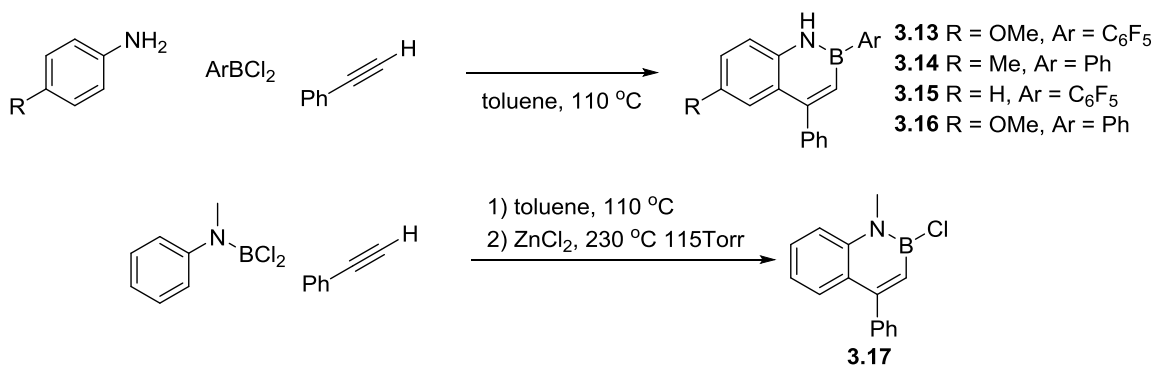
¹⁶⁵ (a) Dewar, M. J. S.; Dietz, R. *J. Chem. Soc.* **1959**, 2728-2730. (b) Dewar, M. J. S.; Dietz, R.; Kubba, V. P.; Lepley, A. R. *J. Am. Chem. Soc.* **1961**, *83*, 1754-1756. (c) Paetzold revisited this synthesis in 2004: Paetzold, P.; Stanescu, C.; Stubenrauch, J. R.; Bienmüller, M.; Englert, U. *Z. anorg. allg. Chem.* **2004**, *630*, 2632-2640.

Scheme 3.1: Dewar's synthesis of 2,1-borazonaphthalenes



In 1968,¹⁶⁶ Paetzold disclosed a similar synthesis of 2,1-borazonaphthalenes **3.13-3.16** from aniline compounds under the action of phenylacetylene and aryl borondichloride reagents (Scheme 3.2).

Scheme 3.2: Paetzold's synthesis of 2,1 borazonaphthalenes



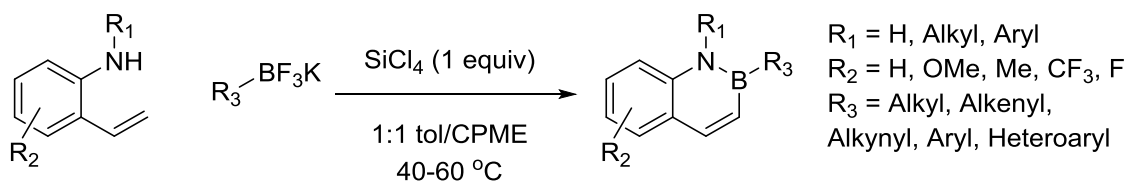
Compounds **3.13-3.16** were synthesized in yields from 43-92%. Using N-methyl aniline the authors were able to generate the B-Cl containing **3.17** in 43% isolated yield. **3.17** can be readily modified through nucleophilic substitution at boron in a similar

¹⁶⁶ Paetzold, P. I.; Stohr, G.; Maisch, H.; Lenz, H. *Chem. Ber.* **1968**, *101*, 2881-2888.

fashion to compound **3.8**. This methodology remains the only example for the synthesis of C(4) substituted 2,1-borazonaphthalenes.

More recently, Molander¹⁶⁷ has greatly expanded the scope of the synthesis of 2,1-borazonaphthalenes. Through a modification of Dewar's original synthetic route, Molander's group was able to utilize their popular organotrifluoroborate¹⁶⁸ reagents in conjunction with 2-vinyl anilines and tetrachlorosilane to generate many (>40) substituted 2,1-borazonaphthalenes through a convergent modular approach (Scheme 3.3). This methodology greatly expanded the accessible 2,1-borazonaphthalenes and was amenable to a large variety of organofluoroborate boron sources including: alkyl, alkenyl, alkynyl, aryl, and heteroaryl B-substituents; -H, alkyl, and aryl N-substituents; as well as electron-rich and electron-poor variation of the starting 2-vinyl aniline.

Scheme 3.3: Molander's modular synthesis of 2,1-borazonaphthalenes



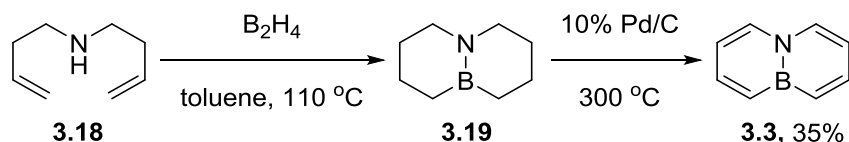
¹⁶⁷ Wisniewski, S. R.; Guenther, C. L.; Argintaru, O. A.; Molander, G. A. *J. Org. Chem.* **2013**, *79*, 365-378.

¹⁶⁸ For reviews of the many uses of organotrifluoroborates see: (a) Molander, G. A.; Figueroa, R. *Aldrichimica Acta* **2005**, *38*, 49-56. (b) Molander, G. A.; Ellis, N. *Acc. Chem. Res.* **2007**, *40*, 275-286. (c) Stefani, H. A.; Cella, R.; Vieira, A. S. *Tetrahedron* **2007**, *63*, 3623-3658. (d) Darses, S.; Genet, J.-P. *Chem. Rev.* **2008**, *108*, 288-325.

3.2.1.2 Synthesis of 10,9-Borazonaphthalenes

Dewar first synthesized 10,9-borazonaphthalene **3.3** through a bis-hydroboration dehydrogenation sequence (Scheme 3.4).¹⁶⁹

Scheme 3.4: Dewar's original synthesis of 10,9-borazonaphthalenes



Treatment of bis-homoallyl amine **3.18** with diborane in refluxing toluene generates BN-decalin **3.19** which was subjected to palladium on carbon oxidation using 1-octene as hydrogen acceptor to generate 10,9-borazonaphthalene **3.3** in 33% yield.

More recently, Ashe has explored the synthesis of compound **3.3** through a ring expansion¹⁷⁰ from BN-indenyl **3.20** in a 5.6% overall yield or from direct ring-closing metathesis¹⁷¹ of tetraallyl **3.21** followed by oxidation of resulting diene **3.22** in an overall yield of 9% (Scheme 3.5), however **3.23** is the major product of this oxidation and difficult to separate from desired **3.3**. By using DDQ as the oxidant and generating the tetraallyl species in a different manner, Fang has optimized the synthesis of **3.3** to a 3-step synthesis with a 10% overall yield.¹⁷²

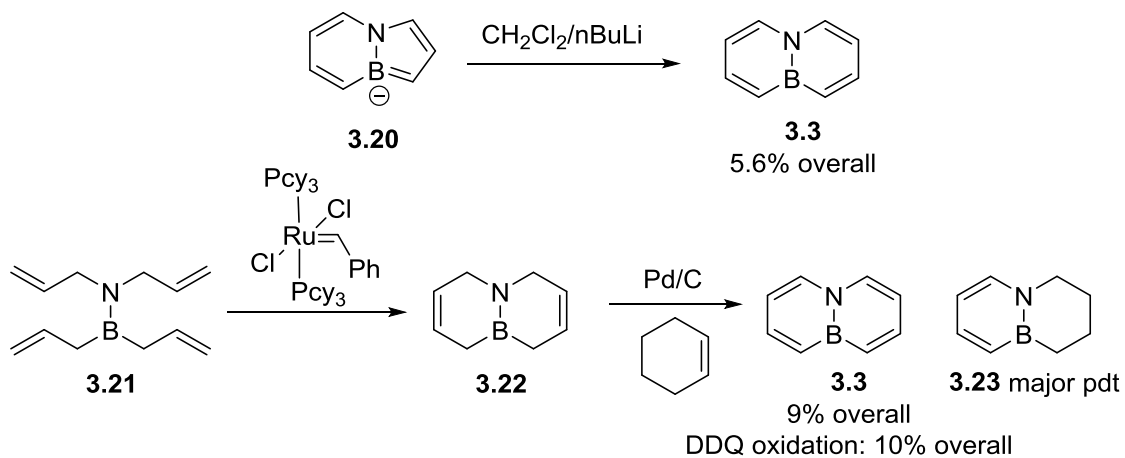
¹⁶⁹Dewar, M.; Jones, R. *J. Am. Chem. Soc.* **1968**, *90*, 2137-2144.

¹⁷⁰Fang, X.; Yang, H.; Kampf, J. W.; Banaszak Holl, M. M.; Ashe, A. J. *Organometallics* **2006**, *25*, 513-518.

¹⁷¹Rohr, A. D.; Kampf, J. W.; Ashe, A. J. *Organometallics* **2014**, *33*, 1318-1321.

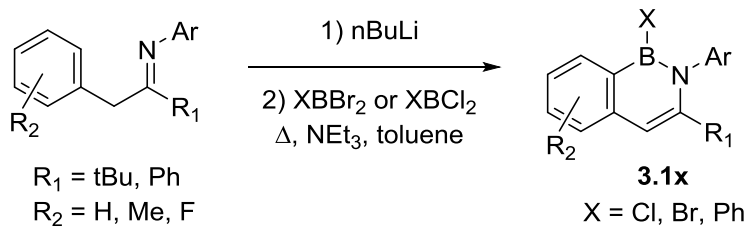
¹⁷²Sun, F.; Lv, L.; Huang, M.; Zhou, Z.; Fang, X. *Org. Lett.* **2014**, *16*, 5024-5027.

Scheme 3.5: Ashe's syntheses of 10,9-borazaronaphthalene



3.2.1.3 Synthesis of 1,2-Borazaronaphthalenes

Scheme 3.6: Cui's synthesis of substituted 1,2-borazaronaphthalenes



Cui has developed the first and only current route to substituted 1,2-borazaronaphthalenes (Scheme 3.6).¹⁷³ By trapping an *in situ* generated enamine with a B–X reagent the system is set up to undergo a directed electrophilic aromatic substitution upon heating and treatment with base. The heavy substitution of **3.1x** may limit the potential for this methodology to generate unsubstituted **3.1**.

¹⁷³Liu, X.; Wu, P.; Li, J.; Cui, C. *J. Org. Chem.* **2015**, *80*, 3737-3744.

3.2.2 BN-Indene

Ashe has synthesized BN-indene **3.24** through a ring-closing metathesis/oxidation strategy from compound **3.25** or through a ring-closing metathesis/carbenoid ring expansion from compound **3.26** (Scheme 3.7).¹⁷⁴

Compound **3.25** can undergo double ring-closing metathesis to generate diene **3.27**. Oxidation with DDQ generates **3.24** in 3% overall yield. Compound **3.26** did not undergo a double ring-closing to the [5,5]-system, even under forcing conditions. After deprotonation, ring-expansion, and ring-closing metathesis, **3.24** can be generated in a much improved 14% overall yield, despite the additional steps. Compound **3.24** can be deprotonated with LDA to generate the BN-Indenyl, which can be complexed to a zirconium center to generate BN-zirconocene **3.31**, which was active in polymerization reactions in a similar fashion to the carbonaceous zirconocene.

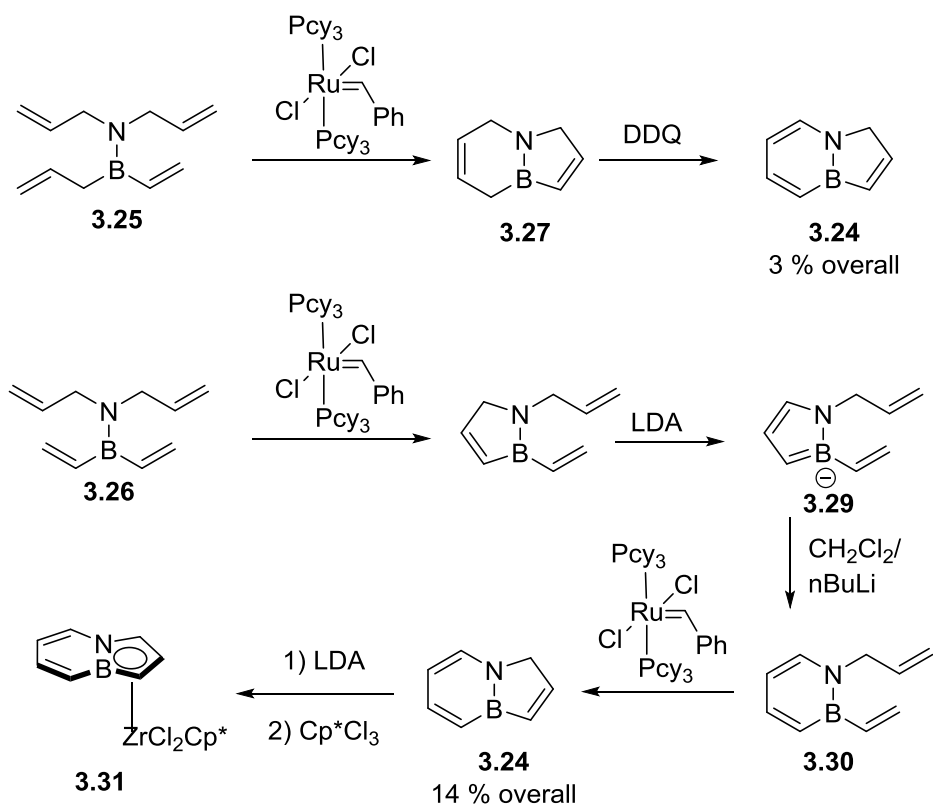
Ashe¹⁷⁵ also found that at low temperatures in solution in the presence of KHMDS the (3.24)Cr(CO)₃ piano-stool complex **3.32** preferred an η^6 -coordination mode over the 6-membered ring. The complex underwent a haptotropic migration to an η^5 -coordination mode over the 5-membered anionic portion of the ring when warmed to room temperature (Scheme 3.8). This proceeds in a similar fashion to the all-carbon indenyl system.¹⁷⁶

¹⁷⁴ (a) Ashe, A. J.; Yang, H.; Fang, X.; Kampf, J. W. *Organometallics* **2002**, *21*, 4578-4580. (b) Fang, X.; Yang, H.; Kampf, J. W.; Banaszak Holl, M. M.; Ashe, A. J. *Organometallics* **2006**, *25*, 513-518.

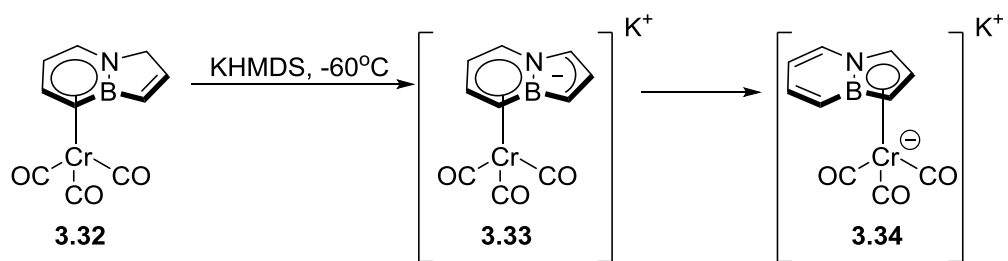
¹⁷⁵ Pan, J.; Wang, J.; Banaszak Holl, M. M.; Kampf, J. W.; Ashe, A. J. *Organometallics* **2006**, *25*, 3463-3467.

¹⁷⁶ Cecon, A.; Gambaro, A.; Gottardi, F.; Santi, S.; Venzo, A. J. *Organomet. Chem.* **1991**, *412*, 85-94.

Scheme 3.7: Ashe's syntheses of BN-indene 3.24



Scheme 3.8: Haptotropic migration of pianostool BN-indene 3.32



3.2.3 Halogenation Reactions of BN-Heterocycles

After demonstrating the synthesis of 2,1-borazaronaphthalenes, Dewar was able to perform electrophilic aromatic substitution using elemental bromine or chlorine in acetic acid to facilitate C(3) selective halogenation in the presence of an *N*-H bond using 2,1 borazaronaphthalene **3.10** to generate halogenated **3.35** (Scheme 3.9, Eq. 1).¹⁷⁷ Decomposition through protodeborylation was an unavoidable side product under these conditions. Ashe later expanded this methodology to include *N*-Et, *B*-Ph monocyclic azaborine **3.36**.¹⁷⁸ By switching the solvent to methylene chloride and cooling the reaction to 0 °C to control the exothermic reaction, Ashe was able to obtain high yields of C(3) brominated azaborine **3.37** (Scheme 3.9, Eq. 2). Our group later expanded this methodology to include the functionalizable *B*-Cl bond by performing the bromination reaction on compound **3.38** generating C(3) brominated monocyclic azaborine **3.39** (Scheme 3.9, Eq. 3).¹⁷⁹

With access to a family of 2,1 borazaronaphthalenes Molander was able to generate a plethora of C(3) brominated systems with a variety of boron and nitrogen substituents by modifying Ashe's optimized procedure to include slow addition of bromine (Scheme 3.9, Eq. 4).¹⁸⁰ Alkenyl boron substitution was not tolerated, instead leading to bromination of the *B*-vinyl species due to the activating nature of boron. In all other cases, the 2,1-borazaronaphthalene core was selectively brominated over

¹⁷⁷ Dewar, M. J. S.; Dietz, R. *J. Org. Chem.* **1961**, *26*, 3253-3256.

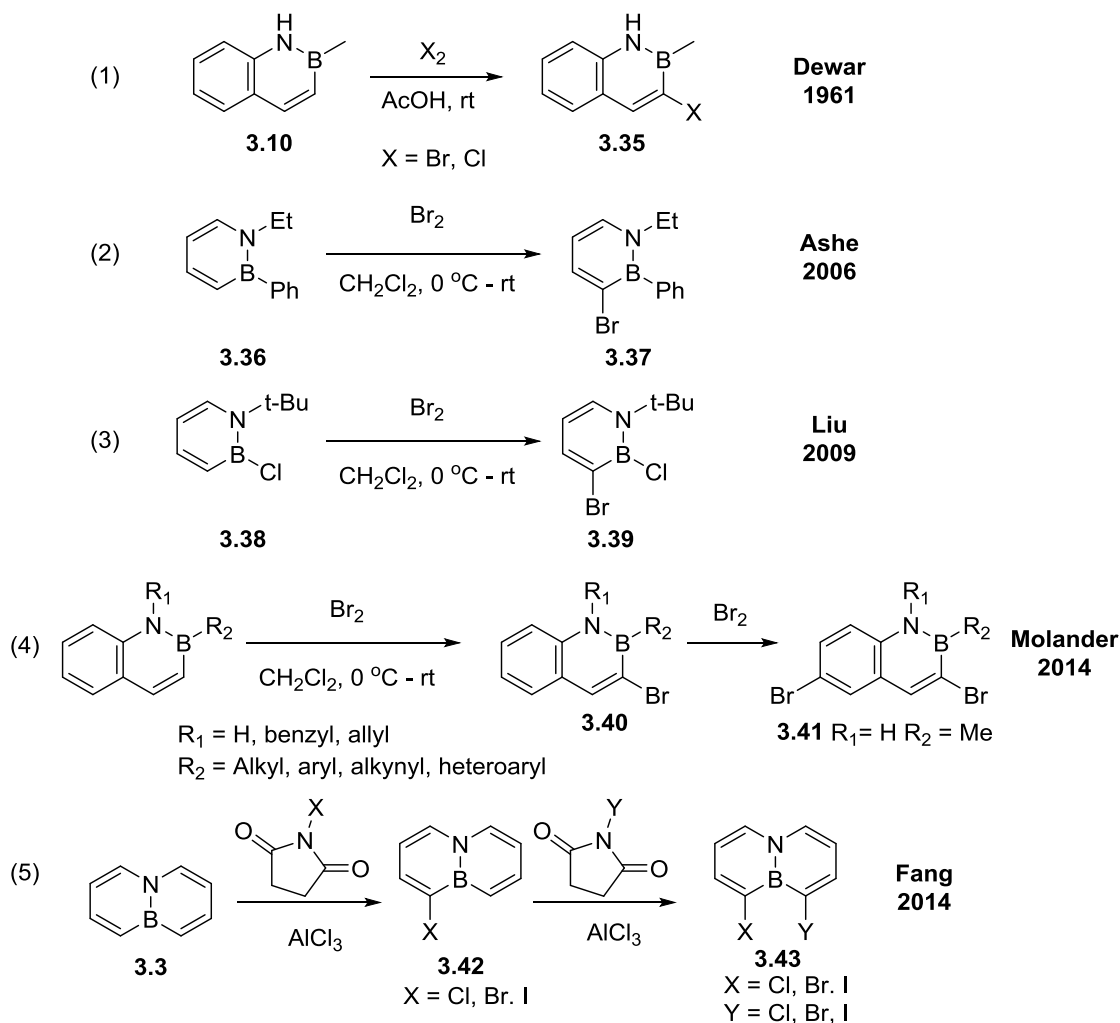
¹⁷⁸ Pan, J.; Kampf, J. W.; Ashe, A. *J. Org. Lett.* **2007**, *9*, 679-681.

¹⁷⁹ Lamm, A. N.; Liu, S.-Y. *Mol. BioSyst.* **2009**, *5*, 1303-1305.

¹⁸⁰ Molander, G. A.; Wisniewski, S. R. *J. Org. Chem.* **2014**, *79*, 6663-6678.

other possible electrophilic sites on the molecule. Molander also synthesized the bis-brominated product **3.41** by using 2 equivalents of elemental bromine.

Scheme 3.9: Halogenation reactions of BN-heterocycles



More recently, Fang has demonstrated the selective mono- and sequential bis-bromination of 10,9-borazonaphthalene **3.3** using aluminum trichloride activated N-halosuccinimide reagents (Scheme 3.9, Eq. 5).¹⁸¹ Using this methodology any

¹⁸¹ Sun, F.; Lv, L.; Huang, M.; Zhou, Z.; Fang, X. *Org. Lett.* **2014**, *16*, 5024-5027.

combination of halogens can be introduced to the ring at the symmetric 1 and 8 positions (which correspond to the 3 position of 2,1 borazaronaphthalenes) with the proper order of addition in order to generate varied halogenated systems **3.42** and **3.43**.

3.2.4 The Application of Cross-Coupling Reactions for the Modification of BN-Heterocycles

The development of metal-catalyzed cross-coupling for carbon-carbon bond formation has had a profound effect on synthetic organic chemistry and was recognized for its impact by the Nobel committee in 2010 "*for palladium-catalyzed cross-couplings in organic synthesis.*" Cross-coupling is especially suited for arene functionalization, and has proven to be a valuable tool for the synthesis of substituted BN-heterocycles.¹⁸²

Molander's group was the first to demonstrate a cross-coupling methodology for carbon-carbon bond formation in a BN-heterocycle. Using their extensive library of C(3) brominated azaborines with core structure **3.40** they were able to demonstrate Suzuki cross-coupling of aryl, heteroaryl, and alkenyl (with a modification of the catalyst system) potassium trifluoroborate reagents to generate new substituted BN arenes of structure **3.44** and **3.45** (Scheme 3.10, Eq. 1).¹⁸³

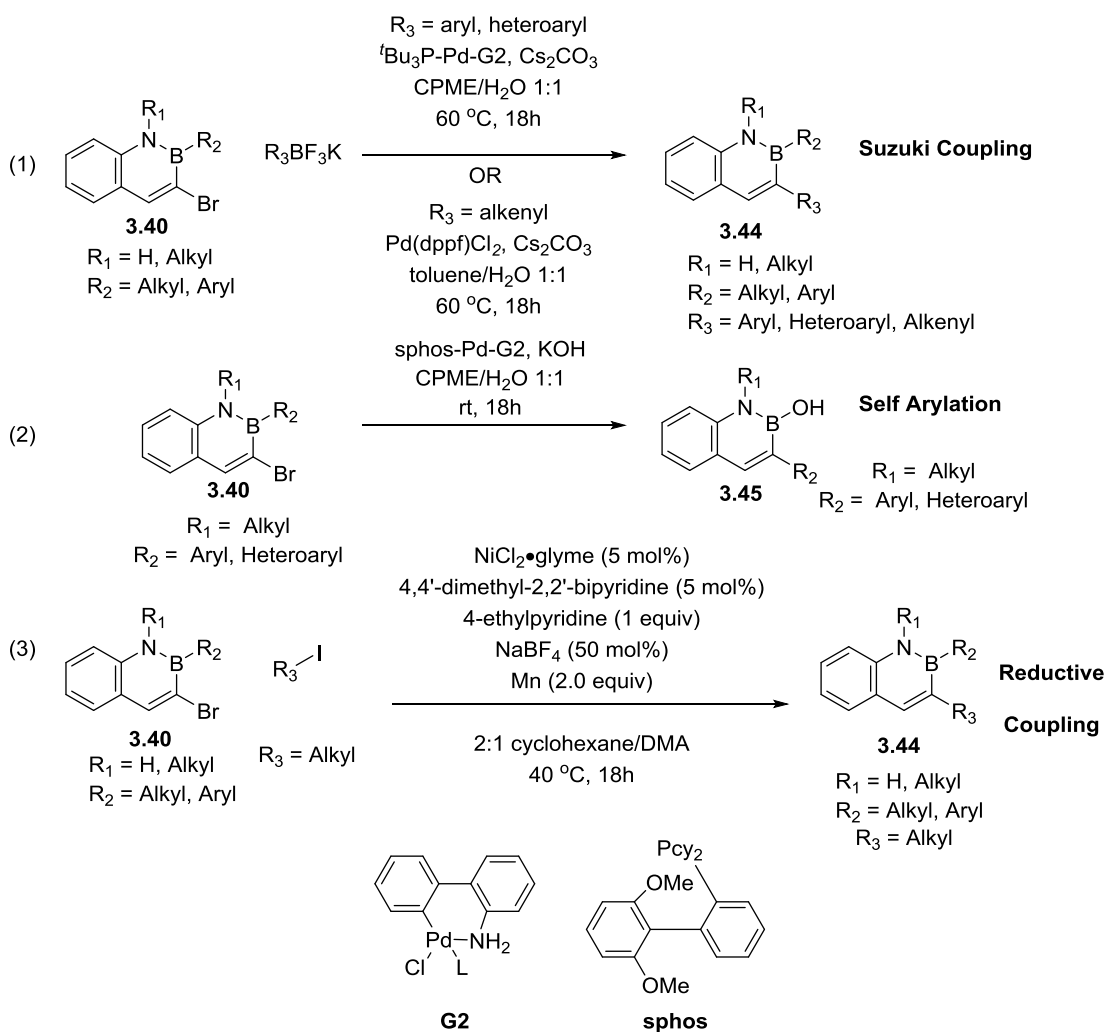
Molander also showed that B-aryl examples of **3.40** undergo a unique self-arylation under appropriately basic conditions to generate B-OH structures **3.45** (Scheme

¹⁸² For recent reviews on modern metal-catalyzed cross-coupling please see: (a) Jana, R.; Pathak, T. P.; Sigman, M. S. *Chem. Rev.* **2011**, *111*, 1417-1492. (b) Johansson Seechurn, C. C. C.; Kitching, M. O.; Colacot, T. J.; Snieckus, V. *Angew. Chem. Int. Ed.* **2012**, *51*, 5062-5085.

¹⁸³ (a) Molander, G. A.; Wisniewski, S. R. *J. Org. Chem.* **2014**, *79*, 6663-6678. (b) Molander, G. A.; Wisniewski, S. R.; Etemadi-Davan, E. *J. Org. Chem.* **2014**, *79*, 11199-11204.

3.10, Eq. 2).¹⁸⁴ This unique reactivity was not amenable to *N*-H bonds, probably due to a competitive deprotonation of the acidic *N*-H moiety. *B*-alkyl species were stable under the reaction conditions, due to either the lower electrophilicity of *B*-alkyl boranes or the lowered propensity for *B*-alkyl bonds to undergo transmetallation.

Scheme 3.10: Cross-coupling reactions of 2,1 borazaronaphthalenes with core 3.40

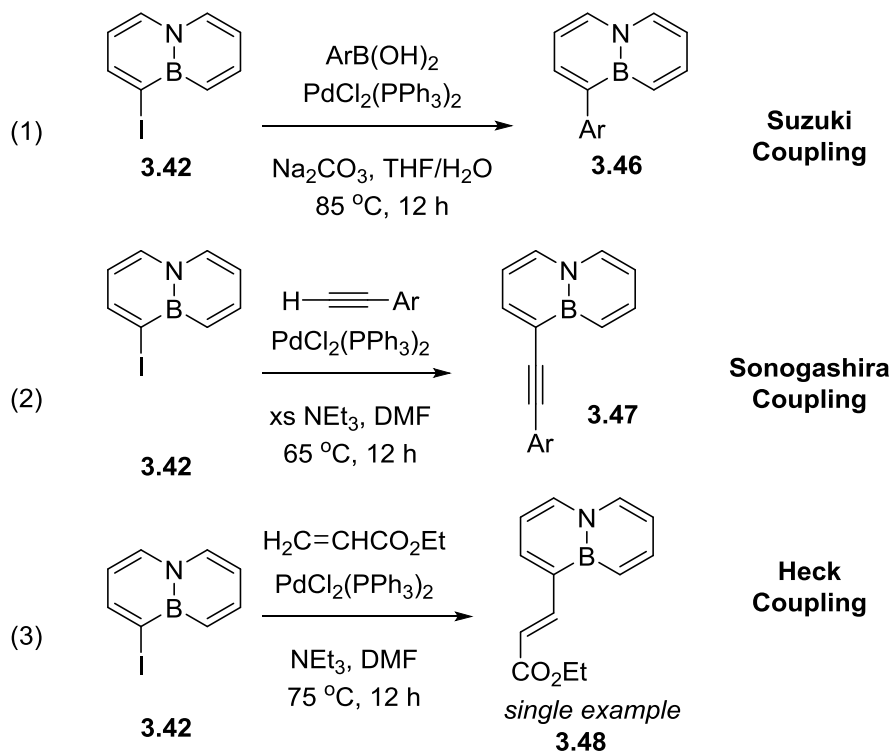


¹⁸⁴ Molander, G. A.; Wisniewski, S. R. *J. Org. Chem.* **2014**, *79*, 8339-8347.

Suzuki coupling of alkyl groups was not demonstrated, however Molander was able to perform a nickel-catalyzed reductive coupling of alkyl iodides with C(3) brominated **3.40** (Scheme 3.10, Eq. 3)¹⁸⁵ which could cross-couple primary and secondary alkyl iodides in acceptable yields.

Recently, Fang¹⁸⁶ has shown that iodinated **3.42** can be cross-coupled under Suzuki, Cassar-Sonogashira, or Heck conditions (Scheme 3.11) to generate aryl (**3.46**, Scheme 3.11, Eq. 1), alkynyl (**3.47**, Scheme 3.11, Eq. 2), and a single example of alkenyl (**3.48**, Scheme 3.11, Eq. 3) substitution respectively.

Scheme 3.11: Fang's cross-coupling of 10,9 borazaronaphthalenes

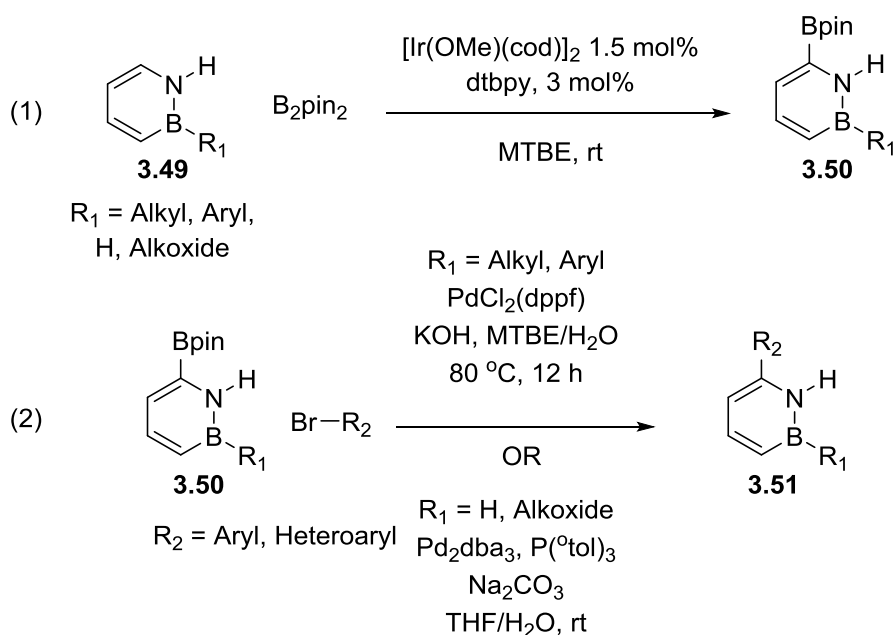


¹⁸⁵ Molander, G. A.; Wisniewski, S. R.; Traister, K. M. *Org. Lett.* **2014**, *16*, 3692-3695.

¹⁸⁶ Sun, F.; Lv, L.; Huang, M.; Zhou, Z.; Fang, X. *Org. Lett.* **2014**, *16*, 5024-5027.

Our group has recently developed a regioselective C(6) borylation of N–H azaborines **3.49** to generate new structures **3.50** (Scheme 3.12, Eq. 1).¹⁸⁷ We also demonstrated the first example of a BN-arene acting as the nucleophile in the Suzuki cross-coupling of borylated azaborines **3.50** to generate C(6) substituted azaborines **3.51** (Scheme 3.12, Eq. 2). This method is amenable to B–alkyl/aryl/alkoxide substitution as well as B–H to a lesser extent. The B–H tolerance is limited to two examples of C(6) aryl bromides and was not successful for the cross-coupling of heteroaryl bromides.

Scheme 3.11: Liu’s C(6) functionalization of monocyclic N–H azaborines



The application of metal-mediated cross-coupling reactions to BN-heterocycles is still an emerging field. Negishi coupling is the only one of the three Nobel Prize winning cross-coupling methodologies that has not been demonstrated previously. By avoiding

¹⁸⁷ Baggett, A. W.; Vasiliu, M.; Li, B.; Dixon, D. A.; Liu, S.-Y. *J. Am. Chem. Soc.* **2015**, *137*, 5536-5541.

the oxygen-bases and aqueous conditions required for Suzuki coupling it should be possible to expand and improve upon the scope of boron functionalities which are tolerated in order to enter new chemical space while accessing previously inaccessible structures. The use of zinc reagents in Negishi coupling is one approach to avoiding side reactivity. The next section details the limited studies on the interaction between boron and zinc reagents in order to outline potential pitfalls and challenges of maintaining reactive functionalities during the Negishi cross-coupling.

3.2.5 Boron-Zinc Exchange

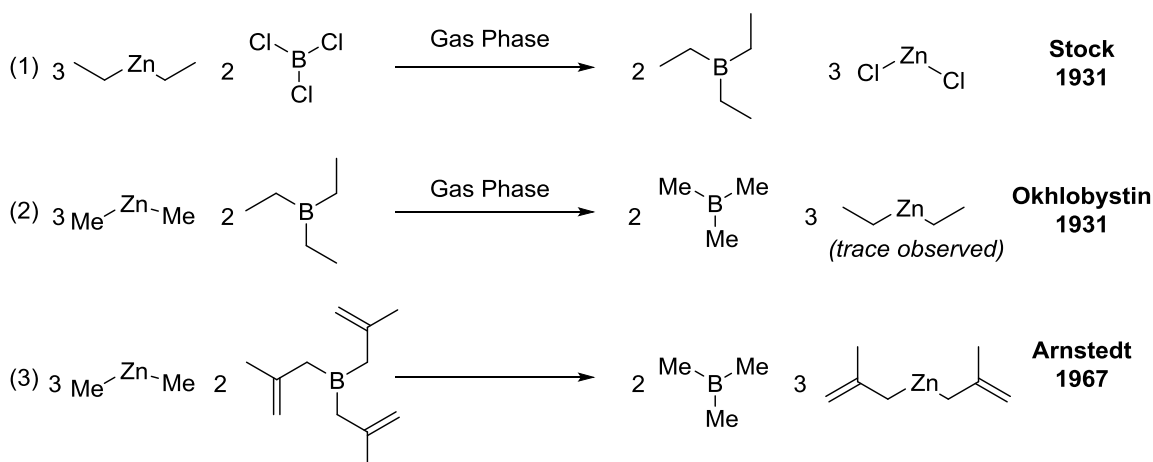
Organozinc and organoboron reagents have a long history of reactivity in transmetallation and exchange reactions. In 1931, Stock synthesized triethyl borane by reacting boron trichloride and diethyl zinc in the gas phase, which after a triple transmetallation generated triethylborane and zinc chloride, suggesting that alkylzinc reagents can readily substitute for $B-X$ bonds (Scheme 3.13, Eq. 1).¹⁸⁸ In 1960, Okhlobystin was able to perform a cross-metathesis of dimethylzinc and triethylborane to generate trimethylborane and some diethylzinc (although the production of diethylzinc was not quantitative, the transmetallation must have taken place to generate BMe_3 , Scheme 3.13, Eq. 2).¹⁸⁹ The boron/zinc exchange reaction was further developed by Arnstedt in the late 1960's to include methallylzinc reagents (Scheme 3.13, Eq. 3).¹⁹⁰

¹⁸⁸ Stock, A.; Zeidler, F. *Ber. dtsh. Chem. Ges. A/B* **1921**, *54*, 531-541.

¹⁸⁹ Zakharkin, L. I.; Okhlobystin, O. Y. *Z. Obshch. Khim.* **1960**, *30*, 2134-2138.

¹⁹⁰ Thiele, K.-H.; Engelhardt, G.; Köhler, J.; Arnstedt, M. *J. Organomet. Chem.* **1967**, *9*, 385-393.

Scheme 3.13: Early boron-zinc transmetallation reactions



The development of the asymmetric addition of dialkylzinc reagents to aldehydes discovered by Omi¹⁹¹ and extensively developed by Noyori¹⁹² and Ogawa¹⁹³ sparked a renewed interest in the synthesis of dialkylzinc compounds through boron-zinc exchange in order to expand the viable nucleophiles for this reaction. Radinov was the first to explore the use of boron-zinc exchange in the context of enantioselective carbonyl addition. After first demonstrating the viability of divinylzinc to undergo enantioselective addition to aldehydes,¹⁹⁴ Radinov expanded the methodology to more complicated alkenyl zinc reagents, available through the hydroboration/boron-zinc exchange of alkynes (Scheme 3.14).¹⁹⁵ Radinov was able to generate the *E*-vinylborane

¹⁹¹ Oguni, N.; Omi, T. *Tetrahedron Letters* **1984**, 25, 2823-2824.

¹⁹² (a) Kitamura, M.; Suga, S.; Kawai, K.; Noyori, R. *J. Am. Chem. Soc.* **1986**, 108, 6071-6072.

(b) Kitamura, M.; Okada, S.; Suga, S.; Noyori, R. *J. Am. Chem. Soc.* **1989**, 111 (11), 4028-4036. (c) for a review covering enantioselective additions of organometallic reagents to carbonyl compounds discovered during this time period please see: Noyori, R.; Kitamura, M. *Angew. Chem. Int. Ed. Engl.* **1991**, 30, 49-69.

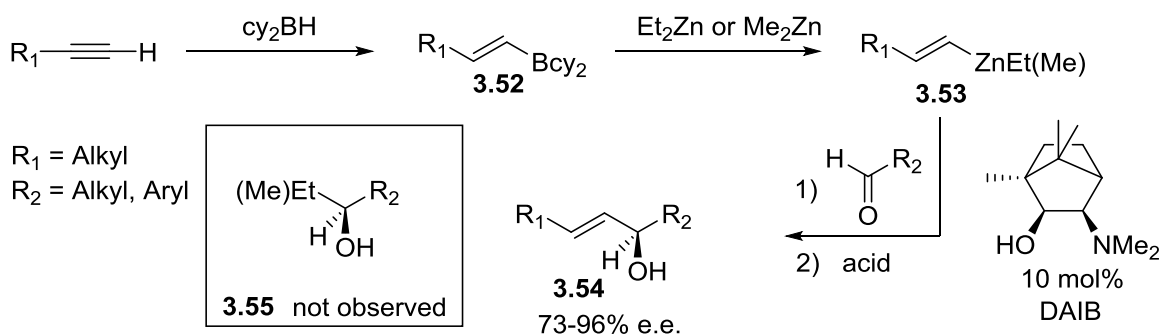
¹⁹³ Soai, K.; Ookawa, A.; Kaba, T.; Ogawa, K. *J. Am. Chem. Soc.* **1987**, 109, 7111-7115.

¹⁹⁴ Oppolzer, W.; Radinov, R. N. *Tetrahedron Lett.* **1988**, 29, 5645-5648.

¹⁹⁵ Oppolzer, W.; Radinov, R. N. *Helv. Chim. Acta* **1992**, 75, 170-173.

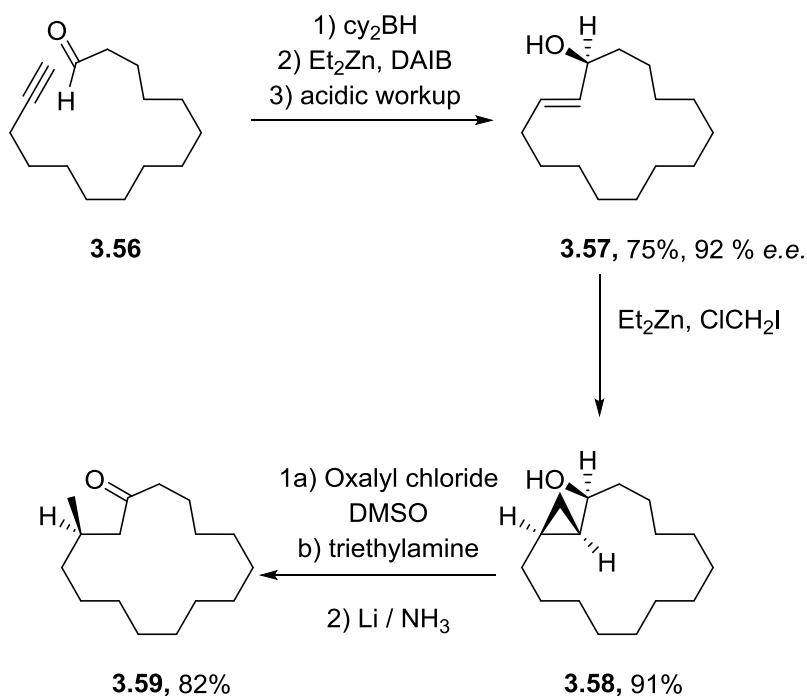
3.52 through hydroboration, which could be followed by boron-zinc exchange to generate the *E*-vinylzinc reagent **3.53**. Treatment of **3.53** with (-)-3-exo-(dimethylamino)isoborneol followed by an alkyl or aryl aldehyde and an acidic workup generated the enantioenriched allylic alcohol **3.54**. The alkenyl group was selectively transferred, as there was no evidence for the formation of **3.55** which would arise upon alkyl transfer from the mixed alkyl/alkenyl zinc species **3.53**.

Scheme 3.14: Application of boron/zinc exchange to aldehyde vinylation



Radinov's contribution to this field culminated in the development of an intramolecular enantioselective macrocyclization as the key step in the synthesis of (R)-(-)-muscone (Scheme 3.15). The boron-zinc exchange followed by intramolecular allylation of **3.56** generated **3.57** in good yield and high enantioselectivity. Hydroxyl-directed Simmons-Smith reaction generated cyclopropanated **3.58**, which underwent Swern oxidation followed by regioselective hydrogenolysis of the cyclopropane to generate (R)-Muscone **3.59** in good yield.

Scheme 3.15: Total synthesis of (R)-muscalone through boron-zinc exchange



Boron-zinc exchange has since become a common method for generating dialkyl, dialkenyl, and diaryl zinc reagents for use in cross-coupling and other zinc-mediated reactions.¹⁹⁶

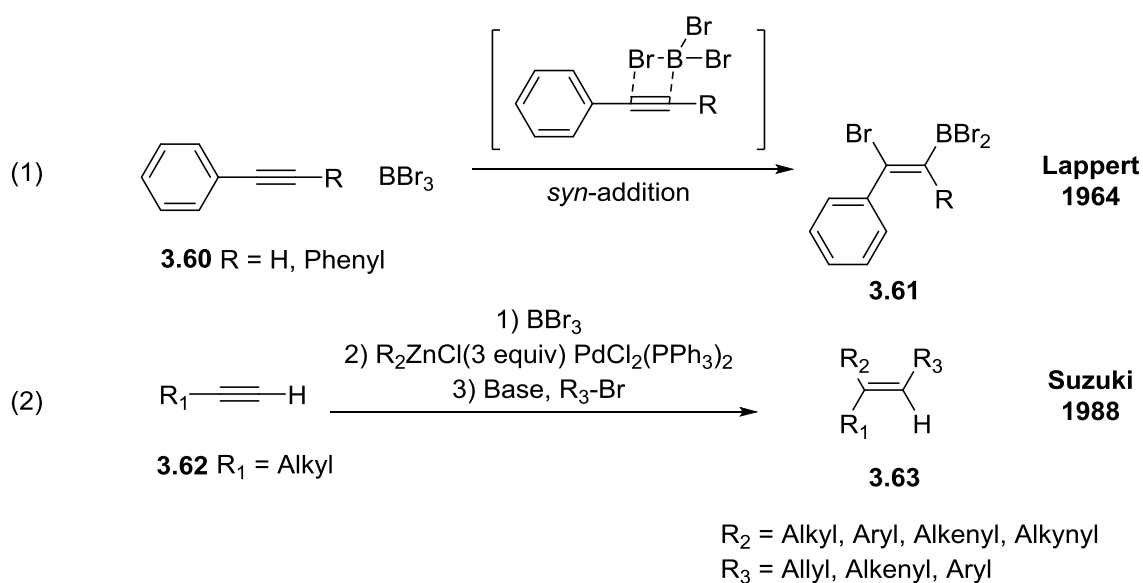
3.2.6 Known Reactivity Between Boron and Zinc Reagents: Boron-Tolerant Negishi Coupling

Despite the propensity for boron-zinc exchange to occur, there are many examples of Negishi coupling being performed in the presence of organoborane functionality. The

¹⁹⁶ Knochel, P.; Leuser, H.; Gong, L.-Z.; Perrone, S.; Kneisel, F. F. In *Patai's Chemistry of Functional Groups*; John Wiley & Sons, Ltd, 2009, pp. 25-30.

haloboration reaction has emerged as a powerful tool for the stereoselective synthesis of highly substituted alkenes.¹⁹⁷

Scheme 3.16: Haloboration/cross-coupling examples



First discovered by Lappert in 1964,¹⁹⁸ the haloboration reaction is the concerted syn-addition of a B–X bond across a triple bond, in an analogous fashion to the hydroboration reaction and is a powerful method for the selective synthesis of tri- and tetrasubstituted alkenes **3.61** from alkynes (Scheme 3.16, Eq. 1). Suzuki later used this haloboration reaction to demonstrate a one-pot haloboration/Negishi coupling/Suzuki coupling sequence to generate trisubstituted alkenes **3.63** from alkyl alkynes **3.62**

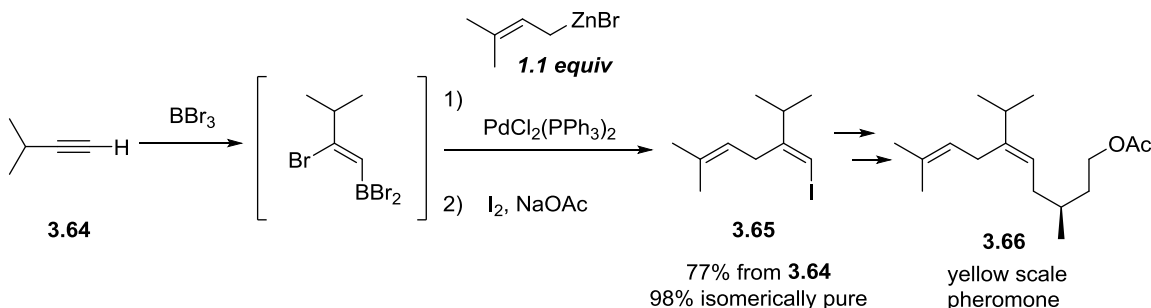
¹⁹⁷ For a review on modern alkynyl borylation methodology see: Barbeyron, R.; Benedetti, E.; Cossy, J.; Vasseur, J.-J.; Arseniyadis, S.; Smietana, M. *Tetrahedron* **2014**, *70*, 8431-8452.

¹⁹⁸ Lappert, M. F.; Prokai, B. *J. Organomet. Chem.* **1964**, *1*, 384-400.

(Scheme 3.16, Eq. 2).¹⁹⁹ Suzuki used excess organozinc chloride (3 equivalents) to account for the probable alkylation of the *B*-X bonds after haloboration.

Negishi later utilized this methodology for the synthesis of key intermediate **3.65** from alkyne **3.64** in a convergent total synthesis of yellow scale pheromone **3.66**, showing that with prenyl zinc bromides the Negishi cross-coupling could outcompete *B*-X alkylation requiring only a slight excess of zinc reagent (Scheme 3.17).²⁰⁰ This is the only verified literature report of Negishi coupling taking place in the presence of a reactive *B*-X bond to selectively generate a *C*-*C* bond.

Scheme 3.17: Negishi's use of haloboration/cross-coupling in total synthesis



Negishi has since modified this approach to generate the isolable Bpin species **3.67** before cross-coupling at the alkenyl halide which prevented post haloboration isomerization, a common stereodegenerating process with this methodology.²⁰¹ By eliminating the reactive *B*-X bonds, this methodology was expanded to include alkyl-

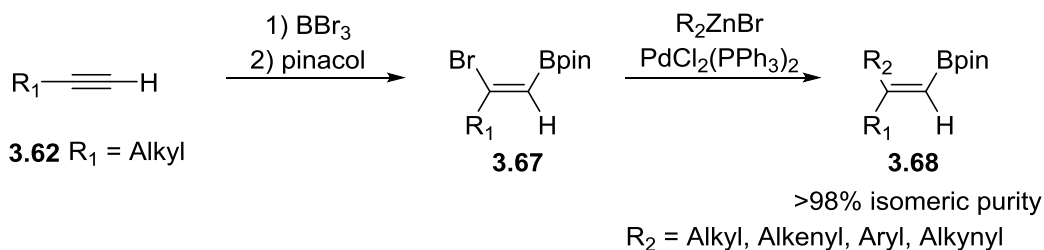
¹⁹⁹ Satoh, Y.; Serizawa, H.; Miyaura, N.; Hara, S.; Suzuki, A. *Tetrahedron Lett.* **1988**, *29*, 1811-1814.

²⁰⁰ Xu, Z.; Negishi, E. *Org. Lett.* **2008**, *10*, 4311-4314.

²⁰¹ Wang, C.; Tobrman, T.; Xu, Z.; Negishi, E. *Org. Lett.* **2009**, *11*, 4092-4095.

aryl-, alkenyl-, and alkynyl- zinc halides and remains the state of the art for this cross-coupling strategy in the rational synthesis of tri-substituted olefins (Scheme 3.18).

Scheme 3.18: State of the art haloboration/Negishi cross-coupling



3.3 Development of Functional Group Tolerant Negishi Cross-Coupling

3.3.1 Synthesis of C(3) Brominated *B*-H and *B*-Cl Azaborines

We were interested in exploring the viability of cross-coupling for C(3) substitution of monocyclic azaborines featuring readily functionalized groups (*B*-H or *B*-Cl) because the synthetic toolbox available for late-stage functionalization of monocyclic BN-heterocycles is still limited and largely unexplored.

Negishi coupling is an attractive strategy for late-stage functionalization of azaborines because: 1) it enables cross-coupling of aryl halides and alkyl, aryl, alkenyl, alkynyl, and heteroaryl zinc halides with a reasonable functional group tolerance;²⁰² 2)

²⁰² (a) Negishi, E. *Acc. Chem. Res.* **1982**, *15*, 340-348. (b) Nicolaou, K. C.; Bulger, P. G.; Sarlah, D. *Angew. Chem. Int. Ed.* **2005**, *44*, 4442-4489. (c) Knochel, P.; Leuser, H.; Gong, L.-Z.; Perrone, S.; Kneisel, F. F. In *Patai's Chemistry of Functional Groups*; John Wiley & Sons, Ltd, **2009**

zinc reagents are nontoxic and readily available;²⁰³ and 3) unlike Suzuki coupling, it does not require borophilic additives as activating agents.²⁰⁴ The use of Suzuki coupling for functionalization of BN-heterocycles, while effective with certain *B*-substitution is limited with *B*-H and likely impossible with *B*-Cl functionality (due to the prevalence of alcoholic and aqueous solvents and additives necessary to promote transmetallation). Negishi's successful cross-coupling in the presence of the reactive *B*-Br bond (Scheme 3.17) led us to believe that cross-coupling using zincates would be possible; however we first needed to establish whether *B*-H and *B*-Cl azaborines were stable towards the nucleophilic carbon-zinc bond. We decided to focus on the use of brominated azaborines **3.70** and **3.71** (Scheme 3.19) as model azaborines to determine the feasibility of Negishi cross-coupling.

The most effective synthesis of *B*-Cl (**3.70**) and *B*-H (**3.71**) C(3) brominated azaborines begins with versatile *B*-Cl intermediate **3.69**. In an analogous fashion to the *N*-^tBu *B*-Cl azaborine **3.38**, **3.69** selectively brominates at the C(3) position yielding **3.70** after distillation (Scheme 3.19). There is an unknown side product (~7-10%)²⁰⁵ to this reaction that has similar chemical shifts and a higher reactivity towards nucleophiles that is separable by fractional distillation if it hinders the desired reaction. Otherwise, it is possible to carry the mixture to *B*-H **3.71** with no deleterious effects by treatment with

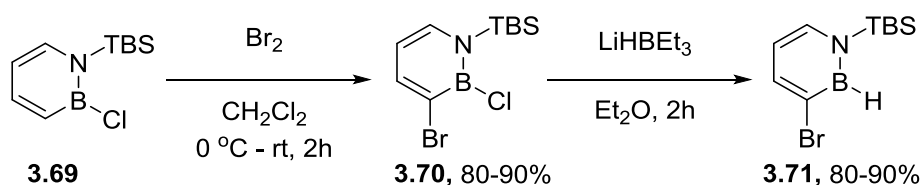
²⁰³ Sigma-Aldrich offers 175 Rieke[®] and organozinc reagents in their online catalogue. (Accessed Mar, 2015) and many are readily available through transmetallation with more available organomagnesium reagents

²⁰⁴ For recent reviews on modern metal-catalyzed cross-coupling please see: (a) Jana, R.; Pathak, T. P.; Sigman, M. S. *Chem. Rev.* **2011**, *111*, 1417-1492. (b) Johansson Seechurn, C. C. C.; Kitching, M. O.; Colacot, T. J.; Snieckus, V. *Angew. Chem. Int. Ed.* **2012**, *51*, 5062-5085.

²⁰⁵ This species is likely the *B*-Br halide exchanged compound.

super hydride, LiHBEt₃. The high isolated yields with no side products suggest the full conversion of the unidentified side product to **3.71**.

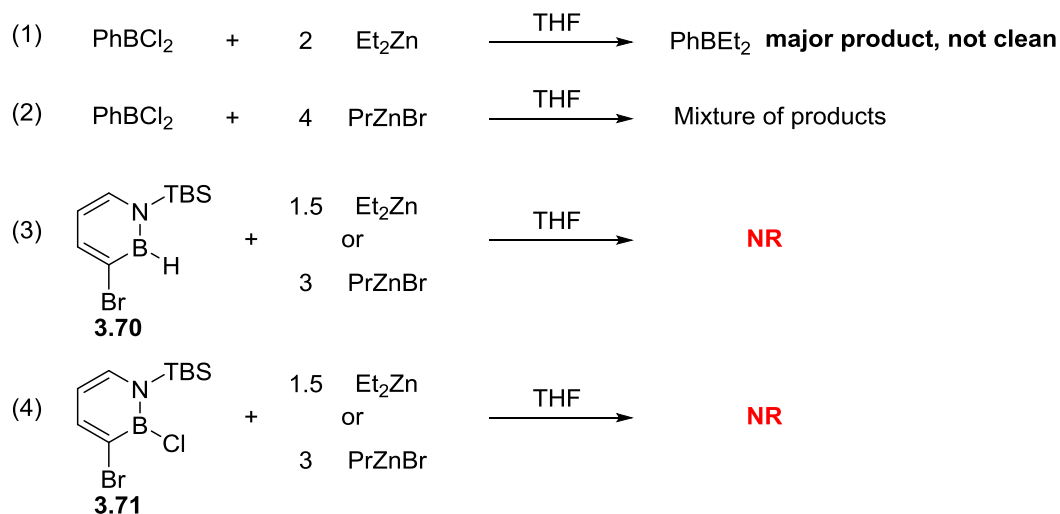
Scheme 3.19: Synthesis of C(3) brominated azaborines



3.3.2 Stability of BN-Arenes to Zinc Reagents

With C(3) brominated azaborines **3.70** and **3.71** in hand, we investigated the stability of the B–H and B–Cl bond towards highly reactive diethylzinc as well as less reactive propylzinc chloride before undertaking an exploration of Negishi cross-coupling.

Scheme 3.20: Stability of B–H and B–Cl bonds to excess alkylzinc reagents



To gauge the reactivity of different *B*–Cl bonds to dialkylzinc and alkylzinc halide reagents, we treated commercially available phenylboron dichloride with diethyl zinc or less reactive propylzinc bromide and monitored the reaction by ¹¹B NMR. We found that diethylzinc gave diethyl phenylborane as the major product (Scheme 3.20, Eq. 1), while propylzinc bromide generated a mixture of products containing multiple 4-coordinate and alkylated boron-containing species (Scheme 3.20, Eq. 2). To probe the viability of Negishi couplings in the presence of reactive boron centers in 1,2-azaborines we also treated **3.70** and **3.71** with excess diethylzinc or propylzinc bromide in THF solution (Scheme 3.20, Eq. 3-4). To our delight, we were unable to observe any alkylation or decomposition of either model reaction at room temperature for 24 hours verifying that Negishi coupling could be viable.

3.3.3 Optimization and Substrate Scope of *B*–H Tolerant Negishi Coupling

We decided first to develop the cross-coupling of compound **3.70** due to the higher stability of the *B*–H bond toward hydrolysis and silica gel. In order to develop a robust system, we chose to optimize our conditions for propylzinc bromide, as alkylzinc halides are generally less reactive than dialkylzinc reagents in cross coupling. By optimizing the conditions for the less reactive system, we would have a higher chance of finding conditions amenable to a range of organozinc reagents. In order to probe this reaction, we screened a variety of electron rich and sterically hindered phosphines (as shown in Table 3.1) for their activity in our model system with Pd (II) source PdCl₂(PhCN)₂.

Table 3.1: Screening of phosphine ligands for *B*-H tolerant Negishi coupling

Entry	Pd Source	Ligand	% yield ^a
1	PdCl ₂ (PhCN) ₂	P ^t BuPh ₂	75
2	PdCl ₂ (PhCN) ₂	P(cy) ₂ mes	70
3	PdCl ₂ (PhCN) ₂	P(cy) ₂ Ph	75
4	PdCl ₂ (PhCN) ₂	orthobiphenylP ^t Bu ₂	73
5	PdCl ₂ (PhCN) ₂	P(cy) ₃	76
6	PdCl ₂ (PhCN) ₂	P(furyl) ₃	53
7	PdCl ₂ (PhCN) ₂	P(^o tol) ₃	72
8	PdCl ₂ (PhCN) ₂	HP ^t Bu ₃ ⁺ BF ₄ ⁻	68
9	PdCl ₂ (PhCN) ₂	HP ^t Bu ₂ Me ⁺ BF ₄ ⁻	77
10	Pd(P ^t Bu ₃) ₂	-	67

^aPercent yield determined by GC-FID with undecane as calibrated internal standard.

Mixed alkyl/aryl phosphines (Table 3.1, entries 1-4) showed similar activity to sterically hindered aryl P(^otol)₃ and electron-rich P(cy)₃ (Table 3.1, entries 5 and 7). Of the phosphines screened, P(furyl)₃ showed the lowest yield of expected product (Table 3.1, entry 6). Trialkylphosphonium phosphine precursors popularized by Fu²⁰⁶ were also active in this transformation (Table 3.1, entries 8 and 9), while Pd(P^tBu₃)₂ showed a relatively low yield for the model reaction (Table 3.1, entry 10). None of the catalysts screened showed a large increase in yield for this cross-coupling, so we further optimized this reaction for the preformed 1 Pd (II): 2 PR₃ PdCl₂(P^otol₃)₂ for operational and economic simplicity (Table 3.2).

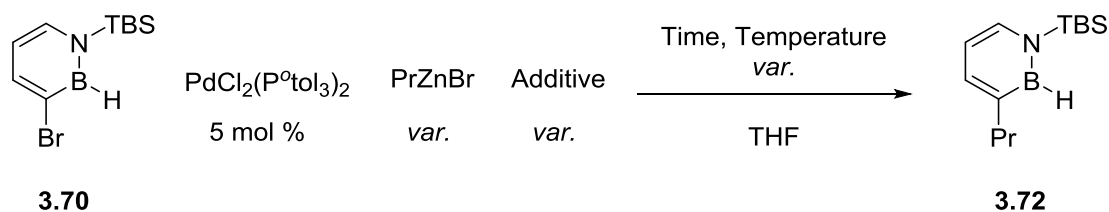
²⁰⁶ Netherton, M. R.; Fu, G. C. *Org. Lett.* **2001**, *3*, 4295-4298.

Using Table 3.1, entry 7 (72%) as a baseline yield for the in-situ generated (after reduction) $\text{Pd}(\text{P}^o\text{tol}_3)_2$ species we screened conditions in order to identify additives that would increase the yield. We screened basic additives in 0.5 and 1.5 equivalents, however only 2,6-lutidine showed a competitive yield to that observed in Table 3.1, entry 7 (Table 3.2, entries 1-10). The addition of lithium bromide in order to raise the dielectric constant of the solvent neither helped nor hindered the reaction (Table 3.2, entries 11-12). Of the cosolvent systems screened (PrZnBr is only available in a THF solution), only Et_2O and toluene did not lower the yield dramatically from that observed in Table 3.1, entry 7 (Table 3.2, entries 13-20).

Heating the reaction had no deleterious effect, with the reaction being complete after 1 hour (Table 3.2, entries 21-22). The addition of either more zincate (Table 3.2, entries 24-25) or less zincate (Table 3.2, entry 23) only lowered the yield of the reaction in comparison to Table 3.1, entry 7. We revisited additives such as 2,6-lutidine as well as LiBr and LiCl , at this higher temperature however none of these additives provided a tangible increase in yield over Table 3.1, entry 7 (Table 3.2, entries 26-29).

For the purposes of our substrate scope, we decided to use the equivalent-yielding to Table 3.1 entry 7 conditions consisting of: 5 mol% $\text{PdCl}_2(\text{P}^o\text{tol}_3)_2$, 1.5 equiv Zincate, THF, 50 °C, 1.5 h (Table 3.2, entries 21-22).

Table 3.2: Optimization of PdCl₂(P^otol₃)₂ catalyst system

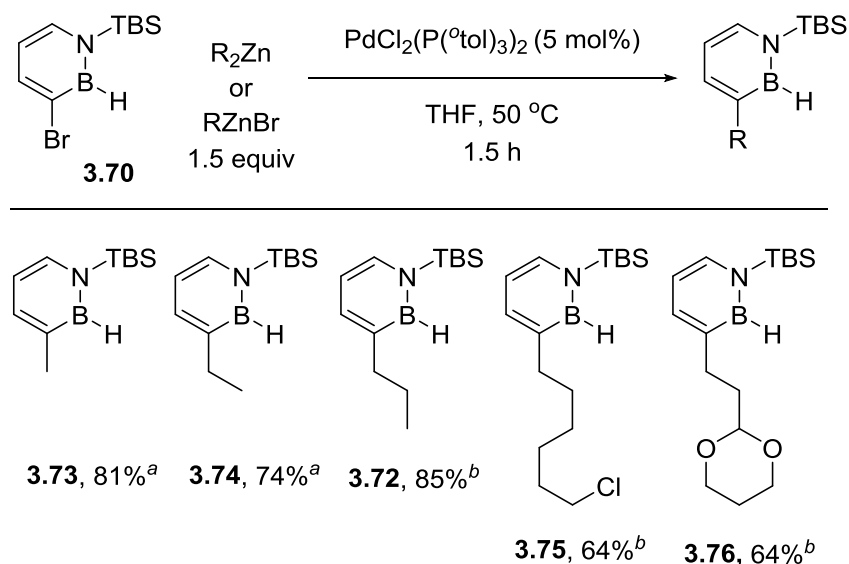


Entry	Additive	Additive Equivalents	Zinc Reagent Equivalents	Temp	Time	% yield ^a
1	NMI	0.5	1.5	rt	20 h	56
2	NMI	1.5	1.5	rt	20 h	56
3	DMA	0.5	1.5	rt	20 h	59
4	DMA	1.5	1.5	rt	20 h	57
5	DMF	0.5	1.5	rt	20 h	55
6	DMF	1.5	1.5	rt	20 h	58
7	TEA	0.5	1.5	rt	20 h	62
8	TEA	1.5	1.5	rt	20 h	61
9	2,6-lutidine	0.5	1.5	rt	20 h	62
10	2,6-lutidine	1.5	1.5	rt	20 h	73
11	LiBr	0.5	1.5	rt	20 h	76
12	LiBr	1.5	1.5	rt	20 h	73
13	Et ₂ O	cosolvent	1.5	rt	20 h	62
14	DMF	cosolvent	1.5	rt	20 h	44
15	DMA	cosolvent	1.5	rt	20 h	48
16	NMI	cosolvent	1.5	rt	20 h	5
17	Toluene	cosolvent	1.5	rt	20 h	61
18	DME	cosolvent	1.5	rt	20 h	26
19	Pentane	cosolvent	1.5	rt	20 h	46
20	Acetonitrile	cosolvent	1.5	rt	20 h	46
21	-	-	1.5	50	1 h	75
22	-	-	1.5	50	3 h	74
23	-	-	1.1	50	1.5 h	64
24	-	-	2	50	1.5 h	63
25	-	-	5	50	1.5 h	52
26	2,6-lutidine	cosolvent	1.5	50	1.5 h	51
27	LiBr	1.5	1.5	50	1.5 h	64
28	2,6-lutidine	1.5	1.5	50	1.5 h	71
29	LiCl	1.5	1.5	50	1.5 h	61

^aPercent yield determined by GC-FID with undecane as calibrated internal standard.

With optimized conditions in hand for the synthesis of **3.72**, we applied these conditions to other alkylzinc halide and dialkylzinc reagents in order to generate C(3) substituted azaborines **3.72-3.76** (Scheme 3.21). Gratifyingly, the reaction with propylzinc bromide gave a higher isolated yield upon scale up than that observed during optimization (**3.72**, 85%).

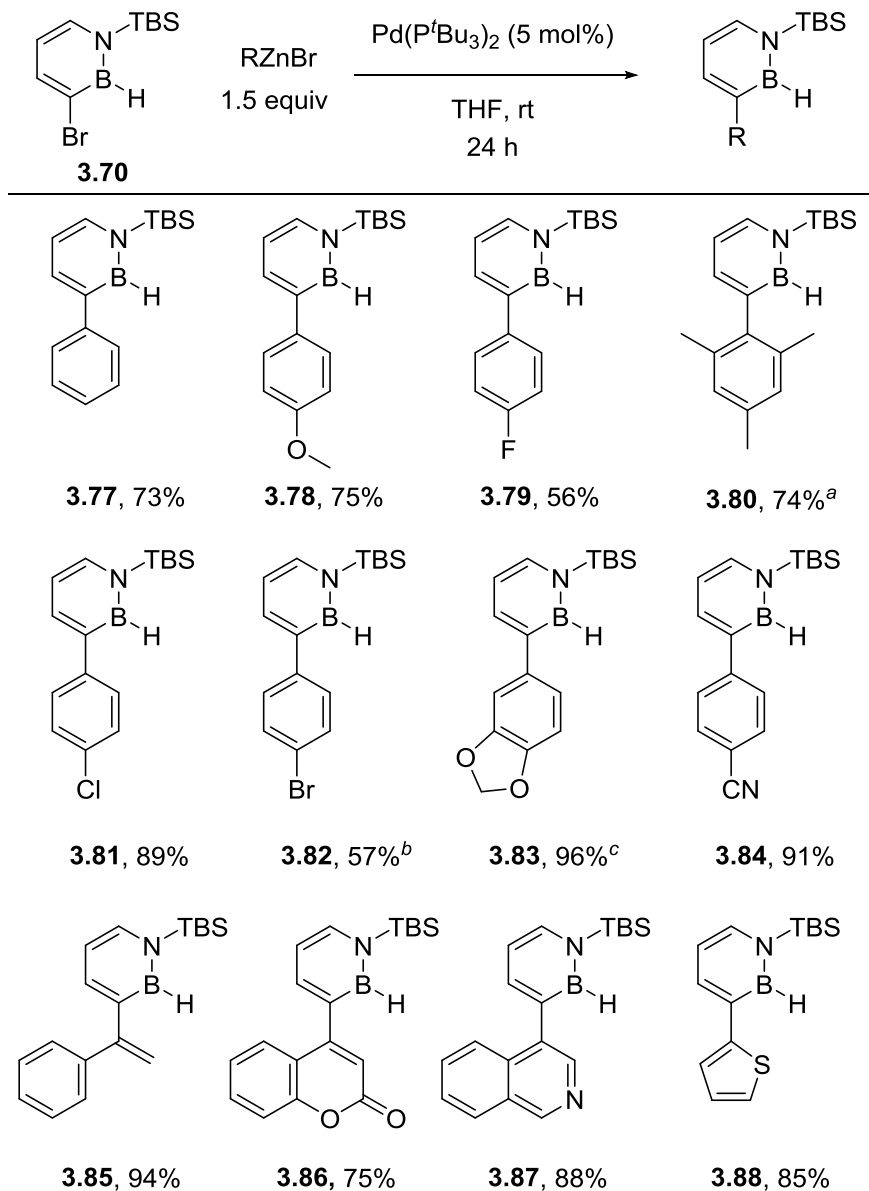
Scheme 3.21: Negishi cross-coupling of 3.70 with alkyl- and dialkyl- zinc reagents



Percent yields are isolated and the average of two runs. ^aDialkylzinc (1.5 equiv) used
^bAlkylzincbromide (1.5 equiv) used.

Reactive dimethyl zinc (**3.73**, 81%) and diethyl zinc (**3.74**, 81%) coupled in good yield without evidence of alkylation at boron, while alkylzinc bromides with either alkyl chloride (**3.75**, 64%) or acetal (**3.76**, 64%) functionalities proceeded in moderate yield.

Scheme 3.22: Negishi cross-coupling of 3.70 with aryl-, alkenyl-, and heteroaryl-, zinc halide reagents.



Percent yields are isolated and the average of two runs. ^a conditions: 3 equiv 2,4,6-trimethylphenylzinc iodide, 0.05 equiv Pd(P^tBu₃)₂, THF, rt, 48 h. ^b4-bromophenylzinc iodide was used. ^c2,3-Methylenedioxyphenylzinc iodide was used.

Azaborines **3.72-3.74** are more volatile than expected, the additional steric bulk of the C(3) substituent may be responsible for lowering the boiling points of **3.72-3.74** when compared to compound **3.70** or when the C(3) substituent is hydrogen.²⁰⁷

Unfortunately, under identical conditions, our preliminary attempts to cross-couple arylzinc halides were not clean or high-yielding. Organ has extensively studied the mechanism and reactivity of alkyl- and aryl- zinc halides in Negishi coupling and has shown that maximizing reactivity can require separate conditions for alkyl- and aryl- zinc reagents due to the different nature of the active transmetallating species in both systems.²⁰⁸

In our system, a switch to the highly active Pd⁽⁰⁾(P^tBu₃)₂ catalyst system popularized by Fu²⁰⁹ was sufficient to facilitate the clean cross-coupling reactions of alkenyl, aryl, and heteroaryl zinc compounds with **3.70**. C(3) substituted azaborines **3.77-3.88** were generated in moderate to excellent yields (Scheme 3.22).

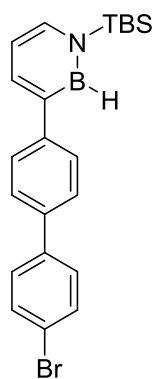
Phenylzinc bromide couples in good yield (**3.77**, 73%), while electron rich 4-methoxy phenylzinc bromide (**3.78**, 75%) and electron deficient 4-fluorophenylzinc bromide (**3.79**, 56%) are also viable coupling partners. Sterically hindered 2,4,6-trimethylphenylzinc iodide coupled sluggishly but in good yield (**3.80**, 74%). Aryl-halide containing 4-chlorophenylzinc bromide (**3.81**, 89%) and 4-bromophenylzinc iodide (**3.82**,

²⁰⁷ Exposure to 300 mTorr vacuum caused loss of products **3.77-3.88** while C(3)=H distills at 300 mTorr at ~60-70 °C. Adding additional substituents to normal arenes generally increases their boiling point, 1,3-dimethylbenzene boils at 139 °C while 1,2,3-trimethylbenzene boils at 176 °C.

²⁰⁸ (a) Achonduh, G. T.; Hadei, N.; Valente, C.; Avola, S.; O'Brien, C. J.; Organ, M. G. *Chem. Commun.* **2010**, 46, 4109-4111. (b) Hadei, N.; Achonduh, G. T.; Valente, C.; O'Brien, C. J.; Organ, M. G. *Angew. Chem. Int. Ed.* **2011**, 50, 3896-3899. (c) McCann, L. C.; Hunter, H. N.; Clyburne, J. A. C.; Organ, M. G. *Angew. Chem. Int. Ed.* **2012**, 51, 7024-7027. (d) McCann, L. C.; Organ, M. G. *Angew. Chem. Int. Ed.* **2014**, 53, 4386-4389.

²⁰⁹ (a) Dai, C.; Fu, G. C. *J. Am. Chem. Soc.* **2001**, 123, 2719-2724. (b) Fu, G. C. *Acc. Chem. Res.* **2008**, 41, 1555-1564.

57%) were also amenable to these conditions, and could be substrates for further cross-coupling. The decreased yield of **3.82** is mainly due to competitive coupling of the aryl bromide in **3.82** with 4-bromophenylzinc iodide to generate terphenyl structure **3.89** which was isolated in 14% yield. Compounds **3.81**, **3.82**, and **3.89** could be potential monomers for the generation of azaborine-capped polymers.



3.89, 14%

Figure 3.3: Side product **3.89** from cross coupling of 4-bromophenylzinc iodide

2,3-Methylenedioxyphenylzinc iodide (**3.83**, 96%), 4-cyanophenylzinc bromide (**3.84**, 91%) and alkenyl (1-phenylvinyl)zinc bromide (**3.85**, 94%) coupled in excellent yield. Cross-coupling with 4-coumarinylzinc bromide generates the neoflavone²¹⁰ structure in good yield (**3.86**, 75%) providing an example of an oxygen-containing heterocycle. We were successful in coupling both isoquinoline (**3.87**, 88%) and thiophene (**3.88**, 85%) containing zinc reagents in good yield as examples of nitrogen and sulfur containing heterocycles.

²¹⁰ Neoflavanoids are 4-phenyl coumarin based natural products: Donnelly, D. M. X.; Boland, G. M. *Nat. Prod. Rep.* **1995**, *12*, 321-338.

We were able to grow crystals suitable for single crystal x-ray diffraction of **3.83** as shown in Figure 3.4. The bond lengths in the azaborine ring are in agreement with those in unsubstituted azaborines.²¹¹ The C(4)-C(5) bond length of 1.485 is similar to that in biphenyl.²¹² The dihedral angle is 37.5° which is consistent with expected angles for typical biaryl compounds.

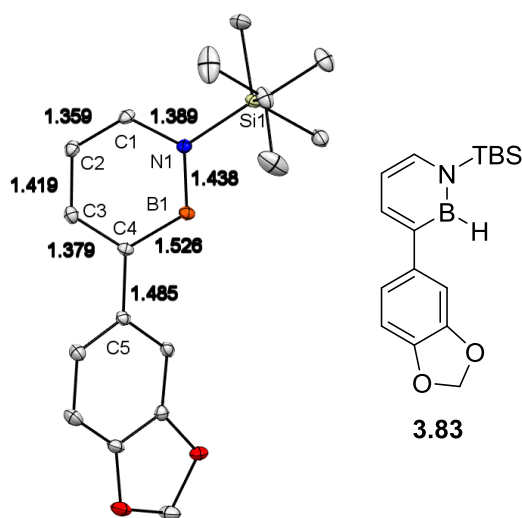


Figure 3.4. X-ray crystal structure of compound **3.83**, ORTEP illustration, with thermal ellipsoids drawn at the 35% probability level of **3.83**; all hydrogen atoms have been omitted for clarity.

Of the cross couplings attempted, there were a few which either did not produce the desired product or need more optimization to be adequate. The attempted cross-coupling of allylzinc bromide gave a mixture of *B*-substituted products, even without the catalyst. The attempted cross coupling of zinc (II) cyanide was inconsistent, giving a large variance in yields and conversions. Further optimization is necessary in order to

²¹¹ For a structural analysis of BN substituted 1,2-azaborines, see: Abbey, E. R.; Zakharov, L. N.; Liu, S. - *Y. J. Am. Chem. Soc.* **2008**, *130*, 7250-7252

²¹² Biphenyl has a bridging C-C bond length of 1.496 Å: Charbonneau, G. P.; Delugeard, Y. *Acta Cryst.*, **1976**, B32, 1420-1423.

make this reaction viable and reproducible. The cross-coupling of 2-pyridyl zinc reagents was successful, although the isolated yields were <10%. Zincates containing an ester moiety gave unidentified *B*-O species. The simplest way to improve these systems would be to move to a more stable *B*-OR azaborine, however the use of other less gentle cross-coupling methodologies may be more attractive with the stable *B*-OR.

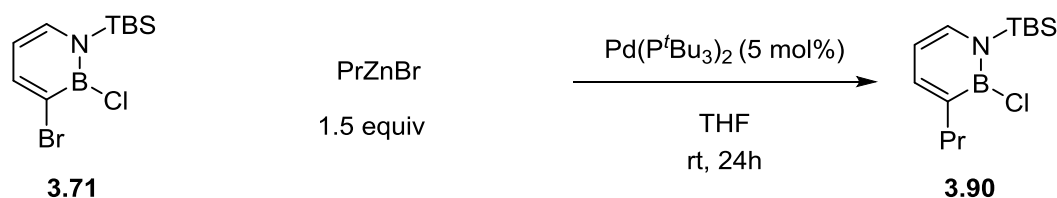
3.3.4 Optimization and Substrate Scope of *B*-Cl Tolerant Negishi Coupling

Having successfully demonstrated that Negishi cross-coupling was viable with compound **3.70** we began to study cross-coupling of the very sensitive *B*-Cl containing **3.71**. The precedent set by Negishi led us to believe that this should be possible, however selective catalytic activation of the C(3)-Br bond would be necessary over the *B*-Cl bond. During our initial screening of this reaction we found that the reaction with PdCl₂(P^{*o*}tol₃)₂ generally gave a more intractable reaction profile than Pd(^{*t*}Bu₃)₂, and it was completely unsuccessful with ArZnX reagents, generating exclusively *B*-O species from the ring opening of THF (unfortunately, the majority of zinc reagents are available only in THF solution, 2-Me THF would be a viable option to avoid this if THF could be completely removed from the reaction). In order to avoid side reactions, we focused on room temperature conditions as shown in Table 3.3.

Gratifyingly, a benchmark NMR yield of 87% for compound **3.90** was obtained by using Fu's Pd(^{*t*}Bu₃)₂ catalyst system (Table 3.3, entry 1). No reaction was observed without palladium catalyst (Table 3.3, entry 2). Other palladium-based precatalysts were active, however the yields were consistently lower than the Pd(^{*t*}Bu₃)₂ system (Table 3.3,

entries 3-5). Nickel-based precatalysts gave poor yields and complex reaction mixtures (Table 3.3, entries 6 and 7).²¹³

Table 3.3: Survey of catalysts and solvents for the Negishi cross-coupling reaction of 1,2-azaborine 3.71.



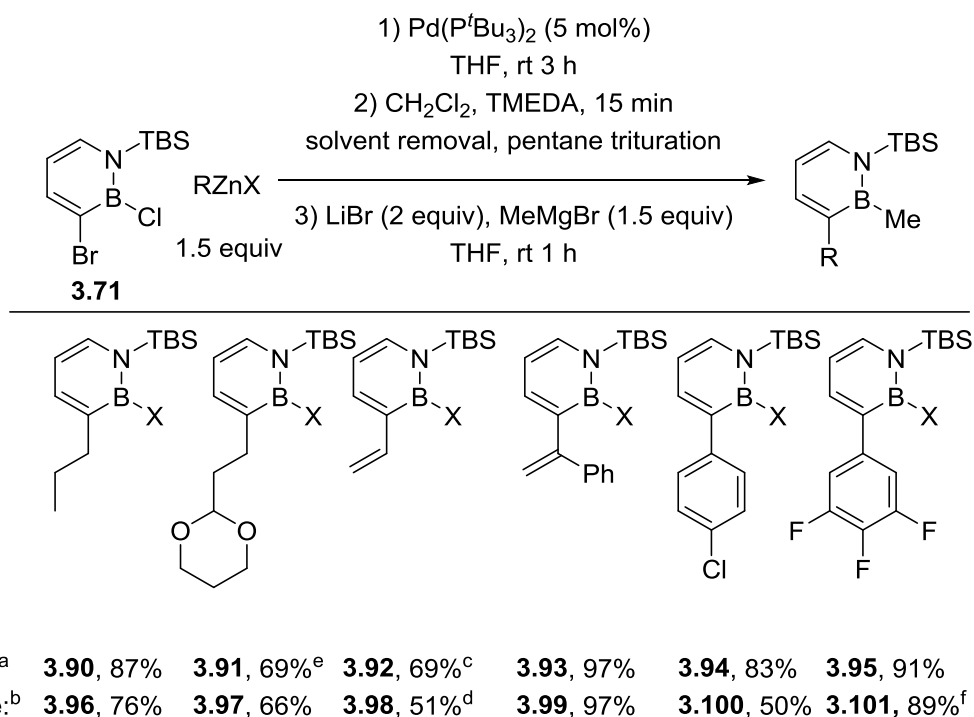
Entry	Deviation from standard conditions	NMR yield (%)
1	No deviation	87
2	No catalyst	NR
3	Catalyst: 5 mol% PdCl ₂ (P ^o tol ₃) ₂	75
4	Catalyst: 5 mol% Xphos Pd G2	79
5	Catalyst: 5 mol% Pcy ₃ Pd G2	63
6	Catalyst: 5 mol% NiCl ₂ (Pcy ₃) ₂	35
7	Catalyst: 5 mol% Ni(cod) ₂ + terpy	31
8	Et ₂ O instead of THF	85
9	Toluene instead of THF	82
10	Additive: N-methyl pyrrolidone	43
11	3 hour reaction time	87

¹H NMR yield determined by the internal standard method against hexamethylbenzene, average of two runs.

²¹³ (a) Huo, S. *Org. Lett.* **2003**, *5*, 423-425. (b) Smith, S. W.; Fu, G. C. *Angew. Chem. Int. Ed.* **2008**, *47*, 9334-9336. (c) for a review of nickel catalyzed cross-coupling please see: Adhikary, A.; Guan, H. In *Pincer and Pincer-Type Complexes*; Szabó, K. J., Wendt, O. F., Eds.; Wiley-VCH Verlag GmbH & Co. KGaA, **2014**; pp 117-148.

A solvent switch to diethyl ether (Table 1, entry 8) or toluene (Table 3.3, entry 9) was not detrimental to the observed yield of **3.90**. Use of N-methyl pyrrolidone as an additive resulted in a decreased yield for the reaction (Table 3.3, entry 10).²¹⁴

Scheme 3.23: Synthesis of *B*-Me 1,2-azaborines through a semi-one pot Negishi coupling substitution sequence.



^a ¹H NMR yields determined in a separate experiment (.0981 mmole scale) by the internal standard method against an internal standard of hexamethylbenzene, average of two runs. Isolated yields (0.654 mmole scale), average of two runs. ^cReaction conditions: 1.2 equivalents vinylzinc bromide generated from 1.2 equivalents vinylmagnesium bromide and 2.4 equivalents zinc bromide, 24 hour reaction time, a significant amount of B-vinyl side product was generated under these conditions. ^d1.01 Equivalents vinylzinc bromide generated from 1.01 equivalents of vinylmagnesium bromide and 2 equivalents of zinc bromide, 22 h reaction time. ^eInternal standard of triphenylmethane was used. ^f1.01 Equivalents methyl magnesium bromide used in order to minimize over-alkylation.

²¹⁴ THF/NMP mixtures are common solvents in Negishi couplings: Jana, R.; Pathak, T. P.; Sigman, M. S. *Chem. Rev.* **2011**, 111, 1417-1492.

The reaction time could be shortened to 3 hours with no significant loss in yield (Table 3.3, entry 11). With optimized conditions in hand, we investigated the scope of the cross-coupling in the presence of a *B*-Cl bond (Scheme 3.23).

We were able to determine yields of the intermediate *B*-Cl compounds by ¹H NMR, however the reactivity of the *B*-Cl bond towards oxygen nucleophiles made small-scale isolation problematic. In order to maximize the reproducibility and practicality of these reactions, we developed a semi-one pot method for the direct two-step preparation of the chromatography-stable *B*-Me 1,2-azaborine (Scheme 3.23). We are able to cleanly generate the *B*-Cl compound (<20% *B*-O and other species). Treatment with excess methylene chloride and TMEDA to quench the catalyst followed by multiple triturations of the resulting oily precipitate under pentane gives *B*-Cl compounds **3.90-3.95**.

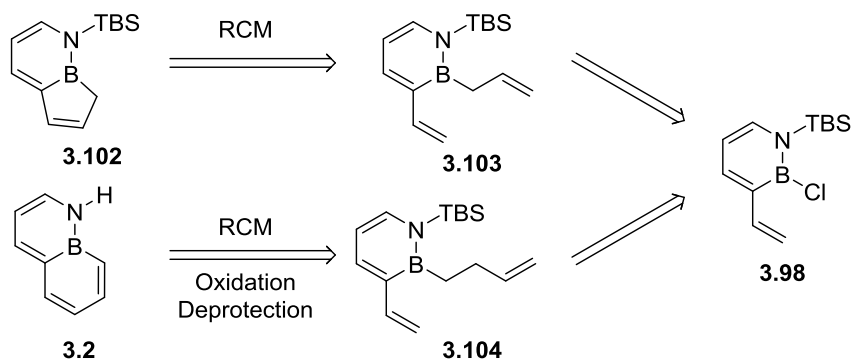
The *B*-Cl compounds can be reacted directly with lithium bromide-activated methyl magnesium bromide²¹⁵ to generate the *B*-Me species **3.96-3.101**. We were able to perform this two-step procedure with alkyl zinc bromide reagents in good yield (**3.96**, 76% and **3.97**, 66%) and with alkenyl zinc bromide reagents in moderate (**3.98**, 51%) to excellent (**3.99**, 97%) yield. Electron deficient aryl zinc iodide or bromide reagents were also tolerated in moderate (**3.100**, 50%) to good (**3.101**, 89%) yield. Compound **3.100** was problematic due to side reactivity of the aryl chloride in the nucleophilic substitution step while compound **3.98** was difficult to isolate due to the reactive nature of styrenyl alkenes.

²¹⁵ Without LiBr the reaction was sluggish (~10h with 4 equiv MeMgBr). The addition of 2 equiv of LiBr increased the rate dramatically (full conversion <1h with 1.5 equiv MeMgBr). The LiBr could be generating a so-called “turbo” grignard reagent (for reviews see: (a) Tilly, D.; Chevallier, F.; Mongin, F.; Gros, P. C. *Chem. Rev.* **2014**, *114*, 1207-1257. (b) Bao, R. L.-Y.; Zhao, R.; Shi, L. *Chem. Commun.* **2015**, retrieved online 3/24/2015, DOI: 10.1039/c4cc10194d.) increasing the reactivity of the Grignard.

3.3.5 Synthesis of and Characterization of New Extended BN-Arenes

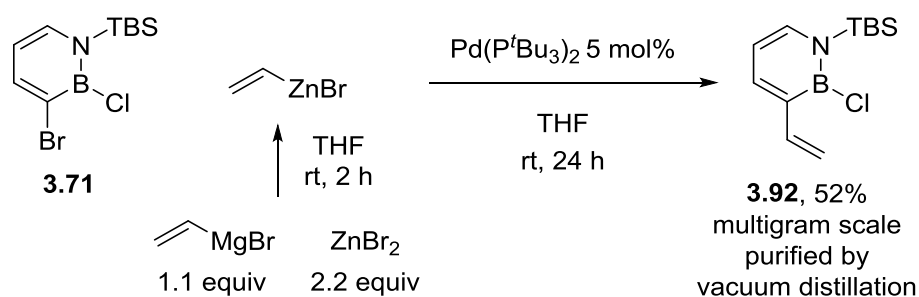
We identified compound **3.98** as a potential common intermediate for the synthesis of new BN-indene (compound **3.102**) and BN-naphthalene (compound **3.2**) isosteres by incorporation of an allylic (compound **3.103**) or homoallylic (compound **3.104**) boron substituent followed by ring closing metathesis (RCM) to generate the 6,5 and 6,6 fused ring systems respectively (Scheme 3.24). In the case of the 6,6 system further oxidation and TBS removal would generate the parental 9,1-borazaronaphthalene **3.2**, while deprotonation of **3.102** would lead to a new BN-indenyl ligand system.

Scheme 3.24: Retrosynthetic analysis of new BN-indene 3.102 and BN-naphthalene 3.2



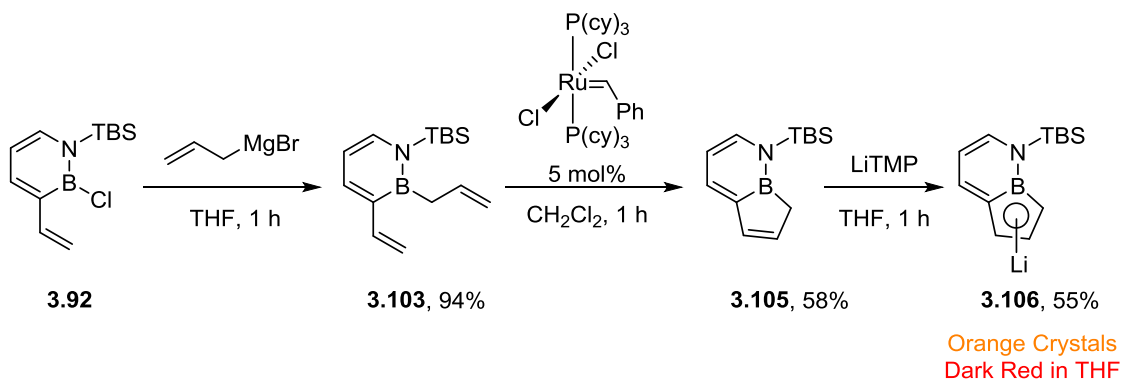
Gratifyingly, the Negishi coupling to generate key intermediate **3.92** was amenable to scale-up where isolation by vacuum distillation was practical on gram scale (Scheme 3.25).

Scheme 3.25: Synthesis of key intermediate 3.92 on gram-scale.



With access to large quantities of **3.92** we began the synthesis of BN indenyl **3.106** by first reacting **3.92** with allyl magnesium bromide to generate **3.103** in excellent yield (Scheme 3.26).

Scheme 3.26: Synthesis of BN-indenyl 3.106 from 3.92.



Ring-closing metathesis with Grubbs' first generation catalyst provided **4** as a single isomer in moderate yield. Lithium tetramethylpiperadine (pK_a~37) readily deprotonated compound **3.105** to generate BN-indenyl **3.106**. LiHMDS (pK_a~30) failed

to deprotonate **3.105**, suggesting a much higher pK_a for **3.105** than indene ($pK_a \sim 20$)
 Ashe's BN indene **3.21** was deprotonated by LDA ($pK_a \sim 36$).

Single-crystal X-ray diffraction analysis of **3.106** unambiguously confirms the indenyl structure (Figure 3.5) which is consistent with the observed upfield ^{11}B NMR shift ($\delta_{3.105} = 43.8$ ppm to $\delta_{3.106} = 28.8$ ppm) as well as the replacement of the methylene group with a new alkenyl resonance in the ^1H NMR spectra.

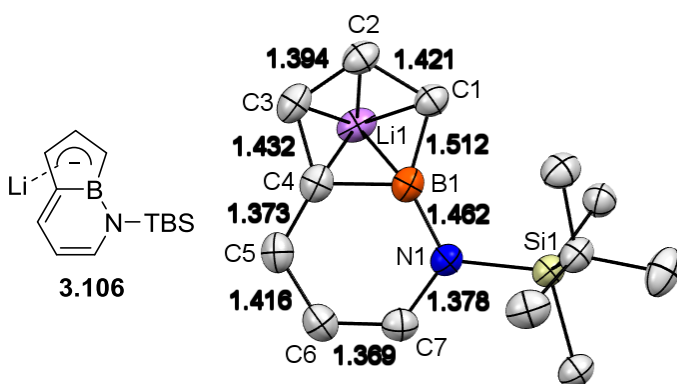


Figure 3.5: X-ray crystal structure of **3.106** ORTEP illustration, with thermal ellipsoids drawn at the 35% probability level of $(\text{THF})_2 \cdot \text{Li BN indenyl}$ **3.106**. All hydrogens and two THF molecules (coordinated to the lithium cation) have been omitted for clarity. Selected bond distances (Å): N–B: 1.462(3), N–C7: 1.378(3), B–C4: 1.568(3), B–C1: 1.512(3), Li–B: 2.458(4), Li–C1: 2.322(4), Li–C2: 2.247(4), Li–C3: 2.296(4) Li–C4: 2.419(4), C1–C2: 1.421(3), C2–C3: 1.394(3), C3–C4: 1.432(3), C4–C5: 1.373(3), C5–C6: 1.416(3), C6–C7: 1.369(3).

In the solid state **3.106** is planar and is bound η -5 to a lithium atom through the “cyclopentadienyl” portion of the ring. The bond distances in the 6-membered azaborine portion are consistent with previously reported bond lengths for monocyclic azaborines

except for the bridging boron carbon bond (B–C(4)), which is significantly longer than that found in typical monocyclic azaborine structures (1.568 Å vs ~1.516 Å). [Li(TMEDA)]₂[2,5-Ph₂C₄H₂BNMe₂], **3.107** a borole dianion, has a more symmetric corresponding B–C(1)-Bond and C(4)-Bond lengths of 1.550 Å and 1.541 Å respectively (Figure 3.6).²¹⁶ The η-5 coordination shows longer bonds for the internal Li–B and Li–C(4) interaction in comparison to the external Li–C(1), Li–C(2), and Li–C(3) interactions, which is similar to a previously reported substituted all-carbon Li–indenyl complex. For the symmetrically substituted carbanaceous 1,3-bis-trimethylsilyl lithium indenyl • 2THF **3.108**, selected bond lengths are as follows (Å) : Li–C(1): 2.244 and Li–C(2): 2.321 and Li–C(3): 2.402 Figure 3.6).²¹⁷

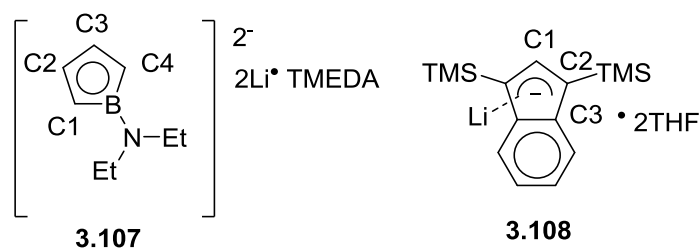


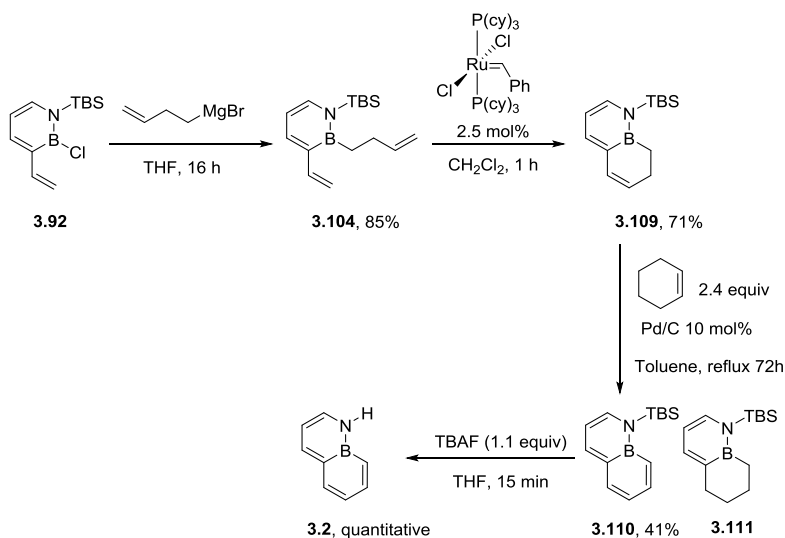
Figure 3.6: Structure of comparative borole dianion **3.107** and Li-indenyl **3.108**.

After the successful synthesis of **3.106**, we targeted **3.2** using methodology previously demonstrated to be viable with 1,2-azaborines (Scheme 3.27). Treatment of compound **3.92** with homoallyl magnesium bromide (the use of LiBr as an activating agent caused isomerization of the primary alkene to an internal alkene) generated **3.104** in good yield.

²¹⁶ Herberich, G. E.; Hostalek, M.; Laven, R.; Boese, R. *Angew. Chem. Int. Ed. Engl.* **1990**, *29*, 317-318.

²¹⁷ Jones, J. N.; Cowley, A. H. *Chem. Commun.* **2005**, *10*, 1300-1302

Scheme 3.27: Synthesis of 9,1-borazonaphthalene 3.2 from 3.92



Compound **3.104** was competent in ring closing metathesis to generate compound **3.109**. The oxidation of this compound using palladium on carbon with cyclohexene as a hydrogen scavenger in refluxing toluene proceeded in moderate yield generating aromatized **3.110** along with a significant amount of reduced product **3.111**. Desilylation using TBAF provided new parental 9,1-borazonaphthalene **3.2** as a crystalline solid that exhibits a strong odor reminiscent of naphthalene.

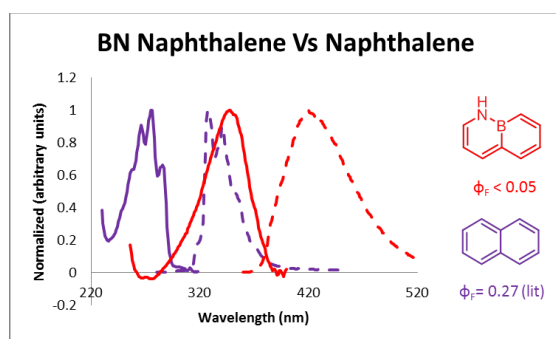


Figure 3.7: Normalized absorption (solid red trace) and emission (dashed red trace) of **3.2**. spectra in cyclohexane at 1×10^{-5} M (red trace) overlaid with naphthalenes absorption (solid purple trace) and emission profiles (dashed purple trace). The quantum yield of **3.2** was determined in cyclohexane at room temperature.

The absorption and emission spectra of compound **3.2** both exhibit a large bathochromic shift compared to naphthalene (λ_{abs} : 347 nm and λ_{em} : 420 nm for **3.2** versus λ_{abs} : 275 nm and λ_{em} : 327 nm for naphthalene). Unfortunately, the quantum yield for **3.2** was much lower than naphthalene.²¹⁸ The Stokes shift of parental naphthalene is 5782.6 cm^{-1} versus the 5008.9 cm^{-1} in **3.2**. This suggests that the initial excited state of **3.2** is closer in energy to the emissive state than that of naphthalene which is consistent with less spatial reorganization of atoms in order to access the emissive state (S_1) from the Franck-Condon excited state.

We were able to grow single-crystals of **3.2** however X-ray diffraction analysis of bond lengths in **3.2** was inconclusive due to a disordered system. The extended packing adopts an edge-to face herringbone fashion similar to that observed in carbonaceous naphthalene (Figure 3.8).²¹⁹

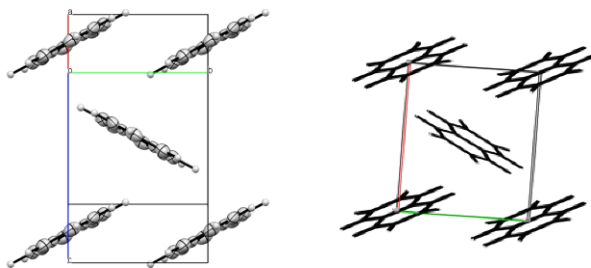


Figure 3.8: Crystal packing of 9,1-borazonaphthalene **3.2** (left) and all-carbon naphthalene (right).

²¹⁸ Suzuki, K.; Kobayashi, A.; Kaneko, S.; Takehira, K.; Yoshihara, T.; Ishida, H.; Shiina, Y.; Oishic, S.; Tobita, S. *Phys. Chem. Chem. Phys.* **2009**, *11*, 9850-9860.

²¹⁹ Alt, H.C.; Kalus, J. *Acta Crystallogr., Sect. B: Struct. Crystallogr. Cryst. Chem.* **1982**, *38*, 2595-2600.

3.4 Summary and Conclusions

We have demonstrated the Negishi cross-coupling at the C(3) position of monocyclic azaborines containing a *B*-H or *B*-Cl bond while maintaining that functionality. This methodology can be applied to the rationally designed synthesis of extended BN-arenes including new BN-indene **3.105** and 9,1-borazaronaphthalene **3.2**. We have demonstrated that BN-indenyl **3.106** is an isolable crystalline solid which should be a suitable starting material to access new BN-indenyl metal complexes. We have developed a new synthetic strategy for accessing the new 9,1-borazaronaphthalene structure and there is ongoing work in our lab using compound **3.92** to generate other new extended BN-arenes.

Metal-catalyzed cross-coupling (especially Negishi) has proven to be a viable and valuable tool for the synthesis of new 1,2-azaborines and enables the synthesis of a variety of previously inaccessible BN-arene containing structures.

3.5 Experimental Section

3.5.0 General Information

All oxygen- and moisture-sensitive manipulations were carried out under an inert atmosphere (N₂) using either standard Schlenk techniques or a glove box. THF, Et₂O, CH₂Cl₂, and pentane were purified by passing through a neutral alumina column under argon. Commercially available zinc reagents were purchased from **Sigma-Aldrich**: 0.5 M (THF) propylzinc bromide solution-499374, 0.5 M (THF) (1-phenylvinyl)zinc

bromide solution-499390, 0.5 M (THF) (4-chloro)phenylzinc iodide solution-497835, 1 M (hexanes) diethyl zinc solution-296112, 1 M (heptane) dimethylzinc solution-417246 0.5M (THF) phenylzincbromide solution-524719 **Alfa Aesar**: 0.5M (THF) (2-(1,3-dioxan-2-yl)ethyl)zinc bromide solution-H58912, 0.5M (THF) 6-chlorohexylzinc bromide-H58330, 0.5M (THF) 4-Fluorophenylzinc bromide-H58780, 0.5M (THF) 4-Methoxyphenylzinc iodide-H58690, 0.5M (THF) 4-Cyanophenylzinc bromide-H58211, 0.5M (THF) 2-Thienylzinc bromide-H58397, 0.5M (THF) 4-Bromophenylzinc iodide-H58429, 0.5 M (THF). (3,4,5-trifluorophenyl)zinc bromide solution-H58581, **Rieke Metals**: 0.5M (THF) 2,4,6-Trimethylphenylzinc iodide-2194, 0.5M (THF) 4-Isoquinolinzinc bromide-2284, 0.5M (THF) 3,4-(Methylenedioxy)phenylzinc iodide-2289, 0.5M (THF) 4-Coumarinylzinc bromide-2310 and used without further purification. All other chemicals were purchased (Sigma-Aldrich or TCI) and used as received. Silica and alumina were dried overnight at 150 °C under high vacuum. NMR spectra were recorded on a Varian VNMRS 600 MHz, VNMRS 500 MHz, INOVA 500 MHz, or VNMRS 400 MHz spectrometer. ¹¹B NMR spectra were externally referenced to BF₃•Et₂O (δ 0). Fluorescence emission spectra were collected on Photon Technology International spectrometer in dry, distilled, and degassed (by 4 freeze-pump-thaw cycles) HPLC grade cyclohexane (Sigma-Aldrich CHROMASOLV[®] plus-650455). Photoluminescence quantum yields were calculated using anthracene and 9,10-diphenylanthracene as external reference standards by literature procedure.²²⁰ 9,10-diphenylanthracene was recrystallized from hot ethanol with a hot polish filtration to

²²⁰ Jobin Yvon Ltd. *A Guide to Recording Fluorescence Quantum Yields* (accessed March 2015). <http://www.horiba.com/fileadmin/uploads/Scientific/Documents/Fluorescence/quantumyieldstrad.pdf>

remove impurities before measurement. UV-Vis spectra were collected on an Agilent Cary 100 spectrophotometer. Recycling HPLC was performed using a Jaigel next recycling preparative HPLC equipped with a Jaigel 2H polystyrene column plumbed into a nitrogen glovebox to enable airfree collection of fractions. High resolution mass spectroscopy was carried out on a JEOL AccuTOF instrument (JEOL USA, Peabody, MA), equipped with a DART ion source (IonSense, Inc., Danvers, MA) in positive ion mode.

3.5.1 Experimental Procedures

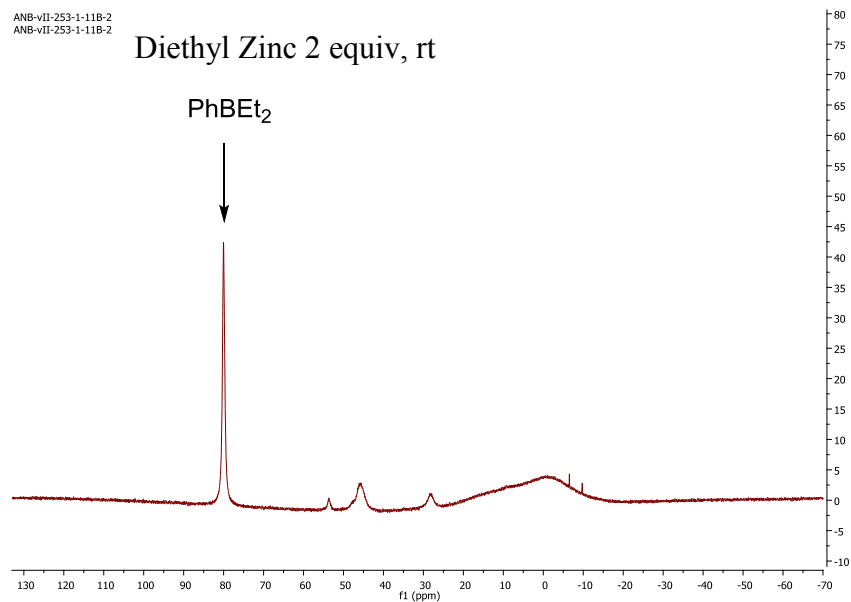
For the synthesis of 1,2-azaborine starting materials please see Appendix 1.

3.5.1.1 Qualitative *B-Cl* Bond Reactivity with Alkyl Zinc Tests (Scheme 2)

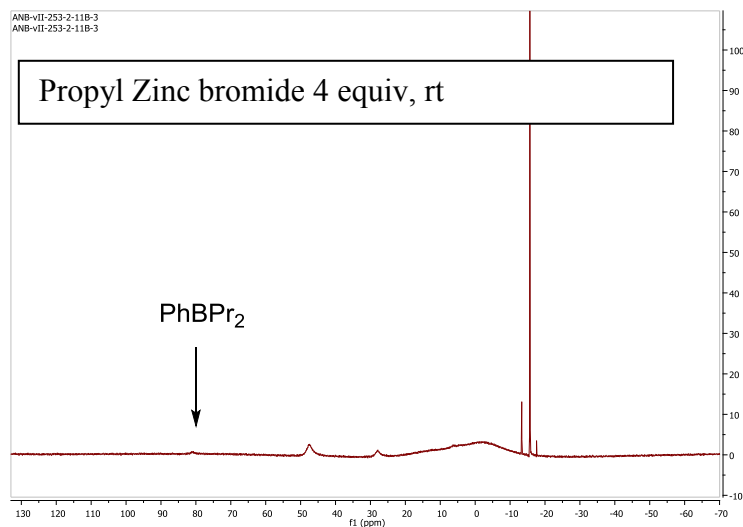
Procedure: A J-Young NMR tube was charged with 1 equiv phenylborondichloride (17.3 mg, 0.109 mmole) and 0.5 mL THF. A ^{11}B NMR was taken to establish the identity of the boron species ($\text{PhBCl}_2 \cdot \text{THF}$ [^{11}B \sim 12] with minor free PhBCl_2 [^{11}B \sim 38]). 2 equiv of the zincate was added and ^{11}B analysis after 10 minutes confirmed a reaction had taken place.

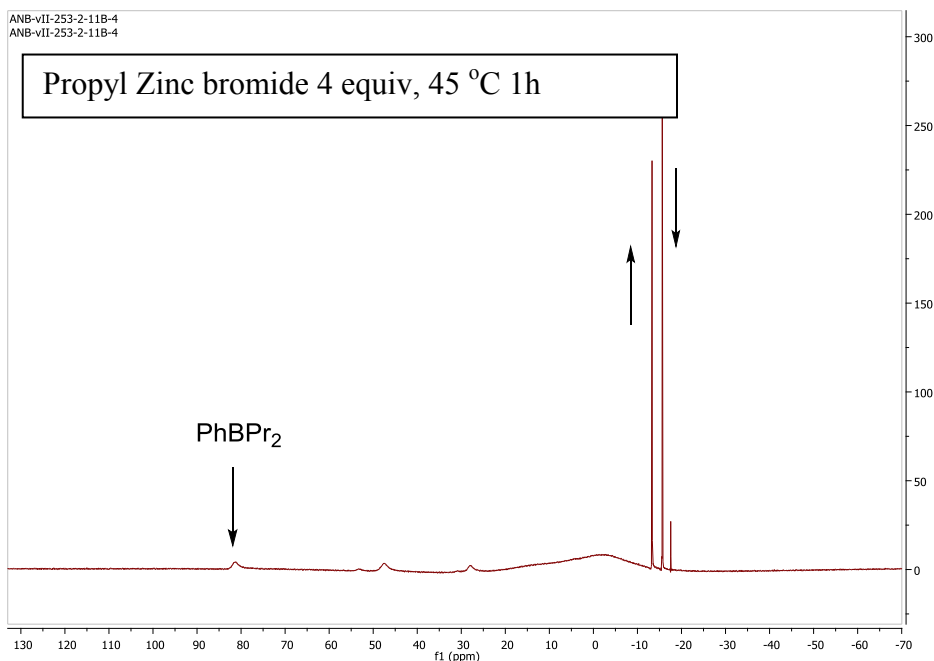
Diethyl Zinc: 0.2 mL of a 1M solution of diethyl zinc in hexanes was added. ^{11}B NMR analysis showed a major product of PhBEt_2 [^{11}B NMR \sim 80ppm]

ANB-vII-253-1-11B-2
ANB-vII-253-1-11B-2



Propylzinc bromide: 0.4 mL of a 0.5 M solution of propylzinc bromide in THF was added. ¹¹B analysis showed the generation of a 4-coordinate boron intermediate [¹¹B NMR ~ -15 ppm) in addition to PhBEtCl [¹¹B NMR ~ 44 ppm]. the addition of 0.4 mL of the 0.5 M solution of propylzinc bromide at room temperature generated a larger portion of 4-coordinate boron peaks (¹¹B ~ -18ppm to -12ppm). The J-Young tube was heated to 45 °C for one hour and NMR analysis indicated minor formation of PhBPr₂.





We saw no change in the spectra of **3.70** or **3.71** upon treatment with either diethyl zinc or propylzinc bromide.

3.5.1.2 Screening of phosphine ligands for *B–H* tolerant cross-coupling (Table 3.1)

General Procedure: In a nitrogen glovebox, a 1 dram scintillation vial was charged with 250 μ L of a stock solution in THF of the following: an internal standard of undecane (286 mg : 5 mL, 14.3 mg, 0.092 mmol : 250 μ L), *N*-TBS *B–H–C3Br–azaborine* **3.70** (500 mg : 5mL, 25 mg, 0.092 mmol : 250 μ L), In cases where an additive was necessary the additive was either weighed (for solids) or added directly via microsyringe (for liquids). To this was added 1.5 equiv of PrZnBr solution (0.5 M in THF, 275 μ L) A solution of an appropriate amount of catalyst (5% loading, 0.5 mL solvent) was then added to this mixture and the mixture stirred for 20 hours sealed in the glovebox.

GC/FID comparison to a calibrated standard curve of product **3.72** versus undecane as internal standard gave the percent yields.

Entry 1: The general procedure was followed, using PdCl₂(PhCN)₂ (1.8 mg, 0.0046 mmol) as precatalyst and P^tBuPh₂ (2.1 mg, 0.0092 mmole) as ligand.. GC/FID analysis after 20 hours indicated 75% product formation.

Entry 2: The general procedure was followed, using PdCl₂(PhCN)₂ (1.8 mg, 0.0046 mmol) as precatalyst and P(cy)₂Mes (2.9 mg, 0.0092 mmole) as ligand. GC/FID analysis after 20 hours indicated 70% product formation.

Entry 3: The general procedure was followed, using PdCl₂(PhCN)₂ (1.8 mg, 0.0046 mmol) as precatalyst and P(cy)₂Ph (2.5 mg, 0.0092 mmole) as ligand. GC/FID analysis after 20 hours indicated 75% product formation.

Entry 4: The general procedure was followed, using PdCl₂(PhCN)₂ (1.8 mg, 0.0046 mmol) as precatalyst and orthobiphenylP^tBu₂ (2.8 mg, 0.0092 mmole) as ligand. GC/FID analysis after 20 hours indicated 73% product formation.

Entry 5: The general procedure was followed, using PdCl₂(PhCN)₂ (1.8 mg, 0.0046 mmol) as precatalyst and P(cy)₃ (2.6 mg, 0.0092 mmole) as ligand. GC/FID analysis after 20 hours indicated 76% product formation.

Entry 6: The general procedure was followed, using PdCl₂(PhCN)₂ (1.8 mg, 0.0046 mmol) as precatalyst and P(furyl)₃ (2.1 mg, 0.0092 mmole) as ligand. GC/FID analysis after 20 hours indicated 76% product formation.

Entry 7: The general procedure was followed, using $\text{PdCl}_2(\text{PhCN})_2$ (1.8 mg, 0.0046 mmol) as precatalyst and P^otol_3 (2.8 mg, 0.0092 mmole) as ligand. GC/FID analysis after 20 hours indicated 72% product formation.

Entry 8: The general procedure was followed, using $\text{PdCl}_2(\text{PhCN})_2$ (1.8 mg, 0.0046 mmol) as precatalyst and $\text{HP}^t\text{Bu}_3 \text{BF}_4$ (2.7 mg, 0.0092 mmole) as ligand. GC/FID analysis after 20 hours indicated 76% product formation.

Entry 9: The general procedure was followed, using $\text{PdCl}_2(\text{PhCN})_2$ (1.8 mg, 0.0046 mmol) as precatalyst and $\text{HP}^t\text{Bu}_2\text{Me} \text{BF}_4$ (2.3 mg, 0.0092 mmole) as ligand. GC/FID analysis after 20 hours indicated 76% product formation.

Entry 10: The general procedure was followed, using $\text{Pd}(\text{P}^t\text{Bu}_3)_2$ (2.4 mg, 0.0046 mmol) as catalyst. GC/FID analysis after 20 hours indicated 67% product formation.

3.5.1.3 Optimization of $\text{PdCl}_2(\text{P}^o\text{tol}_3)_2$ catalyst system (Table 3.2)

General Procedure: In a nitrogen glovebox, a 1 dram scintillation vial was charged with 250 μL of a stock solution in THF of the following: an internal standard of undecane (286 mg : 5 mL, 14.3 mg, 0.092 mmol : 250 μL), N-TBS-B-H-C3Br-azaborine **3.70** (500 mg : 5mL, 25 mg, 0.092 mmol : 250 μL), In cases where an additive was necessary the additive was either weighed (for solids) or added directly via microsyringe (for liquids). To this was added 1.5 equiv of PrZnBr solution (0.5 M in THF, 275 μL) A solution of an appropriate amount of $\text{PdCl}_2(\text{P}^o\text{tol}_3)_2$ (5% loading, 0.5 mL solvent, 3.61 mg, 0.0046 mmole) was then added to this mixture and the mixture stirred for 20 hours

sealed in the glovebox. When heating was necessary the scintillation vials were sealed with Teflon tape and allowed to react outside of a glovebox. GC/FID comparison to a calibrated standard curve of product **3.72** versus undecane as internal standard gave the percent yields.

Entry 1: The general procedure was followed using 0.5 equiv of N-methylimidazole (3.8 mg, 0.046 mmole). GC/FID analysis after 20 hours indicated 56% product formation.

Entry 2: The general procedure was followed using 1.5 equiv of N-methylimidazole (11 mg, 0.138 mmole). GC/FID analysis after 20 hours indicated 56% product formation.

Entry 3: The general procedure was followed using 0.5 equiv of dimethylacetamide (4.0 mg, 0.046 mmole). GC/FID analysis after 20 hours indicated 59% product formation.

Entry 4: The general procedure was followed using 1.5 equiv of dimethylacetamide (12 mg, 0.14 mmole). GC/FID analysis after 20 hours indicated 57% product formation.

Entry 5: The general procedure was followed using 0.5 equiv of dimethylformamide (3.4 mg, 0.046 mmole). GC/FID analysis after 20 hours indicated 55% product formation.

Entry 6: The general procedure was followed using 1.5 equiv of dimethylformamide (10 mg, 0.14 mmole). GC/FID analysis after 20 hours indicated 58% product formation.

Entry 7: The general procedure was followed using 0.5 equiv of triethylamine (4.7 mg, 0.046 mmole). GC/FID analysis after 20 hours indicated 62% product formation.

Entry 8: The general procedure was followed using 1.5 equiv of triethylamine (14 mg, 0.14 mmole). GC/FID analysis after 20 hours indicated 61% product formation.

Entry 9: The general procedure was followed using 0.5 equiv of 2,6-lutidine (4.9 mg, 0.046 mmole). GC/FID analysis after 20 hours indicated 61% product formation.

Entry 10: The general procedure was followed using 1.5 equiv of 2,6-lutidine (15 mg, 0.14 mmole). GC/FID analysis after 20 hours indicated 62% product formation.

Entry 11: The general procedure was followed using 0.5 equiv of LiBr (4.0 mg, 0.046 mmole). GC/FID analysis after 20 hours indicated 73% product formation.

Entry 12: The general procedure was followed using 1.5 equiv of LiBr (12 mg, 0.14 mmole). GC/FID analysis after 20 hours indicated 76% product formation.

Entry 13: The general procedure was followed using diethyl ether as a 1:1 cosolvent. GC/FID analysis after 20 hours indicated 62% product formation.

Entry 14: The general procedure was followed using dimethylformamide as a 1:1 cosolvent. GC/FID analysis after 20 hours indicated 44% product formation.

Entry 15: The general procedure was followed using dimethylacetamide as a 1:1 cosolvent. GC/FID analysis after 20 hours indicated 48% product formation.

Entry 16: The general procedure was followed using N-methylimidazole as a 1:1 cosolvent. GC/FID analysis after 20 hours indicated 5% product formation.

Entry 17: The general procedure was followed using toluene as a 1:1 cosolvent. GC/FID analysis after 20 hours indicated 61% product formation.

Entry 18: The general procedure was followed using dimethoxyethane as a 1:1 cosolvent. GC/FID analysis after 20 hours indicated 26% product formation.

Entry 19: The general procedure was followed using pentane as a 1:1 cosolvent. GC/FID analysis after 20 hours indicated 46% product formation.

Entry 20: The general procedure was followed using acetonitrile as a 1:1 cosolvent. GC/FID analysis after 20 hours indicated 46% product formation.

Entry 21: The general procedure was followed with the following modification: reaction temperature = 50 °C. reaction time = 1 h GC/FID analysis after 20 hours indicated 75% product formation.

Entry 22: The general procedure was followed with the following modification: reaction temperature = 50 °C. reaction time = 3 h GC/FID analysis after 20 hours indicated 74% product formation.

Entry 23: The general procedure was followed with the following modification: reaction temperature = 50 °C. reaction time = 1.5 h Zincate Equivalents = 1.1 GC/FID analysis after 20 hours indicated 64% product formation.

Entry 24: The general procedure was followed with the following modification: reaction temperature = 50 °C. reaction time = 1.5 h Zincate Equivalents = 2 GC/FID analysis after 20 hours indicated 63% product formation.

Entry 25: The general procedure was followed with the following modification: reaction temperature = 50 °C. reaction time = 1.5 h Zincate Equivalents = 5 GC/FID analysis after 20 hours indicated 52% product formation.

Entry 26: The general procedure was followed with the following modification: reaction temperature = 50 °C. reaction time = 1.5 h 2,6-lutidine was used as a 1:1 cosolvent. GC/FID analysis after 20 hours indicated 51% product formation.

Entry 27: The general procedure was followed with the following modification: reaction temperature = 50 °C. reaction time = 1.5 h, 1.5 equiv of LiBr (12 mg, 0.14 mmole). GC/FID analysis after 20 hours indicated 64% product formation.

Entry 28: The general procedure was followed with the following modification: reaction temperature = 50 °C. reaction time = 1.5 h, 1.5 equiv of 2,6-lutidine (15 mg, 0.14 mmole). GC/FID analysis after 20 hours indicated 71% product formation.

Entry 29: The general procedure was followed with the following modification: reaction temperature = 50 °C. reaction time = 1.5 h, 1.5 equiv of LiCl (5.8 mg, 0.14 mmole). GC/FID analysis after 20 hours indicated 61% product formation.

3.5.1.4 Preparation of C3 substituted B–H azaborines (schemes 3.21-3.22)

Procedures for coupling of R₂Zn and RZnX reagents:

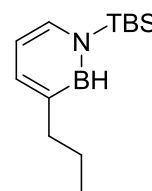
General procedure A: In a nitrogen glovebox a pressure tube equipped with a bar of stirring was charged with 1 equiv **3.70** (150 mg, 0.55 mmol) , 1.5 equiv appropriate zincate and was diluted with THF to a total volume of 5 mL. 0.05 equiv of PdCl₂(P(*o*-tol)₃)₂ (21.7 mg, 0.028 mmol) was added in one portion and the system was sealed and allowed to react at 50 °C for 1.5 hours. The crude reaction mixture was passed through a dry plug of silica (eluent: Et₂O) and the solvent was removed. The product was isolated by silica gel chromatography.

General Procedure B: In a nitrogen glovebox a scintillation vial equipped with a bar of stirring was charged with 1 equiv **3.70** (150 mg, 0.55 mmol) , 1.5 equiv appropriate zincate and was diluted with THF to a total volume of 5 mL. 0.05 equiv of Pd(P(*t*-Bu)₃)₂

(14 mg, 0.028 mmol) was added in one portion and the system was sealed and allowed to react at room temperature for 24 hours. Upon completion the crude reaction mixture was passed through a dry pipette plug of silica (1.5 mL silica, eluent: Et₂O) and the solvent was removed. The crude mixture was stirred over CH₂Cl₂ for 1.5 hours before being passed through another dry plug of silica to provide the desired product (often analytically pure). Any additional required workup is detailed in the specific following entry.

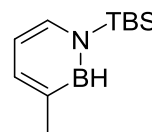
Compound 3.72:

General procedure **A** was followed using 1.5 equiv of a 0.5 M solution of propylzinc bromide (1.7 mL, 0.830 mmol), after the initial plug the solvent was blown down carefully with a stream of nitrogen and a pentane dry-silica plug was run in a pipette (1.5 mL silica, eluent: pentane). Solvent removal yielded volatile compound **3.72** (116 mg, 89% yield, a second run gave 105 mg, 81% yield). ¹H NMR (500 MHz, CD₂Cl₂) δ 7.32 (t, *J* = 10.5 Hz, 1H), 7.24 (d, *J* = 6.5 Hz, 1H), 6.36 (t, *J* = 6.6 Hz, 1H), 2.55 – 2.49 (m, 2H), 1.59 (dq, *J* = 14.6, 7.2 Hz, 2H), 1.06 – 0.82 (m, 12H), 0.47 (s, 6H). ¹¹B NMR (160 MHz, CD₂Cl₂) δ 34.7 (D, *J* = 108 Hz). ¹³C NMR (126 MHz, CD₂Cl₂) δ 140.8, 135.5, 112.5, 39.5, 26.4, 26.0, 18.4, 14.4, -3.9. The quaternary carbon adjacent to boron was not observed. FTIR (ATR): $\tilde{\nu}$ = 2955, 2503 (BH), 1603, 1519, 1463, 1372, 1258, 1147, 998, 828, 805, 782, 695, 616, 400. HRMS (DART+) calculated for C₁₃H₂₇BNSi (M+1): 236.20058; found: 236.19986.



Compound 3.73:

General procedure **A** was followed using 1.5 equiv of a 1.0 M solution of dimethylzinc (0.830 mL, 0.830 mmol), after the initial plug the solvent was

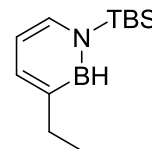


as carefully removed under a stream of nitrogen and an dry-silica plug was

run in a pipette (1.5 mL silica, eluent: pentane). Careful solvent removal under a stream of nitrogen yielded volatile compound **3.73** (95.2 mg, 83% yield, a second run gave 88.6 mg, 78% yield). ^1H NMR (500 MHz, CD_2Cl_2) δ 7.37 (d, $J = 5.8$ Hz, 1H), 7.22 (d, $J = 6.4$ Hz, 1H), 6.35 (t, $J = 6.6$ Hz, 1H), 2.27 (s, 3H), 0.92 (s, 9H), 0.47 (s, 6H). ^{11}B NMR (160 MHz, CD_2Cl_2) δ 34.7 (d, $J = 115.7$ Hz). ^{13}C NMR (126 MHz, CD_2Cl_2) δ 141.2, 135.2, 112.5, 26.4, 22.3, 18.5, -3.9. The quaternary carbon adjacent to boron was not observed. FTIR (ATR): $\tilde{\nu} = 2929, 2857, 2510$ (BH), 1604, 1520, 1470, 1360, 1257, 1172, 1144, 1005, 826, 780, 762, 695, 616. HRMS (DART+) calculated for $\text{C}_{11}\text{H}_{23}\text{BNSi}$ (M+1): 208.16928; found: 208.16897.

Compound 3.74:

General procedure **A** was followed using 1.5 equiv of a 1.0 M solution of diethylzinc (0.830 mL, 0.830 mmol), after the initial plug the solvent was



carefully removed under a stream of nitrogen and a dry-silica plug was run

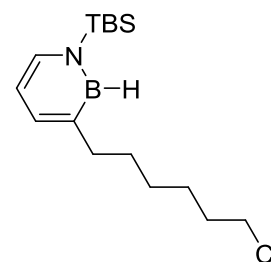
in a pipette (1.5 mL silica, eluent pentane). Careful solvent removal under a stream of nitrogen yielded volatile compound **3.74** (93.7 mg, 77% yield, a second run gave 85.6 mg, 70% yield). ^1H NMR (500 MHz, CD_2Cl_2) δ 7.35 (d, $J = 6.5$ Hz, 1H), 7.24 (d, $J = 6.5$

Hz, 1H), 6.37 (t, $J = 6.6$ Hz, 1H), 2.58 (q, $J = 7.5$ Hz, 2H), 1.19 (t, $J = 7.6$ Hz, 3H), 0.92 (s, 9H), 0.48 (s, 6H). ^{11}B NMR (160 MHz, CD_2Cl_2) δ 34.6 (d, $J = 115.0$ Hz). ^{13}C NMR (126 MHz, CD_2Cl_2) δ 139.9, 135.5, 112.5, 30.1, 26.4, 18.4, 17.0, -3.9. The quaternary carbon adjacent to boron was not observed. FTIR (ATR): $\tilde{\nu} = 2956, 2928, 2885, 2857, 2505$ (BH), 1603, 1519, 1470, 1463, 1390, 1372, 1363, 1271, 1257, 1236, 1172, 1148, 1033, 999, 940, 856, 824, 794, 778, 735, 694, 660, 616, 409.

HRMS (DART+) calculated for $\text{C}_{12}\text{H}_{25}\text{BNSi}$ (M+1): 222.18493; found: 222.18578.

Compound 3.75:

General procedure **B** was followed using 1.5 equiv of a 0.5 M solution of 6-chloro hexylzincbromide (1.7 mL, 0.830 mmol), after the initial plug the product was isolated via recycling preparative HPLC equipped with a Jaigel polystyrene size

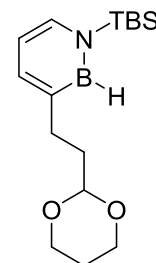


exclusion column (eluent: Toluene) solvent removal yielded compound **3.75**. (111 mg, 64% yield, a second run gave 110 mg, 64% yield). ^1H NMR (600 MHz, CD_2Cl_2) δ 7.29 (d, $J = 6.5$ Hz, 1H), 7.19 (d, $J = 6.5$ Hz, 1H), 6.32 (t, $J = 6.5$ Hz, 1H), 3.53 (t, $J = 6.8$ Hz, 2H), 2.56 – 2.45 (m, 2H), 1.82 – 1.72 (m, 2H), 1.55 (dt, $J = 15.3, 7.6$ Hz, 2H), 1.49 – 1.41 (m, 2H), 1.39 – 1.31 (m, 2H), 0.86 (s, 9H), 0.43 (s, 6H). ^{11}B NMR (160 MHz, CD_2Cl_2) δ 34.5. δ ^{13}C NMR (126 MHz, CD_2Cl_2) δ 140.8, 135.5, 112.5, 45.9, 37.1, 33.3, 32.8, 29.3, 27.4, 26.4, 18.4, -3.9. The quaternary carbon adjacent to boron was not observed. FTIR (ATR): $\tilde{\nu} = 2954, 2927, 2855, 2503$ (BH), 1603, 1517, 1470, 1463, 1371, 1363, 1310,

1271, 1258, 1172, 1149, 1000, 938, 836, 808, 782, 769, 696, 660, 617, 410. HRMS (DART+) calculated for C₁₆H₃₂BClNSi (M+1): 312.20856; found: 312.20901.

Compound 3.76:

General procedure **B** was followed using 1.5 equiv of a 0.5 M solution of the zincate shown (1.7 mL, 0.830 mmol), after the initial plug the product was isolated via recycling preparative HPLC equipped with a Jaigel polystyrene size exclusion column (eluent: Toluene) removal of solvent

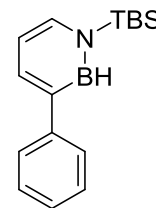


yielded compound **3.76** (101 mg, 60% yield, a second run gave 113 mg, 67% yield). ¹H NMR (500 MHz, CD₂Cl₂) δ 7.33 (d, *J* = 6.5 Hz, 1H), 7.22 (d, *J* = 6.4 Hz, 1H), 6.34 (t, *J* = 6.6 Hz, 1H), 4.53 (t, *J* = 5.2 Hz, 1H), 4.11 – 4.04 (m, 2H), 3.80 – 3.69 (m, 2H), 2.63 – 2.54 (m, 2H), 2.04 (dt, *J* = 17.5, 12.5, 5.0 Hz, 1H), 1.84 – 1.75 (m, 2H), 1.33 (dt, *J* = 13.4, 2.6, 1.4 Hz, 1H), 0.89 (s, 9H), 0.45 (s, 6H). ¹¹B NMR (160 MHz, CD₂Cl₂) δ 34.4. ¹³C NMR (126 MHz, CD₂Cl₂) δ 140.7, 135.5, 112.3, 102.4, 67.2, 38.1, 31.3, 26.4, 26.2, 18.2, -4.1. The quaternary carbon adjacent to boron was not observed. FTIR (ATR): $\tilde{\nu}$ = 2953, 2928, 2885, 2854, 2504(BH), 1602, 1519, 1470, 1431, 1401, 1375, 1270, 1259, 1240, 1172, 1142, 1085, 1029, 998, 971, 958, 924, 884, 832, 806, 783, 697, 662, 617, 423, 409. HRMS (DART+) calculated for C₁₆H₃₁BNO₂Si (M+1): 308.22171; found: 308.22158.

Compound 3.77:

General procedure **B** was followed using 1.5 equiv of a 0.5 M solution of *p*-phenylzincbromide (1.7 mL, 0.830 mmol), after the initial plug the solvent was switched

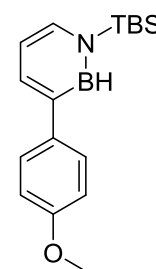
to CH₂Cl₂ and the mixture was allowed to stir for 1.5 hours before being passed through a dry silica plug (30 mL silica, eluent: CH₂Cl₂). Removal of solvent yielded off-white crystalline compound **3.77**. (102.1 mg, 69% yield, a second run gave 112.6 mg, 76% yield).



¹H NMR (400 MHz, CD₂Cl₂) δ 7.78 (d, *J* = 7.0 Hz, 1H), 7.63 – 7.57 (m, 2H), 7.42 – 7.33 (m, 3H), 7.25 – 7.18 (m, 1H), 6.57 – 6.50 (m, 1H), 0.91 (s, 9H), 0.49 (s, 6H). ¹¹B NMR (160 MHz, CD₂Cl₂) δ 33.8. ¹³C NMR (126 MHz, CD₂Cl₂) δ 143.5, 140.1, 138.2, 132.1, 128.9, 128.7, 113.1, 26.4, 18.4, -3.9. The quaternary carbon adjacent to boron was not observed. FTIR (ATR): $\tilde{\nu}$ = 2953, 2928, 2884, 2857, 2522 (BH), 1594, 1516, 1490, 1470, 1391, 1350, 1327, 1303, 1283, 1255, 1207, 1155, 1009, 944, 906, 857, 837, 822, 811, 786, 752, 737, 694, 662, 613, 602, 542, 410. HRMS (DART+) calculated for C₁₆H₂₅BNSi (M+1): 270.18493; found: 270.18420.

Compound 3.78:

General procedure **B** was followed using 1.5 equiv of a 0.5 M solution of 4-methoxyphenyl)zinc bromide (1.7 mL, 0.830 mmol), after the initial plug the solvent was switched to CH₂Cl₂ and the mixture was allowed to stir for 1.5 hours before being passed through a dry silica plug (30 mL

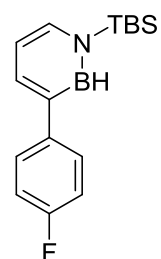


silica, eluent: CH₂Cl₂) **3.78**. (130.5 mg, 79% yield, a second run gave 115.2 mg, 70% yield). ¹H NMR (500 MHz, CD₂Cl₂) δ 7.78 (d, *J* = 6.9 Hz, 1H), 7.60 (d, *J* = 8.9 Hz, 2H), 7.40 (d, *J* = 6.3 Hz, 1H), 6.97 (d, *J* = 8.9 Hz, 2H), 6.55 (t, *J* = 6.7 Hz, 1H), 3.86 (s, 3H), 0.96 (s, 9H), 0.54 (s, 6H). ¹¹B NMR (160 MHz, CD₂Cl₂) δ 34.2. ¹³C NMR (126 MHz, CD₂Cl₂) δ 158.9, 138.9, 137.4, 136.9, 128.3, 114.5, 113.1, 55.8, 26.4, 18.5, -3.9.

The quaternary carbon adjacent to boron was not observed. FTIR (ATR): $\tilde{\nu}$ = 2956, 2931, 2856, 2526 (BH), 1597, 1516, 1505, 1469, 1440, 1344, 1307, 1285, 1275, 1241, 1207, 1178, 1153, 1111, 1088, 1034, 1013, 1002, 939, 870, 858, 839, 821, 811, 781, 773, 732, 694, 682, 658, 635, 614, 561, 545, 405. HRMS (DART+) calculated for C₁₉H₂₇BNOSi (M+1): 300.19550; found: 300.19536.

Compound 3.79:

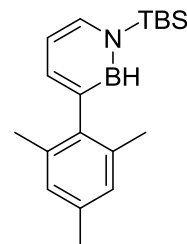
General procedure **B** was followed using 1.5 equiv of a 0.5 M solution of 4-fluoro phenylzincbromide (1.7 mL, 0.830 mmol), after the initial plug the solvent was switched to CH₂Cl₂ and the mixture was allowed to stir for 1.5 hours before being passed through a dry silica plug (30 mL silica, eluent:



CH₂Cl₂). Removal of solvent yielded white crystalline **3.79**. (87.7 mg, 55% yield a second run gave 90.9 mg, 57% yield). ¹H NMR (500 MHz, CD₂Cl₂) δ 7.74 (d, *J* = 7.0 Hz, 1H), 7.64 – 7.48 (m, 2H), 7.39 (d, *J* = 6.3 Hz, 1H), 7.06 (t, *J* = 8.7 Hz, 2H), 6.52 (t, *J* = 6.7 Hz, 1H), 0.91 (s, 9H), 0.49 (s, 6H). ¹¹B NMR (160 MHz, CD₂Cl₂) δ 34.2. ¹³C NMR (151 MHz, CD₂Cl₂) δ 161.7 (d, *J*_{CF} = 243.5 Hz), 140.4, 139.2, 137.1, 128.2 (d, *J*_{CF} = 7.7 Hz), 114.9 (d, *J*_{CF} = 21.2 Hz), 112.4, 25.8, 17.8, -4.5. The quaternary carbon adjacent to boron was not observed. FTIR (ATR): $\tilde{\nu}$ = 2954, 2929, 2884, 2858, 2522 (BH), 1600, 1558, 1540, 1519, 1505, 1489, 1471, 1458, 1417, 1395, 1362, 1340, 1295, 1284, 1257, 1222, 1157, 1009, 945, 861, 827, 809, 785, 776, 740, 688, 614, 547, 417, 409. HRMS (DART+) calculated for C₁₆H₂₄BFNSi (M+1): 288.17551; found: 288.17497.

Compound 3.80:

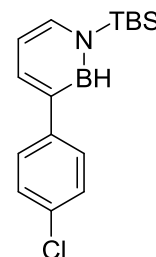
General procedure **B** was followed with the following modifications: 48h reaction time with 2.5 equiv of a 0.5 M solution of mesitylzinc iodide (2.8 mL, 1.4 mmol). The product was purified via silica gel chromatography (eluent: pentane). Removal of solvent yielded



compound **3.80** (132.7 mg, 74% yield a second run gave 132.9 mg, 74% yield). ^1H NMR (500 MHz, CD_2Cl_2) δ 7.39 (d, J = 6.4 Hz, 1H), 7.30 (d, J = 6.6 Hz, 1H), 6.93 (s, 2H), 6.54 (dd, J = 8.2, 5.0 Hz, 1H), 2.31 (s, 3H), 2.04 (s, 6H), 0.92 (s, 9H), 0.49 (s, 6H). ^{11}B NMR (160 MHz, CD_2Cl_2) δ 33.9. ^{13}C NMR (126 MHz, CD_2Cl_2) δ 142.1, 141.7, 135.8, 134.7, 134.6, 127.8, 112.2, 25.8, 21.2, 20.6, 17.9, -4.6. The quaternary carbon adjacent to boron was not observed. FTIR (ATR): $\tilde{\nu}$ = 2953, 2928, 2857, 2516, 1598, 1558, 1540, 1519, 1470, 1406, 1373, 1362, 1339, 1286, 1255, 1204, 1147, 1115, 1074, 1006, 937, 858, 837, 822, 810, 785, 750, 736, 709, 686, 656, 619, 577, 410. HRMS (DART+) calculated for $\text{C}_{19}\text{H}_{31}\text{BNSi}$ ($\text{M}+1$): 312.23188; found: 312.23217.

Compound 3.81:

General procedure **B** was followed using 1.5 equiv of a 0.5 M solution of 4-chloro-phenylzinc iodide (1.7 mL, 0.830 mmol), after the initial plug the solvent was switched to CH_2Cl_2 and the mixture was allowed to stir for 1.5 hours before being passed through a dry silica plug (30 mL silica, eluent:

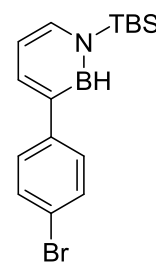


CH_2Cl_2). Removal of solvent yielded compound **3.81**. (149.9 mg, 89% yield, a second run gave 147.7 mg, 88% yield). ^1H NMR (500 MHz, CD_2Cl_2) δ 7.82 (d, J = 6.9 Hz,

1H), 7.64 – 7.57 (m, 2H), 7.46 (t, $J = 7.1$ Hz, 1H), 7.41 – 7.34 (m, 2H), 6.58 (t, $J = 6.7$ Hz, 1H), 0.95 (s, 9H), 0.53 (s, 6H). ^{11}B NMR (160 MHz, CD_2Cl_2) δ 34.2. ^{13}C NMR (126 MHz, CD_2Cl_2) δ 143.5, 140.1, 138.2, 132.1, 128.9, 128.7, 113.1, 26.4, 18.4, -3.9. The quaternary carbon adjacent to boron was not observed. FTIR (ATR): $\tilde{\nu} = 2954, 2928, 2884, 2855, 2517$ (BH), 1593, 1515, 1489, 1480, 1461, 1444, 1405, 1361, 1337, 1297, 1283, 1252, 1206, 1154, 1083, 1003, 942, 859, 838, 822, 810, 783, 716, 702, 671, 645, 632, 614, 572, 540, 488, 467, 426, 407. HRMS (DART+) calculated for $\text{C}_{16}\text{H}_{24}\text{BCINSi}$ (M+1): 304.14596; found: 304.14596.

Compound 3.82:

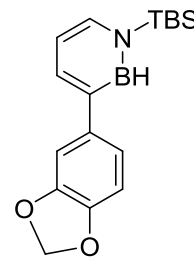
General procedure **B** was followed using 1.5 equiv of a 0.5 M solution of 4-bromo phenylzinc iodide (1.7 mL, 0.830 mmol), after the initial plug the product was isolated via recycling preparative HPLC equipped with a Jaigel polystyrene size exclusion column (eluent: Toluene) removal of solvent



yielded off-white crystalline **3.82**. (111 mg, 58% yield, a second run gave 107 mg, 56% yield). ^1H NMR (500 MHz, CD_2Cl_2) δ 7.77 (d, $J = 7.0$ Hz, 1H), 7.52 – 7.46 (m, 4H), 7.42 (d, $J = 6.4$ Hz, 1H), 6.53 (t, $J = 6.7$ Hz, 1H), 0.90 (s, 9H), 0.49 (s, 6H). ^{11}B NMR (160 MHz, CD_2Cl_2) δ 34.0. ^{13}C NMR (126 MHz, CD_2Cl_2) δ 143.9, 140.2, 138.3, 131.9, 129.2, 120.3, 113.2, 26.4, 18.5, -3.9. The quaternary carbon adjacent to boron was not observed. FTIR (ATR): $\tilde{\nu} = 2953, 2928, 2884, 2857, 2521$ (BH), 1596, 1517, 1487, 1470, 1361, 1338, 1282, 1258, 1207, 1156, 1070, 1004, 945, 860, 838, 821, 811, 787, 774, 699, 667, 613, 538, 416, 407. HRMS (DART+) calculated for $\text{C}_{16}\text{H}_{24}\text{BBrNSi}$ (M+1): 348.09544; found: 348.09466.

Compound 3.83:

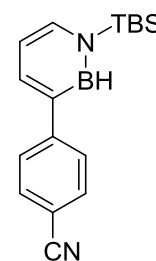
General procedure **B** was followed using 1.5 equiv of a 0.5 M solution of 2,3-methylenedioxyphenylzinc iodide (1.7 mL, 0.830 mmol), after the initial plug the solvent was switched to CH₂Cl₂ and the mixture was allowed to stir for 1.5 hours before being passed through a dry silica



pipette plug (eluent: CH₂Cl₂) removal of solvent yielded compound **4I**. (169.7 mg, 98% yield, a second run gave 161.4 mg, 93% yield). Crystals suitable for x-ray diffraction were grown by slow evaporation from CH₂Cl₂. ¹H NMR (500 MHz, CD₂Cl₂) δ 7.75 (dd, *J* = 6.9, 0.9 Hz, 1H), 7.40 (d, *J* = 6.3 Hz, 1H), 7.19 – 7.12 (m, 2H), 6.88 (d, *J* = 8.0 Hz, 1H), 6.55 (t, *J* = 6.7 Hz, 1H), 6.00 (s, 2H), 0.95 (s, 9H), 0.53 (s, 6H). ¹¹B NMR (160 MHz, CD₂Cl₂) δ 34.0. ¹³C NMR (126 MHz, CD₂Cl₂) δ 148.6, 146.6, 139.3, 139.2, 137.3, 120.6, 113.0, 108.8, 107.8, 101.6, 26.4, 18.5, 1.4. The quaternary carbon adjacent to boron was not observed. FTIR (ATR): $\tilde{\nu}$ = 2951, 2927, 2883, 2855, 2520 (BH), 1596, 1516, 1497, 1480, 1469, 1427, 1408, 1387, 1363, 1316, 1291, 1268, 1255, 1224, 1162, 1141, 1117, 1103, 1038, 1011, 994, 963, 947, 933, 889, 864, 853, 87, 809, 788, 775, 752, 723, 717, 691, 662, 627, 613, 571, 555, 503, 453, 423, 408. HRMS (DART+) calculated for C₁₇H₂₅BNO₂Si (M+1): 314.17476; found: 314.17412.

Compound 3.84:

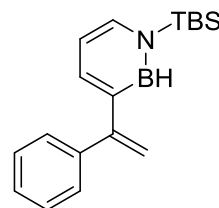
General procedure **B** was followed using 1.5 equiv of a 0.5 M solution of (4-cyanophenyl)zinc bromide (1.7 mL, 0.830 mmol), after the initial plug the solvent was switched to CH₂Cl₂ and the mixture was allowed to stir



for 1.5 hours before being passed through a dry pipette plug (30 mL silica, eluent: CH₂Cl₂) removal of solvent yielded compound **3.84** as a crystalline solid. (151.3 mg, 93% yield, a second run gave 143.4 mg, 88% yield). ¹H NMR (500 MHz, CD₂Cl₂) δ 7.89 (dd, *J* = 6.2, 0.9 Hz, 1H), 7.76 (d, *J* = 8.6 Hz, 2H), 7.69 (d, *J* = 8.6 Hz, 2H), 7.52 (d, *J* = 6.4 Hz, 1H), 6.69 – 6.56 (m, 1H), 0.95 (s, 9H), 0.54 (s, 6H). ¹¹B NMR (160 MHz, CD₂Cl₂) δ 34.1. ¹³C NMR (126 MHz, CD₂Cl₂) δ 149.7, 141.4, 139.5, 132.8, 127.9, 120.0, 113.2, 109.6, 26.3, 18.4, -3.9. The quaternary carbon adjacent to boron was not observed. FTIR (ATR): $\tilde{\nu}$ = 2967, 2952, 2932, 2856, 2523 (BH), 2224 (CN), 1590, 1514, 1464, 1444, 1361, 1343, 1301, 1285, 1251, 1221, 1207, 1178, 1155, 1111, 1003, 945, 874, 861, 833, 822, 811, 784, 733, 719, 684, 653, 613, 563, 508, 425, 408. HRMS (DART+) calculated for C₁₇H₂₄BN₂Si (M+1): 295.18018; found: 295.18067.

Compound 3.85:

General procedure **B** was followed using 1.5 equiv of a 0.5 M solution of (1-phenylvinyl)zinc bromide (1.7 mL, 0.830 mmol), after the initial

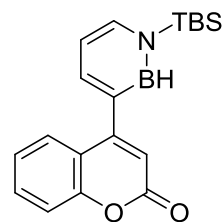


plug the solvent was switched to CH₂Cl₂ and the mixture was allowed to stir for 1.5 hours before being passed through a dry silica plug (30 mL silica, eluent: CH₂Cl₂). Solvent removal yielded compound **3.85** as a colorless oil (153.7 mg, 94% yield, a second run gave 153.8 mg, 94% yield). ¹H NMR (500 MHz, CD₂Cl₂) δ 7.56 – 7.18 (m, 7H), 6.44 (dd, *J* = 8.3, 5.0 Hz, 1H), 5.50 (d, *J* = 1.9 Hz, 1H), 5.31 (d, *J* = 1.9 Hz, 1H), 0.93 (s, 9H), 0.49 (s, 6H). ¹¹B NMR (192 MHz, CD₂Cl₂) δ 34.1 ¹³C NMR (126 MHz, CD₂Cl₂) δ 153.8, 143.6, 141.7, 137.8, 128.8, 128.5, 127.7, 112.6, 112.4, 26.4, 18.5, -3.9. The quaternary carbon adjacent to boron was not observed. FTIR (ATR): $\tilde{\nu}$ = 2953,

2928, 2883, 2857, 2529 (BH), 1600, 1510, 1491, 1470, 1443, 1391, 1361, 1339, 1259, 1220, 1160, 1122, 1057, 1026, 1000, 954, 885, 860, 837, 821, 808, 776, 695, 662, 615, 581, 411. HRMS (DART+) calculated for C₁₈H₂₇BNSi (M+1): 296.20058; found: 296.20012.

Compound 3.86:

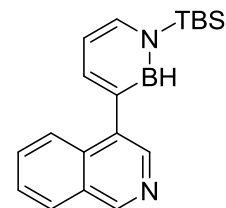
General procedure **B** was followed using 1.5 equiv of a 0.5 M solution of (2-oxo-2H-chromen-4-yl)zinc bromide (1.7 mL, 0.830 mmol), after the initial plug the solvent was switched to CH₂Cl₂ and the mixture was allowed to stir for 1.5 hours before being passed



through a dry silica pipette plug (eluent: CH₂Cl₂) removal of solvent yielded **3.86**. (136.8 mg, 73% yield, a second run gave 144.3 mg 77% yield). ¹H NMR (500 MHz, CD₂Cl₂) δ 7.71 (d, *J* = 7.0 Hz, 1H), 7.63 – 7.58 (m, 1H), 7.57 (d, *J* = 6.4 Hz, 1H), 7.55 – 7.49 (m, 1H), 7.35 (dd, *J* = 8.3, 0.6 Hz, 1H), 7.26 – 7.17 (m, 1H), 6.68 – 6.60 (m, 1H), 6.21 (s, *J* = 14.3 Hz, 1H), 0.92 (s, 9H), 0.49 (s, 6H). ¹¹B NMR (160 MHz, CD₂Cl₂) δ 33.6. ¹³C NMR (126 MHz, CD₂Cl₂) δ 161.5, 160.4, 154.8, 143.7, 140.6, 131.8, 128.0, 124.1, 120.4, 117.4, 113.3, 26.3, 18.5, -3.9. The quaternary carbon adjacent to boron was not observed. FTIR (ATR): $\tilde{\nu}$ = 2953, 2929, 2883, 2857, 2531 (BH), 1715 (C=O), 1652, 1635, 1621, 1605, 1557, 1541, 1516, 1488, 1470, 1451, 1398, 1365, 1337, 1274, 1251, 1227, 1207, 1177, 1151, 1135, 1119, 1101, 1034, 1000, 928, 888, 866, 828, 809, 787, 75, 708, 678, 660, 611, 526, 502, 494, 473, 454, 419, 409. HRMS (DART+) calculated for C₁₉H₂₅BNO₂Si (M+1): 338.17476; found: 338.17605.

Compound 3.87:

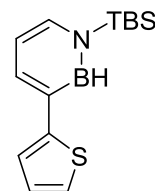
General procedure **B** was followed using 1.5 equiv of a 0.5 M solution of isoquinolin-4-ylzinc bromide (1.7 mL, 0.830 mmol),



after the initial plug the solvent was switched to CH₂Cl₂ and the mixture was allowed to stir for 1.5 hours before being passed through a dry silica pipette plug (eluent: CH₂Cl₂ (3 column volumes) followed by Et₂O (3 column volumes) to obtain product). Removal of ether yielded compound **3.87**. (155.5 mg, 87% yield, a second run gave 135.3 mg, 77% yield). ¹H NMR (500 MHz, CD₂Cl₂) δ 9.47 (s, 1H), 8.48 (s, 1H), 8.17 (d, *J* = 8.1 Hz, 1H), 8.12 (d, *J* = 8.5 Hz, 1H), 7.82 (ddd, *J* = 8.4, 6.9, 1.3 Hz, 1H), 7.73 (dd, *J* = 11.1, 4.0 Hz, 1H), 7.69 (d, *J* = 6.8 Hz, 1H), 7.56 (d, *J* = 6.0 Hz, 1H), 6.66 (t, *J* = 6.6 Hz, 1H), 0.92 (s, 9H), 0.47 (s, 6H). ¹¹B NMR (160 MHz, CD₂Cl₂) δ 34.55. ¹³C NMR (126 MHz, CD₂Cl₂) δ 150.9, 144.6, 140.7, 139.4, 139.1, 136.1, 132.9, 129.5, 129.0, 128.9, 126.2, 113.3, 26.3, 18.5, 15.7. The quaternary carbon adjacent to boron was not observed. FTIR (ATR): $\tilde{\nu}$ = 2952, 2927, 2882, 2856, 2534 (BH), 1623, 1571, 1514, 1496, 1469, 1442, 1392, 1382, 1361, 1347, 1315, 1258, 1217, 1173, 1158, 1151, 1127, 1115, 1084, 1044, 999, 978, 965, 946, 901, 861, 838, 821, 808, 789, 755, 731, 693, 666, 642, 623, 616, 592, 572, 545, 483, 475, 427, 408. HRMS (DART+) calculated for C₁₉H₂₆BN₂Si (M+1): 321.19583; found: 321.19567

Compound 3.88:

General procedure **B** was followed using 1.5 equiv of a 0.5 M solution of 2-thienyl zinc bromide (1.7 mL, 0.830 mmol). After the initial plug the



solvent was switched to CH₂Cl₂ and the mixture was allowed to stir for 1.5 hours before being passed through a dry silica plug (30 mL silica, eluent: CH₂Cl₂) yielding compound **3.88** as a yellow oil. (122.1 mg, 80%, a second run gave 136.2 mg 90% yield) ¹H NMR (500 MHz, CD₂Cl₂) δ 7.85 – 7.79 (m, 1H), 7.41 – 7.32 (m, 1H), 7.23 (d, *J* = 1.1 Hz, 1H), 7.22 (d, *J* = 1.1 Hz, 1H), 7.11 – 7.05 (m, 1H), 6.55 – 6.47 (m, 1H), 0.95 (s, *J* = 2.0 Hz, 9H), 0.53 (s, *J* = 1.6 Hz, 6H). ¹¹B NMR (160 MHz, CD₂Cl₂) δ 33.9 (br s). ¹³C NMR (151 MHz, cd₂cl₂) δ 149.4, 137.9, 137.8, 128.4, 123.9, 122.9, 113.1, 26.4, 18.5, -3.9. The quaternary carbon adjacent to boron was not observed. FTIR (ATR): $\tilde{\nu}$ = 2953, 2928, 2883, 2857, 2525 (BH), 1594, 1522, 1507, 1470, 1445, 1391, 1362, 1334, 1253, 1213, 1154, 1145, 1003, 930, 918, 855, 848, 837, 821, 810, 785, 773, 684, 659, 612, 411. HRMS (DART+) calcd for C₁₄H₂₃BNSSi (M+1): 276.14135; found: 276.14187.

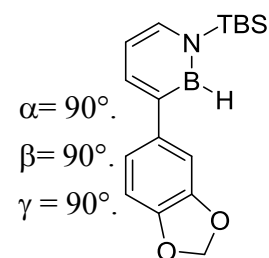
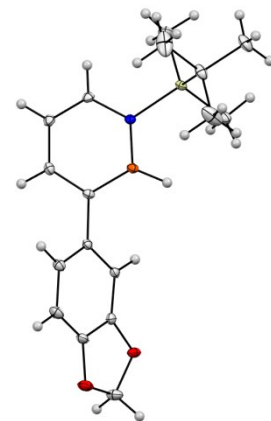
Compound 3.89:

Compound **3.89** was isolated by recycling preparative HPLC from the reaction which produced **3.82** (Scheme 3.22). (32 mg, 14% yield) ¹H NMR (500 MHz, CD₂Cl₂) δ 7.85 (d, *J* = 6.9 Hz, 1H), 7.75 – 7.66 (m, 2H), 7.64 – 7.46 (m, 6H), 7.42 (d, *J* = 5.9 Hz, 1H), 6.56 (td, *J* = 6.7, 2.1 Hz, 1H), 0.92 (d, *J* = 2.2 Hz, 9H), 0.50 (d, *J* = 2.2 Hz, 6H). ¹¹B NMR (160 MHz, CD₂Cl₂) δ 34.0.

3.5.1.5 Crystallographic data for compound 3.83

Crystal data and structure refinement for C₁₇H₂₄BNO₂Si **3.83**.

Identification code	C ₁₇ H ₂₄ BNO ₂ Si
Empirical formula	C ₁₇ H ₂₄ B N O ₂ Si
Formula weight	313.27
Temperature	100(2) K
Wavelength	0.71073 Å
Crystal system	Orthorhombic
Space group	Pna2 ₁
Unit cell dimensions	a = 20.562(3) Å b = 7.0796(10) Å c = 11.9510(17) Å
Volume	1739.7(4) Å ³
Z	4
Density (calculated)	1.196 Mg/m ³
Absorption coefficient	0.141 mm ⁻¹
F(000)	672
Crystal size	0.600 x 0.450 x 0.380 mm ³
Theta range for data collection	1.981 to 28.434°.
Index ranges	0 ≤ h ≤ 27, -9 ≤ k ≤ 9, -15 ≤ l ≤ 15
Reflections collected	8214
Independent reflections	4285 [R(int) = 0.0372]
Completeness to theta = 25.242°	100.0 %
Absorption correction	Semi-empirical from equivalents
Max. and min. transmission	0.7457 and 0.5771
Refinement method	Full-matrix least-squares on F ²
Data / restraints / parameters	4285 / 1 / 208
Goodness-of-fit on F ²	1.049
Final R indices [I > 2σ(I)]	R1 = 0.0345, wR2 = 0.0907
R indices (all data)	R1 = 0.0364, wR2 = 0.0923
Extinction coefficient	na



Largest diff. peak and hole

0.332 and -0.323 e.Å⁻³

Atomic coordinates (x 10⁴) and equivalent isotropic displacement parameters (Å²x 10³)

for C17H24BNO2Si. U(eq) is defined as one third of the trace of the orthogonalized U^{ij} tensor.

	x	y	z	U(eq)
Si(1)	7868(1)	2841(1)	6595(1)	15(1)
O(1)	4785(1)	7277(2)	3547(1)	24(1)
O(2)	4348(1)	5621(2)	2047(1)	28(1)
N(1)	7124(1)	1844(2)	6082(1)	14(1)
B(1)	6707(1)	2884(3)	5338(2)	15(1)
C(1)	6993(1)	-46(3)	6298(2)	17(1)
C(2)	6483(1)	-967(3)	5823(2)	18(1)
C(3)	6057(1)	-34(3)	5070(2)	18(1)
C(4)	6136(1)	1846(3)	4803(2)	14(1)
C(5)	5676(1)	2791(3)	4026(2)	15(1)
C(6)	5416(1)	1830(3)	3106(2)	20(1)
C(7)	4970(1)	2674(3)	2376(2)	24(1)
C(8)	4787(1)	4491(3)	2611(2)	20(1)
C(9)	4298(1)	7321(3)	2692(2)	27(1)
C(10)	5043(1)	5466(3)	3511(2)	17(1)
C(11)	5489(1)	4685(3)	4227(2)	16(1)
C(12)	7751(1)	5422(3)	6821(2)	25(1)
C(13)	8057(1)	1715(3)	7962(2)	28(1)
C(14)	8516(1)	2324(3)	5522(2)	24(1)
C(15)	8344(1)	3207(5)	4385(2)	44(1)
C(16)	8603(1)	173(4)	5400(3)	50(1)
C(17)	9168(1)	3177(4)	5913(2)	32(1)

Bond lengths [Å] and angles [°] for C₁₇H₂₄BNO₂Si.

Si(1)-N(1)	1.7937(17)
Si(1)-C(13)	1.858(2)
Si(1)-C(12)	1.863(2)
Si(1)-C(14)	1.885(2)
O(1)-C(10)	1.388(2)
O(1)-C(9)	1.430(3)
O(2)-C(8)	1.382(2)
O(2)-C(9)	1.433(3)
N(1)-C(1)	1.389(2)
N(1)-B(1)	1.438(3)
B(1)-C(4)	1.526(3)
B(1)-H(1B)	1.09(2)
C(1)-C(2)	1.360(3)
C(1)-H(1)	0.9500
C(2)-C(3)	1.419(3)
C(2)-H(2)	0.9500
C(3)-C(4)	1.378(3)
C(3)-H(3)	0.9500
C(4)-C(5)	1.485(3)
C(5)-C(6)	1.399(3)
C(5)-C(11)	1.416(3)
C(6)-C(7)	1.399(3)
C(6)-H(6)	0.9500
C(7)-C(8)	1.370(3)
C(7)-H(7)	0.9500
C(8)-C(10)	1.383(3)
C(9)-H(9A)	0.9900
C(9)-H(9B)	0.9900
C(10)-C(11)	1.371(3)
C(11)-H(11)	0.9500
C(12)-H(12A)	0.9800

C(12)-H(12B)	0.9800
C(12)-H(12C)	0.9800
C(13)-H(13A)	0.9800
C(13)-H(13B)	0.9800
C(13)-H(13C)	0.9800
C(14)-C(15)	1.537(4)
C(14)-C(16)	1.540(3)
C(14)-C(17)	1.543(3)
C(15)-H(15A)	0.9800
C(15)-H(15B)	0.9800
C(15)-H(15C)	0.9800
C(16)-H(16A)	0.9800
C(16)-H(16B)	0.9800
C(16)-H(16C)	0.9800
C(17)-H(17A)	0.9800
C(17)-H(17B)	0.9800
C(17)-H(17C)	0.9800
N(1)-Si(1)-C(13)	108.03(9)
N(1)-Si(1)-C(12)	108.99(9)
C(13)-Si(1)-C(12)	108.69(11)
N(1)-Si(1)-C(14)	107.08(9)
C(13)-Si(1)-C(14)	111.55(11)
C(12)-Si(1)-C(14)	112.37(10)
C(10)-O(1)-C(9)	105.36(16)
C(8)-O(2)-C(9)	105.67(16)
C(1)-N(1)-B(1)	119.54(16)
C(1)-N(1)-Si(1)	118.72(13)
B(1)-N(1)-Si(1)	121.24(13)
N(1)-B(1)-C(4)	118.14(17)
N(1)-B(1)-H(1B)	114.7(15)
C(4)-B(1)-H(1B)	127.0(14)
C(2)-C(1)-N(1)	122.25(17)
C(2)-C(1)-H(1)	118.9

N(1)-C(1)-H(1)	118.9
C(1)-C(2)-C(3)	121.19(17)
C(1)-C(2)-H(2)	119.4
C(3)-C(2)-H(2)	119.4
C(4)-C(3)-C(2)	121.59(18)
C(4)-C(3)-H(3)	119.2
C(2)-C(3)-H(3)	119.2
C(3)-C(4)-C(5)	120.33(17)
C(3)-C(4)-B(1)	117.27(17)
C(5)-C(4)-B(1)	122.40(16)
C(6)-C(5)-C(11)	119.41(18)
C(6)-C(5)-C(4)	121.05(17)
C(11)-C(5)-C(4)	119.53(17)
C(5)-C(6)-C(7)	122.17(19)
C(5)-C(6)-H(6)	118.9
C(7)-C(6)-H(6)	118.9
C(8)-C(7)-C(6)	116.97(19)
C(8)-C(7)-H(7)	121.5
C(6)-C(7)-H(7)	121.5
C(7)-C(8)-O(2)	128.61(19)
C(7)-C(8)-C(10)	121.57(18)
O(2)-C(8)-C(10)	109.82(18)
O(1)-C(9)-O(2)	108.47(17)
O(1)-C(9)-H(9A)	110.0
O(2)-C(9)-H(9A)	110.0
O(1)-C(9)-H(9B)	110.0
O(2)-C(9)-H(9B)	110.0
H(9A)-C(9)-H(9B)	108.4
C(11)-C(10)-C(8)	122.65(18)
C(11)-C(10)-O(1)	127.47(17)
C(8)-C(10)-O(1)	109.88(17)
C(10)-C(11)-C(5)	117.19(18)
C(10)-C(11)-H(11)	121.4
C(5)-C(11)-H(11)	121.4

Si(1)-C(12)-H(12A)	109.5
Si(1)-C(12)-H(12B)	109.5
H(12A)-C(12)-H(12B)	109.5
Si(1)-C(12)-H(12C)	109.5
H(12A)-C(12)-H(12C)	109.5
H(12B)-C(12)-H(12C)	109.5
Si(1)-C(13)-H(13A)	109.5
Si(1)-C(13)-H(13B)	109.5
H(13A)-C(13)-H(13B)	109.5
Si(1)-C(13)-H(13C)	109.5
H(13A)-C(13)-H(13C)	109.5
H(13B)-C(13)-H(13C)	109.5
C(15)-C(14)-C(16)	110.2(2)
C(15)-C(14)-C(17)	107.9(2)
C(16)-C(14)-C(17)	108.3(2)
C(15)-C(14)-Si(1)	111.10(16)
C(16)-C(14)-Si(1)	109.82(16)
C(17)-C(14)-Si(1)	109.39(16)
C(14)-C(15)-H(15A)	109.5
C(14)-C(15)-H(15B)	109.5
H(15A)-C(15)-H(15B)	109.5
C(14)-C(15)-H(15C)	109.5
H(15A)-C(15)-H(15C)	109.5
H(15B)-C(15)-H(15C)	109.5
C(14)-C(16)-H(16A)	109.5
C(14)-C(16)-H(16B)	109.5
H(16A)-C(16)-H(16B)	109.5
C(14)-C(16)-H(16C)	109.5
H(16A)-C(16)-H(16C)	109.5
H(16B)-C(16)-H(16C)	109.5
C(14)-C(17)-H(17A)	109.5
C(14)-C(17)-H(17B)	109.5
H(17A)-C(17)-H(17B)	109.5
C(14)-C(17)-H(17C)	109.5

H(17A)-C(17)-H(17C) 109.5

H(17B)-C(17)-H(17C) 109.5

Symmetry transformations used to generate equivalent atoms:

Anisotropic displacement parameters ($\text{\AA}^2 \times 10^3$) for C17H24BNO2Si. The anisotropic displacement factor exponent takes the form: $-2\pi^2 [h^2 a^{*2} U^{11} + \dots + 2 h k a^* b^* U^{12}]$

	U11	U22	U33	U23	U13	U12
Si(1)	12(1)	16(1)	15(1)	-1(1)	-2(1)	2(1)
O(1)	23(1)	19(1)	28(1)	4(1)	-9(1)	4(1)
O(2)	28(1)	29(1)	28(1)	1(1)	-15(1)	5(1)
N(1)	13(1)	14(1)	16(1)	0(1)	0(1)	2(1)
B(1)	12(1)	17(1)	16(1)	0(1)	0(1)	1(1)
C(1)	16(1)	15(1)	20(1)	2(1)	1(1)	4(1)
C(2)	18(1)	14(1)	23(1)	1(1)	1(1)	1(1)
C(3)	14(1)	19(1)	20(1)	-3(1)	1(1)	-2(1)
C(4)	12(1)	18(1)	14(1)	0(1)	-1(1)	2(1)
C(5)	11(1)	18(1)	16(1)	2(1)	-1(1)	-1(1)
C(6)	18(1)	21(1)	21(1)	-3(1)	-2(1)	0(1)
C(7)	23(1)	29(1)	20(1)	-4(1)	-7(1)	-1(1)
C(8)	15(1)	26(1)	18(1)	4(1)	-5(1)	0(1)
C(9)	26(1)	31(1)	26(1)	4(1)	-8(1)	8(1)
C(10)	14(1)	17(1)	19(1)	3(1)	0(1)	-2(1)
C(11)	13(1)	18(1)	16(1)	1(1)	-1(1)	-3(1)
C(12)	22(1)	21(1)	32(1)	-6(1)	-7(1)	2(1)
C(13)	28(1)	33(1)	23(1)	5(1)	-10(1)	-1(1)
C(14)	15(1)	29(1)	29(1)	-8(1)	4(1)	-1(1)
C(15)	26(1)	85(2)	21(1)	-1(1)	5(1)	-5(1)
C(16)	33(1)	37(1)	80(2)	-28(2)	28(2)	-2(1)
C(17)	15(1)	42(1)	39(1)	-8(1)	1(1)	-3(1)

Hydrogen coordinates ($\times 10^4$) and isotropic displacement parameters ($\text{\AA}^2 \times 10^3$)
for C₁₇H₂₄BNO₂Si.

	x	y	z	U(eq)
H(1B)	6859(13)	4340(30)	5180(20)	27(6)
H(1)	7270	-718	6795	20
H(2)	6411	-2259	5998	22
H(3)	5708	-721	4743	21
H(6)	5547	563	2972	24
H(7)	4802	2016	1746	28
H(9A)	4365	8435	2204	33
H(9B)	3861	7413	3034	33
H(11)	5665	5386	4834	19
H(12A)	7715	6060	6096	37
H(12B)	8124	5933	7233	37
H(12C)	7353	5632	7254	37
H(13A)	7678	1817	8457	42
H(13B)	8429	2354	8305	42
H(13C)	8162	380	7844	42
H(15A)	8309	4581	4467	66
H(15B)	7929	2696	4123	66
H(15C)	8686	2908	3842	66
H(16A)	8208	-377	5077	75
H(16B)	8683	-385	6138	75
H(16C)	8974	-87	4908	75
H(17A)	9507	2887	5363	48
H(17B)	9288	2635	6639	48
H(17C)	9123	4549	5985	48

Torsion angles [°] for C₁₇H₂₄BNO₂Si.

C(13)-Si(1)-N(1)-C(1)	-34.73(17)
C(12)-Si(1)-N(1)-C(1)	-152.66(15)
C(14)-Si(1)-N(1)-C(1)	85.55(15)
C(13)-Si(1)-N(1)-B(1)	153.38(16)
C(12)-Si(1)-N(1)-B(1)	35.44(18)
C(14)-Si(1)-N(1)-B(1)	-86.35(17)
C(1)-N(1)-B(1)-C(4)	-0.6(3)
Si(1)-N(1)-B(1)-C(4)	171.19(13)
B(1)-N(1)-C(1)-C(2)	0.5(3)
Si(1)-N(1)-C(1)-C(2)	-171.57(15)
N(1)-C(1)-C(2)-C(3)	0.3(3)
C(1)-C(2)-C(3)-C(4)	-1.0(3)
C(2)-C(3)-C(4)-C(5)	-179.08(18)
C(2)-C(3)-C(4)-B(1)	0.7(3)
N(1)-B(1)-C(4)-C(3)	0.0(3)
N(1)-B(1)-C(4)-C(5)	179.85(17)
C(3)-C(4)-C(5)-C(6)	-36.7(3)
B(1)-C(4)-C(5)-C(6)	143.5(2)
C(3)-C(4)-C(5)-C(11)	142.31(19)
B(1)-C(4)-C(5)-C(11)	-37.5(3)
C(11)-C(5)-C(6)-C(7)	-0.6(3)
C(4)-C(5)-C(6)-C(7)	178.5(2)
C(5)-C(6)-C(7)-C(8)	-1.1(3)
C(6)-C(7)-C(8)-O(2)	-178.4(2)
C(6)-C(7)-C(8)-C(10)	1.7(3)
C(9)-O(2)-C(8)-C(7)	175.4(2)
C(9)-O(2)-C(8)-C(10)	-4.6(2)
C(10)-O(1)-C(9)-O(2)	-8.9(2)
C(8)-O(2)-C(9)-O(1)	8.4(2)
C(7)-C(8)-C(10)-C(11)	-0.6(3)
O(2)-C(8)-C(10)-C(11)	179.48(18)

C(7)-C(8)-C(10)-O(1)	179.0(2)
O(2)-C(8)-C(10)-O(1)	-1.0(2)
C(9)-O(1)-C(10)-C(11)	-174.3(2)
C(9)-O(1)-C(10)-C(8)	6.1(2)
C(8)-C(10)-C(11)-C(5)	-1.1(3)
O(1)-C(10)-C(11)-C(5)	179.39(18)
C(6)-C(5)-C(11)-C(10)	1.7(3)
C(4)-C(5)-C(11)-C(10)	-177.41(17)
N(1)-Si(1)-C(14)-C(15)	60.15(19)
C(13)-Si(1)-C(14)-C(15)	178.16(18)
C(12)-Si(1)-C(14)-C(15)	-59.5(2)
N(1)-Si(1)-C(14)-C(16)	-62.0(2)
C(13)-Si(1)-C(14)-C(16)	56.0(2)
C(12)-Si(1)-C(14)-C(16)	178.31(18)
N(1)-Si(1)-C(14)-C(17)	179.21(16)
C(13)-Si(1)-C(14)-C(17)	-62.79(19)
C(12)-Si(1)-C(14)-C(17)	59.56(19)

Symmetry transformations used to generate equivalent atoms:

3.5.1.6 Survey of catalysts and solvents for the Negishi cross-coupling reaction of 1,2-azaborine **3.71** (Table 3.3).

General Procedure: In a nitrogen glovebox, a 1 dram scintillation vial was charged with 100 μ L of a stock solution in THF containing: internal standard hexamethylbenzene (28.8 mg : 3 mL; 0.96 mg, .0059 mmole : 100 μ L) and azaborine **3.71** (902.5 mg : 3 mL; 30.1 mg, 0.0981 mmole : 100 μ L). This was mixed with 1 mL of THF and additives and catalysts (0.05 equiv as noted below) followed by 0.3 mL of a 0.5 M solution of PrZnBr (1.5 equiv, 0.147 mmole) and stirred for 24 hours upon which solvent was removed under

reduced pressure. NMR analysis of the crude reaction mixtures was carried out in dry deuterated benzene. Yields were determined by the internal standard method with a calibration to the measured NMR ratio of the starting material and hexamethylbenzene in the prepared stock solution. Since the reactions were run in duplicate the reported NMR yields are the average of two yields and as such, the yields reported in table xx will not necessarily match the individual yields reported below.

Entry 1: The general procedure was followed with the following modifications: 0.05 equiv Pd(P^tBu₃)₂ (2.3 mg, 0.0049 mmole) was used as the catalyst. NMR analysis of the crude reaction mixture indicated an 89% yield. (a second run indicated an 86% yield)

Entry 2: The general procedure was followed with the following modifications: no catalyst was added. NMR analysis of the crude reaction mixture indicated no reaction.

Entry 3: The general procedure was followed with the following modifications: 0.05 equiv Pd(P^otol₃)₂Cl₂ (3.5 mg, 0.0045 mmole) was used as the catalyst. NMR analysis of the crude reaction mixture indicated a 74% yield. (a second run indicated a 76% yield)

Entry 4: The general procedure was followed with the following modifications: 0.05 equiv Xphos Pd G2 catalyst (3.5 mg, 0.0044 mmole) was used as the catalyst. NMR analysis of the crude reaction mixture indicated a 88% yield. (a second run indicated a 71% yield; this reaction was generally inconsistent with this catalyst system, potentially due to incomplete activation of the catalyst under room temperature conditions.)

Entry 5: The general procedure was followed with the following modifications: 0.05 equiv Pcy₃ Pd G2 (2.9 mg, 0.0049 mmole) and additive Pcy₃ (1.6 mg, 0.0057 mmole)

was used as the catalyst. NMR analysis of the crude reaction mixture indicated a 64% yield. (a second run indicated a 62% yield)

Entry 6: The general procedure was followed with the following modifications: 0.05 equiv NiCl₂(Pcy₃)₂ (3.6 mg, 0.0052 mmole) was used as the catalyst. NMR analysis of the crude reaction mixture indicated a 37% yield. (a second run indicated a 34% yield)

Entry 7: The general procedure was followed with the following modifications: 0.05 equiv Ni(cod)₂ (2.1 mg, 0.0076 mmole) was used as the catalyst with 0.1 equiv of terpyridine (3.0 mg, .0128 mmole) as added ligand. NMR analysis of the crude reaction mixture indicated a 30% yield. (a second run indicated a 31% yield)

Entry 8: The general procedure was followed with the following modifications: Before addition of the zincate the THF solvent was removed under high vacuum from both the stock solution of azaborine and hexamethylbenzene and PrZnBr and replaced with Et₂O. NMR analysis of the crude reaction mixture indicated an 81% yield. (a second run indicated an 89% yield)

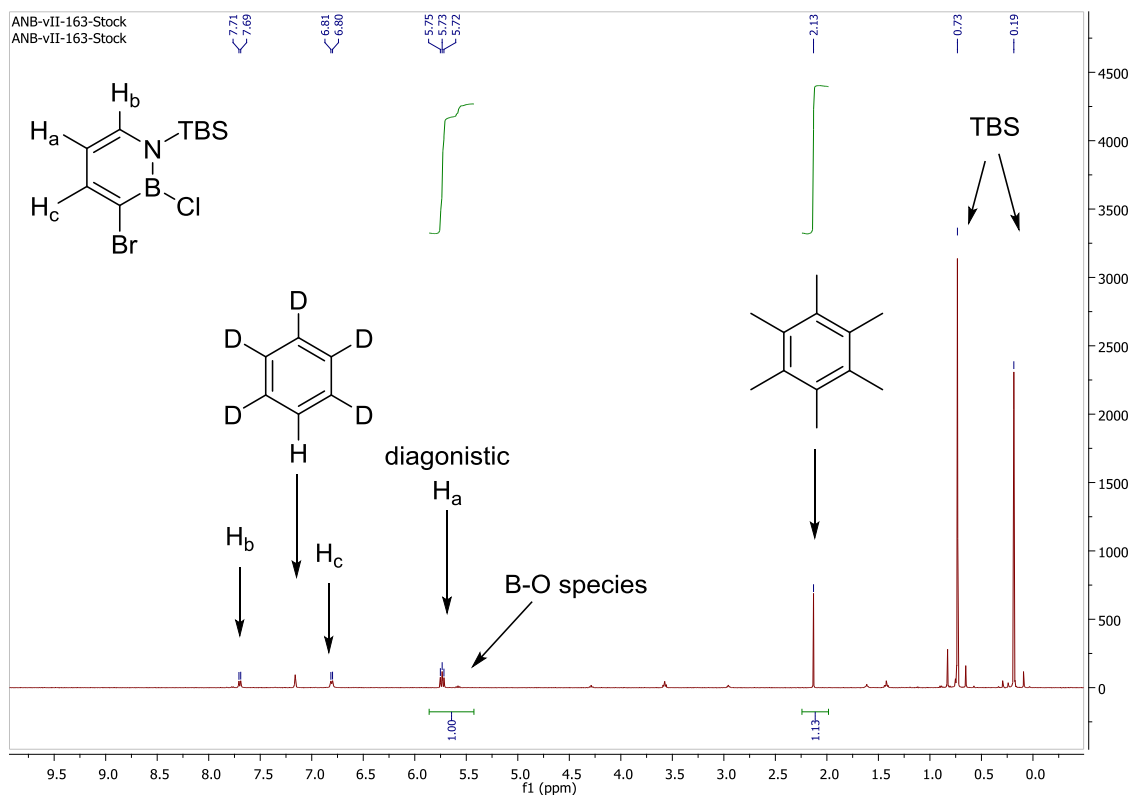
Entry 9: The general procedure was followed with the following modifications: Before addition of the zincate the THF solvent was removed from both the stock solution of azaborine and hexamethylbenzene and replaced with toluene. NMR analysis of the crude reaction mixture indicated an 84% yield. (a second run indicated a 79% yield)

Entry 10: The general procedure was followed with the following modifications: 1.2 equivalents of N-methyl- 2-pyrrolidone (12 μL, 12 mg, 0.121 mmole) was added. NMR analysis of the crude reaction mixture indicated a 42% yield. (a second run indicated a 44% yield)

Entry 11: Please see Scheme 3.23, compound **3.90**.

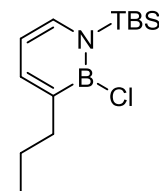
3.5.1.7 NMR yields of *B*-Cl azaborines 3.90-3.95 (Scheme 3.23)

Each stock solution was prepared and calibrated by removing the solvent under a stream of nitrogen followed by nmr analysis to obtain an initial integrative ratio of the starting azaborine **1** versus the internal standard. This ratio was used to determine the nmr yield of the products by comparing the initial ratio of azaborine **2** to internal standard to the final ratio of the C3 functionalized azaborine to internal standard. We also checked the ^{11}B nmr of each sample to verify the major product was not alkylation or B-O bond formation, which are diagnostic in the ^{11}B nmr ($\delta_{\text{alkyl}}\sim 40$, $\delta_{\text{aryl}}\sim 38$, $\delta_{\text{OR}}\sim 29$, $\delta_{\text{Cl}}\sim 35$). The nmr signal for H_a consistently shifts downfield to ~ 6.1 upon C3 substitution.

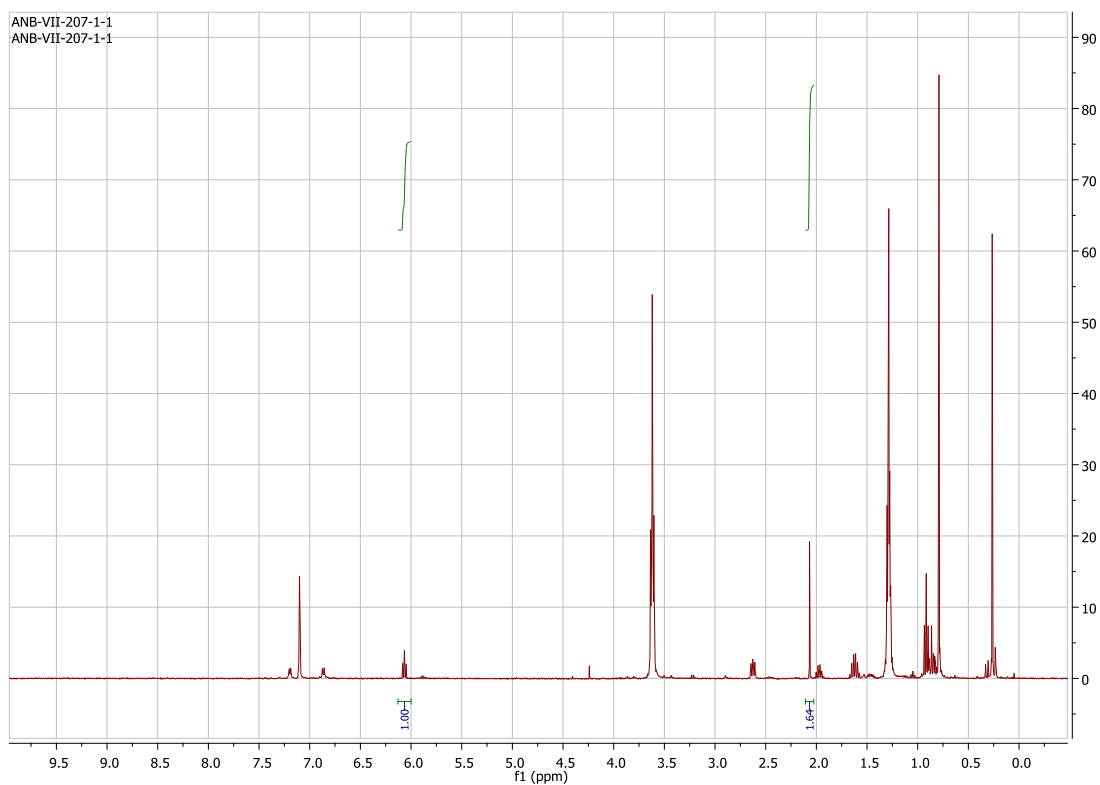


Compound 3.90:

A vial was charged with 1 mL of THF and 300 μ L of a stock solution of azaborine **3.71** (302.5 mg : 3 mL; 30.3 mg, 0.099 mmole : 300 μ L) and hexamethylbenzene (11.1 mg : 3 mL; 1.1 mg, 0.0068 mmole : 300 μ L).



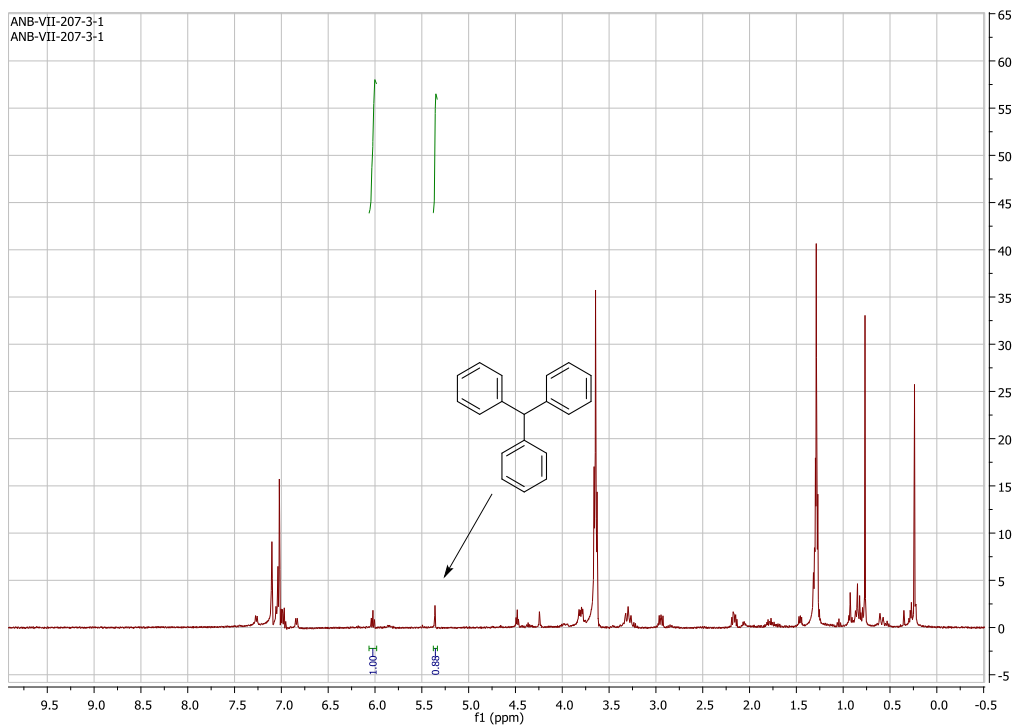
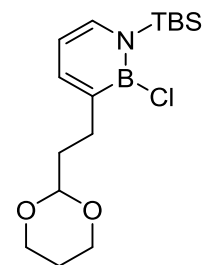
0.05 equiv of Pd(P^tBu₃)₂ (2.5 mg, 0.0050 mmole) in .5 mL of THF was added to this followed by 1.5 equiv propylzinc bromide (0.5 M solution, 0.3 mL, 0.15 mmole). The reaction was stirred for 3 hours and an aliquot was quenched with ~0.1 mL CH₂Cl₂. The solvent was removed under a stream of nitrogen and nmr analysis (stock solution integral ratio of **3.71**:internal standard = 1.00:1.41) of the crude reaction mixture indicated an 86% yield. (A second run gave an 88% yield).



Compound 3.91:

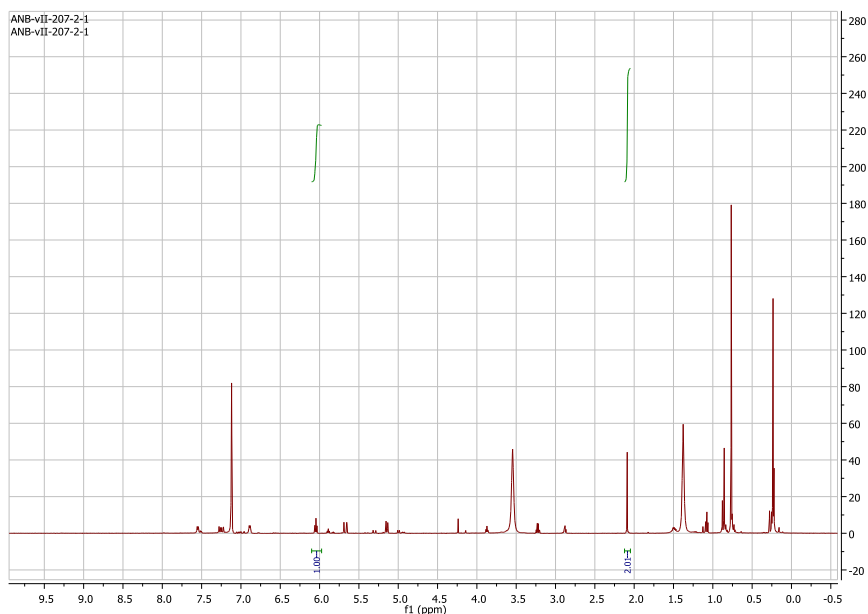
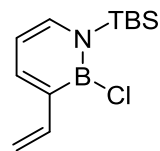
A vial was charged with 1 mL of THF and 300 μ L of a stock solution of azaborine **3.71** (302.3 mg : 3 mL; 30.2 mg, 0.099 mmole : 300 μ L) and triphenylmethane (121.1 mg : 3 mL; 12.1 mg, 0.0491 mmole : 300 μ L).

0.05 equiv of Pd(P^tBu₃)₂ (2.5 mg, 0.0050 mmole) in .5 mL of THF was added to this mixture followed by 1.5 equiv (2-(1,3-dioxan-2-yl)ethyl)zinc bromide (0.5 M solution, 0.3 mL, 0.15 mmole). The reaction was stirred for 3 hours and an aliquot was quenched with ~0.1 mL CH₂Cl₂. The solvent was removed under a stream of nitrogen and nmr analysis (stock solution integral ratio of **3.71**:internal standard = 1.00:0.62) of the crude reaction mixture indicated a 71% yield. (A second run gave a 67% yield). note: triphenylmethane was used due to overlap of signals with hexamethylbenzene leading to inconsistent integrations.



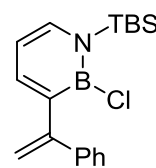
Compound 3.92:

Vinylzinc bromide was prepared by stirring a solution of 1.2 equiv of vinylmagnesium bromide (117 μ L of 1M solution, .117 mmole) with 2 equiv of zinc bromide (51 mg, 0.23 mmole) for 2 hours in 1 mL THF. A vial was charged with 300 μ L of a stock solution of azaborine **3.71** (302.5 mg : 3 mL; 30.3 mg, 0.099 mmole : 300 μ L) and hexamethylbenzene (11.1 mg : 3 mL; 1.1 mg, 0.0068 mmole : 300 μ L). 0.05 equiv of Pd(P^tBu₃)₂ (2.5 mg, 0.0050 mmole) in .5 mL of THF was added to the azaborine mixture and the resulting solution was rinsed into the vinylzinc bromide slurry (total volume ~2.5 mL) with THF. The reaction was allowed to stir for 24 hours and an aliquot was quenched with ~0.1 mL of CH₂Cl₂. The solvent was removed under a stream of nitrogen and nmr analysis (stock solution integral ratio of **3.71**:internal standard = 1.00:1.41) of the crude reaction mixture indicated a 70% yield. (A second run gave a 67% yield). This crude reaction mixture also contained ~20% of the B-Vinyl species.

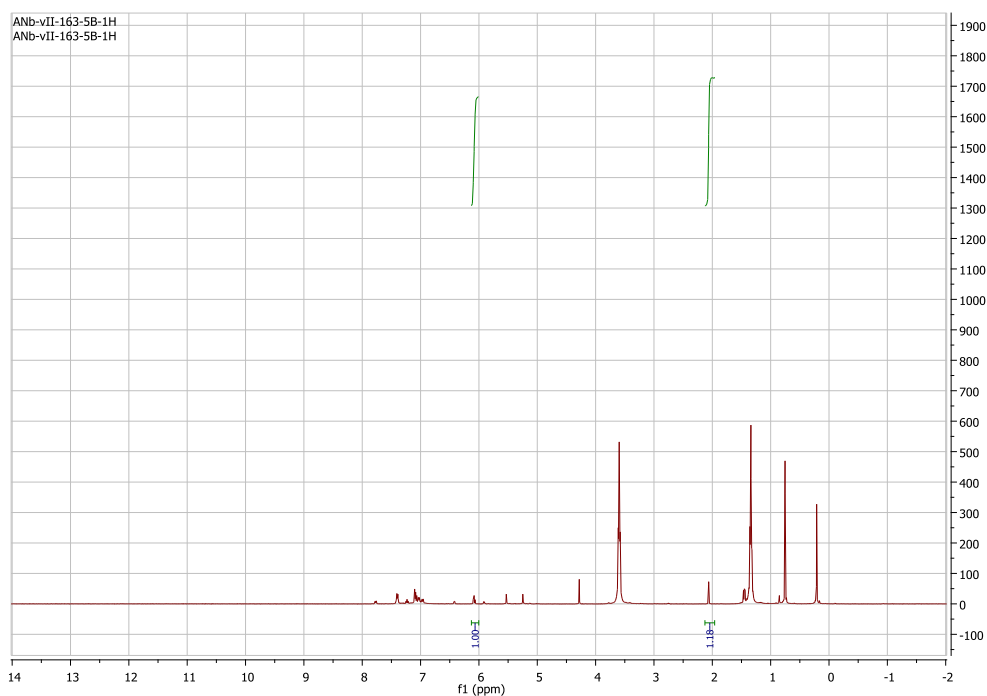


Compound 3.93:

A vial was charged with 1 mL of THF and 200 μ L of a stock solution of azaborine **3.71** (299.2 mg : 2 mL; 29.9 mg, 0.098 mmole : 200 μ L) and hexamethylbenzene (10.4 mg : 2 mL; 1.0 mg, 0.0062 mmole : 200 μ L).



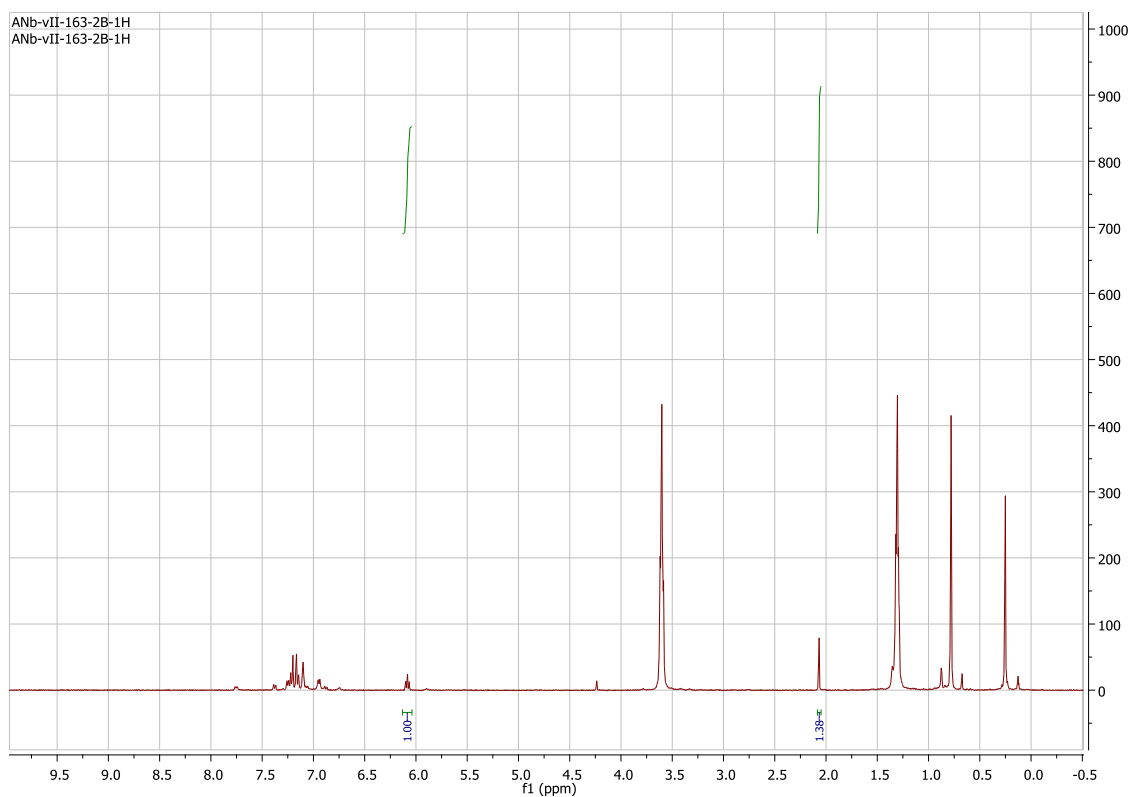
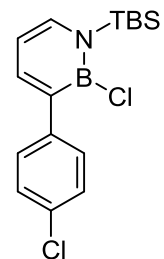
0.05 equiv of $\text{Pd}(\text{P}^t\text{Bu}_3)_2$ (2.5 mg, 0.0050 mmole) in .5 mL of THF was added to this followed by 1.5 equiv (1-phenylvinyl)zinc bromide (0.5 M solution, 0.3 mL, 0.15 mmole). The reaction was stirred for 3 hours and an aliquot was quenched with \sim 0.1 mL CH_2Cl_2 . The solvent was removed under a stream of nitrogen and nmr analysis (stock solution integral ratio of **3.71**:internal standard = 1.00:1.13) indicated of the crude reaction mixture indicated a 97% yield. (A second run gave a 96% yield).



Compound 3.94:

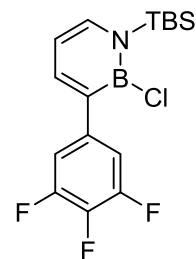
A vial was charged with 1 mL of THF and 200 μ L of a stock solution of azaborine **3.71** (299.2 mg : 2 mL; 29.9 mg, 0.098 mmole : 200 μ L) and hexamethylbenzene (10.4 mg : 2 mL; 1.0 mg, 0.0062 mmole : 200 μ L).

0.05 equiv of Pd(P^tBu₃)₂ (2.5 mg, 0.0050 mmole) in .5 mL of THF was added to this followed by 1.5 equiv (4-chloro)phenylzinc iodide (0.5 M solution, 0.3 mL, 0.15 mmole). The reaction was stirred for 3 hours and an aliquot was quenched with ~0.1 mL CH₂Cl₂. The solvent was removed under a stream of nitrogen and nmr analysis of the crude reaction mixture (stock solution integral ratio of **3.71**:internal standard = 1.00:1.13) indicated an 83% yield. (A second run gave an 82% yield).

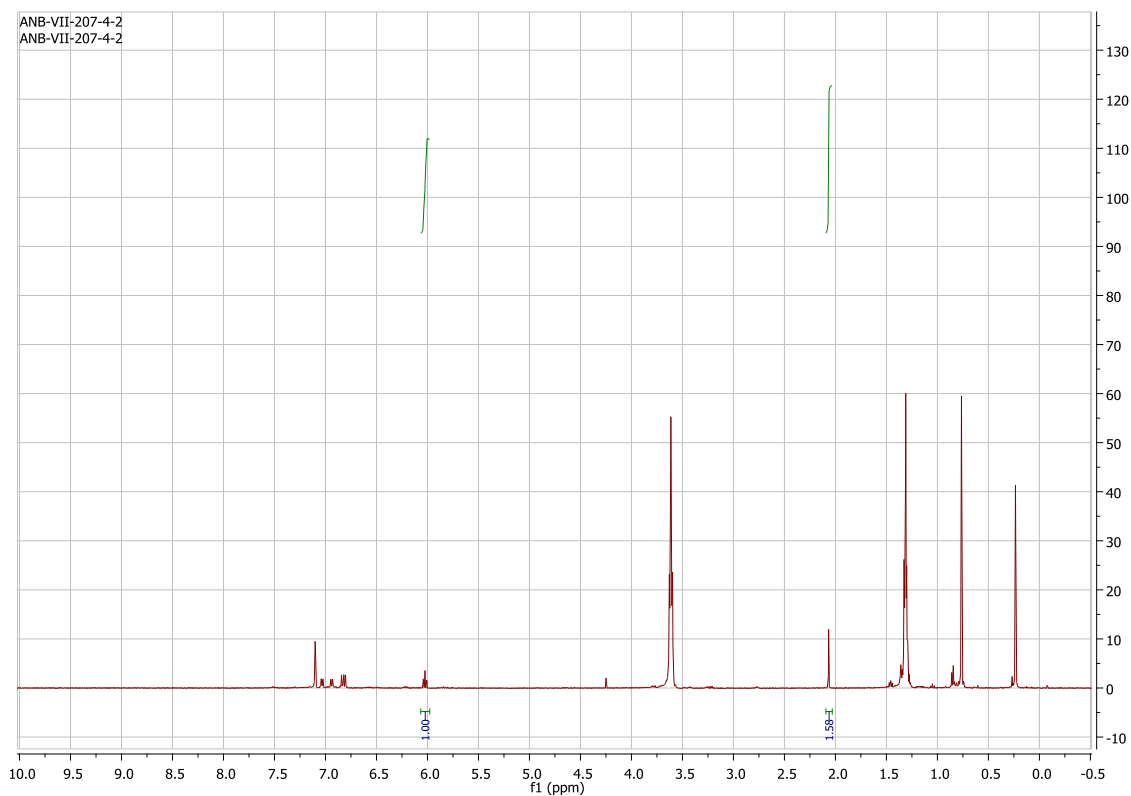


Compound 3.95:

A vial was charged with 1 mL of THF and 300 μ L of a stock solution of azaborine **3.71** (302.5 mg : 3 mL; 30.3 mg, 0.099 mmole : 300 μ L) and hexamethylbenzene (11.1 mg : 3 mL; 1.1 mg, 0.0068 mmole : 300 μ L). 0.05 equiv of Pd(P^tBu₃)₂ (2.5 mg, 0.0050 mmole) in .5 mL of THF was

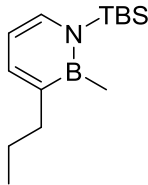


added to this followed by 1.5 equiv (3,4,5-trifluorophenyl)zinc bromide (0.5 M solution, 0.3 mL, 0.15 mmole). The reaction was stirred for 3 hours and an aliquot was quenched with ~0.1 mL CH₂Cl₂. The solvent was removed under a stream of nitrogen and nmr analysis (stock solution integral ratio of **3.71**:internal standard = 1.00:1.41) of the crude reaction mixture indicated an 92% yield. (A second run gave an 89% yield).



3.5.1.8 Preparation of *B*-Me azaborines 3.96-3.101 (Scheme 3.23)

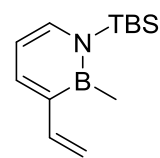
Compound 3.96:

1 Equiv of azaborine **3.71** (200 mg, 0.653 mmole) was dissolved in 3 mL of THF. To this mixture was added 0.05 equiv (17.0 mg, 0.0326 mmole) of  Pd(P^tBu₃)₂ in 1 mL THF followed by 1.5 equiv of propylzinc bromide (2.0 mL of 0.5 M solution in THF, 1.0 mmole). The mixture was stirred for 3 hours and 0.5 mL of CH₂Cl₂ was added followed by 0.2 mL of TMEDA (1.3 mmole). After 15 minutes the reaction was concentrated under reduced pressure. The remaining oily solids were triturated with four portions of ~2 mL of pentane and filtered. Upon solvent removal nmr analysis showed clean conversion to the C3 substituted B-Cl compound. 2 equiv of lithium bromide (120 mg, 1.33 mmole) was added to the B-Cl compound and was dissolved in 3 mL THF. 1.5 equiv of methyl magnesium bromide solution (0.35 mL of 3M solution in Et₂O) was added and was stirred for 30 minutes. The reaction mixture was passed directly through a plug of silica (~35 mL silica gel, eluent: Et₂O) and concentrated. The remaining oil was purified by column chromatography (~3 mL silica gel, eluent: pentane). (colorless oil: 122 mg, 75% yield, a second run gave 127 mg, 78% yield) *Note:* Compound **3.96** is volatile so special care should be taken during solvent removal (significant amounts of **3.96** were lost upon prolong exposure to high vacuum (75-150 mTorr)) The reaction mixture can be quenched with TMS-Cl (0.2 mL) without negative effects. ¹H NMR (500 MHz, CD₂Cl₂) δ 7.16 – 7.09 (m, 2H), 6.12 (t, *J* = 6.6 Hz,

may be unstable upon extended exposure to large excess of silica gel. The reaction mixture can be quenched with 0.2 equiv of TMS-Cl with no negative effects. ^1H NMR (500 MHz, CD_2Cl_2) δ 7.17 – 7.09 (m, 2H), 6.12 (t, J = 6.6 Hz, 1H), 4.50 (t, J = 5.2 Hz, 1H), 4.06 (dd, J = 10.7, 5.0 Hz, 2H), 3.73 (td, J = 12.3, 2.2 Hz, 2H), 2.55 – 2.43 (m, 2H), 2.11 – 1.89 (m, 1H), 1.72 – 1.58 (m, 2H), 1.32 (dd, J = 13.4, 1.2 Hz, 1H), 0.91 (s, 9H), 0.74 (s, 3H), 0.46 (s, 6H). ^{11}B NMR (160 MHz, CD_2Cl_2) δ 40.5 (s). ^{13}C NMR (126 MHz, CD_2Cl_2) δ 139.5, 136.7, 110.5, 102.8, 67.4, 37.4, 30.3, 26.9, 26.6, 19.7, -0.9. The carbons adjacent to boron were not observed. FTIR (ATR): $\tilde{\nu}$ = 2954, 2929, 2855, 1611, 1524, 1470, 1430, 1399, 1367, 1308, 1263, 1240, 1195, 1179, 1145, 1133, 1099, 1082, 1044, 1030, 997, 940, 926, 883, 871, 840, 827, 809, 783, 768, 786, 682, 635. HRMS (DART+) calcd for $\text{C}_{17}\text{H}_{33}\text{BNO}_2\text{Si}$ (M+1): 322.23736; found: 322.23852.

Compound 3.98:

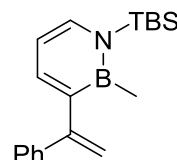
Vinylzinc bromide was generated from 1.02 equiv vinylmagnesium bromide (660 μL of a 1 M solution, 0.660 mmole) and 2.04 equiv Zinc Bromide (305 mg, 1.33 mmole) in 10 mL THF. In a separate vial 1 Equiv of azaborine **3.71** (200 mg, 0.653 mmole) was dissolved in 5 mL of THF. To this mixture was added 0.05 equiv (17.0 mg, 0.0326 mmole) of $\text{Pd}(\text{P}^t\text{Bu}_3)_2$ in 1 mL THF. The azaborine/catalyst mixture was rinsed into the vinylzincbromide slurry with an additional 2 mL of THF (total volume \sim 17 mL THF). The mixture was stirred for 20 hours and the reaction was diluted with 30 mL pentane and filtered and 0.5 mL of CH_2Cl_2 was added to quench the remaining catalyst. Upon solvent removal and a second pentane filtration, nmr analysis showed relatively clean conversion to the C3 substituted B-Cl compound. 2



Equiv of lithium bromide (120 mg, 1.33 mmole) was added to the B-Cl compound and was dissolved in 3 mL THF. 1.15 equiv of methyl magnesium bromide solution (0.25 mL of 3M solution in Et₂O) was added and was stirred for one hour. The reaction mixture was passed directly through a plug of alumina (~35 mL silica gel, eluent: Et₂O) and concentrated. The remaining oil was purified by column chromatography (~1.5 mL alumina, eluent: pentane). (colorless oil: 74.8 mg, 48% yield, a second run gave 81.2 mg, 53% yield) ¹H NMR (600 MHz, CD₂Cl₂) δ 7.50 (d, *J* = 6.7 Hz, 1H), 7.26 (d, *J* = 6.7 Hz, 1H), 6.91 (dd, *J* = 17.5, 10.8 Hz, 1H), 6.23 (t, *J* = 6.7 Hz, 1H), 5.37 (dd, *J* = 17.5, 2.0 Hz, 1H), 5.01 (dd, *J* = 10.8, 1.9 Hz, 1H), 0.94 (s, 9H), 0.82 (s, 3H), 0.48 (s, 6H). ¹¹B NMR (192 MHz, CD₂Cl₂) δ 40.3 (s). ¹³C NMR (151 MHz, CD₂Cl₂) δ 140.9, 138.9, 137.8, 111.7, 110.9, 26.9, 19.7, -0.9. The carbons adjacent to boron were not observed. FTIR (ATR): $\tilde{\nu}$ = 2955, 2930, 2886, 2858, 1614, 1600, 1515, 1471, 1464, 1446, 1391, 1346, 1307, 1262, 1205, 1178, 1116, 1085, 1019, 1005, 992, 895, 875, 839, 820, 808, 783, 768, 728, 683, 626. HRMS (DART+) calcd for C₁₃H₂₅BNSi (M+1): 234.18493; found: 234.18529.

Compound 3.99:

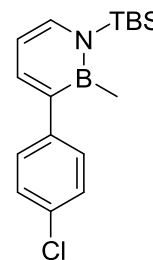
1 Equiv of azaborine **3.71** (200 mg, 0.653 mmole) was dissolved in 3 mL of THF. To this mixture was added 0.05 equiv (17.0 mg, 0.0326 mmole) of Pd(P^tBu₃)₂ in 1 mL THF followed by 1.5 equiv of (1-phenylvinyl)zinc(II) bromide (2.0 mL of 0.5 M solution in THF, 1.0 mmole). The mixture was stirred for 3 hours and 0.5 mL of CH₂Cl₂ was added followed by 0.2 mL of TMEDA (1.3 mmole). After 15 minutes the reaction was concentrated under reduced



pressure. The remaining oily solids were triturated with three portions of ~2 mL of pentane and filtered. upon solvent removal nmr analysis showed clean conversion to the C3 substituted B-Cl compound. 2 equiv of lithium bromide (120 mg, 1.33 mmole) was added to the B-Cl compound and was dissolved in 3 mL THF. 1.5 equiv of methyl magnesium bromide solution (0.35 mL of 3M solution in Et₂O) was added and was stirred for 30 minutes. The reaction mixture was passed directly through a plug of silica (~35 mL silica, eluent: CH₂Cl₂) and concentrated. The remaining oil was purified by column chromatography (silica gel, eluent: CH₂Cl₂). (yellow oil: 193.2 mg, 96% yield, a second run gave 199 mg, 98% yield). ¹H NMR (500 MHz, CD₂Cl₂) δ 7.33 – 7.18 (m, 7H), 6.24 (t, *J* = 6.7 Hz, 1H), 5.44 (d, *J* = 1.9 Hz, 1H), 5.00 (t, *J* = 3.7 Hz, 1H), 0.90 (s, 9H), 0.44 (s, 6H), 0.41 (s, 3H). ¹¹B NMR (160 MHz, CD₂Cl₂) δ 40.2 (s). ¹³C NMR (126 MHz, CD₂Cl₂) δ 155.1, 143.4, 141.4, 138.7, 128.5, 127.6, 127.4, 111.5, 110.5, 26.9, 19.8, -1.0. The carbons adjacent to boron were not observed. FTIR (ATR): $\tilde{\nu}$ = 3077, 2955, 2930, 2885, 2858, 1604, 1519, 1491, 1471, 1444, 1391, 1340, 1308, 1263, 1184, 1162, 1098, 1075, 1062, 1027, 1006, 902, 886, 840, 821, 809, 779, 721, 693, 640. HRMS (DART+) calcd for C₁₉H₂₉BNSi (M+1): 310.21623; found: 310.21612.

Compound 3.100:

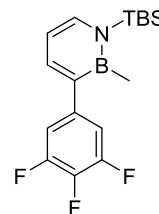
1 Equiv of azaborine **3.71** (200 mg, 0.653 mmole) was dissolved in 3 mL of THF. To this mixture was added 0.05 equiv (17.0 mg, 0.0326 mmole) of Pd(P^tBu₃)₂ in 1 mL THF followed by 1.5 equiv of (4-chlorophenyl)zinc iodide (2.0 mL of 0.5 M solution in THF, 1.0 mmole). The mixture was stirred for 3 hours and 0.5 mL of CH₂Cl₂ was added followed by 0.2 mL



of TMEDA (1.3 mmole). After 15 minutes the reaction was concentrated under reduced pressure. The remaining oily solids were triturated with four portions of ~2 mL of pentane and filtered. Upon solvent removal nmr analysis showed conversion to the C3 substituted B-Cl compound. 2 Equiv of lithium bromide (120 mg, 1.33 mmole) was added to the B-Cl compound and was dissolved in 3 mL THF. 1.5 equiv of methyl magnesium bromide solution (0.3 mL of 3M solution in Et₂O) was added and was stirred for one hour. The reaction mixture was passed directly through a plug of silica (~35 mL silica gel, eluent: Et₂O) and concentrated. The remaining oil was purified by column chromatography (~3 mL silica gel, eluent: pentane (the solubility of this compound in pentane is not fantastic, some addition of CH₂Cl₂ to the eluent would make this a smoother isolation). (white solid: 106.0 mg, 51% yield (90% purity), a second run gave 104.4 mg, 50% yield (90% purity)) ¹H NMR (400 MHz, CD₂Cl₂) δ 7.36 – 7.25 (m, 4H), 7.23 – 7.16 (m, 2H), 6.31 (t, *J* = 6.7 Hz, 1H), 0.95 (s, 9H), 0.74 (s, 3H), 0.51 (s, 6H). ¹¹B NMR (160 MHz, CD₂Cl₂) δ 39.9. ¹³C NMR (126 MHz, CD₂Cl₂) δ 145.8, 141.4, 139.0, 131.5 130.5, 128.4, 110.8, 26.9, 19.8, -0.9. The carbons adjacent to boron were not observed. FTIR (ATR): $\tilde{\nu}$ = 2949, 2930, 2898, 2856, 1600, 1518, 1485, 1471, 1444, 1360, 1340, 1308, 1275, 1260, 1174, 1158, 1133, 1111, 1088, 1011, 992, 872, 840, 821, 807, 775, 725, 690, 663, 640, 627, 557, 504, 464, 451, 429. HRMS (DART+) calcd for C₁₇H₂₆BCINSi (M+1): 318.16161; found: 318.16265.

Compound 3.101:

1 Equiv of azaborine **3.71** (200 mg, 0.653 mmole) was dissolved in 3 mL of THF. To this mixture was added 0.05 equiv (17.0 mg, 0.0326 mmole)

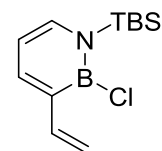


of Pd(P^tBu₃)₂ in 1 mL THF followed by 1.5 equiv of (3,4,5-trifluorophenyl)zinc bromide (2.0 mL of 0.5 M solution in THF, 1.0 mmole). The mixture was stirred for 3 hours and 0.5 mL of CH₂Cl₂ was added followed by 0.2 mL of TMEDA (1.3 mmole). After 15 minutes the reaction was concentrated under reduced pressure. The remaining oily solids were triturated with four portions of ~2 mL of pentane and filtered. Upon solvent removal nmr analysis showed clean conversion to the C3 substituted B-Cl compound. 2 Equiv of lithium bromide (120 mg, 1.33 mmole) was added to the B-Cl compound and was dissolved in 3 mL THF. 0.92 equiv of methyl magnesium bromide solution (0.20 mL of 3M solution in Et₂O) was added and was stirred for 30 minutes. The reaction mixture was passed directly through a plug of silica (~35 mL silica gel, eluent: Et₂O) and concentrated. The remaining oil was purified by column chromatography (~3 mL silica gel, eluent: CH₂Cl₂). (colorless oil: 195.0 mg, 89% yield, a second run gave 195.1 mg, 89% yield) *Note*: This compound was especially sensitive to excess turbo Grignard reagent (when normal amounts were used a large portion of 4-coordinate boron was observed from overaddition) and so a limiting amount of methylmagnesium bromide was used. ¹H NMR (600 MHz, CD₂Cl₂) δ 7.37 (dd, *J* = 6.8, 1.1 Hz, 1H), 7.32 (dd, *J* = 6.7, 1.1 Hz, 1H), 6.89 – 6.83 (m, 2H), 6.31 (t, *J* = 6.7 Hz, 1H), 0.95 (s, 9H), 0.75 (s, 3H), 0.51 (s, 6H). ¹¹B NMR (192 MHz, CD₂Cl₂) δ 39.7 (s). ¹³C NMR (151 MHz, CD₂Cl₂) δ 151.9 (dd, *J*_{CF} = 9.9, 4.3 Hz), 150.4 (dd, *J*_{CF} = 9.8, 4.5 Hz), 143.7 (s), 141.9 (s), 139.8 (s), 112.9 (dd, *J*_{CF} = 16.3, 4.0 Hz), 110.6 (s), 26.9 (s), 19.8 (s), -0.9 (s). The carbons adjacent to boron were not observed. FTIR (ATR): $\tilde{\nu}$ = 2955, 2932, 2886, 2859, 1610, 1525, 1472, 1425, 1393, 1359, 1339, 1309, 1262, 1238, 1201, 1179, 1127, 1107, 1038, 1006, 924,

877, 841, 821, 809, 779, 729, 705, 695, 665, 642, 625. HRMS (DART+) calcd for $C_{17}H_{24}BF_3NSi$ (M+1): 338.17232; found: 338.17327.

3.5.1.9 Large-scale preparation of **3.92** (Scheme 3.25)

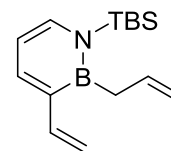
Vinylzincbromide was prepared by stirring 1.2 equiv. vinylmagnesium bromide (7.8 mL of 1M solution in THF, 7.8 mmole) with 2.4 equiv. zinc bromide (3.53g, 15.7 mmole) in 125 mL THF for 2 hours at room temperature. 1 equiv. of **3.71** (2g, 6.54 mmole) and 0.05 equiv. of $Pd(P(t-Bu)_3)_2$ were combined in *c.a.* 20 mL of THF and added to the suspension dropwise. The mixture was allowed to stir at room temperature in a glovebox for 24 h. 125 mL of pentane was added to this suspension and this mixture was filtered. Solvent was removed and the resulting oil was triturated with 25 mL of pentane. The pentane suspension was filtered through an Acros disc and solvent was removed leaving a brown oil. Short-path vacuum distillation (300 mTorr, 85-100 °C) yielded **3.92** as a clear colorless oil in a single fraction (870 mg, 52%). 1H NMR (500 MHz, CD_2Cl_2) δ 7.68 (d, $J = 6.7$ Hz, 1H), 7.25 (d, $J = 6.6$ Hz, 1H), 6.93 (dd, $J = 17.6, 10.9$ Hz, 1H), 6.35 (t, $J = 6.7$ Hz, 1H), 5.59 (dd, $J = 17.6, 1.7$ Hz, 1H), 5.10 (dd, $J = 10.9, 1.7$ Hz, 1H), 0.95 (s, 9H), 0.56 (s, 6H). ^{11}B NMR (160 MHz, CD_2Cl_2) δ 34.9. ^{13}C NMR (126 MHz, CD_2Cl_2) δ 140.5, 139.1, 138.2, 112.9, 111.9, 27.0, 19.8, -1.1. The quaternary carbon adjacent to boron was not observed. FTIR (ATR): $\tilde{\nu} = 2955, 2929, 2884, 2857, 1612, 1527, 1470, 1381, 1362, 1343, 1312, 1287, 1260, 1004, 842, 825, 811, 787, 713$. HRMS (DART+) calcd for $C_{12}H_{22}BCINSi$ (M+1): 254.13031; found: 254.13037.



3.5.1.10 Synthesis of BN-indenyl 3.106 from 3.92 (Scheme 3.26)

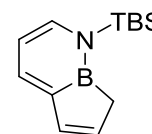
Compound 3.103:

1.1 Equiv. of allylmagnesium bromide (1.0 mL of 1M solution in THF, 1.0 mmole) was added dropwise to a solution of 1 equiv. **3.92** (231.5 mg, 0.914 mmole) in 5 mL THF at -20 °C. The solution was warmed to room temperature and stirred for 2h. The reaction was quenched with 200 μ L TMS-Cl and solvent was removed. The crude mixture was triturated with pentane and filtered and the solvent was removed. (222.2 mg, 94% yield). *Note:* B-allyl compounds have a tendency to isomerize to the B-vinyl on silica or under our cross-coupling conditions. ^1H NMR (500 MHz, CD_2Cl_2) δ 7.62 (d, $J = 6.7$ Hz, 1H), 7.30 (d, $J = 6.7$ Hz, 1H), 7.01 (dd, $J = 17.4, 10.7$ Hz, 1H), 6.30 (t, $J = 6.7$ Hz, 1H), 5.96 (ddt, $J = 16.1, 11.1, 6.8$ Hz, 1H), 5.42 (dd, $J = 17.4, 1.9$ Hz, 1H), 5.00 (dd, $J = 10.7, 1.8$ Hz, 1H), 4.96 – 4.87 (m, 2H), 2.30 (d, $J = 6.8$ Hz, 2H), 0.92 (s, 9H), 0.53 (s, 6H). ^{11}B NMR (160 MHz, CD_2Cl_2) δ 39.1. ^{13}C NMR (126 MHz, CD_2Cl_2) δ 140.4, 139.0, 138.3, 138.2, 115.1, 111.6, 111.8, 26.9, 19.5, -0.8. The carbons adjacent to boron were not observed. HRMS (DART+) calcd for $\text{C}_{15}\text{H}_{27}\text{BNSi}$ ($\text{M}+1$): 260.20058; found: 260.20166.



Compound 3.105:

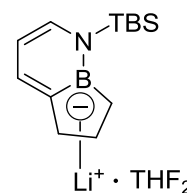
1 Equiv. of compound **3.103** (92.5 mg, 0.357 mmole) was dissolved in 5 mL of CH_2Cl_2 and 0.05 equiv. of Grubbs 1st generation catalyst (15 mg, .0178 mmole) was added in one portion. The resulting purple solution was stirred at room temperature for 2 hours. Solvent was removed under reduced pressure



and the product was isolated by filtration through neutral alumina. (eluent: pentane). (Colorless oil, 49.5 mg, 60% yield). ^1H NMR (500 MHz, CD_2Cl_2) δ 7.27 (d, $J = 6.1$ Hz, 1H), 7.11 (d, $J = 6.7$ Hz, 1H), 6.93 – 6.85 (m, 1H), 6.48 – 6.40 (m, 1H), 6.32 (dd, $J = 9.8$, 3.6 Hz, 1H), 1.89 (s, $J = 2.4$ Hz, 2H), 0.89 (s, 9H), 0.48 (s, 6H). ^{11}B NMR (160 MHz, CD_2Cl_2) δ 43.8. ^{13}C NMR (126 MHz, CD_2Cl_2) δ 138.5, 136.4, 133.6, 129.2, 112.6, 26.6, 19.2, -3.7. The carbons adjacent to boron were not observed. FTIR (ATR): $\tilde{\nu} = 2954$, 2929, 2884, 2857, 1612, 1511, 1471, 1463, 1391, 1363, 1331, 1295, 1257, 1236, 1109, 1072, 1005, 887, 837, 820, 809, 783, 759, 701, 681, 624, 592. HRMS (DART+) calcd for $\text{C}_{19}\text{H}_{23}\text{BNSi}$ (M+1): 232.16928; found: 232.17023.

Compound 3.106:

Lithium tetramethylpiperadine was freshly generated by treatment of 1.2 equiv of 2,2,6,6-tetramethylpiperadine (40 mg, 0.283 mmole) in 1 mL THF with nBuLi (113 μL of 2.5 M solution in hexanes, 0.283 mmole) for

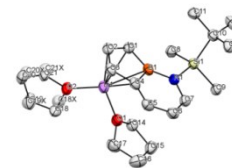


15 minutes with stirring. This solution was added in one portion to a solution of **3.105** in THF and stirred until completion resulting in a blood red solution (followed by ^{11}B nmr and completion took approximately 40 minutes). Upon completion the solvent was removed and the resulting solid was washed thoroughly with a 1:1 diethyl ether:pentane. The resulting orange solid (43.5 mg, 78%) generates a red solution upon dissolution in THF for analysis. Crystals suitable for x-ray diffraction were grown in a -30 °C freezer from a 1:1 mixture of THF to pentane. ^1H NMR (600 MHz, THF) δ 7.38 – 7.36 (m, 2H), 7.03 (d, $J = 6.3$ Hz, 1H), 6.19 (t, $J = 6.4$ Hz, 1H), 5.62 (dd, $J = 3.6$, 1.1 Hz, 1H), 4.52 (d, $J = 5.6$ Hz, 1H), 0.92 (s, 9H), 0.58 (s, 6H). ^{11}B NMR (192 MHz, THF) δ 28.8. ^{13}C NMR

(151 MHz, THF) δ 142.6, 126.2, 122.9, 107.3, 88.5, 26.4, 18.9, -4.1. The carbons adjacent to boron were not observed. FTIR (ATR): $\tilde{\nu}$ = 3036, 2993, 2953, 2927, 2882, 2853, 2241, 2123, 2099, 1613, 1574, 1537, 1513, 1488, 1468, 1392, 1362, 1347, 1298, 1277, 1248, 1210, 1165, 1105, 1092, 1072, 1042, 1023, 1006, 940, 880, 834, 821, 808, 781, 762, 750, 713, 700, 675, 624, 598, 425, 406. We were unable to get HRMS data for compound **3.105** instead generating reprotonated **4** after many attempts.

3.5.1.11 X-ray crystal data for 3.106

Crystal data and structure refinement for compound 3.106.



Identification code	C13H21BLiNSi(C4H8O)2	
Empirical formula	C21 H37 B Li N O2 Si	
Formula weight	381.35	
Temperature	100(2) K	
Wavelength	1.54178 Å	
Crystal system	Monoclinic	
Space group	P2 ₁ /c	3.106
Unit cell dimensions	a = 7.6489(4) Å	α = 90°.
	b = 17.3794(8) Å	β = 96.646(2)°.
	c = 17.2195(8) Å	γ = 90°.
Volume	2273.66(19) Å ³	
Z	4	
Density (calculated)	1.114 Mg/m ³	
Absorption coefficient	1.005 mm ⁻¹	
F(000)	832	
Crystal size	0.480 x 0.170 x 0.060 mm ³	
Theta range for data collection	3.626 to 66.641°.	
Index ranges	-8 ≤ h ≤ 8, 0 ≤ k ≤ 20, 0 ≤ l ≤ 20	
Reflections collected	4005	
Independent reflections	4005 [R(int) = 0.0714]	
Completeness to theta = 66.750°	99.3 %	
Absorption correction	Semi-empirical from equivalents	
Max. and min. transmission	0.7528 and 0.4386	
Refinement method	Full-matrix least-squares on F ²	
Data / restraints / parameters	4005 / 3 / 276	
Goodness-of-fit on F ²	1.024	
Final R indices [I > 2σ(I)]	R1 = 0.0551, wR2 = 0.1555	
R indices (all data)	R1 = 0.0616, wR2 = 0.1645	
Extinction coefficient	na	
Largest diff. peak and hole	0.480 and -0.236 e.Å ⁻³	

Atomic coordinates ($\times 10^4$) and equivalent isotropic displacement parameters ($\text{\AA}^2 \times 10^3$) for twin5. $U(\text{eq})$ is defined as one third of the trace of the orthogonalized U_{ij} tensor.

	x	y	z	$U(\text{eq})$
Si(1)	4650(1)	6064(1)	8369(1)	44(1)
Li(1)	2780(5)	6500(2)	5673(2)	56(1)
N(1)	4771(2)	6751(1)	7615(1)	45(1)
O(1)	1030(2)	7069(1)	6167(1)	56(1)
O(2)	1343(2)	6153(1)	4735(1)	61(1)
B(1)	5031(3)	6548(1)	6813(1)	47(1)
C(1)	5104(3)	5820(1)	6336(1)	49(1)
C(2)	5525(3)	6070(1)	5595(1)	53(1)
C(3)	5598(3)	6866(2)	5507(1)	55(1)
C(4)	5324(3)	7220(1)	6234(1)	50(1)
C(5)	5282(3)	7965(1)	6497(1)	57(1)
C(6)	5020(3)	8102(1)	7286(1)	56(1)
C(7)	4784(3)	7522(1)	7802(1)	51(1)
C(8)	3382(3)	5204(1)	7979(1)	52(1)
C(9)	3416(3)	6498(1)	9137(1)	53(1)
C(10)	6972(3)	5791(1)	8784(1)	51(1)
C(11)	7908(3)	5369(2)	8170(1)	61(1)
C(12)	6928(3)	5260(2)	9493(2)	75(1)
C(13)	8014(3)	6521(2)	9033(2)	66(1)
C(14)	48(3)	6845(1)	6792(1)	56(1)
C(15)	-153(3)	7569(2)	7260(2)	67(1)
C(16)	130(4)	8213(2)	6703(2)	84(1)
C(17)	482(4)	7833(2)	5965(2)	78(1)
C(18)	-468(4)	6352(4)	4534(3)	65(2)
C(19)	-1158(17)	5813(7)	3916(7)	82(4)
C(20)	414(7)	5514(4)	3563(3)	67(1)
C(21)	1945(7)	5918(4)	4011(3)	55(1)
C(18X)	-559(15)	5961(10)	4720(7)	66(3)

C(19X)	-1280(40)	5839(12)	3859(17)	56(6)
C(20X)	370(20)	5313(9)	3738(10)	62(4)
C(21X)	1840(30)	5701(11)	4107(12)	74(6)

Bond lengths [Å] and angles [°] for 3.106.

Si(1)-N(1)	1.7737(17)
Si(1)-C(8)	1.864(2)
Si(1)-C(9)	1.870(2)
Si(1)-C(10)	1.897(2)
Li(1)-O(1)	1.938(4)
Li(1)-O(2)	1.941(4)
Li(1)-C(2)	2.247(4)
Li(1)-C(3)	2.296(4)
Li(1)-C(1)	2.322(4)
Li(1)-C(4)	2.419(4)
Li(1)-B(1)	2.458(4)
N(1)-C(7)	1.378(3)
N(1)-B(1)	1.462(3)
O(1)-C(17)	1.423(3)
O(1)-C(14)	1.436(3)
O(2)-C(18)	1.431(4)
O(2)-C(21)	1.438(4)
B(1)-C(1)	1.512(3)
B(1)-C(4)	1.568(3)
C(1)-C(2)	1.421(3)
C(1)-H(1)	0.944(16)
C(2)-C(3)	1.394(3)
C(2)-H(2)	0.971(16)
C(3)-C(4)	1.432(3)
C(3)-H(3)	0.966(16)
C(4)-C(5)	1.373(3)
C(5)-C(6)	1.416(3)

C(5)-H(5)	0.9500
C(6)-C(7)	1.369(3)
C(6)-H(6)	0.9500
C(7)-H(7)	0.9500
C(8)-H(8A)	0.9800
C(8)-H(8B)	0.9800
C(8)-H(8C)	0.9800
C(9)-H(9A)	0.9800
C(9)-H(9B)	0.9800
C(9)-H(9C)	0.9800
C(10)-C(11)	1.531(3)
C(10)-C(13)	1.532(3)
C(10)-C(12)	1.534(3)
C(11)-H(11A)	0.9800
C(11)-H(11B)	0.9800
C(11)-H(11C)	0.9800
C(12)-H(12A)	0.9800
C(12)-H(12B)	0.9800
C(12)-H(12C)	0.9800
C(13)-H(13A)	0.9800
C(13)-H(13B)	0.9800
C(13)-H(13C)	0.9800
C(14)-C(15)	1.512(3)
C(14)-H(14A)	0.9900
C(14)-H(14B)	0.9900
C(15)-C(16)	1.506(4)
C(15)-H(15A)	0.9900
C(15)-H(15B)	0.9900
C(16)-C(17)	1.484(4)
C(16)-H(16A)	0.9900
C(16)-H(16B)	0.9900
C(17)-H(17A)	0.9900
C(17)-H(17B)	0.9900
C(18)-C(19)	1.469(12)

C(18)-H(18A)	0.9900
C(18)-H(18B)	0.9900
C(19)-C(20)	1.501(15)
C(19)-H(19A)	0.9900
C(19)-H(19B)	0.9900
C(20)-C(21)	1.500(8)
C(20)-H(20A)	0.9900
C(20)-H(20B)	0.9900
C(21)-H(21A)	0.9900
C(21)-H(21B)	0.9900
N(1)-Si(1)-C(8)	110.21(9)
N(1)-Si(1)-C(9)	108.62(9)
C(8)-Si(1)-C(9)	107.11(10)
N(1)-Si(1)-C(10)	108.52(9)
C(8)-Si(1)-C(10)	111.14(10)
C(9)-Si(1)-C(10)	111.21(10)
O(1)-Li(1)-O(2)	99.81(18)
O(1)-Li(1)-C(2)	153.3(2)
O(2)-Li(1)-C(2)	106.83(17)
O(1)-Li(1)-C(3)	128.2(2)
O(2)-Li(1)-C(3)	115.60(18)
C(2)-Li(1)-C(3)	35.72(10)
O(1)-Li(1)-C(1)	124.88(18)
O(2)-Li(1)-C(1)	125.4(2)
C(2)-Li(1)-C(1)	36.18(10)
C(3)-Li(1)-C(1)	61.70(12)
O(1)-Li(1)-C(4)	97.19(17)
O(2)-Li(1)-C(4)	147.7(2)
C(2)-Li(1)-C(4)	58.83(12)
C(3)-Li(1)-C(4)	35.24(10)
C(1)-Li(1)-C(4)	62.09(12)
O(1)-Li(1)-B(1)	95.03(15)
O(2)-Li(1)-B(1)	162.1(2)

C(2)-Li(1)-B(1)	59.09(12)
C(3)-Li(1)-B(1)	60.60(12)
C(1)-Li(1)-B(1)	36.74(10)
C(4)-Li(1)-B(1)	37.50(9)
C(7)-N(1)-B(1)	117.24(17)
C(7)-N(1)-Si(1)	118.91(14)
B(1)-N(1)-Si(1)	123.58(14)
C(17)-O(1)-C(14)	105.72(18)
C(17)-O(1)-Li(1)	124.60(19)
C(14)-O(1)-Li(1)	129.67(18)
C(18)-O(2)-C(21)	104.9(3)
C(18)-O(2)-Li(1)	124.4(2)
C(21)-O(2)-Li(1)	127.0(3)
C(18X)-O(2)-Li(1)	122.8(5)
N(1)-B(1)-C(1)	137.1(2)
N(1)-B(1)-C(4)	117.72(19)
C(1)-B(1)-C(4)	105.16(18)
N(1)-B(1)-Li(1)	127.13(17)
C(1)-B(1)-Li(1)	66.73(15)
C(4)-B(1)-Li(1)	69.89(15)
C(2)-C(1)-B(1)	105.0(2)
C(2)-C(1)-Li(1)	69.05(15)
B(1)-C(1)-Li(1)	76.53(15)
C(2)-C(1)-H(1)	119.6(14)
B(1)-C(1)-H(1)	134.9(14)
Li(1)-C(1)-H(1)	123.7(15)
C(3)-C(2)-C(1)	114.6(2)
C(3)-C(2)-Li(1)	74.04(17)
C(1)-C(2)-Li(1)	74.78(16)
C(3)-C(2)-H(2)	122.2(15)
C(1)-C(2)-H(2)	123.1(15)
Li(1)-C(2)-H(2)	115.6(15)
C(2)-C(3)-C(4)	108.69(19)
C(2)-C(3)-Li(1)	70.24(17)

C(4)-C(3)-Li(1)	77.07(15)
C(2)-C(3)-H(3)	126.1(15)
C(4)-C(3)-H(3)	125.1(15)
Li(1)-C(3)-H(3)	122.4(15)
C(5)-C(4)-C(3)	134.8(2)
C(5)-C(4)-B(1)	118.87(19)
C(3)-C(4)-B(1)	106.34(19)
C(5)-C(4)-Li(1)	124.82(18)
C(3)-C(4)-Li(1)	67.68(15)
B(1)-C(4)-Li(1)	72.60(15)
C(4)-C(5)-C(6)	119.1(2)
C(4)-C(5)-H(5)	120.5
C(6)-C(5)-H(5)	120.5
C(7)-C(6)-C(5)	122.9(2)
C(7)-C(6)-H(6)	118.6
C(5)-C(6)-H(6)	118.6
C(6)-C(7)-N(1)	124.2(2)
C(6)-C(7)-H(7)	117.9
N(1)-C(7)-H(7)	117.9
Si(1)-C(8)-H(8A)	109.5
Si(1)-C(8)-H(8B)	109.5
H(8A)-C(8)-H(8B)	109.5
Si(1)-C(8)-H(8C)	109.5
H(8A)-C(8)-H(8C)	109.5
H(8B)-C(8)-H(8C)	109.5
Si(1)-C(9)-H(9A)	109.5
Si(1)-C(9)-H(9B)	109.5
H(9A)-C(9)-H(9B)	109.5
Si(1)-C(9)-H(9C)	109.5
H(9A)-C(9)-H(9C)	109.5
H(9B)-C(9)-H(9C)	109.5
C(11)-C(10)-C(13)	108.73(19)
C(11)-C(10)-C(12)	108.4(2)
C(13)-C(10)-C(12)	109.5(2)

C(11)-C(10)-Si(1)	110.62(14)
C(13)-C(10)-Si(1)	109.43(16)
C(12)-C(10)-Si(1)	110.13(15)
C(10)-C(11)-H(11A)	109.5
C(10)-C(11)-H(11B)	109.5
H(11A)-C(11)-H(11B)	109.5
C(10)-C(11)-H(11C)	109.5
H(11A)-C(11)-H(11C)	109.5
H(11B)-C(11)-H(11C)	109.5
C(10)-C(12)-H(12A)	109.5
C(10)-C(12)-H(12B)	109.5
H(12A)-C(12)-H(12B)	109.5
C(10)-C(12)-H(12C)	109.5
H(12A)-C(12)-H(12C)	109.5
H(12B)-C(12)-H(12C)	109.5
C(10)-C(13)-H(13A)	109.5
C(10)-C(13)-H(13B)	109.5
H(13A)-C(13)-H(13B)	109.5
C(10)-C(13)-H(13C)	109.5
H(13A)-C(13)-H(13C)	109.5
H(13B)-C(13)-H(13C)	109.5
O(1)-C(14)-C(15)	105.54(19)
O(1)-C(14)-H(14A)	110.6
C(15)-C(14)-H(14A)	110.6
O(1)-C(14)-H(14B)	110.6
C(15)-C(14)-H(14B)	110.6
H(14A)-C(14)-H(14B)	108.8
C(16)-C(15)-C(14)	104.4(2)
C(16)-C(15)-H(15A)	110.9
C(14)-C(15)-H(15A)	110.9
C(16)-C(15)-H(15B)	110.9
C(14)-C(15)-H(15B)	110.9
H(15A)-C(15)-H(15B)	108.9
C(17)-C(16)-C(15)	105.5(2)

C(17)-C(16)-H(16A)	110.6
C(15)-C(16)-H(16A)	110.6
C(17)-C(16)-H(16B)	110.6
C(15)-C(16)-H(16B)	110.6
H(16A)-C(16)-H(16B)	108.8
O(1)-C(17)-C(16)	106.6(2)
O(1)-C(17)-H(17A)	110.4
C(16)-C(17)-H(17A)	110.4
O(1)-C(17)-H(17B)	110.4
C(16)-C(17)-H(17B)	110.4
H(17A)-C(17)-H(17B)	108.6
O(2)-C(18)-C(19)	106.1(6)
O(2)-C(18)-H(18A)	110.5
C(19)-C(18)-H(18A)	110.5
O(2)-C(18)-H(18B)	110.5
C(19)-C(18)-H(18B)	110.5
H(18A)-C(18)-H(18B)	108.7
C(18)-C(19)-C(20)	106.0(8)
C(18)-C(19)-H(19A)	110.5
C(20)-C(19)-H(19A)	110.5
C(18)-C(19)-H(19B)	110.5
C(20)-C(19)-H(19B)	110.5
H(19A)-C(19)-H(19B)	108.7
C(21)-C(20)-C(19)	104.2(5)
C(21)-C(20)-H(20A)	110.9
C(19)-C(20)-H(20A)	110.9
C(21)-C(20)-H(20B)	110.9
C(19)-C(20)-H(20B)	110.9
H(20A)-C(20)-H(20B)	108.9
O(2)-C(21)-C(20)	105.6(4)
O(2)-C(21)-H(21A)	110.6
C(20)-C(21)-H(21A)	110.6
O(2)-C(21)-H(21B)	110.6
C(20)-C(21)-H(21B)	110.6

Symmetry transformations used to generate equivalent atoms:

Anisotropic displacement parameters ($\text{\AA}^2 \times 10^3$) for 8. The anisotropic displacement factor exponent takes the form: $-2\pi^2 [h^2 a^{*2} U^{11} + \dots + 2 h k a^* b^* U^{12}]$

	U ¹¹	U ²²	U ³³	U ²³	U ¹³	U ¹²
Si(1)	42(1)	52(1)	39(1)	0(1)	6(1)	1(1)
Li(1)	47(2)	76(2)	45(2)	-6(2)	6(1)	2(2)
N(1)	42(1)	49(1)	43(1)	0(1)	4(1)	0(1)
O(1)	52(1)	70(1)	46(1)	-2(1)	8(1)	6(1)
O(2)	47(1)	88(1)	47(1)	-16(1)	6(1)	4(1)
B(1)	40(1)	56(1)	44(1)	4(1)	3(1)	-1(1)
C(1)	44(1)	58(1)	46(1)	-1(1)	6(1)	1(1)
C(2)	44(1)	71(1)	47(1)	-3(1)	8(1)	3(1)
C(3)	44(1)	77(2)	44(1)	10(1)	6(1)	-2(1)
C(4)	41(1)	62(1)	48(1)	7(1)	2(1)	-2(1)
C(5)	54(1)	56(1)	60(1)	12(1)	4(1)	-1(1)
C(6)	55(1)	49(1)	64(1)	2(1)	1(1)	-1(1)
C(7)	47(1)	55(1)	50(1)	-4(1)	2(1)	1(1)
C(8)	55(1)	52(1)	50(1)	2(1)	6(1)	-2(1)
C(9)	49(1)	64(1)	47(1)	-2(1)	10(1)	2(1)
C(10)	45(1)	65(1)	44(1)	5(1)	6(1)	4(1)
C(11)	51(1)	74(2)	58(1)	0(1)	7(1)	12(1)
C(12)	51(1)	109(2)	64(1)	31(1)	7(1)	11(1)
C(13)	46(1)	86(2)	65(1)	-11(1)	0(1)	-3(1)
C(14)	47(1)	71(1)	49(1)	1(1)	9(1)	0(1)
C(15)	52(1)	88(2)	62(1)	-17(1)	9(1)	2(1)
C(16)	72(2)	63(2)	122(2)	-8(2)	27(2)	1(1)
C(17)	80(2)	88(2)	65(2)	20(1)	5(1)	18(2)
C(18)	42(2)	85(3)	67(2)	-21(2)	-2(2)	10(2)
C(19)	54(4)	130(7)	61(4)	-25(3)	-1(2)	-12(3)

C(20)	83(3)	71(3)	48(2)	-10(2)	8(2)	-5(2)
C(21)	54(2)	72(3)	40(2)	-7(2)	13(1)	2(2)

**Hydrogen coordinates ($\times 10^4$) and isotropic displacement parameters ($\text{\AA}^2 \times 10^3$)
for **3.106**.**

	x	y	z	U(eq)
H(1)	5060(30)	5288(10)	6445(13)	59
H(2)	5650(30)	5719(13)	5166(12)	64
H(3)	5880(30)	7138(13)	5048(11)	66
H(5)	5427	8382	6154	69
H(6)	5009	8619	7465	68
H(7)	4617	7660	8322	61
H(8A)	2231	5367	7723	78
H(8B)	3217	4853	8410	78
H(8C)	4032	4939	7600	78
H(9A)	4159	6882	9433	79
H(9B)	3099	6094	9492	79
H(9C)	2344	6746	8888	79
H(11A)	7935	5699	7710	91
H(11B)	7273	4893	8018	91
H(11C)	9115	5245	8390	91
H(12A)	8133	5117	9698	112
H(12B)	6253	4796	9335	112
H(12C)	6371	5530	9900	112
H(13A)	7420	6800	9423	99
H(13B)	8083	6851	8576	99
H(13C)	9204	6380	9261	99
H(14A)	690	6446	7122	67
H(14B)	-1118	6639	6583	67
H(15A)	-1343	7599	7432	81
H(15B)	735	7588	7726	81

H(16A)	-930	8543	6614	101
H(16B)	1144	8536	6913	101
H(17A)	-596	7826	5587	93
H(17B)	1417	8110	5727	93
H(18A)	-578	6889	4343	78
H(18B)	-1123	6301	4995	78
H(19A)	-1975	6079	3516	99
H(19B)	-1796	5385	4139	99
H(20A)	521	4949	3628	81
H(20B)	332	5640	3000	81
H(21A)	2966	5567	4109	66
H(21B)	2298	6371	3716	66
H(18C)	-1193	6387	4948	79
H(18D)	-707	5488	5025	79
H(19C)	-1346	6318	3545	68
H(19D)	-2418	5561	3788	68
H(20C)	254	4800	3976	74
H(20D)	474	5245	3174	74
H(21C)	2339	6037	3725	89
H(21D)	2748	5324	4308	89

Torsion angles [°] for 3.106.

C(8)-Si(1)-N(1)-C(7)	146.68(16)
C(9)-Si(1)-N(1)-C(7)	29.62(18)
C(10)-Si(1)-N(1)-C(7)	-91.41(17)
C(8)-Si(1)-N(1)-B(1)	-39.49(19)
C(9)-Si(1)-N(1)-B(1)	-156.55(17)
C(10)-Si(1)-N(1)-B(1)	82.42(18)
C(7)-N(1)-B(1)-C(1)	-179.2(2)
Si(1)-N(1)-B(1)-C(1)	6.9(4)
C(7)-N(1)-B(1)-C(4)	0.7(3)
Si(1)-N(1)-B(1)-C(4)	-173.23(14)
C(7)-N(1)-B(1)-Li(1)	-84.2(3)
Si(1)-N(1)-B(1)-Li(1)	101.9(2)
N(1)-B(1)-C(1)-C(2)	-176.3(2)
C(4)-B(1)-C(1)-C(2)	3.9(2)
Li(1)-B(1)-C(1)-C(2)	63.58(18)
N(1)-B(1)-C(1)-Li(1)	120.2(3)
C(4)-B(1)-C(1)-Li(1)	-59.72(17)
B(1)-C(1)-C(2)-C(3)	-4.8(3)
Li(1)-C(1)-C(2)-C(3)	64.0(2)
B(1)-C(1)-C(2)-Li(1)	-68.84(18)
C(1)-C(2)-C(3)-C(4)	3.7(3)
Li(1)-C(2)-C(3)-C(4)	68.13(18)
C(1)-C(2)-C(3)-Li(1)	-64.5(2)
C(2)-C(3)-C(4)-C(5)	178.8(2)
Li(1)-C(3)-C(4)-C(5)	-117.5(3)
C(2)-C(3)-C(4)-B(1)	-0.8(2)
Li(1)-C(3)-C(4)-B(1)	62.80(17)
C(2)-C(3)-C(4)-Li(1)	-63.65(19)
N(1)-B(1)-C(4)-C(5)	-1.6(3)
C(1)-B(1)-C(4)-C(5)	178.4(2)
Li(1)-B(1)-C(4)-C(5)	120.7(2)
N(1)-B(1)-C(4)-C(3)	178.17(18)

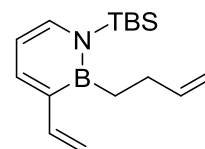
C(1)-B(1)-C(4)-C(3)	-1.9(2)
Li(1)-B(1)-C(4)-C(3)	-59.57(17)
N(1)-B(1)-C(4)-Li(1)	-122.3(2)
C(1)-B(1)-C(4)-Li(1)	57.65(17)
C(3)-C(4)-C(5)-C(6)	-178.1(2)
B(1)-C(4)-C(5)-C(6)	1.6(3)
Li(1)-C(4)-C(5)-C(6)	89.7(3)
C(4)-C(5)-C(6)-C(7)	-0.8(4)
C(5)-C(6)-C(7)-N(1)	-0.1(4)
B(1)-N(1)-C(7)-C(6)	0.1(3)
Si(1)-N(1)-C(7)-C(6)	174.31(17)
N(1)-Si(1)-C(10)-C(11)	-65.89(18)
C(8)-Si(1)-C(10)-C(11)	55.46(19)
C(9)-Si(1)-C(10)-C(11)	174.69(16)
N(1)-Si(1)-C(10)-C(13)	53.88(17)
C(8)-Si(1)-C(10)-C(13)	175.22(15)
C(9)-Si(1)-C(10)-C(13)	-65.54(17)
N(1)-Si(1)-C(10)-C(12)	174.24(17)
C(8)-Si(1)-C(10)-C(12)	-64.4(2)
C(9)-Si(1)-C(10)-C(12)	54.8(2)
C(17)-O(1)-C(14)-C(15)	-34.4(2)
Li(1)-O(1)-C(14)-C(15)	144.8(2)
O(1)-C(14)-C(15)-C(16)	20.9(3)
C(14)-C(15)-C(16)-C(17)	-0.4(3)
C(14)-O(1)-C(17)-C(16)	34.5(3)
Li(1)-O(1)-C(17)-C(16)	-144.7(2)
C(15)-C(16)-C(17)-O(1)	-20.6(3)
C(21)-O(2)-C(18)-C(19)	35.4(9)
Li(1)-O(2)-C(18)-C(19)	-164.8(6)
O(2)-C(18)-C(19)-C(20)	-21.2(11)
C(18)-C(19)-C(20)-C(21)	-0.4(10)
C(18)-O(2)-C(21)-C(20)	-35.6(6)
Li(1)-O(2)-C(21)-C(20)	165.4(4)
C(19)-C(20)-C(21)-O(2)	21.8(7)

Symmetry transformations used to generate equivalent atoms:

3.5.1.12 Synthesis of 9,1-borazaronaphthalene 3.2 from 3.92 (Scheme 3.27)

Compound 3.104:

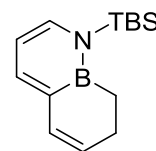
4.0 Equiv of homoallylmagnesium bromide (3 mL of 0.5M solution in Et₂O, 1.5 mmole) was added in one portion to 1 equiv. **3.92** (100 mg, 0.394 mmole) at rt. The solution was stirred for 12 h at which point



approximately half of the solvent was removed and magnesium salts were precipitated with 10 mL pentane. The solvent was removed from the filtrate under reduced pressure. The product was isolated by passing through a pipette plug of silica gel (eluent: pentane). (Colorless oil, 65 mg, 60% yield). ¹H NMR (500 MHz, CD₂Cl₂) δ 7.58 (d, *J* = 6.7 Hz, 1H), 7.26 (d, *J* = 6.6 Hz, 1H), 6.94 (dd, *J* = 17.4, 10.8 Hz, 1H), 6.26 (t, *J* = 6.7 Hz, 1H), 5.96 (ddt, *J* = 16.6, 10.2, 6.2 Hz, 1H), 5.41 (dd, *J* = 17.3, 1.9 Hz, 1H), 5.11 – 4.95 (m, 2H), 4.91 (ddd, *J* = 10.1, 1.8, 1.1 Hz, 1H), 2.17 – 2.00 (m, 2H), 1.45 – 1.36 (m, 2H), 0.91 (s, 9H), 0.50 (s, 6H). ¹¹B NMR (160 MHz, CD₂Cl₂) δ 40.2. ¹³C NMR (126 MHz, CD₂Cl₂) δ 142.34, 140.4, 138.9, 138.2, 112.7, 111.4, 111.3, 31.6, 26.9, 19.4, -0.9. The carbons adjacent to boron were not observed. HRMS (DART+) calcd for C₁₆H₂₉BNSi (M+1): 274.21623; found: 274,21728.

Compound 3.109:

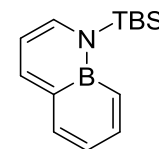
1 Equiv. of compound **3.104** (182.5 mg, 0.668 mmole) was dissolved in 5 mL of CH₂Cl₂ and 0.05 equiv. of Grubbs 1st generation catalyst (27.4 mg, .0334 mmole) was added in one portion. The resulting solution was stirred



at room temperature for 25 minutes. Solvent was removed under reduced pressure and the product was isolated by filtration through neutral alumina. (eluent: pentane). (Colorless oil, 116.1 mg, 71% yield). ¹H NMR (500 MHz, CD₂Cl₂) δ 7.07 (d, *J* = 6.8 Hz, 1H), 6.94 (d, *J* = 6.3 Hz, 1H), 6.46 (d, *J* = 9.6 Hz, 1H), 6.16 (t, *J* = 6.6 Hz, 1H), 5.87 – 5.75 (m, 1H), 2.32 (dt, *J* = 7.6, 6.0 Hz, 2H), 1.41 (t, *J* = 7.7 Hz, 2H), 0.94 (s, 9H), 0.44 (s, 6H). ¹¹B NMR (160 MHz, CD₂Cl₂) δ 41.5. ¹³C NMR (126 MHz, CD₂Cl₂) δ 137.0, 134.9, 132.7, 130.2, 111.6, 26.7, 24.9, 19.4, -1.8. The carbons adjacent to boron were not observed. HRMS (DART+) calcd for C₁₄H₂₅BNSi (M+1): 246.18493; found: 246.18617.

Compound 3.110:

1 Equiv. of compound **3.109** (455 mg, 1.90 mmole) was mixed with 2.4 equiv. of cyclohexene (375 mg, 4.57 mmole) and 0.1 equivalents of 10% palladium on carbon (200 mg, 0.187 mmole) in 30 mL of toluene and

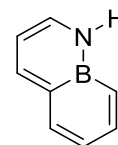


refluxed for 72 hours. Upon completion the reaction was filtered and the solids were washed with 50 mL thf and solvent was removed under reduced pressure. A significant amount of fully reduced product was observed (¹¹B NMR ~40, pdt:reduced 1:0.8). Compound **10** was isolated by column chromatography (neutral alumina, ~20 mL) (190.9 mg, 41%). ¹H NMR (500 MHz, CD₂Cl₂) δ 8.33 (d, *J* = 7.0 Hz, 1H), 8.00 (d, *J* = 6.2 Hz, 1H), 7.75 (dd, *J* = 11.6, 6.4 Hz, 1H), 7.62 (d, *J* = 8.4 Hz, 1H), 7.35 (dd, *J* = 11.7, 0.7 Hz,

1H), 6.99 – 6.90 (m, 2H), 0.94 (s, 9H), 0.71 (s, 6H). ¹¹B NMR (160 MHz, CD₂Cl₂) δ 29.5. ¹³C NMR (126 MHz, CD₂Cl₂) δ 146.7, 142.9, 140.6, 132.7, 123.5, 113.2, 26.9, 19.1, -1.1. The carbons adjacent to boron were not observed. FTIR (ATR): $\tilde{\nu}$ = 3042, 2952, 2928, 2883, 2855, 1591, 1568, 1531, 1471, 1462, 1444, 1426, 1374, 1358, 1249, 1217, 1191, 1147, 1109, 1066, 1048, 1036, 1006, 977, 938, 834, 819, 809, 781, 749, 738, 725, 683, 617, 574, 490, 460, 410. HRMS (DART+) calcd for C₁₄H₂₃BNSi (M+1): 244.16928; found: 244.16911.

Compound 3.2:

Compound **3.110** (40 mg, 0.164 mmole) was dissolved in 3 mL of THF. 1.05 equiv. of a 1M TBAF solution (175 μ L, .175 mmole) was added and the mixture was stirred for 10 minutes. Final product **3.2** was isolated by column



chromatography (silica gel, eluent Et₂O) (21.2 mg, quantitative yield). ¹H NMR (500 MHz, CD₂Cl₂) δ 9.31 (t, *J* = 53.8 Hz, 1H), 8.41 (d, *J* = 7.1 Hz, 1H), 7.94 (t, *J* = 7.1 Hz, 1H), 7.82 (dd, *J* = 10.4, 6.1 Hz, 1H), 7.65 (d, *J* = 8.5 Hz, 1H), 7.23 (d, *J* = 11.3 Hz, 1H), 7.05 (dd, *J* = 8.4, 6.4 Hz, 1H), 6.93 (t, *J* = 6.6 Hz, 1H). ¹¹B NMR (160 MHz, CD₂Cl₂) δ 26.7. ¹³C NMR (126 MHz, CD₂Cl₂) δ 145.7, 141.7, 136.9, 131.7, 126.7 (br), 124.8, 112.2. The quaternary carbon adjacent to boron was not observed. FTIR (ATR): $\tilde{\nu}$ = 3226 (NH), 3009, 2991, 2957, 1567, 1540, 1497, 1451, 1427, 1388, 1318, 1245, 1208, 1121, 1091, 1018, 959, 937, 903, 756, 718, 701, 681, 593, 567, 448, 421, 414. HRMS (DART+) calcd for C₈H₉BN (M+1): 130.08280; found: 130.08289.

3.5.1.13 Procedure for the determination of the quantum yield of 3.2²²¹:

Fluorescence quantum yield, Φ , was measured according to the principles outlined in “*A Guide to Recording Fluorescence Quantum Yields*” from Horiba Inc. Measurements were taken in degassed cyclohexane with constant slit widths (3 nm) with an excitation wavelength of 350 nm and measurement and integration from 360-550 nm for all compounds measured. Two compounds of known quantum yield in cyclohexane (anthracene ($\Phi=0.36$ ²²²) and 9-10-diphenyl anthracene ($\Phi=0.97$ ²²³)) were used to calibrate the measurement following the outlined procedure and equations below.

$$\Phi_{\text{standard1}}/\Phi_{\text{standard2}} \sim (\text{slope}_{\text{standard1}}/\text{slope}_{\text{standard2}})$$

All compounds were excited at 350 nm at different concentrations to have a range of absorbancies below 0.1. A linear response ($R^2 \geq 0.95$) of absorbance vs integrated fluorescence over 5 points with a zero intercept indicated reliable data. The quantum yield was calculated from the following relationship

$$\Phi_{\text{azaborine}} = \Phi_{\text{standard}}(\text{slope}_{\text{azaborine}}/\text{slope}_{\text{standard}})$$

where $\text{slope}_{\text{azaborine}}$ is the slope of the linear plot of absorbance vs integrated fluorescence for the azaborine sample and $\text{slope}_{\text{standard}}$ is the slope of the linear plot of absorbance vs. integrated fluorescence for calibrated 9,10 diphenylanthracene sample. Since the solvent was always the same, no correction factor for the refractive index of the solvent was necessary. For the calibration run, the slopes of the two standards (anthracene and 9,10-diphenylanthracene) were

²²¹ Jobin Yvon Ltd. *A Guide to Recording Fluorescence Quantum Yields* (accessed March 2015).

<http://www.horiba.com/fileadmin/uploads/Scientific/Documents/Fluorescence/quantumyieldstrad.pdf>

²²² Suzuki, K.; Kobayashi, A.; Kaneko, S.; Takehira, K.; Yoshihara, T.; Ishida, H.; Shiina, Y.; Oishic, S.; Tobita, S. *Phys. Chem. Chem. Phys.* **2009**, *11*, 9850.

²²³ I. B. Berlman. *Handbook of Fluorescence Spectra of Aromatic Molecules*, Academic Press, New York (1971). compiled by: Brouwer, A. M. *Pure and Applied Chemistry* **2011**, *83*, 2213-2228.

compared with the above relationship and an agreement within 10% of the published quantum yields was considered to be good data. Upon collection of reliable calibration data, the quantum yield of compound **5** was measured under identical conditions and was found to be ~0.01.

Using

$$\Phi_{\text{standard1}}/\Phi_{\text{standard2}} \sim (\text{slope}_{\text{standard1}}/\text{slope}_{\text{standard2}})$$

(actual values)

$$.36/.97 = 2.235\text{E}10 / 7.767\text{E}9$$

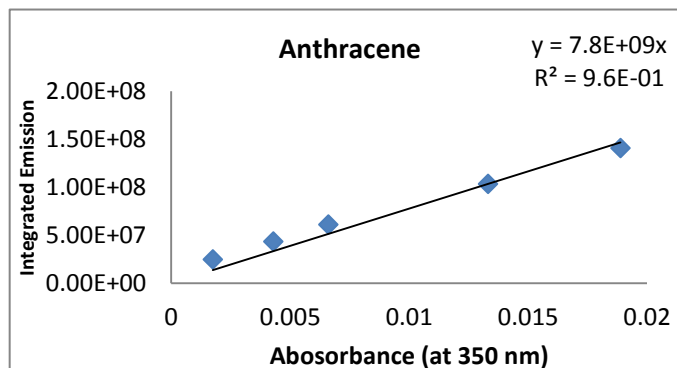
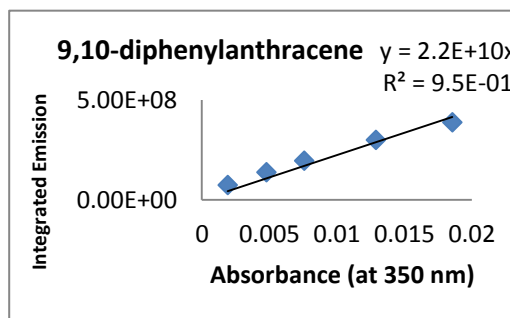
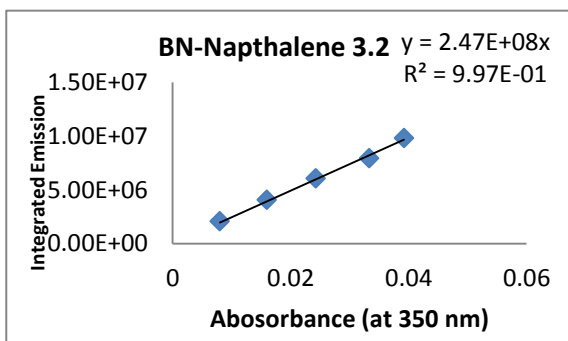
$$.371 = .348 \quad \text{These are within 10\% of each other, so valid method.}$$

Using

$$\Phi_{\text{azaborine}} = \Phi_{\text{standard}}(\text{slope}_{\text{azaborine}}/\text{slope}_{\text{standard}})$$

$$X = .97 (2.47\text{E}8/2.24\text{E}10)$$

$$X = .011$$

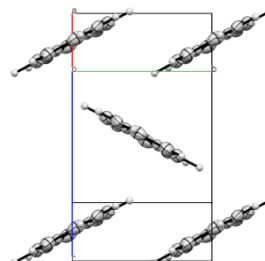


3.5.1.13 Crystallographic information for 3.2

* crystals of 3.2 were disordered so the good data for bond lengths is not obtainable

Crystal data and structure refinement for c8h8bn.

Identification code	C8H8BN	
Empirical formula	C8 H8 B N	
Formula weight	128.96	
Temperature	100(2) K	
Wavelength	1.54178 Å	
Crystal system	Monoclinic	
Space group	P2 ₁ /c	
Unit cell dimensions	a = 8.1542(6) Å	α = 90°.
	b = 5.7395(4) Å	β = 107.059(6)°.
	c = 7.7590(5) Å	γ = 90°.
Volume	347.15(4) Å ³	
Z	2	
Density (calculated)	1.234 Mg/m ³	
Absorption coefficient	0.541 mm ⁻¹	
F(000)	136	
Crystal size	0.120 x 0.040 x 0.030 mm ³	
Theta range for data collection	5.675 to 66.487°.	
Index ranges	-9 ≤ h ≤ 9, -6 ≤ k ≤ 6, -9 ≤ l ≤ 9	
Reflections collected	3226	
Independent reflections	616 [R(int) = 0.0336]	
Completeness to theta = 67.679°	98.1 %	
Absorption correction	Semi-empirical from equivalents	
Max. and min. transmission	0.7528 and 0.6336	
Refinement method	Full-matrix least-squares on F ²	
Data / restraints / parameters	616 / 0 / 62	
Goodness-of-fit on F ²	1.076	
Final R indices [I > 2σ(I)]	R1 = 0.0566, wR2 = 0.1557	
R indices (all data)	R1 = 0.0666, wR2 = 0.1641	
Extinction coefficient	na	



Largest diff. peak and hole

0.497 and -0.186 e.Å⁻³

Atomic coordinates (x 10⁴) and equivalent isotropic displacement parameters (Å²x 10³) for c8h8bn. U(eq) is defined as one third of the trace of the orthogonalized U^{ij} tensor.

	x	y	z	U(eq)
N(1)	6285(3)	2507(3)	4400(3)	42(1)
B(1)	4838(3)	3876(4)	4497(3)	33(1)
C(1)	6285(3)	2507(3)	4400(3)	42(1)
C(2)	4838(3)	3876(4)	4497(3)	33(1)
C(3)	7870(3)	3221(4)	5226(3)	45(1)
C(4)	8243(3)	5287(4)	6204(3)	42(1)
C(5)	6967(3)	6800(4)	6397(3)	46(1)

Bond lengths [Å] and angles [°] for c8h8bn.

N(1)-C(3)	1.328(3)
N(1)-B(1)	1.438(3)
N(1)-H(2)	1.06(3)
B(1)-C(5)#1	1.483(3)
B(1)-C(2)#1	1.492(4)
C(1)-C(3)	1.328(3)
C(1)-C(2)	1.438(3)
C(1)-H(2)	1.06(3)
C(2)-C(5)#1	1.483(3)
C(3)-C(4)	1.392(3)
C(3)-H(4)	0.99(3)
C(4)-C(5)	1.397(3)
C(4)-H(3)	0.99(3)
C(5)-C(2)#1	1.483(3)
C(5)-H(1)	0.89(4)
C(3)-N(1)-B(1)	120.2(2)
C(3)-N(1)-H(2)	116.9(15)

B(1)-N(1)-H(2)	122.8(15)
N(1)-B(1)-C(5)#1	123.4(2)
N(1)-B(1)-C(2)#1	118.6(2)
C(5)#1-B(1)-C(2)#1	118.0(3)
C(3)-C(1)-C(2)	120.2(2)
C(3)-C(1)-H(2)	116.9(15)
C(2)-C(1)-H(2)	122.8(15)
C(1)-C(2)-C(5)#1	123.4(2)
C(1)-C(2)-B(1)#1	118.6(2)
C(5)#1-C(2)-B(1)#1	118.0(3)
C(1)-C(3)-C(4)	123.5(2)
C(1)-C(3)-H(4)	115.9(17)
C(4)-C(3)-H(4)	120.6(17)
C(3)-C(4)-C(5)	122.5(2)
C(3)-C(4)-H(3)	114.3(15)
C(5)-C(4)-H(3)	123.1(16)
C(4)-C(5)-B(1)#1	117.1(2)
C(4)-C(5)-H(1)	122.7(19)
B(1)#1-C(5)-H(1)	120.2(19)

Symmetry transformations used to generate equivalent atoms:

#1 -x+1,-y+1,-z+1

Anisotropic displacement parameters ($\text{\AA}^2 \times 10^3$) for c8h8bn. The anisotropic displacement factor exponent takes the form: $-2\pi^2 [h^2 a^{*2} U^{11} + \dots + 2 h k a^* b^* U^{12}]$

	U ¹¹	U ²²	U ³³	U ²³	U ¹³	U ¹²
N(1)	64(1)	29(1)	34(1)	4(1)	15(1)	4(1)
B(1)	51(1)	24(1)	25(1)	6(1)	12(1)	-3(1)
C(1)	64(1)	29(1)	34(1)	4(1)	15(1)	4(1)
C(2)	51(1)	24(1)	25(1)	6(1)	12(1)	-3(1)
C(3)	56(1)	42(1)	37(1)	9(1)	15(1)	5(1)
C(4)	37(1)	52(2)	36(1)	12(1)	8(1)	-6(1)
C(5)	70(2)	34(1)	33(1)	6(1)	16(1)	-12(1)

Hydrogen coordinates ($\times 10^4$) and isotropic displacement parameters ($\text{\AA}^2 \times 10^3$) for c8h8bn.

	x	y	z	U(eq)
H(1)	7200(40)	8120(70)	7020(40)	73(10)
H(2)	6160(30)	890(50)	3730(40)	61(8)
H(3)	9480(30)	5580(50)	6760(40)	53(7)
H(4)	8800(40)	2160(50)	5150(40)	59(8)

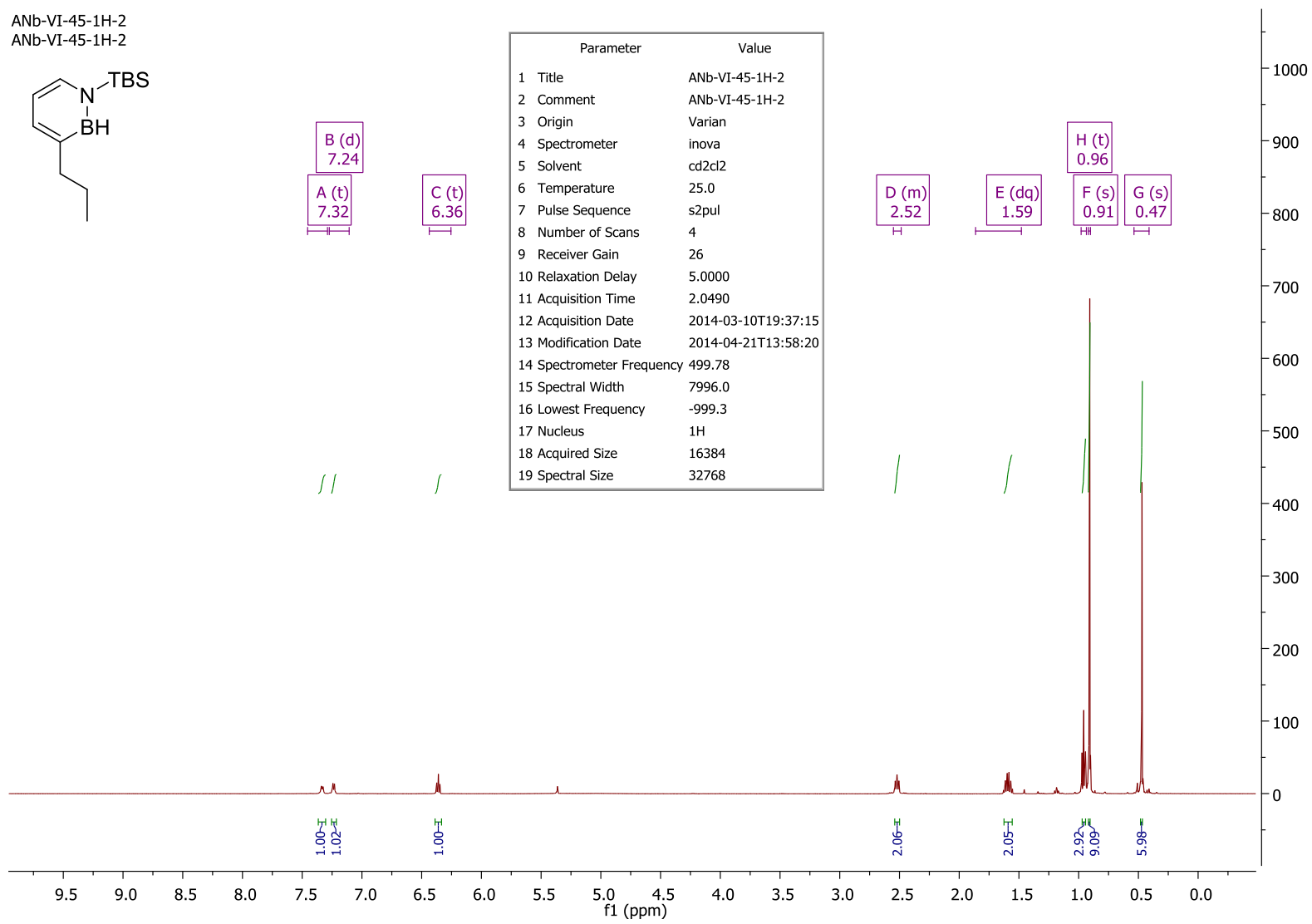
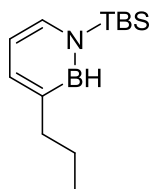
Torsion angles [$^\circ$] for c8h8bn.

C(3)-C(1)-C(2)-C(5)#1	179.6(2)
C(3)-C(1)-C(2)-B(1)#1	1.4(3)
C(2)-C(1)-C(3)-C(4)	-0.5(3)
N(1)-C(3)-C(4)-C(5)	-0.2(3)
C(3)-C(4)-C(5)-B(1)#1	-0.1(3)

Symmetry transformations used to generate equivalent atoms:
#1 $-x+1, -y+1, -z+1$

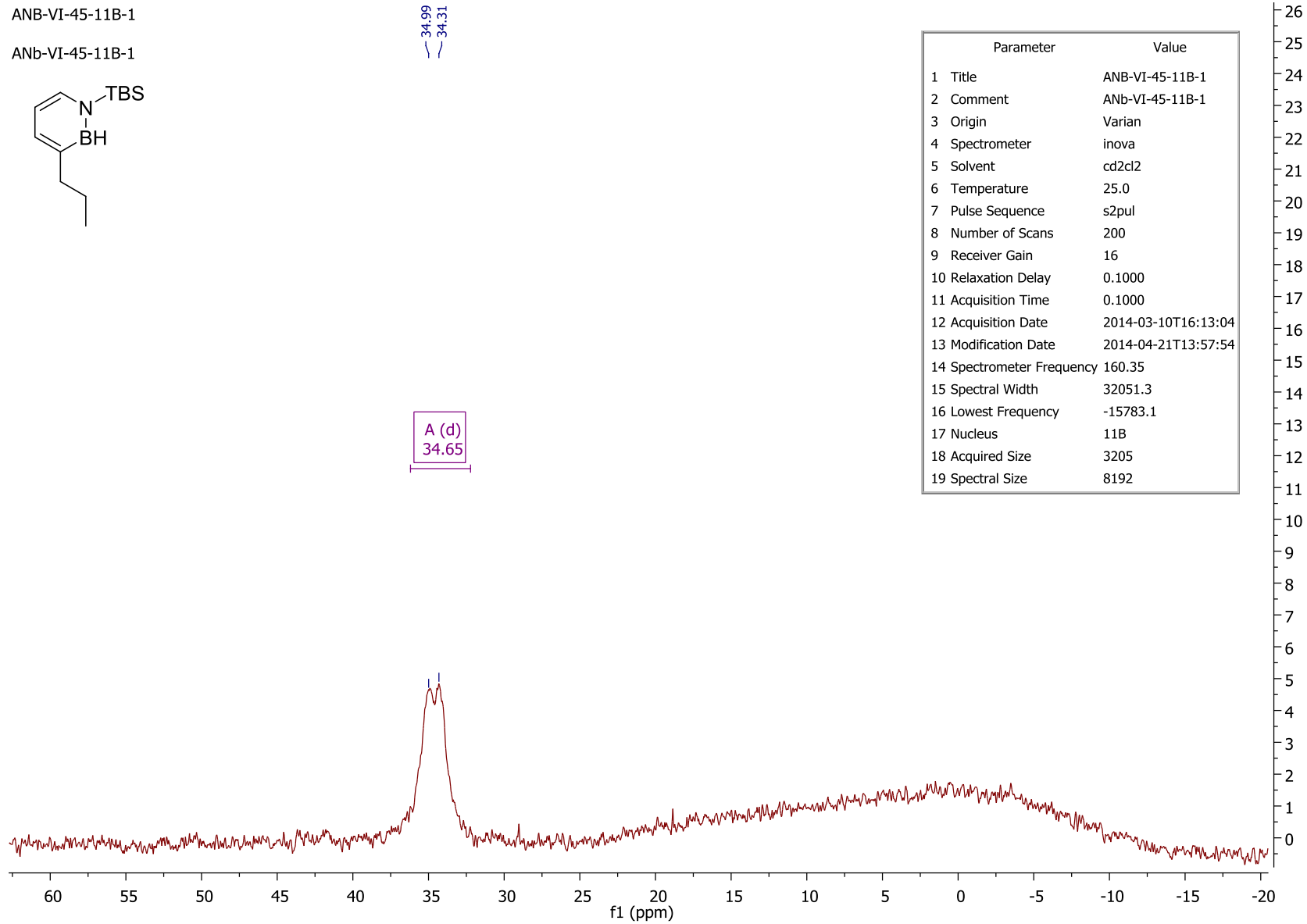
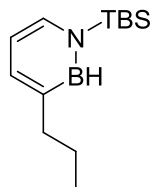
3.6 NMR Spectral Library

ANb-VI-45-1H-2
ANb-VI-45-1H-2



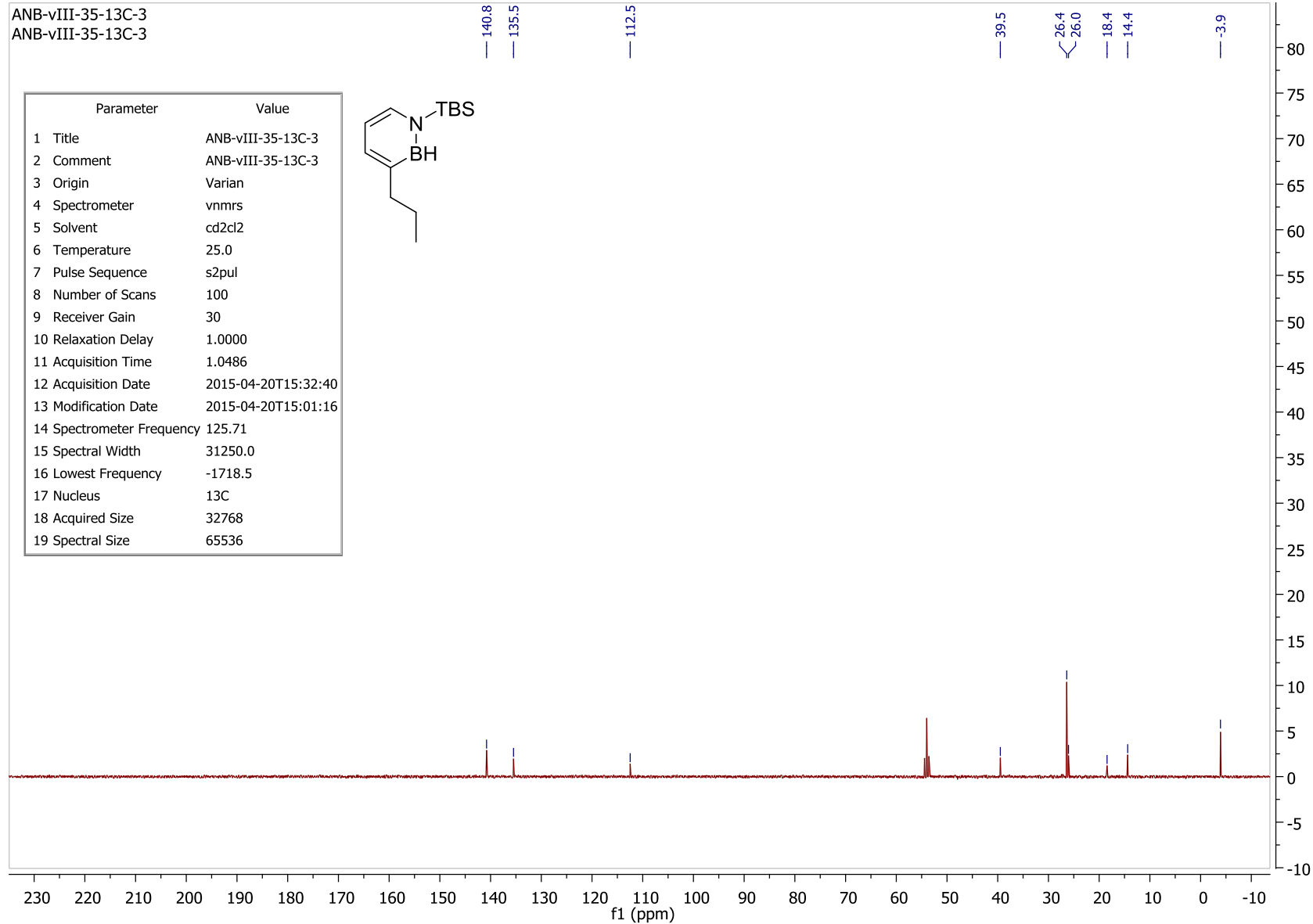
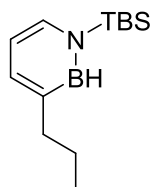
ANB-VI-45-11B-1

ANb-VI-45-11B-1

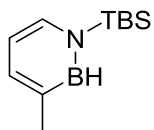


ANB-vIII-35-13C-3
ANB-vIII-35-13C-3

Parameter	Value
1 Title	ANB-vIII-35-13C-3
2 Comment	ANB-vIII-35-13C-3
3 Origin	Varian
4 Spectrometer	vnmrs
5 Solvent	cd2cl2
6 Temperature	25.0
7 Pulse Sequence	s2pul
8 Number of Scans	100
9 Receiver Gain	30
10 Relaxation Delay	1.0000
11 Acquisition Time	1.0486
12 Acquisition Date	2015-04-20T15:32:40
13 Modification Date	2015-04-20T15:01:16
14 Spectrometer Frequency	125.71
15 Spectral Width	31250.0
16 Lowest Frequency	-1718.5
17 Nucleus	13C
18 Acquired Size	32768
19 Spectral Size	65536



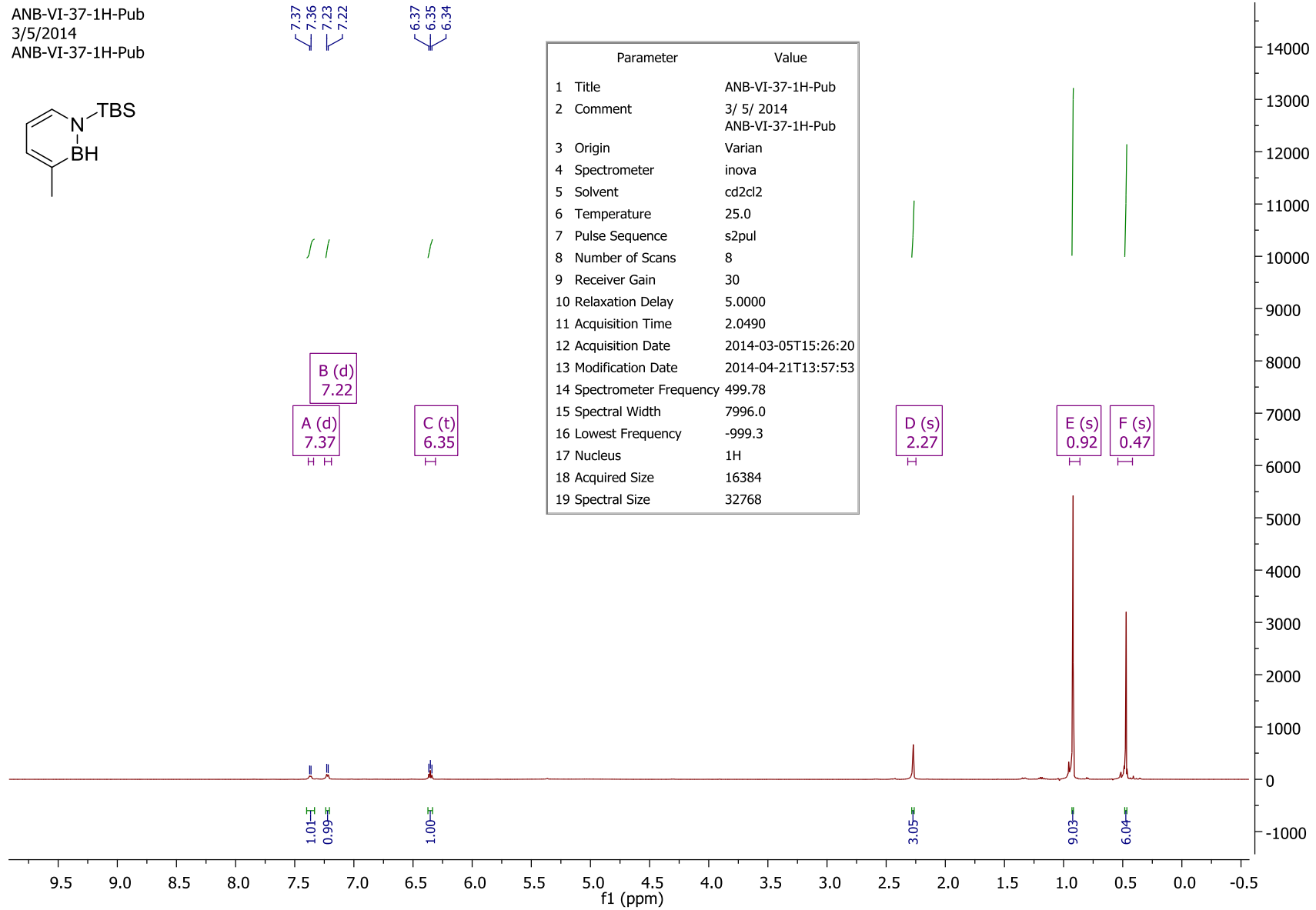
ANB-VI-37-1H-Pub
 3/5/2014
 ANB-VI-37-1H-Pub



7.37
 7.36
 7.23
 7.22

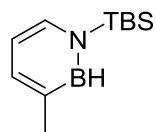
6.37
 6.35
 6.34

Parameter	Value
1 Title	ANB-VI-37-1H-Pub
2 Comment	3/ 5/ 2014 ANB-VI-37-1H-Pub
3 Origin	Varian
4 Spectrometer	inova
5 Solvent	cd2cl2
6 Temperature	25.0
7 Pulse Sequence	s2pul
8 Number of Scans	8
9 Receiver Gain	30
10 Relaxation Delay	5.0000
11 Acquisition Time	2.0490
12 Acquisition Date	2014-03-05T15:26:20
13 Modification Date	2014-04-21T13:57:53
14 Spectrometer Frequency	499.78
15 Spectral Width	7996.0
16 Lowest Frequency	-999.3
17 Nucleus	1H
18 Acquired Size	16384
19 Spectral Size	32768

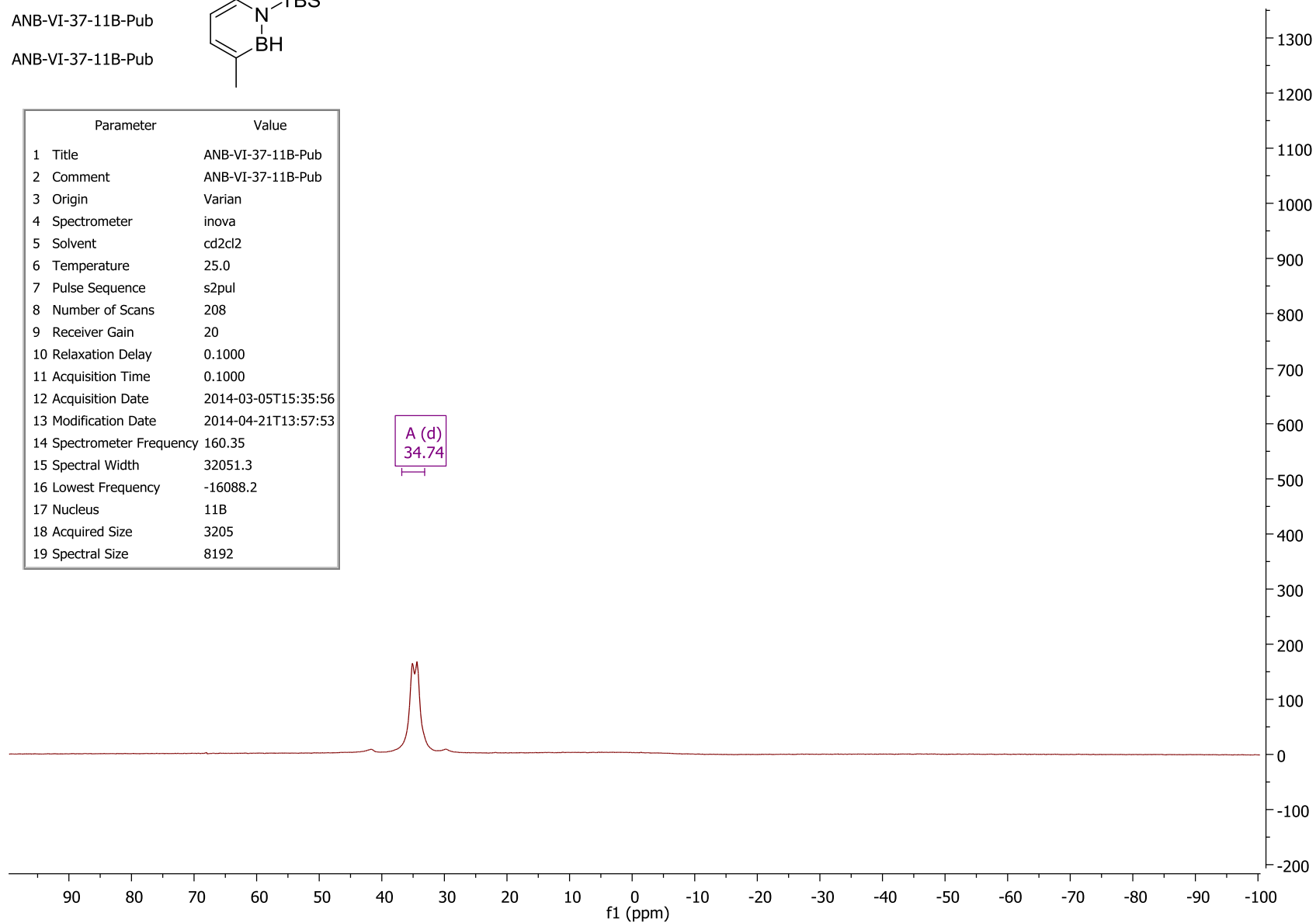


ANB-VI-37-11B-Pub

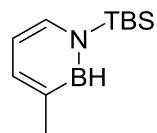
ANB-VI-37-11B-Pub



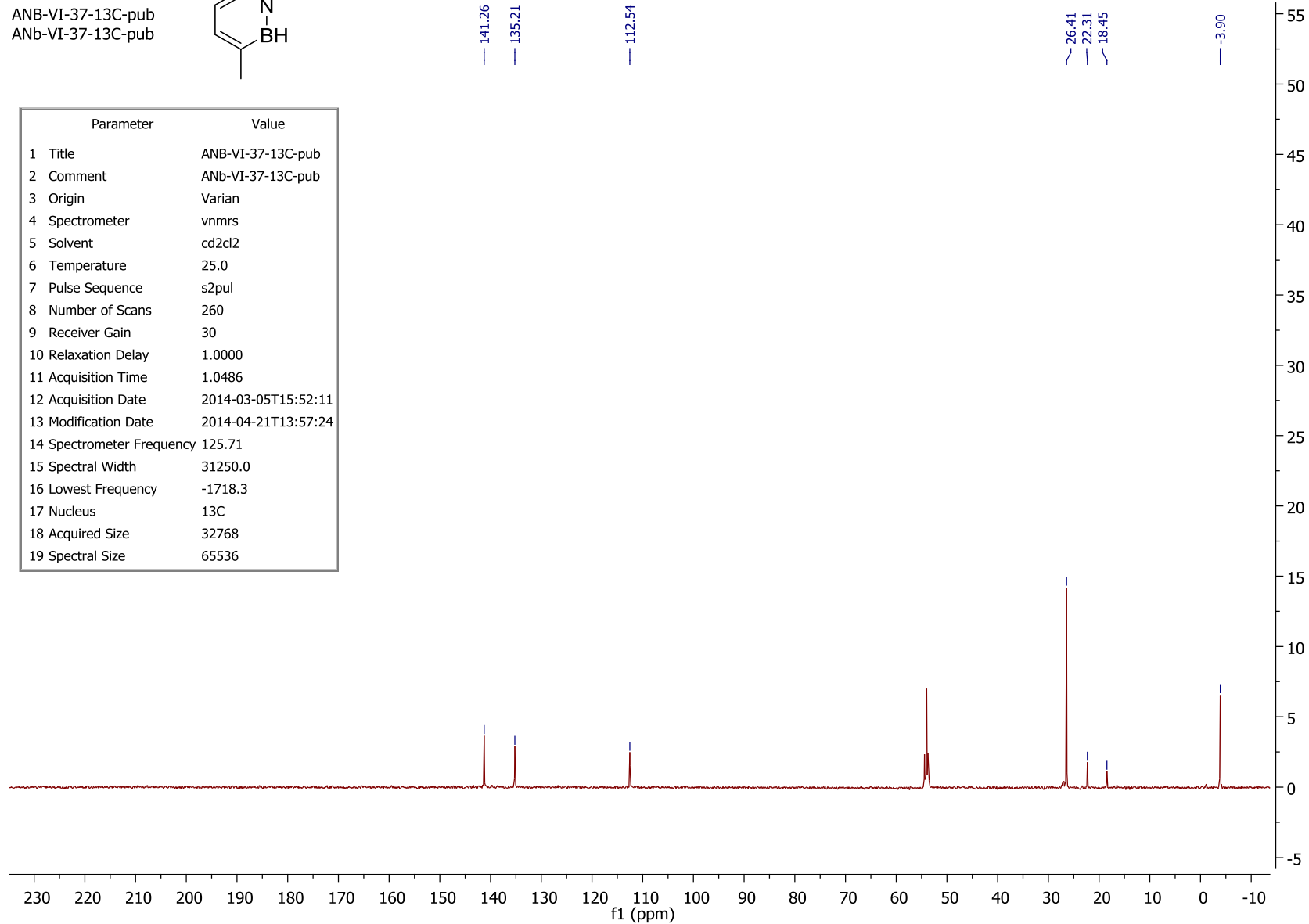
Parameter	Value
1 Title	ANB-VI-37-11B-Pub
2 Comment	ANB-VI-37-11B-Pub
3 Origin	Varian
4 Spectrometer	inova
5 Solvent	cd2cl2
6 Temperature	25.0
7 Pulse Sequence	s2pul
8 Number of Scans	208
9 Receiver Gain	20
10 Relaxation Delay	0.1000
11 Acquisition Time	0.1000
12 Acquisition Date	2014-03-05T15:35:56
13 Modification Date	2014-04-21T13:57:53
14 Spectrometer Frequency	160.35
15 Spectral Width	32051.3
16 Lowest Frequency	-16088.2
17 Nucleus	11B
18 Acquired Size	3205
19 Spectral Size	8192



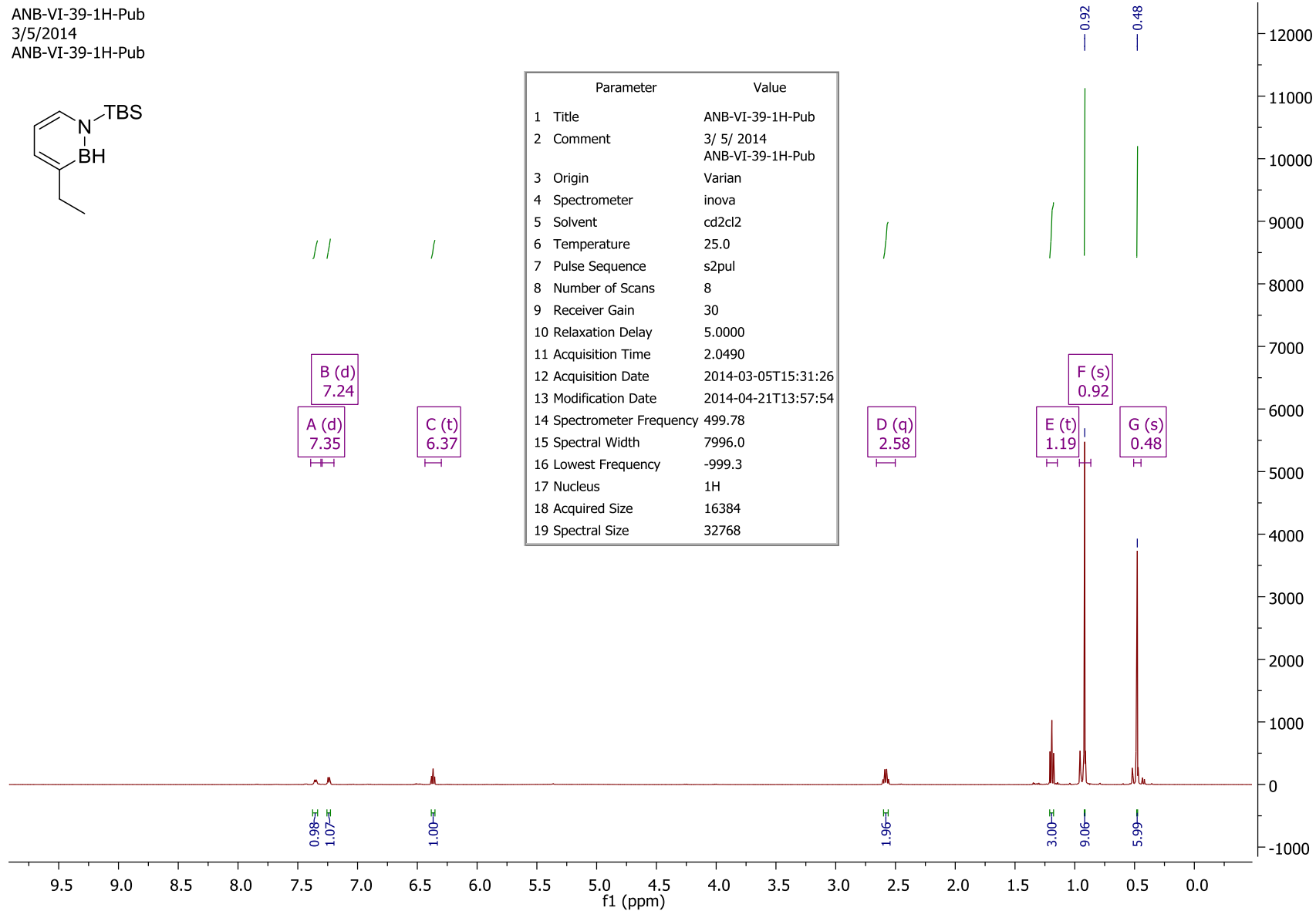
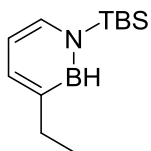
ANB-VI-37-13C-pub
ANb-VI-37-13C-pub



Parameter	Value
1 Title	ANB-VI-37-13C-pub
2 Comment	ANb-VI-37-13C-pub
3 Origin	Varian
4 Spectrometer	vnmrs
5 Solvent	cd2cl2
6 Temperature	25.0
7 Pulse Sequence	s2pul
8 Number of Scans	260
9 Receiver Gain	30
10 Relaxation Delay	1.0000
11 Acquisition Time	1.0486
12 Acquisition Date	2014-03-05T15:52:11
13 Modification Date	2014-04-21T13:57:24
14 Spectrometer Frequency	125.71
15 Spectral Width	31250.0
16 Lowest Frequency	-1718.3
17 Nucleus	13C
18 Acquired Size	32768
19 Spectral Size	65536



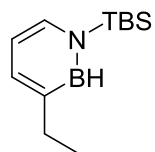
ANB-VI-39-1H-Pub
 3/5/2014
 ANB-VI-39-1H-Pub



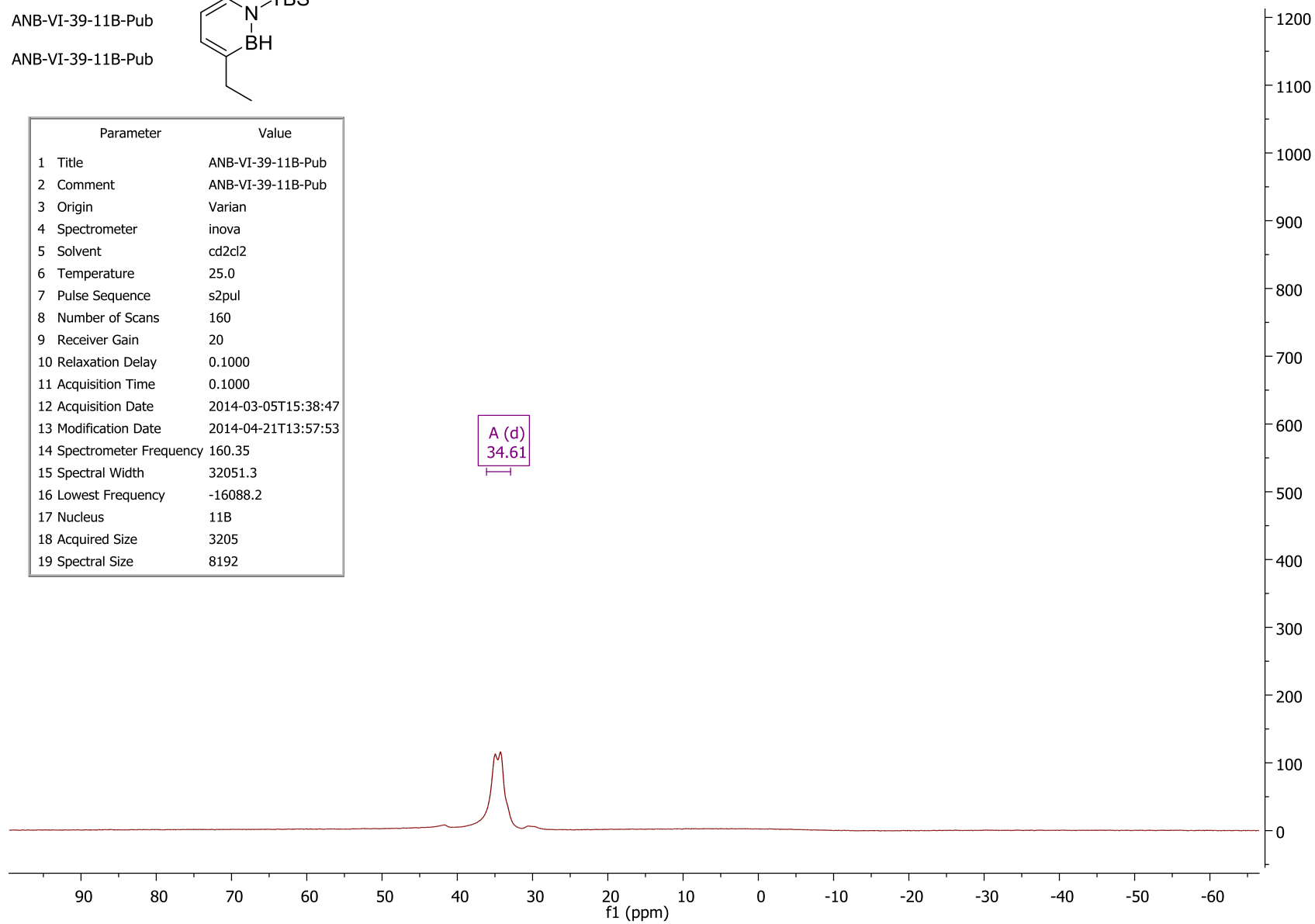
Parameter	Value
1 Title	ANB-VI-39-1H-Pub
2 Comment	3/ 5/ 2014 ANB-VI-39-1H-Pub
3 Origin	Varian
4 Spectrometer	inova
5 Solvent	cd2cl2
6 Temperature	25.0
7 Pulse Sequence	s2pul
8 Number of Scans	8
9 Receiver Gain	30
10 Relaxation Delay	5.0000
11 Acquisition Time	2.0490
12 Acquisition Date	2014-03-05T15:31:26
13 Modification Date	2014-04-21T13:57:54
14 Spectrometer Frequency	499.78
15 Spectral Width	7996.0
16 Lowest Frequency	-999.3
17 Nucleus	1H
18 Acquired Size	16384
19 Spectral Size	32768

ANB-VI-39-11B-Pub

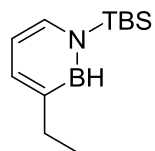
ANB-VI-39-11B-Pub



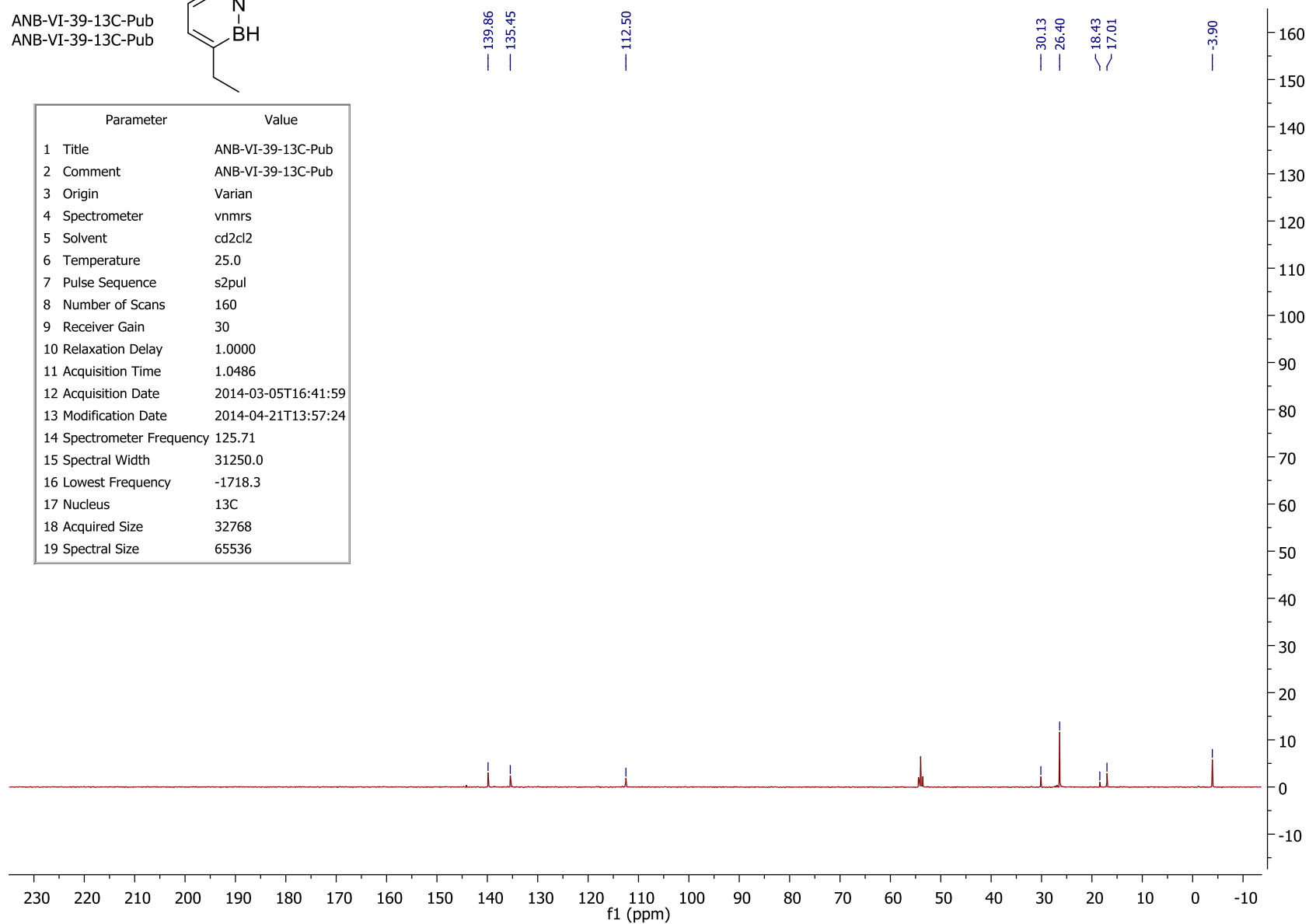
Parameter	Value
1 Title	ANB-VI-39-11B-Pub
2 Comment	ANB-VI-39-11B-Pub
3 Origin	Varian
4 Spectrometer	inova
5 Solvent	cd2cl2
6 Temperature	25.0
7 Pulse Sequence	s2pul
8 Number of Scans	160
9 Receiver Gain	20
10 Relaxation Delay	0.1000
11 Acquisition Time	0.1000
12 Acquisition Date	2014-03-05T15:38:47
13 Modification Date	2014-04-21T13:57:53
14 Spectrometer Frequency	160.35
15 Spectral Width	32051.3
16 Lowest Frequency	-16088.2
17 Nucleus	11B
18 Acquired Size	3205
19 Spectral Size	8192



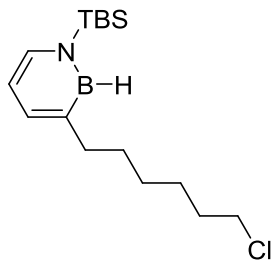
ANB-VI-39-13C-Pub
ANB-VI-39-13C-Pub



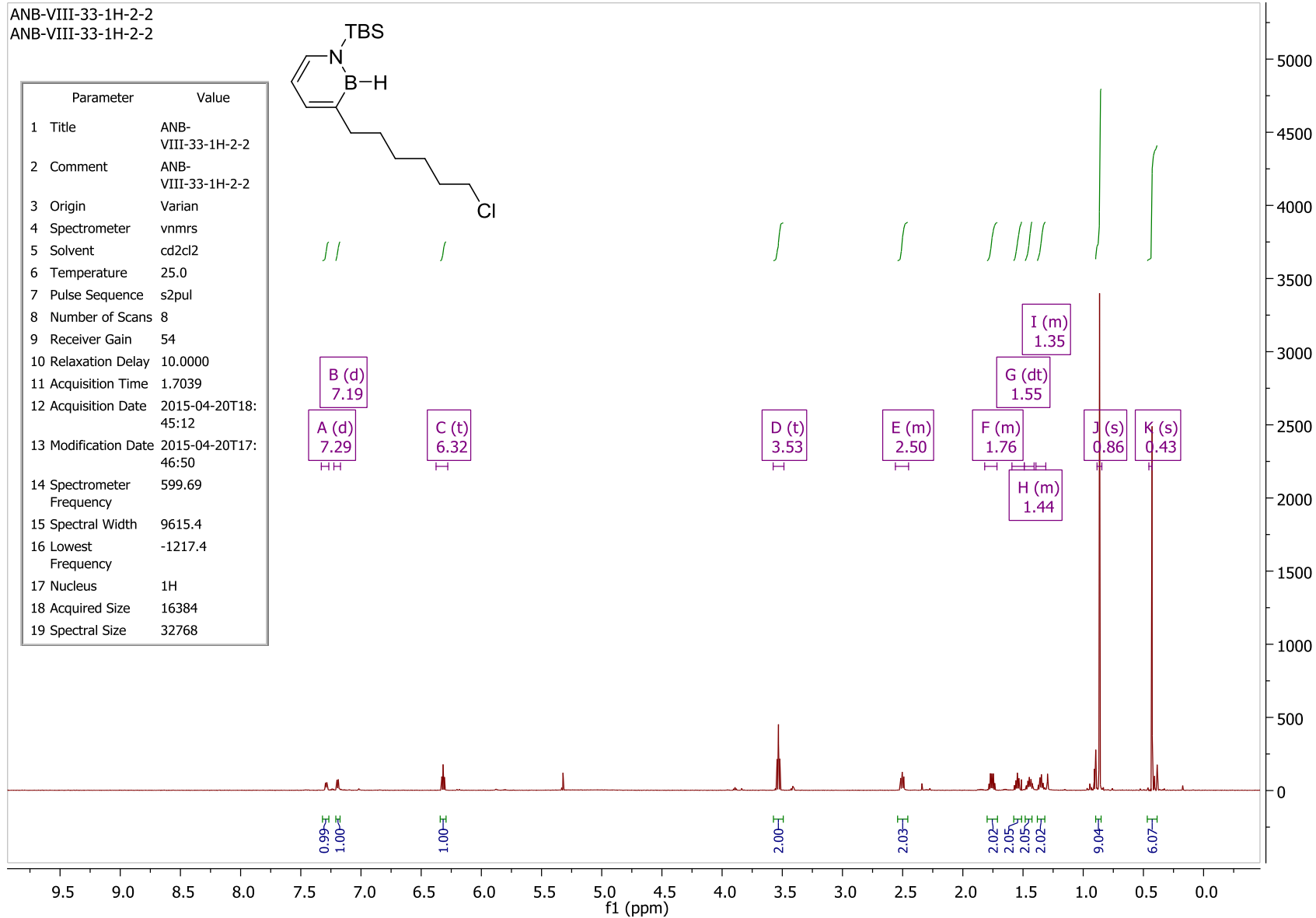
Parameter	Value
1 Title	ANB-VI-39-13C-Pub
2 Comment	ANB-VI-39-13C-Pub
3 Origin	Varian
4 Spectrometer	vnmrs
5 Solvent	cd2cl2
6 Temperature	25.0
7 Pulse Sequence	s2pul
8 Number of Scans	160
9 Receiver Gain	30
10 Relaxation Delay	1.0000
11 Acquisition Time	1.0486
12 Acquisition Date	2014-03-05T16:41:59
13 Modification Date	2014-04-21T13:57:24
14 Spectrometer Frequency	125.71
15 Spectral Width	31250.0
16 Lowest Frequency	-1718.3
17 Nucleus	¹³ C
18 Acquired Size	32768
19 Spectral Size	65536



ANB-VIII-33-1H-2-2
ANB-VIII-33-1H-2-2



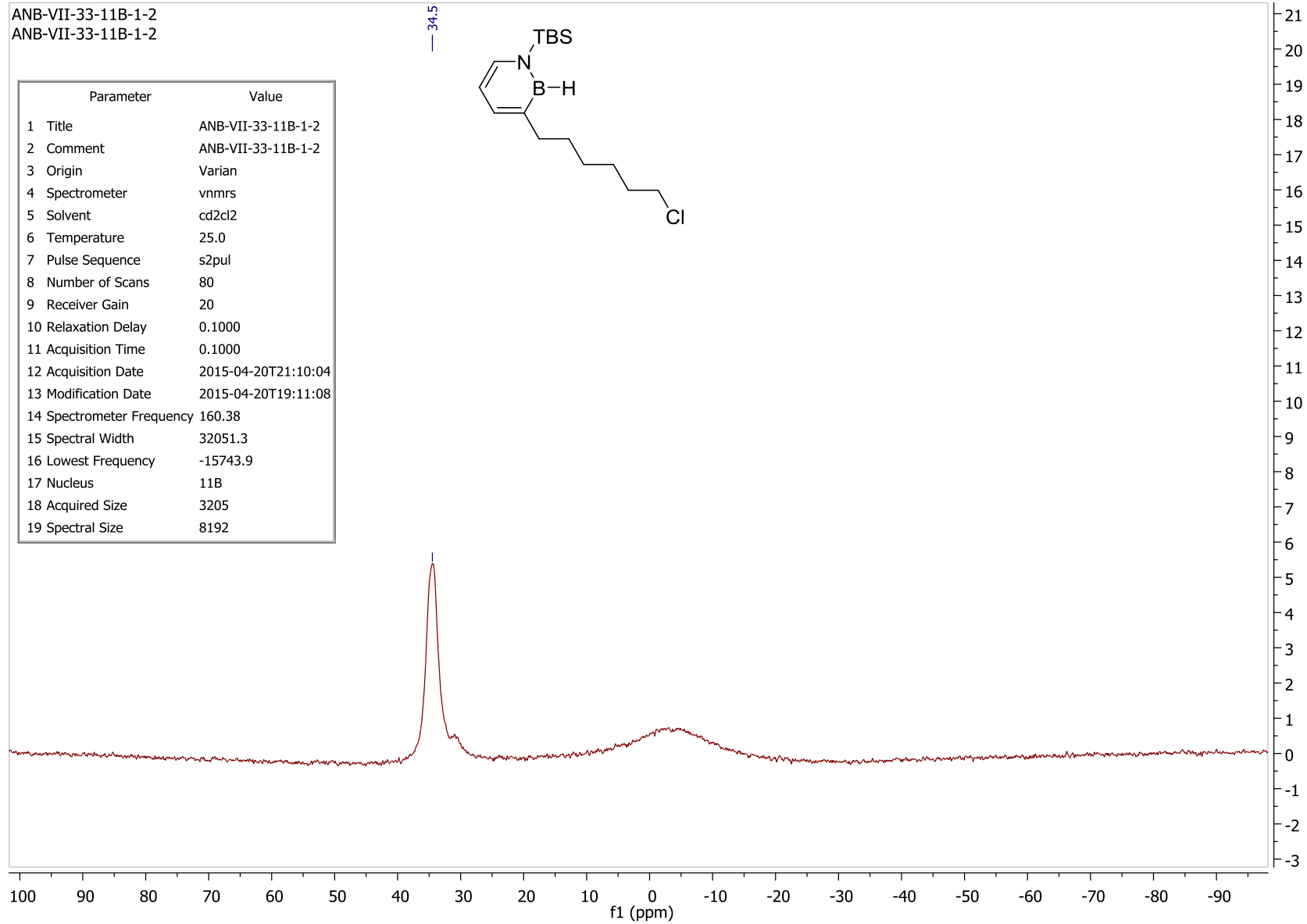
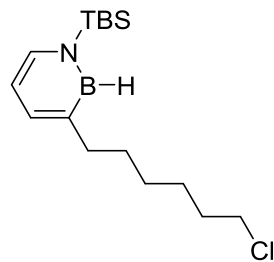
Parameter	Value
1 Title	ANB-VIII-33-1H-2-2
2 Comment	ANB-VIII-33-1H-2-2
3 Origin	Varian
4 Spectrometer	vnmrs
5 Solvent	cd2cl2
6 Temperature	25.0
7 Pulse Sequence	s2pul
8 Number of Scans	8
9 Receiver Gain	54
10 Relaxation Delay	10.0000
11 Acquisition Time	1.7039
12 Acquisition Date	2015-04-20T18:45:12
13 Modification Date	2015-04-20T17:46:50
14 Spectrometer Frequency	599.69
15 Spectral Width	9615.4
16 Lowest Frequency	-1217.4
17 Nucleus	1H
18 Acquired Size	16384
19 Spectral Size	32768



ANB-VII-33-11B-1-2
ANB-VII-33-11B-1-2

Parameter	Value
1 Title	ANB-VII-33-11B-1-2
2 Comment	ANB-VII-33-11B-1-2
3 Origin	Varian
4 Spectrometer	vnmrs
5 Solvent	cd2cl2
6 Temperature	25.0
7 Pulse Sequence	s2pul
8 Number of Scans	80
9 Receiver Gain	20
10 Relaxation Delay	0.1000
11 Acquisition Time	0.1000
12 Acquisition Date	2015-04-20T21:10:04
13 Modification Date	2015-04-20T19:11:08
14 Spectrometer Frequency	160.38
15 Spectral Width	32051.3
16 Lowest Frequency	-15743.9
17 Nucleus	11B
18 Acquired Size	3205
19 Spectral Size	8192

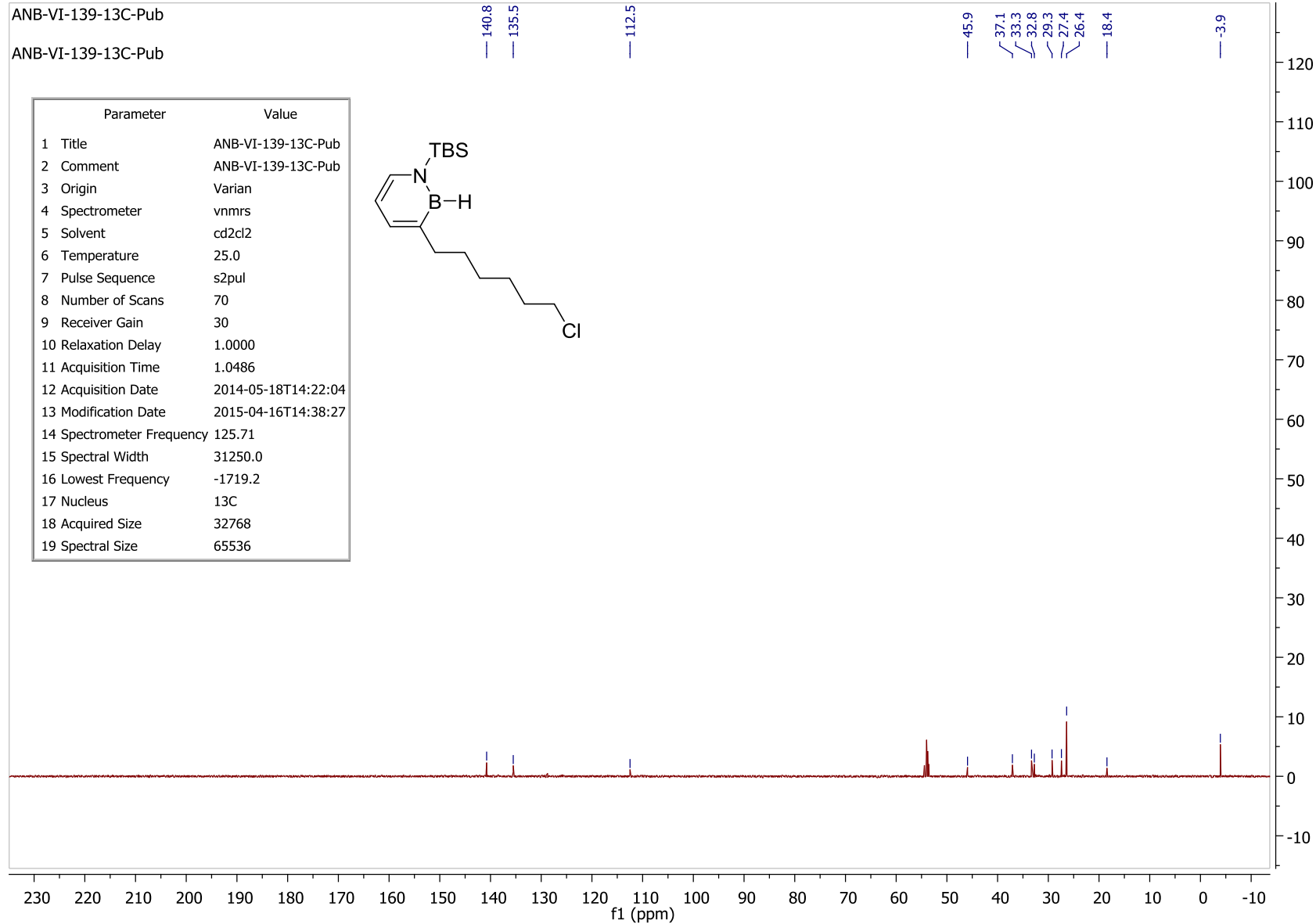
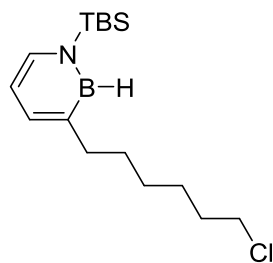
— 34.5



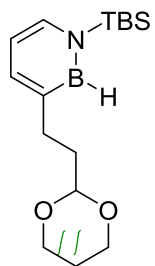
ANB-VI-139-13C-Pub

ANB-VI-139-13C-Pub

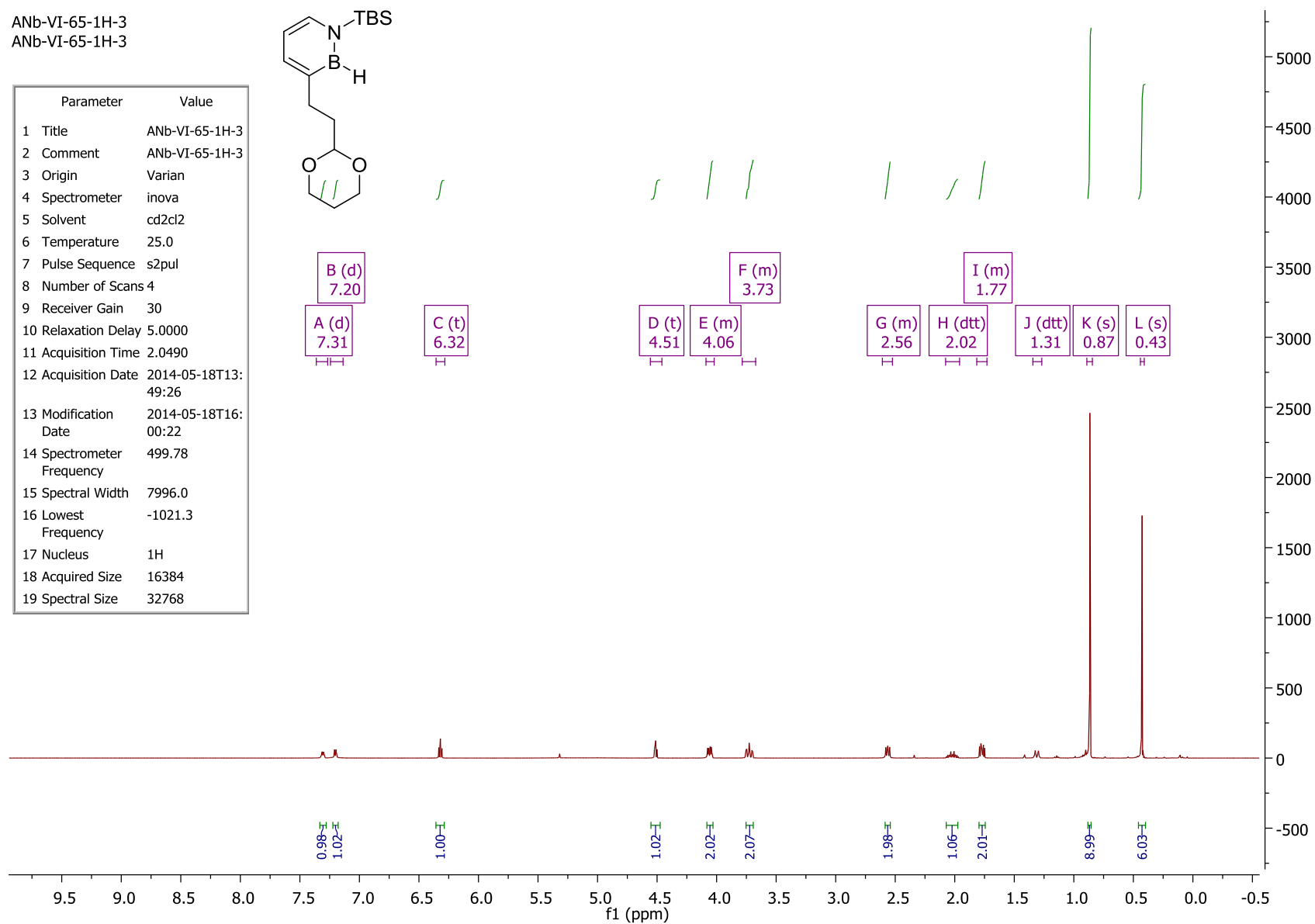
Parameter	Value
1 Title	ANB-VI-139-13C-Pub
2 Comment	ANB-VI-139-13C-Pub
3 Origin	Varian
4 Spectrometer	vnmrs
5 Solvent	cd2cl2
6 Temperature	25.0
7 Pulse Sequence	s2pul
8 Number of Scans	70
9 Receiver Gain	30
10 Relaxation Delay	1.0000
11 Acquisition Time	1.0486
12 Acquisition Date	2014-05-18T14:22:04
13 Modification Date	2015-04-16T14:38:27
14 Spectrometer Frequency	125.71
15 Spectral Width	31250.0
16 Lowest Frequency	-1719.2
17 Nucleus	13C
18 Acquired Size	32768
19 Spectral Size	65536



ANb-VI-65-1H-3
ANb-VI-65-1H-3

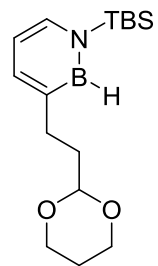


Parameter	Value
1 Title	ANb-VI-65-1H-3
2 Comment	ANb-VI-65-1H-3
3 Origin	Varian
4 Spectrometer	inova
5 Solvent	cd2cl2
6 Temperature	25.0
7 Pulse Sequence	s2pul
8 Number of Scans	4
9 Receiver Gain	30
10 Relaxation Delay	5.0000
11 Acquisition Time	2.0490
12 Acquisition Date	2014-05-18T13:49:26
13 Modification Date	2014-05-18T16:00:22
14 Spectrometer Frequency	499.78
15 Spectral Width	7996.0
16 Lowest Frequency	-1021.3
17 Nucleus	1H
18 Acquired Size	16384
19 Spectral Size	32768

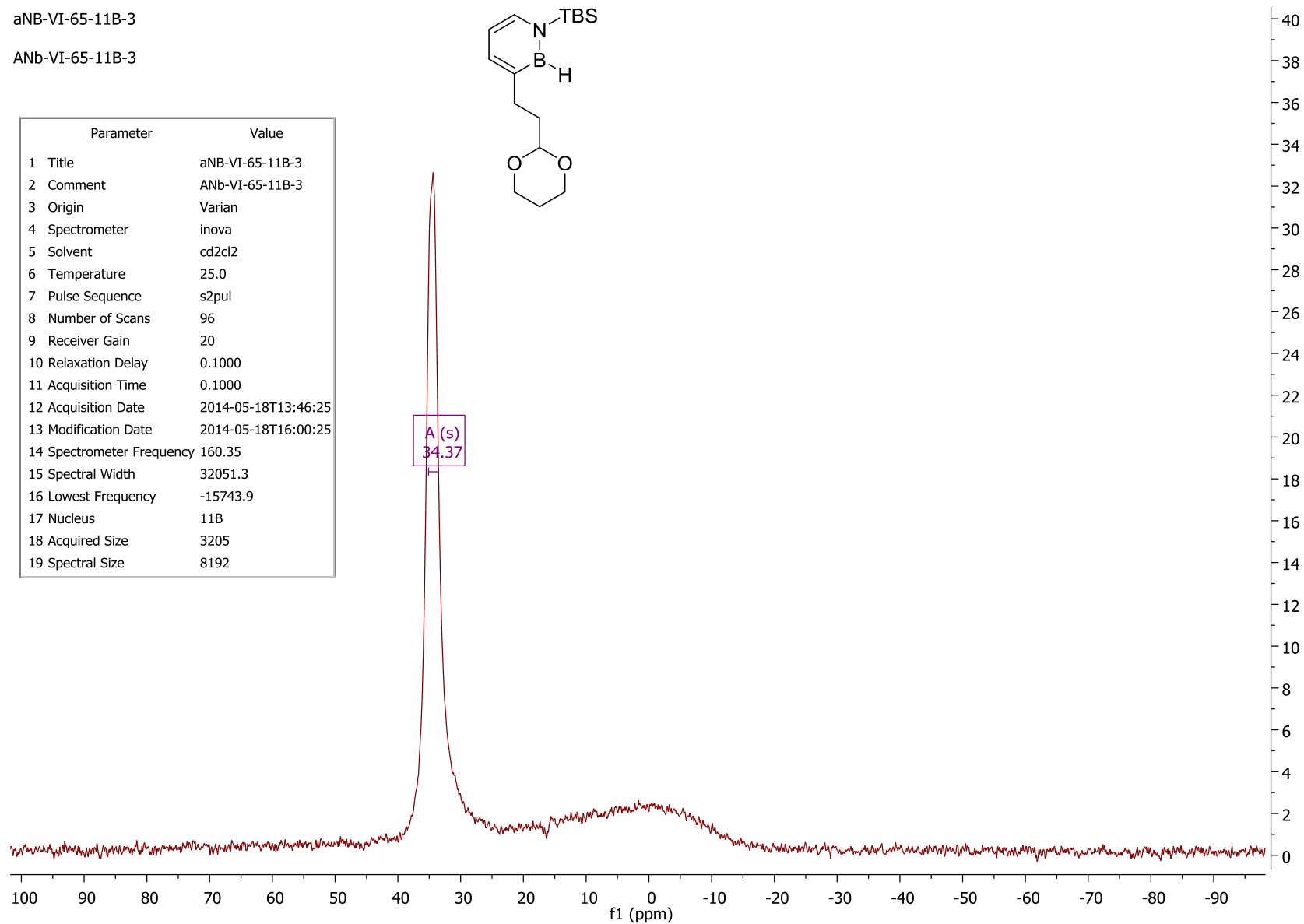


aNB-VI-65-11B-3

ANb-VI-65-11B-3

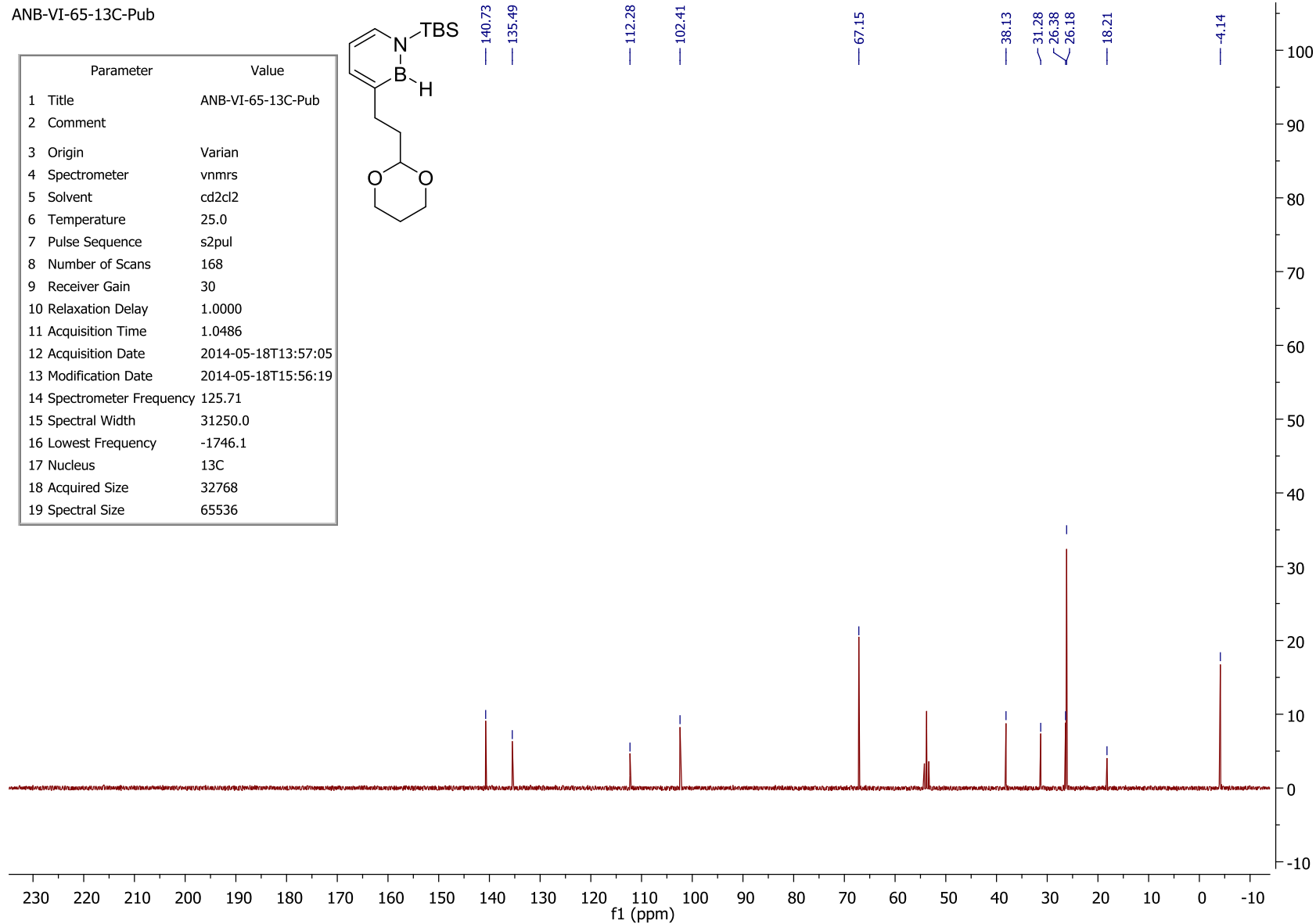
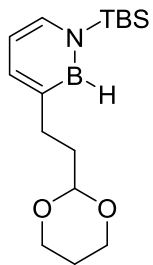


Parameter	Value
1 Title	aNB-VI-65-11B-3
2 Comment	ANb-VI-65-11B-3
3 Origin	Varian
4 Spectrometer	inova
5 Solvent	cd2cl2
6 Temperature	25.0
7 Pulse Sequence	s2pul
8 Number of Scans	96
9 Receiver Gain	20
10 Relaxation Delay	0.1000
11 Acquisition Time	0.1000
12 Acquisition Date	2014-05-18T13:46:25
13 Modification Date	2014-05-18T16:00:25
14 Spectrometer Frequency	160.35
15 Spectral Width	32051.3
16 Lowest Frequency	-15743.9
17 Nucleus	11B
18 Acquired Size	3205
19 Spectral Size	8192

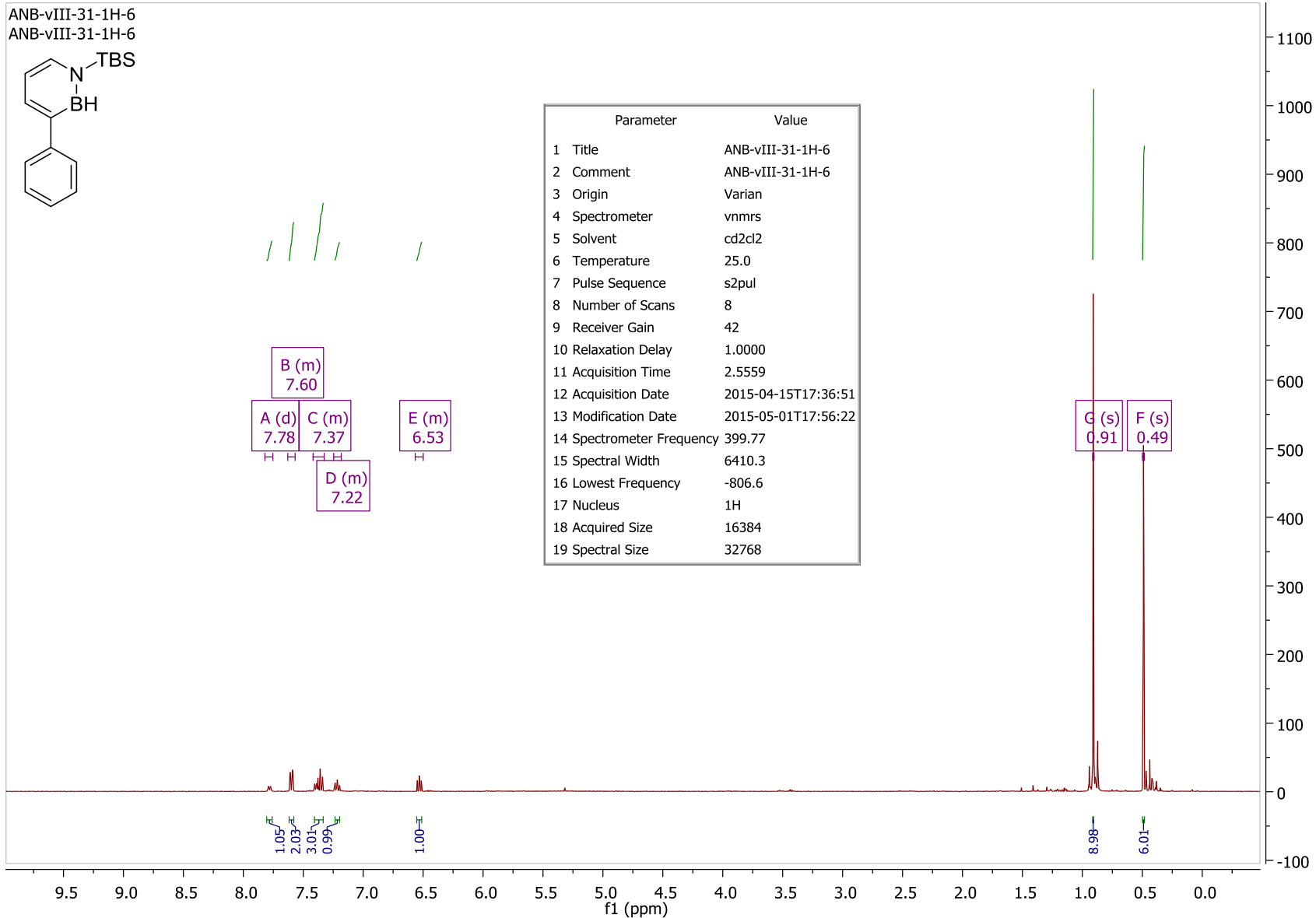
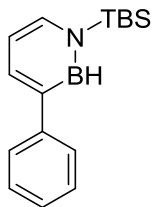


ANB-VI-65-13C-Pub

Parameter	Value
1 Title	ANB-VI-65-13C-Pub
2 Comment	
3 Origin	Varian
4 Spectrometer	vnmrs
5 Solvent	cd2cl2
6 Temperature	25.0
7 Pulse Sequence	s2pul
8 Number of Scans	168
9 Receiver Gain	30
10 Relaxation Delay	1.0000
11 Acquisition Time	1.0486
12 Acquisition Date	2014-05-18T13:57:05
13 Modification Date	2014-05-18T15:56:19
14 Spectrometer Frequency	125.71
15 Spectral Width	31250.0
16 Lowest Frequency	-1746.1
17 Nucleus	13C
18 Acquired Size	32768
19 Spectral Size	65536

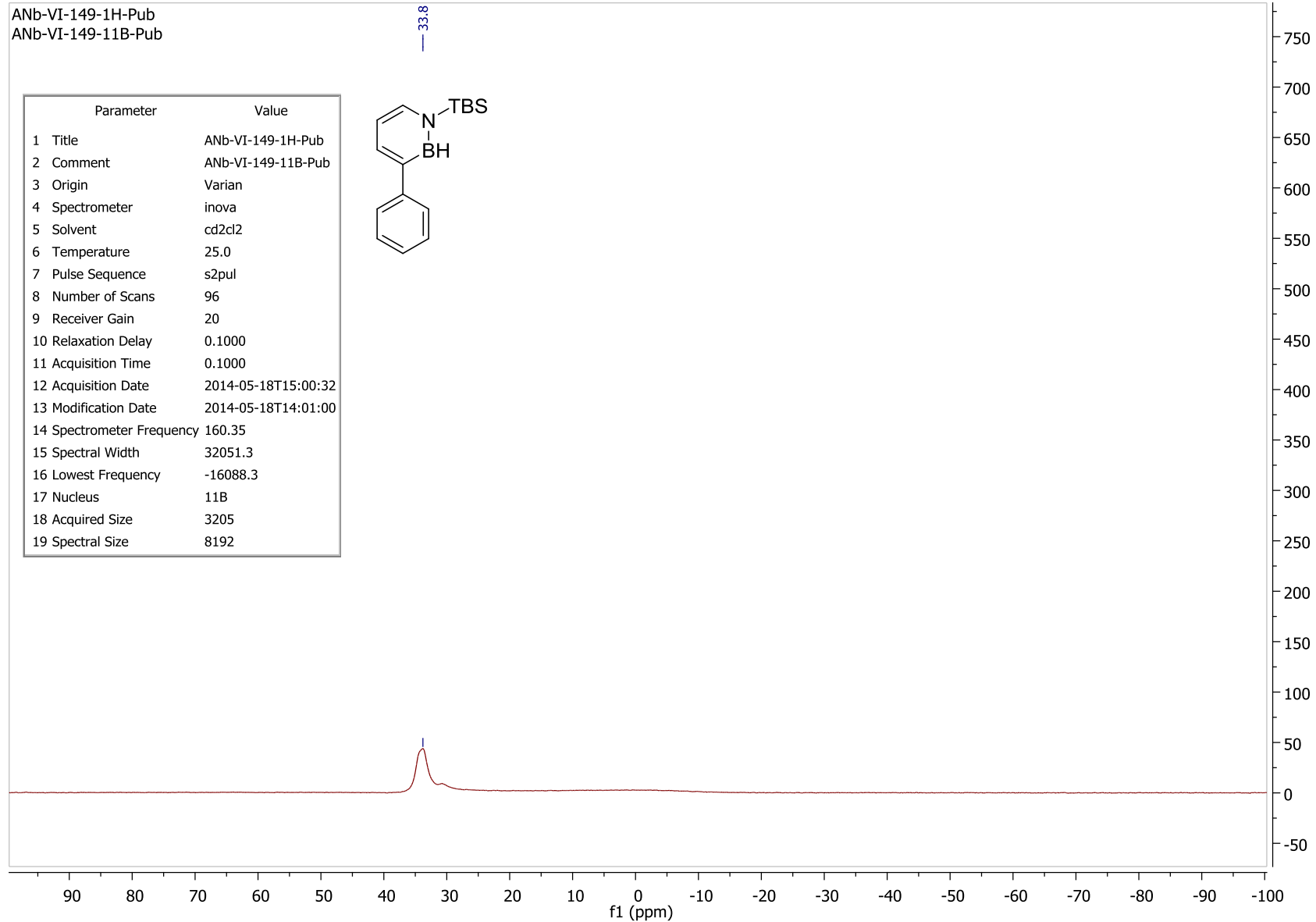
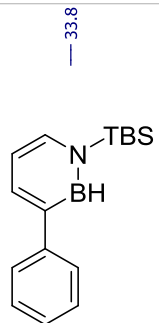


ANB-vIII-31-1H-6
ANB-vIII-31-1H-6



ANb-VI-149-1H-Pub
ANb-VI-149-11B-Pub

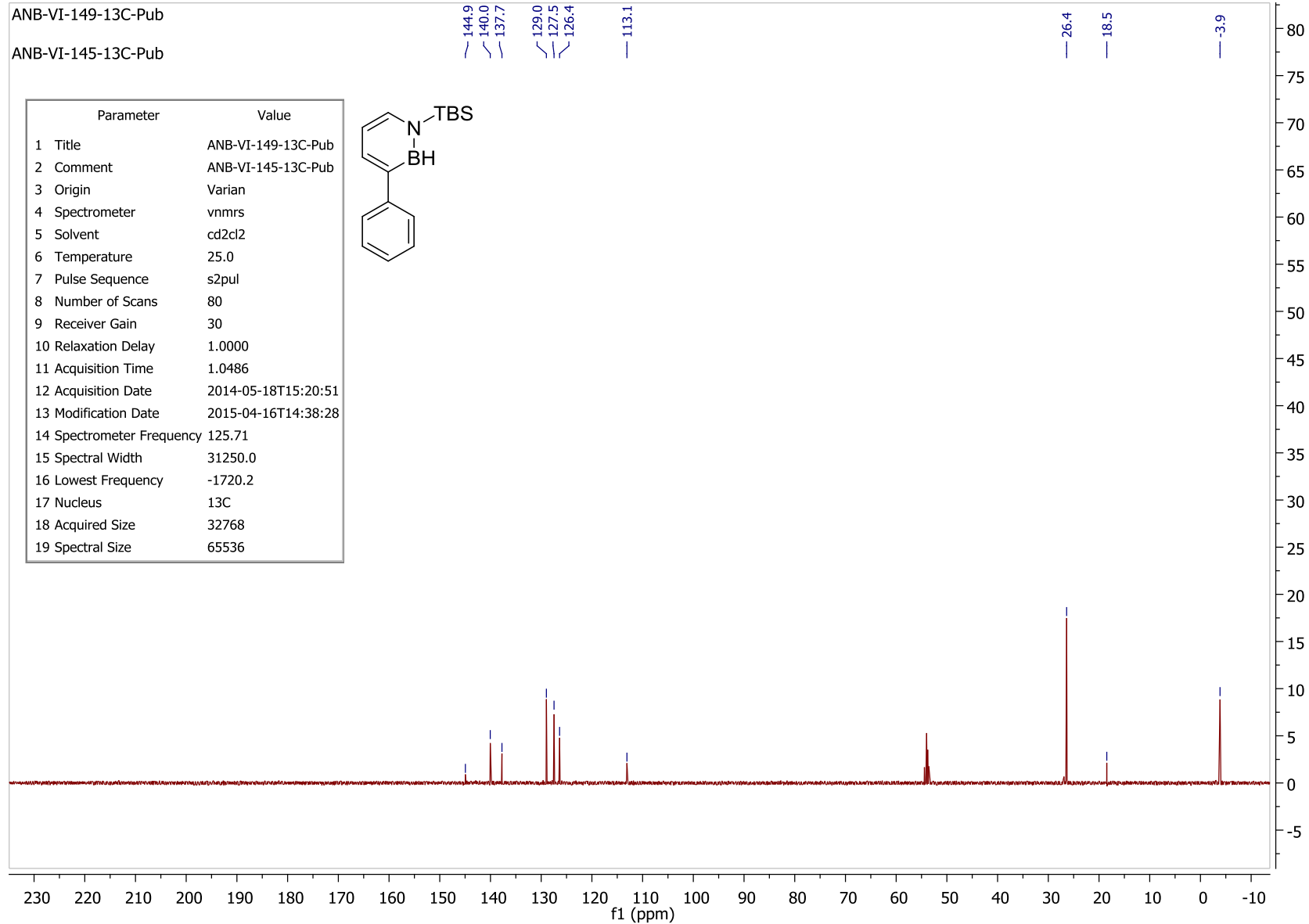
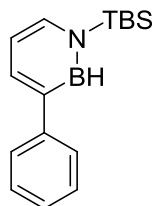
Parameter	Value
1 Title	ANb-VI-149-1H-Pub
2 Comment	ANb-VI-149-11B-Pub
3 Origin	Varian
4 Spectrometer	inova
5 Solvent	cd2cl2
6 Temperature	25.0
7 Pulse Sequence	s2pul
8 Number of Scans	96
9 Receiver Gain	20
10 Relaxation Delay	0.1000
11 Acquisition Time	0.1000
12 Acquisition Date	2014-05-18T15:00:32
13 Modification Date	2014-05-18T14:01:00
14 Spectrometer Frequency	160.35
15 Spectral Width	32051.3
16 Lowest Frequency	-16088.3
17 Nucleus	11B
18 Acquired Size	3205
19 Spectral Size	8192



ANB-VI-149-13C-Pub

ANB-VI-145-13C-Pub

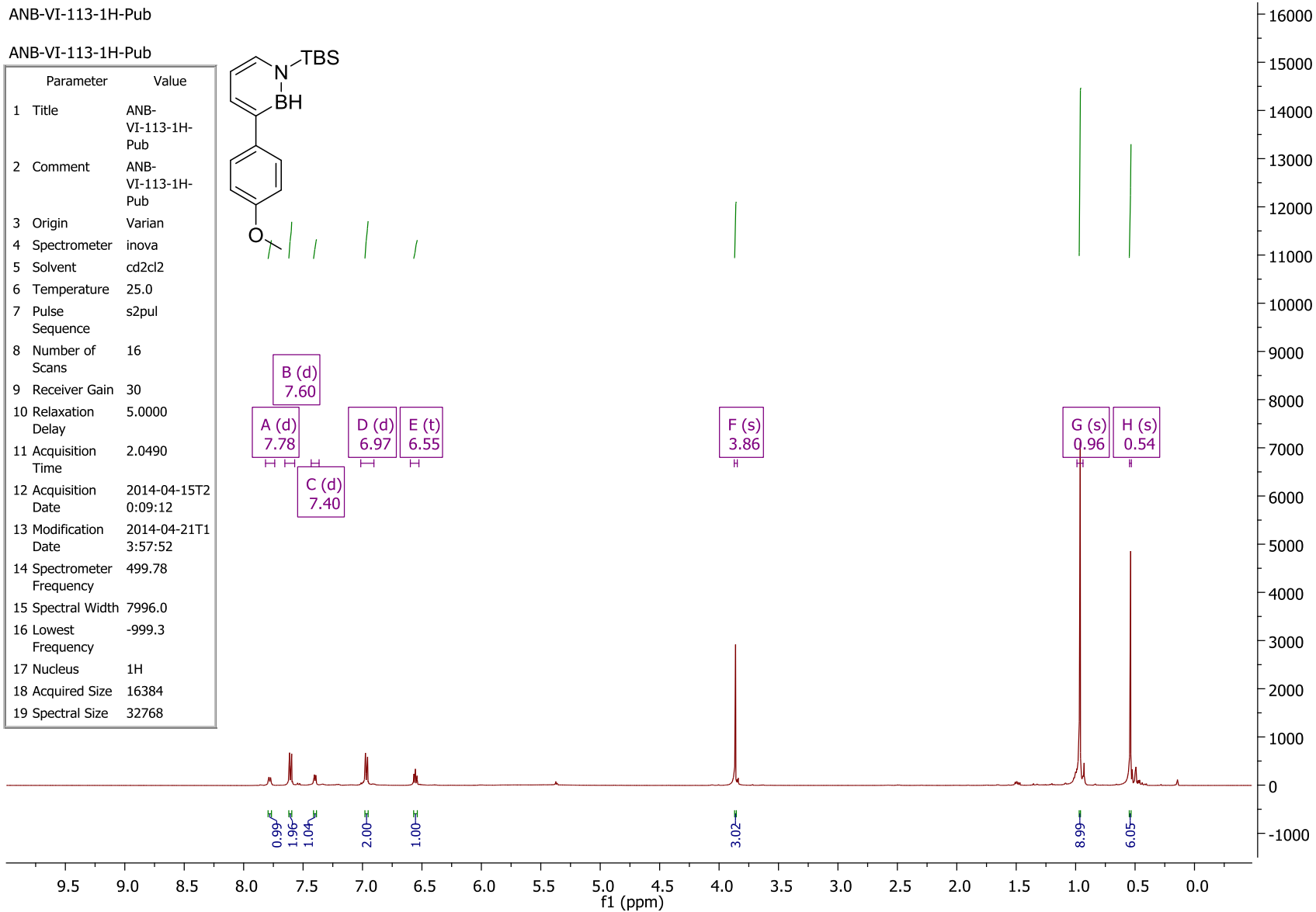
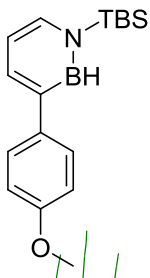
Parameter	Value
1 Title	ANB-VI-149-13C-Pub
2 Comment	ANB-VI-145-13C-Pub
3 Origin	Varian
4 Spectrometer	nmrs
5 Solvent	cd2cl2
6 Temperature	25.0
7 Pulse Sequence	s2pul
8 Number of Scans	80
9 Receiver Gain	30
10 Relaxation Delay	1.0000
11 Acquisition Time	1.0486
12 Acquisition Date	2014-05-18T15:20:51
13 Modification Date	2015-04-16T14:38:28
14 Spectrometer Frequency	125.71
15 Spectral Width	31250.0
16 Lowest Frequency	-1720.2
17 Nucleus	13C
18 Acquired Size	32768
19 Spectral Size	65536



ANB-VI-113-1H-Pub

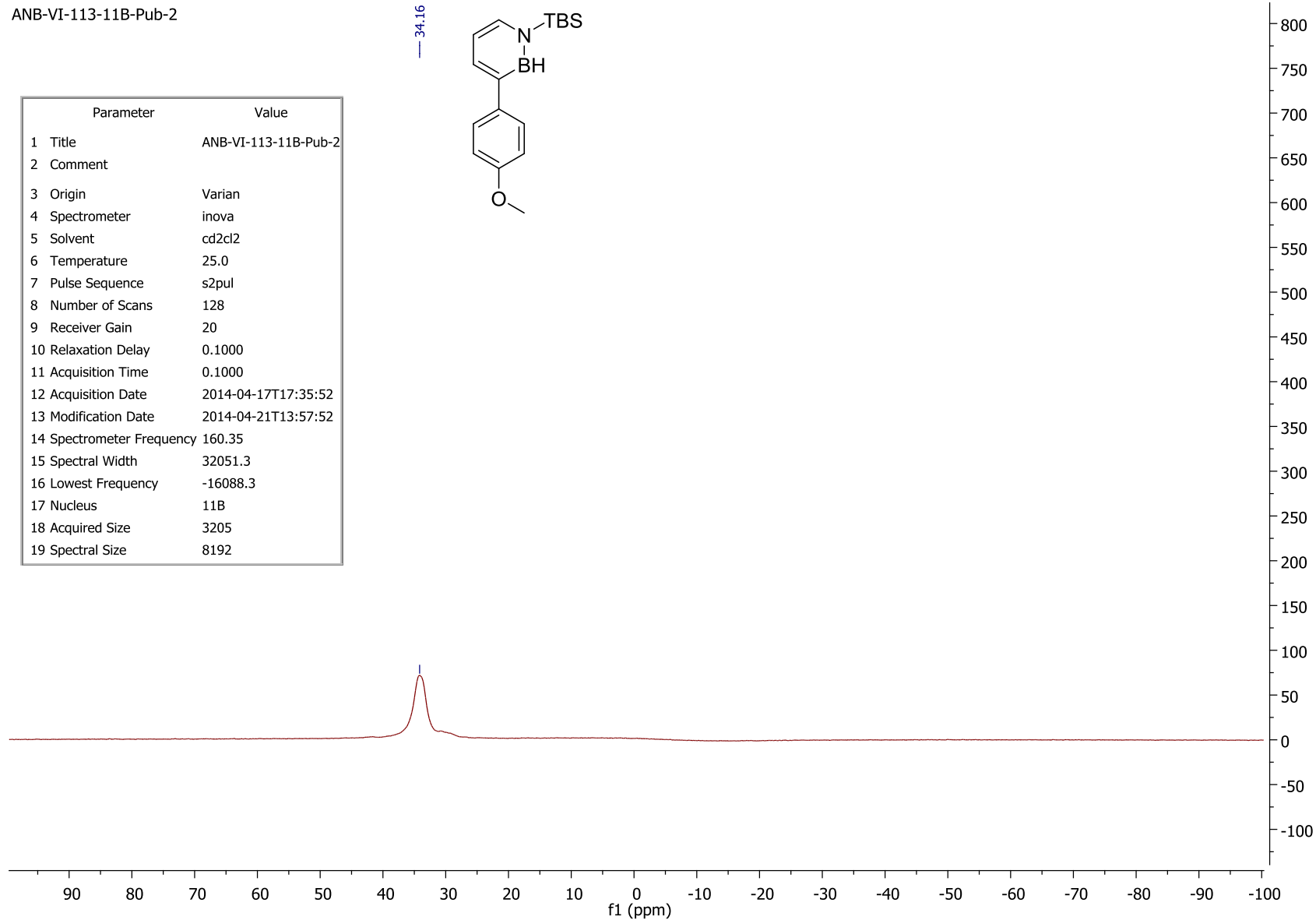
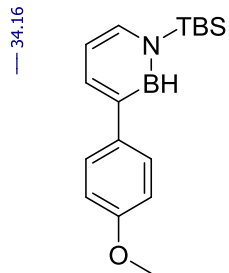
ANB-VI-113-1H-Pub

Parameter	Value
1 Title	ANB-VI-113-1H-Pub
2 Comment	ANB-VI-113-1H-Pub
3 Origin	Varian
4 Spectrometer	inova
5 Solvent	cd2cl2
6 Temperature	25.0
7 Pulse Sequence	s2pul
8 Number of Scans	16
9 Receiver Gain	30
10 Relaxation Delay	5.0000
11 Acquisition Time	2.0490
12 Acquisition Date	2014-04-15T2 0:09:12
13 Modification Date	2014-04-21T1 3:57:52
14 Spectrometer Frequency	499.78
15 Spectral Width	7996.0
16 Lowest Frequency	-999.3
17 Nucleus	1H
18 Acquired Size	16384
19 Spectral Size	32768



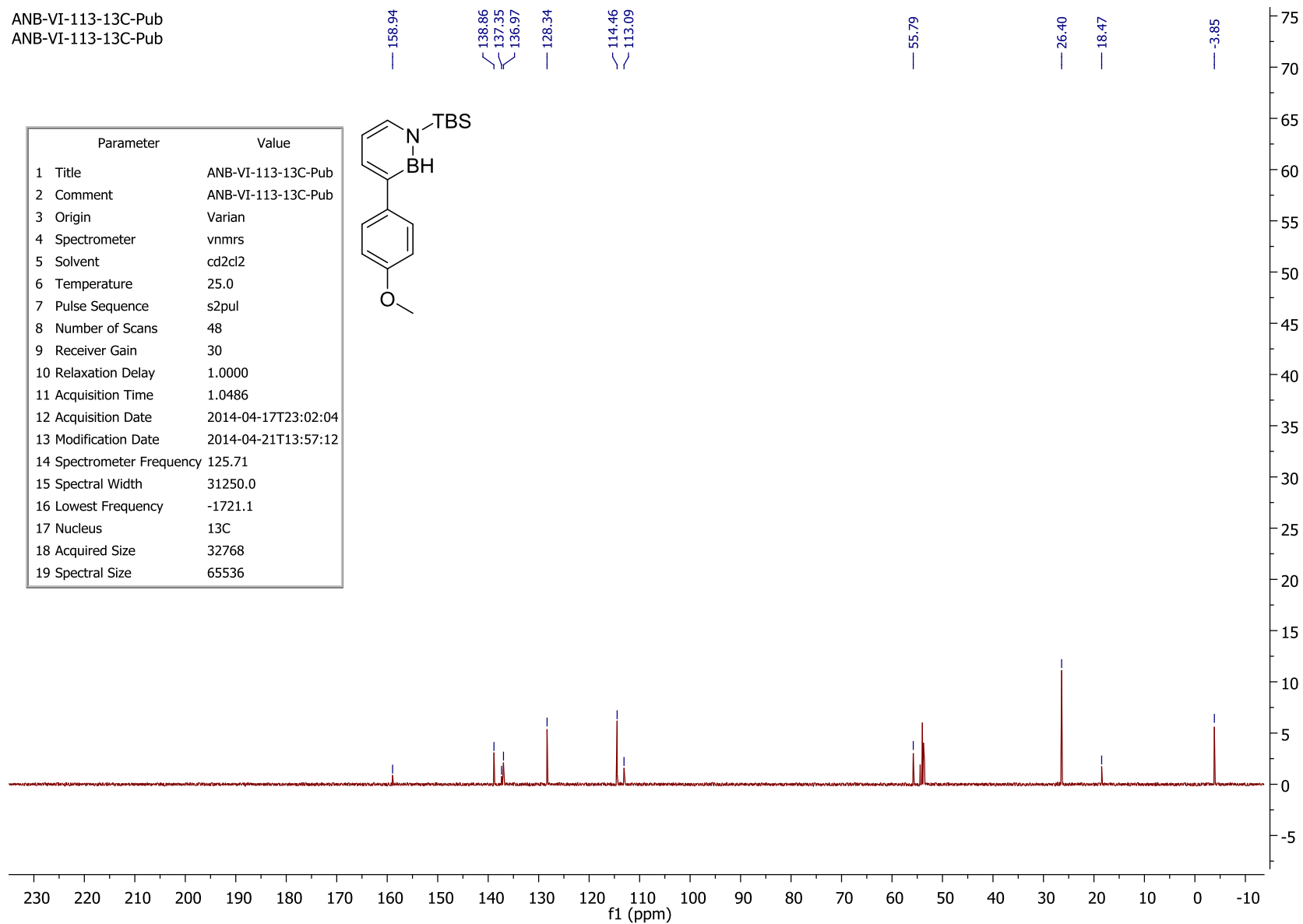
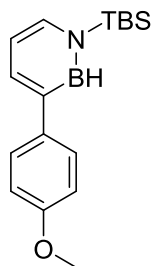
ANB-VI-113-11B-Pub-2

Parameter	Value
1 Title	ANB-VI-113-11B-Pub-2
2 Comment	
3 Origin	Varian
4 Spectrometer	inova
5 Solvent	cd2cl2
6 Temperature	25.0
7 Pulse Sequence	s2pul
8 Number of Scans	128
9 Receiver Gain	20
10 Relaxation Delay	0.1000
11 Acquisition Time	0.1000
12 Acquisition Date	2014-04-17T17:35:52
13 Modification Date	2014-04-21T13:57:52
14 Spectrometer Frequency	160.35
15 Spectral Width	32051.3
16 Lowest Frequency	-16088.3
17 Nucleus	11B
18 Acquired Size	3205
19 Spectral Size	8192



ANB-VI-113-13C-Pub
ANB-VI-113-13C-Pub

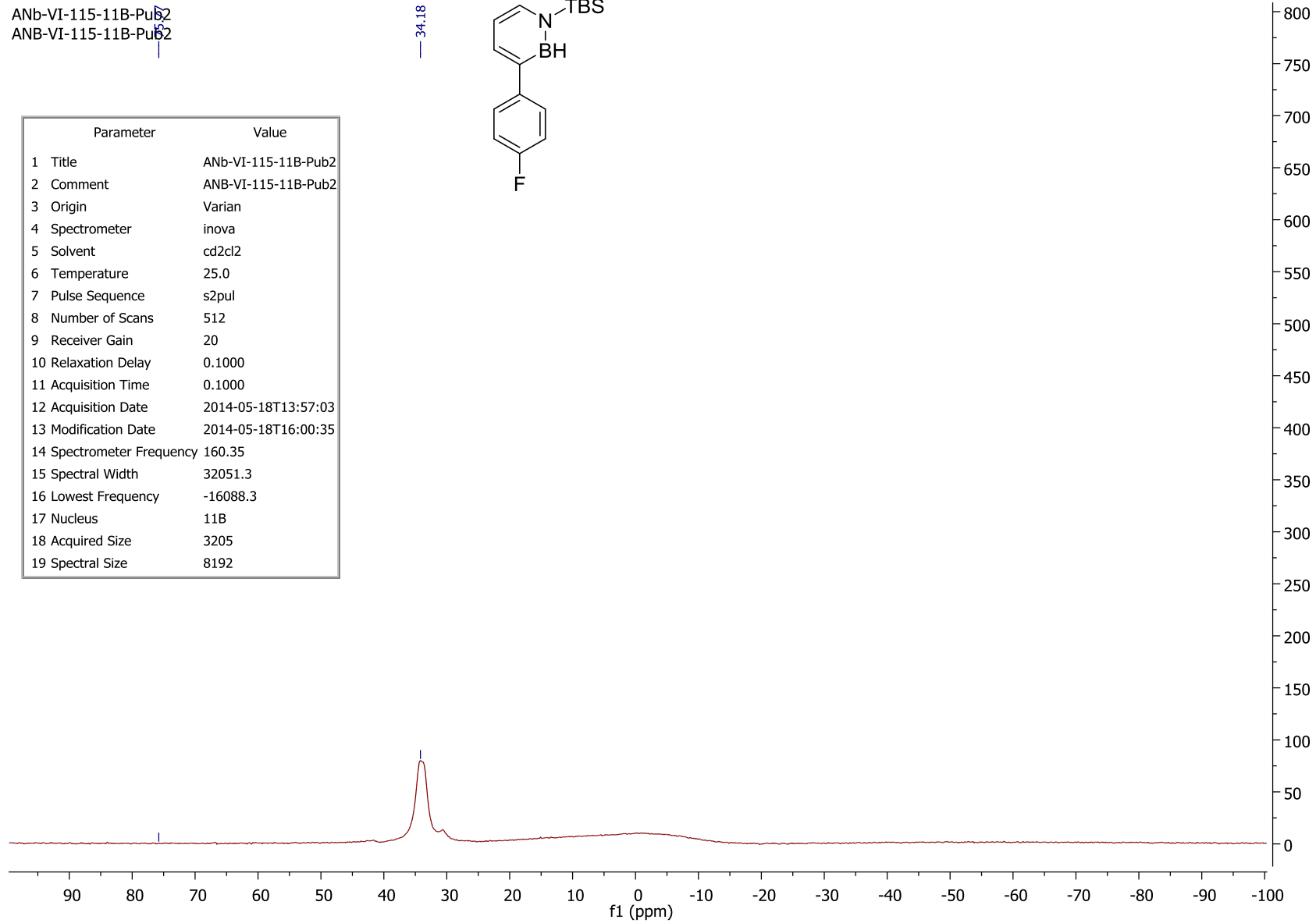
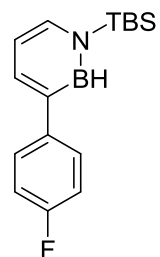
Parameter	Value
1 Title	ANB-VI-113-13C-Pub
2 Comment	ANB-VI-113-13C-Pub
3 Origin	Varian
4 Spectrometer	vnmrs
5 Solvent	cd2cl2
6 Temperature	25.0
7 Pulse Sequence	s2pul
8 Number of Scans	48
9 Receiver Gain	30
10 Relaxation Delay	1.0000
11 Acquisition Time	1.0486
12 Acquisition Date	2014-04-17T23:02:04
13 Modification Date	2014-04-21T13:57:12
14 Spectrometer Frequency	125.71
15 Spectral Width	31250.0
16 Lowest Frequency	-1721.1
17 Nucleus	13C
18 Acquired Size	32768
19 Spectral Size	65536



ANb-VI-115-11B-Pub2
ANB-VI-115-11B-Pub2

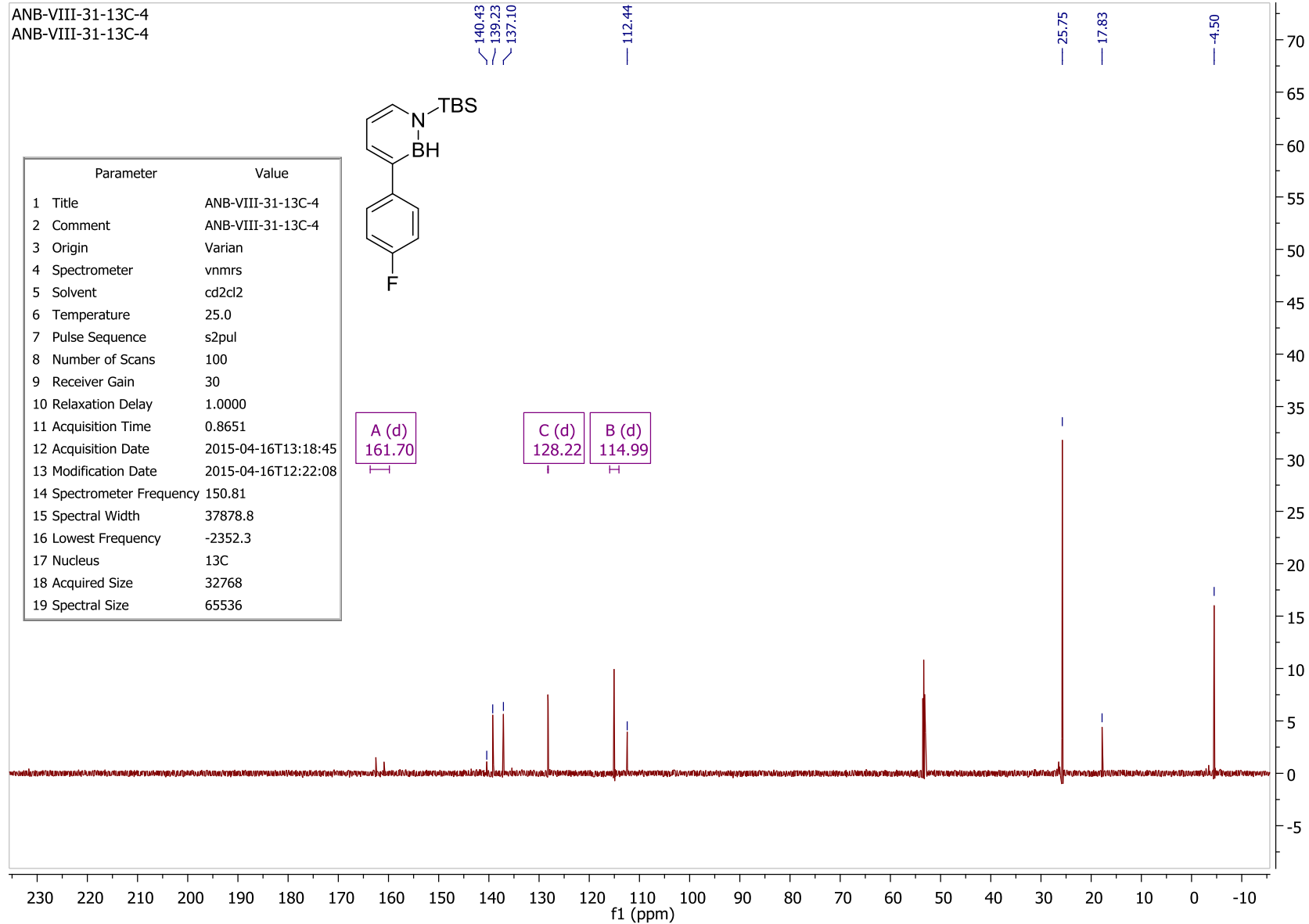
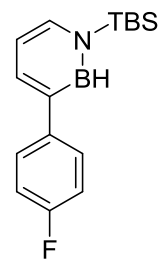
Parameter	Value
1 Title	ANb-VI-115-11B-Pub2
2 Comment	ANB-VI-115-11B-Pub2
3 Origin	Varian
4 Spectrometer	inova
5 Solvent	cd2cl2
6 Temperature	25.0
7 Pulse Sequence	s2pul
8 Number of Scans	512
9 Receiver Gain	20
10 Relaxation Delay	0.1000
11 Acquisition Time	0.1000
12 Acquisition Date	2014-05-18T13:57:03
13 Modification Date	2014-05-18T16:00:35
14 Spectrometer Frequency	160.35
15 Spectral Width	32051.3
16 Lowest Frequency	-16088.3
17 Nucleus	11B
18 Acquired Size	3205
19 Spectral Size	8192

34.18

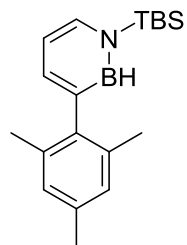


ANB-VIII-31-13C-4
ANB-VIII-31-13C-4

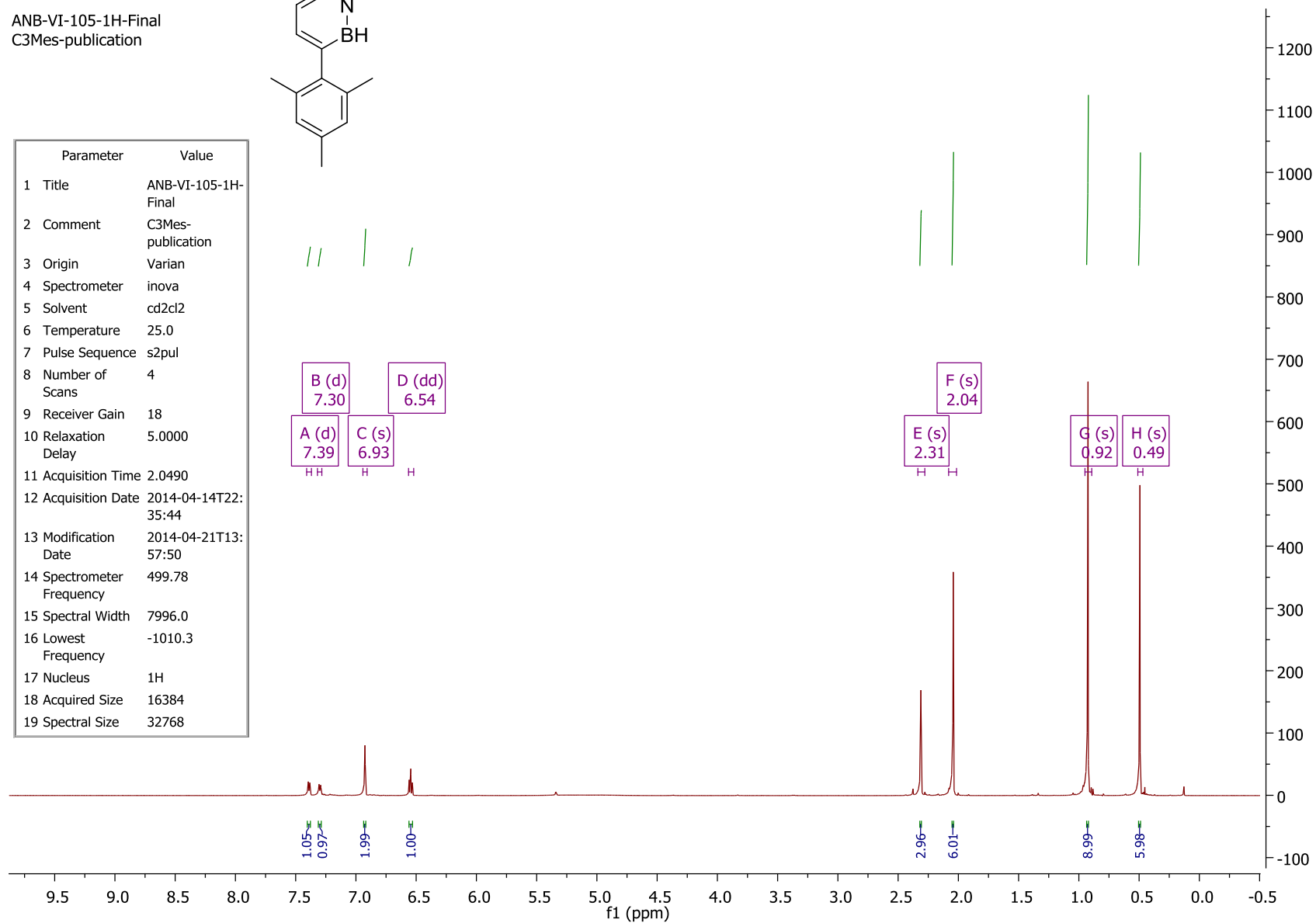
Parameter	Value
1 Title	ANB-VIII-31-13C-4
2 Comment	ANB-VIII-31-13C-4
3 Origin	Varian
4 Spectrometer	vnmrs
5 Solvent	cd2cl2
6 Temperature	25.0
7 Pulse Sequence	s2pul
8 Number of Scans	100
9 Receiver Gain	30
10 Relaxation Delay	1.0000
11 Acquisition Time	0.8651
12 Acquisition Date	2015-04-16T13:18:45
13 Modification Date	2015-04-16T12:22:08
14 Spectrometer Frequency	150.81
15 Spectral Width	37878.8
16 Lowest Frequency	-2352.3
17 Nucleus	13C
18 Acquired Size	32768
19 Spectral Size	65536



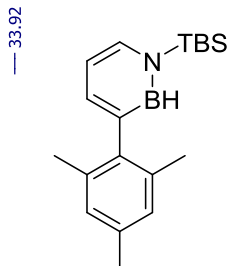
ANB-VI-105-1H-Final
C3Mes-publication



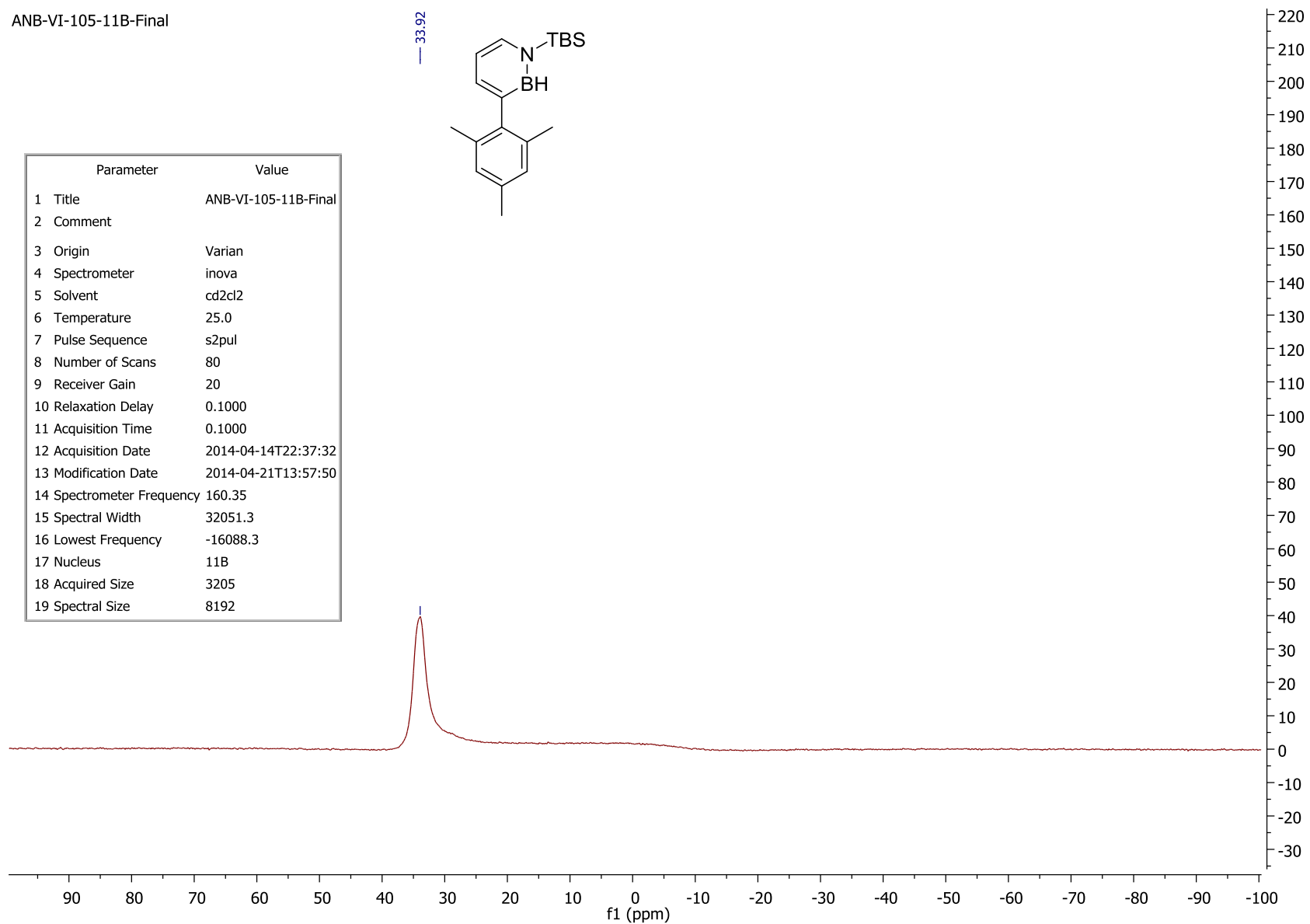
Parameter	Value
1 Title	ANB-VI-105-1H-Final
2 Comment	C3Mes-publication
3 Origin	Varian
4 Spectrometer	inova
5 Solvent	cd2cl2
6 Temperature	25.0
7 Pulse Sequence	s2pul
8 Number of Scans	4
9 Receiver Gain	18
10 Relaxation Delay	5.0000
11 Acquisition Time	2.0490
12 Acquisition Date	2014-04-14T22:35:44
13 Modification Date	2014-04-21T13:57:50
14 Spectrometer Frequency	499.78
15 Spectral Width	7996.0
16 Lowest Frequency	-1010.3
17 Nucleus	1H
18 Acquired Size	16384
19 Spectral Size	32768



ANB-VI-105-11B-Final

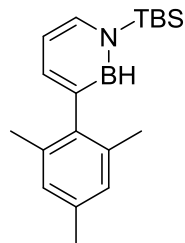


Parameter	Value
1 Title	ANB-VI-105-11B-Final
2 Comment	
3 Origin	Varian
4 Spectrometer	inova
5 Solvent	cd2cl2
6 Temperature	25.0
7 Pulse Sequence	s2pul
8 Number of Scans	80
9 Receiver Gain	20
10 Relaxation Delay	0.1000
11 Acquisition Time	0.1000
12 Acquisition Date	2014-04-14T22:37:32
13 Modification Date	2014-04-21T13:57:50
14 Spectrometer Frequency	160.35
15 Spectral Width	32051.3
16 Lowest Frequency	-16088.3
17 Nucleus	11B
18 Acquired Size	3205
19 Spectral Size	8192

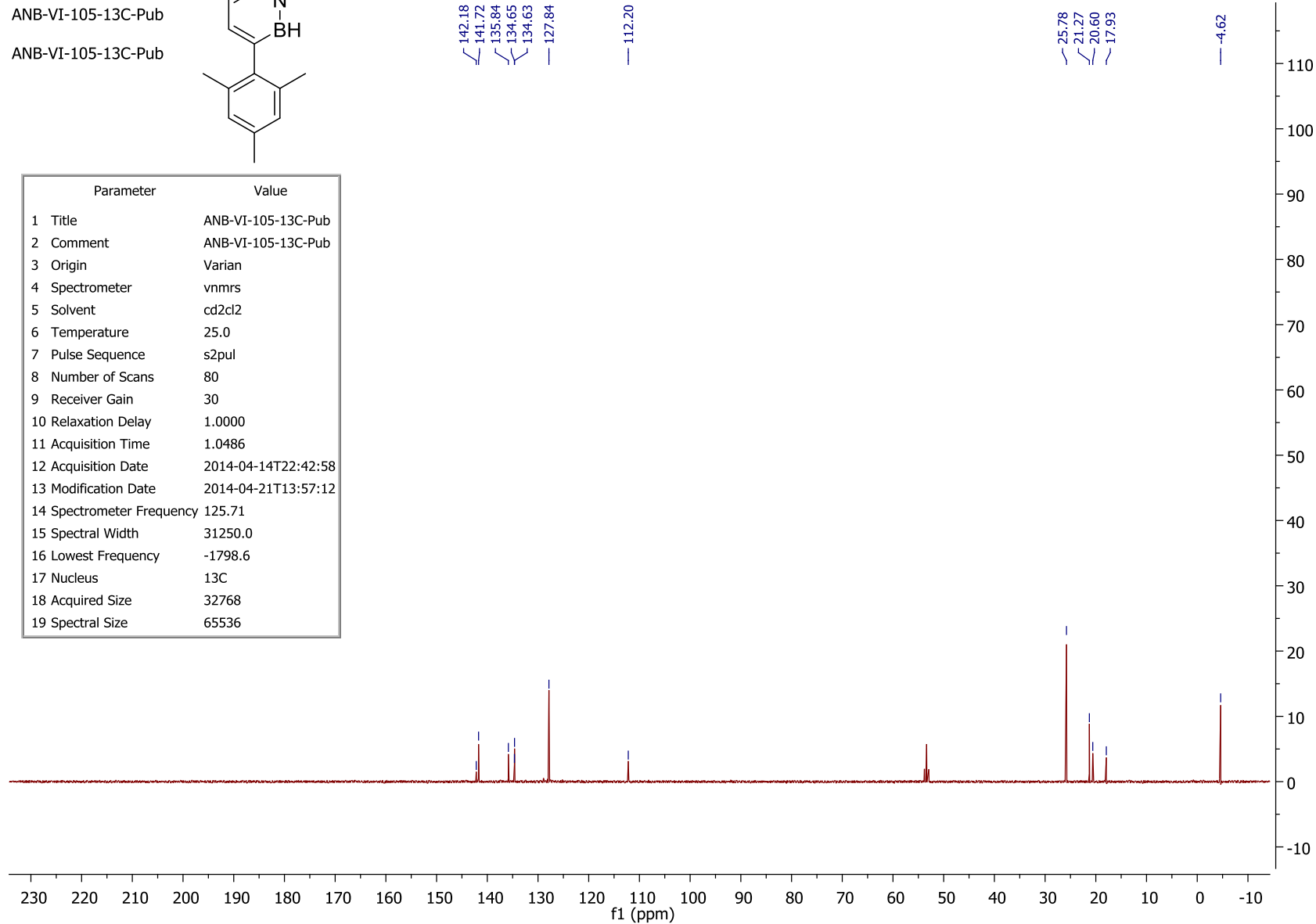


ANB-VI-105-13C-Pub

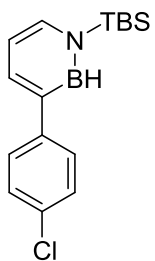
ANB-VI-105-13C-Pub



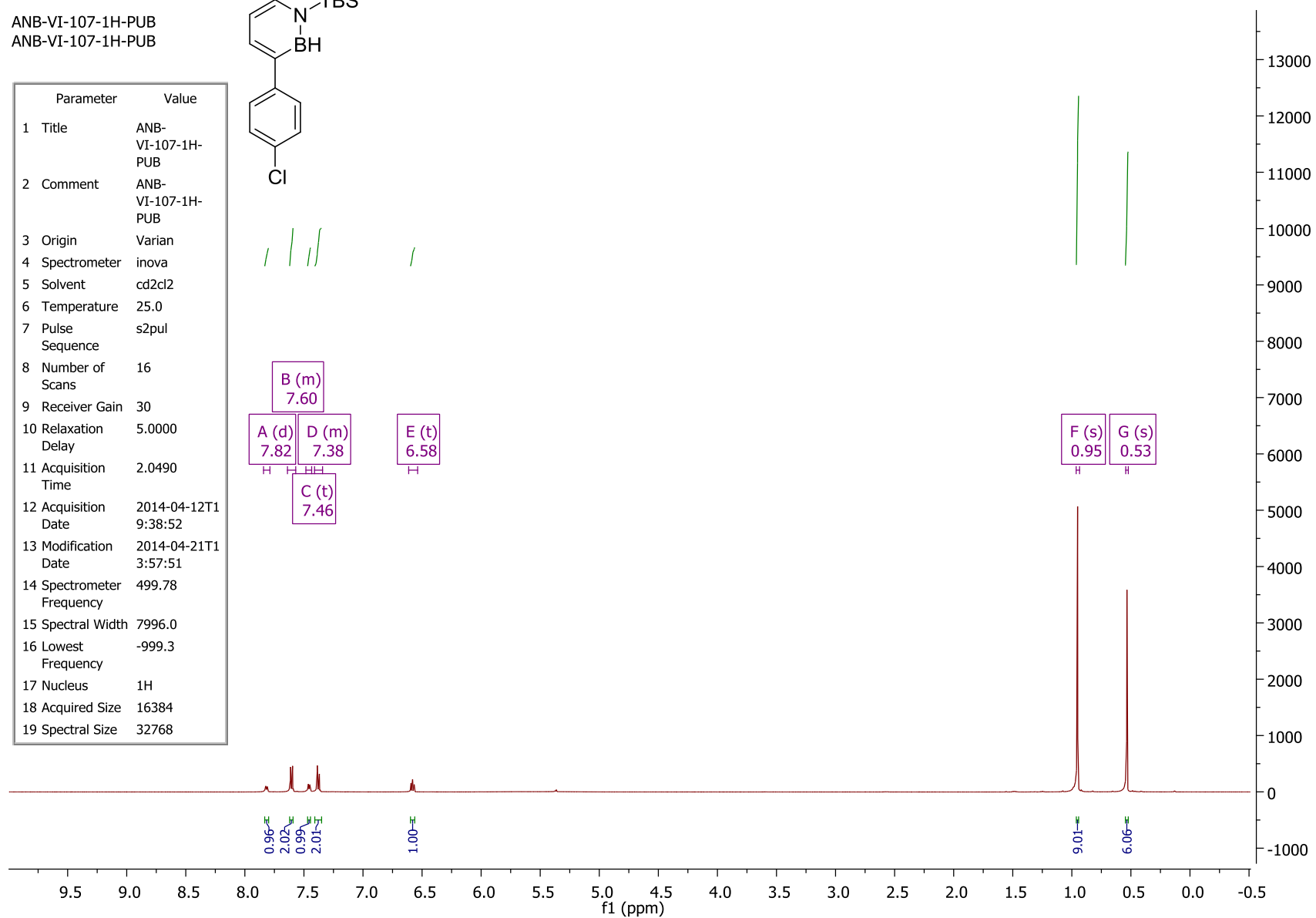
Parameter	Value
1 Title	ANB-VI-105-13C-Pub
2 Comment	ANB-VI-105-13C-Pub
3 Origin	Varian
4 Spectrometer	vnmrs
5 Solvent	cd2cl2
6 Temperature	25.0
7 Pulse Sequence	s2pul
8 Number of Scans	80
9 Receiver Gain	30
10 Relaxation Delay	1.0000
11 Acquisition Time	1.0486
12 Acquisition Date	2014-04-14T22:42:58
13 Modification Date	2014-04-21T13:57:12
14 Spectrometer Frequency	125.71
15 Spectral Width	31250.0
16 Lowest Frequency	-1798.6
17 Nucleus	13C
18 Acquired Size	32768
19 Spectral Size	65536



ANB-VI-107-1H-PUB
ANB-VI-107-1H-PUB

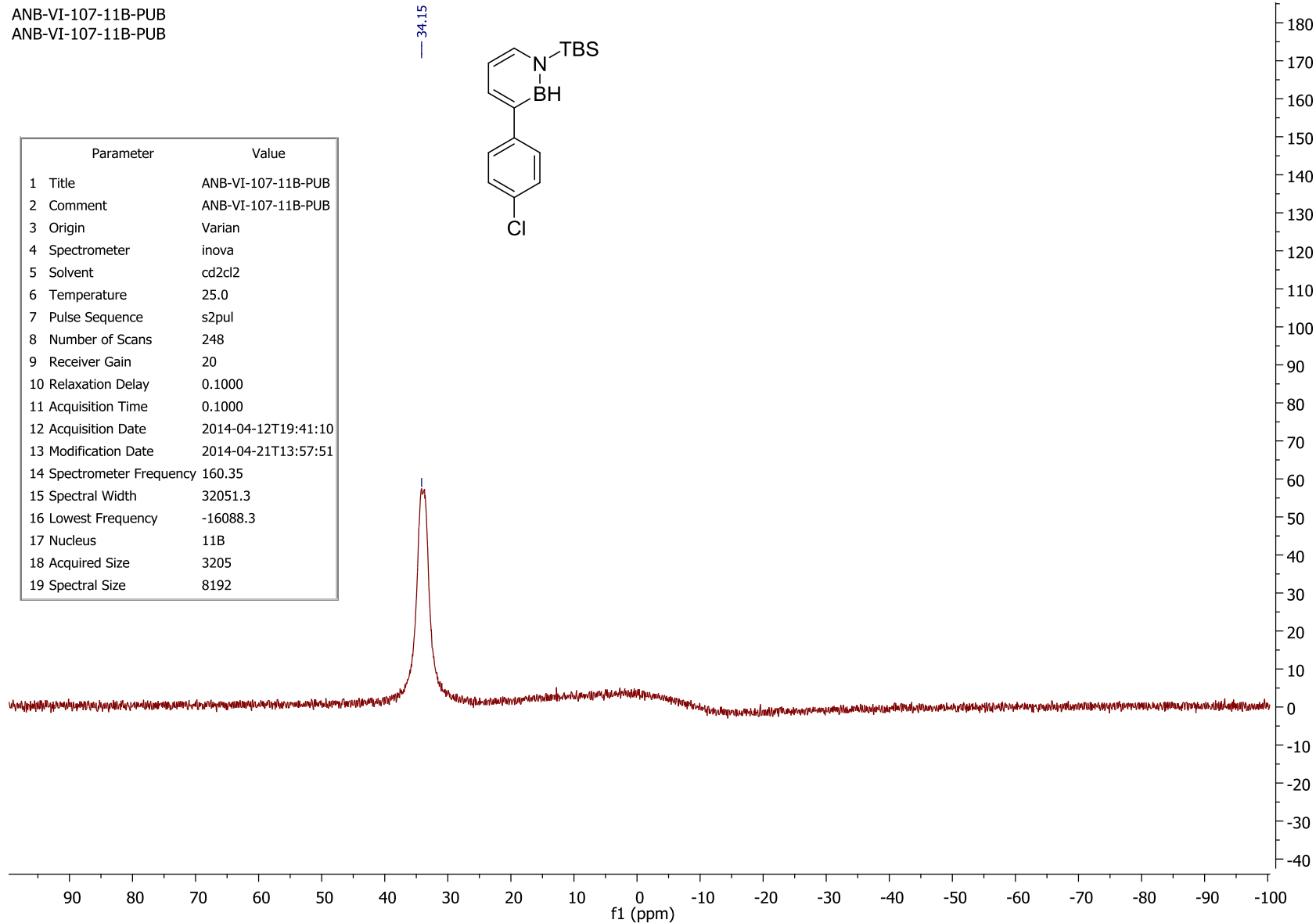
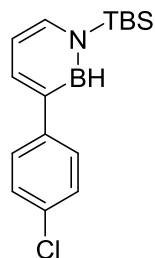


Parameter	Value
1 Title	ANB-VI-107-1H-PUB
2 Comment	ANB-VI-107-1H-PUB
3 Origin	Varian
4 Spectrometer	inova
5 Solvent	cd2cl2
6 Temperature	25.0
7 Pulse Sequence	s2pul
8 Number of Scans	16
9 Receiver Gain	30
10 Relaxation Delay	5.0000
11 Acquisition Time	2.0490
12 Acquisition Date	2014-04-12T1 9:38:52
13 Modification Date	2014-04-21T1 3:57:51
14 Spectrometer Frequency	499.78
15 Spectral Width	7996.0
16 Lowest Frequency	-999.3
17 Nucleus	1H
18 Acquired Size	16384
19 Spectral Size	32768



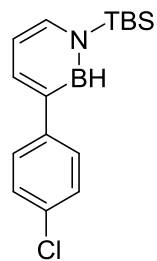
ANB-VI-107-11B-PUB
ANB-VI-107-11B-PUB

Parameter	Value
1 Title	ANB-VI-107-11B-PUB
2 Comment	ANB-VI-107-11B-PUB
3 Origin	Varian
4 Spectrometer	inova
5 Solvent	cd2cl2
6 Temperature	25.0
7 Pulse Sequence	s2pul
8 Number of Scans	248
9 Receiver Gain	20
10 Relaxation Delay	0.1000
11 Acquisition Time	0.1000
12 Acquisition Date	2014-04-12T19:41:10
13 Modification Date	2014-04-21T13:57:51
14 Spectrometer Frequency	160.35
15 Spectral Width	32051.3
16 Lowest Frequency	-16088.3
17 Nucleus	11B
18 Acquired Size	3205
19 Spectral Size	8192

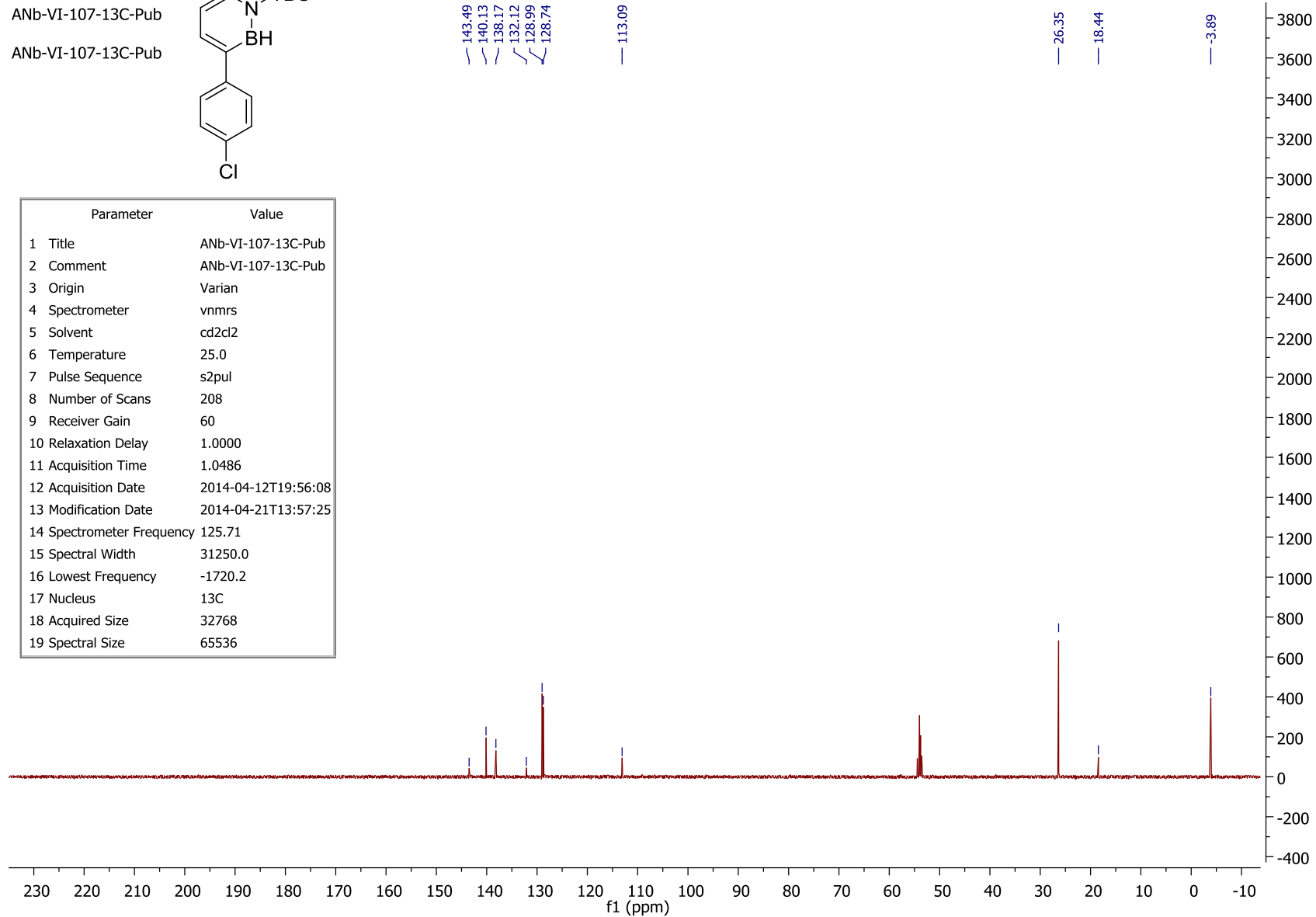


ANb-VI-107-13C-Pub

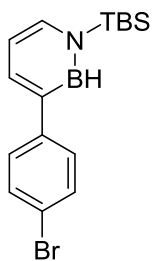
ANb-VI-107-13C-Pub



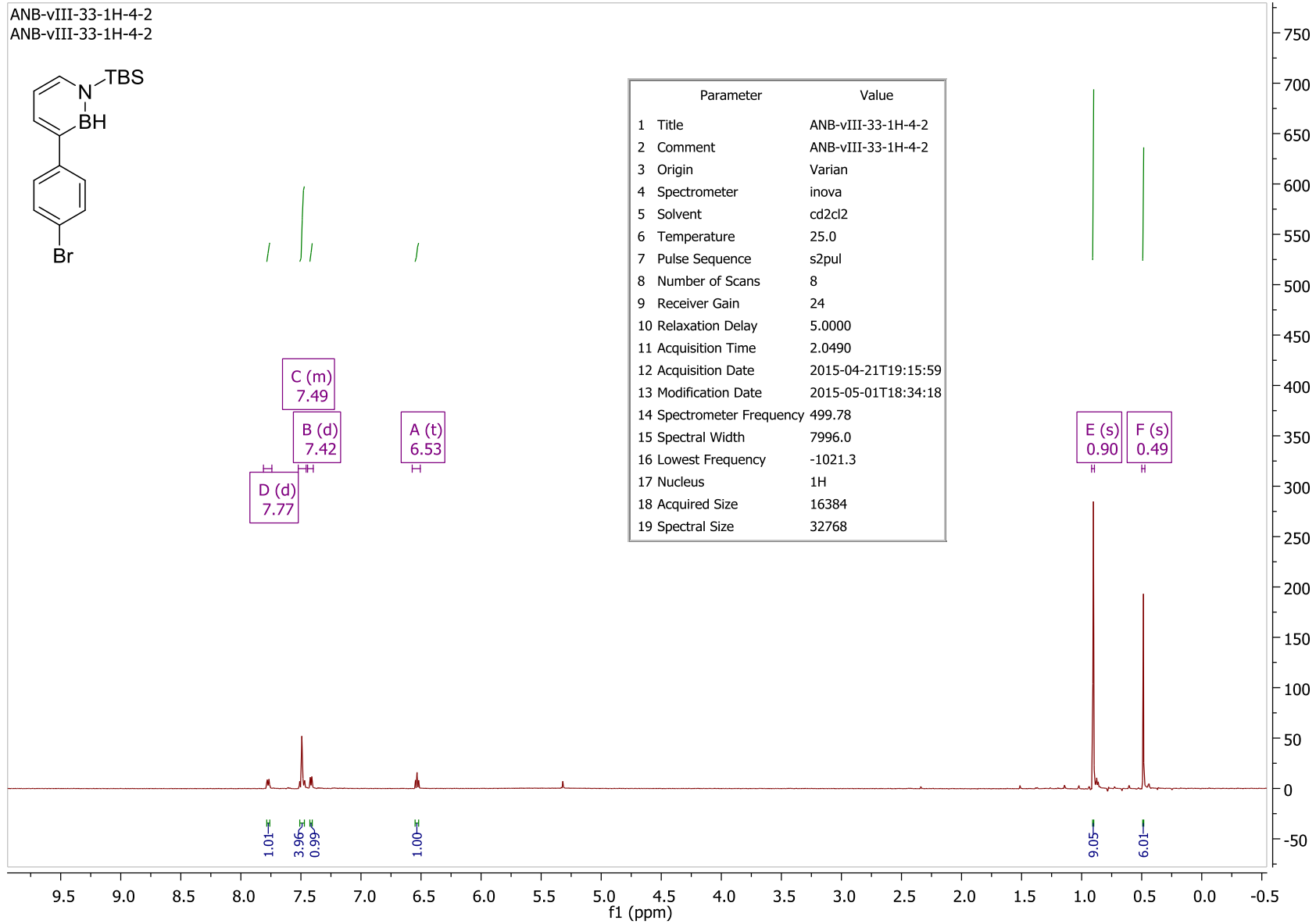
Parameter	Value
1 Title	ANb-VI-107-13C-Pub
2 Comment	ANb-VI-107-13C-Pub
3 Origin	Varian
4 Spectrometer	vnmrs
5 Solvent	cd2cl2
6 Temperature	25.0
7 Pulse Sequence	s2pul
8 Number of Scans	208
9 Receiver Gain	60
10 Relaxation Delay	1.0000
11 Acquisition Time	1.0486
12 Acquisition Date	2014-04-12T19:56:08
13 Modification Date	2014-04-21T13:57:25
14 Spectrometer Frequency	125.71
15 Spectral Width	31250.0
16 Lowest Frequency	-1720.2
17 Nucleus	¹³ C
18 Acquired Size	32768
19 Spectral Size	65536



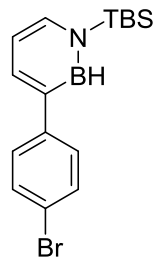
ANB-vIII-33-1H-4-2
ANB-vIII-33-1H-4-2



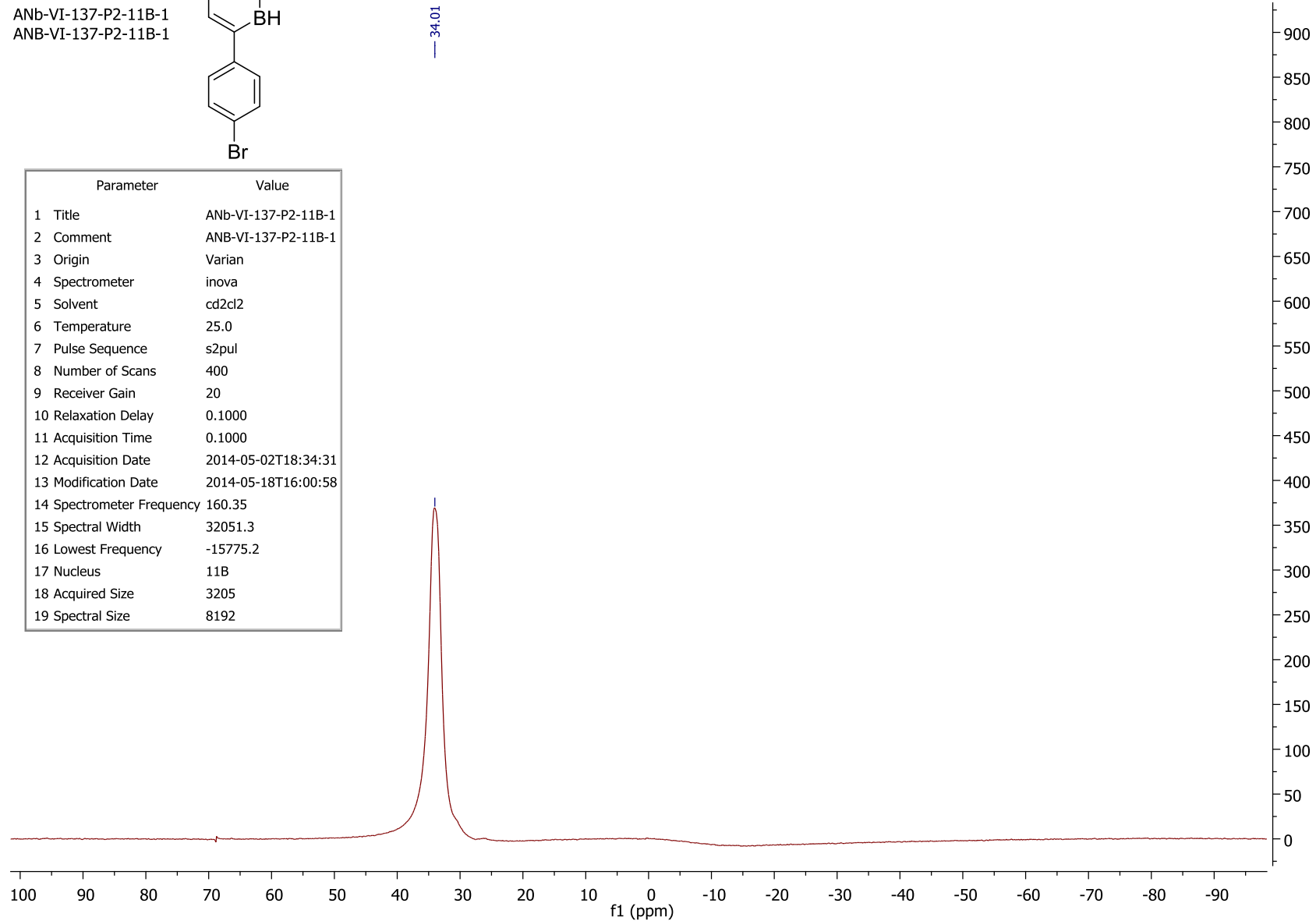
Parameter	Value
1 Title	ANB-vIII-33-1H-4-2
2 Comment	ANB-vIII-33-1H-4-2
3 Origin	Varian
4 Spectrometer	inova
5 Solvent	cd2cl2
6 Temperature	25.0
7 Pulse Sequence	s2pul
8 Number of Scans	8
9 Receiver Gain	24
10 Relaxation Delay	5.0000
11 Acquisition Time	2.0490
12 Acquisition Date	2015-04-21T19:15:59
13 Modification Date	2015-05-01T18:34:18
14 Spectrometer Frequency	499.78
15 Spectral Width	7996.0
16 Lowest Frequency	-1021.3
17 Nucleus	1H
18 Acquired Size	16384
19 Spectral Size	32768



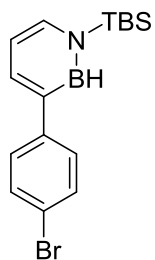
ANb-VI-137-P2-11B-1
ANb-VI-137-P2-11B-1



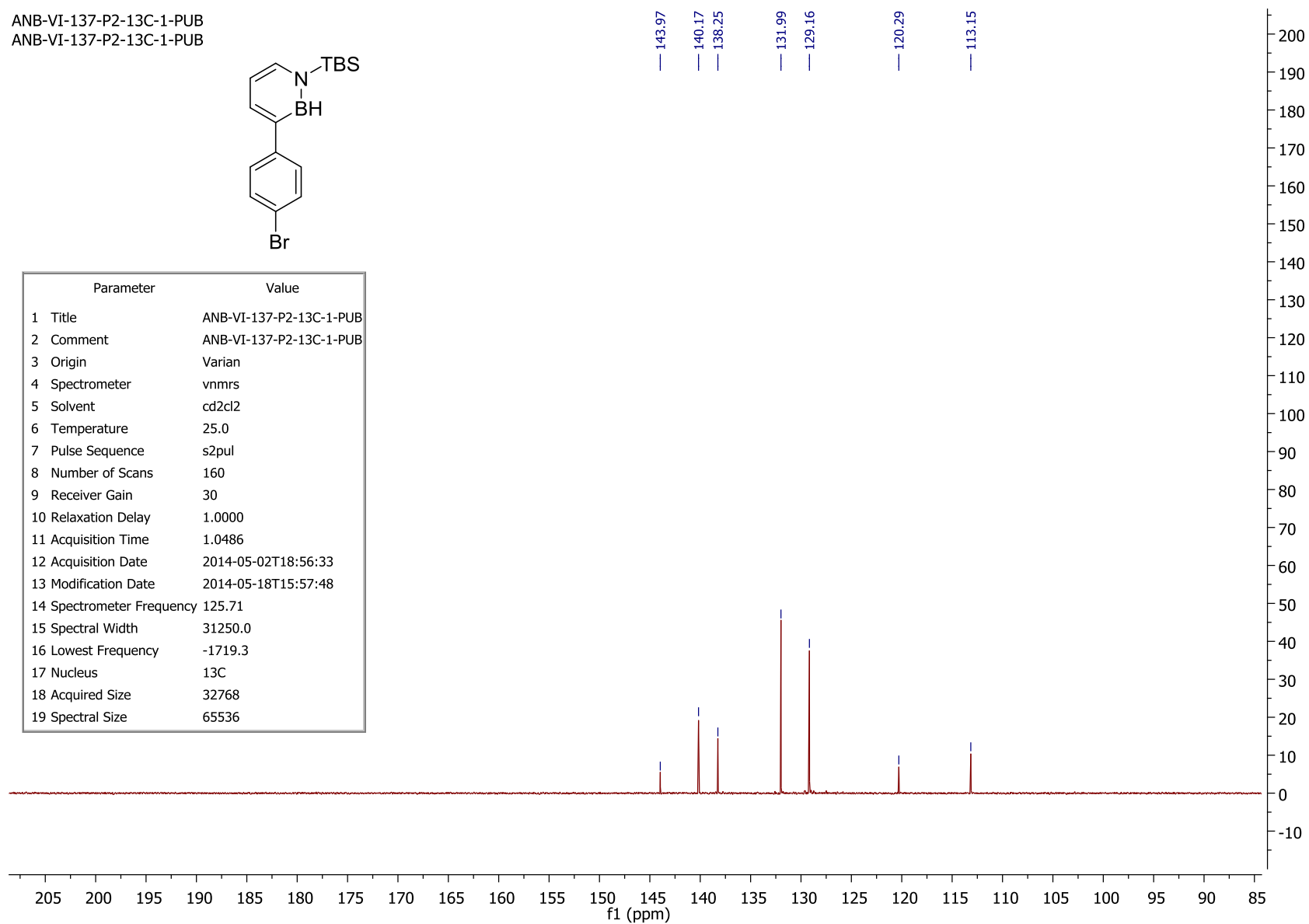
Parameter	Value
1 Title	ANb-VI-137-P2-11B-1
2 Comment	ANb-VI-137-P2-11B-1
3 Origin	Varian
4 Spectrometer	inova
5 Solvent	cd2cl2
6 Temperature	25.0
7 Pulse Sequence	s2pul
8 Number of Scans	400
9 Receiver Gain	20
10 Relaxation Delay	0.1000
11 Acquisition Time	0.1000
12 Acquisition Date	2014-05-02T18:34:31
13 Modification Date	2014-05-18T16:00:58
14 Spectrometer Frequency	160.35
15 Spectral Width	32051.3
16 Lowest Frequency	-15775.2
17 Nucleus	11B
18 Acquired Size	3205
19 Spectral Size	8192



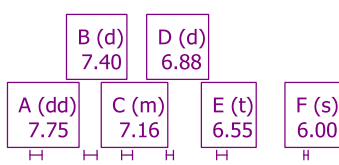
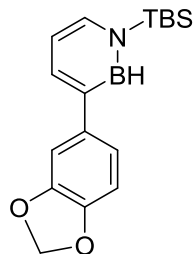
ANB-VI-137-P2-13C-1-PUB
ANB-VI-137-P2-13C-1-PUB



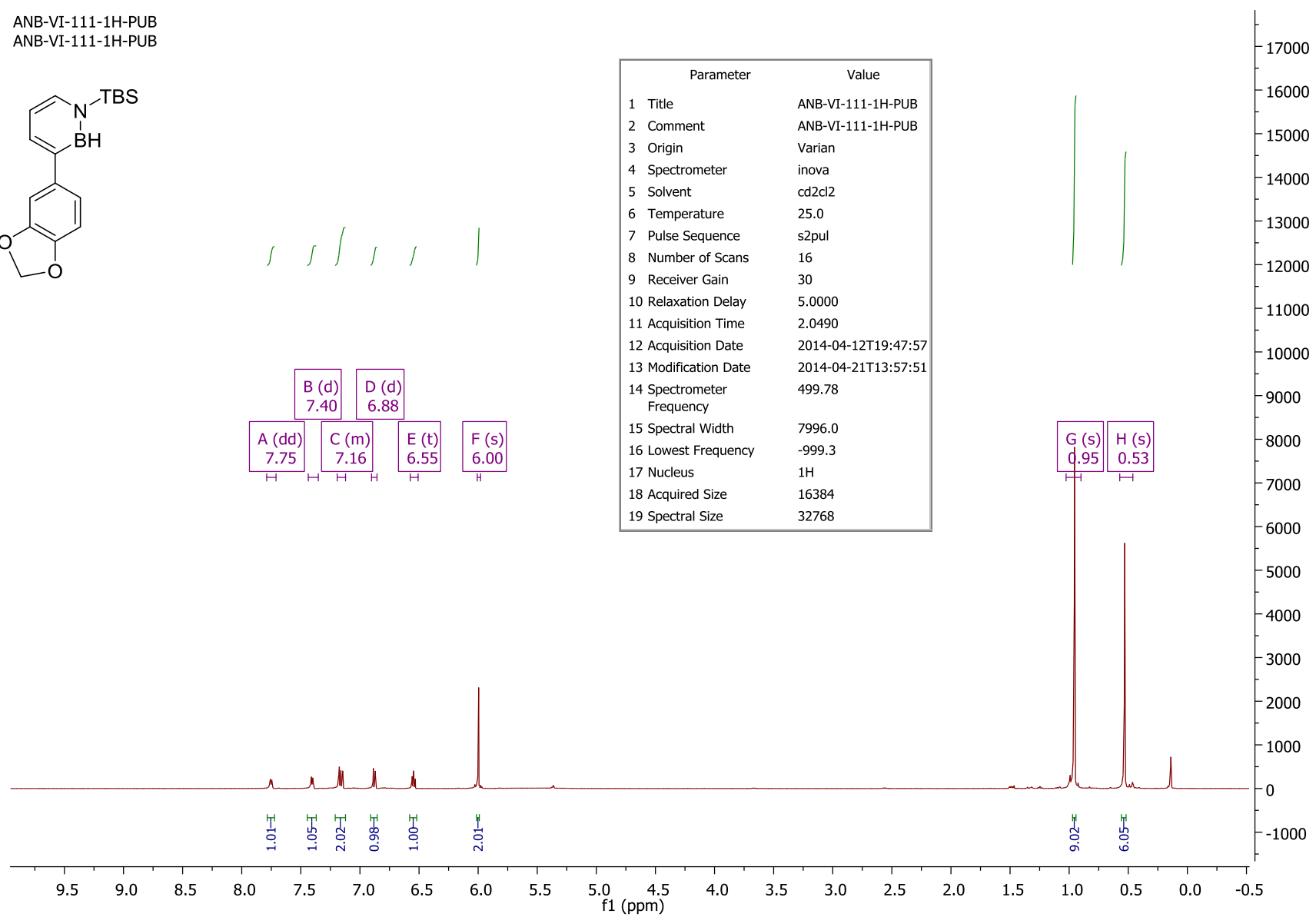
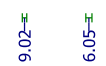
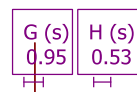
Parameter	Value
1 Title	ANB-VI-137-P2-13C-1-PUB
2 Comment	ANB-VI-137-P2-13C-1-PUB
3 Origin	Varian
4 Spectrometer	vnmrs
5 Solvent	cd2cl2
6 Temperature	25.0
7 Pulse Sequence	s2pul
8 Number of Scans	160
9 Receiver Gain	30
10 Relaxation Delay	1.0000
11 Acquisition Time	1.0486
12 Acquisition Date	2014-05-02T18:56:33
13 Modification Date	2014-05-18T15:57:48
14 Spectrometer Frequency	125.71
15 Spectral Width	31250.0
16 Lowest Frequency	-1719.3
17 Nucleus	13C
18 Acquired Size	32768
19 Spectral Size	65536



ANB-VI-111-1H-PUB
ANB-VI-111-1H-PUB



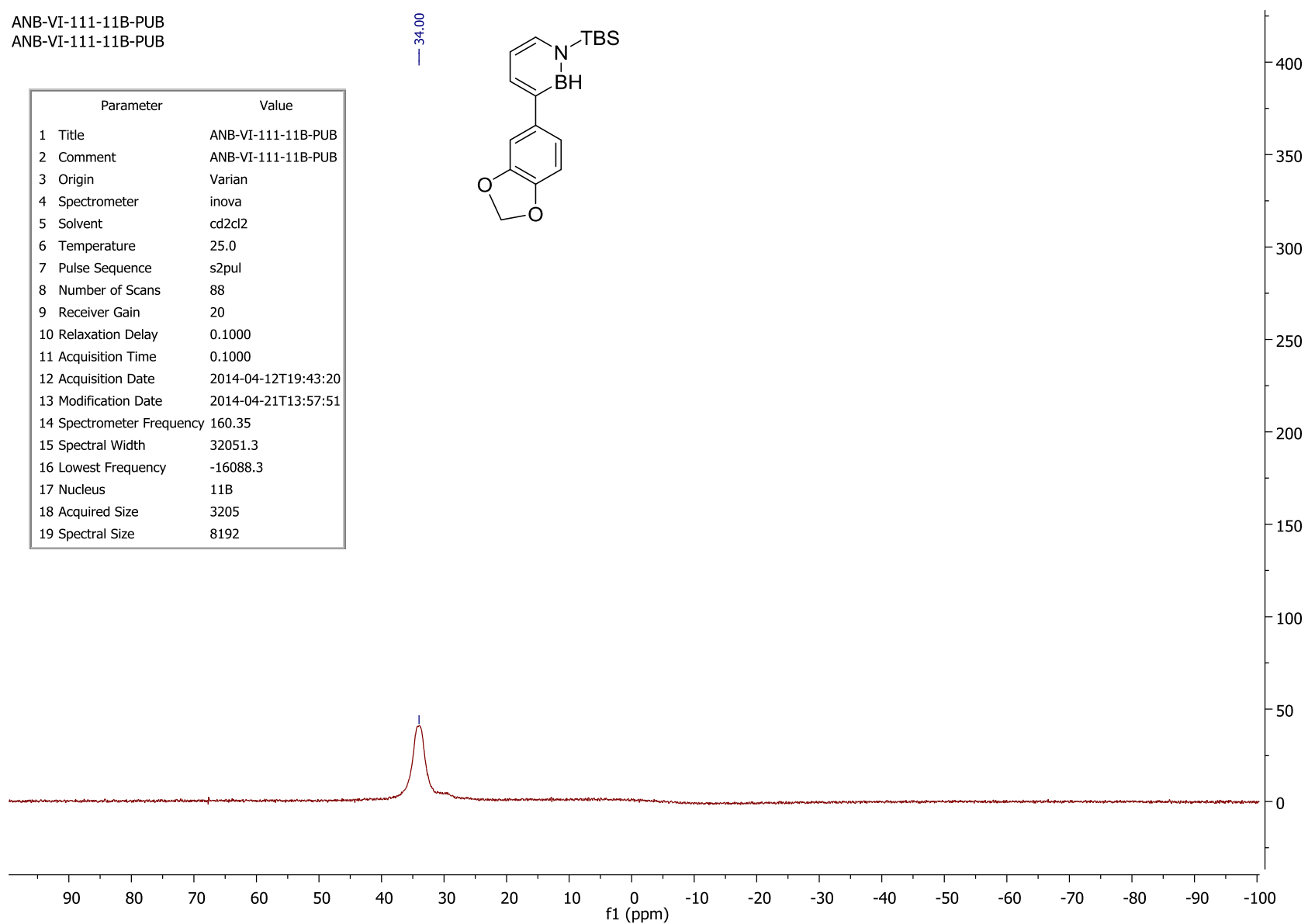
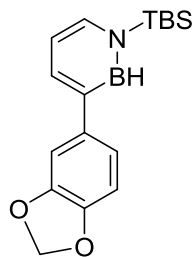
Parameter	Value
1 Title	ANB-VI-111-1H-PUB
2 Comment	ANB-VI-111-1H-PUB
3 Origin	Varian
4 Spectrometer	inova
5 Solvent	cd2cl2
6 Temperature	25.0
7 Pulse Sequence	s2pul
8 Number of Scans	16
9 Receiver Gain	30
10 Relaxation Delay	5.0000
11 Acquisition Time	2.0490
12 Acquisition Date	2014-04-12T19:47:57
13 Modification Date	2014-04-21T13:57:51
14 Spectrometer Frequency	499.78
15 Spectral Width	7996.0
16 Lowest Frequency	-999.3
17 Nucleus	1H
18 Acquired Size	16384
19 Spectral Size	32768



ANB-VI-111-11B-PUB
ANB-VI-111-11B-PUB

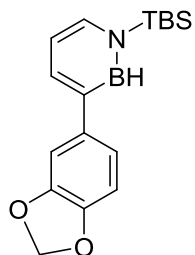
Parameter	Value
1 Title	ANB-VI-111-11B-PUB
2 Comment	ANB-VI-111-11B-PUB
3 Origin	Varian
4 Spectrometer	inova
5 Solvent	cd2cl2
6 Temperature	25.0
7 Pulse Sequence	s2pul
8 Number of Scans	88
9 Receiver Gain	20
10 Relaxation Delay	0.1000
11 Acquisition Time	0.1000
12 Acquisition Date	2014-04-12T19:43:20
13 Modification Date	2014-04-21T13:57:51
14 Spectrometer Frequency	160.35
15 Spectral Width	32051.3
16 Lowest Frequency	-16088.3
17 Nucleus	11B
18 Acquired Size	3205
19 Spectral Size	8192

— 34.00

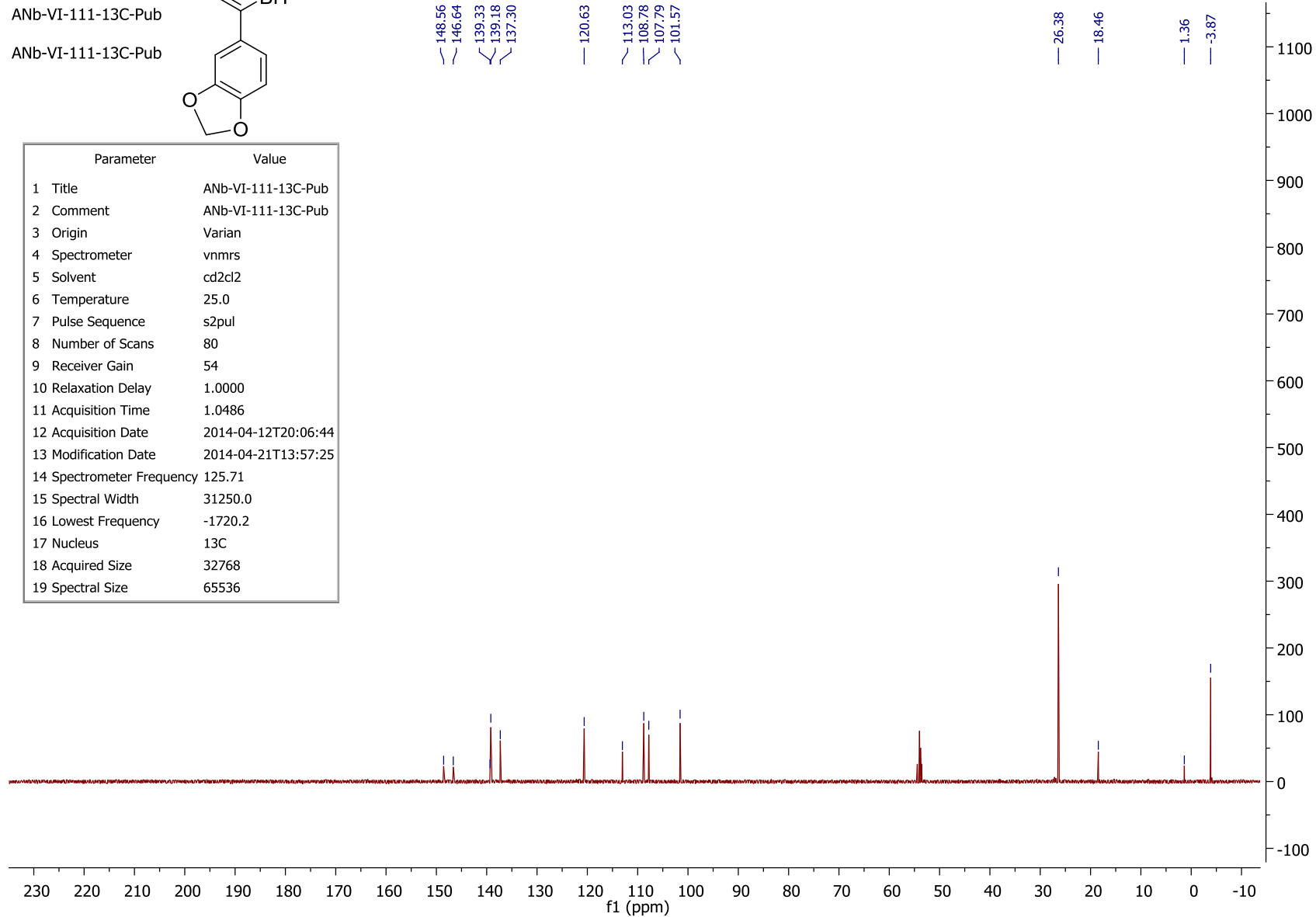


ANb-VI-111-13C-Pub

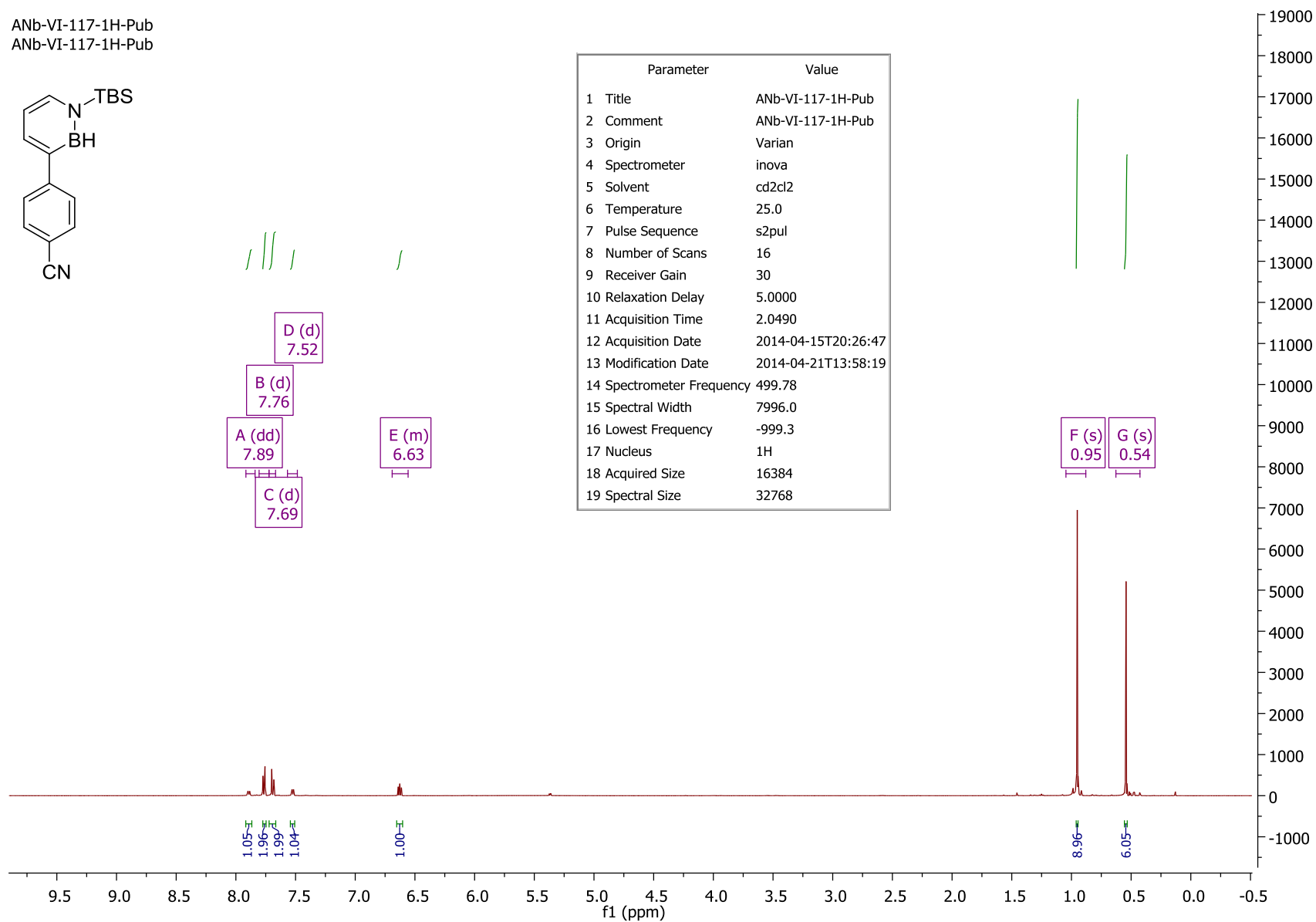
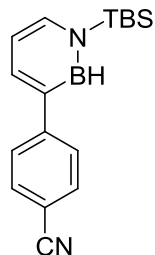
ANb-VI-111-13C-Pub



Parameter	Value
1 Title	ANb-VI-111-13C-Pub
2 Comment	ANb-VI-111-13C-Pub
3 Origin	Varian
4 Spectrometer	vnmrs
5 Solvent	cd2cl2
6 Temperature	25.0
7 Pulse Sequence	s2pul
8 Number of Scans	80
9 Receiver Gain	54
10 Relaxation Delay	1.0000
11 Acquisition Time	1.0486
12 Acquisition Date	2014-04-12T20:06:44
13 Modification Date	2014-04-21T13:57:25
14 Spectrometer Frequency	125.71
15 Spectral Width	31250.0
16 Lowest Frequency	-1720.2
17 Nucleus	13C
18 Acquired Size	32768
19 Spectral Size	65536

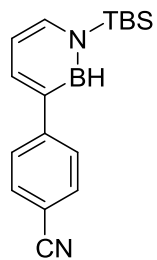


ANb-VI-117-1H-Pub
ANb-VI-117-1H-Pub

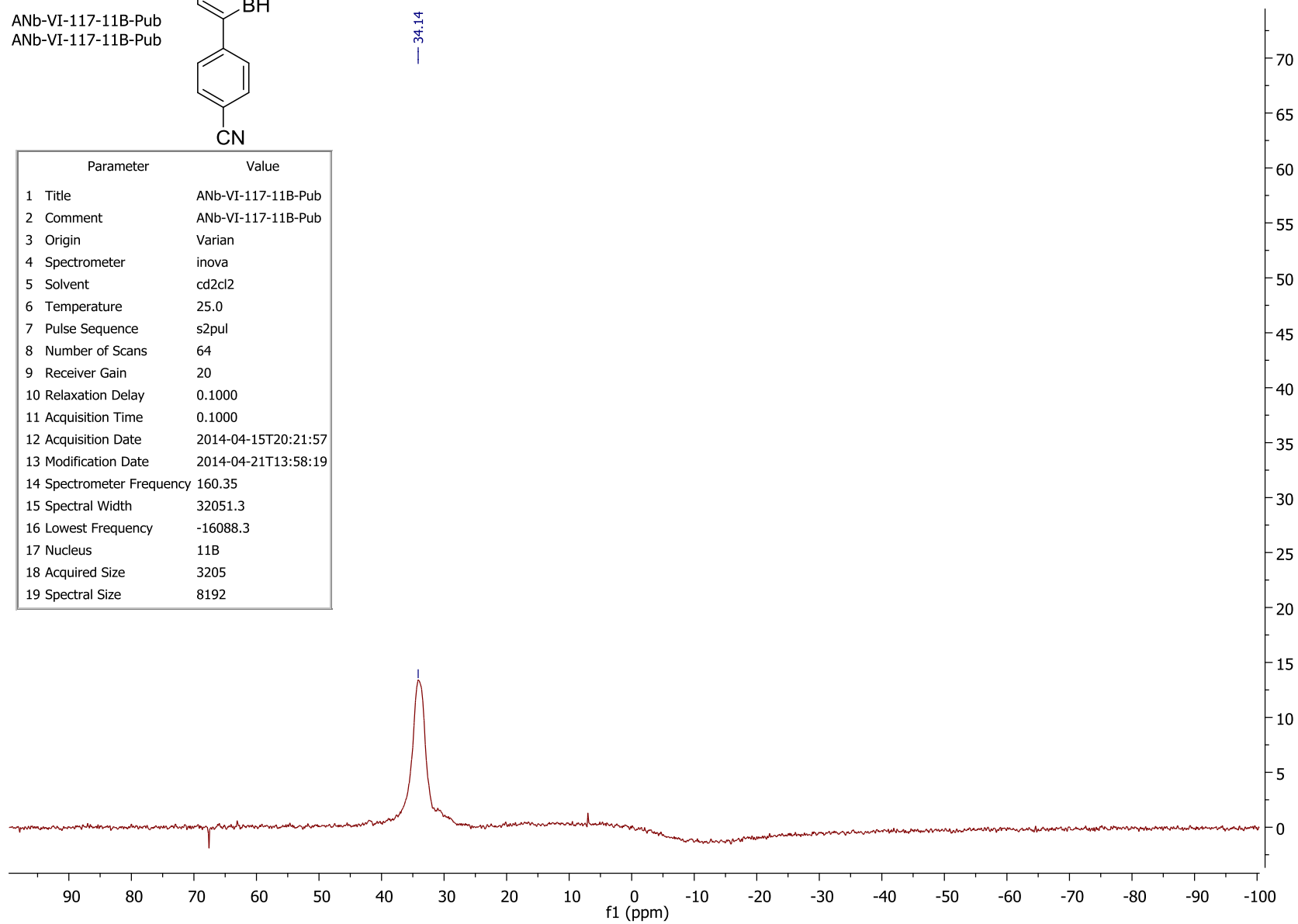


Parameter	Value
1 Title	ANb-VI-117-1H-Pub
2 Comment	ANb-VI-117-1H-Pub
3 Origin	Varian
4 Spectrometer	inova
5 Solvent	cd2cl2
6 Temperature	25.0
7 Pulse Sequence	s2pul
8 Number of Scans	16
9 Receiver Gain	30
10 Relaxation Delay	5.0000
11 Acquisition Time	2.0490
12 Acquisition Date	2014-04-15T20:26:47
13 Modification Date	2014-04-21T13:58:19
14 Spectrometer Frequency	499.78
15 Spectral Width	7996.0
16 Lowest Frequency	-999.3
17 Nucleus	1H
18 Acquired Size	16384
19 Spectral Size	32768

ANb-VI-117-11B-Pub
ANb-VI-117-11B-Pub

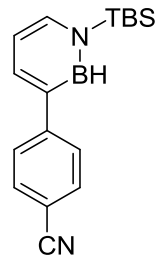


Parameter	Value
1 Title	ANb-VI-117-11B-Pub
2 Comment	ANb-VI-117-11B-Pub
3 Origin	Varian
4 Spectrometer	inova
5 Solvent	cd2cl2
6 Temperature	25.0
7 Pulse Sequence	s2pul
8 Number of Scans	64
9 Receiver Gain	20
10 Relaxation Delay	0.1000
11 Acquisition Time	0.1000
12 Acquisition Date	2014-04-15T20:21:57
13 Modification Date	2014-04-21T13:58:19
14 Spectrometer Frequency	160.35
15 Spectral Width	32051.3
16 Lowest Frequency	-16088.3
17 Nucleus	11B
18 Acquired Size	3205
19 Spectral Size	8192

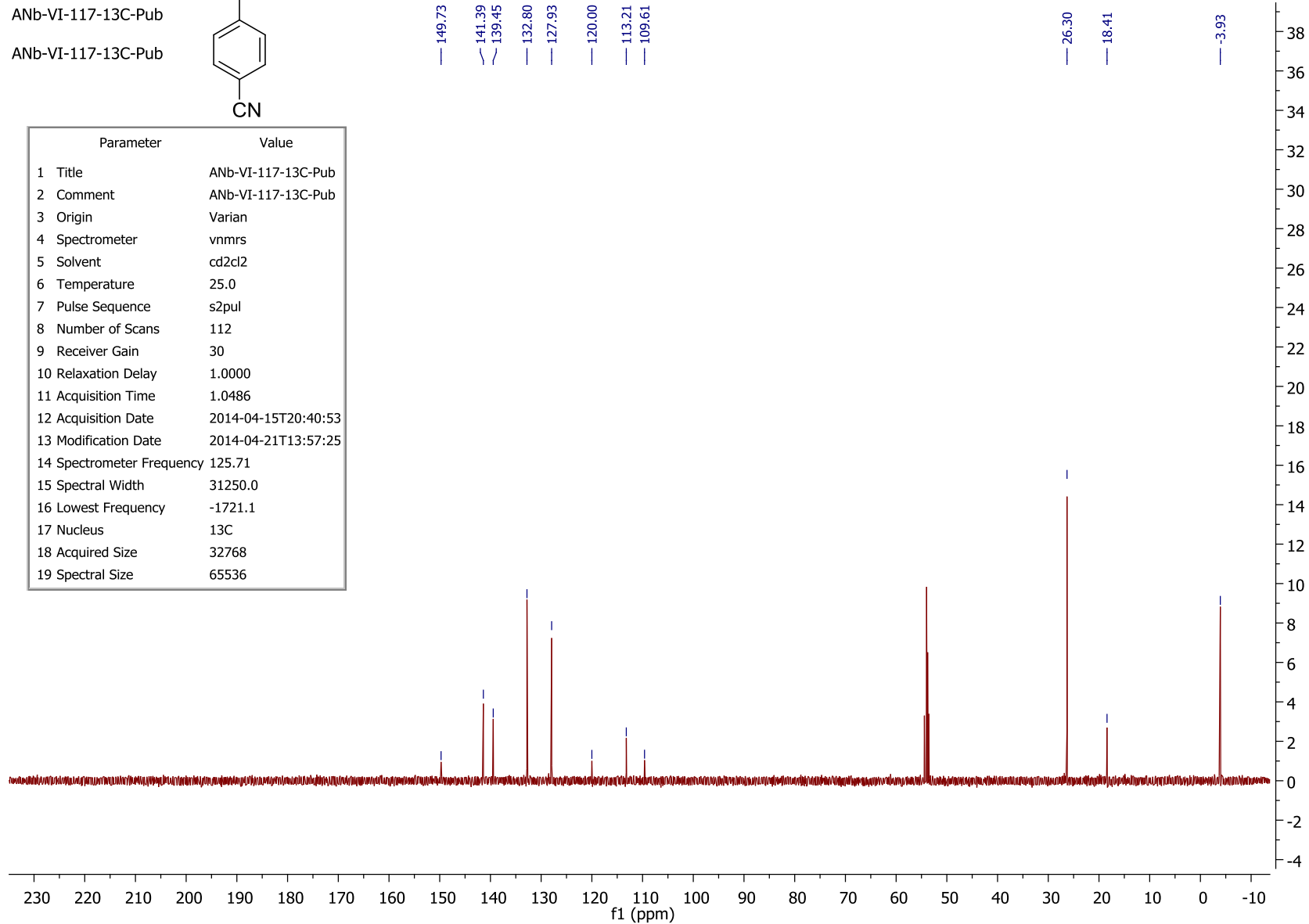


ANb-VI-117-13C-Pub

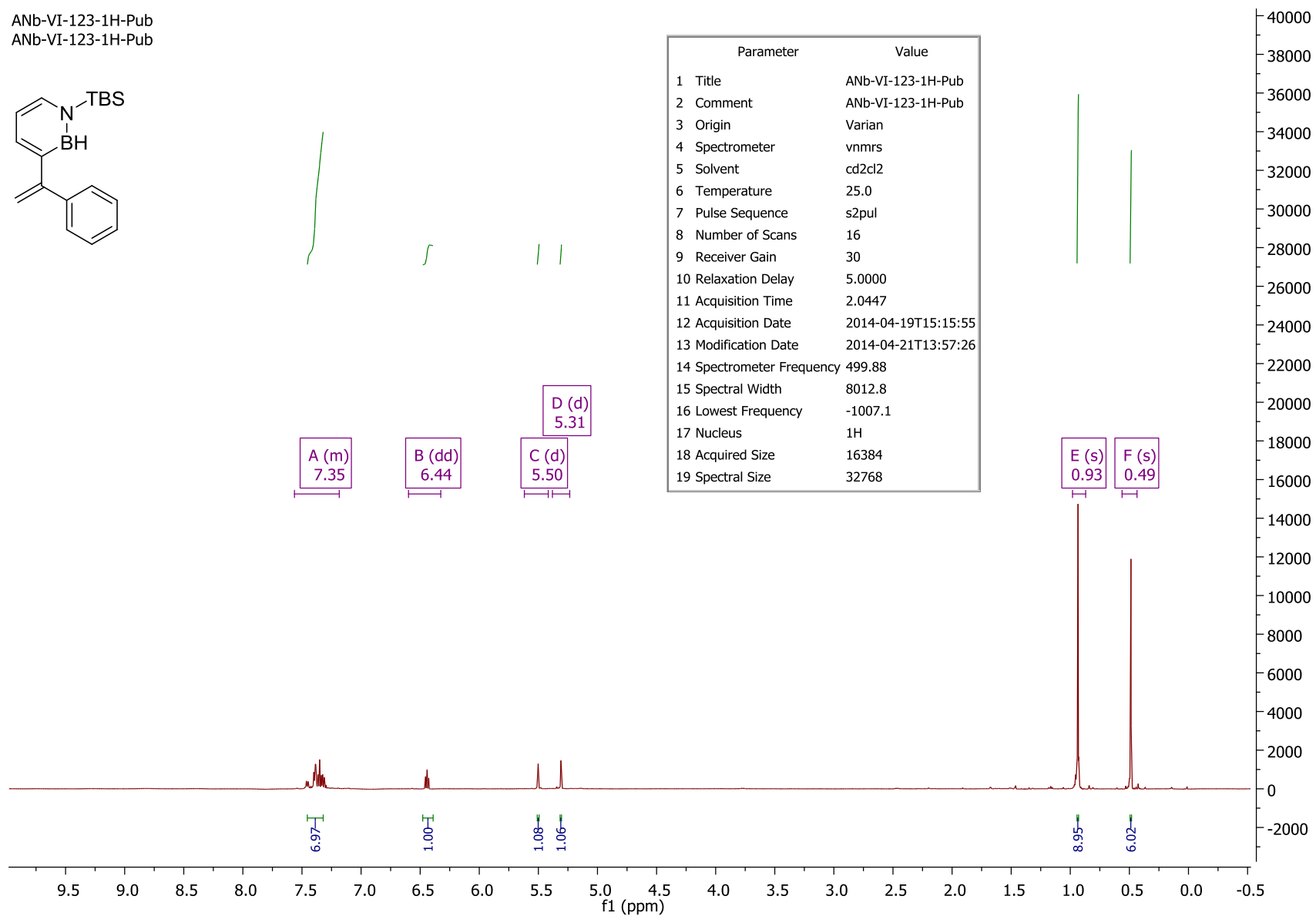
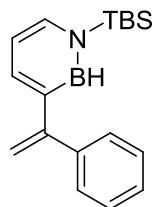
ANb-VI-117-13C-Pub



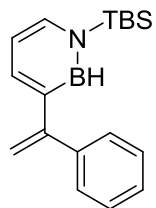
Parameter	Value
1 Title	ANb-VI-117-13C-Pub
2 Comment	ANb-VI-117-13C-Pub
3 Origin	Varian
4 Spectrometer	nmrs
5 Solvent	cd2cl2
6 Temperature	25.0
7 Pulse Sequence	s2pul
8 Number of Scans	112
9 Receiver Gain	30
10 Relaxation Delay	1.0000
11 Acquisition Time	1.0486
12 Acquisition Date	2014-04-15T20:40:53
13 Modification Date	2014-04-21T13:57:25
14 Spectrometer Frequency	125.71
15 Spectral Width	31250.0
16 Lowest Frequency	-1721.1
17 Nucleus	13C
18 Acquired Size	32768
19 Spectral Size	65536



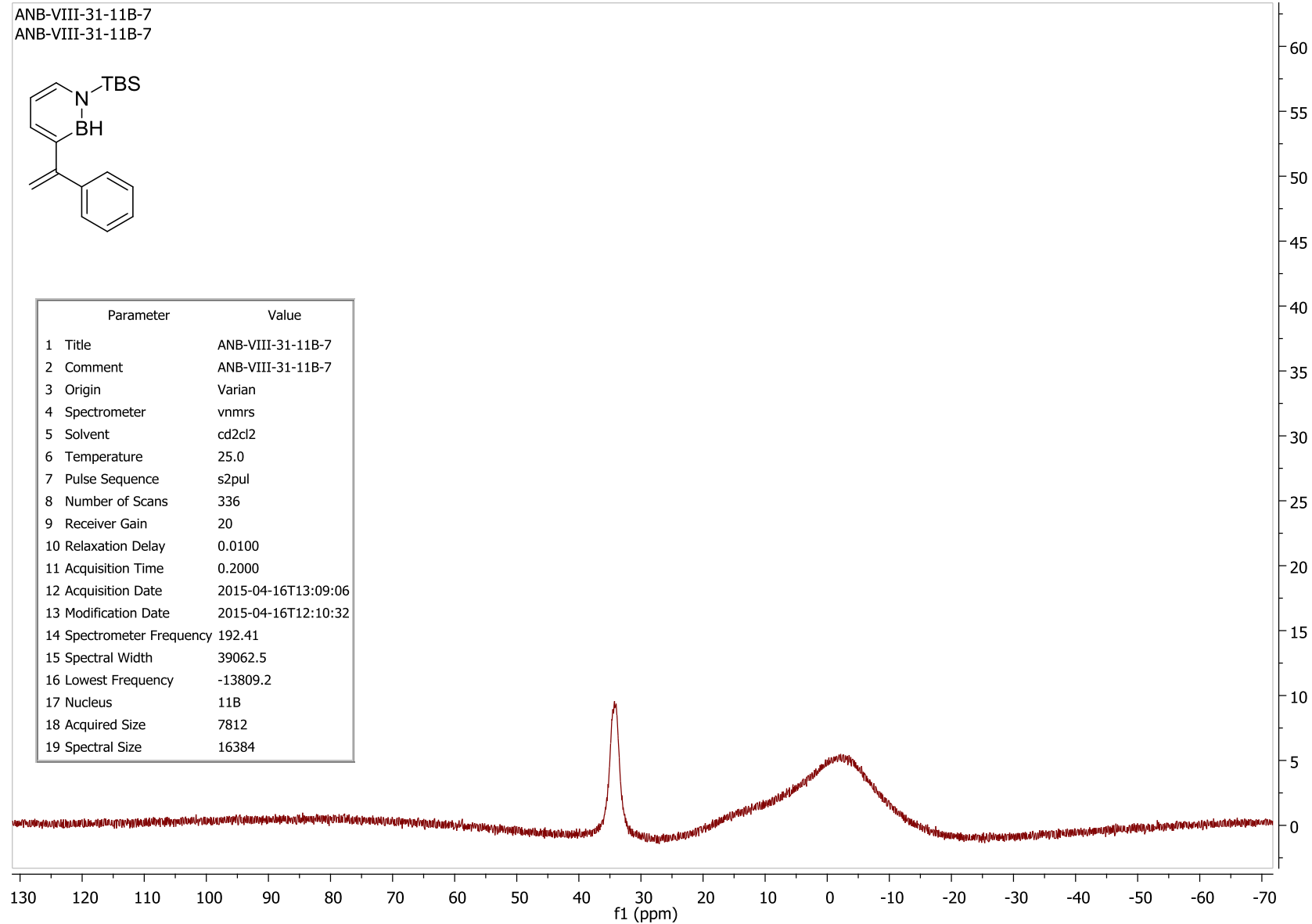
ANb-VI-123-1H-Pub
ANb-VI-123-1H-Pub



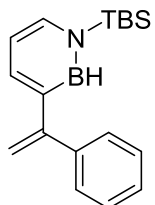
ANB-VIII-31-11B-7
ANB-VIII-31-11B-7



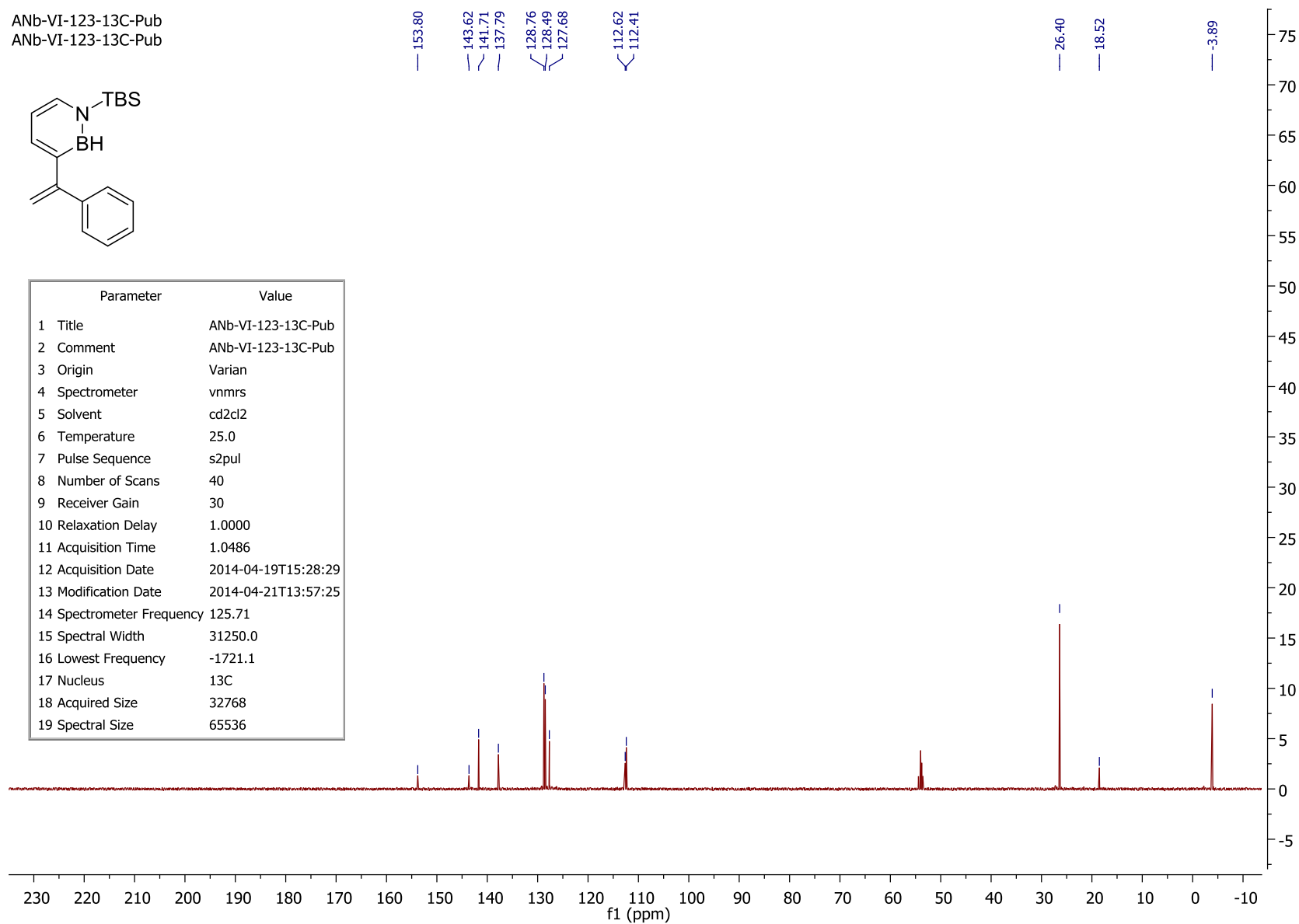
Parameter	Value
1 Title	ANB-VIII-31-11B-7
2 Comment	ANB-VIII-31-11B-7
3 Origin	Varian
4 Spectrometer	vnmrs
5 Solvent	cd2cl2
6 Temperature	25.0
7 Pulse Sequence	s2pul
8 Number of Scans	336
9 Receiver Gain	20
10 Relaxation Delay	0.0100
11 Acquisition Time	0.2000
12 Acquisition Date	2015-04-16T13:09:06
13 Modification Date	2015-04-16T12:10:32
14 Spectrometer Frequency	192.41
15 Spectral Width	39062.5
16 Lowest Frequency	-13809.2
17 Nucleus	11B
18 Acquired Size	7812
19 Spectral Size	16384



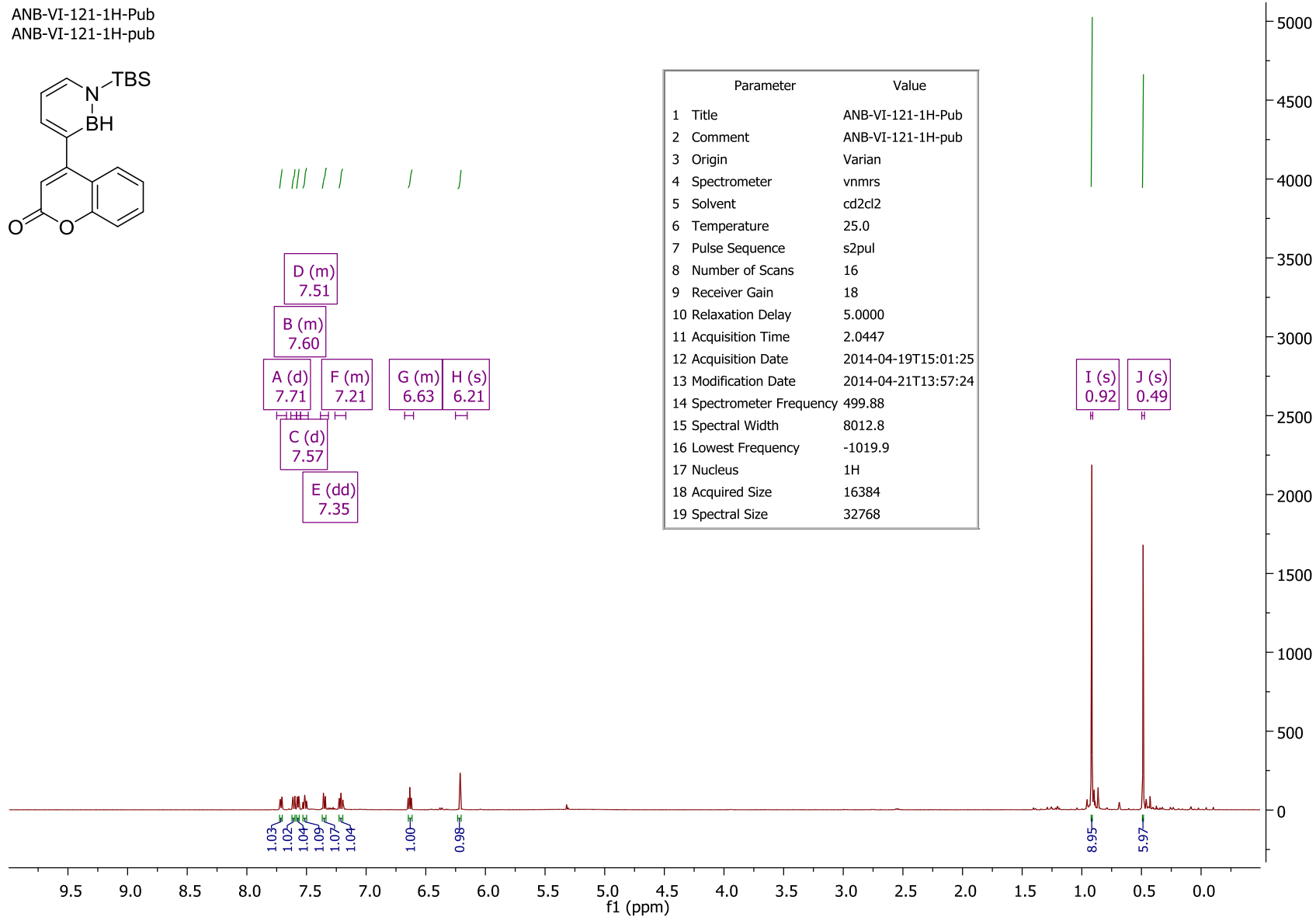
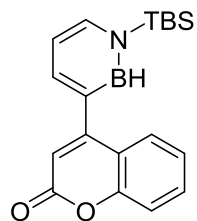
ANb-VI-123-13C-Pub
ANb-VI-123-13C-Pub



Parameter	Value
1 Title	ANb-VI-123-13C-Pub
2 Comment	ANb-VI-123-13C-Pub
3 Origin	Varian
4 Spectrometer	vnmrs
5 Solvent	cd2cl2
6 Temperature	25.0
7 Pulse Sequence	s2pul
8 Number of Scans	40
9 Receiver Gain	30
10 Relaxation Delay	1.0000
11 Acquisition Time	1.0486
12 Acquisition Date	2014-04-19T15:28:29
13 Modification Date	2014-04-21T13:57:25
14 Spectrometer Frequency	125.71
15 Spectral Width	31250.0
16 Lowest Frequency	-1721.1
17 Nucleus	13C
18 Acquired Size	32768
19 Spectral Size	65536

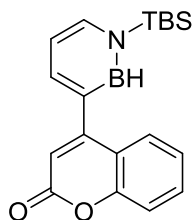


ANB-VI-121-1H-Pub
ANB-VI-121-1H-pub

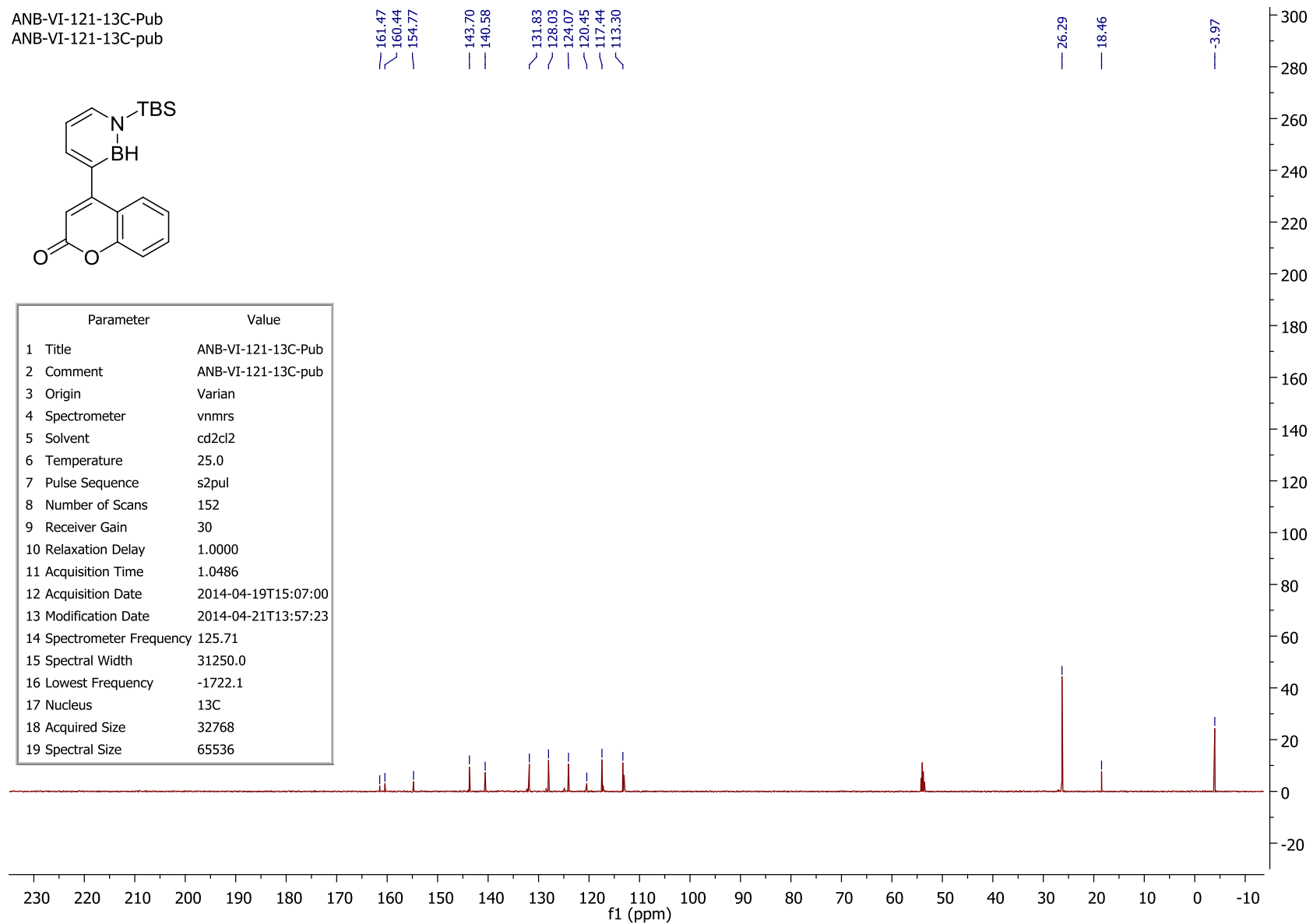


Parameter	Value
1 Title	ANB-VI-121-1H-Pub
2 Comment	ANB-VI-121-1H-pub
3 Origin	Varian
4 Spectrometer	vnmrs
5 Solvent	cd2cl2
6 Temperature	25.0
7 Pulse Sequence	s2pul
8 Number of Scans	16
9 Receiver Gain	18
10 Relaxation Delay	5.0000
11 Acquisition Time	2.0447
12 Acquisition Date	2014-04-19T15:01:25
13 Modification Date	2014-04-21T13:57:24
14 Spectrometer Frequency	499.88
15 Spectral Width	8012.8
16 Lowest Frequency	-1019.9
17 Nucleus	1H
18 Acquired Size	16384
19 Spectral Size	32768

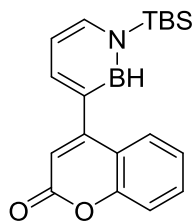
ANB-VI-121-13C-Pub
ANB-VI-121-13C-pub



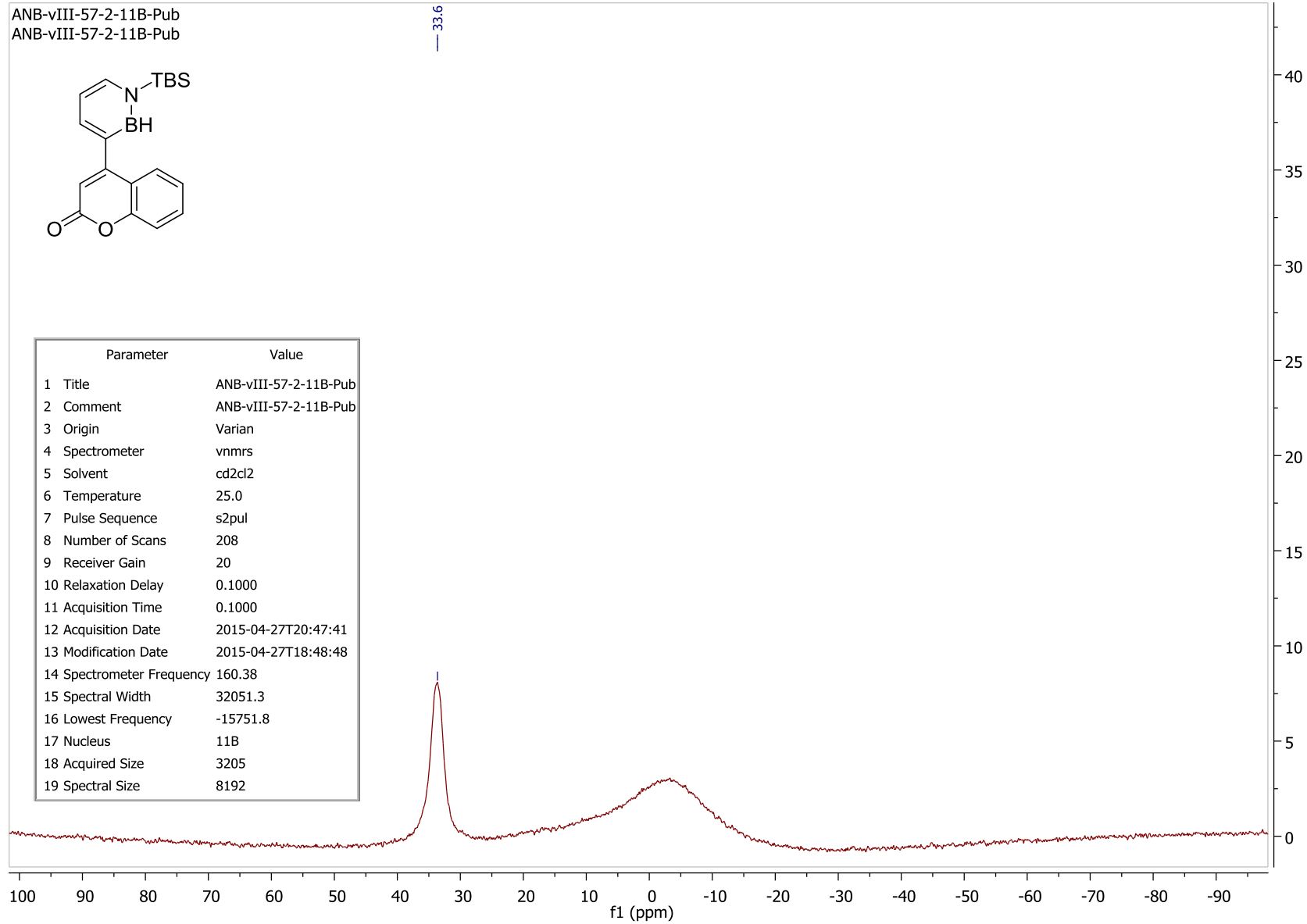
Parameter	Value
1 Title	ANB-VI-121-13C-Pub
2 Comment	ANB-VI-121-13C-pub
3 Origin	Varian
4 Spectrometer	vnmrs
5 Solvent	cd2cl2
6 Temperature	25.0
7 Pulse Sequence	s2pul
8 Number of Scans	152
9 Receiver Gain	30
10 Relaxation Delay	1.0000
11 Acquisition Time	1.0486
12 Acquisition Date	2014-04-19T15:07:00
13 Modification Date	2014-04-21T13:57:23
14 Spectrometer Frequency	125.71
15 Spectral Width	31250.0
16 Lowest Frequency	-1722.1
17 Nucleus	13C
18 Acquired Size	32768
19 Spectral Size	65536



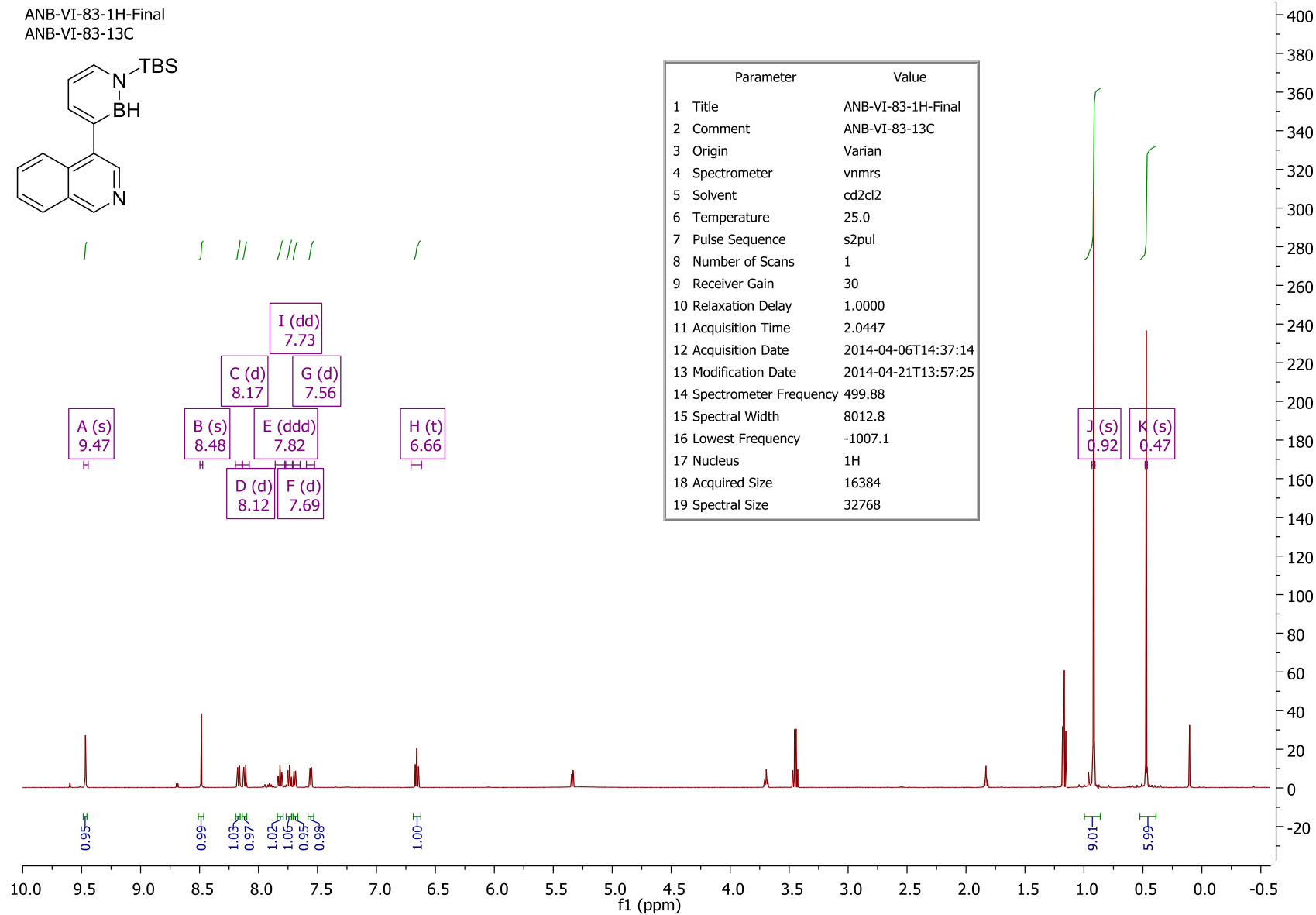
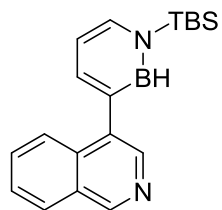
ANB-vIII-57-2-11B-Pub
ANB-vIII-57-2-11B-Pub



Parameter	Value
1 Title	ANB-vIII-57-2-11B-Pub
2 Comment	ANB-vIII-57-2-11B-Pub
3 Origin	Varian
4 Spectrometer	vnmrs
5 Solvent	cd2cl2
6 Temperature	25.0
7 Pulse Sequence	s2pul
8 Number of Scans	208
9 Receiver Gain	20
10 Relaxation Delay	0.1000
11 Acquisition Time	0.1000
12 Acquisition Date	2015-04-27T20:47:41
13 Modification Date	2015-04-27T18:48:48
14 Spectrometer Frequency	160.38
15 Spectral Width	32051.3
16 Lowest Frequency	-15751.8
17 Nucleus	11B
18 Acquired Size	3205
19 Spectral Size	8192



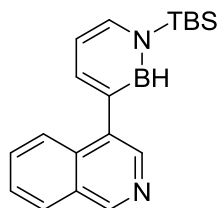
ANB-VI-83-1H-Final
ANB-VI-83-13C



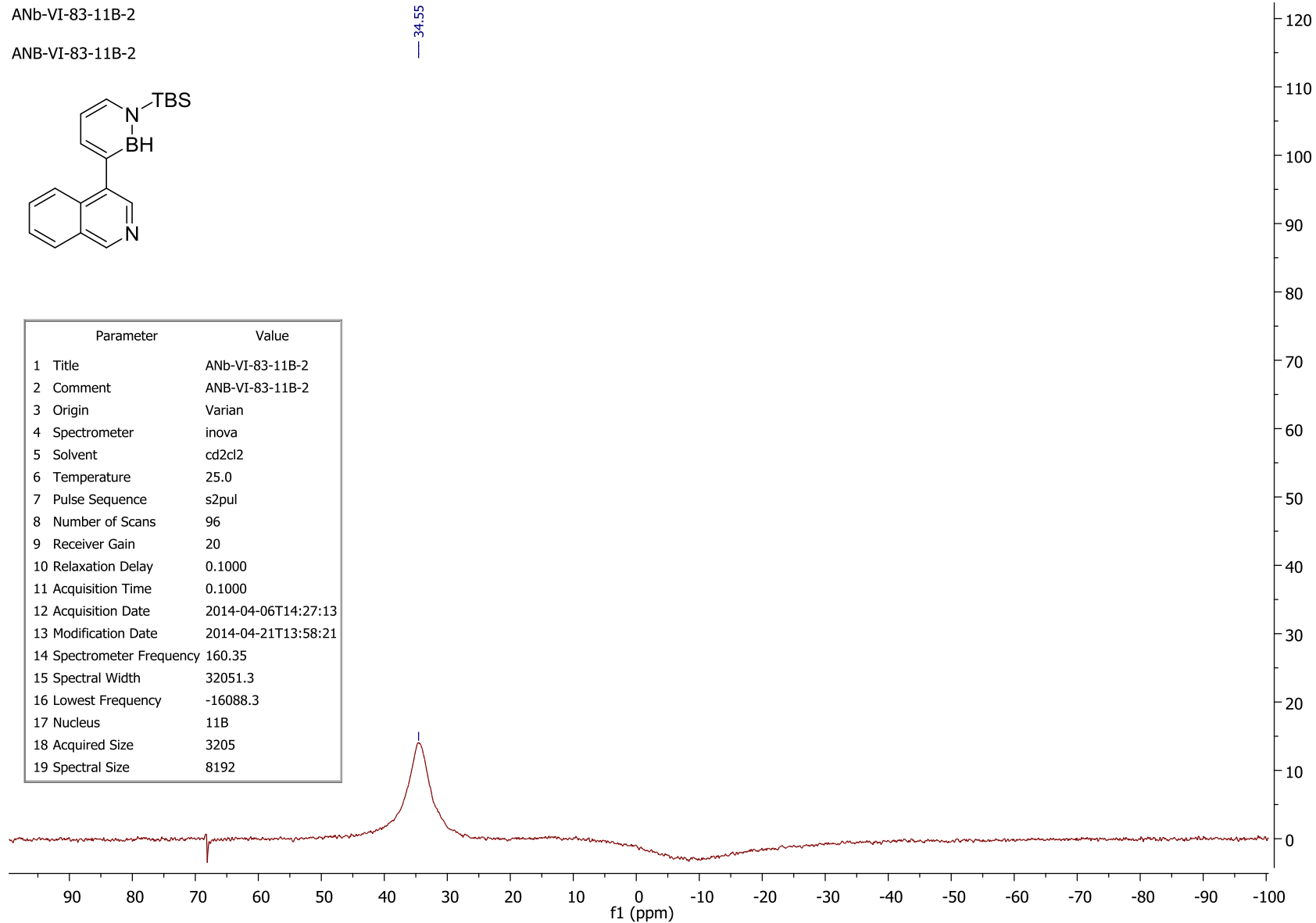
Parameter	Value
1 Title	ANB-VI-83-1H-Final
2 Comment	ANB-VI-83-13C
3 Origin	Varian
4 Spectrometer	vnmrs
5 Solvent	cd2cl2
6 Temperature	25.0
7 Pulse Sequence	s2pul
8 Number of Scans	1
9 Receiver Gain	30
10 Relaxation Delay	1.0000
11 Acquisition Time	2.0447
12 Acquisition Date	2014-04-06T14:37:14
13 Modification Date	2014-04-21T13:57:25
14 Spectrometer Frequency	499.88
15 Spectral Width	8012.8
16 Lowest Frequency	-1007.1
17 Nucleus	1H
18 Acquired Size	16384
19 Spectral Size	32768

ANb-VI-83-11B-2

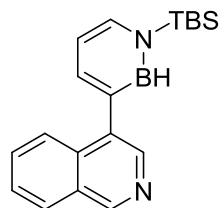
ANB-VI-83-11B-2



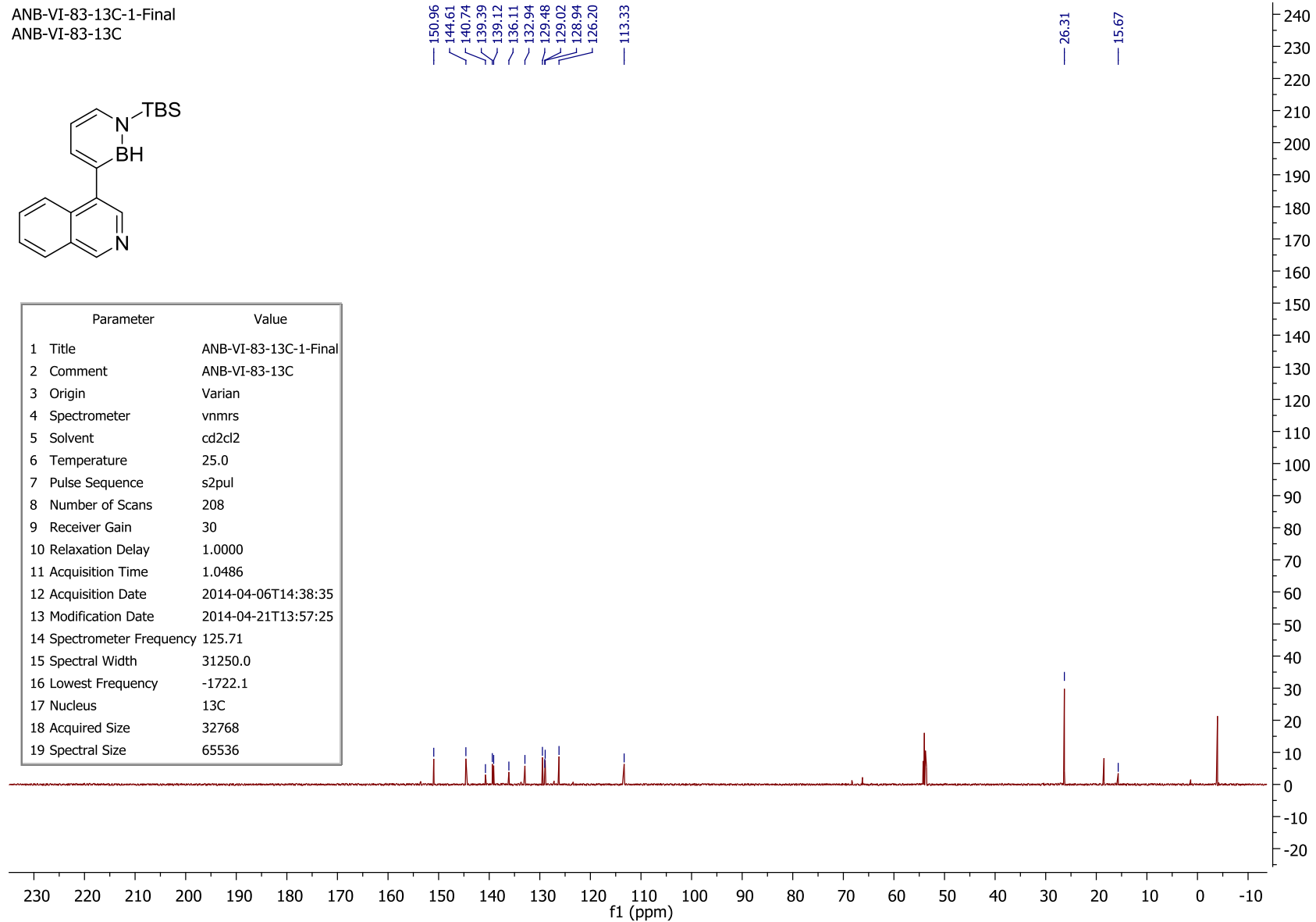
Parameter	Value
1 Title	ANb-VI-83-11B-2
2 Comment	ANB-VI-83-11B-2
3 Origin	Varian
4 Spectrometer	inova
5 Solvent	cd2cl2
6 Temperature	25.0
7 Pulse Sequence	s2pul
8 Number of Scans	96
9 Receiver Gain	20
10 Relaxation Delay	0.1000
11 Acquisition Time	0.1000
12 Acquisition Date	2014-04-06T14:27:13
13 Modification Date	2014-04-21T13:58:21
14 Spectrometer Frequency	160.35
15 Spectral Width	32051.3
16 Lowest Frequency	-16088.3
17 Nucleus	11B
18 Acquired Size	3205
19 Spectral Size	8192



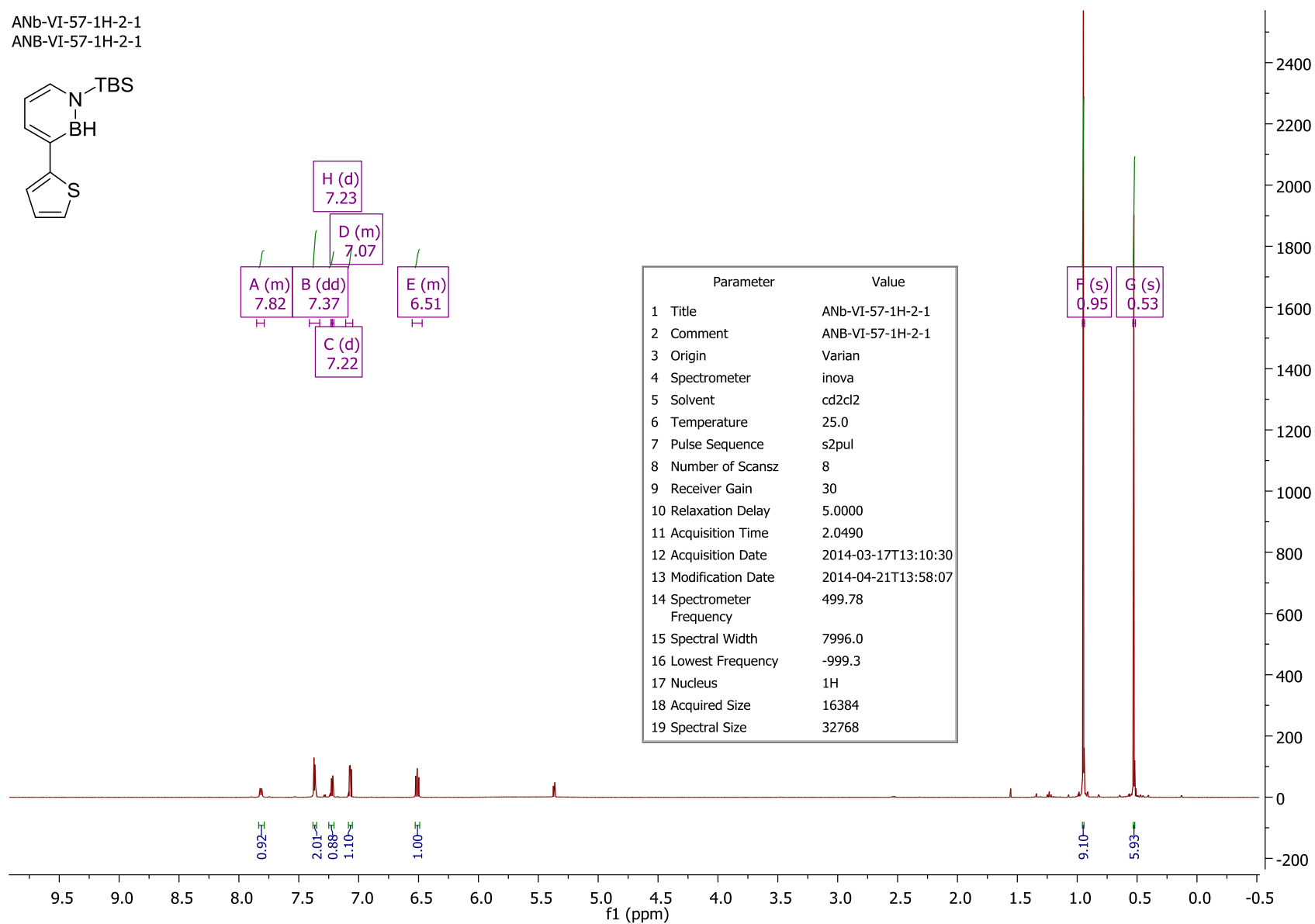
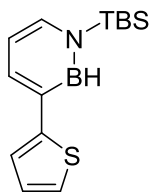
ANB-VI-83-13C-1-Final
ANB-VI-83-13C



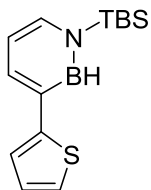
Parameter	Value
1 Title	ANB-VI-83-13C-1-Final
2 Comment	ANB-VI-83-13C
3 Origin	Varian
4 Spectrometer	vnmrs
5 Solvent	cd2cl2
6 Temperature	25.0
7 Pulse Sequence	s2pul
8 Number of Scans	208
9 Receiver Gain	30
10 Relaxation Delay	1.0000
11 Acquisition Time	1.0486
12 Acquisition Date	2014-04-06T14:38:35
13 Modification Date	2014-04-21T13:57:25
14 Spectrometer Frequency	125.71
15 Spectral Width	31250.0
16 Lowest Frequency	-1722.1
17 Nucleus	13C
18 Acquired Size	32768
19 Spectral Size	65536



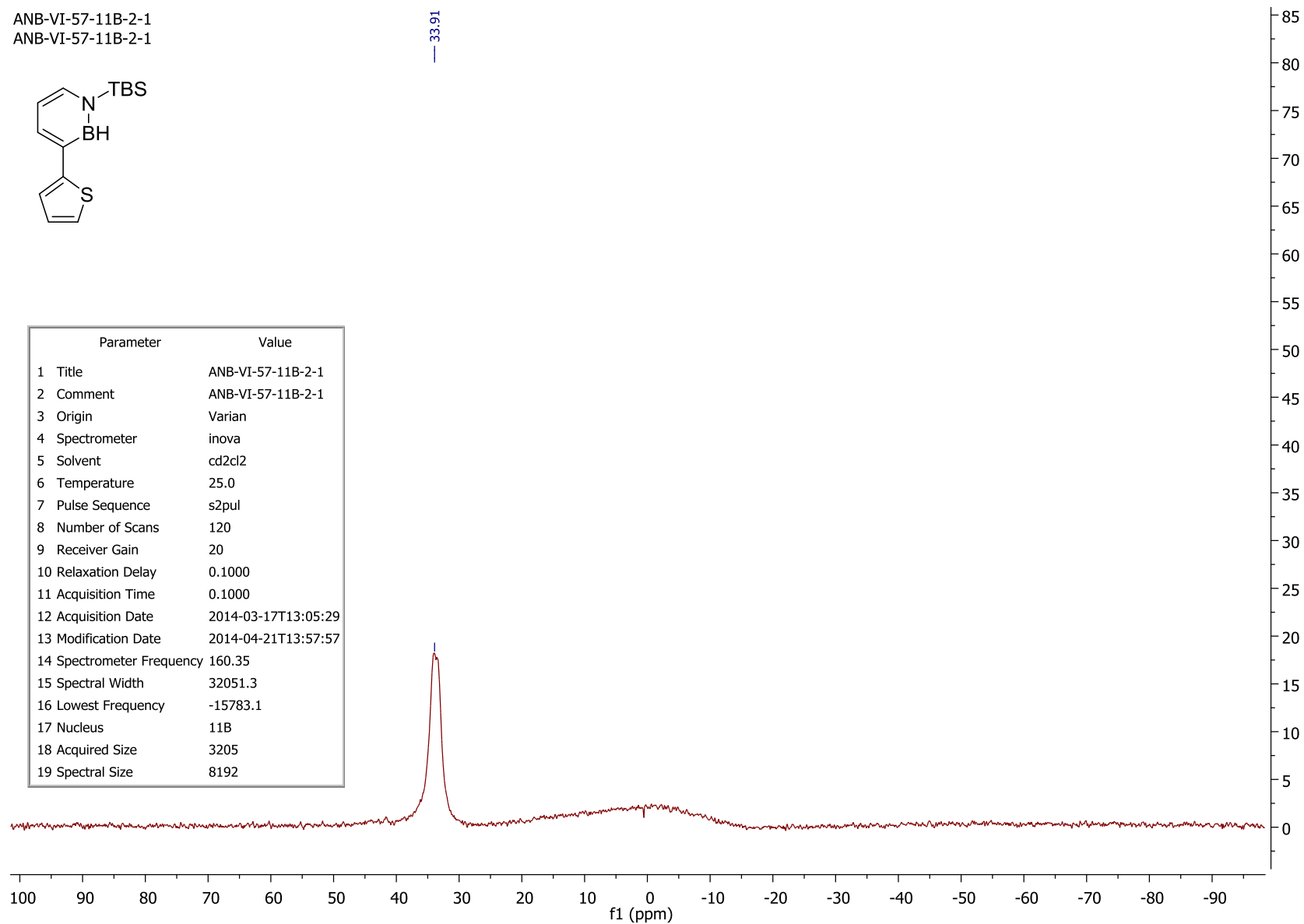
ANb-VI-57-1H-2-1
ANB-VI-57-1H-2-1



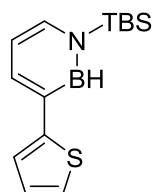
ANB-VI-57-11B-2-1
ANB-VI-57-11B-2-1



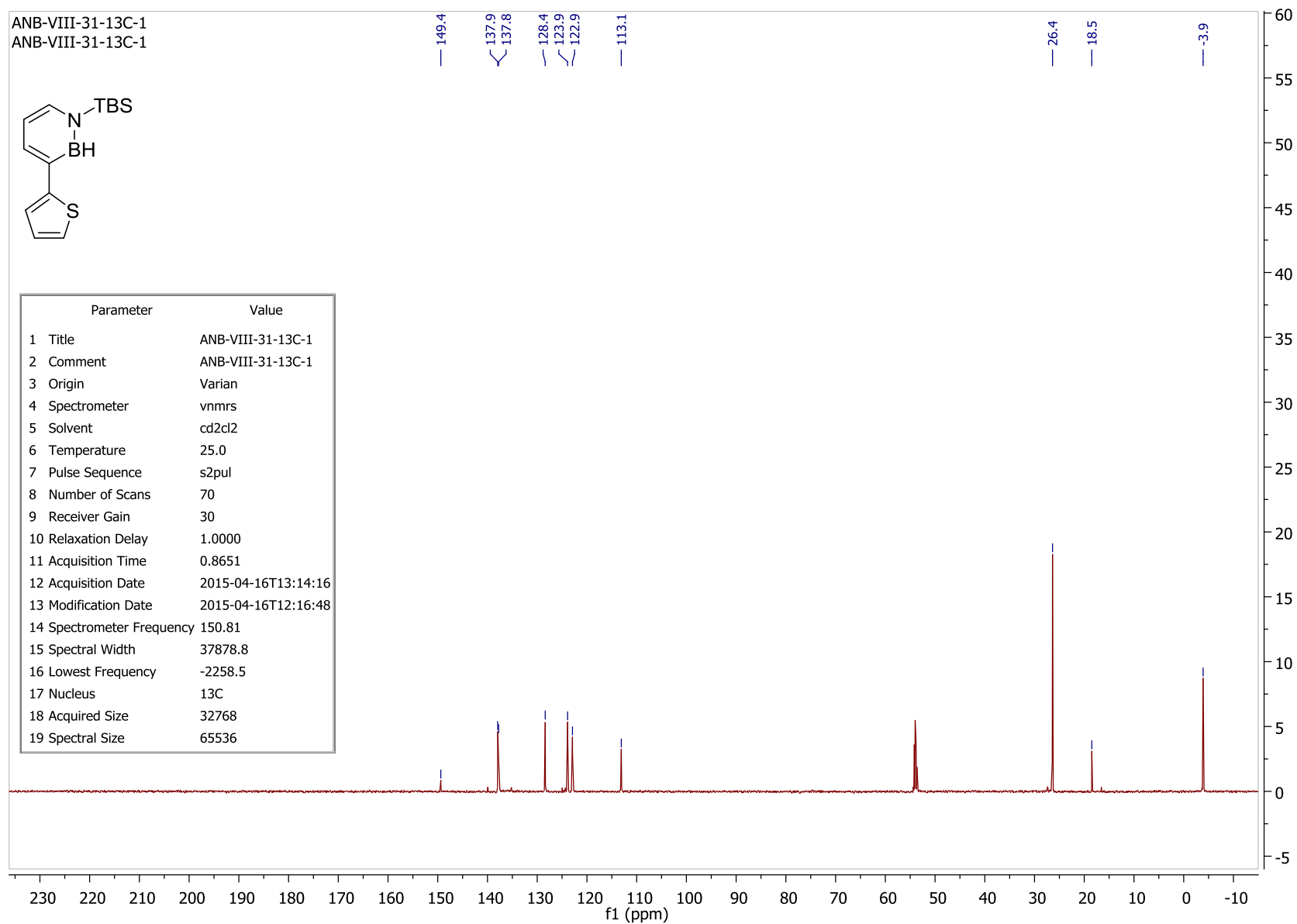
Parameter	Value
1 Title	ANB-VI-57-11B-2-1
2 Comment	ANB-VI-57-11B-2-1
3 Origin	Varian
4 Spectrometer	inova
5 Solvent	cd2cl2
6 Temperature	25.0
7 Pulse Sequence	s2pul
8 Number of Scans	120
9 Receiver Gain	20
10 Relaxation Delay	0.1000
11 Acquisition Time	0.1000
12 Acquisition Date	2014-03-17T13:05:29
13 Modification Date	2014-04-21T13:57:57
14 Spectrometer Frequency	160.35
15 Spectral Width	32051.3
16 Lowest Frequency	-15783.1
17 Nucleus	11B
18 Acquired Size	3205
19 Spectral Size	8192



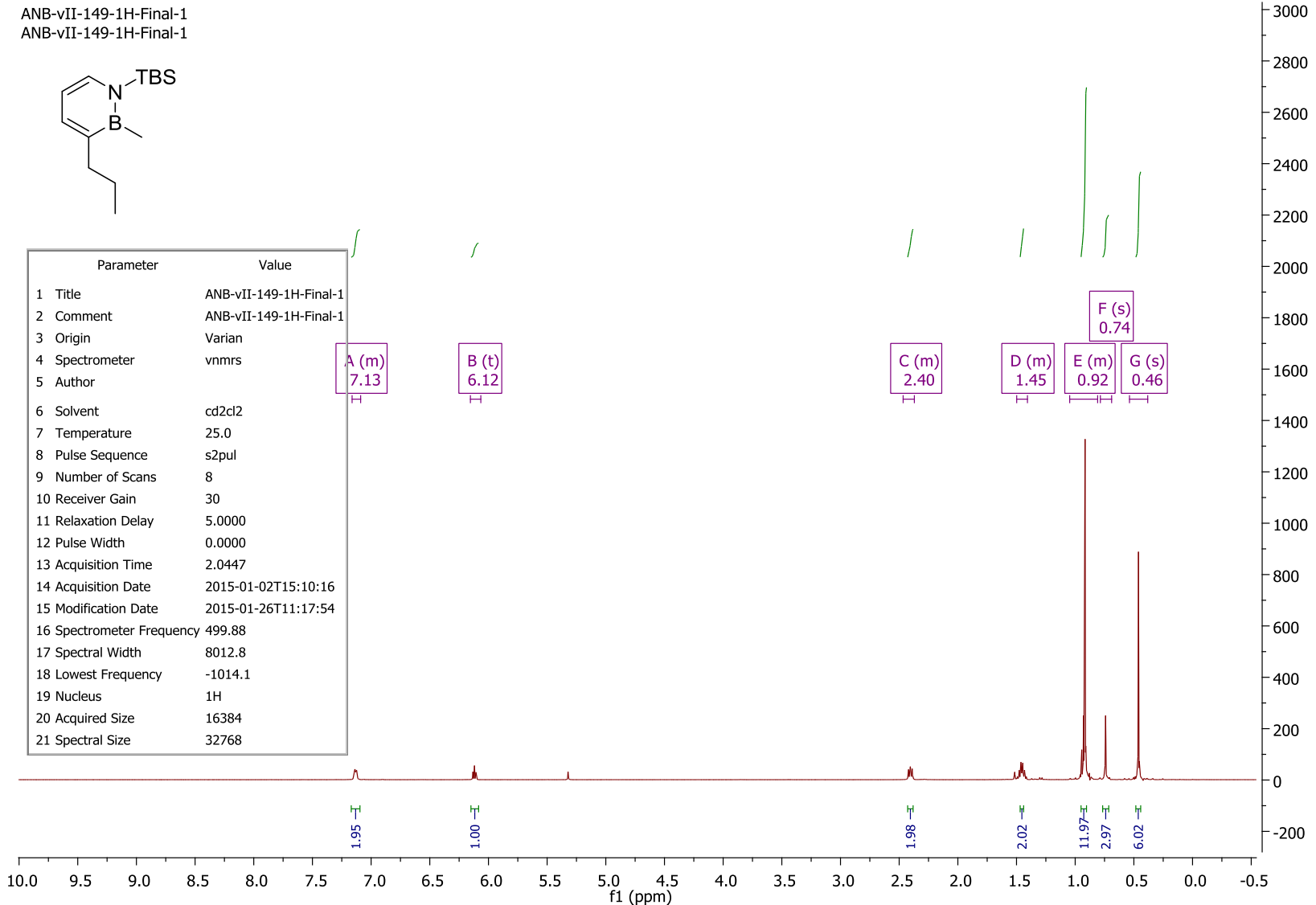
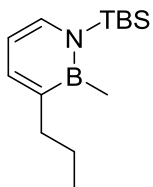
ANB-VIII-31-13C-1
ANB-VIII-31-13C-1



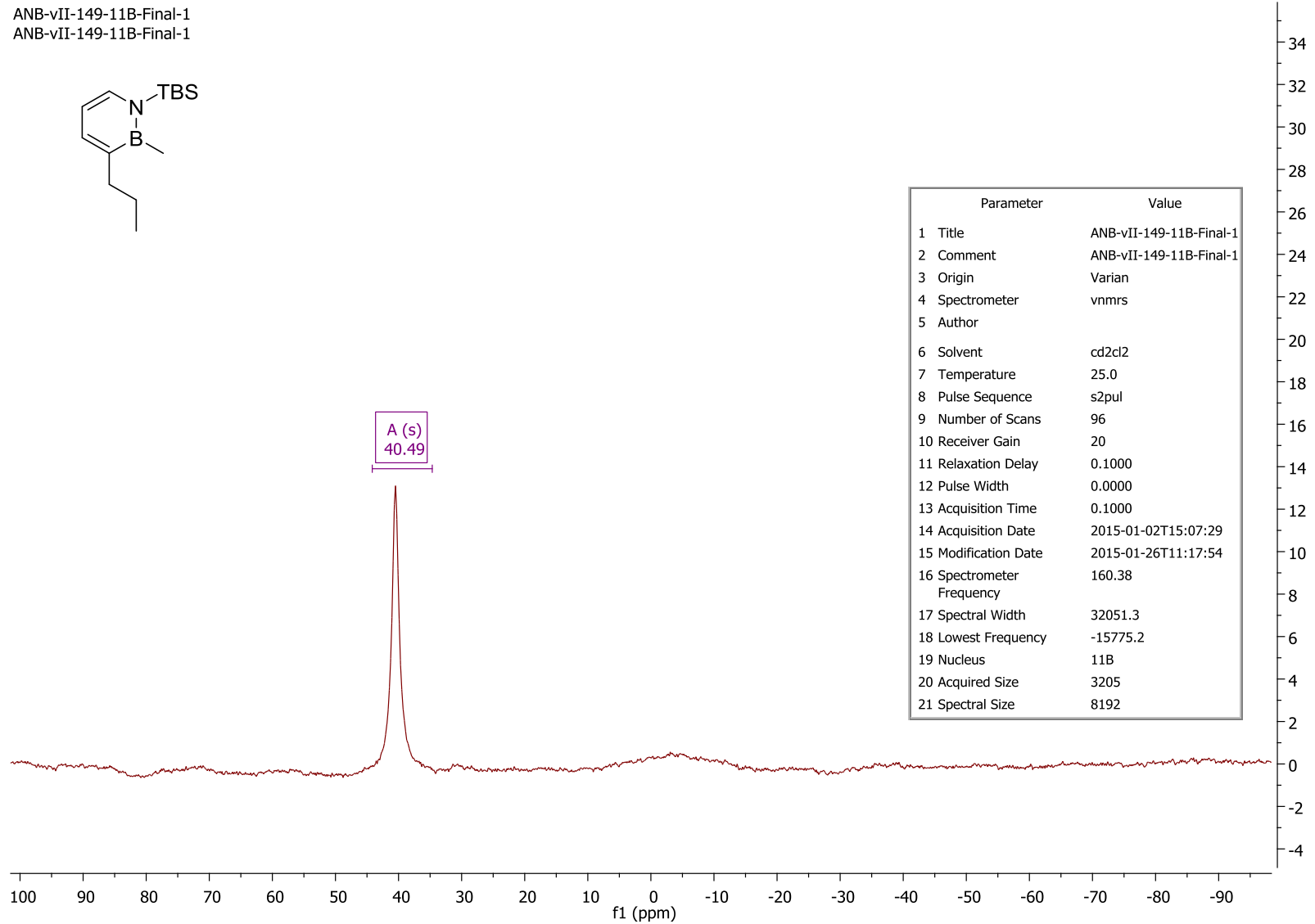
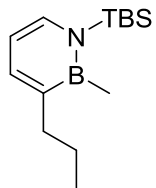
Parameter	Value
1 Title	ANB-VIII-31-13C-1
2 Comment	ANB-VIII-31-13C-1
3 Origin	Varian
4 Spectrometer	nmrs
5 Solvent	cd2cl2
6 Temperature	25.0
7 Pulse Sequence	s2pul
8 Number of Scans	70
9 Receiver Gain	30
10 Relaxation Delay	1.0000
11 Acquisition Time	0.8651
12 Acquisition Date	2015-04-16T13:14:16
13 Modification Date	2015-04-16T12:16:48
14 Spectrometer Frequency	150.81
15 Spectral Width	37878.8
16 Lowest Frequency	-2258.5
17 Nucleus	13C
18 Acquired Size	32768
19 Spectral Size	65536



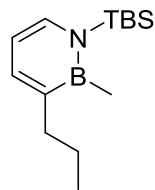
ANB-vII-149-1H-Final-1
 ANB-vII-149-1H-Final-1



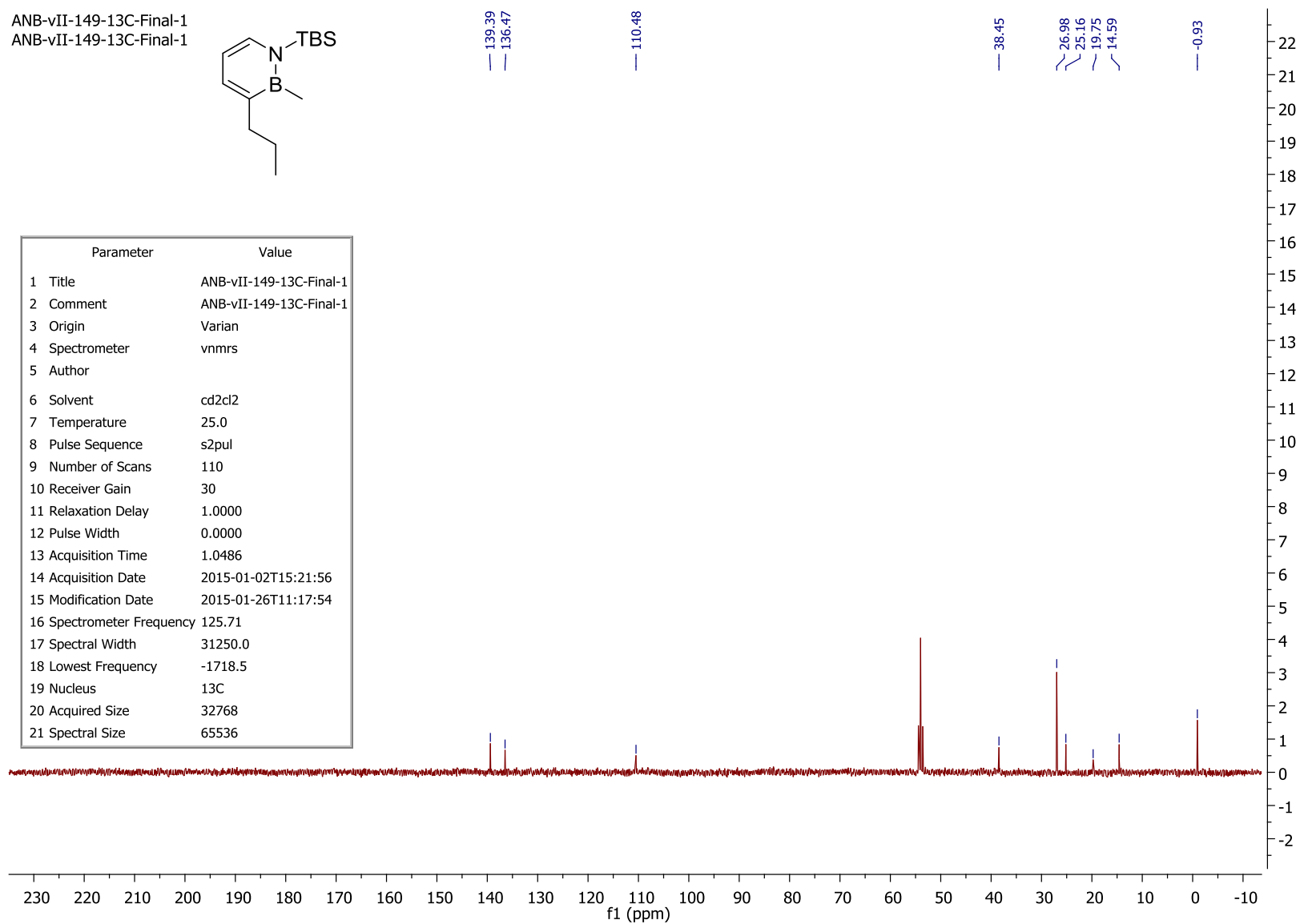
ANB-vII-149-11B-Final-1
ANB-vII-149-11B-Final-1



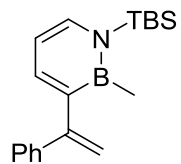
ANB-vII-149-13C-Final-1
ANB-vII-149-13C-Final-1



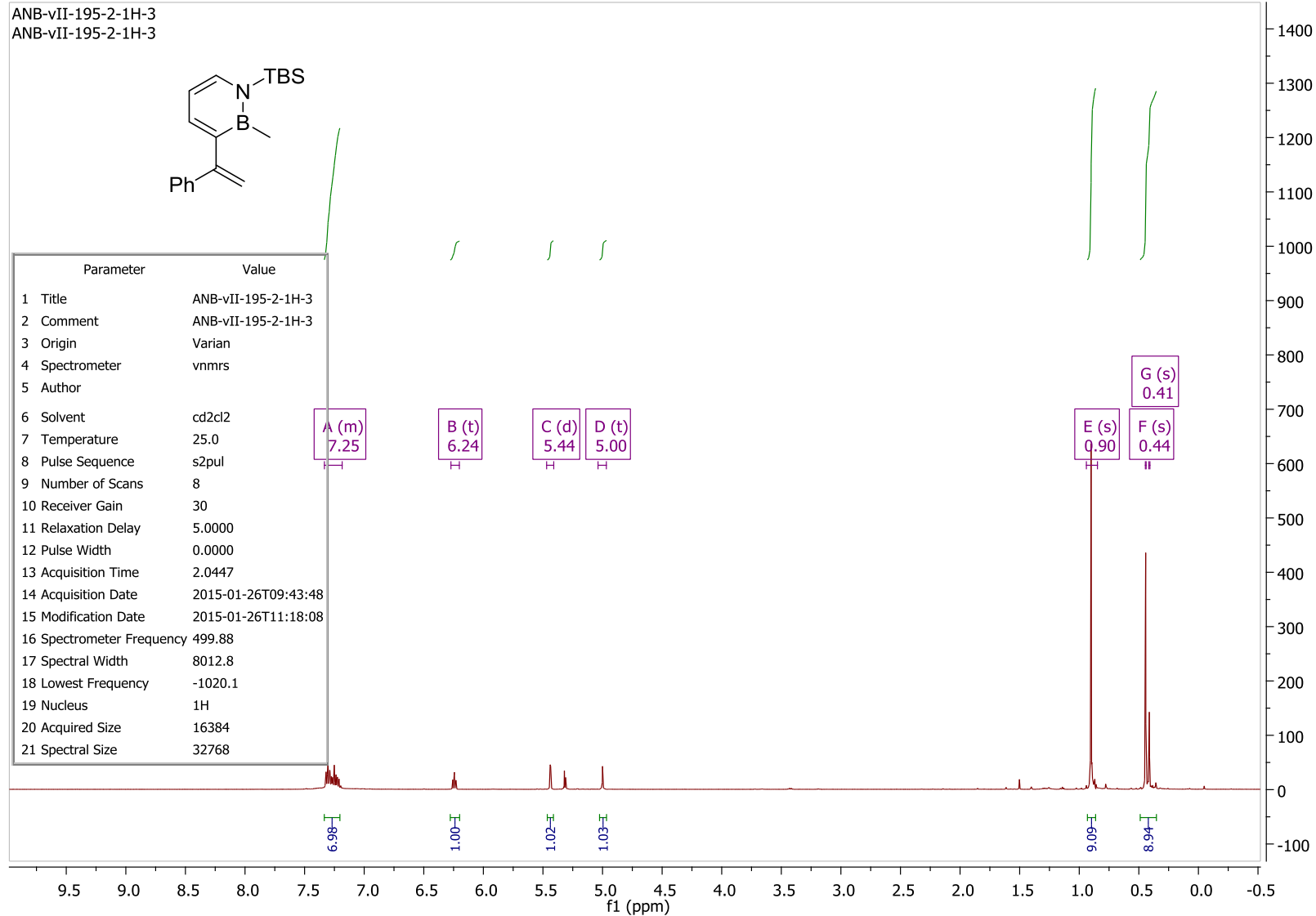
Parameter	Value
1 Title	ANB-vII-149-13C-Final-1
2 Comment	ANB-vII-149-13C-Final-1
3 Origin	Varian
4 Spectrometer	nmrs
5 Author	
6 Solvent	cd2cl2
7 Temperature	25.0
8 Pulse Sequence	s2pul
9 Number of Scans	110
10 Receiver Gain	30
11 Relaxation Delay	1.0000
12 Pulse Width	0.0000
13 Acquisition Time	1.0486
14 Acquisition Date	2015-01-02T15:21:56
15 Modification Date	2015-01-26T11:17:54
16 Spectrometer Frequency	125.71
17 Spectral Width	31250.0
18 Lowest Frequency	-1718.5
19 Nucleus	13C
20 Acquired Size	32768
21 Spectral Size	65536



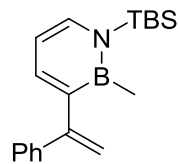
ANB-vII-195-2-1H-3
ANB-vII-195-2-1H-3



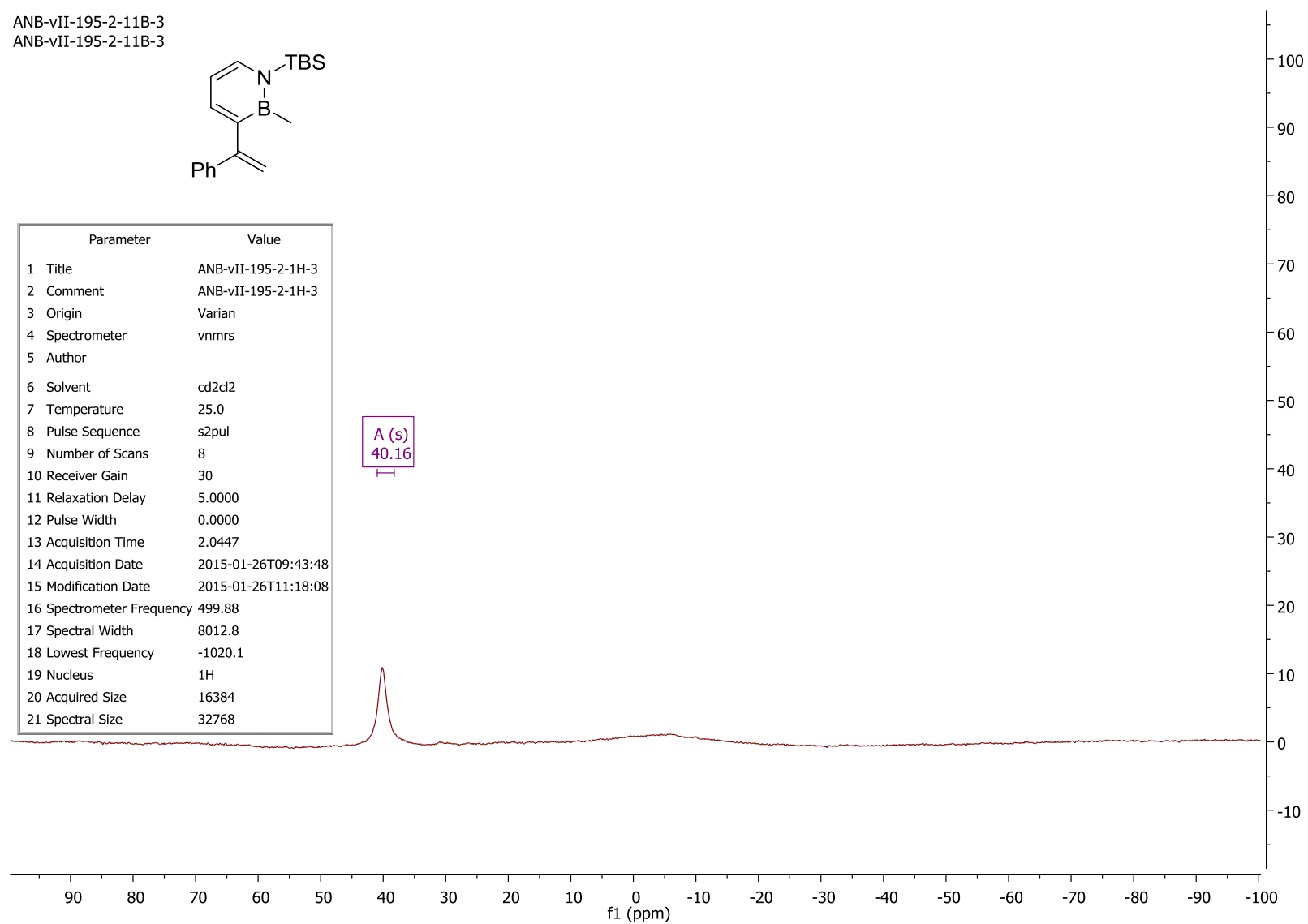
Parameter	Value
1 Title	ANB-vII-195-2-1H-3
2 Comment	ANB-vII-195-2-1H-3
3 Origin	Varian
4 Spectrometer	vnmrs
5 Author	
6 Solvent	cd2cl2
7 Temperature	25.0
8 Pulse Sequence	s2pul
9 Number of Scans	8
10 Receiver Gain	30
11 Relaxation Delay	5.0000
12 Pulse Width	0.0000
13 Acquisition Time	2.0447
14 Acquisition Date	2015-01-26T09:43:48
15 Modification Date	2015-01-26T11:18:08
16 Spectrometer Frequency	499.88
17 Spectral Width	8012.8
18 Lowest Frequency	-1020.1
19 Nucleus	1H
20 Acquired Size	16384
21 Spectral Size	32768



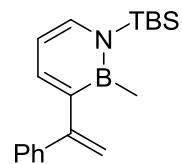
ANB-vII-195-2-11B-3
ANB-vII-195-2-11B-3



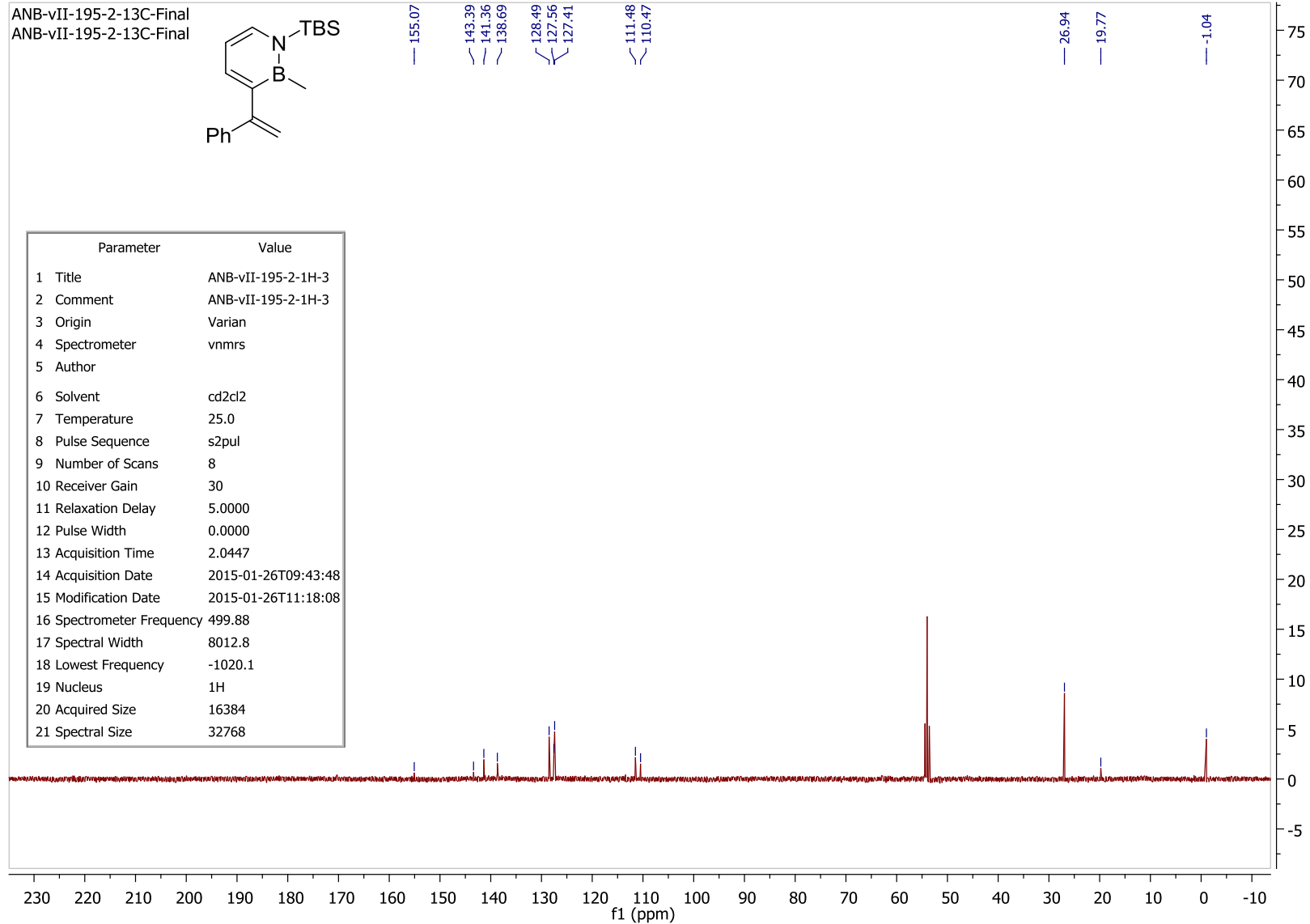
Parameter	Value
1 Title	ANB-vII-195-2-1H-3
2 Comment	ANB-vII-195-2-1H-3
3 Origin	Varian
4 Spectrometer	vnmrs
5 Author	
6 Solvent	cd2cl2
7 Temperature	25.0
8 Pulse Sequence	s2pul
9 Number of Scans	8
10 Receiver Gain	30
11 Relaxation Delay	5.0000
12 Pulse Width	0.0000
13 Acquisition Time	2.0447
14 Acquisition Date	2015-01-26T09:43:48
15 Modification Date	2015-01-26T11:18:08
16 Spectrometer Frequency	499.88
17 Spectral Width	8012.8
18 Lowest Frequency	-1020.1
19 Nucleus	1H
20 Acquired Size	16384
21 Spectral Size	32768



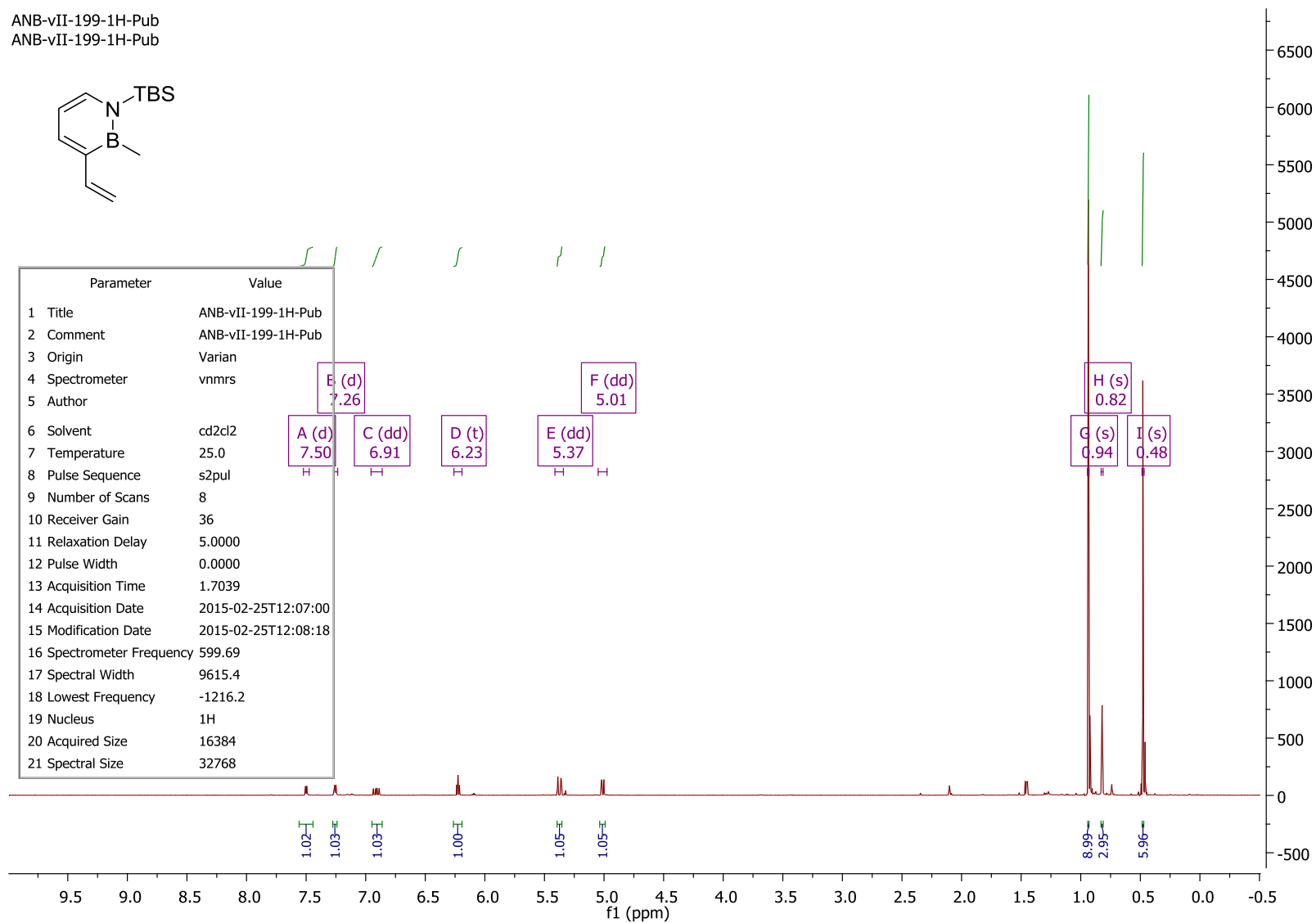
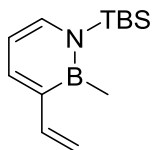
ANB-vII-195-2-13C-Final
ANB-vII-195-2-13C-Final



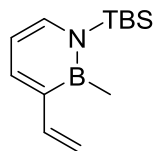
Parameter	Value
1 Title	ANB-vII-195-2-1H-3
2 Comment	ANB-vII-195-2-1H-3
3 Origin	Varian
4 Spectrometer	vnmrs
5 Author	
6 Solvent	cd2cl2
7 Temperature	25.0
8 Pulse Sequence	s2pul
9 Number of Scans	8
10 Receiver Gain	30
11 Relaxation Delay	5.0000
12 Pulse Width	0.0000
13 Acquisition Time	2.0447
14 Acquisition Date	2015-01-26T09:43:48
15 Modification Date	2015-01-26T11:18:08
16 Spectrometer Frequency	499.88
17 Spectral Width	8012.8
18 Lowest Frequency	-1020.1
19 Nucleus	1H
20 Acquired Size	16384
21 Spectral Size	32768



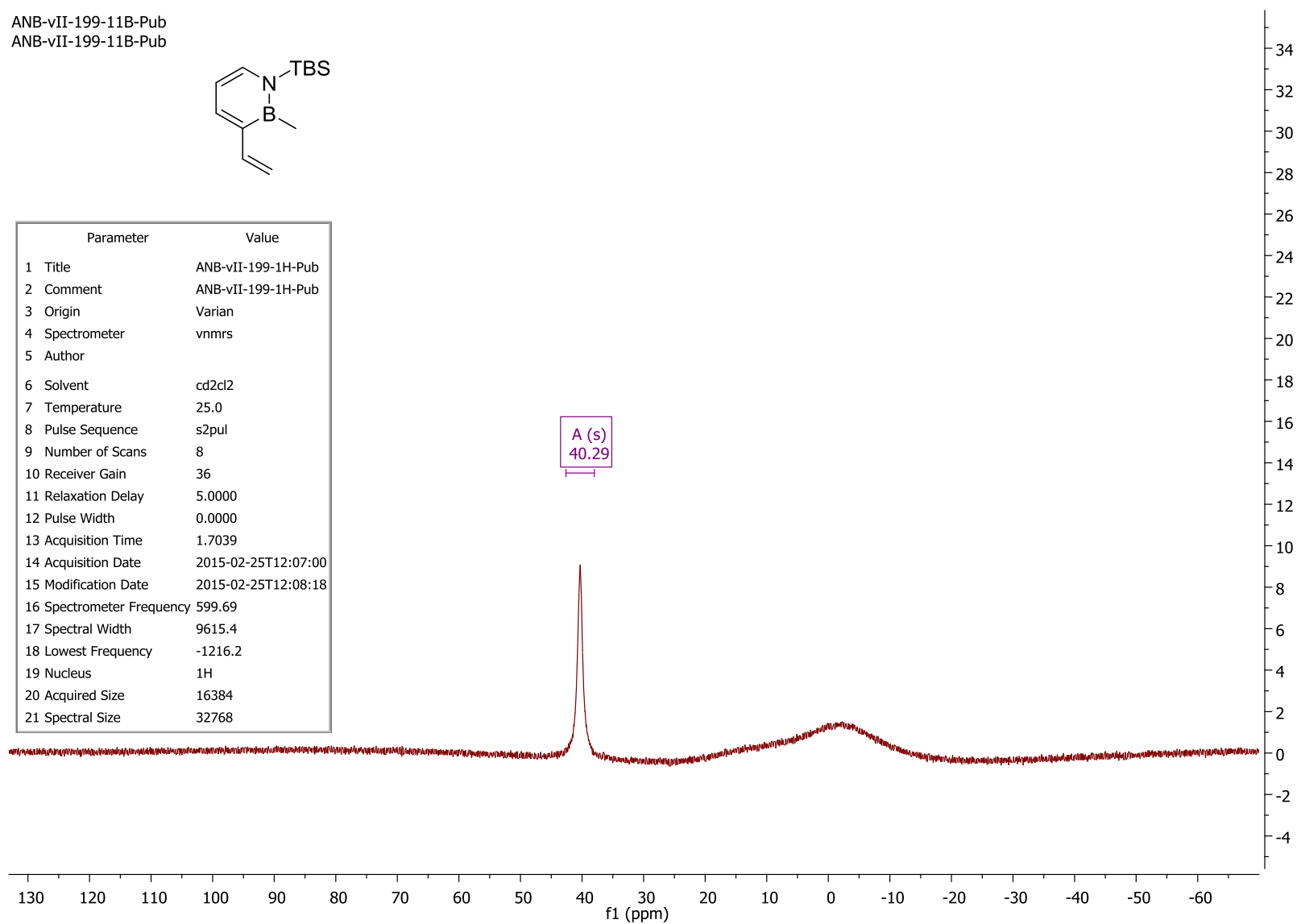
ANB-vII-199-1H-Pub
ANB-vII-199-1H-Pub



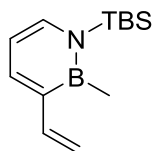
ANB-vII-199-11B-Pub
ANB-vII-199-11B-Pub



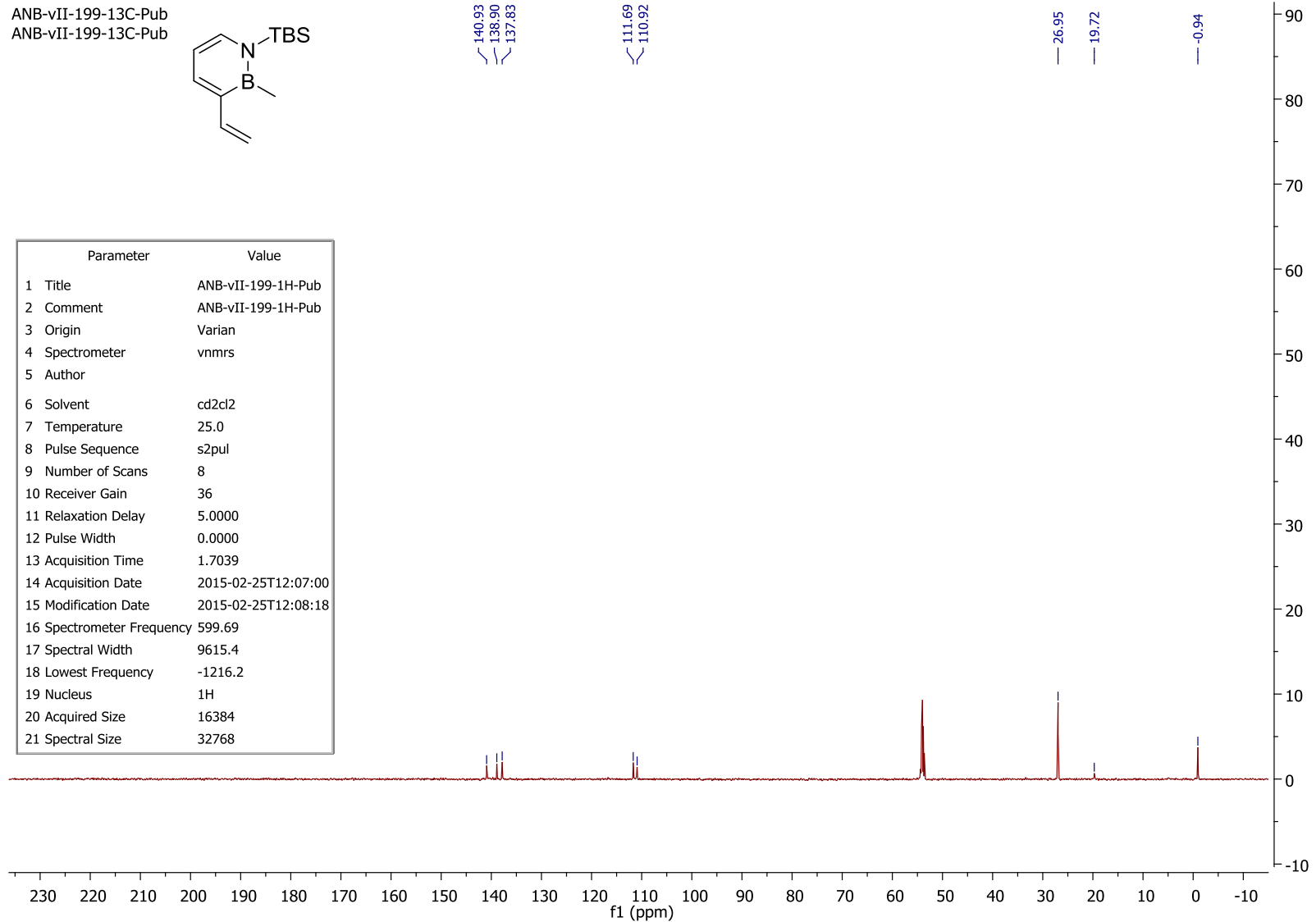
Parameter	Value
1 Title	ANB-vII-199-1H-Pub
2 Comment	ANB-vII-199-1H-Pub
3 Origin	Varian
4 Spectrometer	vnmrs
5 Author	
6 Solvent	cd2cl2
7 Temperature	25.0
8 Pulse Sequence	s2pul
9 Number of Scans	8
10 Receiver Gain	36
11 Relaxation Delay	5.0000
12 Pulse Width	0.0000
13 Acquisition Time	1.7039
14 Acquisition Date	2015-02-25T12:07:00
15 Modification Date	2015-02-25T12:08:18
16 Spectrometer Frequency	599.69
17 Spectral Width	9615.4
18 Lowest Frequency	-1216.2
19 Nucleus	1H
20 Acquired Size	16384
21 Spectral Size	32768



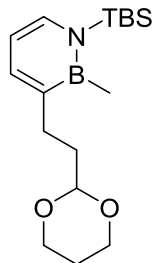
ANB-vII-199-13C-Pub
ANB-vII-199-13C-Pub



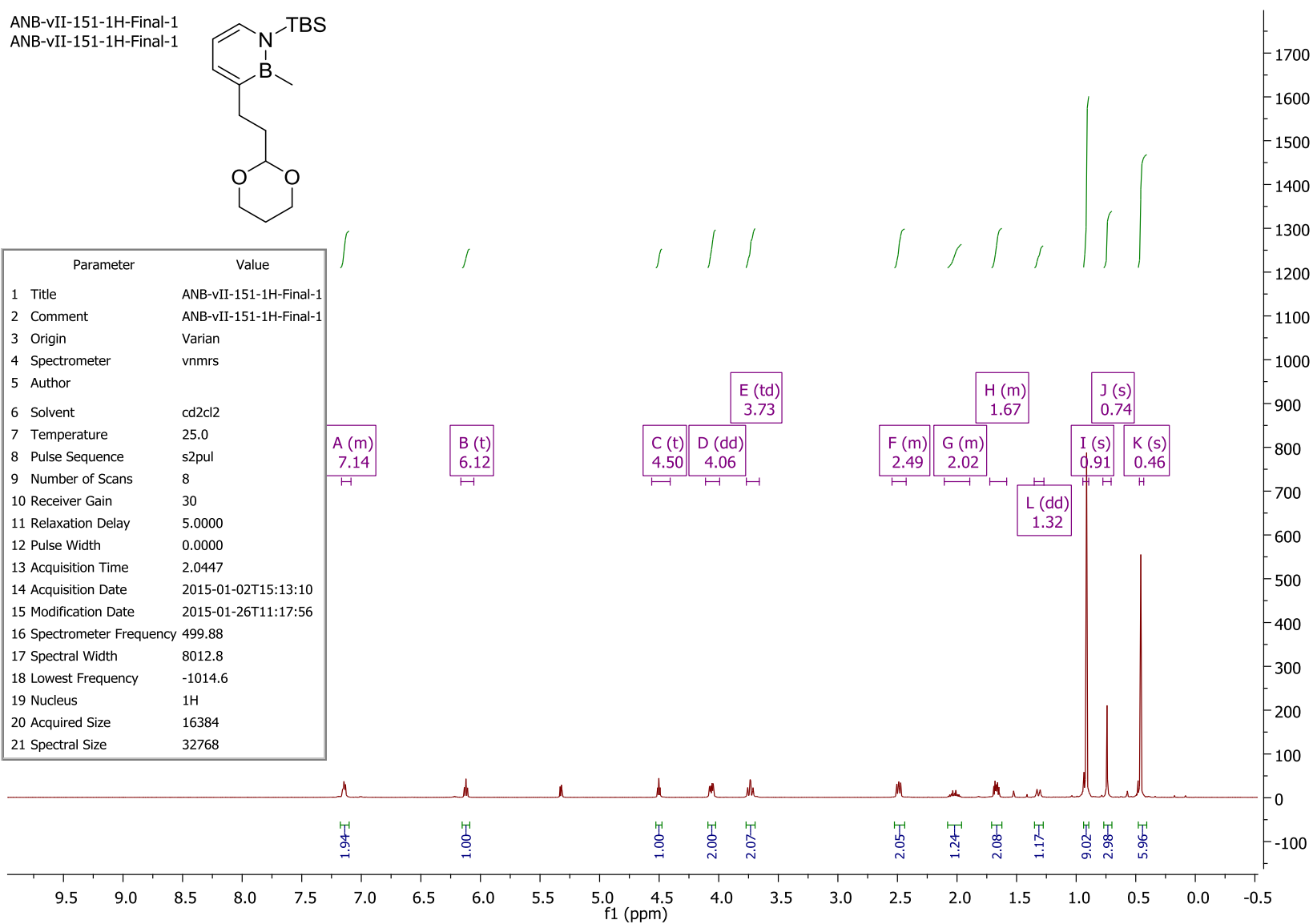
Parameter	Value
1 Title	ANB-vII-199-1H-Pub
2 Comment	ANB-vII-199-1H-Pub
3 Origin	Varian
4 Spectrometer	vnmrs
5 Author	
6 Solvent	cd2cl2
7 Temperature	25.0
8 Pulse Sequence	s2pul
9 Number of Scans	8
10 Receiver Gain	36
11 Relaxation Delay	5.0000
12 Pulse Width	0.0000
13 Acquisition Time	1.7039
14 Acquisition Date	2015-02-25T12:07:00
15 Modification Date	2015-02-25T12:08:18
16 Spectrometer Frequency	599.69
17 Spectral Width	9615.4
18 Lowest Frequency	-1216.2
19 Nucleus	1H
20 Acquired Size	16384
21 Spectral Size	32768



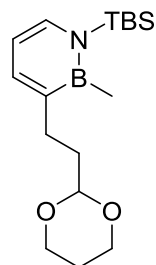
ANB-vII-151-1H-Final-1
ANB-vII-151-1H-Final-1



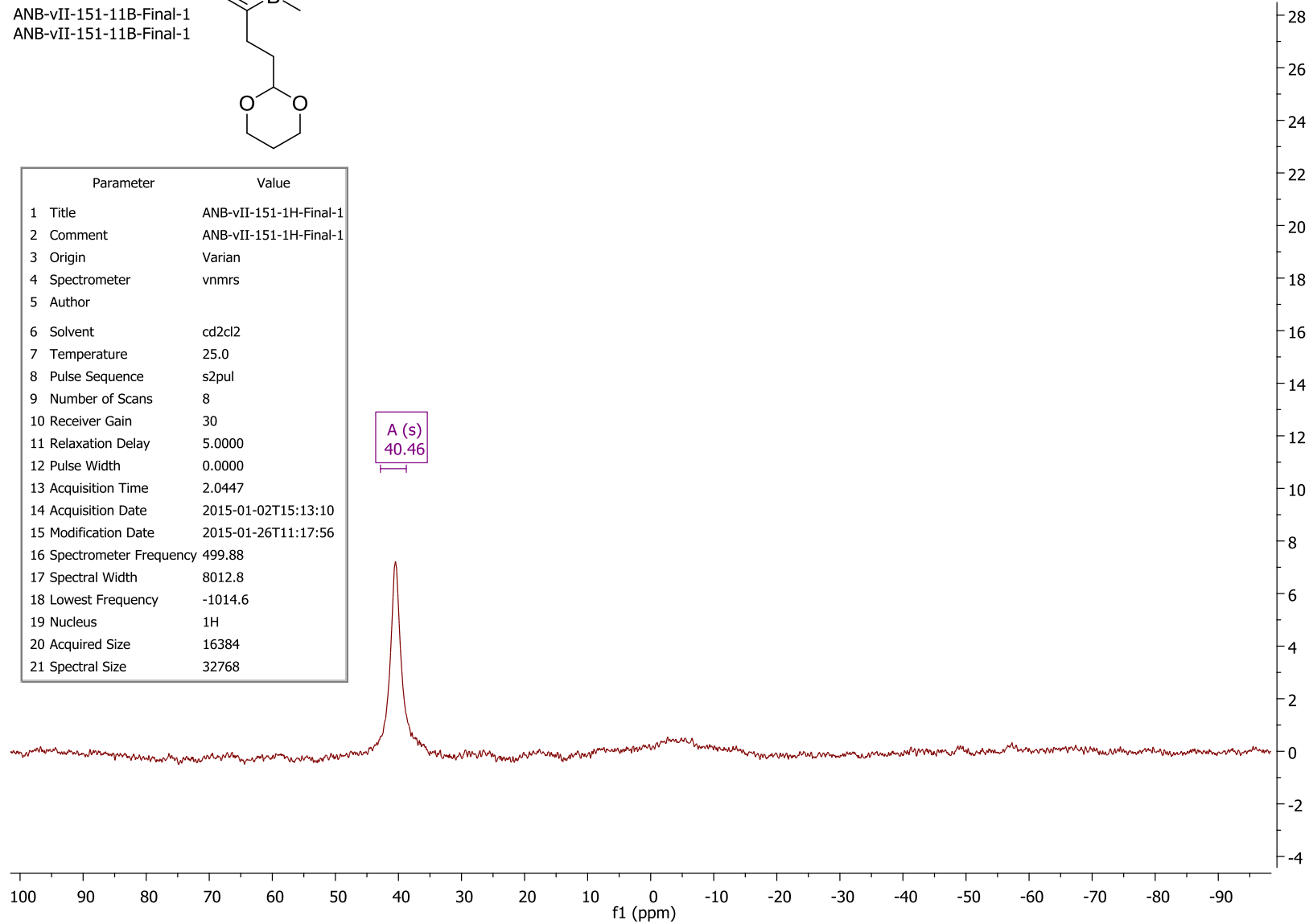
Parameter	Value
1 Title	ANB-vII-151-1H-Final-1
2 Comment	ANB-vII-151-1H-Final-1
3 Origin	Varian
4 Spectrometer	vnmrs
5 Author	
6 Solvent	cd2cl2
7 Temperature	25.0
8 Pulse Sequence	s2pul
9 Number of Scans	8
10 Receiver Gain	30
11 Relaxation Delay	5.0000
12 Pulse Width	0.0000
13 Acquisition Time	2.0447
14 Acquisition Date	2015-01-02T15:13:10
15 Modification Date	2015-01-26T11:17:56
16 Spectrometer Frequency	499.88
17 Spectral Width	8012.8
18 Lowest Frequency	-1014.6
19 Nucleus	1H
20 Acquired Size	16384
21 Spectral Size	32768



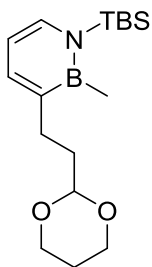
ANB-vII-151-11B-Final-1
ANB-vII-151-11B-Final-1



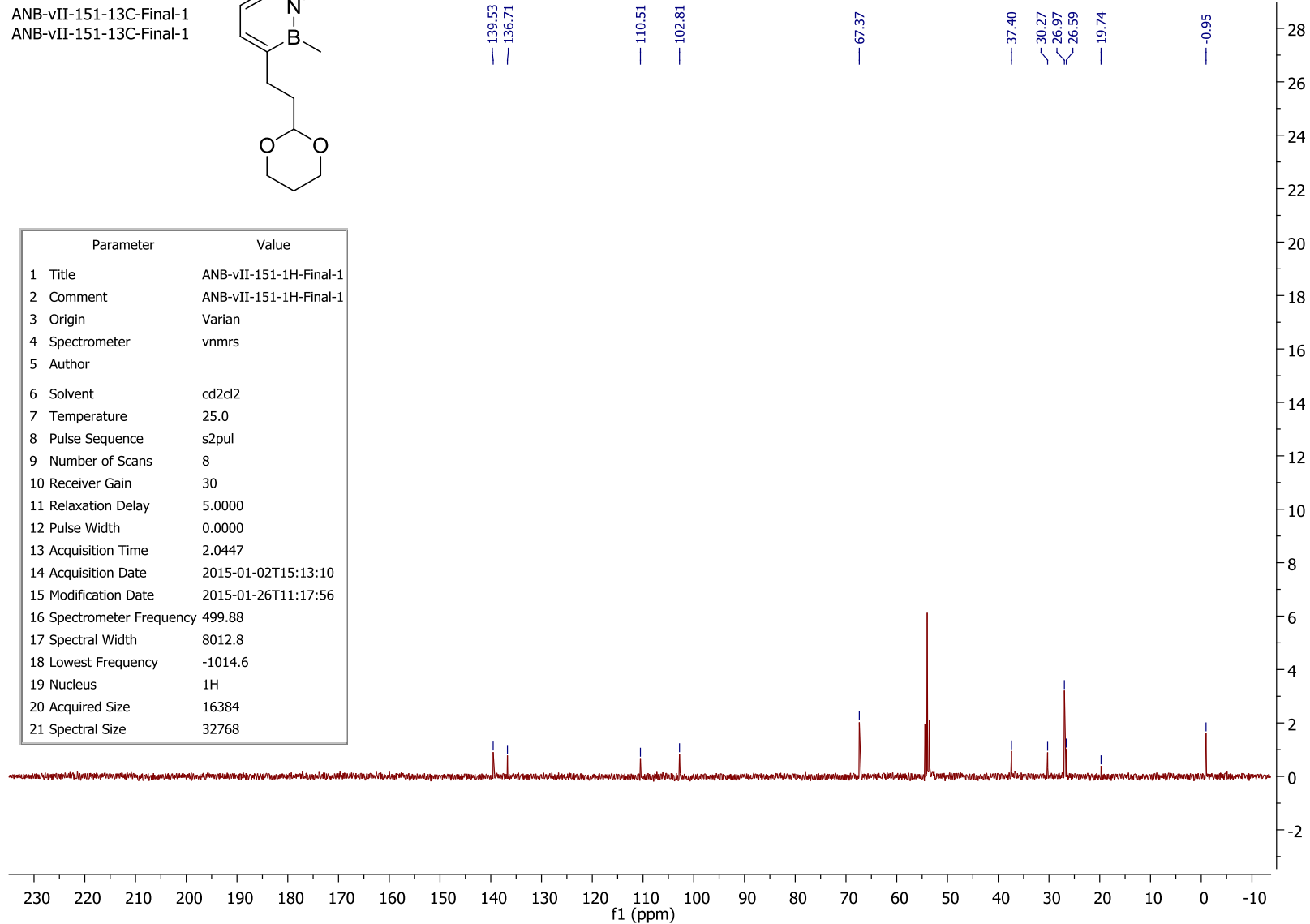
Parameter	Value
1 Title	ANB-vII-151-1H-Final-1
2 Comment	ANB-vII-151-1H-Final-1
3 Origin	Varian
4 Spectrometer	vnmrs
5 Author	
6 Solvent	cd2cl2
7 Temperature	25.0
8 Pulse Sequence	s2pul
9 Number of Scans	8
10 Receiver Gain	30
11 Relaxation Delay	5.0000
12 Pulse Width	0.0000
13 Acquisition Time	2.0447
14 Acquisition Date	2015-01-02T15:13:10
15 Modification Date	2015-01-26T11:17:56
16 Spectrometer Frequency	499.88
17 Spectral Width	8012.8
18 Lowest Frequency	-1014.6
19 Nucleus	1H
20 Acquired Size	16384
21 Spectral Size	32768



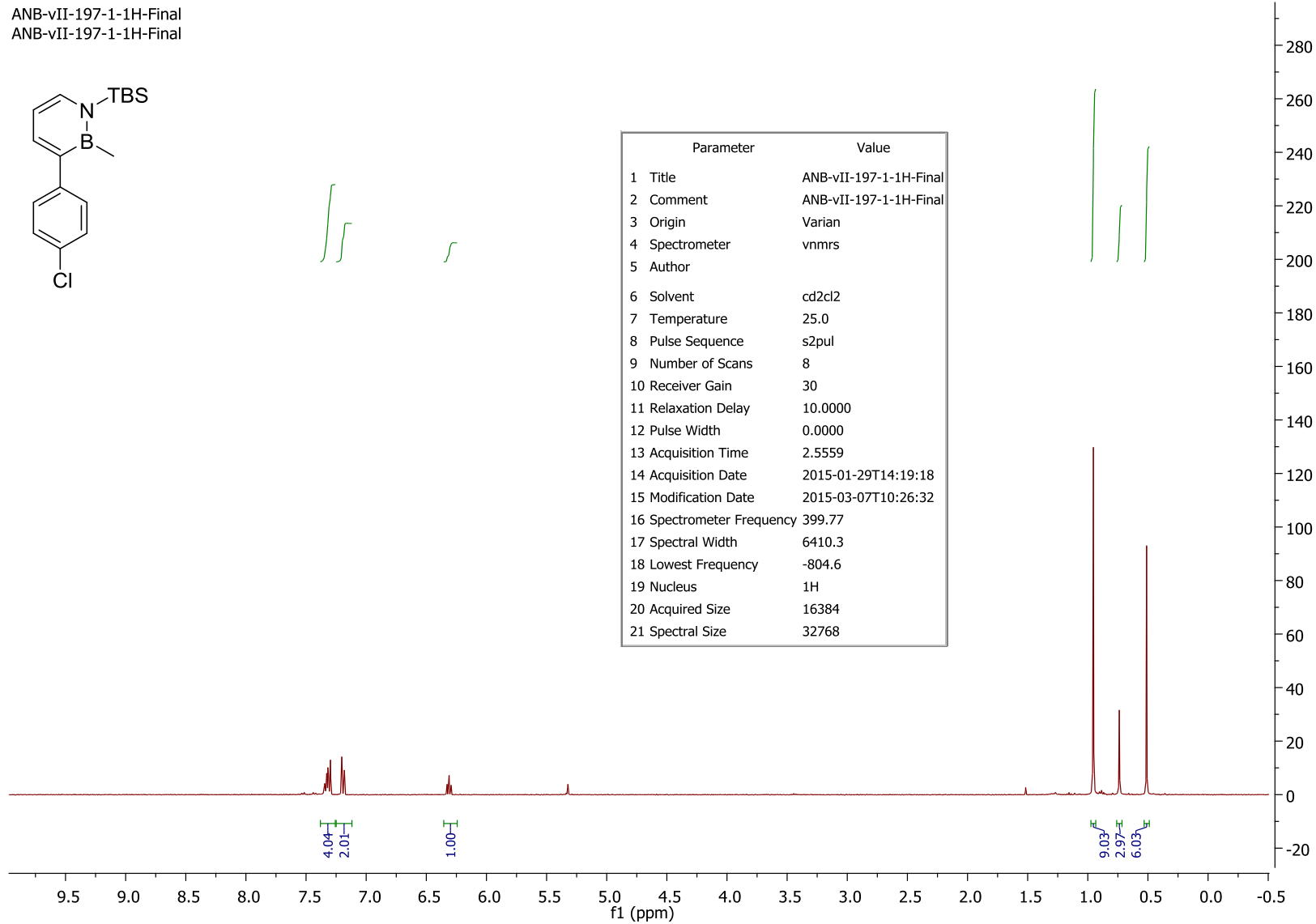
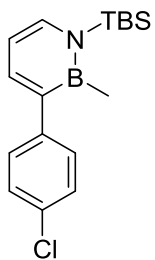
ANB-vII-151-13C-Final-1
ANB-vII-151-13C-Final-1



Parameter	Value
1 Title	ANB-vII-151-1H-Final-1
2 Comment	ANB-vII-151-1H-Final-1
3 Origin	Varian
4 Spectrometer	vnmrs
5 Author	
6 Solvent	cd2cl2
7 Temperature	25.0
8 Pulse Sequence	s2pul
9 Number of Scans	8
10 Receiver Gain	30
11 Relaxation Delay	5.0000
12 Pulse Width	0.0000
13 Acquisition Time	2.0447
14 Acquisition Date	2015-01-02T15:13:10
15 Modification Date	2015-01-26T11:17:56
16 Spectrometer Frequency	499.88
17 Spectral Width	8012.8
18 Lowest Frequency	-1014.6
19 Nucleus	1H
20 Acquired Size	16384
21 Spectral Size	32768

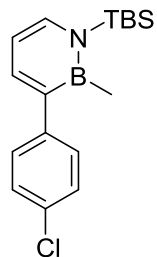


ANB-vII-197-1-1H-Final
ANB-vII-197-1-1H-Final



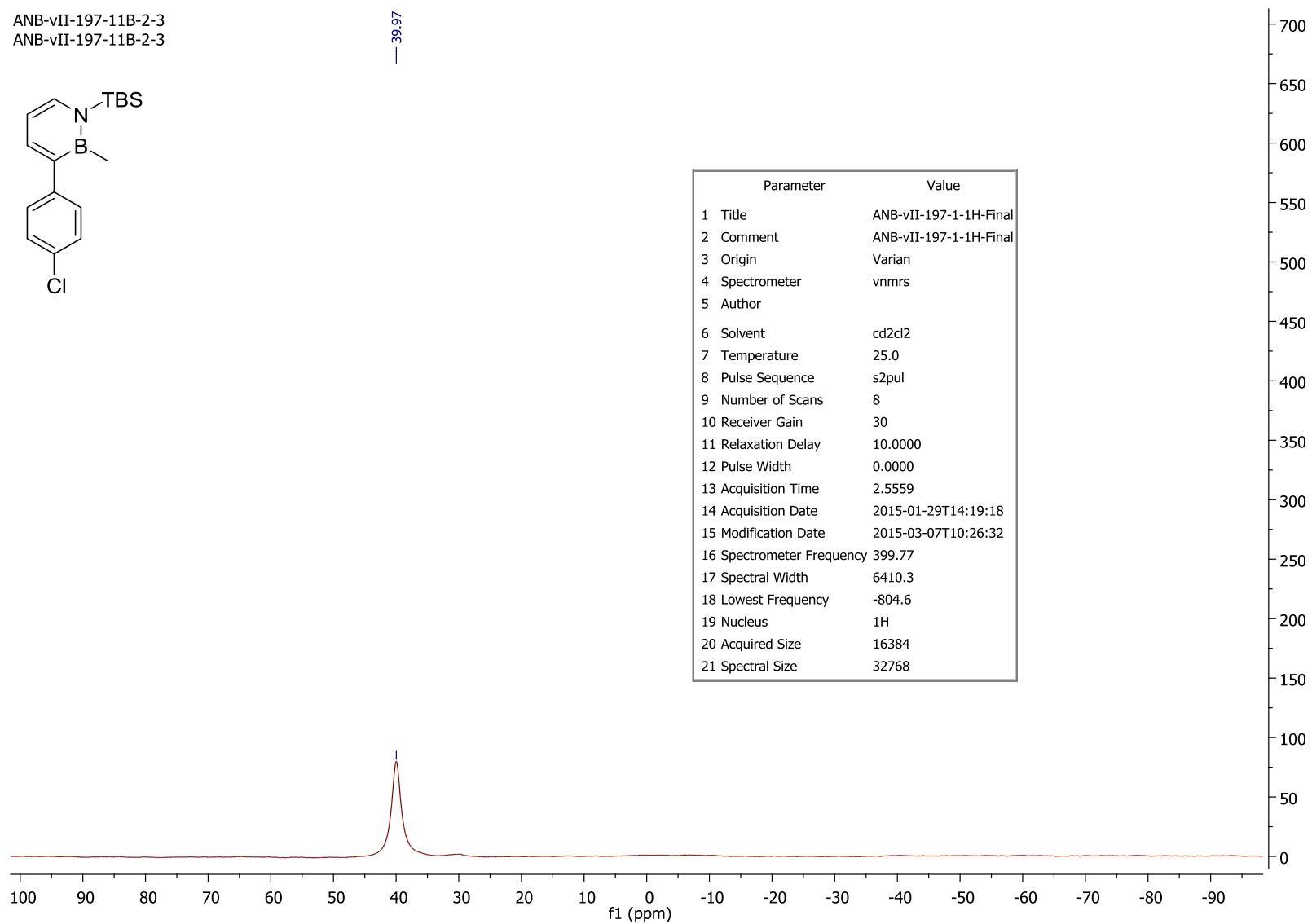
Parameter	Value
1 Title	ANB-vII-197-1-1H-Final
2 Comment	ANB-vII-197-1-1H-Final
3 Origin	Varian
4 Spectrometer	vnms
5 Author	
6 Solvent	cd2cl2
7 Temperature	25.0
8 Pulse Sequence	s2pul
9 Number of Scans	8
10 Receiver Gain	30
11 Relaxation Delay	10.0000
12 Pulse Width	0.0000
13 Acquisition Time	2.5559
14 Acquisition Date	2015-01-29T14:19:18
15 Modification Date	2015-03-07T10:26:32
16 Spectrometer Frequency	399.77
17 Spectral Width	6410.3
18 Lowest Frequency	-804.6
19 Nucleus	1H
20 Acquired Size	16384
21 Spectral Size	32768

ANB-vII-197-11B-2-3
ANB-vII-197-11B-2-3

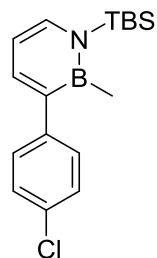


— 39.97

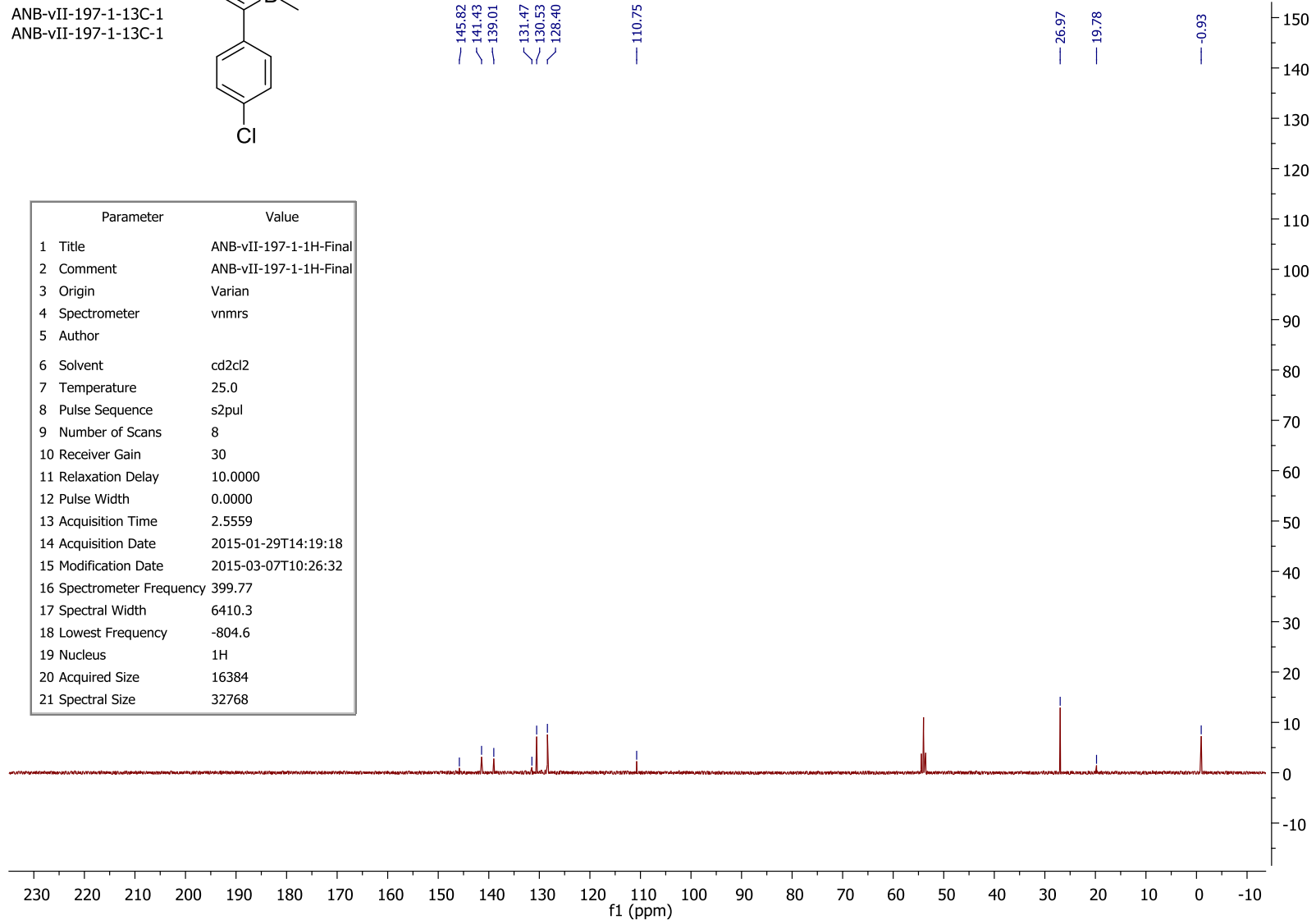
Parameter	Value
1 Title	ANB-vII-197-1-1H-Final
2 Comment	ANB-vII-197-1-1H-Final
3 Origin	Varian
4 Spectrometer	nmrs
5 Author	
6 Solvent	cd2cl2
7 Temperature	25.0
8 Pulse Sequence	s2pul
9 Number of Scans	8
10 Receiver Gain	30
11 Relaxation Delay	10.0000
12 Pulse Width	0.0000
13 Acquisition Time	2.5559
14 Acquisition Date	2015-01-29T14:19:18
15 Modification Date	2015-03-07T10:26:32
16 Spectrometer Frequency	399.77
17 Spectral Width	6410.3
18 Lowest Frequency	-804.6
19 Nucleus	1H
20 Acquired Size	16384
21 Spectral Size	32768



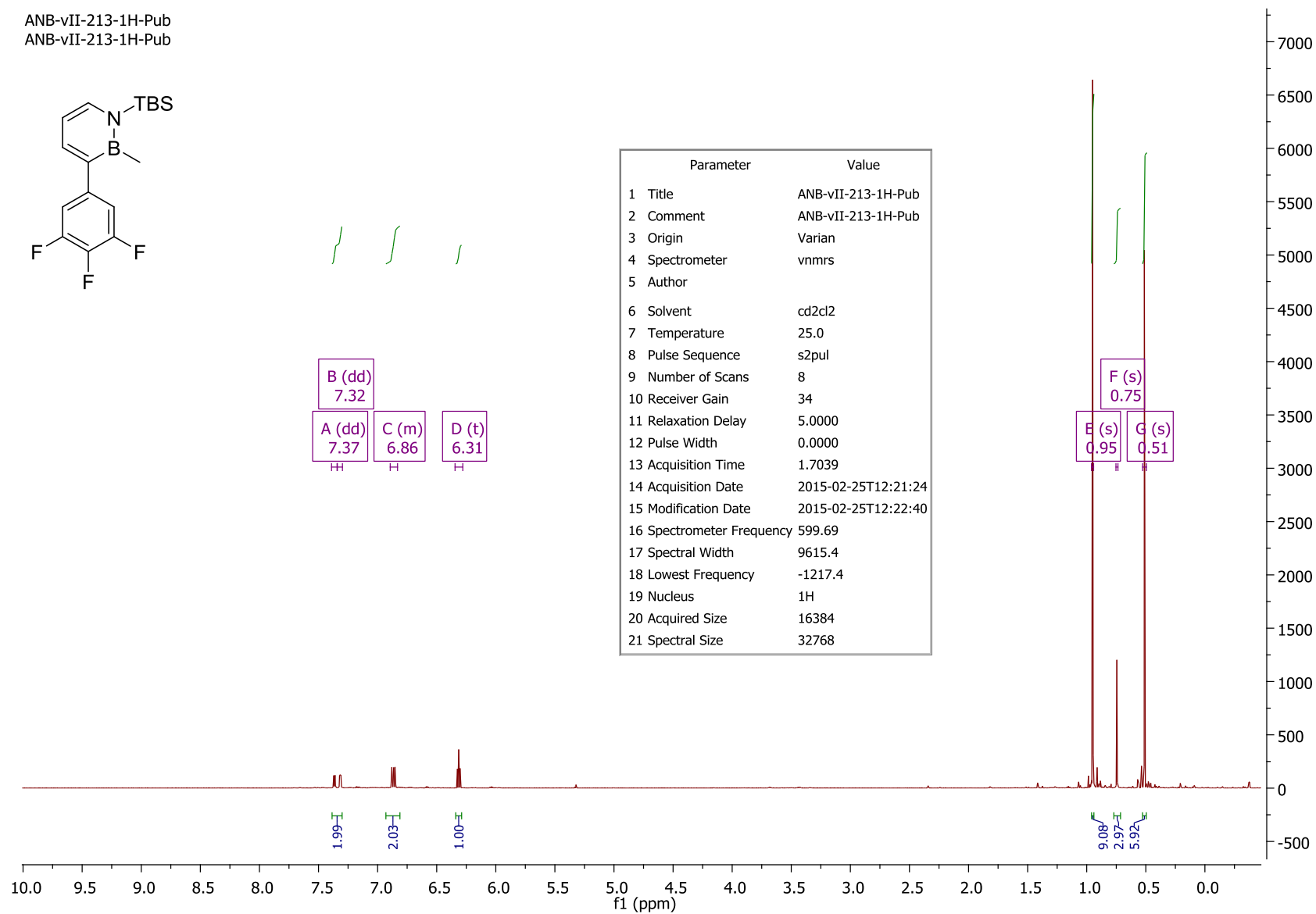
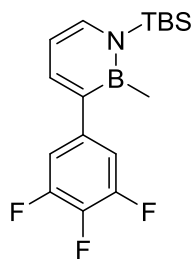
ANB-vII-197-1-13C-1
ANB-vII-197-1-13C-1



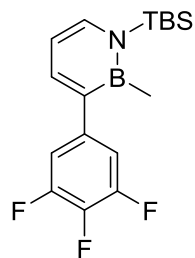
Parameter	Value
1 Title	ANB-vII-197-1-1H-Final
2 Comment	ANB-vII-197-1-1H-Final
3 Origin	Varian
4 Spectrometer	vnmrs
5 Author	
6 Solvent	cd2cl2
7 Temperature	25.0
8 Pulse Sequence	s2pul
9 Number of Scans	8
10 Receiver Gain	30
11 Relaxation Delay	10.0000
12 Pulse Width	0.0000
13 Acquisition Time	2.5559
14 Acquisition Date	2015-01-29T14:19:18
15 Modification Date	2015-03-07T10:26:32
16 Spectrometer Frequency	399.77
17 Spectral Width	6410.3
18 Lowest Frequency	-804.6
19 Nucleus	1H
20 Acquired Size	16384
21 Spectral Size	32768



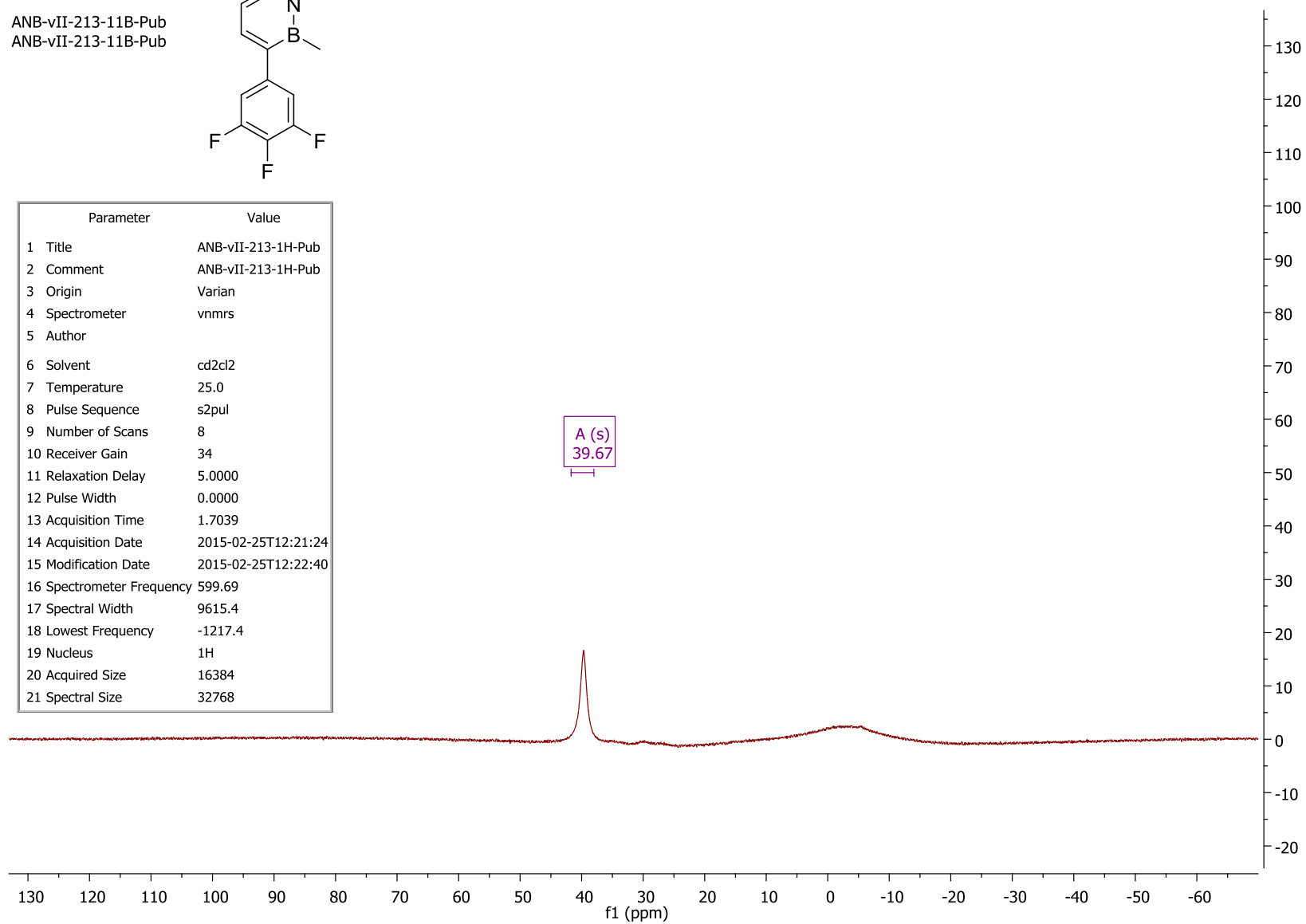
ANB-vII-213-1H-Pub
ANB-vII-213-1H-Pub



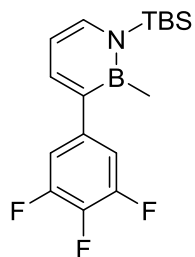
ANB-vII-213-11B-Pub
ANB-vII-213-11B-Pub



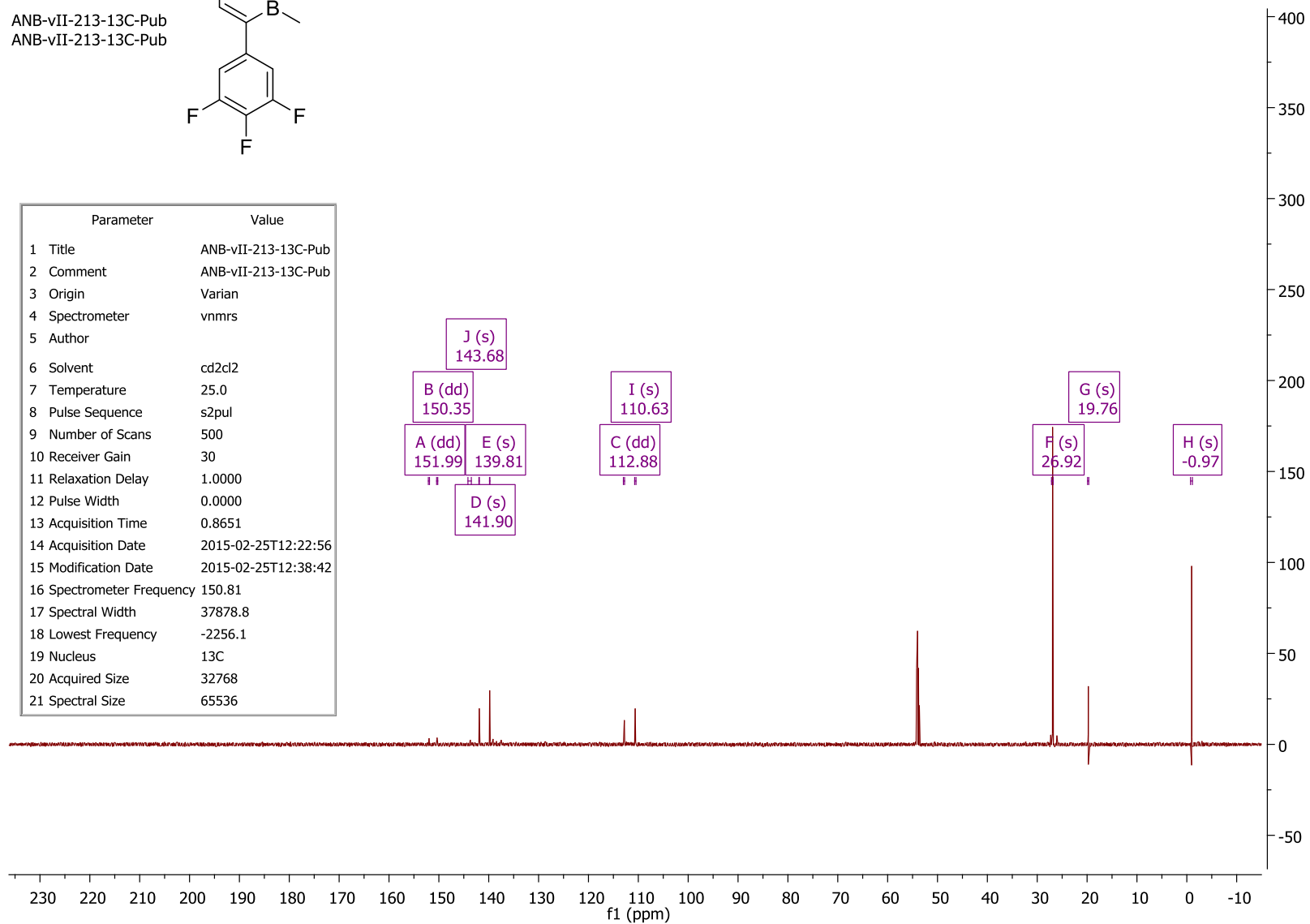
Parameter	Value
1 Title	ANB-vII-213-1H-Pub
2 Comment	ANB-vII-213-1H-Pub
3 Origin	Varian
4 Spectrometer	nmrs
5 Author	
6 Solvent	cd2cl2
7 Temperature	25.0
8 Pulse Sequence	s2pul
9 Number of Scans	8
10 Receiver Gain	34
11 Relaxation Delay	5.0000
12 Pulse Width	0.0000
13 Acquisition Time	1.7039
14 Acquisition Date	2015-02-25T12:21:24
15 Modification Date	2015-02-25T12:22:40
16 Spectrometer Frequency	599.69
17 Spectral Width	9615.4
18 Lowest Frequency	-1217.4
19 Nucleus	1H
20 Acquired Size	16384
21 Spectral Size	32768



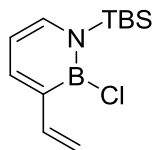
ANB-vII-213-13C-Pub
ANB-vII-213-13C-Pub



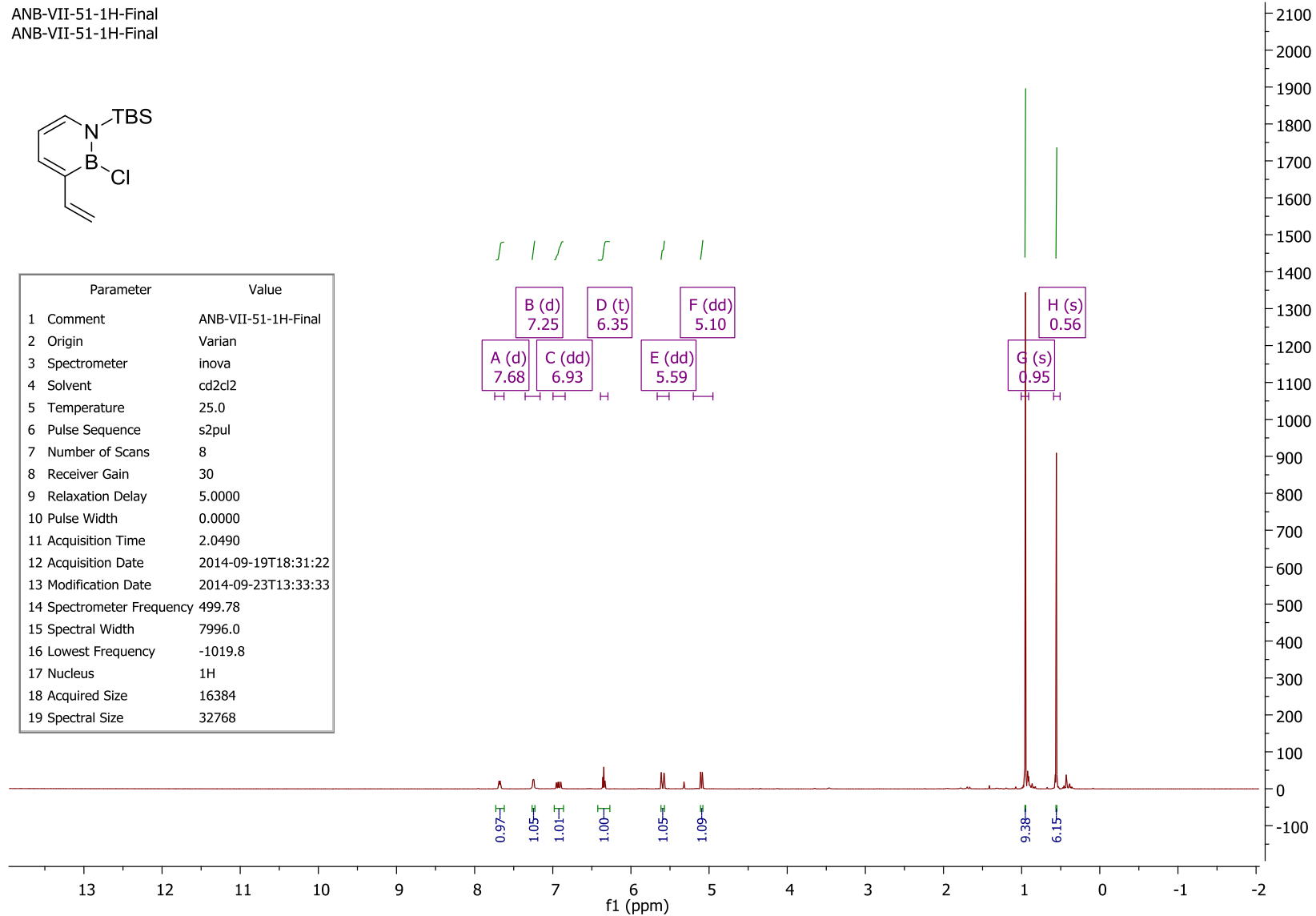
Parameter	Value
1 Title	ANB-vII-213-13C-Pub
2 Comment	ANB-vII-213-13C-Pub
3 Origin	Varian
4 Spectrometer	vnmrs
5 Author	
6 Solvent	cd2cl2
7 Temperature	25.0
8 Pulse Sequence	s2pul
9 Number of Scans	500
10 Receiver Gain	30
11 Relaxation Delay	1.0000
12 Pulse Width	0.0000
13 Acquisition Time	0.8651
14 Acquisition Date	2015-02-25T12:22:56
15 Modification Date	2015-02-25T12:38:42
16 Spectrometer Frequency	150.81
17 Spectral Width	37878.8
18 Lowest Frequency	-2256.1
19 Nucleus	13C
20 Acquired Size	32768
21 Spectral Size	65536



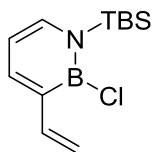
ANB-VII-51-1H-Final
 ANB-VII-51-1H-Final



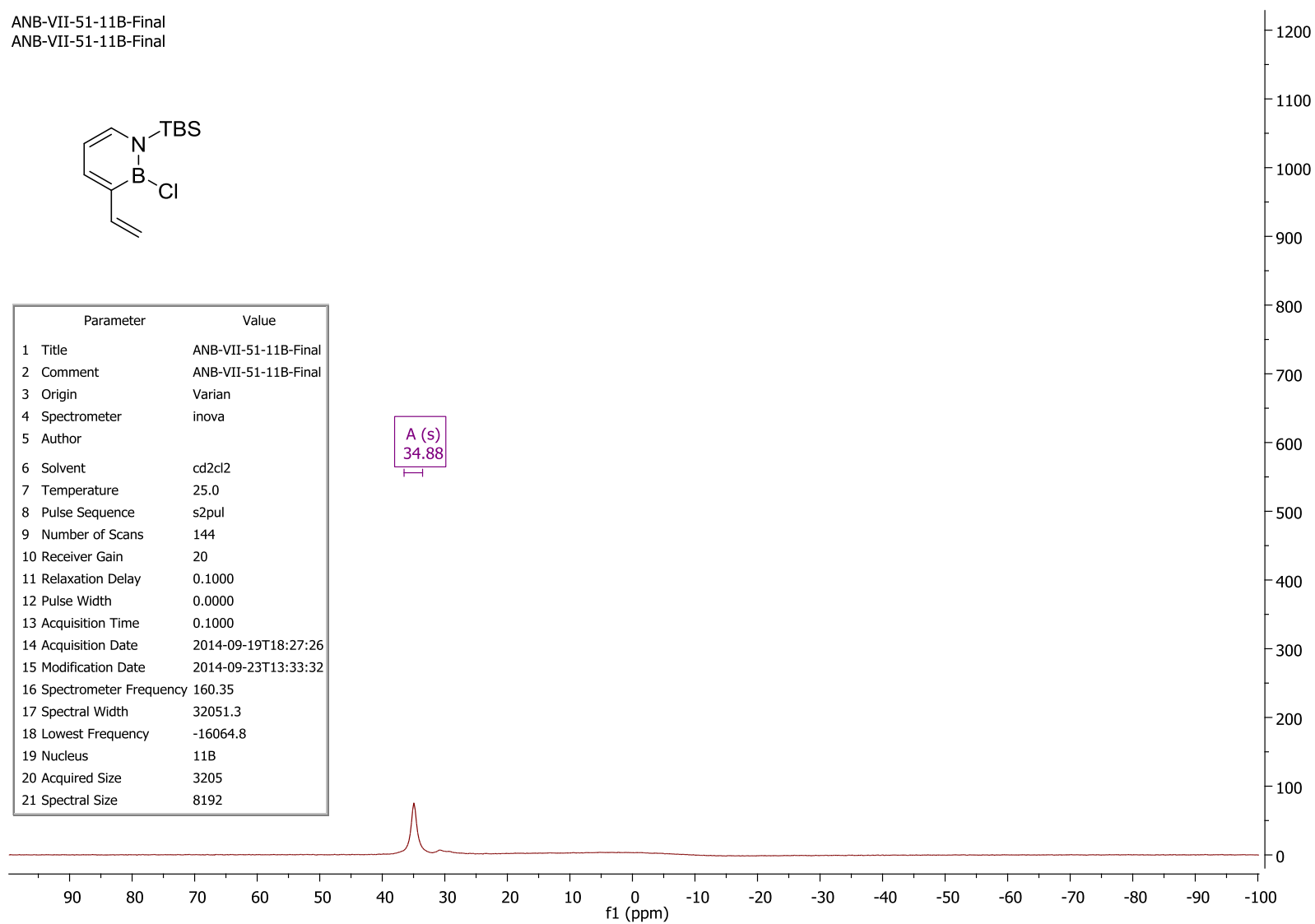
Parameter	Value
1 Comment	ANB-VII-51-1H-Final
2 Origin	Varian
3 Spectrometer	inova
4 Solvent	cd2cl2
5 Temperature	25.0
6 Pulse Sequence	s2pul
7 Number of Scans	8
8 Receiver Gain	30
9 Relaxation Delay	5.0000
10 Pulse Width	0.0000
11 Acquisition Time	2.0490
12 Acquisition Date	2014-09-19T18:31:22
13 Modification Date	2014-09-23T13:33:33
14 Spectrometer Frequency	499.78
15 Spectral Width	7996.0
16 Lowest Frequency	-1019.8
17 Nucleus	1H
18 Acquired Size	16384
19 Spectral Size	32768



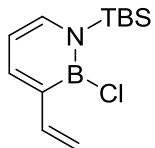
ANB-VII-51-11B-Final
ANB-VII-51-11B-Final



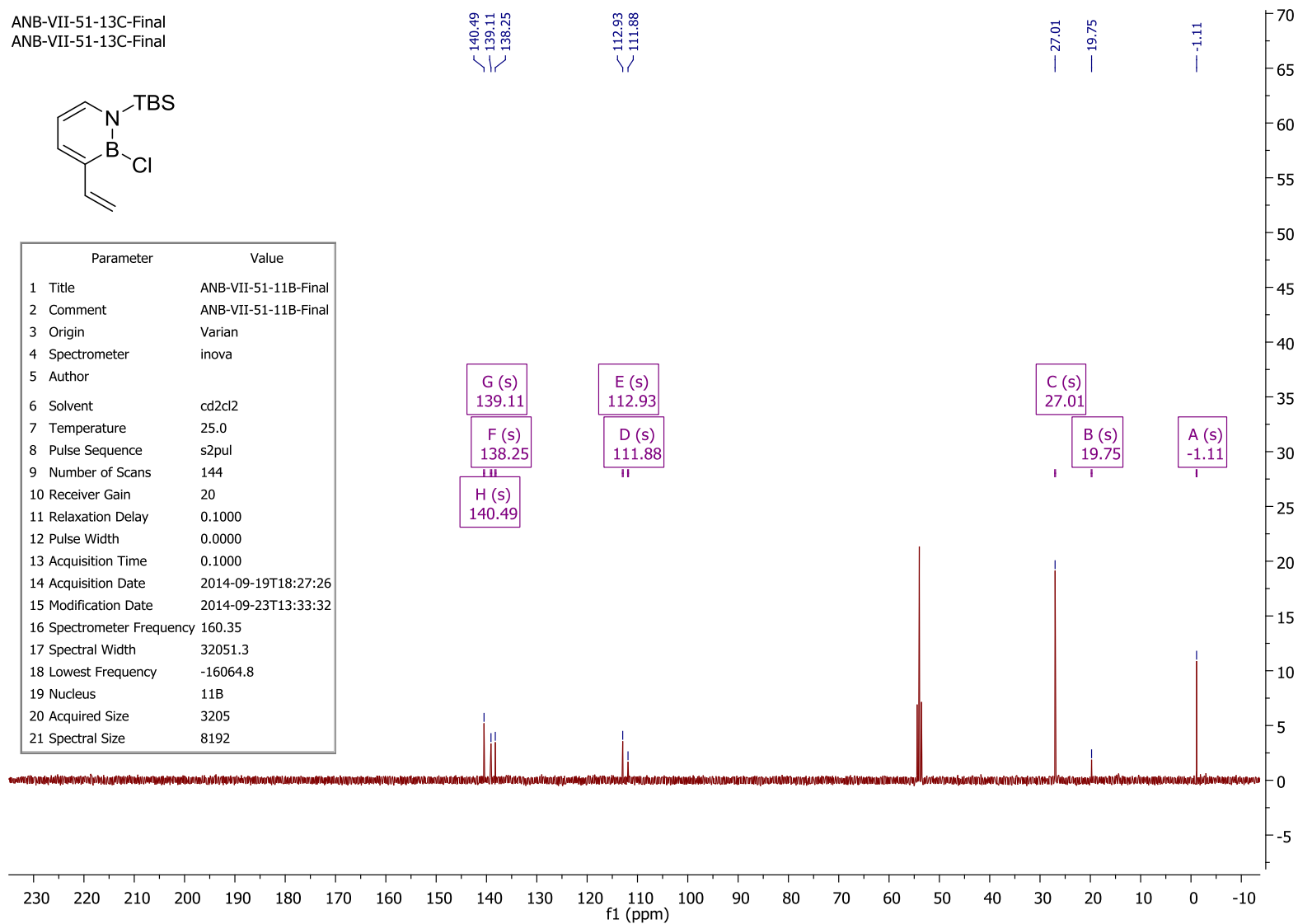
Parameter	Value
1 Title	ANB-VII-51-11B-Final
2 Comment	ANB-VII-51-11B-Final
3 Origin	Varian
4 Spectrometer	inova
5 Author	
6 Solvent	cd2cl2
7 Temperature	25.0
8 Pulse Sequence	s2pul
9 Number of Scans	144
10 Receiver Gain	20
11 Relaxation Delay	0.1000
12 Pulse Width	0.0000
13 Acquisition Time	0.1000
14 Acquisition Date	2014-09-19T18:27:26
15 Modification Date	2014-09-23T13:33:32
16 Spectrometer Frequency	160.35
17 Spectral Width	32051.3
18 Lowest Frequency	-16064.8
19 Nucleus	11B
20 Acquired Size	3205
21 Spectral Size	8192



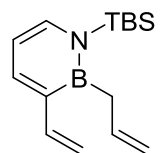
ANB-VII-51-13C-Final
ANB-VII-51-13C-Final



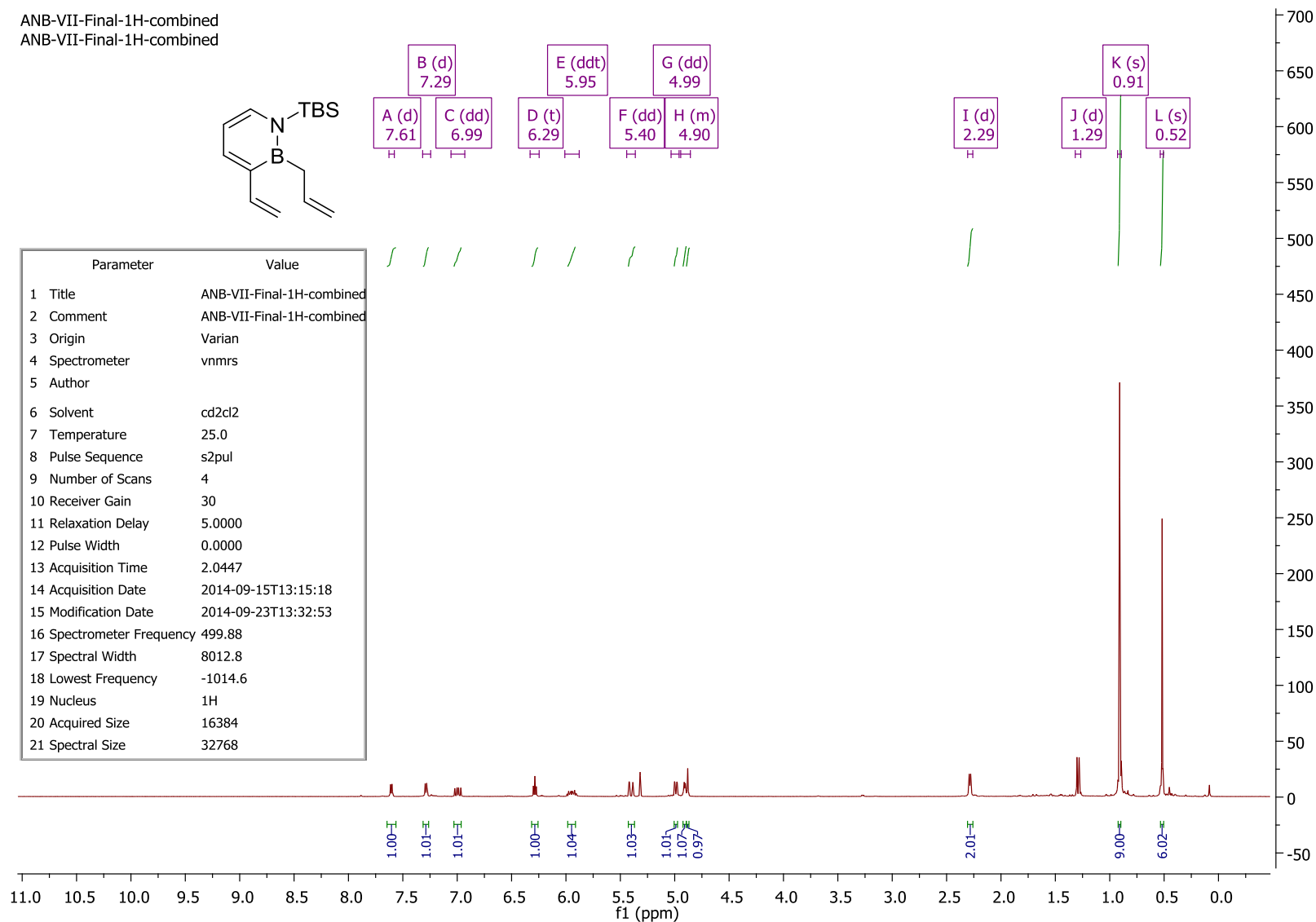
Parameter	Value
1 Title	ANB-VII-51-11B-Final
2 Comment	ANB-VII-51-11B-Final
3 Origin	Varian
4 Spectrometer	inova
5 Author	
6 Solvent	cd2cl2
7 Temperature	25.0
8 Pulse Sequence	s2pul
9 Number of Scans	144
10 Receiver Gain	20
11 Relaxation Delay	0.1000
12 Pulse Width	0.0000
13 Acquisition Time	0.1000
14 Acquisition Date	2014-09-19T18:27:26
15 Modification Date	2014-09-23T13:33:32
16 Spectrometer Frequency	160.35
17 Spectral Width	32051.3
18 Lowest Frequency	-16064.8
19 Nucleus	11B
20 Acquired Size	3205
21 Spectral Size	8192



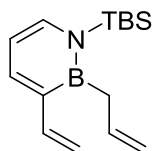
ANB-VII-Final-1H-combined
 ANB-VII-Final-1H-combined



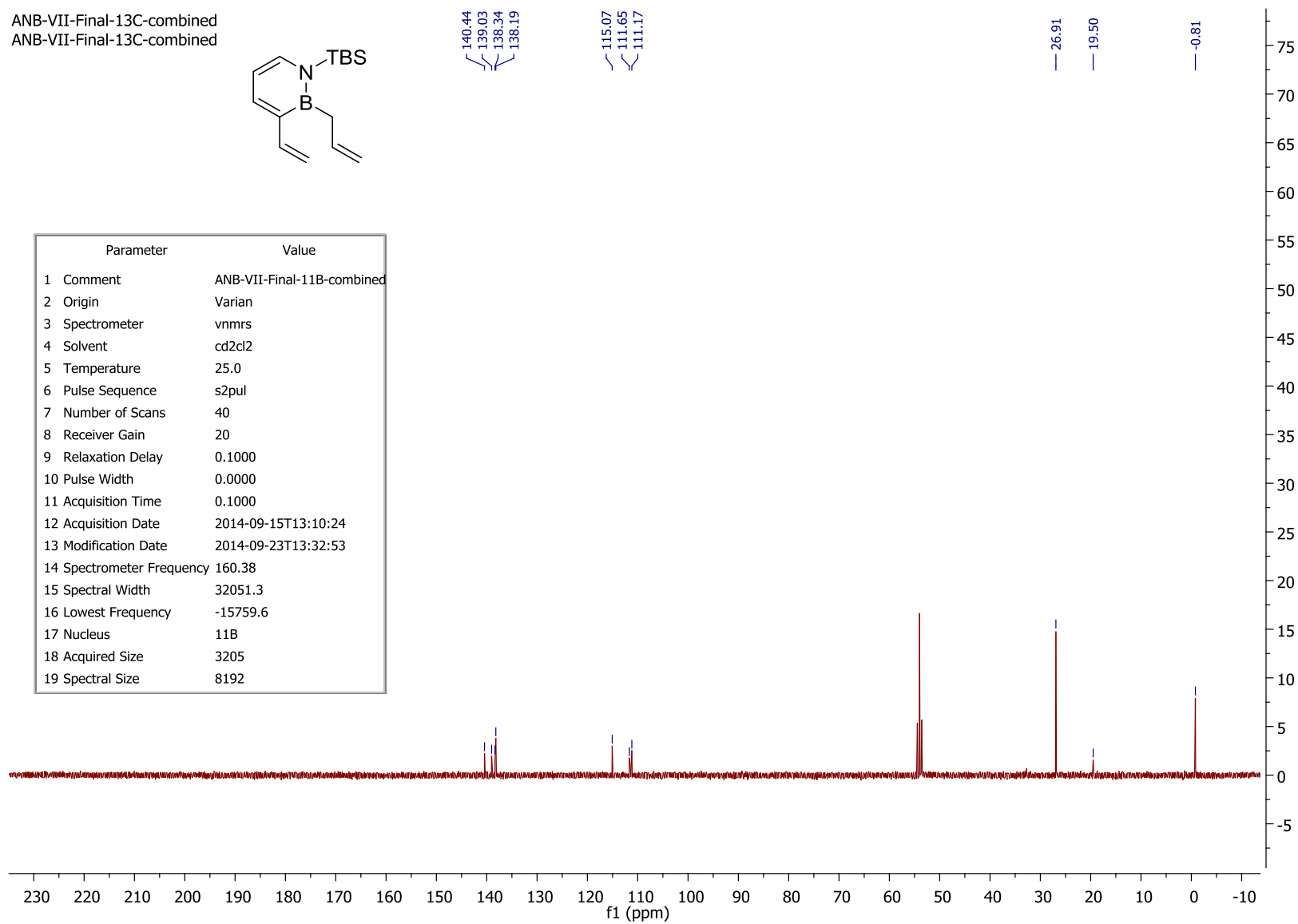
Parameter	Value
1 Title	ANB-VII-Final-1H-combined
2 Comment	ANB-VII-Final-1H-combined
3 Origin	Varian
4 Spectrometer	vnmrs
5 Author	
6 Solvent	cd2cl2
7 Temperature	25.0
8 Pulse Sequence	s2pul
9 Number of Scans	4
10 Receiver Gain	30
11 Relaxation Delay	5.0000
12 Pulse Width	0.0000
13 Acquisition Time	2.0447
14 Acquisition Date	2014-09-15T13:15:18
15 Modification Date	2014-09-23T13:32:53
16 Spectrometer Frequency	499.88
17 Spectral Width	8012.8
18 Lowest Frequency	-1014.6
19 Nucleus	1H
20 Acquired Size	16384
21 Spectral Size	32768



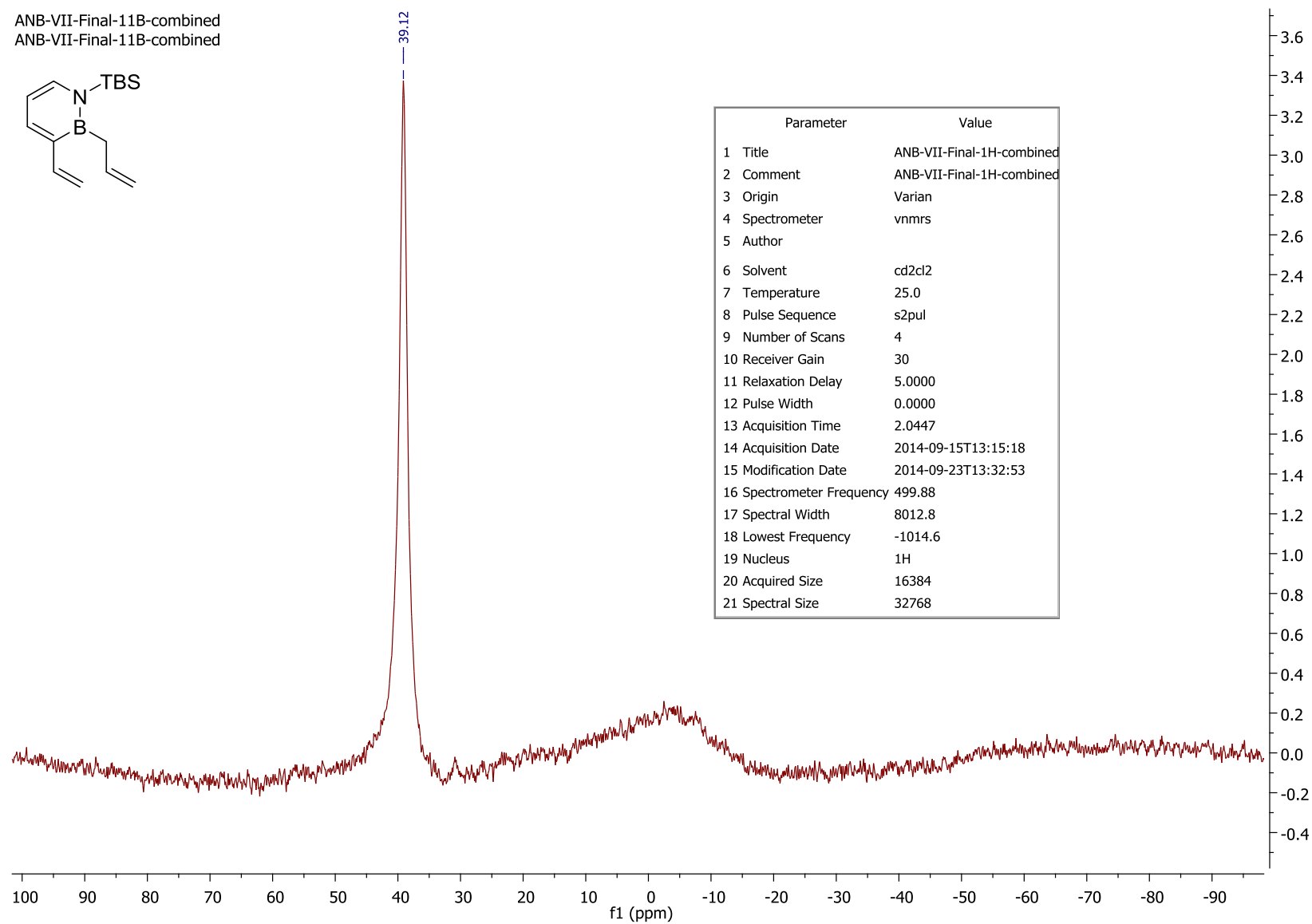
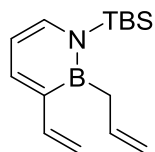
ANB-VII-Final-13C-combined
ANB-VII-Final-13C-combined



Parameter	Value
1 Comment	ANB-VII-Final-11B-combined
2 Origin	Varian
3 Spectrometer	vnmrs
4 Solvent	cd2cl2
5 Temperature	25.0
6 Pulse Sequence	s2pul
7 Number of Scans	40
8 Receiver Gain	20
9 Relaxation Delay	0.1000
10 Pulse Width	0.0000
11 Acquisition Time	0.1000
12 Acquisition Date	2014-09-15T13:10:24
13 Modification Date	2014-09-23T13:32:53
14 Spectrometer Frequency	160.38
15 Spectral Width	32051.3
16 Lowest Frequency	-15759.6
17 Nucleus	11B
18 Acquired Size	3205
19 Spectral Size	8192

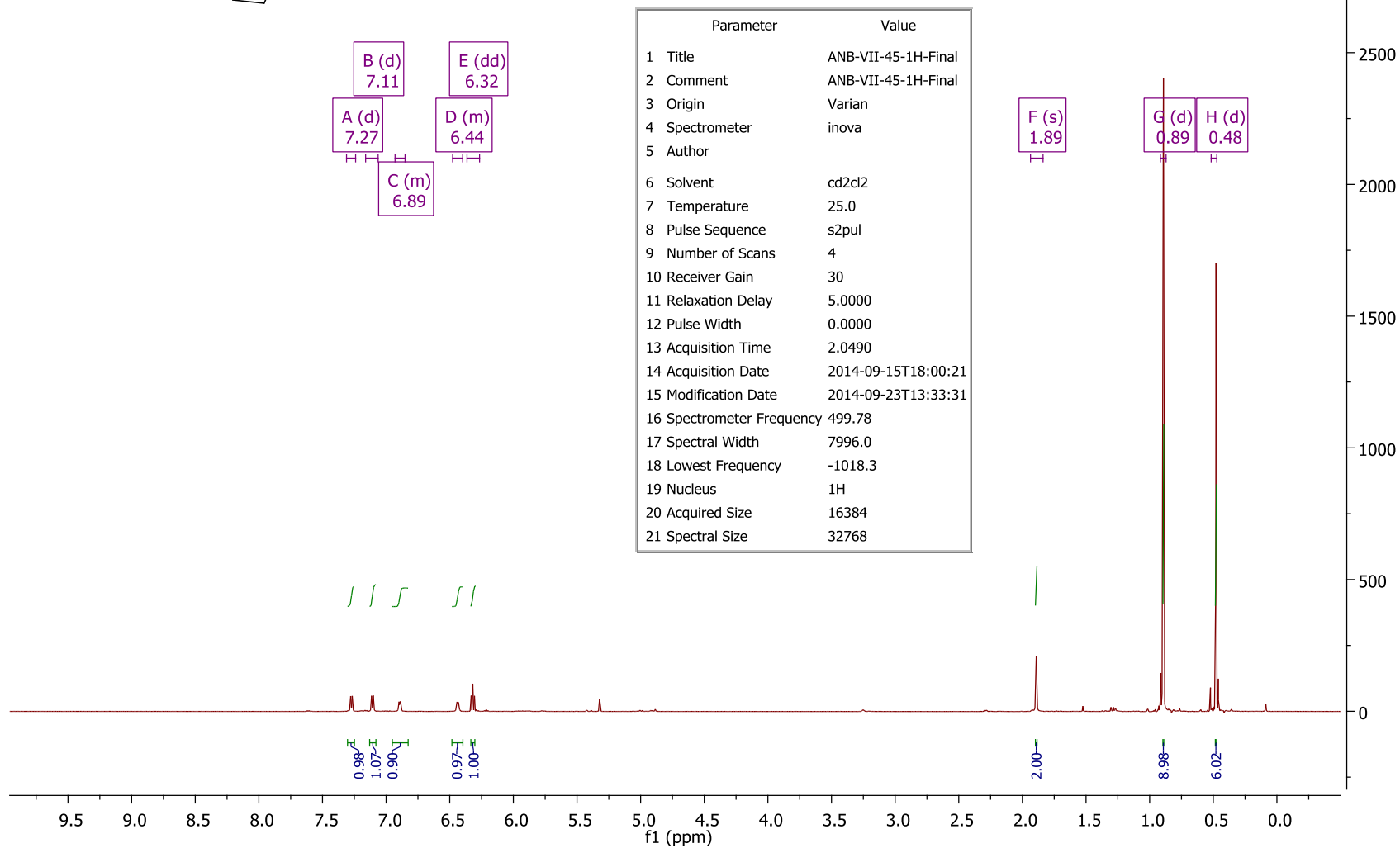
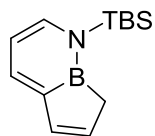


ANB-VII-Final-11B-combined
ANB-VII-Final-11B-combined

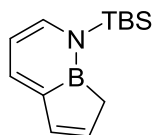


ANB-VII-45-1H-Final

ANB-VII-45-1H-Final

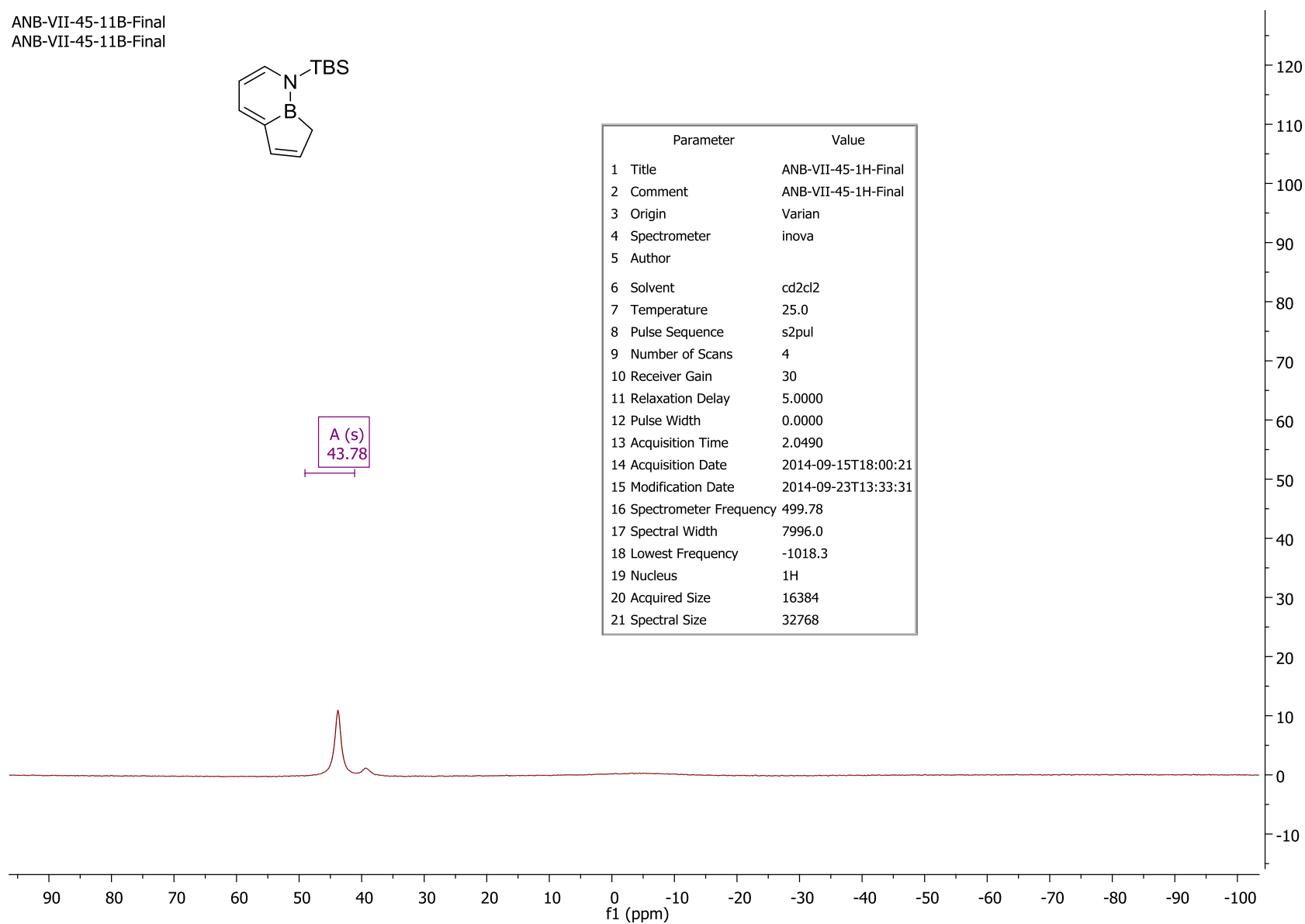


ANB-VII-45-11B-Final
ANB-VII-45-11B-Final

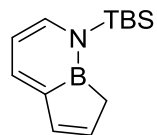


A (s)
43.78

Parameter	Value
1 Title	ANB-VII-45-1H-Final
2 Comment	ANB-VII-45-1H-Final
3 Origin	Varian
4 Spectrometer	inova
5 Author	
6 Solvent	cd2cl2
7 Temperature	25.0
8 Pulse Sequence	s2pul
9 Number of Scans	4
10 Receiver Gain	30
11 Relaxation Delay	5.0000
12 Pulse Width	0.0000
13 Acquisition Time	2.0490
14 Acquisition Date	2014-09-15T18:00:21
15 Modification Date	2014-09-23T13:33:31
16 Spectrometer Frequency	499.78
17 Spectral Width	7996.0
18 Lowest Frequency	-1018.3
19 Nucleus	1H
20 Acquired Size	16384
21 Spectral Size	32768



ANB-VII-45-13C-Final
ANB-VII-45-13C-Final



138.53
136.44
133.61
129.18

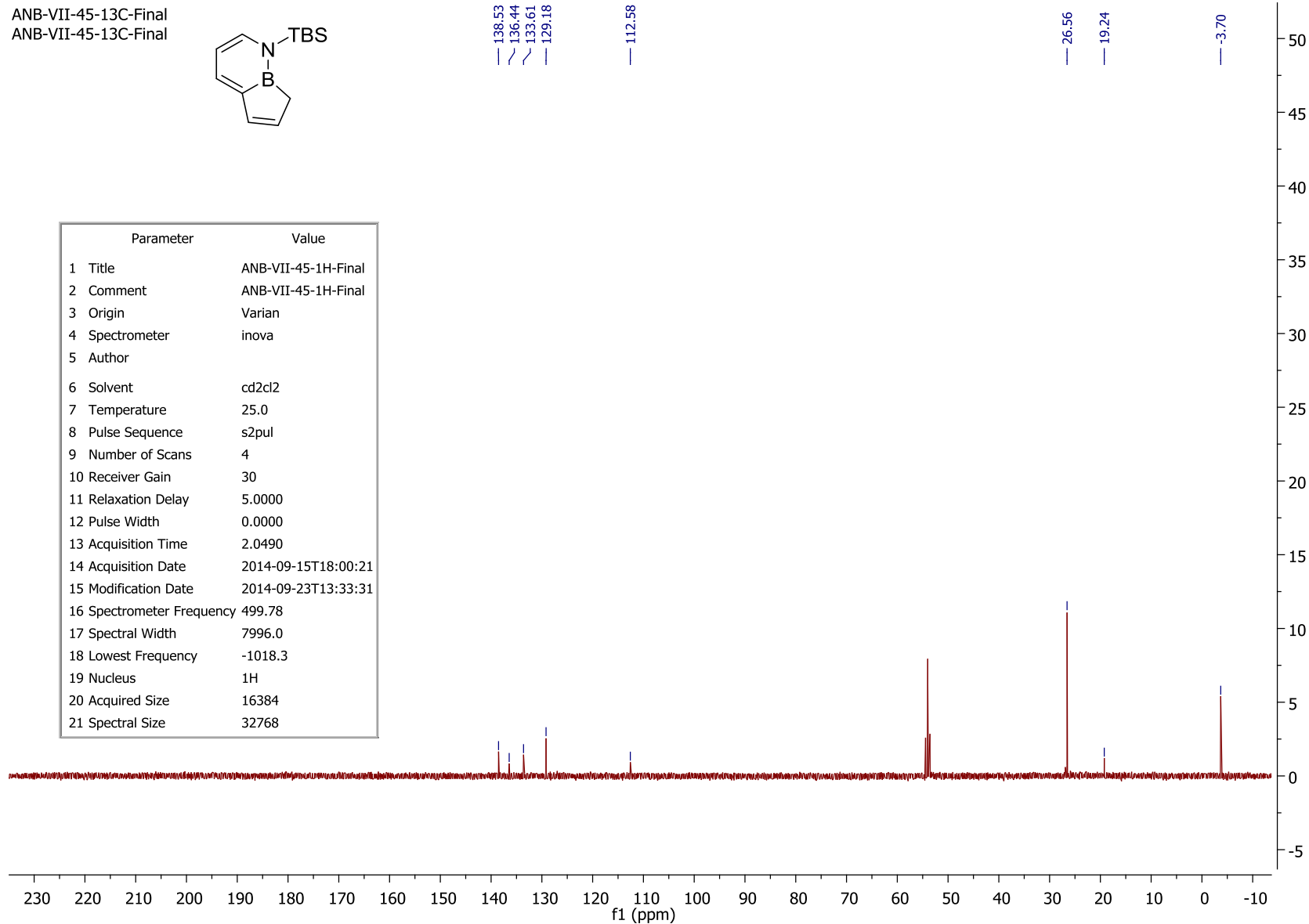
112.58

26.56

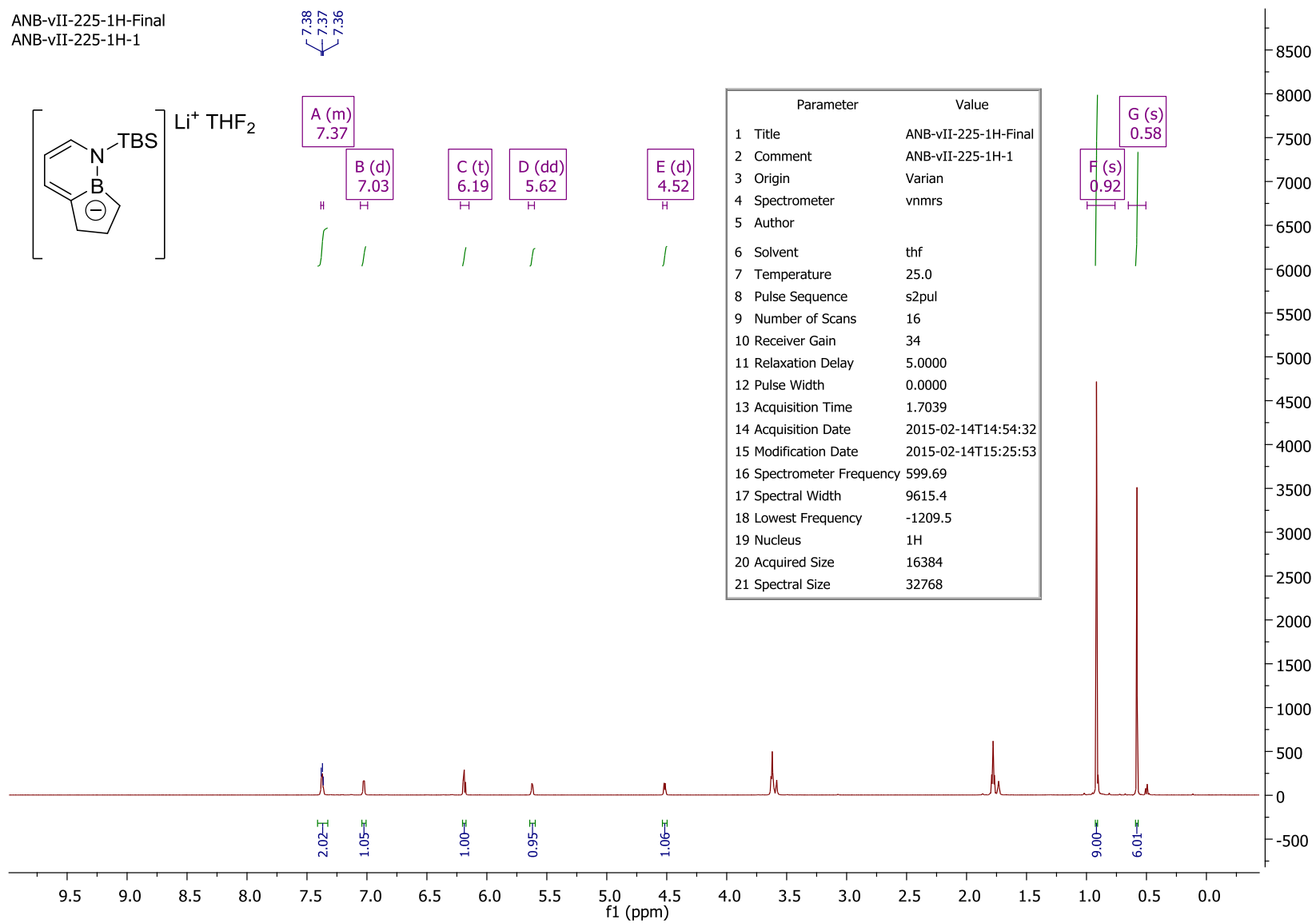
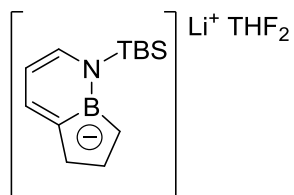
19.24

-3.70

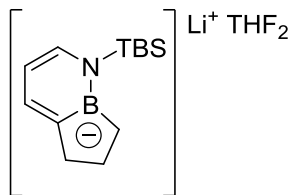
Parameter	Value
1 Title	ANB-VII-45-1H-Final
2 Comment	ANB-VII-45-1H-Final
3 Origin	Varian
4 Spectrometer	inova
5 Author	
6 Solvent	cd2cl2
7 Temperature	25.0
8 Pulse Sequence	s2pul
9 Number of Scans	4
10 Receiver Gain	30
11 Relaxation Delay	5.0000
12 Pulse Width	0.0000
13 Acquisition Time	2.0490
14 Acquisition Date	2014-09-15T18:00:21
15 Modification Date	2014-09-23T13:33:31
16 Spectrometer Frequency	499.78
17 Spectral Width	7996.0
18 Lowest Frequency	-1018.3
19 Nucleus	1H
20 Acquired Size	16384
21 Spectral Size	32768



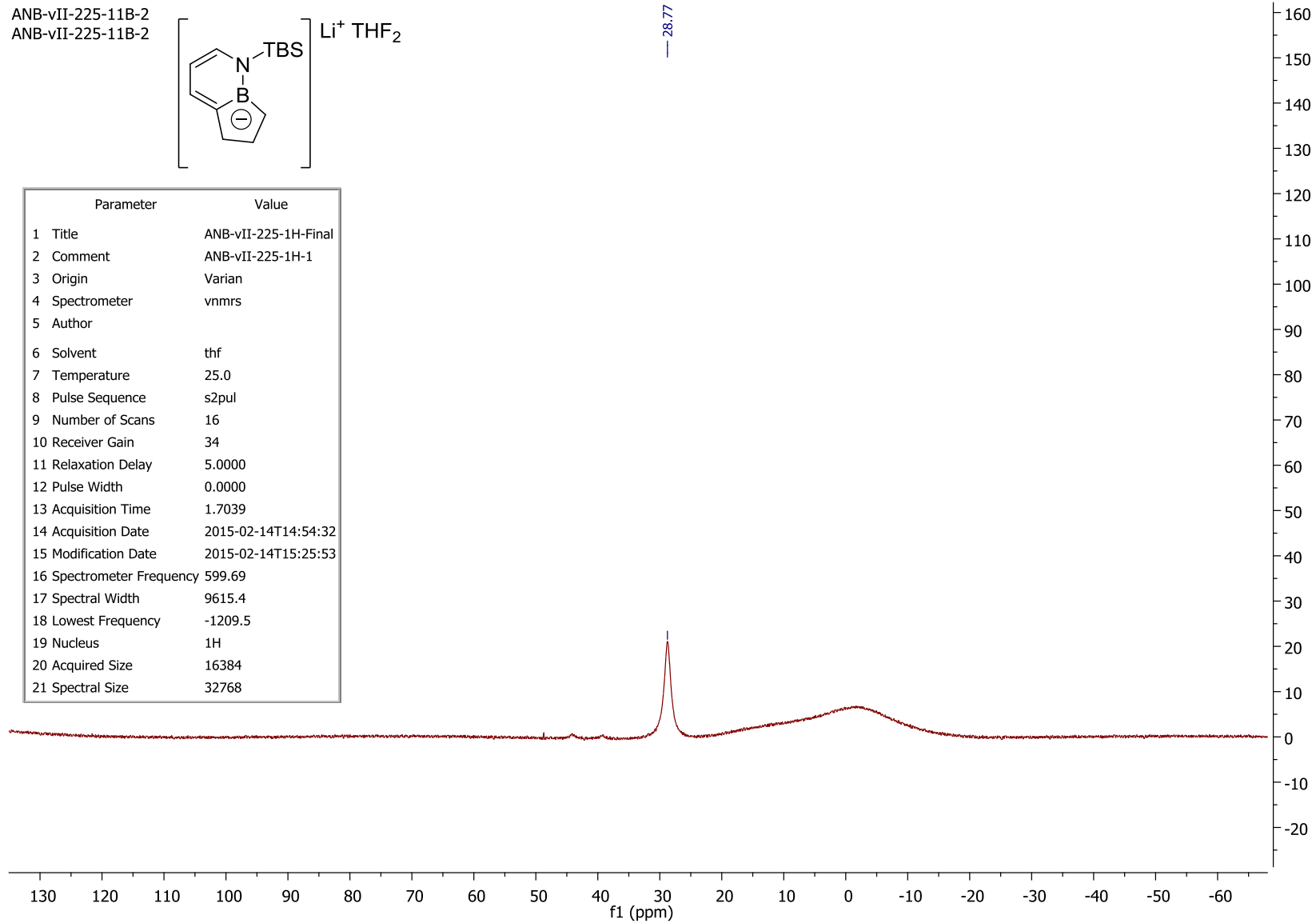
ANB-vII-225-1H-Final
ANB-vII-225-1H-1



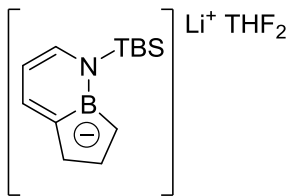
ANB-vII-225-11B-2
ANB-vII-225-11B-2



Parameter	Value
1 Title	ANB-vII-225-1H-Final
2 Comment	ANB-vII-225-1H-1
3 Origin	Varian
4 Spectrometer	vnmrs
5 Author	
6 Solvent	thf
7 Temperature	25.0
8 Pulse Sequence	s2pul
9 Number of Scans	16
10 Receiver Gain	34
11 Relaxation Delay	5.0000
12 Pulse Width	0.0000
13 Acquisition Time	1.7039
14 Acquisition Date	2015-02-14T14:54:32
15 Modification Date	2015-02-14T15:25:53
16 Spectrometer Frequency	599.69
17 Spectral Width	9615.4
18 Lowest Frequency	-1209.5
19 Nucleus	1H
20 Acquired Size	16384
21 Spectral Size	32768

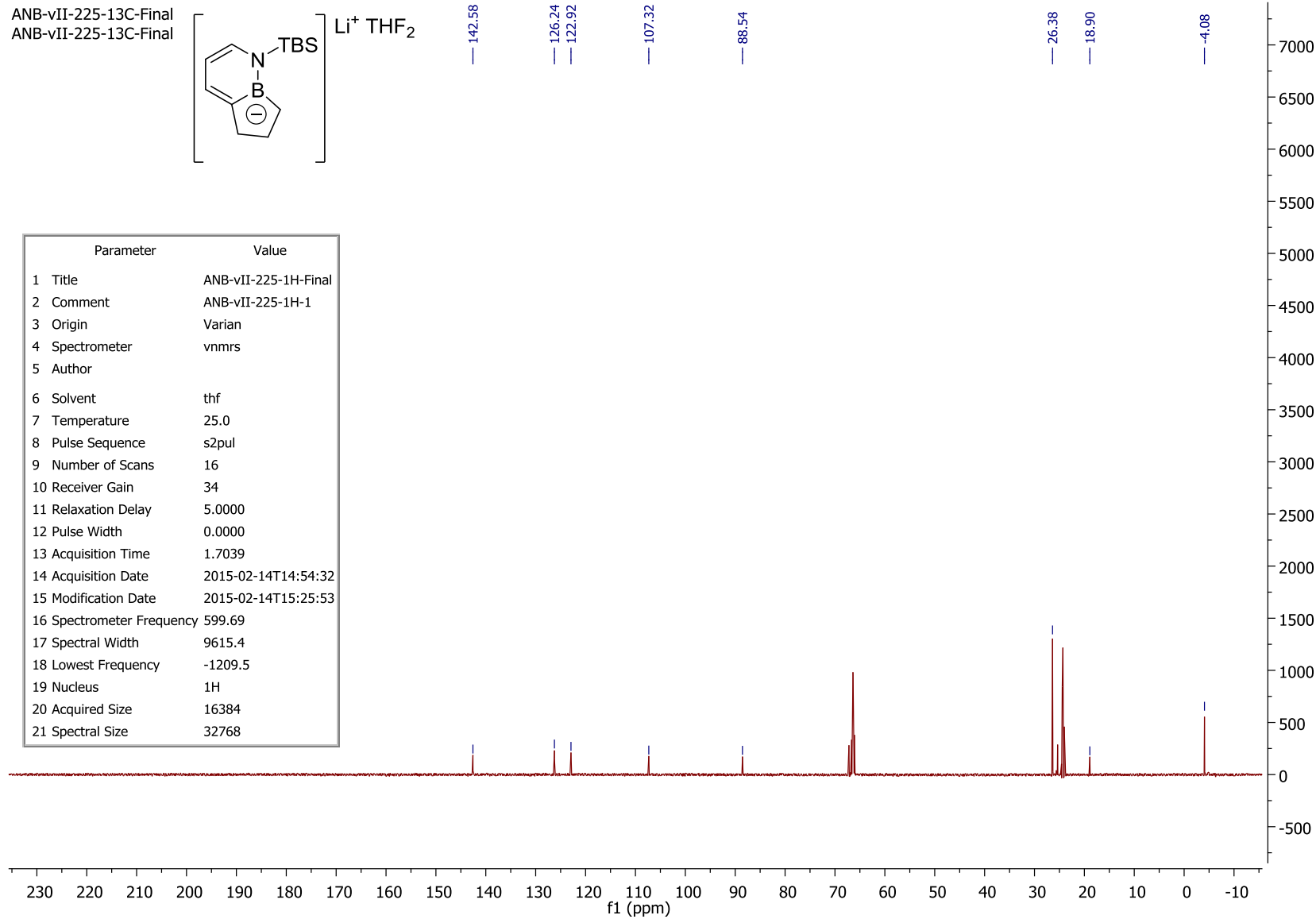


ANB-vII-225-13C-Final
ANB-vII-225-13C-Final

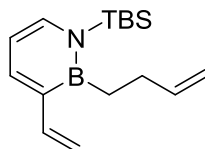


142.58
126.24
122.92
107.32
88.54
26.38
18.90
-4.08

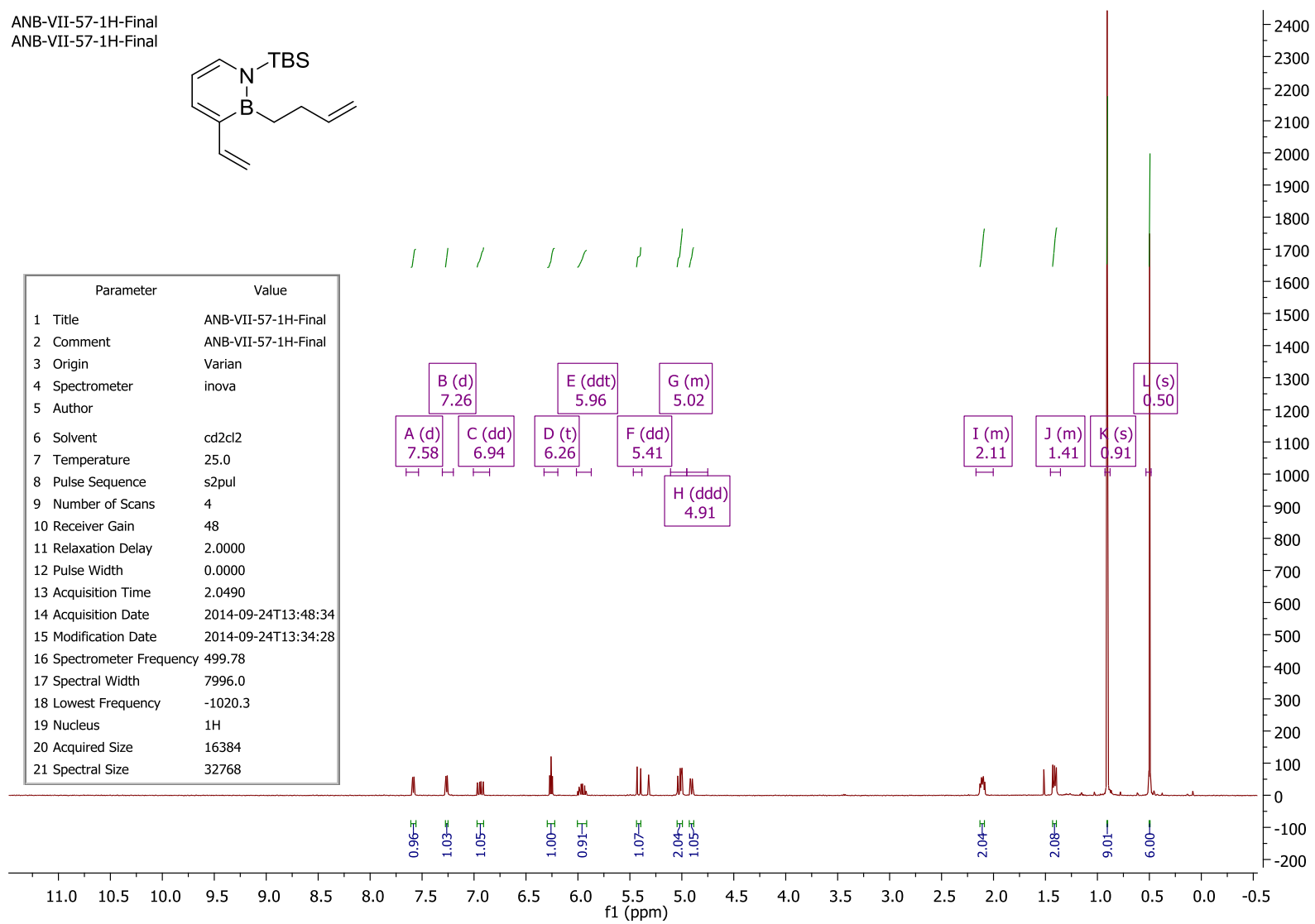
Parameter	Value
1 Title	ANB-vII-225-1H-Final
2 Comment	ANB-vII-225-1H-1
3 Origin	Varian
4 Spectrometer	vnmrs
5 Author	
6 Solvent	thf
7 Temperature	25.0
8 Pulse Sequence	s2pul
9 Number of Scans	16
10 Receiver Gain	34
11 Relaxation Delay	5.0000
12 Pulse Width	0.0000
13 Acquisition Time	1.7039
14 Acquisition Date	2015-02-14T14:54:32
15 Modification Date	2015-02-14T15:25:53
16 Spectrometer Frequency	599.69
17 Spectral Width	9615.4
18 Lowest Frequency	-1209.5
19 Nucleus	1H
20 Acquired Size	16384
21 Spectral Size	32768



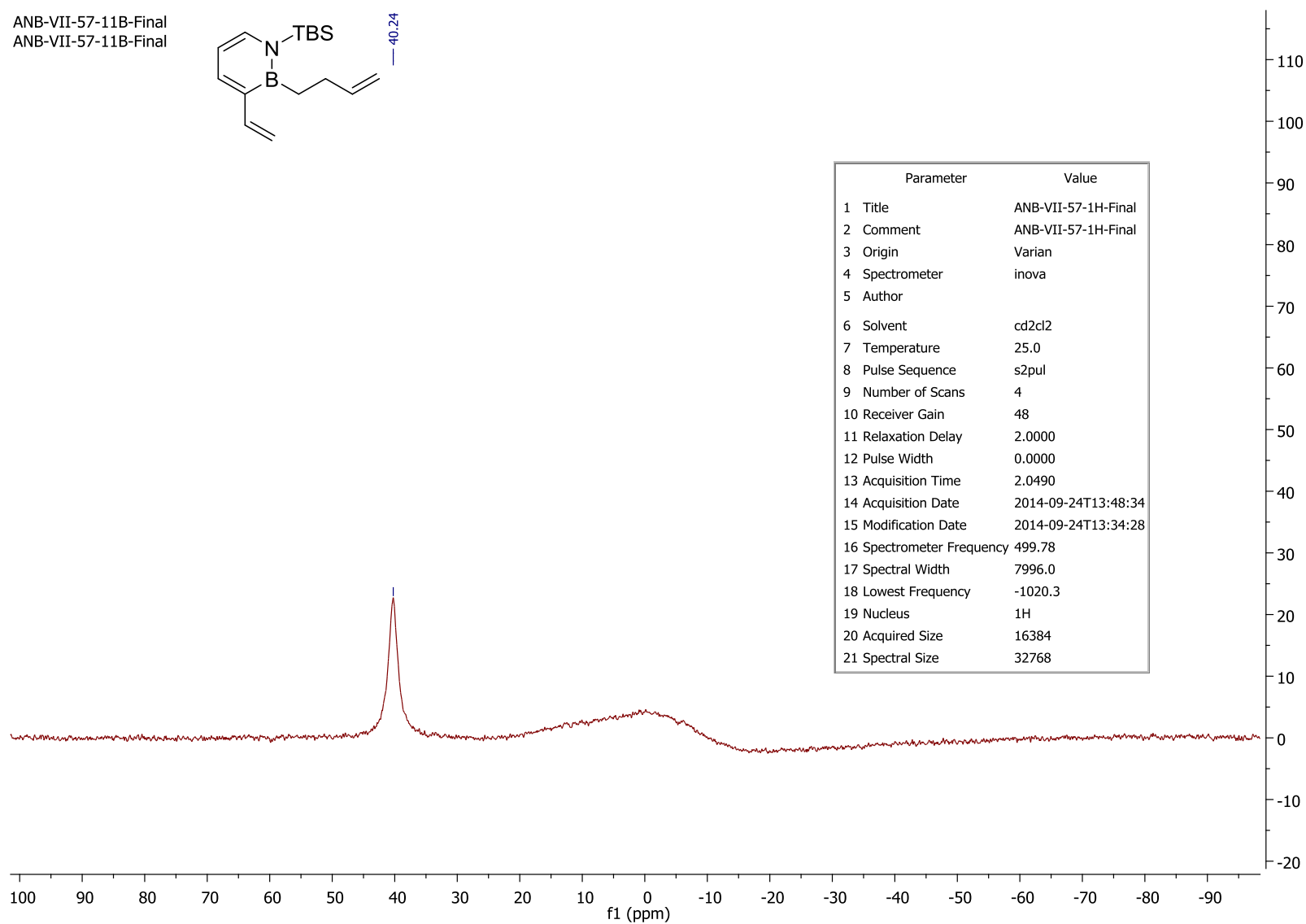
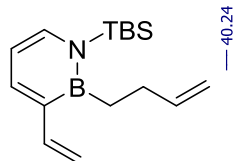
ANB-VII-57-1H-Final
 ANB-VII-57-1H-Final



Parameter	Value
1 Title	ANB-VII-57-1H-Final
2 Comment	ANB-VII-57-1H-Final
3 Origin	Varian
4 Spectrometer	inova
5 Author	
6 Solvent	cd2cl2
7 Temperature	25.0
8 Pulse Sequence	s2pul
9 Number of Scans	4
10 Receiver Gain	48
11 Relaxation Delay	2.0000
12 Pulse Width	0.0000
13 Acquisition Time	2.0490
14 Acquisition Date	2014-09-24T13:48:34
15 Modification Date	2014-09-24T13:34:28
16 Spectrometer Frequency	499.78
17 Spectral Width	7996.0
18 Lowest Frequency	-1020.3
19 Nucleus	1H
20 Acquired Size	16384
21 Spectral Size	32768

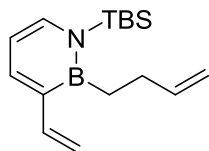


ANB-VII-57-11B-Final
ANB-VII-57-11B-Final



Parameter	Value
1 Title	ANB-VII-57-1H-Final
2 Comment	ANB-VII-57-1H-Final
3 Origin	Varian
4 Spectrometer	inova
5 Author	
6 Solvent	cd2cl2
7 Temperature	25.0
8 Pulse Sequence	s2pul
9 Number of Scans	4
10 Receiver Gain	48
11 Relaxation Delay	2.0000
12 Pulse Width	0.0000
13 Acquisition Time	2.0490
14 Acquisition Date	2014-09-24T13:48:34
15 Modification Date	2014-09-24T13:34:28
16 Spectrometer Frequency	499.78
17 Spectral Width	7996.0
18 Lowest Frequency	-1020.3
19 Nucleus	1H
20 Acquired Size	16384
21 Spectral Size	32768

ANB-VII-57-13C-Final
ANB-VII-57-13C-Final

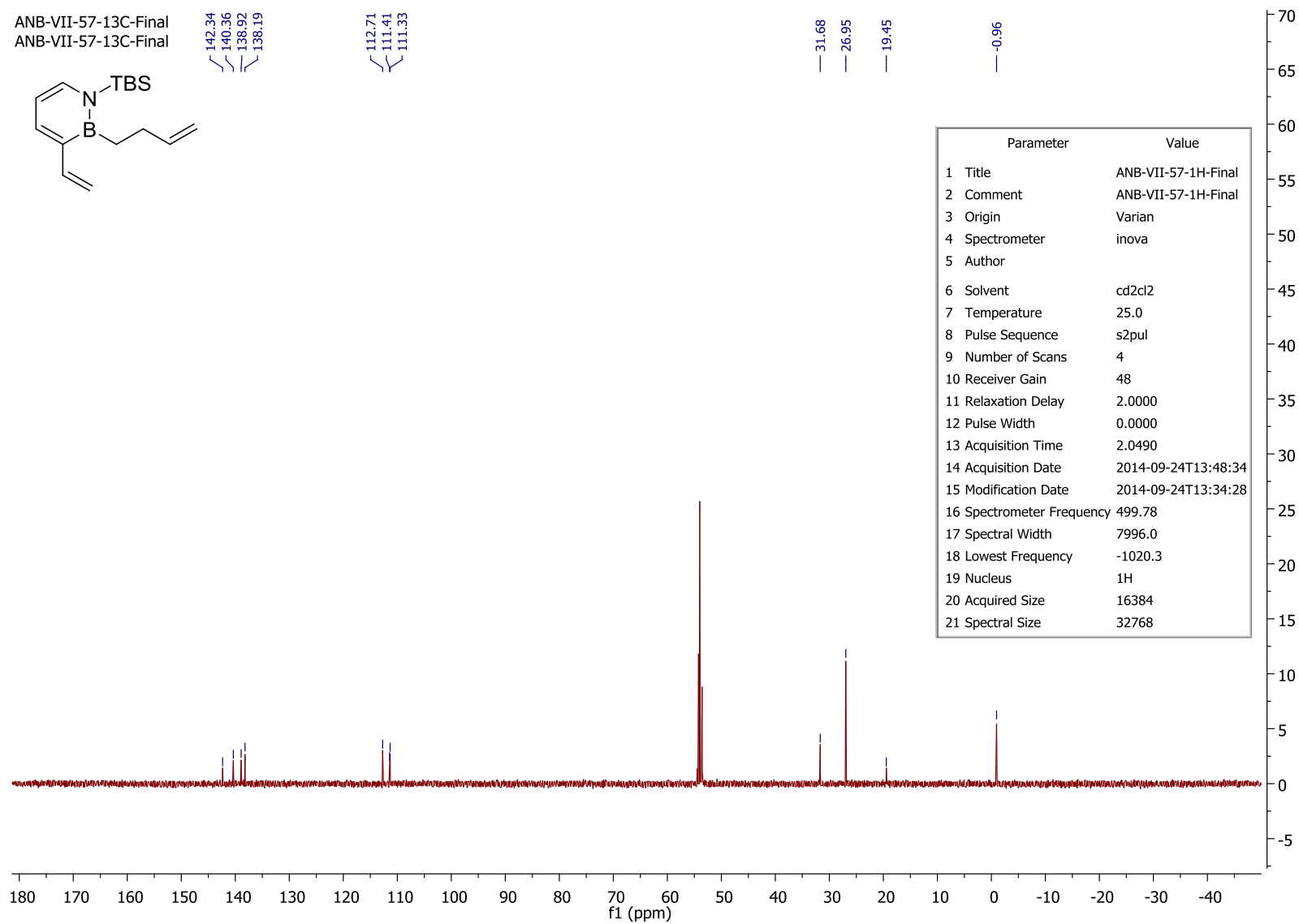


142.34
140.36
138.92
138.19

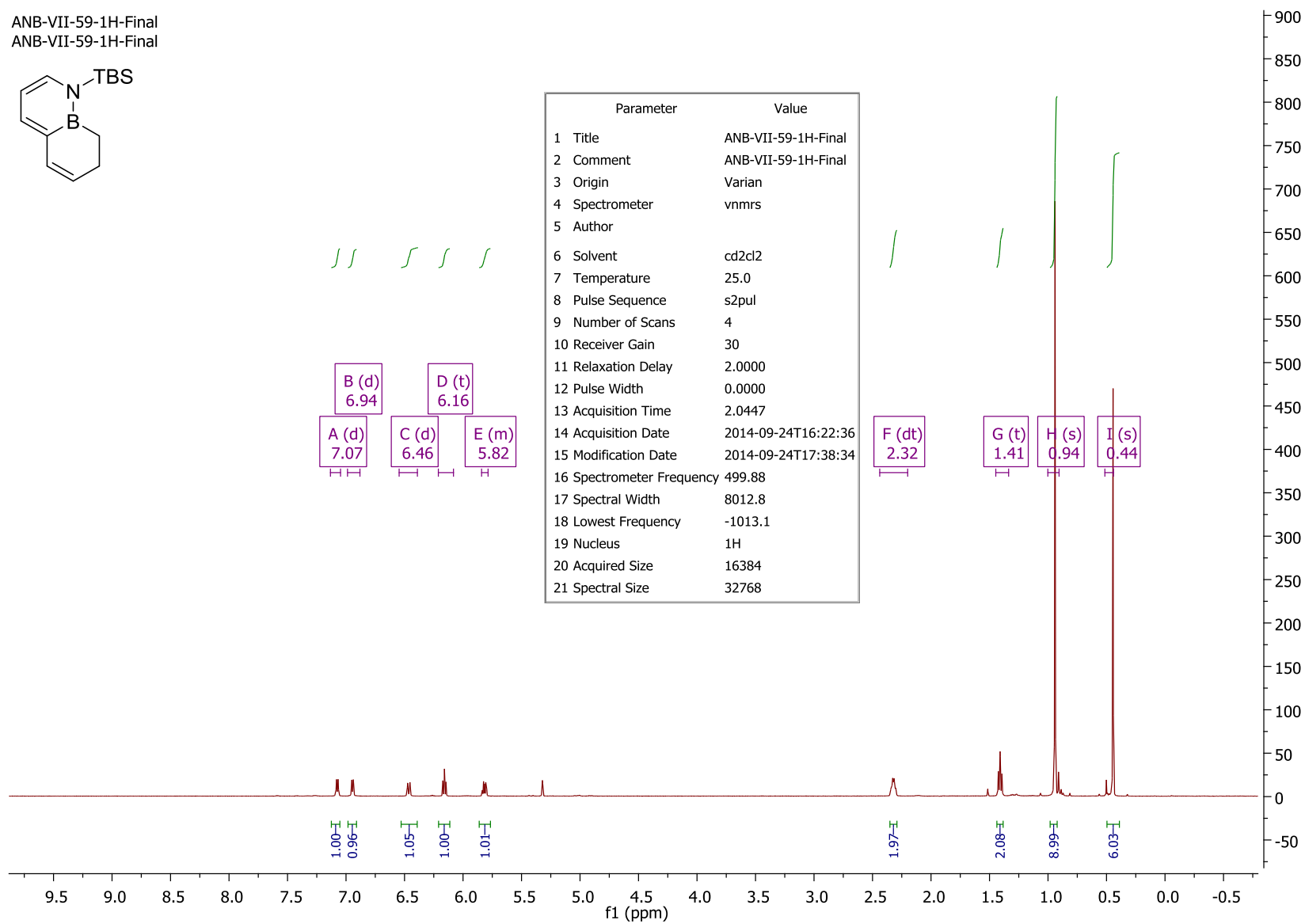
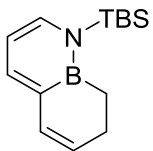
112.71
111.41
111.33

31.68
26.95
19.45

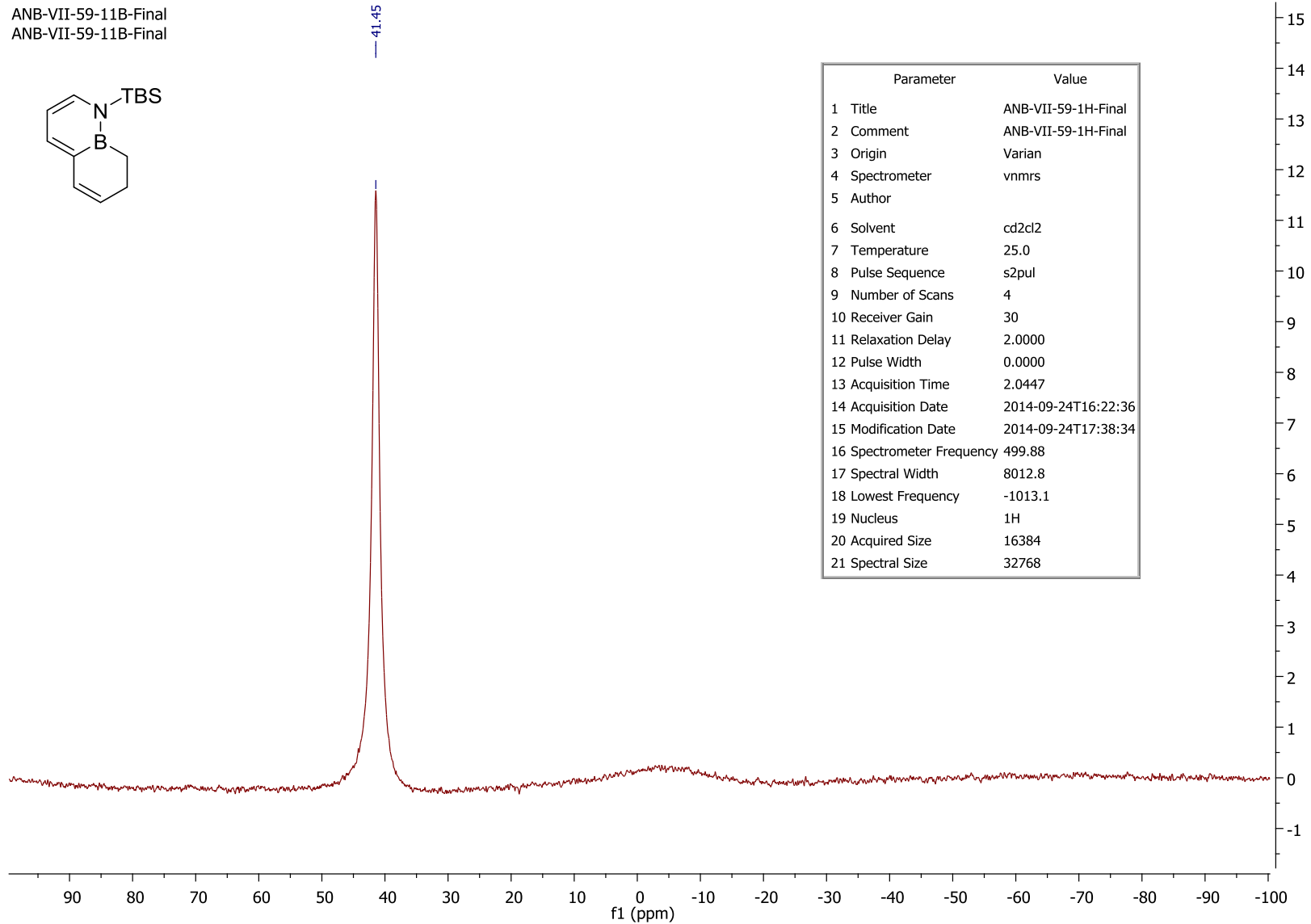
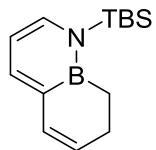
-0.96



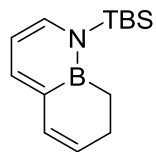
ANB-VII-59-1H-Final
 ANB-VII-59-1H-Final



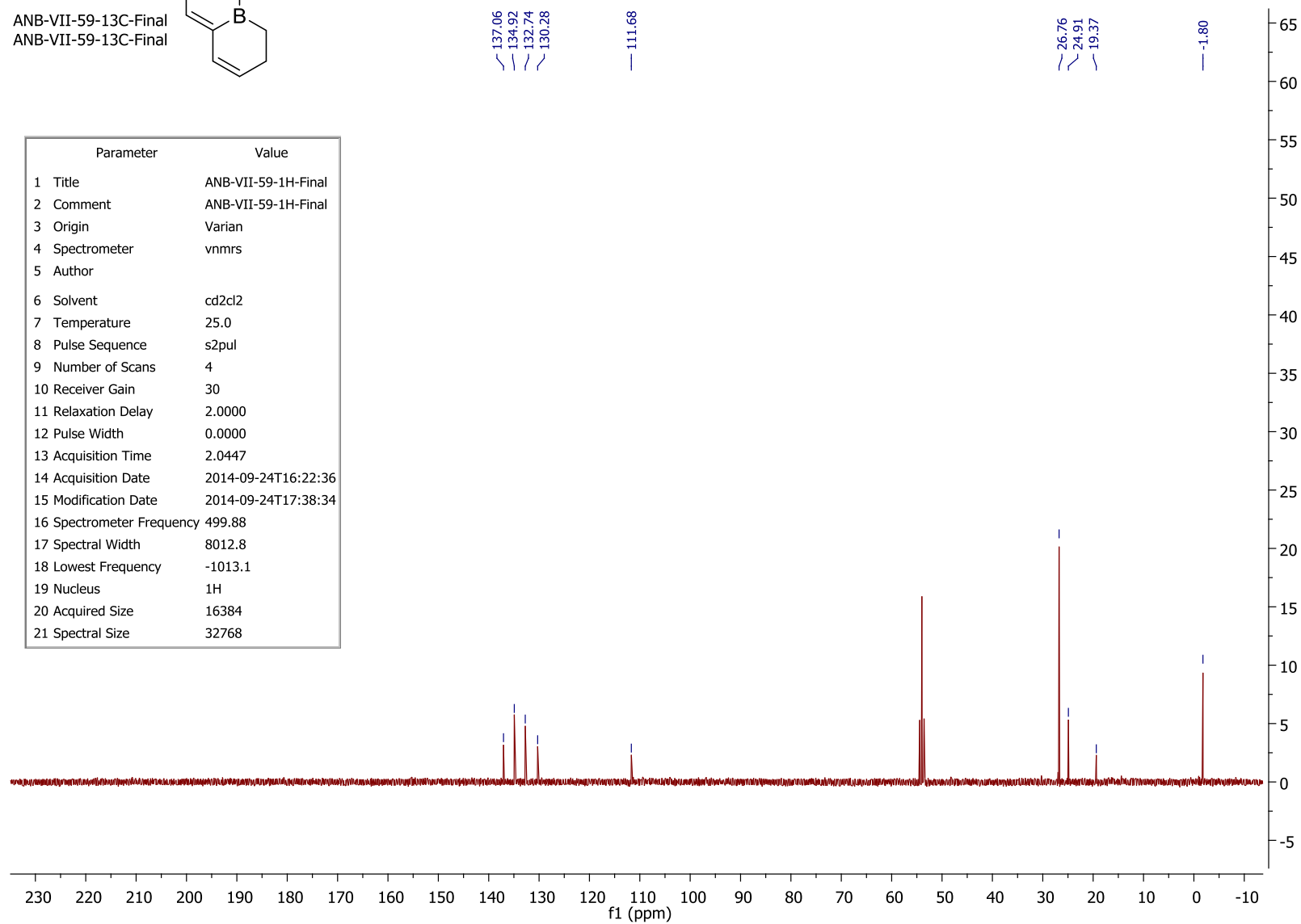
ANB-VII-59-11B-Final
ANB-VII-59-11B-Final



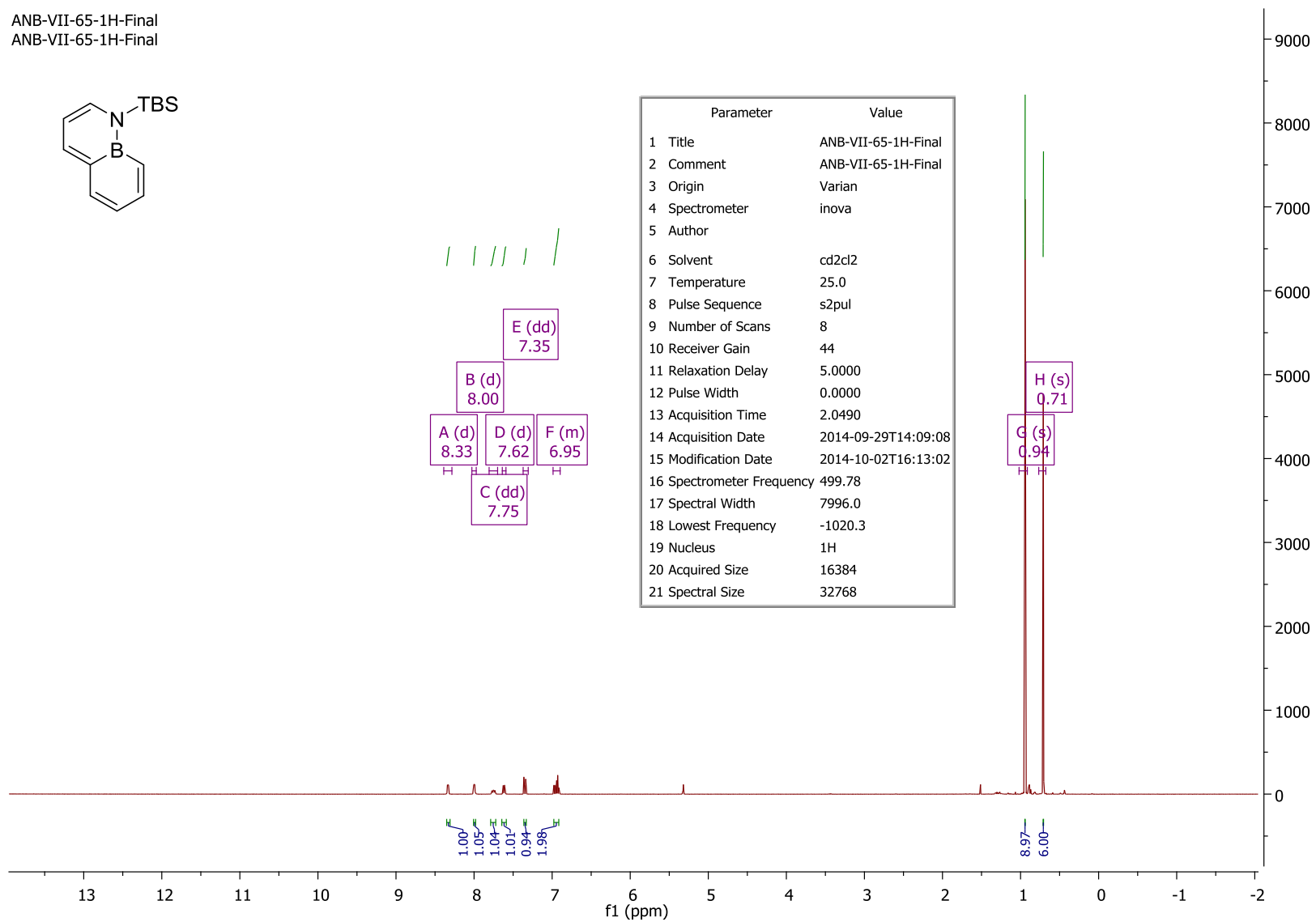
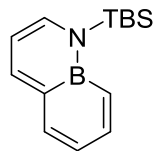
ANB-VII-59-13C-Final
ANB-VII-59-13C-Final



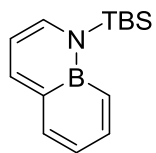
Parameter	Value
1 Title	ANB-VII-59-1H-Final
2 Comment	ANB-VII-59-1H-Final
3 Origin	Varian
4 Spectrometer	vnmrs
5 Author	
6 Solvent	cd2cl2
7 Temperature	25.0
8 Pulse Sequence	s2pul
9 Number of Scans	4
10 Receiver Gain	30
11 Relaxation Delay	2.0000
12 Pulse Width	0.0000
13 Acquisition Time	2.0447
14 Acquisition Date	2014-09-24T16:22:36
15 Modification Date	2014-09-24T17:38:34
16 Spectrometer Frequency	499.88
17 Spectral Width	8012.8
18 Lowest Frequency	-1013.1
19 Nucleus	1H
20 Acquired Size	16384
21 Spectral Size	32768



ANB-VII-65-1H-Final
ANB-VII-65-1H-Final

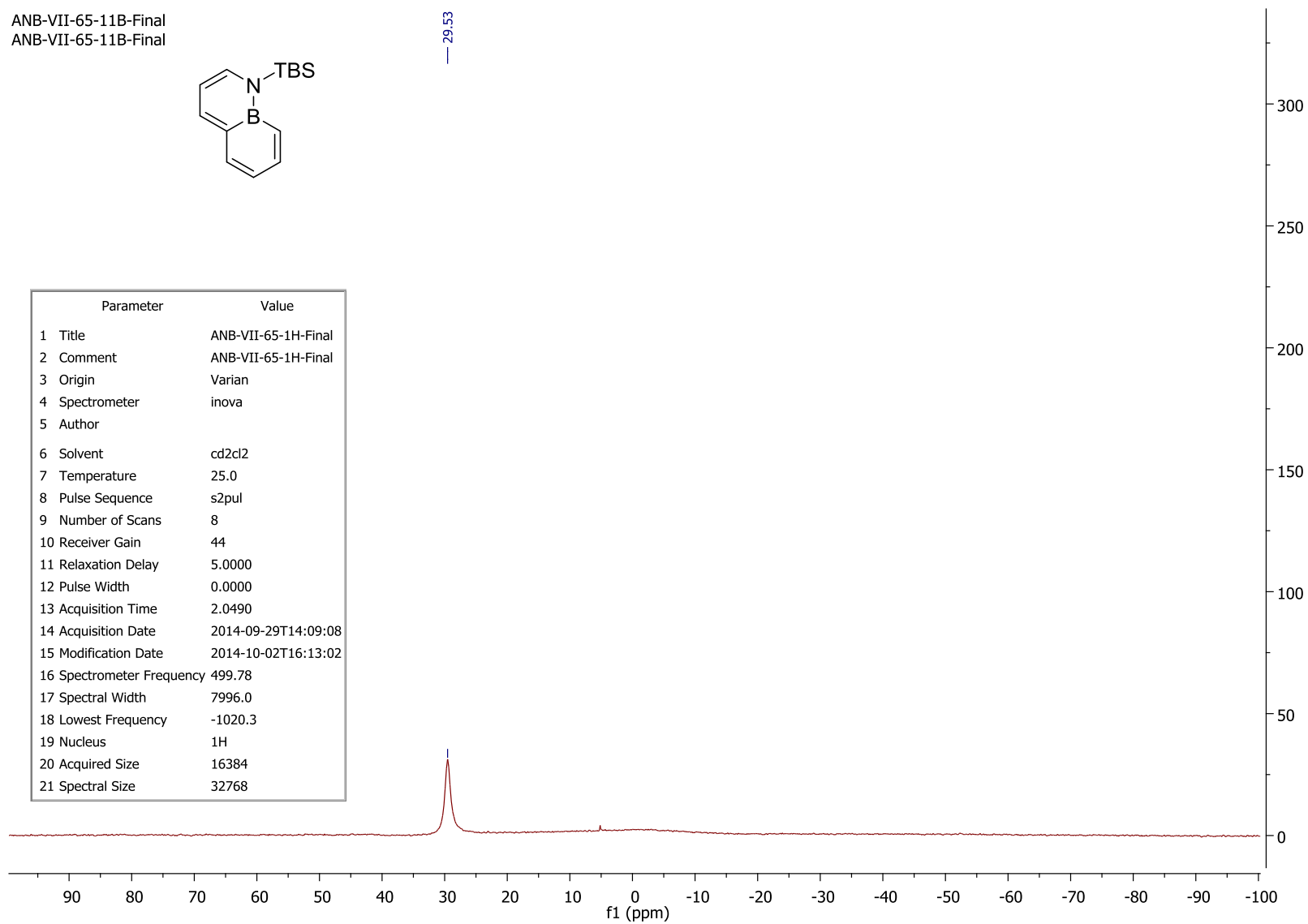


ANB-VII-65-11B-Final
ANB-VII-65-11B-Final

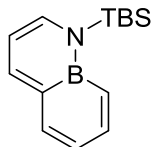


— 29.53

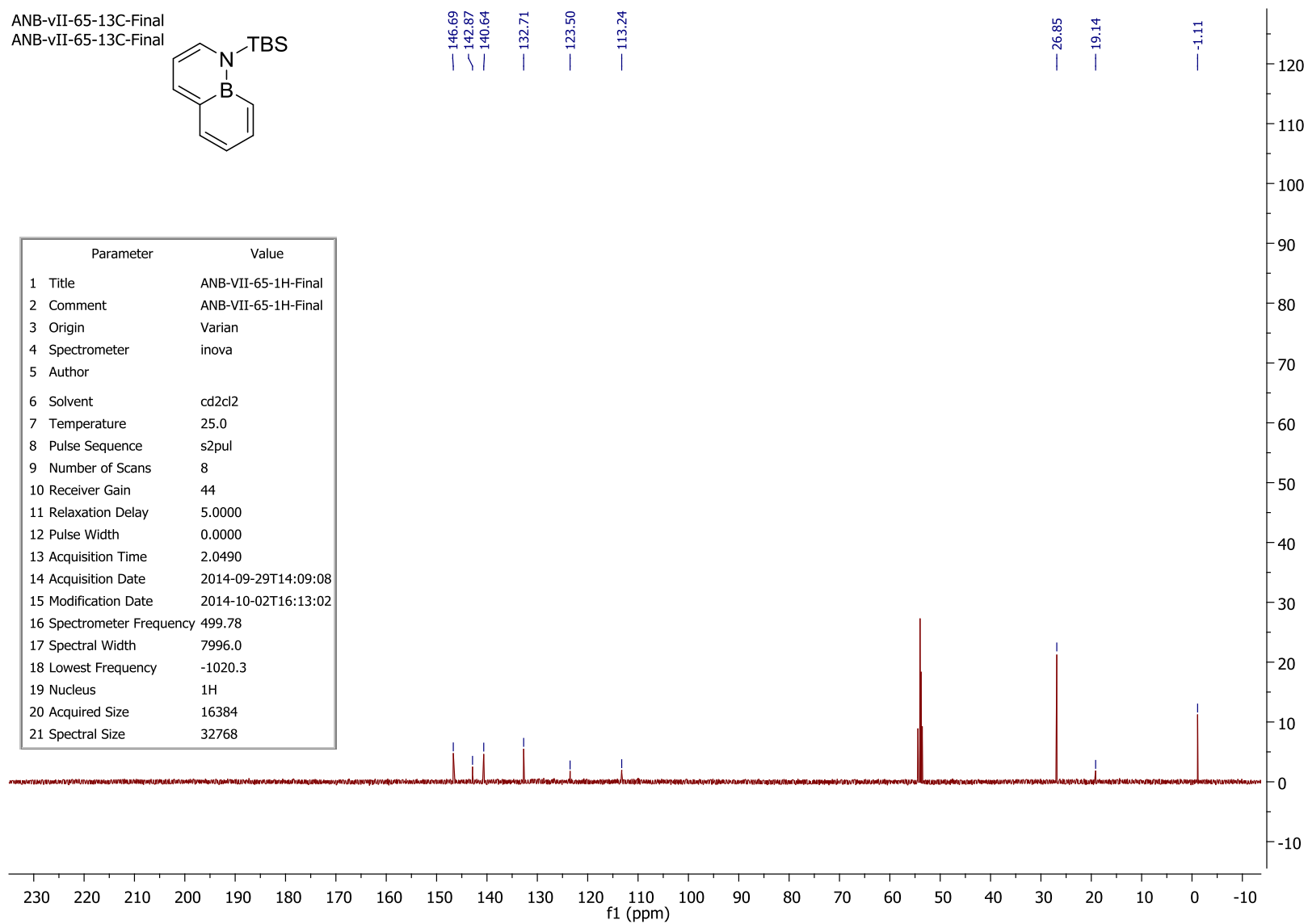
Parameter	Value
1 Title	ANB-VII-65-1H-Final
2 Comment	ANB-VII-65-1H-Final
3 Origin	Varian
4 Spectrometer	inova
5 Author	
6 Solvent	cd2cl2
7 Temperature	25.0
8 Pulse Sequence	s2pul
9 Number of Scans	8
10 Receiver Gain	44
11 Relaxation Delay	5.0000
12 Pulse Width	0.0000
13 Acquisition Time	2.0490
14 Acquisition Date	2014-09-29T14:09:08
15 Modification Date	2014-10-02T16:13:02
16 Spectrometer Frequency	499.78
17 Spectral Width	7996.0
18 Lowest Frequency	-1020.3
19 Nucleus	1H
20 Acquired Size	16384
21 Spectral Size	32768



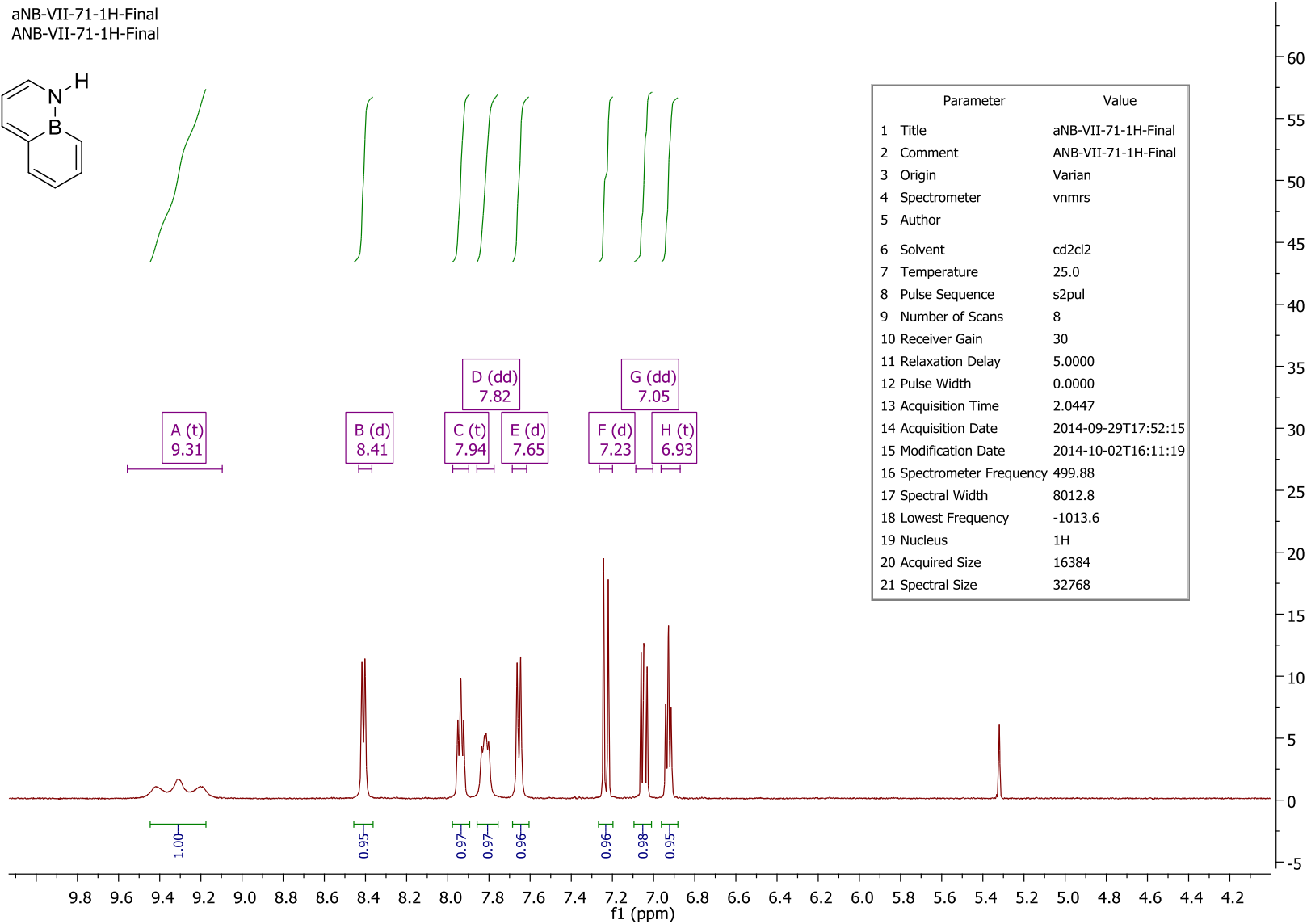
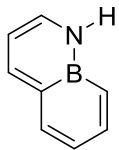
ANB-vII-65-13C-Final
ANB-vII-65-13C-Final



Parameter	Value
1 Title	ANB-VII-65-1H-Final
2 Comment	ANB-VII-65-1H-Final
3 Origin	Varian
4 Spectrometer	inova
5 Author	
6 Solvent	cd2cl2
7 Temperature	25.0
8 Pulse Sequence	s2pul
9 Number of Scans	8
10 Receiver Gain	44
11 Relaxation Delay	5.0000
12 Pulse Width	0.0000
13 Acquisition Time	2.0490
14 Acquisition Date	2014-09-29T14:09:08
15 Modification Date	2014-10-02T16:13:02
16 Spectrometer Frequency	499.78
17 Spectral Width	7996.0
18 Lowest Frequency	-1020.3
19 Nucleus	1H
20 Acquired Size	16384
21 Spectral Size	32768

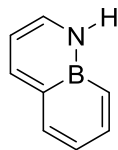


aNB-VII-71-1H-Final
 ANB-VII-71-1H-Final



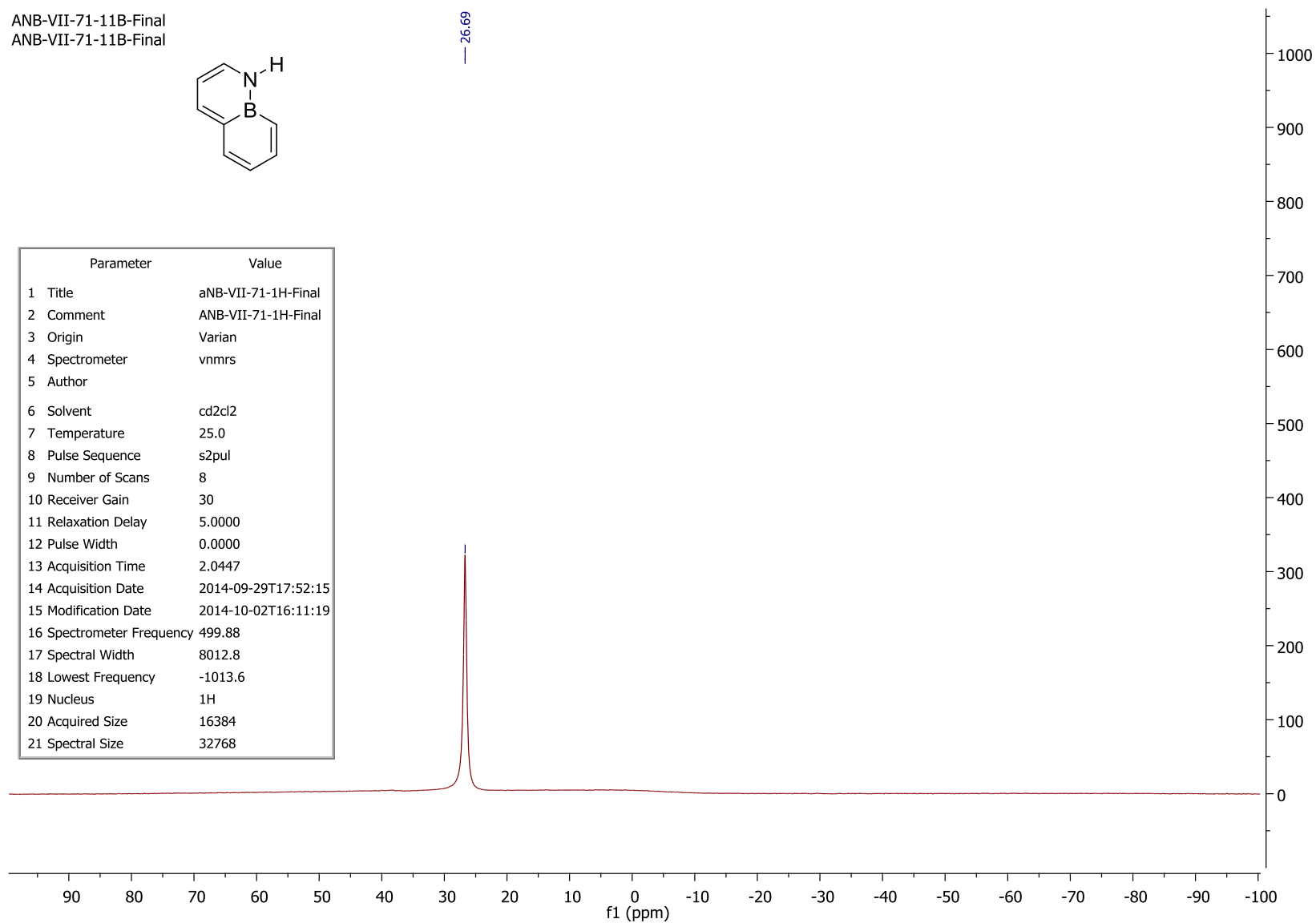
Parameter	Value
1 Title	aNB-VII-71-1H-Final
2 Comment	ANB-VII-71-1H-Final
3 Origin	Varian
4 Spectrometer	vnmrs
5 Author	
6 Solvent	cd2cl2
7 Temperature	25.0
8 Pulse Sequence	s2pul
9 Number of Scans	8
10 Receiver Gain	30
11 Relaxation Delay	5.0000
12 Pulse Width	0.0000
13 Acquisition Time	2.0447
14 Acquisition Date	2014-09-29T17:52:15
15 Modification Date	2014-10-02T16:11:19
16 Spectrometer Frequency	499.88
17 Spectral Width	8012.8
18 Lowest Frequency	-1013.6
19 Nucleus	1H
20 Acquired Size	16384
21 Spectral Size	32768

ANB-VII-71-11B-Final
ANB-VII-71-11B-Final

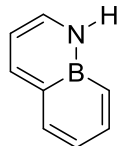


— 26.69

Parameter	Value
1 Title	aNB-VII-71-1H-Final
2 Comment	ANB-VII-71-1H-Final
3 Origin	Varian
4 Spectrometer	vnmrs
5 Author	
6 Solvent	cd2cl2
7 Temperature	25.0
8 Pulse Sequence	s2pul
9 Number of Scans	8
10 Receiver Gain	30
11 Relaxation Delay	5.0000
12 Pulse Width	0.0000
13 Acquisition Time	2.0447
14 Acquisition Date	2014-09-29T17:52:15
15 Modification Date	2014-10-02T16:11:19
16 Spectrometer Frequency	499.88
17 Spectral Width	8012.8
18 Lowest Frequency	-1013.6
19 Nucleus	1H
20 Acquired Size	16384
21 Spectral Size	32768

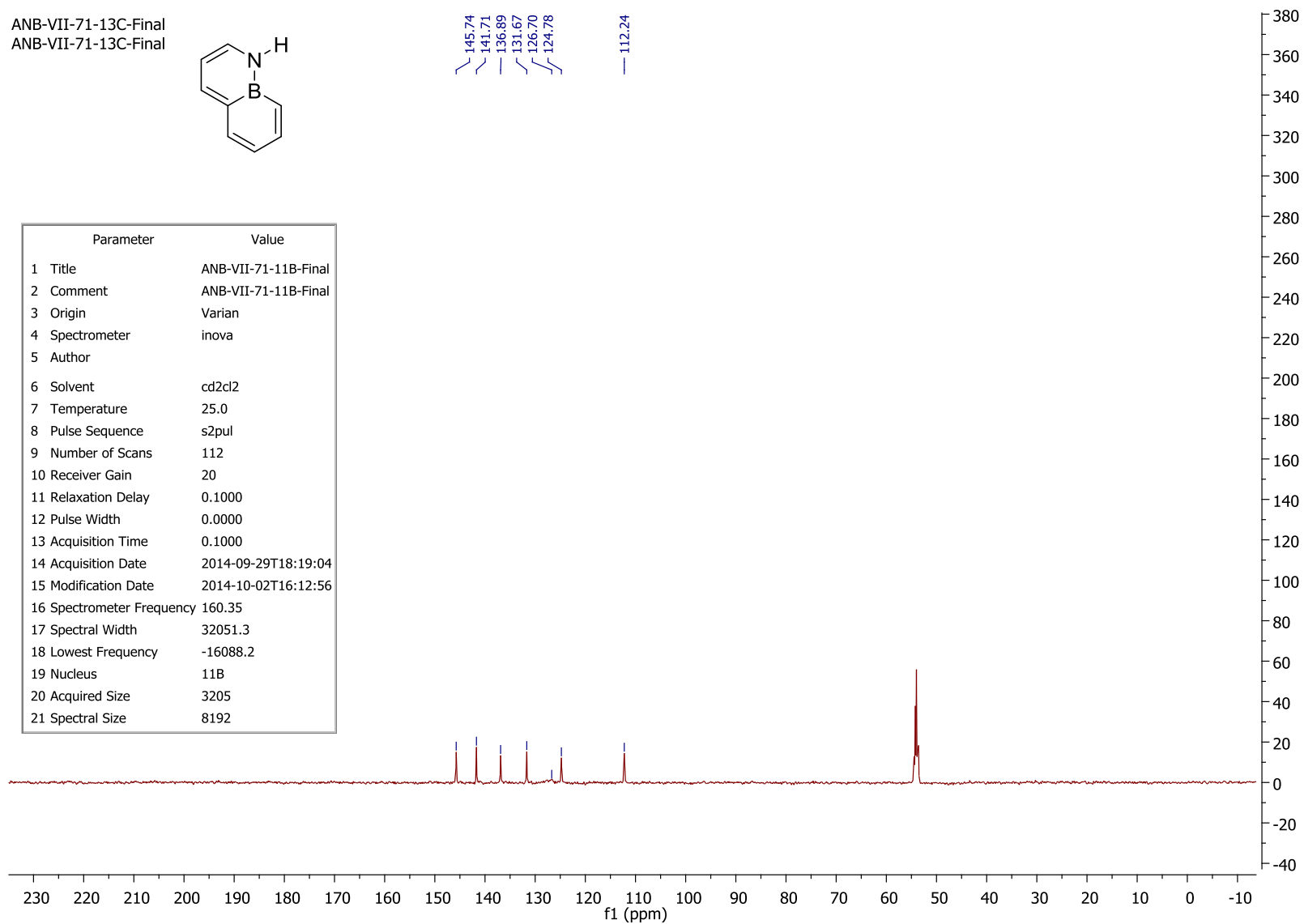


ANB-VII-71-13C-Final
ANB-VII-71-13C-Final



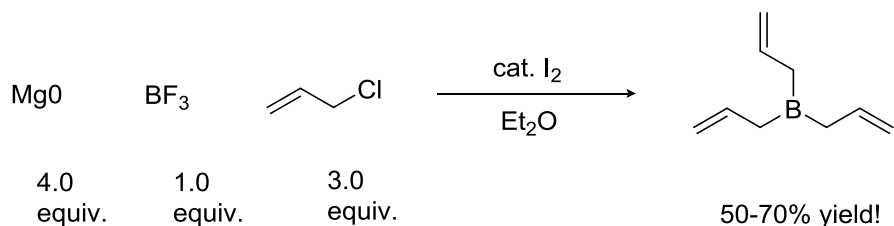
145.74
141.71
136.89
131.67
126.70
124.78
112.24

Parameter	Value
1 Title	ANB-VII-71-11B-Final
2 Comment	ANB-VII-71-11B-Final
3 Origin	Varian
4 Spectrometer	inova
5 Author	
6 Solvent	cd2cl2
7 Temperature	25.0
8 Pulse Sequence	s2pul
9 Number of Scans	112
10 Receiver Gain	20
11 Relaxation Delay	0.1000
12 Pulse Width	0.0000
13 Acquisition Time	0.1000
14 Acquisition Date	2014-09-29T18:19:04
15 Modification Date	2014-10-02T16:12:56
16 Spectrometer Frequency	160.35
17 Spectral Width	32051.3
18 Lowest Frequency	-16088.2
19 Nucleus	11B
20 Acquired Size	3205
21 Spectral Size	8192



Appendix 1: Standard Operating Procedures for the Synthesis of Azaborines Used Throughout This Work

A.1 Synthesis of Triallylborane



We run this reaction on multimole scale—it requires your utmost attention and care.

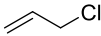
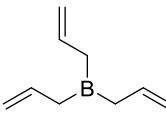
Necessary prep-work before reaction

- Allyl chloride (MW: 76.52 density: 0.94 g/mL bp: 45 °C) should be distilled under inert gas immediately before use.
- BF₃ etherate (MW: 141.93 density: 1.15 g/mL bp: 126-129 °C) should be stirred and distilled over CaH₂ under inert gas and stored away from light in a Schlenk flask.
- Aldrich anhydrous inhibitor-free sureseal ether (what we get for the solvent system) is of sufficient quality to perform the reaction with no further purification.
- All necessary glassware and magnesium should be oven-dried and cooled under a stream of inert gas.
- It is imperative to keep the reagents airfree as the reaction is very sensitive to the initial purity of allyl chloride and BF₃ etherate used—proper syringe/cannula technique is required.

Safety Considerations

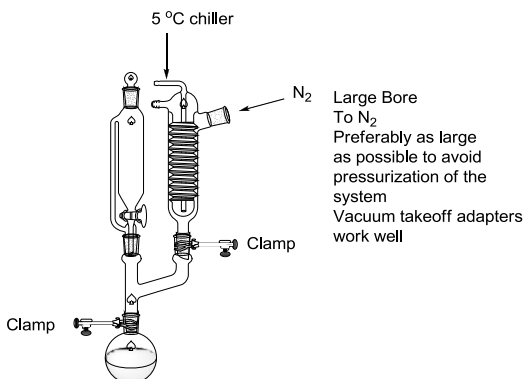
- **Diethyl Ether is Highly Flammable**
- **Overall Reaction is Exothermic**
- **Improper Stirring Can Lead to Runaway Reactions Extreme
Care Should be Taken During the Addition of Allyl Chloride**
- **Ice and Liquid Nitrogen Should be Available to Slow the
Reaction if Necessary**
- **If Set-Up and Performed Carefully and Correctly, This
Reaction can be Carried Out With no Problems, However
the Margin-For-Error is not Large.**

A.1.1 Introductory Scale Procedure for Triallylborane

	Mg0	BF ₃ Etherate		I ₂	$\xrightarrow{\text{Et}_2\text{O}}$	
MW	24.31	141.93	76.52		300 mL for reaction 50 mL for addition	134.03
Mass	9.73g	14.2g=12.3mL	22.5g=24mL	1 crystal	300 mL for washing =650 mL Et ₂ O	
Mmole.	400	100	300			
Equiv.	4.0	1.0	3.0			

Glassware Needed For Reaction Setup:

- 1L Single-Necked RBF 24/40
- Large Football Bar of Stirring
- Claisen Adapter 24/40
- Large Volume Reflux Condenser
24/40
- Pressure equalizing addition funnel
24/40
- Nitrogen Inlet Adapter/Vacuum Takeoff Adapter (same thing)
- Stainless Steel Bowl for Secondary Containment.



Materials Needed For Workup:

- 2x 1L Single-Necked RBF 24/40
- Medium Football Bar of Stirring
- 1L Dry Ice Trap for Low Vacuum Pump
- 1x Schlenk Filter Funnel

- Large-Bore Cannula Needle
- Distillation apparatus and Storage Flask for Distillation

CAUTION: Before beginning this reaction make sure that all safety equipment such as ice, liquid nitrogen, and a fire extinguisher is available and understood. Make sure there are no ready sources of ignition as we are working with large volumes of refluxing diethyl ether. Do not perform this reaction alone in the lab.

An oven-dried 1L round bottom flask containing 9.73 g of magnesium turnings and a large football bar of stirring was cooled under nitrogen. This system was equipped with a Claisen adapter and a large-volume reflux condenser fitted with a nitrogen inlet on the sidearm port. The flask was charged with diethyl ether (300 mL), BF₃ OEt₂ (14.2 g, 12.3 mL) via syringe, and a crystal of iodine. This system was fitted with an addition funnel which was then charged with allyl chloride (22.5 g, 24 mL). The well-stirred reaction was initiated by addition of approximately 4 mL of neat allyl chloride. The reaction was allowed to reflux smoothly by the controlled monitored dropwise addition of the allyl chloride over ca. 1 hour (the addition speed is defined by the safe refluxing of the ether).

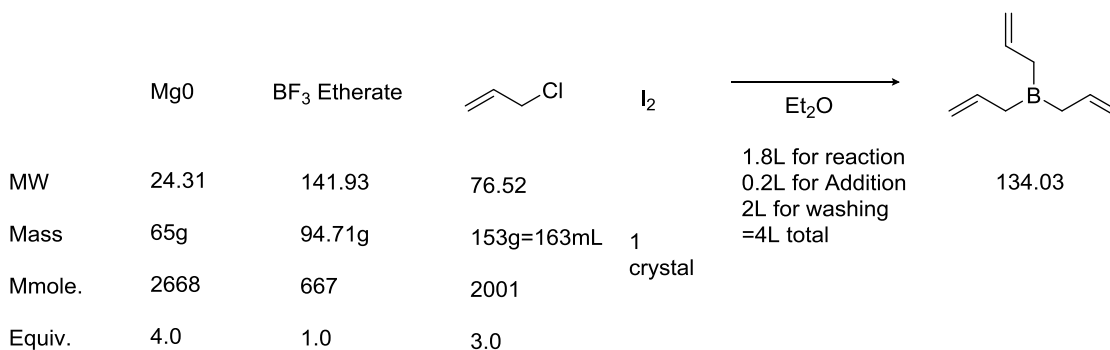
CAUTION: The initial addition of allyl chloride is a possible place for the reaction to run away. If the reflux line reaches the halfway point up the condenser the addition is too fast. If the line is at the top of the condenser cool the flask with ice or liquid nitrogen. If you feel the reaction is unstoppable, do not try to stop it, stay calm, close your hood, inform the rest of the lab, and walk away— it is not worth your safety. If proper care is taken any runaway reaction can be safely stopped— this is why constant monitoring is essential during the beginning of this reaction.

Upon complete addition the addition funnel is replaced by a septum and ¹¹B nmr checkpoints are taken until the reaction is >95 % complete (No remaining BF₃, only

small amounts of intermediate BR_xF_x)— continued reaction is evinced by continued condensation of ether. Upon completion the reaction mixture can be directly filtered via cannula through a schlenk filter into a 1L round bottom flask, and the remaining diethyl ether can be removed via a diaphragm pump equipped with an in-line dry ice trap. The reaction mixture is then washed with 3x 100 mL portions of anhydrous ether and filtered in the same manner. Triallylborane can be distilled into a storage flask under diaphragm pump vacuum at $\sim 65-85$ °C however generally all readily distilled (oil bath <110 °C) product is triallylborane.

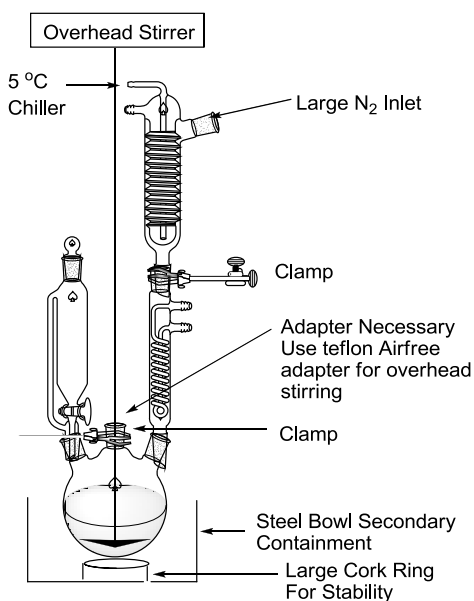
CAUTION: Quenching of the distillation pot should be done with extreme care. A large excess of isopropanol (100-200 mL) at 0 °C under nitrogen (alkylboranes combust on contact with air) followed by bleach quenching works well—*do not quench directly with water or ice it will catch fire*. All borane-contaminated glassware should be bleached and washed appropriately.

A.1.2 Large-scale Synthesis of Triallylborane



Glassware Needed For Reaction Setup:

- 5L Three-Necked RBF
- Overhead Stirrer
- Condenser 24/40
- Large Volume Reflux Condenser 24/40
- Pressure equalizing addition funnel 24/40
- Nitrogen Inlet Adapter/Vacuum Takeoff Adapter (same thing)



Materials Needed For Workup:

- 2x 1L Single-Necked RBF 24/40
- Medium Football Bar of Stirring
- 1L Dry Ice Trap for Low Vacuum Pump
- Schlenk Filter Funnel
- Large-Bore Cannula Needle
- Distillation apparatus and Storage Flask for Distillation

- Nitrogen Inlet Adapter/Vacuum Takeoff Adapter (same thing)

Large scale synthesis takes ~twice as long to run/workup, so be prepared for a long day. On this scale the consequences of inattention are much more; the stakes are higher Pay Attention and do not run this reaction when not in top form.

An oven-dried 5L three-necked round bottom flask containing 65 g of magnesium turnings and an overhead stirrer was cooled under nitrogen. This system was equipped with two sequential reflux condensers with a nitrogen inlet on the sidearm port. The flask was charged with diethyl ether (1.8 L), $\text{BF}_3 \cdot \text{OEt}_2$ (94.71 g, 82 mL) via cannula, and a crystal of iodine. This system was fitted with an addition funnel which was then charged with allyl chloride (163 mL, 153 g). The well-stirred reaction was initiated by addition of approximately 5 mL of neat allyl chloride. Once initiated, the reaction was allowed to reflux smoothly by the controlled monitored dropwise addition of the allyl chloride over ca. 1.5-3 hours (the addition speed is defined by the safe refluxing of the ether, approximately 80% of the lowermost reflux condenser should be where the vapor line is maintained).

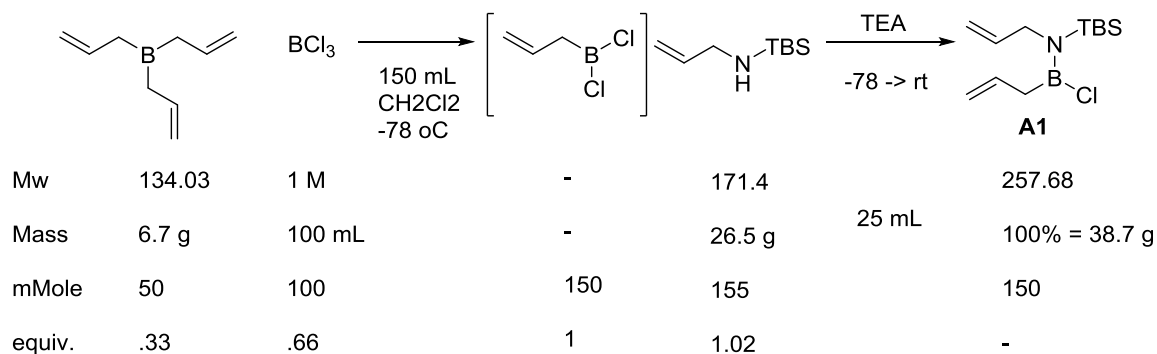
CAUTION: The initial addition of allyl chloride is a possible place for the reaction to run away. If the reflux line reaches the second condenser the addition is too fast. If the line is at the top of the second condenser cool the flask with ice or liquid nitrogen. If you feel the reaction is unstoppable, do not try to stop it, stay calm, close your hood, inform the rest of the lab, and walk away— it is not worth your safety. If proper care is taken any runaway reaction can be safely stopped— this is why constant monitoring is essential during the beginning of this reaction.

Upon complete addition the addition funnel is replaced by a septum and ^{11}B nmr checkpoints are taken until the reaction is >95 % complete (No remaining BF_3 , only small amounts of intermediate BR_xF_x)— continued reaction is evinced by continued condensation of ether. Upon completion the reaction mixture can be directly filtered via cannula through a schlenk filter (when the filter is near to capacity the solids can be rinsed with diethyl ether and the filter can be replaced with another schlenk filter) into a 1L round bottom flask, and the remaining diethyl ether can be removed via a diaphragm pump equipped with an in-line dry ice trap. The reaction mixture is then washed with 3x 500 mL portions of anhydrous ether and filtered in the same manner. Triallylborane can be distilled into a storage flask under diaphragm pump vacuum at $\sim 65\text{-}85\text{ }^\circ\text{C}$ however generally all readily distilled (oil bath $<110\text{ }^\circ\text{C}$) product is triallylborane.

CAUTION: Quenching of the distillation pot should be done with extreme care. A large excess of isopropanol (700-800 mL) at $0\text{ }^\circ\text{C}$ under nitrogen (alkylboranes combust on contact with air) followed by bleach quenching works well—do not quench directly with water or ice: it will catch fire. All borane-contaminated glassware should be bleached and washed appropriately.

A.2 Synthesis of 1,2-Azaborines

A.2.1 Synthesis of ring-closing precursor A1



Glassware required:

For Reaction:

1 L RBF (for reaction)

Large bar of stirring

Vacuum filtration adapter

250 or 100 mL RBF (for amine)

Cannula (not wider than 18 gauge)

Large Dewar Flask for 1L (our lab has ~4 of these)

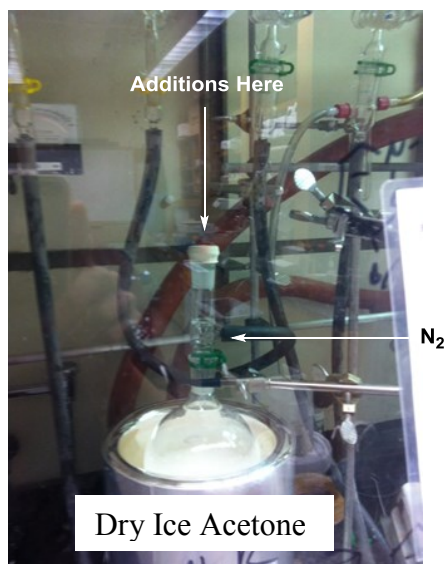
For Workup:

1L RBF

Stirbar

Large Sintered Glass Funnel (M)

Vacuum filtration adaptor that can fit your sintered glass funnel



vacuum filtration
adapter

Distillation setup (24/40 with ~250 mL RBF to collect PDT

(when running 2-4 reactions in parallel))

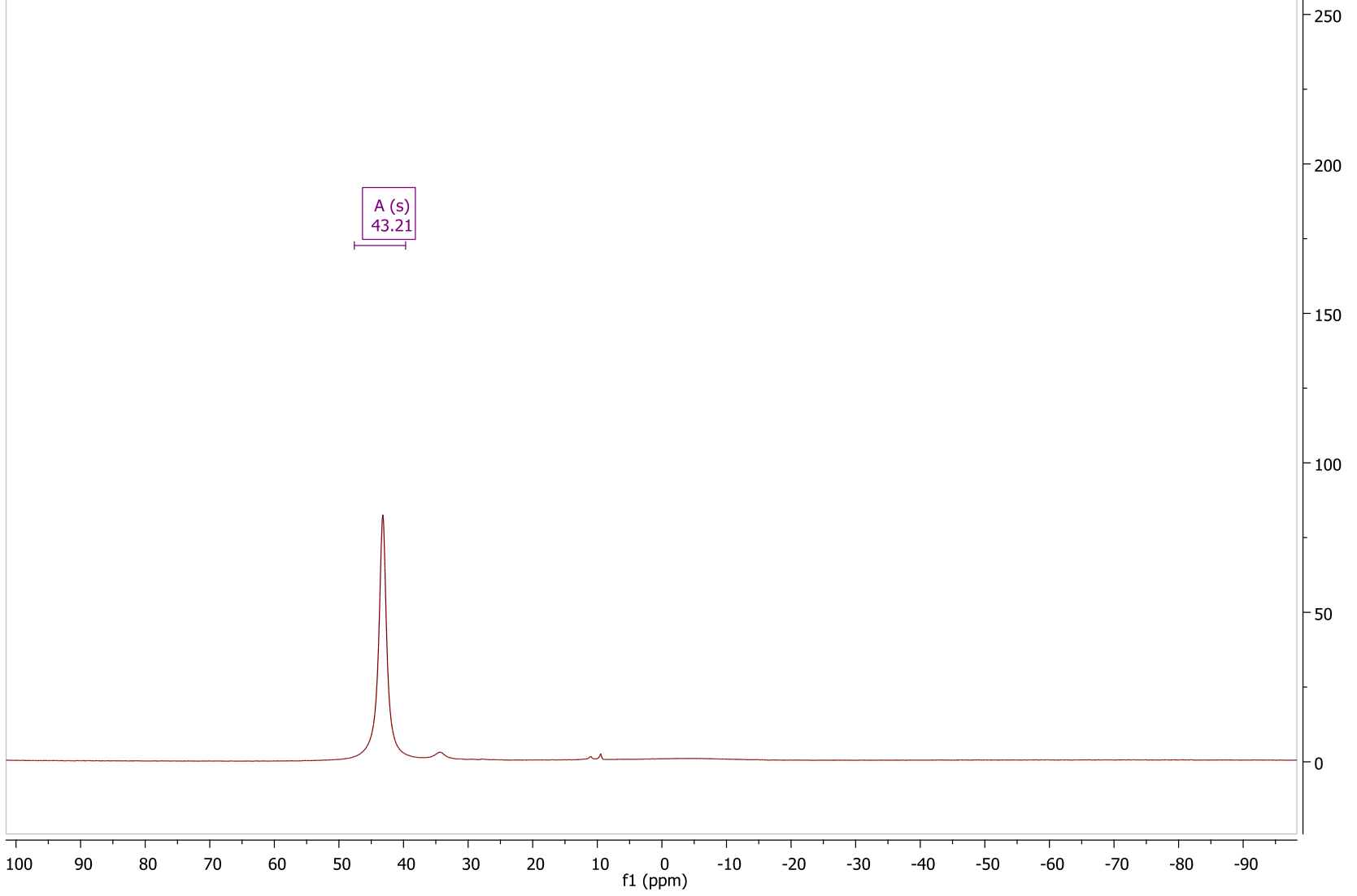
- 6.7 g (50 mmole) of triallylborane is added to 1L flask in glove box
- 150 mL of Methylene chloride is added to this
- bring out of box sealed
- quick switch to vacuum adaptor
- purge system with nitrogen for 10 minutes (via large needle outlet with high flow)
- remove needle outlet
- cool system to -78°C for 45 minutes to ensure complete cooling
- Cannula (not wider than 18 gauge) 1 Bottle (100 mL, 100 mmol) of BCl_3 solution in hexanes into 1L flask with triallylborane
- Stir at -78°C minimum of 3 hours
 - **WAIT TO ADD AMINES**
 - **Make sure there is efficient stirring**
- Weigh TBS allyl amine (26.5 g) into round bottom flask (under N_2 and dilute ~ 1:1 v/v with methylene chloride
- After waiting the appropriate time, make sure there is still sufficient dry ice to maintain the temperature, then cannula (not wider than 18 gauge) TBS allyl amine into 1L containing allyl BCl_2
- upon complete addition of TBS allyl amine add triethylamine (25 mL) directly via syringe (I wait ~10 minutes)

- Make sure there is still dry ice in the Dewar flask
- Let warm to room temperature naturally overnight while remaining in the Dewar flask
- After stirring overnight it is OK to remove the Dewar.
- Allow to warm to room temperature before checking the reaction via ^{11}B nmr
- A completed reaction has no peak at ~ 10 ppm and should be cleanly a peak at 43 ppm
- upon completion remove $\sim 3/4$ of the solvent on the high vacuum line
 - While solvent is being removed bring hot 1L flask, vacuum adaptor, and stir bar into box
- Rinse salts well with pentane through fritted funnel
 - (I rinse the salts into the funnel with ~ 2 -300 mL of pentane (total volume) then wash the salts with smaller amounts)
- Remove pentane and distill (~ 70 °C at 300mtorr)
- Yield should be ~ 75 -90%

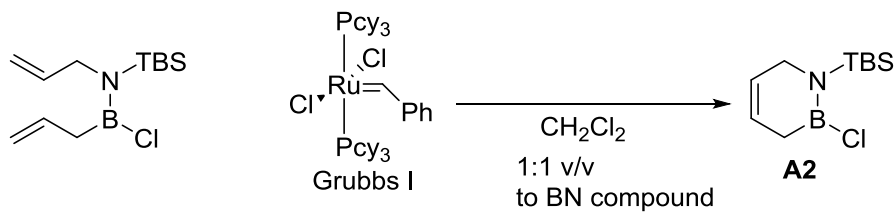
Efficient stirring is essential for this reaction to go to completion cleanly. Large football stirbars seem to work the best, and make sure it can stir before cooling the reaction as sometimes it can be hard to tell when the cold bath is loaded.

If you are unsure of a step above ask an experienced group member.

ANB-vII-241-1-11B-1
ANB-vII-241-1-11B-1



A.2.2 Synthesis of ring-closed A2



MW	257.68	822.96	229.63
mass	38.7 g	0.6-1.2 g	100% = 34.4 g
mmole	150	0.75-1.5	150
equiv.	1	0.002-0.01	-

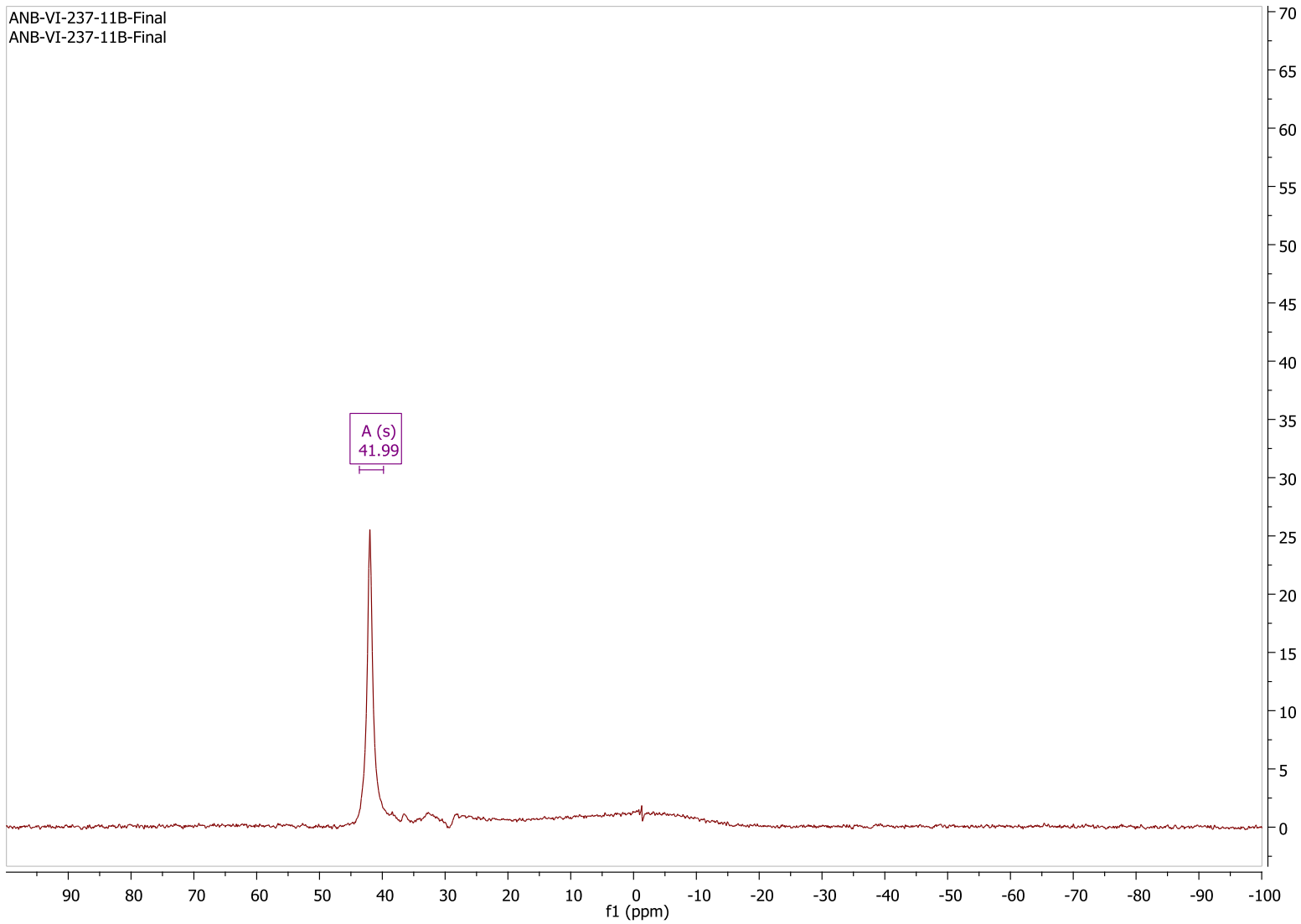
Glassware required:

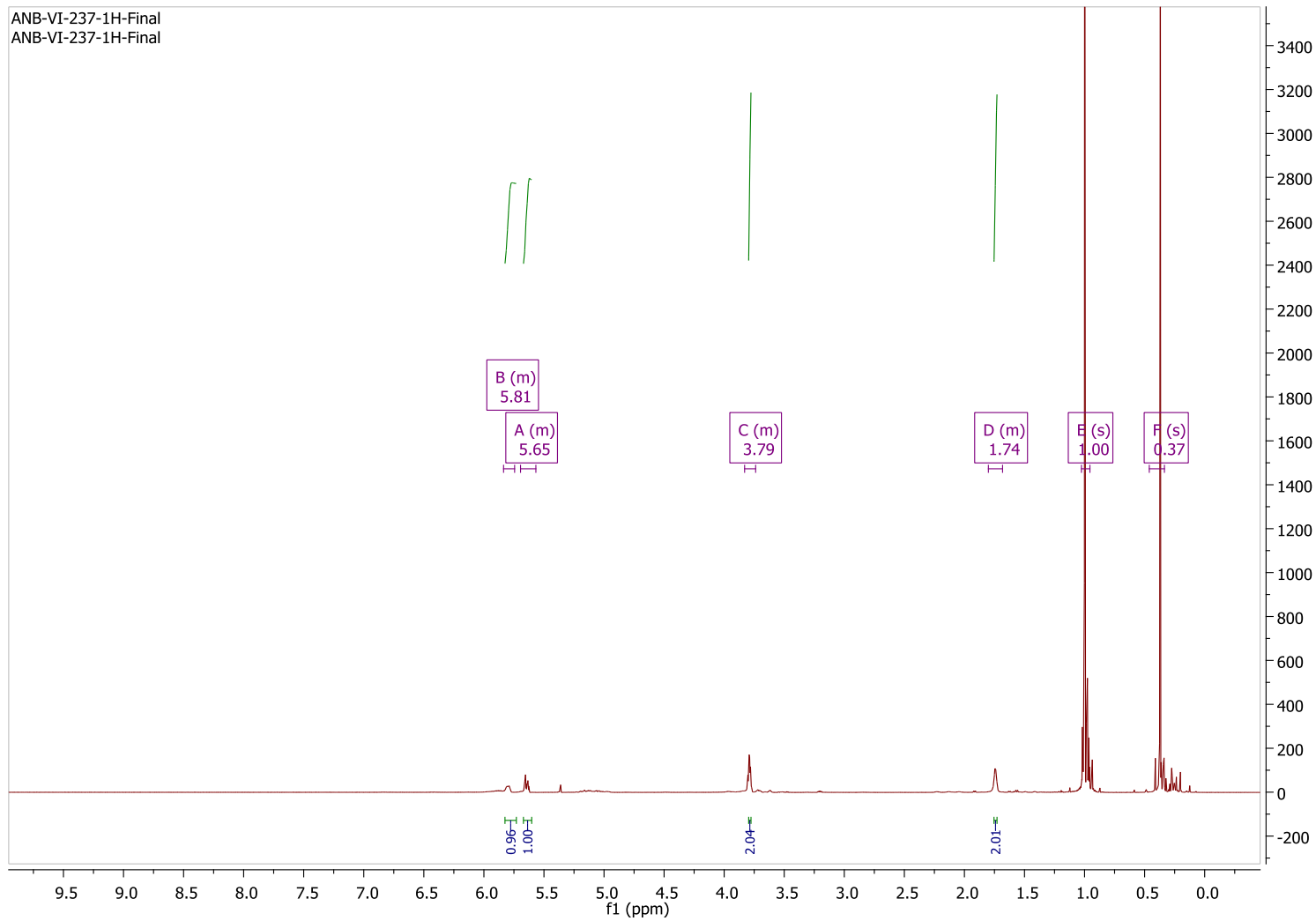
500 mL RBF or 1L (~4 volumes headspace is recommended as this can bubble over)

Stirbar

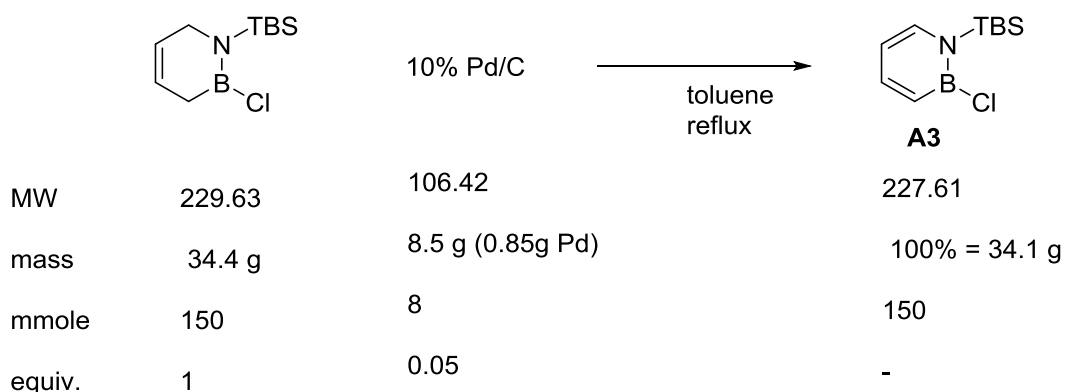
Vacuum distillation setup (24/40)

- Measure azaborine into large flask with 1:1 v/v CH₂Cl₂
- Add Grubb's I in ~75 mg portions while making sure the reaction does not bubble over
- start with 0.2 mol % Grubb's I, check reaction by proton nmr (workup aliquot) at 30 minutes after addition
- if necessary add more Grubb's I
- if not, remove solvent on high vacuum line and distill product
- Yield should be 85-95%





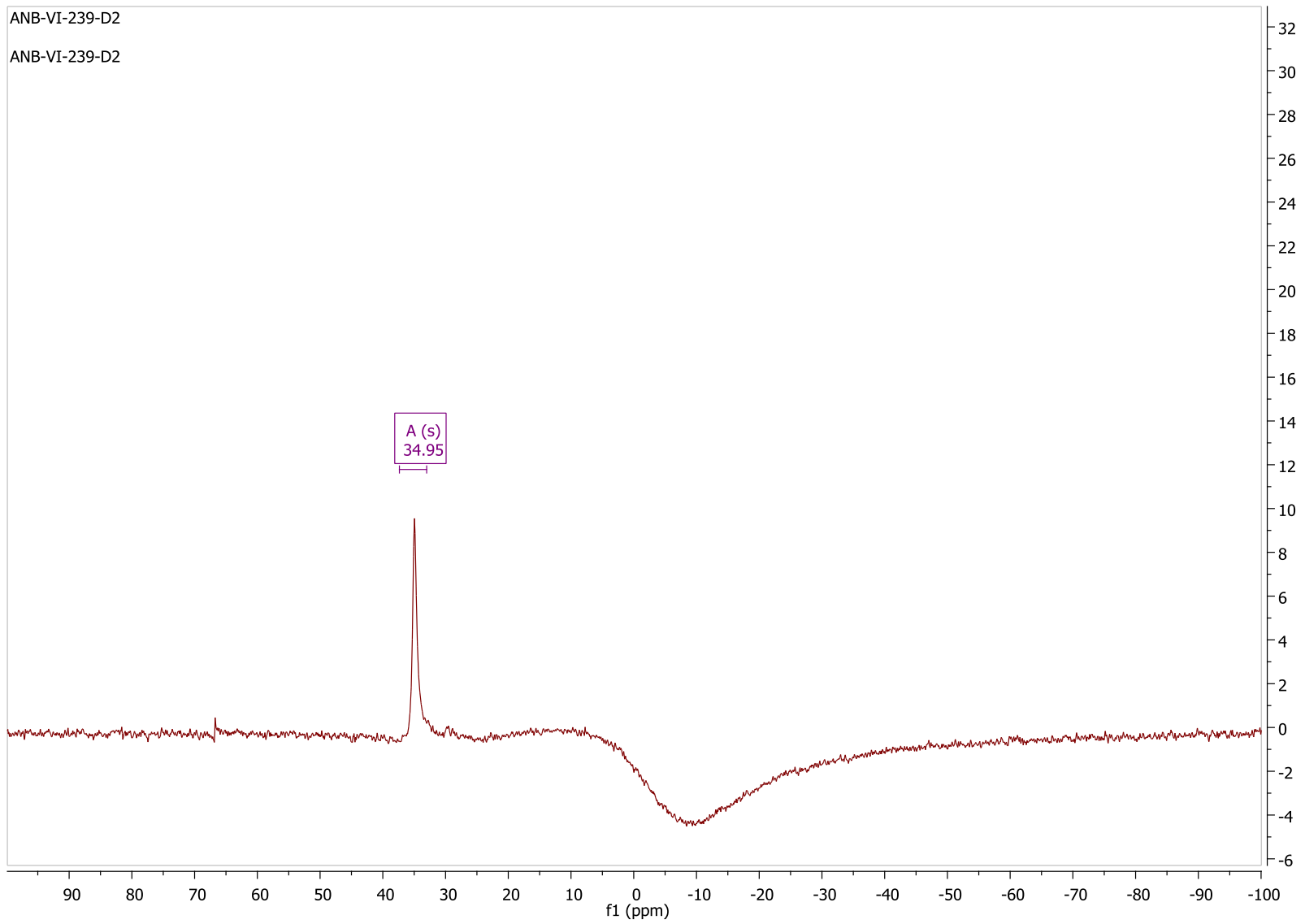
A.2.3 Synthesis of N-TBS B-Cl A3



- Reaction is carried out in a 1L RBF equipped with a water-cooled condenser
- Oil bath is 130 °C for strong reflux
- Reflux until completion, there should be no starting material (¹¹B 43 ppm) and should only have product (¹¹B 35 ppm).
- Palladium is filtered through a sintered glass funnel (M porosity) and rinsed with plenty of solvent (I use THF) (The sintered glass funnel is cleaned by flowing acetone followed by water through the funnel in the opposite direction of initial flow)
- Solvent is removed (high-vac)
- product distills at ~70 °C @ 300 mtorr
- 50-75% yield

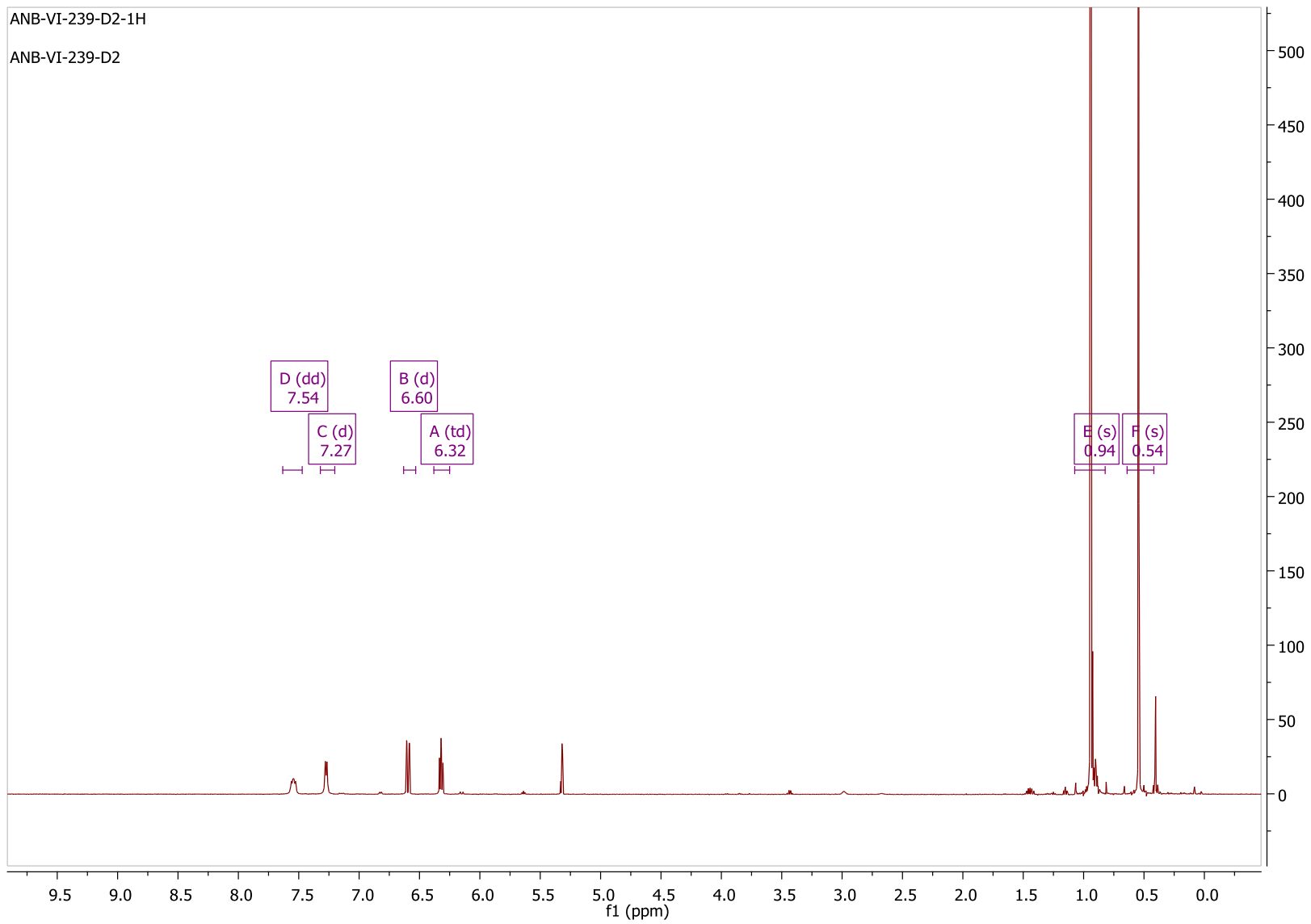
ANB-VI-239-D2

ANB-VI-239-D2

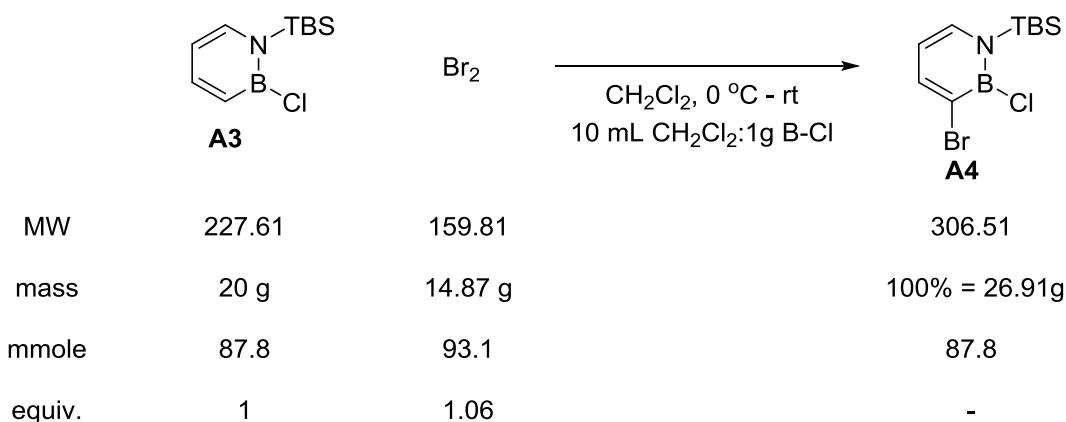


ANB-VI-239-D2-1H

ANB-VI-239-D2



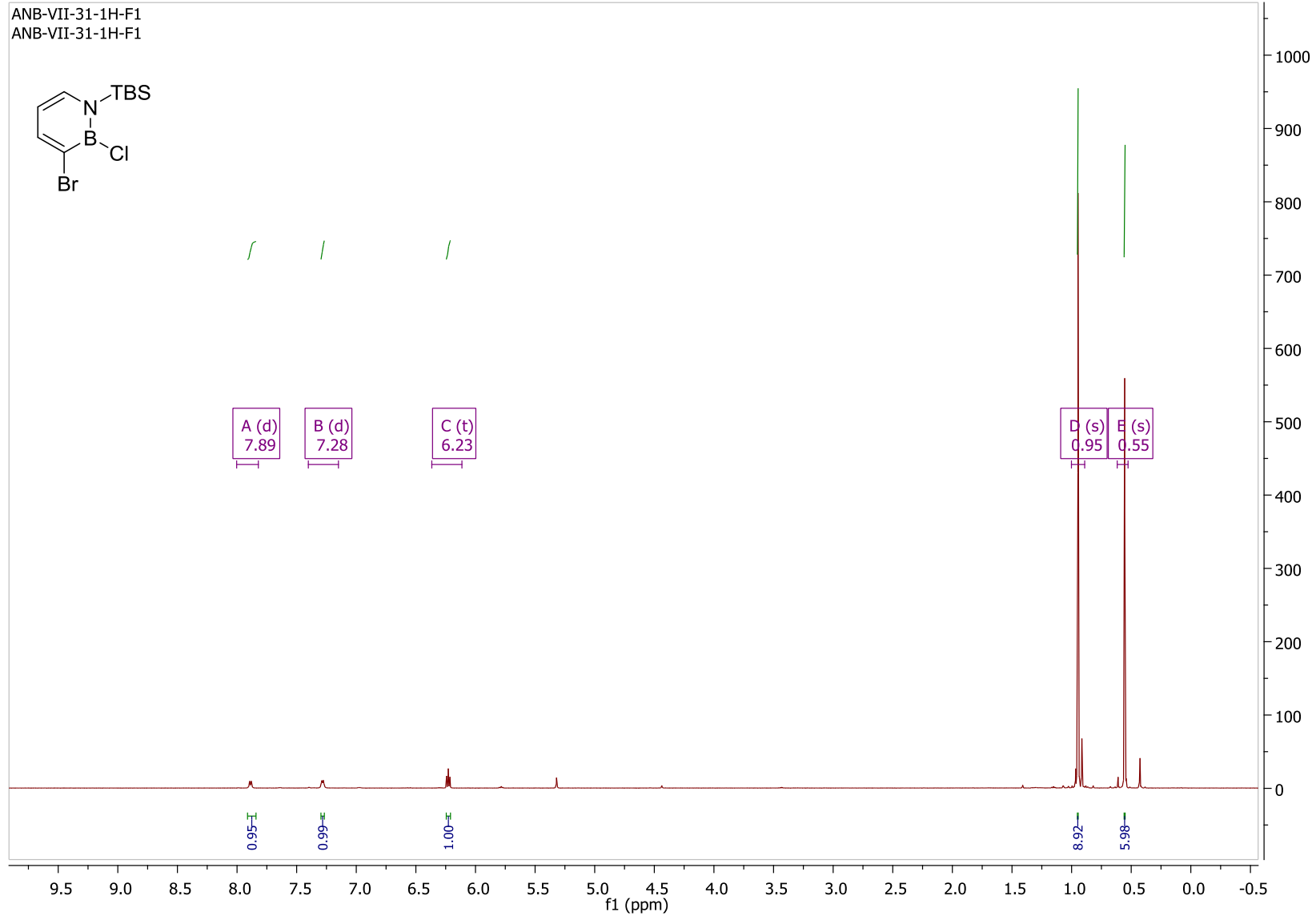
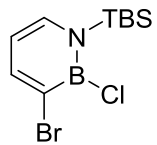
A.2.4 Synthesis of C(3) brominated B–Cl azaborine **A4**



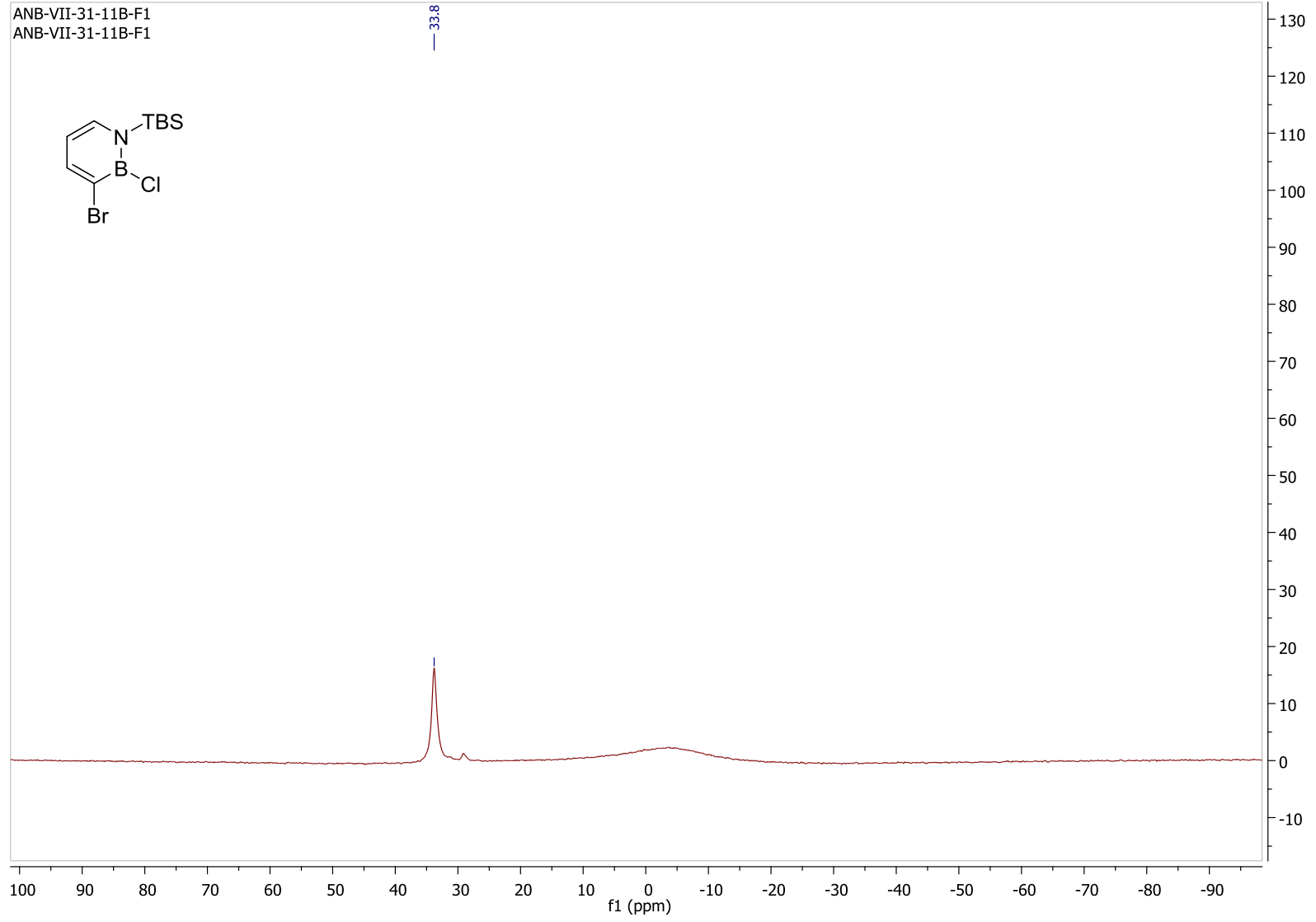
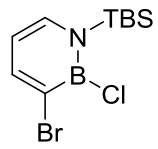
A 100 mL round bottom flask was charged with 1 equiv of **A3** (5g, 21.97 mmole), a bar of stirring, and 50 mL of CH₂Cl₂. This mixture was cooled to 0 °C in an ice/water bath. In a separate vessel, 1.05 equiv Br₂ (3.58g, 23.1 mmole) was diluted in 2 parts methylene chloride: 1 part Br₂. This mixture was added dropwise to the azaborine solution over 15 minutes. The reaction was stirred for 15 additional minutes at 0 °C and was allowed to warm to room temperature and continued until ¹H NMR analysis indicated completion (30 min-2 h). Solvent was removed under reduced pressure and 30 mL pentane was added. Solids were removed by filtration and the filtrate was concentrated. Vacuum distillation (62-65 °C, 120 mT) provided brominated **A4** as a clear, colorless liquid which solidifies upon standing at -30 °C (18.8 g, 70%). ¹H NMR (300 MHz, CH₂Cl₂): δ 7.89 (d, *J* = 7.0 Hz, 1H), 7.28 (d, *J* = 6.7 Hz, 1H), 6.23 (app t, *J* = 6.7 Hz, 1H), 0.95 (s, 9H), 0.55 (s, 6H). ¹¹B NMR (192.5 MHz, CD₂Cl₂): δ 37.4. ¹³C NMR (75.4 MHz, CD₂Cl₂): δ 147.0, 139.0, 111.8, 26.8, 19.7, -1.3. The quaternary carbon adjacent to boron was not observed. FTIR (ATR): $\tilde{\nu}$ = 2956, 2931, 2883, 2858, 1597, 1492, 1466, 1439, 1332, 1262, 1252, 1189, 1137, 1122, 1087, 1032, 994, 943, 844,

823, 808, 790, 762, 741, 711, 692, 671, 653, 577, 439, 422. HRMS (EI) calcd for $C_{10}H_{18}BNSiCl^{\delta 1}Br(M^+)$ 307.01530, found 307.01500.

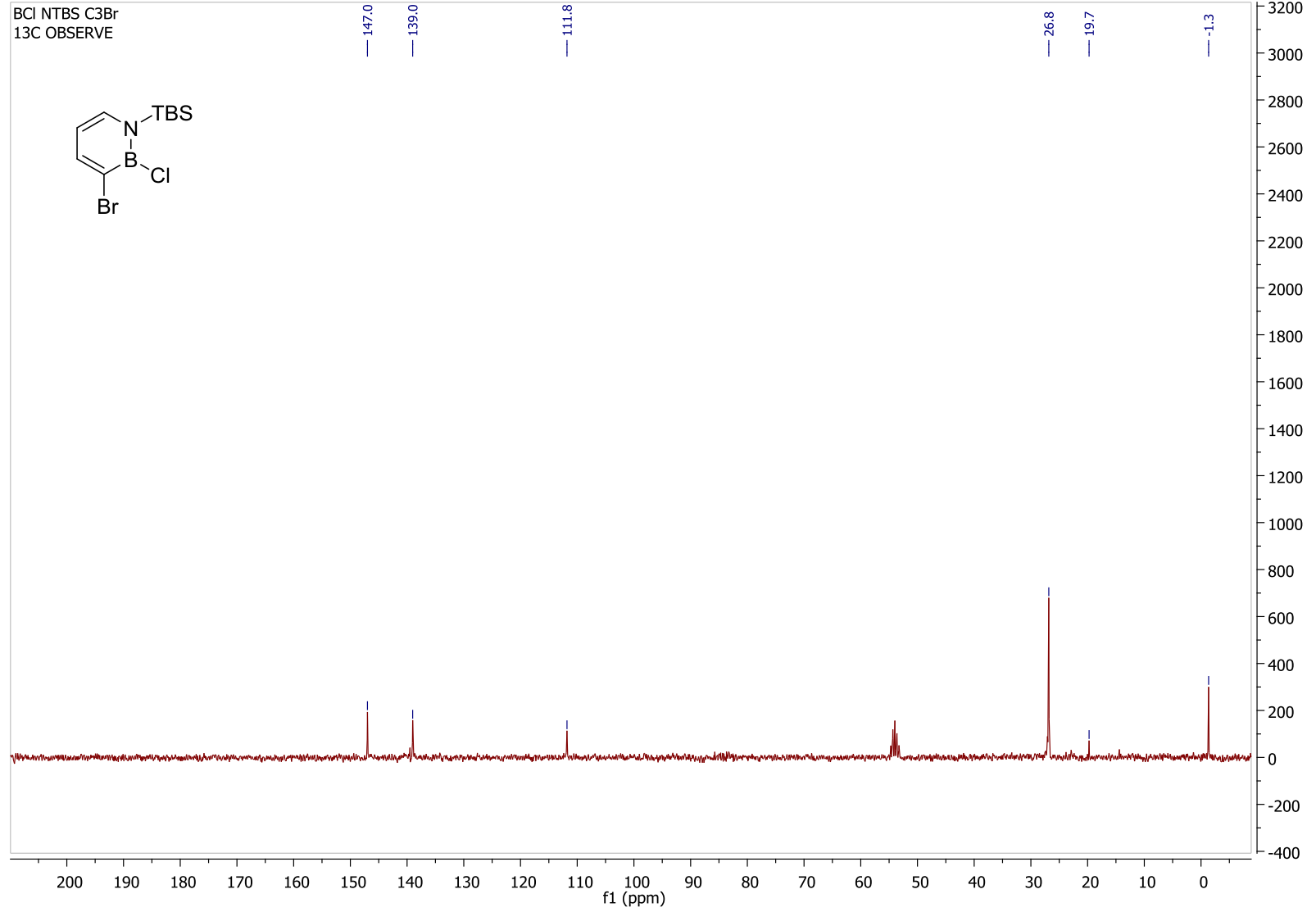
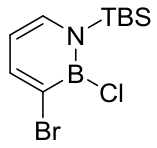
ANB-VII-31-1H-F1
ANB-VII-31-1H-F1



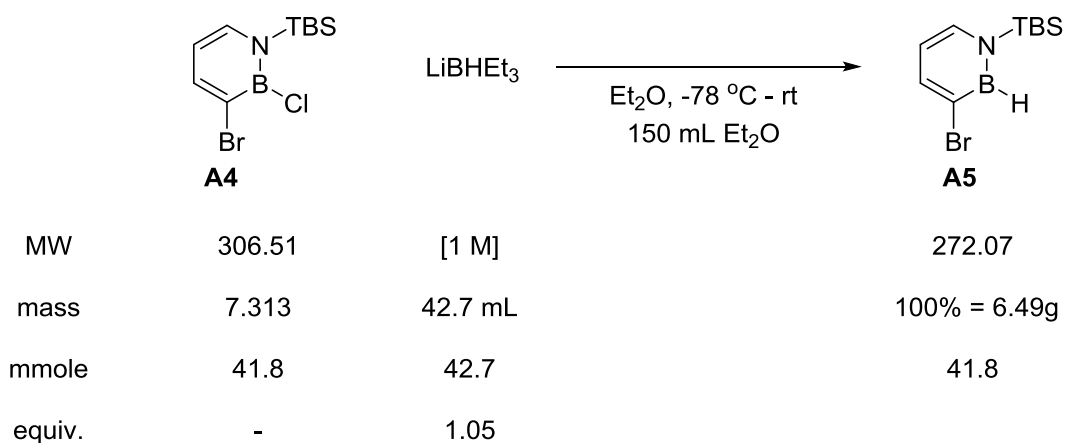
ANB-VII-31-11B-F1
ANB-VII-31-11B-F1



BCI NTBS C3Br
13C OBSERVE



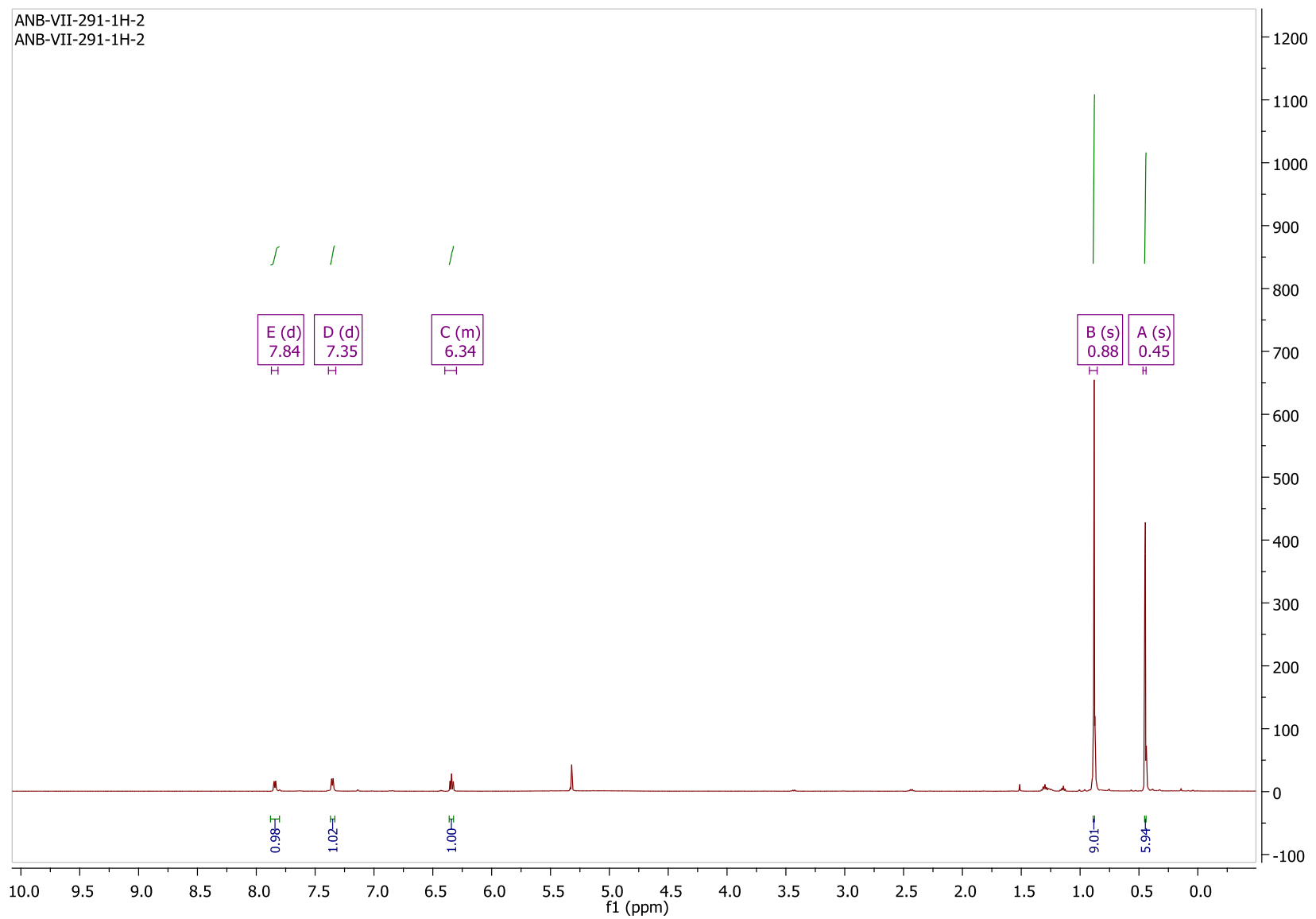
A.2.4 Synthesis of C(3) brominated B–H azaborine **A5**



A 500 mL round bottomed flask was charged with 1 equiv (7.31 g, 41.8 mmole) N–TBS, B–Cl C(3)–Br **A4**, a bar of stirring, and 150 mL Et₂O. This mixture was cooled to -78 °C and 1.05 equiv LiBHET₃ solution (1M, 42.7 mL, 42.7 mmole) was added via syringe. After complete addition the reaction was stirred for 1 hour at -78 °C then allowed to warm to room temperature until ¹H NMR analysis of an aliquot indicated completion (approximately 4 hours). The reaction mixture was filtered directly through silica with Et₂O followed by silica gel chromatography to obtain **A5** as a clear colorless oil which solidifies upon standing at -30 °C (5.79g, 90% yield). ¹H NMR (500 MHz, CD₂Cl₂) δ 7.84 (d, *J* = 6.7 Hz, 1H), 7.35 (d, *J* = 6.3 Hz, 1H), 6.40 – 6.30 (m, 1H), 0.88 (s, 9H), 0.45 (s, 6H). ¹¹B NMR (160 MHz, CD₂Cl₂) δ 34.1 (d, *J* = 127.4 Hz). ¹³C NMR (151 MHz, CD₂Cl₂) δ 144.8, 137.6, 113.2, 26.2, 18.4, -4.0. The quaternary carbon adjacent to boron was not observed.

FTIR (ATR): $\tilde{\nu}$ = 2954, 2929, 2884, 2858, 2562 (BH), 2530 (BH), 1598, 1488, 1470, 1440, 1392, 1362, 1337, 1262, 1223, 1205, 1154, 1073, 1005, 986, 953, 938, 847, 837, 822, 810, 787, 768, 717, 676, 637, 610, 408.

ANB-VII-291-1H-2
ANB-VII-291-1H-2



ANB-VII-291-11B-2
ANB-VII-291-11B-2

